Antiviral and immunomodulatory activities of iminosugars: candidate therapeutics for arbovirus infections

Beatrice E. Tyrrell

St Edmund Hall
University of Oxford

A thesis submitted for the degree of
Doctor of Philosophy

Michaelmas Term 2018

Acknowledgements

I owe great thanks to many people for making this thesis possible. Firstly, Nicole, you have been a wonderfully supportive supervisor, encouraging me to pursue interesting things, both in terms of experiments but also all of the wonderful opportunities for conferences, travel, public engagement and other activities I have been involved in during the course of my DPhil. Jo and Drew, you introduced me to the world of dengue and BSL3 work, and for that and all of your help, support and scientific conversation ever since, I am truly thankful. To all of the other Zitzmannians – you have made the lab a lovely place to work and all of your insights and assistance are much appreciated.

I would also like to thank all of my collaborators, both in Oxford and further afield. To the Virology and Pathogenesis Group at Porton Down, thank you for being so welcoming. I also have to thank the UNIL Summer Undergraduate Research Programme, particularly Thierry and Eleonora, as well as the Goodall group in Cambridge for launching me into the world of innate immunity and infectious disease research. Thank you to the Wellcome Trust for the generous funding but also for enabling the existence of the IITM community.

Thank you to my parents and my sister for supporting me in all of my endeavours and for everything that you have sacrificed to help make me the person I am today. To the Spice Girls, Teddy Hall and 26 community, Will, and Zafar, thank you for keeping me sane through almost eight years at Oxbridge and for all of the amazing experiences we have had. Your friendships mean the world to me. Finally, thank you to Mittens for the fluffy cuddles and to Pip for always making me laugh.

Table of Contents

Table of Figures

Table of Tables

List of Abbreviations

2-AA	2-aminobenzoic acid
2THO-DNJ	*N*-8′-(2′′-tetrahydrofuranyl)-octyl-DNJ; UV-12
2THO-DGJ	*N*-8′-(2′′-tetrahydrofuranyl)-octyl-DGJ
5F-DNJ	*N*-pentafluorobenzyl-1-DNJ
ACE2	angiotensin-I converting enzyme 2
ADE	antibody-dependent enhancement
AFRIMS	US Armed Forces Research Institute of Medical Sciences, Thailand
ATCC	American Type Culture Collection
ATF6	activating transcription factor 6
BHK-21	baby hamster kidney-21 cell
BID	*bis in die* (twice daily)
BiP	binding immunoglobulin protein
BLAST	Basic Local Alignment Search Tool
BSL	Biological Safety Level
BuCAST	6-*O*-butanoyl CAST; celgosivir
BUNV	Bunyamwera virus
BVDV	bovine viral diarrhoea virus
c-di-GMP	bis-(3'-5')-cyclic dimeric guanosine monophosphate
C	capsid
CAST	castanospermine
$CC_{10/50}$	compound concentration resulting in 10 or 50% cytotoxicity
CCHF	Crimean-Congo haemorrhagic fever
CCHFV	Crimean-Congo haemorrhagic fever virus
CDG	congenital disorders of glycosylation
CHIKV	Chikungunya virus

CHOP	CCAAT-enhancer-binding protein homologous protein
CLEC5A	C-type lectin domain containing 5A
CNX	calnexin
CPE	cytopathic effect
CRISPR/Cas9	clustered regularly interspaced short palindromic repeats/CRISPR-associated 9
CRT	calreticulin
Cryo-EM	cryogenic electron microscopy
CZS	congenital Zika syndrome
DC	dendritic cell
DC-SIGN	dendritic cell-specific intercellular adhesion molecule-3-grabbing non-integrin
DENV	dengue virus
DF	dengue fever
DGJ	deoxygalactonojirimycin
DHF	dengue haemorrhagic fever
DMEM	Dulbecco's modified Eagle medium
DMSO	dimethyl sulfoxide
DMJ	deoxymannojirimycin
DNJ	deoxynojirimycin
DSO_2-ONJ	1-dodecylsulfonyl-5N,6O-oxomethylidenenojirimycin
DSS	dengue shock syndrome
E	envelope protein
EBOV	Ebola virus
ECACC	European Collection of Authenticated Cell Cultures
EDTA	ethylenediaminetetraacetic acid
Endo H	endoglycosidase H
ER	endoplasmic reticulum

ERAD	ER-associated degradation
EU	endotoxin units
FLA-BS	Flagellin from *Bacillus subtilis*
FOS	free oligosaccharide
GCS	glucosylceramide synthase; ceramide-specific glucosyltransferase
GE	genome equivalents
Glc	glucose
GlcNAc	N-acetylglucosamine
HAZV	Hazara virus
HBSS	Hank's balanced salt solution
HCoV-NL63	human coronavirus NL63
HCV	hepatitis C virus
HEK	human embryonic kidney
HI-FBS	heat-inactivated foetal bovine serum
HIV	human immunodeficiency virus
HKCA	heat-killed *Candida albicans*
HMGB1	high mobility group box protein 1
IAV	influenza A virus
i.c.	intracranial
$IC_{50/90}$	compound concentration reducing infectious virus secretion by 50 or 90%
IFN	interferon
IFN-α/β	type I interferon; interferon-alpha/beta
Ig	immunoglobulin
IL	interleukin
imDC	immature monocyte-derived dendritic cell
INFV	influenza virus

i.p.	intraperitoneal
IP-10	interferon-inducible protein 10
IRE1α	inositol-requiring enzyme 1α
IRF	interferon regulatory factor
ISG	interferon-stimulated gene
i.v.	intravenous
JAK	Janus kinase
JEV	Japanese encephalitis virus
LASV	Lassa fever virus
LPS	lipopolysaccharide
LPS-EB	lipopolysaccharide from *Escherichia coli* O111:B4
LPS-ST	lipopolysaccharide from *Salmonella enterica* serotype typhimurium
M	membrane protein
Man	mannose
MCP-1	monocyte chemoattractant protein 1
MDA5	melanoma differentiation-associated protein 5
MDBK	Madin-Darby bovine kidney cell
MDDC	monocyte-derived dendritic cell
MDMΦ	monocyte-derived macrophage
MEM	Modified Eagle medium
MIP-1α	macrophage inhibitory protein 1 alpha
MLV	Moloney murine leukaemia virus
MOGS	mannosyl-oligosaccharide glucosidase; ER α-glucosidase I
M*O*N-DNJ	*N*-(9-methoxynonyl)-DNJ; UV-4
M*O*N-6d-DGJ	*N*-(9'-methoxynonyl)-1,6-dideoxygalactonojirimycin
MOI	multiplicity of infection

MSD	mean survival days
MTS	3-(4,5-dimethyl-2-yl)-5-(3-carboxymethoxyphenyl)-2-(4-sulfophenyl)-2H-tetrazolium
MYD88	myeloid differentiation primary response 88
*N*AP-DNJ	*N*-(N-4-azido-2-nitrophenyl)-6-aminohexyl-DNJ; UV-5
*N*B-DNJ	*N*-butyl-DNJ; UV-1
NB-DGJ	*N*-butyl-DGJ
NCBI	National Center for Biotechnology Information
NEAA	non-essential amino acids
NF-κB	nuclear factor kappa B
NGC	New Guinea C
NHSBT	National Health Service Blood and Transplant service
NLRP3	NACHT, LRR and PYD domains-containing protein 3
*N*N-DNJ	*N*-nonyl-DNJ; UV-2
*N*N-DGJ	*N*-nonyl-DGJ
NOD	nucleotide oligomerisation domain
NP-HPLC	normal phase-high performance liquid chromatography
Nrf2	nuclear factor (erythroid-derived 2)-like 2
NS1	non-structural protein 1
PAF	platelet-activating factor
PAMP	pathogen-associated molecular pattern
PBMC	peripheral blood mononuclear cell
PBS	phosphate buffered saline
Pepinh-Control	control peptide inhibitor
Pepinh-MYD	peptide inhibitor of MyD88
Pepinh-TRIF	peptide inhibitor of TRIF

PERK	protein kinase R-like ER kinase
PERL	polyunsaturated ER-targeting liposome
pfu	plaque forming units
PGN-SAndi	peptidoglycan from *Staphylococcus aureus*
p.i.	post-infection
PMA	phorbol-12-myristate-13-acetate
PNGase F	peptide:N-glycosidase F
Poly(A:U)	polyadenylic–polyuridylic acid
Poly(I:C)	polyinosinic-polycytidylic acid
prM	precursor of the membrane protein
PRR	pattern recognition receptor
RANTES	regulated on activation, normal T cell expressed and secreted
RIG-I	retinoic acid-inducible gene I
ROS	reactive oxygen species
RPLP2	ribosomal protein lateral stalk subunit P2
RVFV	Rift Valley fever virus
SARS-CoV	severe acute respiratory syndrome coronavirus
s.c.	subcutaneous
SEAP	secreted alkaline phosphatase
STAT	signal transducers and activators of transcription
STING	stimulator of interferon genes
TACE	tumour necrosis factor converting enzyme
TID	*ter in die* (thrice daily)
TLR	Toll-like receptor
TNF-α	tumour necrosis factor alpha
ToP-DNJ	5’-tocopheroxypentyl-DNJ

TRIF	TIR-domain-containing adapter-inducing interferon-β
TRIM	tripartite motif
UGGT	UDP-glucose:glycoprotein glucosyltransferase
UniProtKB	UniProt Knowledge Base
UPR	unfolded protein resonse
UVi	ultraviolet-inactivated
VEGF	vascular endothelial growth factor
Vero-GluI	ER α-glucosidase I knockout Vero cells
Vero-GluII	ER α-glucosidase II knockout Vero cells
Vero-WT	wild-type Vero cells
VHF	viral haemorrhagic fever
VLP	viral-like particle
VLR	virological log reduction
VSV	vesicular stomatitis virus
WHO	World Health Organization
WNV	West Nile virus
WST-1	4-[3-(4-iodophnyl)-2-(4-nitrophenyl)-2H-5-tetrazolio]-1,3-benzene disulfonate
XBP1	X-box binding protein 1
ZIKV	Zika virus

Abstract

The antiviral efficacy of iminosugars with glucose-stereochemistry has been demonstrated against a broad range of enveloped viruses possessing N-glycoproteins. This antiviral activity is primarily understood to be mediated by competitive inhibition of endoplasmic reticulum (ER) α-glucosidases, leading to a reduction in functional viral glycoprotein folding and infectious virion production.

Dengue virus (DENV) is one such virus for which iminosugar efficacy has previously been established. Here, the antiviral efficacy of *N*-8'-2''-tetrahydrofuranyl-octyl-deoxynojirimycin (2THO-DNJ) is evaluated against DENV infection of primary human monocyte-derived macrophages (MDMΦs). The potential for iminosugars to impact stages of the DENV infection cycle in addition to virion secretion is considered, and DNJ-derivative iminosugars are demonstrated to inhibit DENV replication in primary human immune cells for the first time. Alongside DENV, iminosugar efficacy against Zika virus (ZIKV) is investigated, finding important differences in the iminosugar susceptibility and ER α-glucosidase dependence of the two viruses.

Moving away from flaviviruses, the potential for iminosugars to be employed against the emerging Crimean-Congo haemorrhagic fever virus is considered, through use of the little-characterised 'surrogate' Hazara virus (HAZV). Despite possession of N-glycoproteins, a lack of iminosugar antiviral activity is observed in HAZV-infected SW13 cells.

Common to viral haemorrhagic fevers and certain other disease states is a strong pro-inflammatory, pathological immune response. Immunomodulatory activity of iminosugars has previously been reported, but with a limited range of stimuli used. Here, the impact of iminosugars on cytokine responses to both viral infection and stimulation of MDMΦs with a

spectrum of pattern-associated molecular patterns (PAMPs) is investigated, with secretion of biologically functional TNF-α the major read-out. The suppressive effects of DNJ-derivative iminosugars on TNF-α secretion are broadly conserved across stimuli, supporting previous findings that iminosugar immunomodulatory activity is not dependent on viral replication or restricted to PAMPs of a viral origin. In contrast, the galactostereochemistry iminosugar *N*-nonyl-deoxygalactonojirimycin had more selective effects on cytokine production than the corresponding DNJ-derivative. Preliminary mechanistic investigations considering potential effects of iminosugars on TLR signalling pathways are conducted.

Overall, this thesis explores exciting new features and nuances of iminosugar activities relevant for treating viral infections and combatting a wider range of inflammatory conditions.

Chapter 1. Introduction

1.1 Dengue virus, Zika virus and Crimean-Congo haemorrhagic fever virus

Dengue virus (DENV), Zika virus (ZIKV) and Crimean-Congo haemorrhagic fever virus (CCHFV) are arboviruses of global public health concern. Dengue virus, a flavivirus, and Crimean-Congo haemorrhagic fever virus, a bunyavirus, are both haemorrhagic fever viruses. Infection can cause life-threatening viral haemorrhagic fevers (VHFs): multi-organ system diseases characterised by vascular system damage, often accompanied by haemorrhage, and immune system dysregulation [1]. ZIKV, in contrast, is not a causative agent of VHF. Rather, ZIKV infection during pregnancy is associated with congenital Zika syndrome (CZS), including microcephaly in newborns, and Guillain-Barré syndrome in adults [2]. Both CCHFV and ZIKV represent priority diseases for research and development named in the most recent World Health Organization (WHO) Research & Development Blueprint, while DENV was recognised as a disease continuing to pose a major public health problem [3].

1.1.1 DENV

1.1.1.1 Virology

There are four established serotypes of DENV (DENV-1, -2, -3, and -4) which are genetically diverse, with 63-68% sequence homology, and antigenically distinct [4, 5]. Recently, a fifth serotype has been reported, identified in one human case but circulating in a sylvatic rather than human cycle [6]. The DENV genome is approximately 11 kilobases of single-stranded positive-sense RNA, encoding a single polyprotein which is translated and cleaved by host and viral proteases to produce three structural proteins (capsid, C; precursor of the membrane protein, prM; envelope, E) and seven non-structural proteins (NS1, NS2A, NS2B, NS3, NS4A, NS4B, NS5).

Cellular infection by DENV is mediated by E protein binding to a broad range of receptor molecules, including the mannose receptor [7], dendritic cell-specific intercellular adhesion molecule-3-grabbing non-integrin (DC-SIGN) [8, 9], C-type lectin domain containing 5A (CLEC5A) [10], heparan sulfate [11], heat-shock proteins [12] and TIM and TAM family receptors [13]. In secondary infection, antibodies may also bind to virions, allowing uptake via Fc receptors in antibody-dependent enhancement (ADE) [14-16]. Following receptor binding, the virion is endocytosed, the mechanism dependent on cell type, virus serotype and strain, although clathrin-mediated endocytosis plays a major role [17-19]. Endosomes traffic to the perinuclear region on microtubules, and endosomal maturation and acidification allow E-mediated fusion to occur [18, 20]. This movement to the perinuclear region is important but not essential for productive infection [20]. Upon fusion, viral RNA is released to the cytosol for viral protein synthesis by host machinery and genome replication by the viral NS5 polymerase, occurring on virus-induced endoplasmic reticulum (ER)-derived membranous structures [21]. After nucleocapsid budding into the ER, 90 dimers of E and 180 copies of prM insert into a host cell membrane-derived envelope to form immature virions around the nucleocapsid core [22, 23]. PrM is cleaved to M by a host furin protease in the Golgi apparatus to generate mature virions, although pr remains associated with the virion as it continues through the secretory pathway, dissociating after release from the cell [24]. Uncleaved prM can be retained in secreted virions, however, leading to a spiky rather than smooth icosahedral structure [25]. These immature virions may still be infectious, if their prM is processed by furin following virion binding to DC-SIGN and internalisation [26], or through association with anti-prM or anti-E antibodies allowing virion uptake via Fc receptors [16, 27-31].

1.1.1.2 N-glycosylation of DENV glycoproteins

N-glycosylation is a host cell-derived post-translational modification of many host and viral proteins, detailed in 1.2.1. Of the ten DENV proteins, four are glycoproteins possessing N-linked glycans: prM, E, and NS1, all reviewed in [32], and the more recently identified NS4B.

The exterior of DENV virions is composed of 180 copies of the E protein, arranged in dimers, with each monomer containing the receptor-binding DIII domain and a fusion peptide at the tip of DI, sequestered in a hydrophobic pocket formed by DI and DIII of the adjacent E monomer [33]. The DENV E protein differs from other flaviviruses in that it contains two N-linked glycosylation sites at N67 and N153 [34], rather than the N153 site alone. Functional roles have been ascribed to both glycosylation sites. Glycosylation at N67 underlies binding to the DC-SIGN receptor [35] and is required for infection of mammalian but not mosquito cells in the DENV-2 16681 strain, with a role in either virion morphogenesis or release [36, 37]. However, this requirement for glycosylation is strain-dependent since in a chimeric New Guinea C (NGC)/PUO-218 prM-E infectious clone, loss of either glycan inhibited virion release from both mammalian and mosquito cells, while infectivity for mosquito cells only was enhanced [38]. Although the N153 site is traditionally associated with neurovirulence of flaviviruses such as West Nile virus (WNV) [39], neurological symptoms are not associated with typical DENV infection although these may be present [40, 41]. Occupation of the glycosylation sites can differ between serotypes, with one study identifying that the E protein of DENV-1 produced from *Aedes albopictus*-derived C6/36 cell infection was glycosylated at both sites, whereas DENV-2 E was glycosylated at N67 alone [42]. Heterogeneity in the structure and composition of glycans present on E is also seen in virus derived from mammalian or insect cells [43, 44]. A mixture of high-mannose and complex glycans have been found on DENV-2 E derived from infection of Vero cells, compared to high-mannose and paucimannose glycans when the virus originated from C6/36 cells [45], in keeping with differences between mammalian and insect N-glycan processing

[46]. The presence of high-mannose glycans on E in virus derived from both mammalian and mosquito cells [45] is important for receptor binding, since DC-SIGN and the mannose receptor preferentially interact with high-mannose glycans [47, 48]. In addition to the cell type-dependent differences in glycan composition, differences between serotypes have also been identified. Glycan compositions for E of DENV-2 differed compared to DENV-1, -3 and -4 derived from infected Vero or C6/36 cells [45]. Furthermore, glycan analysis of the Sanofi Pasteur tetravalent vaccine viruses CYD1-4 found that while the E proteins of the different vaccine viruses were fully glycosylated at N67 and N153, glycan compositions differed [49]. Heterogeneity is also likely to be more significant than previously appreciated since different DENV-4 genotypes were found to differ with respect to possession of the N153 site [50].

PrM associates with E in the ER [51] and may act a chaperone to assist E protein folding as in other flaviviruses [52, 53]. PrM overlies the fusion loop to prevent premature fusion during the secretory pathway, until it is cleaved by furin in the Golgi and dissociates from the virion shortly after secretion [54]. However, inefficient cleavage of prM means that virions ranging in maturity level are routinely secreted from infected cells, impacting infectivity and antibody responses to the virus, recently reviewed in [55]. Glycosylation of prM is less well-studied than for E, but one N-glycosylation site at N64-69 (serotype-dependent) is occupied [32, 56, 57]. Processing of the attached glycan is suggested to be important for prM-E dimer formation [51] and for association with the lectin chaperone calnexin [58]. The removal of the glycan from Japanese encephalitis virus (JEV) prM completely impaired E folding [53]: a similar significance could be possible for the DENV prM glycan.

DENV NS1 is a multifunctional protein, as reviewed in [59, 60]. Intracellular dimeric NS1 has a role in the viral replication complex [61-65], as well as membrane remodelling activity [62] which may contribute to forming the ER-derived membranous structures critical for viral replication

[21]. Secreted hexameric NS1 is evident in patient serum during the acute phase of infection [66, 67]. This can interact with complement pathways, and cross-reactive anti-NS1 antibodies can mediate platelet and endothelial cell damage leading to vascular leak [59, 68-73]. Activation of TLR4 signalling by NS1 also leads to pro-inflammatory cytokine production, endothelial cell damage and vascular leak [74, 75]. NS1 can also stimulate IL-10 production from monocytes, which may suppress protective T cell responses [76, 77], and directly disrupt the endothelial glycocalyx, enhancing permeability [78]. However, there is conflicting evidence from patient studies with respect to the correlation between circulating NS1 level and disease severity as well as the timing of peak NS1 levels and vascular leak [79]. A recent study evaluating anti-NS1 antibodies in acute secondary dengue infection found that anti-NS1 antibody titres were higher and rose more quickly in patients who went on to develop DHF compared to DF, as well as identifying serotype-specificity in the responses [80], adding further complexity to the story. In terms of N-glycosylation, NS1 has two conserved glycan sites at N130 and N207 [81-83]. Analysis of the glycan compositions has shown that for secreted NS1, N130- and N207-glycans are complex and high-mannose, respectively [83, 84]. NS1 glycosylation is important for its role in viral replication [43, 85-87]. The N130 glycan has been implicated in virus production [88] and the stability and complement-interacting activity of the secreted NS1 hexamer [89], while the N207 glycan facilitates NS1 secretion [84, 89].

NS4B is a component of the replication complex alongside NS1 and may increase the productivity of replication [90]. DENV NS4B might also contribute to virus-induced membrane remodelling as reported for NS4B from WNV [91] and hepatitis C virus (HCV) [92]. NS4B possesses two N-glycosylation sites at the N58 and N62 residues, and exists in glycosylated and unglycosylated forms in DENV-infected baby hamster kidney (BHK)-21 cells. This glycosylation is functionally important for DENV replication and virus production in BHK-21 or C6/36 mosquito cells. Mutation of the N62 residue had a greater effect than mutating N58, while a double

mutant had a greater effect still [93]. Therefore, the N-glycosylation of multiple DENV proteins is of functional significance in productive infection.

1.1.1.3 Epidemiology

DENV is transmitted ubiquitously across the tropics by *Aedes* species mosquitos: the zones of highest risk being Asia and the Americas, with 3.97 billion people in 128 countries at risk of infection [94]. Modelling predicts that around 294 million inapparent cases occurred in 2010, on top of 96 million symptomatic infections [95]. Other mechanisms contribute to DENV dissemination, including vertical transmission which may be more prevalent than currently appreciated [96]. Case fatality rates range from approximately 0.2-3.5% [97], in line with the spectrum of disease caused by infection. Traditionally, disease was classified as dengue fever (DF), dengue haemorrhagic fever (DHF) or dengue shock syndrome (DSS). In the last ten years, the WHO has introduced a new classification system aiming to improve the triage of patients at risk of developing the haemorrhagic and vascular shock manifestations of severe dengue (Figure 1). The system relies on clinical and laboratory 'warning signs' due to the absence of a validated biomarker able to discriminate those at risk of disease progression. However, the utility of the new system remains controversial and the traditional classification system is often still used.

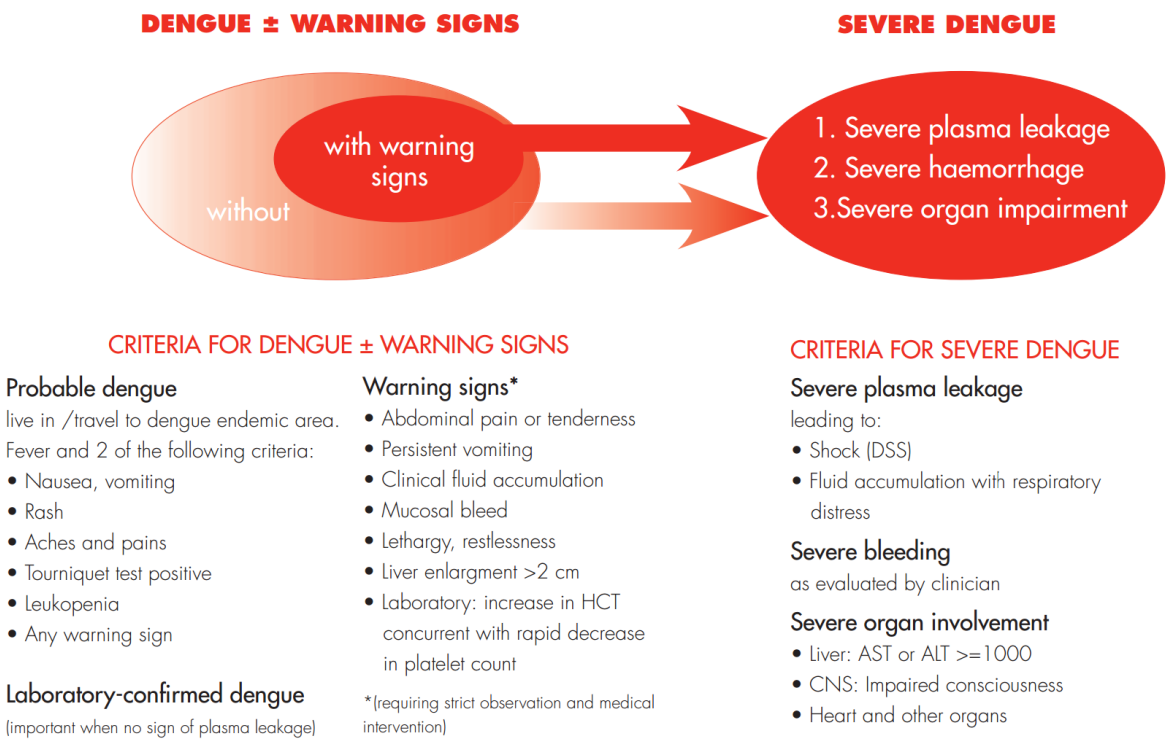

Figure 1. WHO criteria for dengue classification, reprinted with permission from [97].

The multiple serotypes of DENV lead to complex epidemiology, recently reviewed in [98]. Briefly, primary infection leads to the generation of antibody responses that are cross-protective between serotypes. However, in the absence of DENV re-exposure, cross-protective responses wane and responses become more type-specific. This can lead to ADE where, in a heterologous DENV infection, sub-neutralising antibodies may enhance the uptake of virions by Fcγ receptor-expressing cells, leading to higher viral loads, T cell activation and pro-inflammatory cytokine secretion. However, following a secondary heterologous infection, neutralising antibody responses broaden, which may reduce the risk of severe infection in subsequent infections although homologous reinfections can also be symptomatic. The incidence of severe disease in infants in endemic areas is age-dependent, correlating with the decay of maternal antibodies and titres of enhancing antibodies. The roles of DENV re-exposure boosting antibody responses and the possible waning of T cell memory responses over time are still being elucidated. In addition, the effects of original antigenic sin on both antibody and T cell responses are likely to

hamper the development of effective adaptive immune responses to heterotypic secondary infection [99, 100].

1.1.1.4 The role of cellular tropism and cytokines in disease pathogenesis

DENV is primarily inoculated into the dermis during feeding of the mosquito vector. At the inoculation site, myeloid immune cells including Langerhans cells, several other dendritic cell (DC) subsets and macrophages constitute the major targets [101-103], while keratinocytes and fibroblasts are also infected in human skin explants *ex vivo* [103, 104]. Infection of interferon (IFN)-α/β receptor knockout (*Ifnar*$^{-/-}$) mice demonstrates that monocytes recruited from the circulation and resulting monocyte-derived DCs (MDDCs) form a significant proportion of the infected cells in the dermis [101]. Mast cells can be DENV-infected, degranulate and produce pro-inflammatory cytokines and other products including vascular endothelial growth factor (VEGF) and histamine which may play a role in vascular leak [79]. The mosquito saliva introduced concomitant with virions can influence DENV infection. Mosquito salivary gland extracts increased infection in the dermis, immune cell migration and endothelial cell permeability in mice [105], although evidence exists for both proviral and antiviral effects of mosquito saliva [106]. Murine studies suggest that there is significant IL-4 production and a shift from Th1 to Th2 cytokine responses at the site of mosquito bites, contributed to by mosquito salivary proteins [107, 108]. Beyond the skin, circulating myeloid cells, tissue macrophages, endothelial cells and hepatocytes have been identified as targets of DENV infection in post-mortem human tissues [109-115]. DENV infection of platelets and B cells derived from patients has also been reported [116, 117], as well as DENV in the brain in the few cases with neurologic involvement [40, 41].

Many cytokines are implicated in dengue infection, including IFN-α, IFN-γ, interleukin (IL)-1β, IL-4, IL-6, IL-7, IL-8, IL-10, IL-12, IL-13, IL-17, IL-18 and tumour necrosis factor (TNF)-α [118-127]. However, there can be serotype specificity in cytokine responses: in one study, significantly

higher IL-12, TNF-α and IL-6 in the sera of DHF versus DF patients was only seen for DENV-2 but not DENV-1 infections [128]. Cytokine responses to DENV infection are likely to vary with age, partly linked to the infection history of the individual. In addition, monocyte/macrophage cultures from seronegative neonates and elderly individuals produced less TNF-α, IL-1β and IL-6 on DENV infection compared to cells derived from adults [129]. Multiple lines of evidence suggest a protective role for type I IFN (IFN-α/β) responses [118, 130, 131], both through the induction of an antiviral state restricting viral replication and through direct effects on the endothelium [132, 133]. However, the production of and response to IFN-α/β are antagonised by the virus [134, 135]. In contrast, evidence places TNF-α as a leading cause of pathogenesis: it increases endothelial cell permeability leading to vascular leak [136] and anti-TNF-α antibodies are protective in murine ADE models [137]. The 308A allele linked to greater TNF-α responses was identified as a risk factor for severe dengue in some patient populations [138, 139], but this has not been replicated in many subsequent studies [140]. Lipid inflammatory mediators are also important in pathogenesis, with platelet-activating factor (PAF) implicated in increased endothelial permeability, reviewed in [79].

Cytokine induction is mediated by multiple pattern recognition receptor (PRR) pathways, identified in diverse systems. CLEC5A recognition of as yet unidentified epitopes on DENV virions leads to TNF-α, IL-6, IL-8, macrophage inflammatory protein (MIP)-1α and interferon-inducible protein (IP)-10 production from macrophages [141, 142]. Anti-CLEC5A antibodies were protective in DENV-challenged mice, lowering serum TNF-α and IP-10 [141]. CLEC5A surface expression is increased on DENV infection through activation of nuclear factor (erythroid-derived 2)-like 2 (Nrf2), leading to increased TNF-α secretion [143]. CLEC5A ligation also leads to activation of the NACHT, LRR and PYD domains-containing protein 3 (NLRP3) inflammasome in human monocyte-derived macrophages (MDMΦs), enabling secretion of IL-1β and IL-18 [144].

Furthermore, a single nucleotide polymorphism in CLEC5A has been linked to disease severity [145].

Considering other PRRs, recognition of DENV viral RNA by retinoic acid-inducible gene I (RIG-I) and melanoma differentiation-associated protein 5 (MDA5) [146] and Toll-like receptor 4 (TLR4) recognition of NS1 [75] have also been implicated in TNF-α production. Direct activation of nuclear factor-kappa B (NF-κB) by the NS2B3 viral protease can also lead to TNF-α production [147, 148]. Recognition of viral RNA by TLR7 [141, 149-151], TLR3 [152-154], RIG-I [152, 153, 155-157] and MDA5 [152, 157], and TLR4 recognition of NS1 [75] have all been shown to mediate IFN-α/β production. In dengue patients 5 days post-symptom onset, TLR3 and TLR9 expression in DCs was significantly higher in individuals with DF compared to DHF or healthy controls, indicating that upregulation of these TLRs may play a protective role [158]. DC-SIGN and the mannose receptor can also modulate cytokine responses downstream of binding DENV [159]. On top of this, the immune response to DENV infection can be influenced by intrinsic ADE, whereby ligation of Fcγ receptors with DENV-bound immunoglobulin G (IgG) leads to suppression of antiviral responses and pro-inflammatory cytokine production alongside enhanced anti-inflammatory IL-10 secretion, reviewed in [160].

1.1.1.5 Current therapeutic landscape

Currently there is no specific antiviral available for dengue: clinicians must rely on supportive therapy. Several candidate therapeutics have been evaluated in clinical trials, with limited success. The strategy of repurposing drugs approved for other indications has led to several clinical trials: balapiravir, chloroquine, lovastatin, and prednisolone had acceptable safety profiles but failed to meet their primary endpoints in acute dengue patients [161]. The antihistamine and PAF antagonist rupatadine was recently evaluated in a clinical trial for its ability to reduce fluid leakage in acute DENV infection. While the primary endpoint was not met,

post-hoc analysis indicated that there could be beneficial effects with early treatment [162]. Drug repurposing has resulted in other compounds of interest, some of which are currently undergoing pre-clinical investigation [163], alongside many other newly developed candidate antivirals. Some of these target the N-glycosylation pathway, including iminosugars (discussed in 1.2) and sulfonium ions [164], both targeting the ER α-glucosidases. High-dose dexamethasone treatment was evaluated in acute dengue patients with thrombocytopenia, but there was no significant difference in platelet count compared to the control group receiving standard supportive care [165]. Doxycycline was evaluated in DHF patients, reducing mortality by 46% and reducing serum levels of TNF and IL-6 [166]. Ivermectin, an antiparasitic drug, and ketotifen, an antihistamine, are reportedly in clinical trials (ClinicalTrials.gov identifiers NCT02045069 and NCT02673840, respectively). Members of the iminosugar class of compounds have also undergone evaluation in clinical trials for dengue, as discussed in 1.2.4.

Demonstrating efficacy of an antiviral in dengue patients presents many challenges, since presentation to clinic and thus the opportunity for trial enrolment often occurs after peak viraemia and days after fever onset. In addition, there are technical limitations in determining circulating infectious virus levels, and variation in viral clearance between patients mandates large sample sizes to meet statistical significance [161].

Dengue vaccine development has made substantial progress in recent years, with the first vaccine licensed at the end of 2015, the recombinant live attenuated tetravalent vaccine CYD-TDV (Dengvaxia®). The vaccine was licensed for use in individuals aged 9-45 years and the WHO Strategic Advisory Group of Experts on Immunisation recommended that countries introduce vaccination accordingly in high endemicity areas, alongside vector control programmes [167, 168]. Efficacy was demonstrated through seroconversion and reduced hospitalisation across several clinical trials [169], although the low efficacy against DENV-2 remains a cause for concern

[170]. Safety concerns persist over the increased risk of hospitalisation for severe dengue in those aged under nine reported in an interim analysis [169], although longer-term follow up data showed that the overall risk was reduced [171]. Additional vaccine candidates using multiple technologies are under development, recently reviewed in [172]. Thus, while a dengue vaccine has been licensed, the development of vaccine candidates aiming for improved efficacy and safety profiles, as well as antiviral therapeutics, continues.

1.1.2 ZIKV

1.1.2.1 Virology

ZIKV, like DENV, is a flavivirus, and thus has a similar genome structure and replication cycle (1.1.1.1). The structure of ZIKV was solved by cryogenic electron microscopy (cryo-EM) and found to be broadly similar to DENV [173, 174]. Rather than serotypes, ZIKV strains fall into two major lineages: African and Asian, with the American clade derived from Asian strains. Strains from each lineage differ with respect to infectivity, stimulation of immune responses and pathogenesis in mouse models, reviewed in [175].

Like DENV, ZIKV appears to use a multitude of receptors for cellular entry. AXL has been identified as a major receptor, but roles for DC-SIGN, TIM-1, and Tyro3 have been identified in human embryonic kidney (HEK) 293T cells expressing these receptors [176]. AXL and Tyro3 are members of the TAM family of receptors and also play a role in DENV entry [13]. AXL can mediate ZIKV infection of human microglia and astrocytes through the interaction of the AXL ligand Gas6 with virions, leading to clathrin-mediated endocytosis and productive infection, as well as downmodulation of IFN-α/β responses [177]. A role for Tyro3 in infection of human spermatozoa was also identified [178].

1.1.2.2 N-glycosylation of ZIKV glycoproteins

Like DENV, ZIKV possesses N-glycosylated E, prM and NS1 proteins, and may possess N-glycosylated NS4B although this is yet to be reported. The E protein of ZIKV contains a loop encompassing the single N154 glycosylation site, although this site is absent in some strains [174, 179, 180]. This loop structure was initially proposed to increase the thermal stability of ZIKV and underlie the enhanced transmissibility of ZIKV over DENV in body fluids [174], although it has subsequently been shown that mutation of this region does not impact ZIKV thermal stability and that variation between ZIKV strains renders ZIKV and DENV more similar than originally thought [181]. One analysis of 33 ZIKV strains found that the N154 site was broadly conserved across Asian and American strains, while it was mostly absent in African strains analysed [182]. However, the prototype African MR766 strain can contain this site, although extensive passaging has resulted in substrains with and without [180]. N154 glycosylation has a role in E secretion and the production and infectivity of E-pseudotyped particles [183]. N154 glycosylation is also important for virulence of some ZIKV strains in mammalian and mosquito hosts [184, 185], although reports differ with respect to its role in neurovirulence [184, 185]. Recently, the glycosylation site was demonstrated to be important for midgut invasion, an essential step for mosquito-borne transmission, despite having no effect on mammalian cell infection or *in vitro* viral replication [186].

Besides the E protein, functional significance has been attributed to glycosylation of prM and NS1. While both DENV and ZIKV bind to DC-SIGN, the N67 glycan responsible for binding in DENV E is absent in ZIKV, and as such, glycans on prM present on immature ZIKV virions have been proposed to underlie this interaction [35, 176, 187]. ZIKV NS1 is N-glycosylated at N130 and N207, as for DENV [188], with this glycosylation important for viral replication [189]. Thus, the N-glycosylation of ZIKV proteins plays multiple roles in the viral life cycle.

1.1.2.3 Epidemiology

Serological evidence for human ZIKV infection dates from 1952, with the first human isolate obtained soon after [190-192], although ZIKV came to prominence during the recent outbreak beginning in Brazil in 2015 that led to the WHO declaring a Public Health Emergency of International Concern [193]. Like DENV, ZIKV is transmitted by multiple *Aedes* species mosquitos, dependent on location [175]. In addition, *Culex quinquefasciatus* mosquitos are permissive for ZIKV replication and the virus has been isolated from wild-caught mosquitos [194]. However, the viral range is not restricted to that of mosquitos, as vertical and sexual human-to-human transmission occurs. Multiple cases of sexual transmission have been identified, some resulting in infection of pregnant women [195, 196]. ZIKV RNA has been detected in semen for up to 281 days post-symptom onset, although in most cases this resolved within 3 months and infectious virus shedding was limited to weeks [197, 198]. ZIKV infection during pregnancy and vertical transmission to the foetus is of particular interest since this is associated with CZS, which includes microcephaly in newborns. Symptomatic ZIKV infection of non-pregnant individuals is generally relatively mild, involving fever and maculopapular rash, although neurological involvement may manifest as Guillain-Barré syndrome [2].

While ZIKV lacks serotypes, the potential for ADE to occur with anti-DENV antibodies, and the reality of this occurring in populations where ZIKV has spread into DENV endemic areas, has been hotly debated over the last few years. ADE of ZIKV with anti-DENV antibodies occurs *in vitro* in physiological models such as primary human macrophages infected in the presence of human sera from individuals in DENV-endemic regions [199] and in primary Hofbauer cells (placental macrophages) or placental explants [200]. In Rhesus macaques that were DENV-1 or DENV-2 infected 2.8 years prior to ZIKV challenge, ZIKV pathogenesis was not enhanced *in vivo* and in fact the viraemic period was reduced, despite macaque sera inducing ADE *in vitro* [201]. Clinically, a Brazilian study of febrile patients found that prior DENV infection was not associated

with signs of ADE in acute ZIKV infection [202], and analysis of a Nicaraguan paediatric cohort found that prior DENV infection protected individuals from symptomatic ZIKV infections, although the rate of total ZIKV infections was unaffected [203]. This emerging evidence from human studies suggests that this may not be the cause for concern once thought. Evaluation of the reciprocal ADE relationship is ongoing in animal models, with recent findings that prior ZIKV exposure in Rhesus macaques significantly enhances peak viraemia on subsequent DENV-2 challenge [204], and maternal antibodies transmitted from ZIKV-immune mice enhanced DENV infection in their pups [205]. This remains to be evaluated in the human population however.

1.1.2.4 The role of cellular tropism and cytokines in pathogenesis

In mosquito-borne infection, ZIKV initially infects cells in the skin, and infection of human dermal fibroblasts, epidermal keratinocytes and immature dendritic cells has been shown with a clinical ZIKV isolate [176]. In the bloodstream, $CD14^+$ monocytes appear to be the major target of infection [206, 207]. The striking appearance of CZS resulting from ZIKV infection of pregnant women suggested ZIKV tropism for placental cells. Indeed, ZIKV infects cytotrophoblasts and Hofbauer cells in chorionic villus explants from first-trimester human placentas as well as several cell types in tissues formed later in pregnancy [208]. Microcephaly and other neurological features of CZS have been related to infection and attenuated growth of cortical neural progenitor cells as well as infection of glial cells and astrocytes [209, 210]. Ocular abnormalities present in infants with CZS may be related to the lytic infection of retinal endothelial cells, retinal pericytes, and retinal pigmented epithelial cells [211].

The cytokine response to ZIKV infection has been described in longitudinal studies, with IFN-α, IFN-β, IL-1β, IL-2, IL-4, IL-5, IL-6, IL-7, IL-8, IL-9, IL-10, IL-12p70, IL-13, IL-17, IL-18, IL-20, IL-21, IL-22, IL-27, IL-32, and IL-34 all reported to be significantly elevated in serum compared to healthy controls, although the cytokines identified differ between studies and some report reductions

in some of these cytokines [212-214]. An early study found that TNF-α and IFN-γ levels were not significantly increased in the acute phase [212], unlike in DENV, although subsequent larger studies have found significant inductions in both of these cytokines [213-215]. In a study comparing one ZIKV-infected pregnant woman carrying a foetus with developmental abnormalities and five ZIKV-infected women with developmentally normal foetuses, serum concentrations of IL-4, IL-8, IL-18, IL-22, IL-23, IL-27 and TNF-α were found to be significantly higher in the CZS case [213]. Differential effects of African and Asian lineage ZIKV infections have also been proposed, with Asian strain infection immunosuppressive compared to pro-inflammatory responses to African strains [206]. Growth factors and chemokines are also implicated in ZIKV pathogenesis. Significant increases in chemokines including IP-10, regulated on activation, normal T cell expressed and secreted (RANTES), macrophage inflammatory protein 1α (MIP-1α), MIP-1β, monocyte chemoattractant protein 1 (MCP-1), eotaxin and stromal cell-derived factor 1α have been reported in the acute phase across multiple studies [212-216].

Compared to DENV, characterisation of the PRRs activated by ZIKV is more restricted. However, activation of the NLRP3 inflammasome leading to the secretion of IL-1β was shown to involve ZIKV NS5 binding to inflammasome components [217]. Upregulation and activation of TLR3 by ZIKV infection has been implicated in the dysregulation of neurogenesis [218]. ZIKV infection can induce type I, II and III IFN responses, and IFN-α/β responses are antagonised on ZIKV infection by NS1, NS2A, NS2B, NS4A, NS4B and NS5, as reviewed in [175], and by subgenomic flavivirus RNA (sfRNA) [219]. RIG-I activation has been implicated in the IFN-α/β response [220-223], as has MDA5 [219, 223].

1.1.2.5 Current therapeutic landscape

Intense research efforts following the 2015 outbreak lead to the development of multiple new animal models for ZIKV infection, some attempting to replicate ZIKV pathogenesis during pregnancy [224]. In addition, clinical trials of several vaccine candidates have commenced or been conducted (ClinicalTrials.gov identifiers NCT03014089, NCT02887482, NCT02809443). However, there are no specific therapeutics available or undergoing clinical trial (registered with ClinicalTrials.gov), but many compounds, both direct-acting and host-targeted, are under development as summarised in a recent review [225]. Host-targeted antivirals with efficacy demonstrated against ZIKV include those that target viral processes in the ER, including the DNJ-derivative iminosugar IHVR19029 that inhibits ER α-glucosidases [226] (discussed in 1.2), suramin, whose multiple mechanisms of action include interference with glycosylation [227], and the ER signal peptidase inhibitor cavinafungin [228]. Other candidate antiviral strategies have targeted cellular lipid metabolism, including PF-06409577, a pharmacological activator of AMP-activated protein kinase [229] and nordihydroguaiaretic acid, which interferes with the sterol regulatory element-binding protein pathway among other activities [230]. Regardless of the approach, the particular requirement for safety in pregnant women presents an additional challenge for drug development.

1.1.3 CCHFV

1.1.3.1 Virology

CCHFV has similar morphology and characteristics to other members of the *Bunyaviridae* family, although the absence of a central hole in the closely-packed surface subunits when viewed by negative-stain electron microscopy appears to be a distinguishing feature [231, 232]. The replication cycle occurs as for other bunyaviruses, with cell surface receptor binding leading to endocytosis, and endosomal fusion allowing cytoplasmic replication. Virions assemble in the ER

and mature as they are trafficked through the Golgi prior to the fusion of cytoplasmic vesicles with the plasma membrane to release virions [233]. The enveloped virions of CCHFV are 80-120 nm in diameter and contain a tripartite single-stranded negative-sense RNA genome with large (L), medium (M) and small (S) segments. L encodes the RNA-dependent RNA polymerase, S the nucleoprotein and M the glycoprotein precursor, which is processed to produce the two spike glycoproteins Gn and Gc [234] along with non-structural proteins [235], one of which functions to induce apoptosis in infected cells [236].

1.1.3.2 N-glycosylation of CCHFV glycoproteins

The surface glycoproteins of CCHFV have important functional roles, with Gc responsible for receptor binding, possibly to cell-surface nucleolin [237]. Gn is important for virion formation, with conserved electrostatic charges likely to provide a binding site for viral RNA during assembly [238]. Analysis of the CCHFV Matin strain M segment polyprotein indicated 10 potential N-glycosylation sites, with 6 conserved between strains [239]. However, in the mature glycoproteins, Gn is N-glycosylated at one of its two potential sites, the extracellular site at N557, but not N755 [240]. Gc is N-glycosylated at both N1054 and N1563 [240]. The occupied N-glycosylation sites in Gn and Gc are conserved between 32 known CCHFV strains [241]. The glycosylation of Gn is functionally important, determining transport of both Gn and Gc to the Golgi apparatus [240]. Since the glycan on Gn of the prototype bunyavirus Bunyamwera virus (BUNV) has equivalent importance in determining Gn and Gc trafficking, it is possible that the Gn glycan is crucial for virus production for CCHFV as it is for BUNV [242]. The glycans on Gc of BUNV were also shown to contribute to virus infectivity, which might also hold true for CCHFV [242].

1.1.3.3 Epidemiology

CCHFV causes the severe and potentially fatal Crimean-Congo haemorrhagic fever (CCHF). Case fatality rates range widely from 0-80% in outbreaks with more than one case, although average mortality rates are often stated as 30-50% [233, 243, 244]. CCHFV is the most widespread tick-borne disease in humans, and multiple European countries reported their first autochthonous cases within the last 20 years, and Spain as recently as 2016 [245, 246]. Ixodid (hard-bodied) ticks, primarily of the *Hyalomma* genus, support CCHFV replication and are the main cause of CCHFV transmission to vertebrate hosts, of which humans are the only ones to suffer severe pathology [247]. However, nosocomial transmission and contact with the blood of viraemic livestock are also important transmission routes: CCHF outbreaks have been associated with cattle and sheep sacrifice during the Eid-Al-Adha festival [233, 248]. The calendrical shift of the festival to the summer months over the next 10-15 years necessitates additional vigilance during this period of increased tick activity and CCHFV transmission risk [248].

In infected individuals, clinical disease may develop after a short incubation period, before a pre-haemorrhagic phase characterised by symptoms including headache, fever, chills, dizziness, photophobia and vomiting. Haemorrhagic manifestations can develop after 3-6 days, including cerebral haemorrhage in severe cases. If a patient survives, the convalescent period begins after 15-20 days, although generalised weakness and other symptoms may persist for at least a year [233, 249, 250]. Viral load is currently the most reliable predictor of a fatal versus non-fatal outcome [251], while antibody responses also appear to be weaker in fatal cases [252].

1.1.3.4 The role of cellular tropism and cytokines in CCHF pathogenesis

The pathogenesis of CCHF is not entirely well-characterised, however infection of mononuclear phagocytes, hepatocytes and endothelial cells has been shown by *in situ* hybridisation and

immunohistochemistry in patient tissues [253]. *In vitro*, infection of MDDCs [254, 255], MDMΦs [255] and endothelial cells [256] has been demonstrated, leading to their activation. Infection of the Huh7 hepatocarcinoma cell line causes activation of ER stress pathways, IL-8 secretion and apoptosis [257], which could underlie clinical manifestations of liver pathology [253, 258-260].

A major feature of CCHF pathogenesis is dysregulation of the vascular system and disseminated intravascular coagulation, a systemic activation of pathways regulating coagulation that leads to clot formation, multiple organ failure and haemorrhage [243]. This may be due to direct infection of endothelial cells [253] as well as indirect activities of viral-induced cytokines and chemokines. Increased serum IFN-γ, IL-1β, IL-5, IL-6, IL-8, IL-9, IL-10, IL-15, IP-10, MCP-1 and TNF-α have all been associated with fatal outcomes [252, 261, 262]. The involvement of TNF-α in CCHF cases, particularly severe ones, has been found in many studies [252, 261, 263-265], although paediatric studies have found TNF-α not to be increased [266] or not to differ between mild and severe cases [267]. There is conflicting evidence for the role of IL-10, with studies reporting IL-10 to be both lower [264, 265] and higher [263, 267, 268] in severe relative to mild cases. IFN-γ does not seem to correlate with severity [265]. In terms of chemokines, patterns of elevation differ between paediatric and adult patients [269], but IP-10, a chemoattractant for monocytes/macrophages, dendritic, T and natural killer cells, has been shown to positively correlate with viral load [270].

The viral determinants of cytokine induction have not been well-defined. RIG-I and MDA5 are upregulated in infected A549 cells, and RIG-I-mediated detection of CCHFV was demonstrated to be important for IFN-β secretion and the type I IFN-dependent response, while MDA5 did not play a role [271]. However, an earlier report had shown that CCHFV cleaves the 5'-triphosphate motif recognised by RIG-I to a 5'-monophosphate, evading detection [272]. CCHFV infection is

sensitive to IFN-α/β treatment early on, but not after infection is established, with infection delaying interferon regulatory factor (IRF)-3 nuclear translocation and IFN-α/β responses [273]. In MDDCs and MDMΦs, IFN-α secretion was reduced but not abrogated by UV-inactivation of the virus [255], indicating that viral replication plays a significant but not essential role in stimulating this response. The ovarian tumour domain of the viral L protein inhibits NF-κB activation and can cleave ubiquitin and interferon-stimulated gene product 15 (ISG15) from cellular proteins [274], as well as inhibit RIG-I signalling [275]. Mechanisms underlying potential TLR-mediated recognition of CCHFV have not been investigated, but certain genetic polymorphisms in TLR7, 8, 9 and 10 have been implicated in CCHF cases and/or disease severity [276-278].

1.1.3.5 Hazara virus

Hazara virus (HAZV) was isolated from *Ixodes redikorzevi* ticks in Western Pakistan in 1964 [279, 280] and is both genetically [281, 282] and serologically [280, 283-286] closely related to CCHFV. While the severity of CCHF poses a considerable risk to laboratory study, HAZV is not reported to cause pathogenic human infection and thus may be manipulated at Biological Safety Level (BSL) 2, rather than the BSL4 required for CCHFV [286, 287]. One serological survey of rodents, domestic animals and humans in Pakistan found antibodies against HAZV in rodent sera only whereas anti-CCHFV antibodies were found in sera from all sources [288]. Infection of cell lines with HAZV has been proposed as a model for studying CCHFV infection and antivirals targeting viral replication [287, 289, 290], while a murine infection model was suggested as a surrogate for testing antivirals and vaccine development [291]. HAZV is little studied, with few descriptions made of the viral glycoproteins [281, 286, 292] which are discussed further in 5.2.

1.1.3.6 Current therapeutic landscape for CCHFV

Among antivirals tested, ribavirin is the only one that has been recommended by the WHO for the treatment of viral haemorrhagic fevers including CCHF [293]. However, while the efficacy of ribavirin has been demonstrated *in vitro*, *in vivo* and in some patient studies, the benefits of ribavirin are disputed [245, 294] and the sole randomised controlled trial [295] as well as meta-analyses [296-298] have demonstrated a lack of clinical benefit and indicated that adverse events may be more common with ribavirin treatment. High-dose methylprednisolone appears to be beneficial in combination with ribavirin [299, 300]. Besides ribavirin, relatively small studies have suggested benefits of immunoglobulin preparations [301-303]. Other antivirals have been evaluated pre-clinically, reviewed in [304]. Vaccine development is an area of active research, with many approaches under investigation [305]. Currently, the only vaccine in use is prepared using virus cultivated in suckling mouse brain, implemented in Bulgaria but unlikely to ever obtain international regulatory approval [305]. A viral-vectored vaccine candidate, modified vaccinia virus Ankara expressing the M segment open reading frame, demonstrated 100% protective efficacy in a mouse model [306] and is reportedly under evaluation in clinical trials [305].

1.2 Iminosugars as antivirals

1.2.1 Mammalian N-linked glycosylation pathways as an antiviral target

Glycosylation is a fundamental cellular process: around two-thirds of ER-derived proteins are glycosylated [307], with the most common form being N-linked glycosylation. N-glycosylation is initiated by the addition of the oligosaccharide $Glc_3Man_9GlcNAc_2$ (Glc, glucose; Man, mannose; GlcNAc, N-acetylglucosamine) to an asparagine (N) residue of the nascent polypeptide in the ER lumen [308]. The asparagine residue is usually found in the sequon asparagine-X-serine/threonine (NXS/T), where X represents any amino acid except proline. Sequons differ in

glycosylation efficiency, with those containing threonine being efficiently glycosylated, and serine, inefficiently so [309]. Polypeptides may also be O-glycosylated, by glycan attachment to the side chains of serine, threonine, hydroxylysine or tyrosine, or C-mannosylated, by glycan attachment to tryptophan residues, reviewed in [310].

During N-glycosylation, sequential processing of the precursor oligosaccharide by α-glucosidases I and II determines polypeptide interaction with ER chaperones required for correct protein folding (Figure 2; reviewed in [310]). α-glucosidase I cleaves the α-1,2-glycosidic bond to remove the outermost glucose residue, followed by α-glucosidase II-mediated removal of the two inner α-1,3-linked glucoses [308]. The chaperones calnexin (CNX) and calreticulin (CRT) associate with monoglucosylated glycans, promoting correct disulfide bond formation through interaction with ERp57 [311-313]. If folding is incomplete, UDP-Glc:glycoprotein glucosyltransferase (UGGT) can reglucosylate the glycoprotein, enabling cyclical interaction with chaperones until the native conformation is achieved [311]. Alternatively, persistently misfolded proteins enter the ER-associated degradation (ERAD) pathway for proteasomal degradation. Following transport from the ER to the Golgi apparatus, N-linked oligosaccharides undergo further processing by mannosidases followed by the addition of galactose, GlcNAc, fucose and sialic acid residues resulting in hybrid or complex glycans, or receive minimal processing and remain as high-mannose glycans, reviewed in [310].

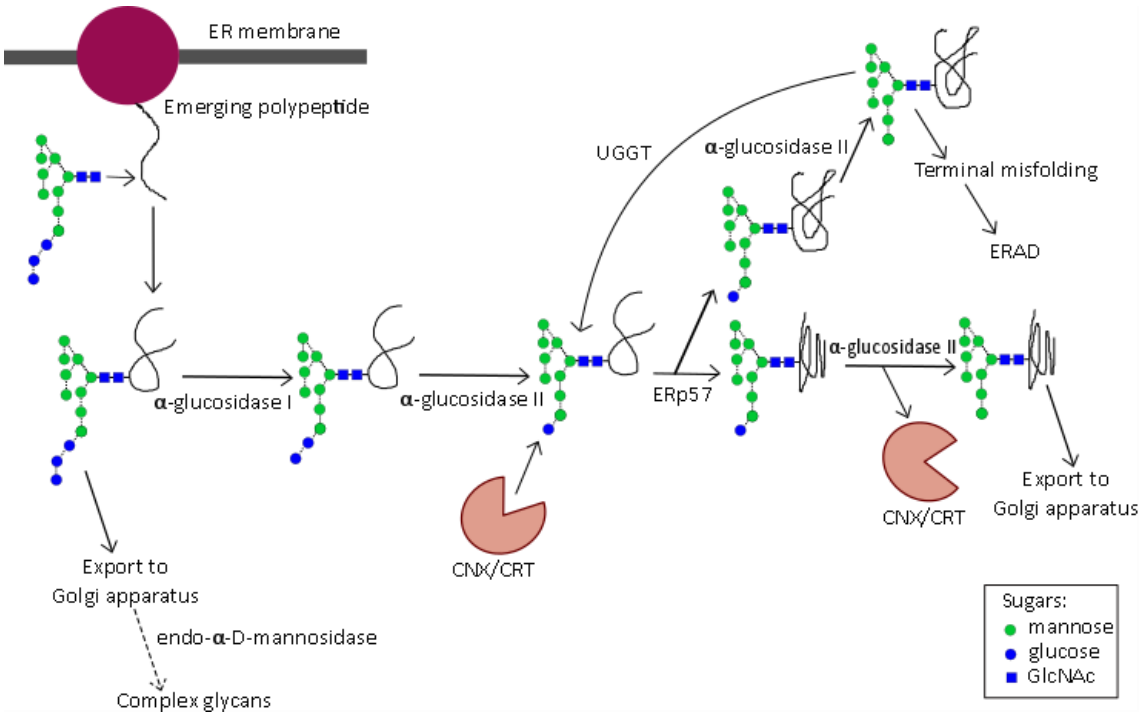

Figure 2. N-linked oligosaccharide processing in the endoplasmic reticulum, reproduced from publication in [314] under CC-BY 4.0 license.

Abbreviations: CNX/CRT, calnexin/calreticulin; ERAD, endoplasmic reticulum-associated degradation; GlcNAc, N-acetylglucosamine; UGGT, UDP-Glc:glycoprotein glucosyltransferase.

As well as host glycoproteins, many enveloped viruses possess N-glycosylated glycoproteins, as described in 1.1 and 1.2.3; thus, the N-glycosylation pathway represents an antiviral target. This is supported by evidence obtained in cells derived from individuals with mannosyl-oligosaccharide glucosidase (MOGS)-congenital disorders of glycosylation (CDG) type II, a rare genetic deficiency in ER α-glucosidase I, described in only six patients to date [315-318]. In cells derived from the two individuals to survive beyond infancy, productive human immunodeficiency virus (HIV) infection was reduced concomitant with glycosylation changes in the virus, and influenza virus (INFV) infection was also inhibited. In contrast, the susceptibility of patient cells to the non-enveloped adenovirus, vaccinia virus and poliovirus was unaffected, indicating that the resistance to viral infection was specific to enveloped viruses [316]. The rarity of this disorder suggests that the complete absence of ER α-glucosidase I is detrimental during

development, whereas drugs targeting this pathway, including the iminosugars discussed in 1.2, would aim for a transient and partial inhibition of α-glucosidase function.

1.2.2 Structural basis of iminosugar inhibition of ER α-glucosidases and glucosylceramide synthase

Iminosugars are polyhydroxylated carbohydrate mimics where the endocyclic oxygen atom is replaced by a nitrogen atom, to which additional moieties may be attached [319]. This project focuses on iminosugars with six-membered rings. Selected structures of iminosugars used in this project are shown in Figure 3.

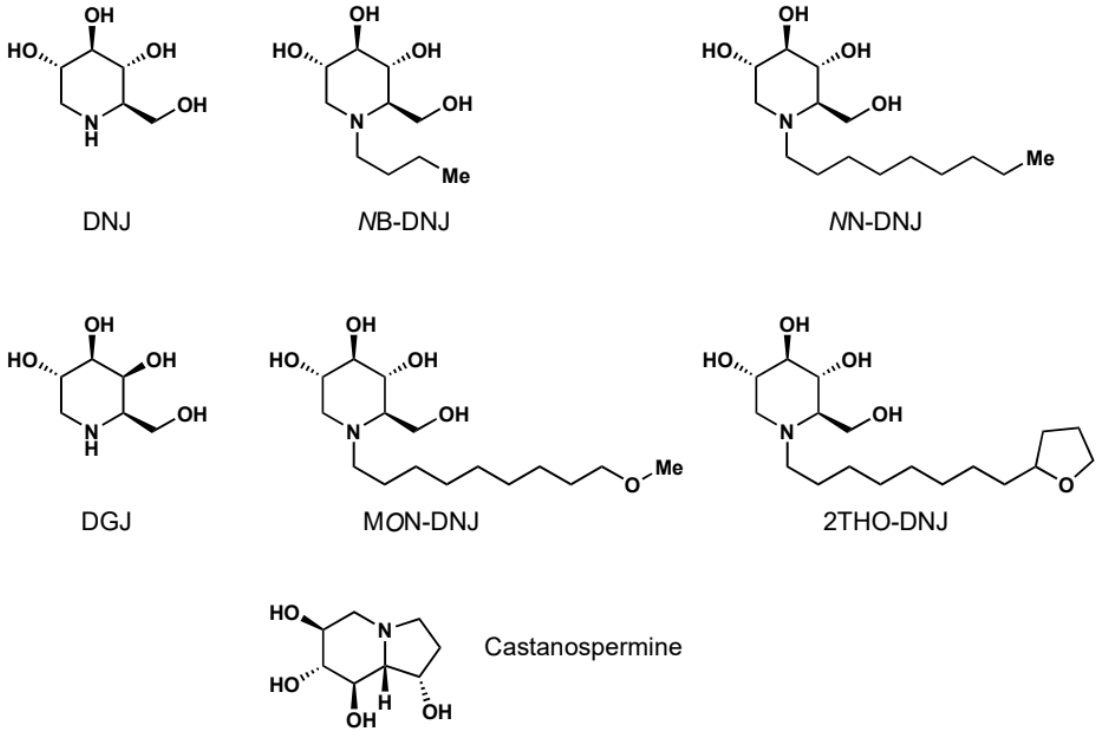

Figure 3. Selected iminosugar structures.

Abbreviations: DNJ, deoxynojirimycin; DGJ, deoxygalactonojirimycin; N*B-DNJ,* N*-butyl-DNJ;* N*N-DNJ,* N*-nonyl-DNJ; M*ON*-DNJ,* N*-(9-methoxynonyl)-DNJ; 2THO-DNJ, N-8'-(2''-tetrahydrofuranyl)-octyl-DNJ.*

Structural mimicry of terminal sugar moieties in natural substrates underlies iminosugar biological activity. Certain iminosugars with glucose stereochemistry, such as deoxynojirimycin (DNJ)-derivatives, can competitively inhibit the ER α-glucosidases. DNJ itself is not a specific inhibitor of these enzymes within the N-glycosylation pathway, since it also inhibits the formation of the oligosaccharide precursors required [320]. The crystal structure of mammalian ER α-glucosidase II, including complexes with four iminosugars, has recently been solved, revealing binding mechanisms and enabling future structure-based inhibitor development [321]. The inhibition of ER α-glucosidases by iminosugars prevents glucose trimming and interaction with CNX/CRT, thus representing a potential antiviral strategy for infections with viruses requiring interaction with CNX/CRT for functional glycoprotein folding [322]. Even a single N-linked glycan can be sufficient to render a glycoprotein susceptible to iminosugar activity [323]. However, N-glycosylation does not mandate dependence on CNX/CRT for glycoprotein folding. The detection of tri-glucosylated viral glycoproteins on iminosugar treatment indicates the presence of a pathway whereby mis- or partially-folded glycoproteins can be produced in the absence of CNX/CRT interaction, as alternative chaperones such as binding immunoglobulin protein (BiP) may be utilised by some glycoproteins [324, 325]. In addition, iminosugars can enhance secretion of high-mannose glycoproteins, indicating that ER quality control may be bypassed, such as by Golgi-resident endo-α-D-mannosidase, which cleaves mannosidase linkages internally, within the first branch of a glucosylated N-glycan chain, although utilisation of this pathway is cell type-specific [326-328].

The structural mimicry of glucose by DNJ-derivative iminosugars means that several intestinal α-glucosidase enzymes are also inhibited. While the ensuing poor absorption of monosaccharides has led to some gastrointestinal side effects evident in clinical trials (Table 5), this is exploited therapeutically in the treatment of type II diabetes with *N*-hydroxyethyldeoxynojirimycin (Miglitol) [329]. Considering other iminosugar stereochemistries,

deoxygalactonojirimycin (DGJ)-derivatives, galactose mimics, predominantly inhibit galactosidases while deoxymannojirimycin (DMJ)-derivatives inhibit mannosidases. Iminosugars with stereochemistries differing from those of natural substrates, like 'talo' stereochemistry, show poor inhibitory activity [330].

N-alkylation of the iminosugar ring structure can enhance antiviral potency, through increased cellular uptake, inhibition of ER α-glucosidases, and inhibition of glucosylceramide synthase (GCS; ceramide-specific glucosyltransferase) [331-334]. The inhibition of GCS, the enzyme catalysing glucosylation of ceramide in the generation of glycosphingolipids, is shared by N-alkylated DNJ- and DGJ-derivatives [335-337] and underpins the clinical use of *N*-butyl-DNJ (*N*B-DNJ; Miglustat) as a substrate-reduction therapy for the lysosomal storage disorders Gaucher disease [338] and Niemann-Pick disease type C [339]. Bicyclic iminosugars do not inhibit glycolipid processing, exemplified by 6-*O*-butanoyl castanospermine (BuCAST; celgosivir) [337]. However, increased alkyl chain length is associated with increased cytotoxicity mediated by cell lysis and fragmentation [333, 340], although this can be ameliorated by inclusion of oxygen atoms in the alkyl chain [341].

1.2.3 Broad-spectrum antiviral activity

Targeting a host process enables broad-spectrum antiviral efficacy, and protection from resistance developing [342, 343]. This is particularly relevant for RNA viruses which rely upon error-prone viral RNA-dependent RNA-polymerases for replication [344] meaning that the development of resistance against direct-acting antivirals is an ever-present challenge. Despite targeting a host process, the sensitivity of viruses to iminosugar treatment appears to exceed that of host proteins, as antiviral effects can be achieved without detrimental effects on the host, perhaps due to vulnerabilities of the complex multimeric virion structure to viral

glycoprotein misfolding [345]. Virus susceptibility to iminosugars requires an aspect of the viral life cycle, such as infectivity or morphogenesis, to be dependent on correctly folded N-glycoproteins, and for that folding to be dependent on CNX/CRT. Thus, the presence of N-glycoproteins alone is not sufficient. Despite this, six-membered ring iminosugars have shown antiviral efficacy *in vitro* and *in vivo* against viruses of multiple families (Table 1). Clinical trials have also been conducted for HIV, HCV and DENV, outlined in 1.2.6.

The consequences of iminosugar-induced glycoprotein misfolding can vary between viruses, possibly because different life cycle stages are dependent on the glycoprotein for different viruses. Iminosugar treatment can reduce virion formation and secretion and/or the infectivity of secreted virions (specific infectivity). While this has not been evaluated for all of the viruses susceptible to iminosugar treatment, reductions in specific infectivity have been demonstrated for HIV-1 [346-348], cytomegalovirus [349] and Kunjin virus [350]. In contrast, a dominant effect on secretion was described for hepatitis B virus [323], INFV [324] and DENV [337].

Table 1. Antiviral efficacy of six-membered ring and bicyclic derivative iminosugars against viruses relevant for human health.

Adapted from publication in [345] to provide additional detail; adapted by permission from Springer Nature Customer Service Centre GmbH: Springer Nature Springer eBook Mechanisms of Antiviral Activity of Iminosugars Against Dengue Virus, Joanna L. Miller, Beatrice E. Tyrrell, Nicole Zitzmann, 2018.

Investigations using only native viruses are included (those considering viral glycoproteins, pseudotyped viruses or replicon systems only are excluded). Effects on viral glycoproteins do not include effects on oligosaccharide processing.

Abbreviations: BID, bis in die *(twice daily); CPE, cytopathic effect; FT, 1,5-dideoxy-1,5-imino-L-fucitol; i.p., intraperitoneal;* N*AP-DNJ,* N-*(N-4-azido-2-nitrophenyl)-6-aminohexyl-DNJ; ND, not determined; NE-DNJ, N-ethyl-DNJ; ToP-DNJ, 5'-tocopheroxypentyl-DNJ.* N-*7-oxadecyl-DNJ is also known as UV-3.*

Virus (N-linked glycoproteins)	Iminosugar	Effect on			Ref.
		Viral glycoprotein	Virion formation/function	Animal model	
Flaviviridae					
Dengue (E, prM, NS1, NS4b)	See Table 2 and Table 3				
Japanese encephalitis (E, prM, NS1)	*N*N-DNJ	↓ secretion and association of NS1 and E with calnexin	↓ antigen expression, infectious virus secretion and virus-induced CPE	↑ survival	[58]
West Nile (E, prM, NS1)	*N*N-DNJ, *N*-propylcyclohexyl-DNJ, *N*-butyl cyclohexyl-DNJ, *N*-pentylcyclo hexyl-DNJ, N-hexyl-(1-hydroxycyclohexyl)-DNJ, N-Pentyl-(1-hydroxycyclo hexyl)-DNJ	ND	↓ infectious virus secretion	ND	[351]
	CAST	ND	No effect on infectious virus secretion	ND	[351]
		ND	Little if any effect on replicon reporter gene expression; slight reduction in infectious virus secretion and no effect on specific infectivity of secreted virions	No effect	[352]
	PBDNJ0801	ND	↓ infectious virus secretion	ND	[353]
	PBDNJ0803				
	PBDNJ0804				

Kunjin (E, prM)	DNJ	No change in E distribution or prM cleavage	No effect on total or infectious virus secretion	ND	[350]
	*N*N-DNJ	No change in E distribution or prM processing	No effect on total virus secretion, but 99.9% reduction in virion specific infectivity	ND	[350]
Hepatitis C (E1, E2, NS4B)	DNJ	ND	Minimal reduction in intracellular NS3	ND	[354]
	*N*B-DNJ	ND	Minimal reduction in intracellular NS3	ND	[354]
	*N*N-DNJ	ND	↓ intracellular viral NS3 protein	ND	[354]
	ToP-DNJ	ND	No effect	ND	[355]
	OSL-95II	Degradation of E2 and E2-p7	↓ infectious virus secretion; no effect on virus replication	ND	[354]
	CM-10-18				[354]
	CM-9-78				[354]
	PBDNJ0802	ND	↓ intracellular viral NS3 protein	ND	[354]
	PBDNJ0803				[354]
	PBDNJ0804	Degradation of E2 and E2-p7	↓ intracellular viral RNA (4 days post-infection) and NS3 protein, ↓ infectious virus secretion	ND	[354]
	*N*B-DNJ	No effect on entry	No effect on replicon replication; ↓ infectious virus secretion	ND	[356]
	*N*N-DNJ	↓ cell entry	No effect on replicon replication; ↓ infectious virus secretion; inhibition of p7 ion channel		[356]
	*N*N-DGJ				[356]
Yellow fever (E, prM, NS1)	CAST	↓ antigen expression	↓ infectious virus secretion	ND	[352]
	IHVR19029	ND	↓ intracellular viral RNA (EC_{50} 21.5 μM)	ND	[226]
ZIKV (E, prM, NS1)	IHVR19029	ND	↓ intracellular viral RNA (EC_{50} 30 μM)	ND	[226]
Bunyaviridae					
Rift Valley fever (Gn, Gc, LGp)	*N*B-DNJ	ND	↓ infectious virus secretion (IC_{50} 250 μM)	ND	[357]
	*N*N-DNJ	ND	↓ infectious virus secretion (IC_{50} 58 μM)	ND	[357]
	N-7-oxadecyl-DNJ	ND	↓ infectious virus secretion (IC_{50} 220 μM)	ND	[357]
	M*O*N-DNJ	ND	↓ infectious virus secretion (IC_{50} 250 μM)	ND	[357]
	*N*AP-DNJ	ND	↓ infectious virus secretion (IC_{50} 49 μM)	ND	[357]

	IHVR11029, IHVR17028, IHVR19029	ND	↓ infectious virus secretion	ND	[358]
Filoviridae					
Ebola (GP, sGP)	*N*B-DNJ	No effect on secretion of GP-pseudotyped lentiviral particles	ND	Reduced clinical signs and histopathology; no significant survival benefit	[359]
		ND	↓ infectious virus secretion (IC_{50} 32.95 µM)	ND	[360]
	*N*B-DGJ	No effect on secretion of GP-pseudotyped lentiviral particles	ND	ND	[359]
	*N*N-DNJ	No effect on secretion of GP-pseudotyped lentiviral particles	ND	ND	[359]
		ND	↓ infectious virus secretion (IC_{50} 15.22 µM)	ND	[360]
	*N*N-DGJ	No effect on secretion of GP-pseudotyped lentiviral particles	ND	ND	[359]
	N-7-oxadecyl-DNJ	ND	↓ infectious virus secretion (IC_{50} 34.98 µM)	ND	[360]
	M*O*N-DNJ	ND	ND	No effect	[359]
		ND	↓ infectious virus secretion (IC_{50} 29.97 µM)	No survival benefit in mouse, guinea pig or Rhesus macaque models	[360]
	*N*AP-DNJ	ND	↓ infectious virus secretion (IC_{50} 7.859 µM)	No survival benefit in mouse model	[360]
	IHVR11029, IHVR17028, IHVR19029	↓ secretion of GP-pseudotyped lentiviral particles	ND	↑ survival	[358]

	IHVR19029	ND	↓ immunostaining for GP in HeLa cells (EC_{50} 16.9 μM); potentiated with favipiravir	↑ survival, potentiated with favipiravir	[226]
Marburg (GP)	*N*B-DNJ	ND	↓ infectious virus secretion (IC_{50} 47.72 μM)	ND	[360]
	*N*N-DNJ		↓ infectious virus secretion (IC_{50} 28.66 μM)		
	N-7-oxadecyl-DNJ		↓ infectious virus secretion (IC_{50} 47.72 μM)		
	M*O*N-DNJ		↓ infectious virus secretion (IC_{50} 47.72 μM)	Little to no survival benefit	
	*N*AP-DNJ		↓ infectious virus secretion (IC_{50} 6.359 μM)	Survival benefit with 10 mg/kg BID i.p. only in mouse model; no survival benefit in guinea pigs	
	IHVR11029, IHVR17028, IHVR19029	ND	ND	↑ survival	[358]
Togaviridae					
Sindbis (E1, PE2)	DNJ	↓ PE2 processing & secretion	↓ release of radiolabelled virions	ND	[361]
	*N*M-DNJ	↓ PE2 processing	↓ virion formation and infectious virus release	ND	[362]
	DMJ	No effect on PE2 cleavage; virions bud internally	↓ virion formation and infectious virus release	ND	[362]
		ND	No effect on parental strain; ↓ infectious virus secretion of PE2 cleavage mutant virus in mammalian and C6/36 cells	ND	[363]
	CAST	↓ PE2 processing & secretion	↓ release of radiolabelled virions	ND	[361]
Semliki forest (E1, E2, E3)	DNJ	Maturation unaffected	No effect in C6/36 cells	ND	[364]
	*N*M-DNJ	↓ E2/E3 cleavage	Slightly ↓ infectious virus secretion	ND	[365]
	DMJ	Maturation unaffected	No effect in C6/36 cells	ND	[364]
	Swainsonine				
Chikungunya (E1, E3E2)	*N*B-DNJ	ND	IC_{50} >500 μM)	ND	[357]
	*N*N-DNJ		↓ infectious virus secretion (IC_{50} 56 μM)		

	N-7-oxadecyl-DNJ		↓ infectious virus secretion (IC_{50} 500 µM)		
	M*O*N-DNJ		↓ infectious virus secretion (IC_{50} 500 µM)		
	*N*AP-DNJ		↓ infectious virus secretion (IC_{50} 22 µM)		
Venezuelan equine encephalitis (E1, E2, E3)	*N*B-DNJ	ND	↓ infectious virus secretion (IC_{50} 156 µM)	ND	[357]
	*N*N-DNJ		↓ infectious virus secretion (IC_{50} 12 µM)		
	N-7-oxadecyl-DNJ		IC_{50} >250 µM		
	M*O*N-DNJ		IC_{50} >250 µM		
	*N*AP-DNJ		↓ infectious virus secretion (IC_{50} 2 µM)		
Orthomyxoviridae					
Influenza A and B (HA, NA)	*Reviewed extensively in [314]*				
Paramyxoviridae					
Measles (F, H)	CAST	Surface expression unchanged; reduced F antigenicity	↓ virion and infectious virion secretion	ND	[366]
	DMJ	No effect	↓ infectious virus secretion		
	Swainsonine		Mostly ↑ infectious virus secretion		
Newcastle disease (F, HANA)	DNJ	ND	↓ syncytia formation	ND	[367]
	CAST	F-mediated haemolysis suppressed			
	DMJ	ND	No effect on syncytia		
	Swainsonine				
	Kifunensine	No effect on F-mediated haemolysis			
Herpesviridae					
Herpes simplex type 1 (gB, gC, gD, gE, gG, gH, gI, gJ, gK, gL)	BuCAST	ND	↓ infectious virus secretion	↓ brain virus; delayed lesion progression	[368]
Herpes simplex type 2 (gB, gC, gD, gE, gG, gH, gI, gJ, gK, gL)	*N*M-DNJ, *N*B-DNJ, *N*H-DNJ, CAST	ND	↓ infectious virus secretion	ND	[369]
	BuCAST	↓ gB processing	↓ infectious virus secretion	ND	[370]
Cytomegalo virus (gN)	DNJ	ND	↓ infectious virus secretion	ND	[349]
	*N*B-DNJ	ND	↓ infectious virus secretion	ND	[369]
		↓ gcI complex 2	No effect on total virion secretion, but ↓ infectious virus	ND	[349]

			secretion (reduced specific infectivity); no virucidal activity		
		ND	↓ infectious virus secretion	ND	[369]
	Fagomine	ND	↓ infectious virus secretion	ND	[349]
Retroviridae					
Human immune deficiency 1 (gp160 → gp120)	DNJ	ND	↓ infectious virus secretion	ND	[348]
		ND	↓ infectious virus secretion	ND	[371]
		ND	↓ CPE, virion formation & infectious virus secretion	ND	[372]
		Still expressed	No effect on virion secretion but virion specific infectivity ↓	ND	[346]
		ND	↓ CPE	ND	[373]
		ND	Slight ↓ CPE	ND	[374]
		ND	↓ CPE	ND	[375]
		ND	↓ CPE	ND	[376]
		↓ processing	↓ CPE	ND	[377]
	DNJ derivatives 1 & 2	ND	↓ CPE & infectious virus release	ND	[375]
	DNJ derivatives 3-8 & 10-11	ND	↓ CPE	ND	[375]
	*N*M-DNJ	ND	↓ infectious virus secretion	ND	[371]
		ND	↓ CPE	ND	[373]
		ND	↓ CPE	ND	[374]
	*N*E-DNJ	ND	↓ infectious virus secretion	ND	[371]
		ND	↓ CPE	ND	[373]
	*N*B-DNJ	↓ envelope protein synthesis; increased molecular weight	↓ CPE; ↓ infectious virion secretion from acutely- or chronically-infected cells; specific infectivity reduced for chronically-infected cells; ↓ virus binding to CD4+ lymphoid cells	ND	[347]
		ND	↓ infectious virus secretion	ND	[348]
		↓ processing	↓ CPE and virion specific infectivity	ND	[378]
		ND	↓ infectious virus secretion & elimination from cell culture	ND	[371]
		ND	↓ CPE	ND	[373]
		ND	↓ CPE	ND	[374]
		ND	↓ CPE	ND	[375]
	*N*B-DNJ free and in liposomes	Variation in sensitivity	↓ virion secretion, enhanced 100,000-fold	ND	[342]

		correlates with number of occupied glycosylation sites in gp120	with liposome-mediated delivery after 3 rounds of treatment; no development of viral resistance to *N*B-DNJ after 15 weeks' treatment		
	*N*B-DNJ + nucleoside analogues or azido thymidine	gp120 V3 loop cleavage ↓ by *N*B-DNJ	↓ virion secretion and infectious virion secretion; no effects on CD4 binding	ND	[379]
	N-(3-phenyl-2-propenyl)-1-DNJ	ND	↓ CPE & infectious virus secretion	ND	[380]
	CAST	↓ processing	↓ infectious virus secretion	ND	[348]
		ND	↓ CPE, virion formation & infectious virus secretion	ND	[372]
		ND	No effect on virion secretion but virion infectivity ↓	ND	[346]
		↓ cellular processing, but virions only have cleaved gp120	↓ CPE; ↓ total and infectious virion secretion	ND	[381]
		ND	↓ CPE	ND	[373]
		ND	↓ CPE	ND	[375]
		ND	↓ CPE	ND	[376]
	CAST + azido thymidine	ND	Synergistic ↓ of total and infectious virion secretion	ND	[382]
	L-6-epiCAST	ND	No effect on infectious virus	ND	[373]
	L-1,6-diepiCAST	ND	No effect on infectious virus	ND	[373]
	BuCAST	↓ processing	↓ infectious virus secretion	ND	[348]
		ND	↓ infectious virus secretion	ND	[383]
	MDL 43 305				
	MDL 28 653				
	MDL 29 435				
	MDL 29 204				
	MDL 44 370				
	MDL 29 270				
	DMJ	ND	No effect on infectious virus secretion	ND	[346]
		ND	Slight ↓ CPE	ND	[373]
		ND	↑ infectious virion secretion for virus grown with DMJ and infecting in presence of serum	ND	[376]
	*N*M-DMJ	ND	↓ CPE	ND	[373]
	HNJ	ND	No effect on CPE	ND	[384]

	*N*M-HNJ				
	*N*B-HNJ				
	Swainsonine	ND	↑ infectious virion secretion for virus grown with swainsonine and infecting in presence of serum	ND	[376]
	Fagomine	ND	↓ CPE but no effect on infectious virion secretion	ND	[372]
		ND	No effect on CPE	ND	[373]
	2-acetamido-1,5-imino-1,2,5-trideoxy-D-glucitol				
	2-acetamido-l,5-imino-l,2,5-trideoxy-D-galactitol				
	L-fuconic-1,5-lactam		↓ CPE		
	FT		No effect on CPE		
	N-methyl-FT		Slight ↓ CPE		
	N-acetyl-FT		Slight ↓ CPE		
	N-(5-carboxy methyl-1-pentyl)-FT		↓ CPE		
Human immune deficiency 2 (gp160 → gp120)	*N*B-DNJ free and in liposomes	ND	↓ virion secretion	ND	[342]
Arenaviridae					
Lymphocytic chorio meningitis (GPC → GP1, GP2)	CAST	Slightly ↓ GP-C cleavage	No effect on infectious virus secretion	ND	[385]
	Swainsonine	No effect			
Junin (GPC → GP1, GP2)	DNJ	ND	No effect on infectious virus secretion	ND	[386]
	DMJ				
	Swainsonine				
Hepadnaviridae					
Hepatitis B (S, M, L)	*N*B-DNJ	ND	↓ viral secretion; intracellular retention of HBV DNA	ND	[387]
Rhabdoviridae					
Vesicular stomatitis (G)	DNJ	No effect on trafficking	Secretion and infectious titres of San Juan strain ↓ at 40°C, not 30°C; Orsay strain unaffected	ND	[388]
		No effect on trafficking	Little effect on total and infectious virion secretion	ND	[389]

	DMJ	No effect on trafficking	Little effect on total and infectious virion secretion	ND	[389]
	CAST	ND	Secretion of San Juan strain ↓ at 40°C; Orsay strain unaffected	ND	[388]
	Miglitol	ND	↓ virus secretion	ND	[390]
Coronaviridae					
Severe acute respiratory syndrome (M, S)	*N*B-DNJ	↓ infectivity of S-pseudotyped virus	↓ plaque size	ND	[391]
		ND	↓ CPE	ND	[392]
	*N*N-DNJ	↓ infectivity of S-pseudotyped virus	↓ infectious virus	ND	[391]
	CAST	↓ infectivity of S-pseudotyped virus	↓ plaque size	ND	[391]
	Compound 7, 15	ND	↓ CPE	ND	[393]

1.2.4 Iminosugars as antivirals for DENV

Considerable research has been conducted into the potential use of iminosugars as antivirals against DENV, with multiple iminosugars demonstrating *in vitro* (Table 2) and *in vivo* (Table 3) efficacy. While most studies have used laboratory strains of DENV-2 and this is almost exclusively the case for animal studies, efficacy has been demonstrated across all four serotypes *in vitro* for *N*-(9-methoxynonyl)-DNJ (M*O*N-DNJ) [394], castanospermine (CAST) [352] and BuCAST [395]. The antiviral efficacy of iminosugars has been linked to viral glycoprotein misfolding [51, 58, 396] and to inhibition of ER α-glucosidases [337, 394, 397]. Phase I clinical trials have been conducted with M*O*N-DNJ and Phase II trials with BuCAST (discussed in 1.2.6).

Table 2. Antiviral efficacy of six-membered ring iminosugars and their bicyclic derivatives against DENV in in vitro *experiments in mammalian cells.*

Adapted from publication in [345]; adapted by permission from Springer Nature Customer Service Centre GmbH: Springer Nature Springer eBook Mechanisms of Antiviral Activity of Iminosugars Against Dengue Virus, Joanna L. Miller, Beatrice E. Tyrrell, Nicole Zitzmann, 2018.

Abbreviations: EC_{50} and IC_{50}, concentration giving a 50% inhibitory effect; ND, not determined; ToP-DNJ, 5'-tocopheroxypentyl-DNJ. N*-7-oxadecyl-DNJ is also known as UV-3.*

Imino-sugar	DENV serotype (strain)	Cell type (MOI)	Effect on			Ref.
			Viral glycoproteins	Viral replication	Infectious virus secretion	
DNJ-derivative iminosugars						
DNJ	1 (FGA/89)	Neuro 2a (400)	prME dimer formation impaired	ND	Reduced to 20% control at 500 μM	[51]
	2 (16681)	MDMΦ (1)	ND	ND	EC_{50} 308 μM	[337]
*N*B-DNJ	2 (16681)	MDMΦ (1)	ND	ND	IC_{50} 6 ± 7.31 μM; IC_{90} 62.1 ± 60.7 μM	[398]
	2 (NGC)	Vero	ND	ND	IC_{50} 162 μM	[399]
	2 (16681)	MDMΦ (1)	ND	Secreted DENV reduced in 1:1 ratio with infectious DENV	EC_{50} 10.6 μM	[337]
*N*N-DNJ	2 (PL046)	BHK-21 (0.1)	Reduced intracellular and secreted E and NS1	Reduced RNA replication (16-fold at 100 μM)	Reduced to plaque assay limit of detection with 5 μM; only significantly antiviral when drug added post-infection	[58]
	2	BHK-21 (0.05)	ND	ND	EC_{50} 1.1 μM; EC_{90} 3.3 μM	[353]
			ND	ND	IC_{50} 1 μM	[351]
	2 (16681)	MDMΦ (1)	ND	ND	IC_{50} 0.91 ± 0.40 μM; IC_{90} 8.02 ± 4.14 μM	[398]
	2 (NGC)	Vero	ND	ND	IC_{50} 9 μM	[400]
	2 (16681)	MDMΦ (1)	ND	ND	EC_{50} 1.25 μM	[337]
N-7-oxadecyl-DNJ	2 (NGC)	Vero	ND	ND	IC_{50} 41 μM	[399]
M*ON*-DNJ	1 (779,172)	Vero (0.01)	ND	ND	IC_{50} 5.15 ± 3.85 μM	[394]
	1 (SH 29177)				IC_{50} 2.10 ± 2.50 μM	
	1 (PRS 41393)				IC_{50} 37.69 ± 10.95 μM	

	2 (16681)	MDMΦ (1)	ND	ND	IC_{50} 3.09 ± 3.93 μM; IC_{90} 7.74 ± 3.63 μM	[398]
			ND	1:1 ratio in reduction of secreted total and infectious virus		[394]
	2 (NGC)	Vero	ND	ND	IC_{50} 17 μM	[399]
		Vero (0.01)	ND	ND	IC_{50} 6.49 ± 1.65 μM	[394]
	2 (SL 5-17-04)				IC_{50} 22.34 ± 16.36 μM	
	2 (UIS 1288)				IC_{50} 18.69 ± 7.21 μM	
	3 (SL 5-29-04)				IC_{50} 3.64 ± 1.39 μM	
	3 (UIS 776)				IC_{50} 6.56 ± 2.80 μM	
	3 (H87)				IC_{50} 86.49 ± 1.58 μM	
	4 (779,157)				IC_{50} 18.18 ± 24.44 μM	
	4 (C258/97)				IC_{50} 8.95 ± 1.25 μM	
	4 (H241)				IC_{50} 2.78 ± 1.42 μM	
*N*AP-DNJ	2 (16681)	MDMΦ (1)	ND	ND	IC_{50} 0.04 ± 0.01 μM; IC_{90} 0.28 ± 0.14 μM	[398]
	2 (NGC)	Vero	ND	ND	IC_{50} 2 μM	[400]
ToP-DNJ	2 (16681)	MDMΦ (1)	ND	ND	IC_{50} 12.7 μM	[355]
		Huh7.5 (0.1)			No antiviral effect	
2THO-DNJ	2 (NGC)	Vero (0.01)	ND	ND	IC_{50} 21.71 μM	[397]
CM-9-78	2 (TSV01)	A549 (0.3)	ND	EC_{50} 1.5 μM	ND	[400]
	2	BHK-21 (0.05)	ND	ND	EC_{50} 6.75 μM; EC_{90} 13 μM	[353]
CM-10-18	2 (TSV01)	A549 (0.3)	ND	EC_{50} 1.1 μM	ND	[400]
	2 (NGC)	BHK-21 (0.01)	ND	ND	EC_{50} 4.5 ± 2.0 μM; EC_{90} 47.2 ± 27.6 μM	[358]
CM-10-18 plus ribavirin	2 (TSV01)	A549	ND	Synergistic antiviral effect	ND	[400]
IHVR 11029	2 (NGC)	BHK-21 (0.01)	ND	ND	EC_{50} 0.75 ± 0.06 μM; EC_{90} 6.3 ± 3.5 μM	[358]
IHVR 17028	2 (NGC)				EC_{50} 0.3 ± 0.03 μM; EC_{90} 1.7 ± 0.8 μM	
IHVR 19029	2 (NGC)				EC_{50} 1.25 ± 1.1 μM; EC_{90} 22.5 ± 10.6 μM	
		HEK293 (0.1)	ND	EC_{50} 1.7 μM	ND	[226]
OSL95-II	2	BHK-21 (0.05)	ND	ND	EC_{50} 4 μM; EC_{90} 8.7 μM	[353]

	2	BHK-21 (0.05)	ND	ND	IC_{50} 2 µM	[351]
PBDNJ 0801	2	BHK-21 (0.05)	ND	ND	EC_{50} 0.1 µM; EC_{90} 0.2 µM	[353]
PBDNJ 0803	2				EC_{50} 0.1 µM; EC_{90} 0.6 µM	
PBDNJ 0804	2				EC_{50} 0.075 µM; EC_{90} 0.6 µM	
N-butyl-cyclo hexyl-DNJ	2	BHK-21 (0.05)	ND	ND	IC_{50} 3 µM	[351]
N-propyl-cyclo hexyl-DNJ	2				IC_{50} 1.5 µM	
DNJ-deriv-ative panel	2 (NGC)	BHK-21 (0.01)	Reduced intracellular E protein (compounds 2l, 3j, 3v, 4b, 3l, 7)	ND	EC_{50} values in the µM range (compounds 1c, 2a, 2d, 2h, 2k–2l, 3a–3c, 3j–3l, 3n, 3p–3t, 3v, 4a–4b, 5c–5e, 7)	[401]
DNJ-deriv-ative panel	Not stated	BHK	ND	ND	EC_{50} values in the µM range	[402]
Bicyclic iminosugars						
CAST	1 (Brazil)	BHK-21 (0.01)	ND	ND	IC_{90} < 50 µM	[352]
	1 (FGA/89)	Neuro 2a (400)	E protein misfolded; prME dimer formation impaired	ND	Reduced to 5% control at 500 µM	[51]
	2	BHK-21 (0.05)	ND	ND	IC_{50} 6 µM	[351]
	2 (16681)	BHK-21 (0.1-10)	prM glycosylation affected	Replicon expression reduced by <40%	IC_{50} 1 µM; IC_{90} < 50 µM; specific infectivity of virions decreased markedly	[352]
		Huh7 (0.1-10)	ND	ND	IC_{50} 85.7 µM	[352]
		MDMΦ (1)	ND	ND	EC_{50} 36.4 µM	[337]
	2 (N1042)	BHK-21	ND	ND	IC_{90} < 50 µM	[352]
	3 (Sri Lanka)					
	4 (Tahiti)					

BuCAST	1 (2402)	BHK-21 (0.3)	ND	EC_{50} 0.65 ± 0.16 µM	ND	[395]
			ND	ND	EC_{50} 0.105 ± 0.059 µM	[403]
		BHK-21 (0.01)			EC_{50} 0.066 ± 0.019 µM	
		Huh7 (0.3)			EC_{50} 17.430 ± 4.921 µM	
		Huh7 (0.01)			EC_{50} 5.961 ± 1.258 µM	
		Vero (0.3)			EC_{50} 51.035 ± 14.47 µM	
		Vero (0.01)			EC_{50} 13.805 ± 1.902 µM	
		THP-1 (2)			EC_{50} 3.236 µM	
	2 (3295)	BHK-21 (0.3)	Intracellular E and NS1 reduced; NS1 molecular weight affected; E and NS1 retained in ER	EC_{50} 0.22 ± 0.01 µM	ND	[395]
			ND	ND	EC_{50} 0.061 ± 0.003 µM	[403]
		Huh7 (0.3)			EC_{50} 0.824 ± 0.109 µM	
		Vero (0.3)			EC_{50} 2.434 ± 0.773 µM	
		THP-1 (50)			EC_{50} 0.756 µM	
	2 (S221)	BHK-21 (0.3)			EC_{50} 0.119 ± 0.000 µM	
		Huh7 (0.3)			EC_{50} 5.093 ± 1.036 µM	
		Vero (0.3)			EC_{50} 8.336 ± 0.773 µM	
		THP-1 (2)			EC_{50} 2.135 µM	
	16 DENV-1 and -2 isolates from CELADEN trial	Huh7 (varied)			Only one strain less sensitive to 3 µM BuCAST than DENV-1 (2402)	
	2 (16681)	MDMΦ (1)	ND	Secreted DENV reduced in 1:1 ratio with infectious DENV	EC_{50} 5.17 µM	[337]

	3 (863)	BHK-21 (0.3)	ND	EC_{50} 0.68 ± 0.02 μM	ND	[395]
	4 (2270)	BHK-21 (0.3)	ND	EC_{50} 0.31 ± 0.12 μM	ND	[395]
DGJ-derivative iminosugars						
*N*B-DGJ	2 (16681)	MDMΦ (1)	ND	ND	No inhibition	[337]
*N*N-DGJ	2 (16681)					[337]
M*O*N-6d-DGJ	2 (16681)	MDMΦ (1)	ND	ND	No inhibition	[394]

Table 3. Iminosugar antiviral efficacy against DENV in in vivo *experiments.*

Adapted from publication in [345]; adapted by permission from Springer Nature Customer Service Centre GmbH: Springer Nature Springer eBook Mechanisms of Antiviral Activity of Iminosugars Against Dengue Virus, Joanna L. Miller, Beatrice E. Tyrrell, Nicole Zitzmann, 2018.

Abbreviations: BID, bis in die *(twice daily); i.c., intracranial; i.p., intraperitoneal; i.v., intravenous; MSD, mean survival days; PERL, polyunsaturated ER-targeting liposome; p.i., post-infection; TID,* ter in die *(thrice daily); VLR, virological log reduction.*

Iminosugar	DENV infection	Animal model	Outcome	Ref.
*N*B-DNJ	10^5 pfu i.v. DENV-2 (D2S10) with ADE (4G2 anti-E antibody)	AG129 mice; n=5-18/group	PBS or PBS-containing PERLs: death at day 4-5 p.i. Non-significant reduction in liver and spleen viral titres. 0.088 mg/kg/day: no effect on survival. Non-significant reduction in liver and spleen virus titres. 250 mg/kg/day: 20% survival 1000 mg/kg/day: 90% survival. Significant viral load reduction in liver, small intestine, serum and spleen at day 3.5 p.i. 0.094 mg/kg/day encapsulated in PERLs: 20% survival, with encapsulation providing >1900-reduction in dose able to increase survival. Non-significant reduction in liver and spleen viral titres.	[398]
	2 x 10^6 pfu i.v. DENV-2 (S221)	AG129 mice; n=23 (water), 10 (drug), 5 (ribavirin)	Water or ribavirin 100 mg/kg daily: euthanised day 4-6 p.i., median survival 4 days 100 mg/kg BID orally for 7 days: no significant difference	[399]
*N*N-DNJ	2 x 10^6 pfu i.p. DENV-2 (TSV01)	7-9-week old AG129 mice; n=8/ group	75 mg/kg orally BID for 3 days: 93% reduced viraemia, 68% reduced splenomegaly	[404]

	2 x 10^6 pfu i.v. DENV-2 (S221)	AG129 mice; n=23 (water), 13 (drug), 5 (ribavirin)	Water or ribavirin 100 mg/kg daily: euthanised day 4-6 p.i., median survival 4 days 100 mg/kg BID orally for 7 days: median survival 8 days, gradual decrease in mean group weight	[399]
N-7-oxadecyl-DNJ	2 x 10^6 pfu i.v. DENV-2 (S221)	AG129 mice; n=23 (water), 5 (drug or ribavirin)	Water or ribavirin 100 mg/kg daily: euthanised day 4-6 p.i., median survival 4 days 100 mg/kg BID orally for 7 days: no significant difference	[399]
M*O*N-DNJ	2 x 10^6 pfu i.v. DENV-2 (S221)	AG129 mice; n=23 (water), 18 (drug), 5 (ribavirin)	Water or ribavirin 100 mg/kg daily: euthanised day 4-6 p.i., median survival 4 days 100 mg/kg BID orally for 7 days: median survival 7.5 days, mean weight significantly higher than control group throughout	[399]
	2 x 10^4 pfu i.v. DENV-2 (S221) with ADE (2H2 anti-prM antibody)	AG129 mice; n=33 (water), 29 (drug)	Water: 10% survival at day 9 p.i., median survival 4 days 100 mg/kg TID orally for 7 days: 89% survival at day 9 p.i. with no symptoms. Serum viral RNA and titres reduced four-fold at 48h p.i., equivalent at 72h p.i., and 100-fold lower at 96h p.i. Viral RNA levels reduced 100-1000-fold in liver, small intestine and kidney. Lower but significant reduction in viral titre in liver and kidney. No effect on DENV-specific IgM or IgG.	
	2 x 10^4 pfu i.v. DENV-2 (S221) with ADE (2H2 anti-prM antibody)	AG129 mice; n=11 (water), 10/drug group	Water: 0% survival at day 5 p.i. 2.5 mg/kg TID orally for 7 days: 30% survival at day 9 p.i. (time point for all iminosugar doses) 5 mg/kg TID orally for 7 days: 50% survival 10 mg/kg TID orally for 7 days: 90% survival 100 mg/kg TID orally for 7 days: 100% survival	
	2 x 10^4 pfu i.v. DENV-2 (S221) with ADE (2H2 anti-prM antibody)	AG129 mice; n=10 (water), 8/drug group	Water: 0% survival at day 9 p.i. Drug dosing 100 mg/kg TID orally for 7 days. From challenge: 90% survival at day 12 p.i. From 24h p.i.: 100% survival at day 12 p.i. From 48h p.i.: 40% survival at day 12 p.i., median survival 11 days From 72h p.i.: 0% survival at day 10 p.i., no significant difference from control	
	1 x 10^{10} GEs in 1^{st} passage, 1 x 10^8 GEs for 2^{nd}-4^{th} passage DENV-2 (S221)	STAT1$^{-/-}$/ 2$^{-/-}$ 129/Sv mice	100 mg/kg orally TID for 72h beginning -1h from infection. 19 nonsynonymous mutations identified in glycoproteins after four serial passages in mice; no true escape mutants	[343]

	10^9 GEs DENV-2 (S221) with ADE (2H2 anti-prM antibody)	AG129 mice; n=10/ group	Vehicle: 10-20% survival, significantly worse clinical scores and weight loss than drug-treated. 10 mg/kg TID orally for 7 days: from -1h relative to infection, 60% survival; from 24h p.i., 56% survival; from 48h p.i., 36% survival 20 mg/kg TID orally for 7 days: from -1h relative to infection, 85% survival; from 24h p.i., 100% survival; from 48h p.i., 70% survival. 40 mg/kg TID orally for 7 days: from -1h relative to infection, 100% survival; from 24h p.i., 100% survival; from 48h p.i., 90% survival 100 mg/kg TID orally for 7 days: from -1h relative to infection, 90% survival; from 24h p.i., 90% survival; from 48h p.i., 100% survival 100 mg/kg M*O*N-6d-DGJ TID orally for 7 days: no protection	[394]
*N*AP-DNJ	2 x 10^6 pfu i.v. DENV-2 (S221)	AG129 mice; n=23 (water), 10 (drug), 5 (ribavirin)	Water or ribavirin 100 mg/kg daily: euthanised day 4-6 p.i., MSD 4 days 100 mg/kg BID orally for 7 days: no significant difference	[399]
2THO-DNJ	1 x 10^4 pfu i.v. DENV-2 (S221) with ADE (2H2 anti-prM antibody)	5-6 week old AG129 mice	Vehicle: 0% survival, MSD 5 days 20 mg/kg TID for 7 days, starting 1 hour pre-infection: 100% survival to day 9 p.i. 100 mg/kg TID for 7 days, starting 1 hour pre-infection: 100% survival to day 9 p.i. Viral loads reduced in kidney (12.9-fold at 72h p.i., 5.23-fold at 96h p.i.) and small intestine (6.1-fold at 72h p.i.), but not in serum or liver at 72 or 96h p.i. Spleen viral load increased 5-fold at 72h p.i. but no difference at 96h p.i.	[397]
CAST	10^5 pfu i.c. DENV-2 (mouse-adapted NGC)	4-week old A/J mice; n = 30-45/ group	Vehicle: 0% survival 10 mg/kg (10 days i/p): 20% survival 50 mg/kg (10 days i/p): 90% survival 250 mg/kg (10 days i/p): 85% survival	[352]
	2 x 10^5 pfu i.p. DENV-2 (S221) with ADE (4G2 anti-E antibody)	AG129 mice; n=8 (vehicle), 10 (drug)	Vehicle: 0% survival at day 5 p.i. 50 mg/kg BID for 5 days: 60% survival at day 10 p.i.	[405]
BuCAST	2 x 10^6 pfu i.p. DENV-2 (TSV01)	7-9-week old AG129 mice; n=8/group	7.5 mg/kg orally BID for 3 days: 62% reduced viraemia 75 mg/kg orally BID for 3 days: 88% reduced viraemia 75 mg/kg orally BID for 2 days, starting 1 day p.i.: 55% reduced viraemia	[404]

	2 x 10^5 pfu i.p. DENV-2 (S221)	AG129 mice; n=8/group	Vehicle: 75% survival at day 10 p.i. 50 mg/kg i/p BID for 5 days: 100% survival at day 10 p.i.	[395]
	2 x 10^5 pfu i.p. DENV-2 (S221) with ADE (4G2 anti-E antibody)	AG129 mice; n=8/group	Vehicle: 0% survival at day 5 p.i. 50 mg/kg i/p BID for 5 days: 100% survival at day 10 p.i., reduced to 50% survival if administered from day 2 p.i.	[395]
	2 x 10^5 pfu i.p. DENV-2 (S221) with ADE (4G2 anti-E antibody)	AG129 mice; n=7 (50 mg/kg) or 8/group	Vehicle: 0% survival at day 5 p.i. 10 mg/kg BID for 5 days: 13% survival at day 10 p.i. 25 mg/kg BID for 5 days: 63% survival at day 10 p.i., reduced viraemia at day 3 p.i. 50 mg/kg BID for 5 days: 100% survival at day 10 p.i., reduced viraemia at day 3 p.i. 100 mg/kg daily for 5 days: 0% survival at day 6 p.i., no viraemia reduction	[405]
	10^5 pfu i.v. DENV-2 (D2S10) with ADE (4G2 anti-E antibody)	AG129 mice	33.3 mg/kg every 8 hours until sacrifice at 80h p.i. Viral RNA load significantly reduced, trend towards reduced circulating infectious virus and viral RNA in kidney, parenteral lymph nodes, liver and small intestine. Enhanced viral RNA levels in spleen	[337]
	7 x 10^7 pfu i.v. DENV-1 (2402) with ADE (4G2 antibody)	AG129 mice; n=5-6/group	Vehicle: 0% survival at day 5 p.i. 10 mg/kg orally BID: 0% survival at day 6 p.i., 1.8-fold viraemia reduction at day 3 p.i. 50 mg/kg orally BID: 100% survival at day 10 p.i., viraemia reduced 4.3-fold. No additional reduction in viraemia if treatment started at peak viraemia	[403]
	1 x 10^8 pfu i.v. DENV-2 (3295) with ADE (4G2 antibody)	AG129 mice; n=5-6/group	Vehicle: 0% survival at day 5 p.i. 10 mg/kg orally BID: 100% survival at day 10 p.i.; 3.7-fold viraemia reduction at day 3 p.i. 50 mg/kg orally BID: 100% survival at day 10 p.i.; 16.5-fold viraemia reduction. No additional reduction in viraemia if treatment started at peak viraemia	[403]
	2 x 10^4 pfu i.v. DENV-2 (S221) with ADE (4G2 antibody)	AG129 mice; n=5-6/group	Vehicle: 0% survival at day 5 p.i. 10 mg/kg orally BID: 0% survival at day 6 p.i., 1.4-fold viraemia reduction at day 3 p.i. 50 mg/kg orally BID: 100% survival at day 10 p.i., viraemia reduced 2.4-fold	[403]
	2 x 10^7 pfu i.v. DENV-2 DENV-2 (#013)	AG129 mice; n=6/group	50 mg/kg orally BID: from infection, viraemia on day 3 p.i. reduced 6.8-fold; from 3 days p.i., VLR from day 3 to day 6 not significantly different from control	[403]

	1 x 10^7 pfu i.v. DENV-2 (#031)	AG129 mice; n=6/group	50 mg/kg orally BID: from infection, viraemia on day 3 p.i. reduced 7.8-fold; from 3 days p.i., VLR from day 3 to day 6 not significantly different from control	[403]
	2 x 10^7 pfu i.v. DENV-2 (#036)	AG129 mice; n=6/group	50 mg/kg orally BID: from infection, viraemia on day 3 p.i. reduced 12.5-fold; from 3 days p.i., VLR from day 3 to day 6 not significantly different from control	[403]
CM-9-78	5 x 10^6 pfu i.p. DENV-2 (TSV01)	7-8 week old AG129 mice; n=6/group	75 mg/kg orally BID for 3 days: 2.3-fold viraemia reduction at 3 days p.i. 25 and 10 mg/kg orally BID for 3 days: no significant effects on viraemia	[400]
CM-10-18	5 x 10^6 pfu i.p. DENV-2 (TSV01)	7-8 week old AG129 mice; n=6/group	75 mg/kg orally BID for 3 days: 1.8-fold viraemia reduction at 3 days p.i.	[400]
	2 x 10^7 pfu i.v. DENV-2 (mouse-adapted D2S10)	AG129 mice; n=5/group	PBS: euthanised day 6 p.i. 40 mg/kg/day ribavirin: euthanised day 5 p.i. 75 mg/kg or 150 mg/kg orally BID for 3 days: 100% survival to day 15	[406]
	10^7 pfu i.p. DENV-2 (D2Y98P-rc)	AG129 mice; n=5/group	PBS: MSD 9±2.2 25 mg/kg BID NITD008: 100% survival at day 24 p.i. 3 mg/kg orally BID for 3 days: MSD 12±2.0 10 mg/kg orally BID for 3 days: MSD 14±1.1 25 mg/kg orally BID for 3 days: MSD 17±2.3 75 mg/kg orally BID for 3 days: 40% survival at day 24 p.i.	[406]
CM-10-18 plus ribavirin	5 x 10^6 pfu i.p. DENV-2 (TSV01)	7-8 week old AG129 mice; n=6/group	CM-10-18 75 mg/kg orally BID for 3 days p.i.: 1.9-fold viraemia reduction at day 3 p.i. Ribavirin 40 mg/kg daily for 3 days p.i.: no effect on viraemia at day 3 p.i. Combination: 4.7-fold viraemia reduction at day 3 p.i.	[400]

1.2.5 Additional antiviral mechanisms of iminosugars

Besides the antiviral effects of iminosugars disrupting the morphogenesis or infectivity of virions, discussed in 1.2.3, other properties of iminosugars can impact viral infection.

1.2.5.1 Viral receptors

Iminosugar treatment may affect the expression or function of cellular receptors where this depends on N-glycosylation or another process inhibited by these compounds. Since *N*B-DNJ treatment reduced HIV cellular entry, the possibility that iminosugar treatment was disrupting the CD4 receptor was considered. However, reduced inclusion of gp120 in virions, combined with a defect in gp120 rearrangement post-CD4 binding were found to be responsible, rather than effects on CD4 itself [381, 407, 408]. Other DNJ-derivative iminosugars have been shown to reduce CD4 expression, however [409]. DNJ-derivatives inhibit cellular entry of lentiviral particles pseudotyped with the envelope proteins of H1N1 influenza A virus (IAV), severe acute respiratory syndrome coronavirus (SARS-CoV) and the human coronavirus NL63 (HCoV-NL63). The latter two viruses share the angiotensin-I converting enzyme 2 (ACE2) entry receptor, the N-glycosylation and membrane fusion capacity of which was compromised by iminosugar treatment [410]. No effect on the entry of lentiviral particles pseudotyped for HCV, vesicular stomatitis virus (VSV), Moloney murine leukaemia virus (MLV), Ebola virus (EBOV) or Lassa fever virus (LASV) was found, indicating the specificity of these effects [410].

1.2.5.2 Viral ion channels

Iminosugars with long alkyl chains can inhibit the activity of viral ion channels. In HCV, the p7 protein can form cation-conducting ion channels [411] and is important for viral infection [412, 413]. *N*-nonyl-DNJ (*N*N-DNJ), *N*-nonyl-DGJ (*N*N-DGJ) and *N*-7-oxanonyl-6-deoxy-DGJ can inhibit the activity of p7 ion channels, with blocking of the channel pore and disrupting channel formation suggested as potential mechanisms of action under ongoing investigation [356, 414, 415]. Besides HCV, intercalation of iminosugar alkyl chains between monomers has been proposed to underpin iminosugar-mediated inhibition of human papillomavirus E5 viroporin function [416].

1.2.5.3 Immunomodulatory activity in viral infections

PRR signalling pathways are required to detect and initiate antiviral responses to viral infection, often leading to the production of IFN-α/β and pro-inflammatory cytokines, as described for DENV, ZIKV and CCHFV in 1.1. These cytokines also play roles in the pathogenesis of these viral infections. Among six-membered ring iminosugars, DNJ-derivatives have been shown to affect cytokine and chemokine responses in the context of DENV infection *in vitro* and *in vivo* while *N*B-DGJ lacked effects (Table 4). Interestingly, a Th1 to Th2 shift in circulating cytokines was observed in BuCAST-treated patients in the CELADEN trial [417]. The antiviral efficacy of the DNJ-derivative iminosugars is likely to contribute to these effects, but this cannot be the sole determinant since iminosugar modulation of cytokines is evident in settings lacking infectious, replicating stimuli, as discussed in 1.3. Furthermore, the effects of iminosugars on cytokines are not evident with all viral infections [359] and bidirectional modulation of different cytokines can occur within one experimental setting (seen in most DENV studies in Table 4), indicating some complexity in the underlying mechanism(s).

Table 4. Effects of six-membered ring iminosugars on cytokines and chemokines in the context of viral infection.

Abbreviations: BID, bis in die *(twice daily); G-CSF, granulocyte-colony stimulating factor; KC, keratinocyte chemoattractant (murine IL-8); MIF, macrophage migration inhibitory factor; MIP-1β, macrophage inflammatory protein-1β; p.i., post-infection; TGF-β, transforming growth factor β; TID,* ter in die *(thrice daily).*

Iminosugar	Conc.	System	Cytokine	Effect	Ref
DNJ-derivatives					
*N*B-DNJ	100 µM	DENV-infected MDMΦs	IFN-γ	Significant reduction in secretion	[418]
			TNF-α		
			MIP-1β	Significant increase in secretion	
			IL-6	No effect	
			IL-8		
			IL-10		
			IL-17A		
			G-CSF		
			IP-10		
			MCP-1		
			MIF		
			RANTES		
			TNF-α		

	1850 mg/kg/ day	EBOV-infected Guinea pigs	TGF-β	No significant effect on mRNA levels in blood at necropsy	[359]
			IL-12		
*N*N-DNJ	75 mg/kg orally BID for 3 days	DENV-infected A129 mice	TNF-α	Reduced plasma levels 3 days p.i.	[404]
			IFN-γ		
			IL-6		
			IL-12		
			MCP-1		
M*O*N-DNJ	100 mg/kg TID	ADE-DENV infection of A129 mice	TNF	Delayed increase until 72 h p.i.. Remained below 150 pg/ml to 96 h p.i. compared to >500 pg/ml in control mice. At day 4 p.i. treated mice had <20% TNF of controls	[399]
			IFN-γ	Delayed increase until 96 h p.i. when levels increased but remained below control	
			IL-12	Delayed increase until 96 h p.i.	
			IP-10		
			IL-6		
			MCP-1	Delayed increase until 72 h p.i.	
			KC	Significantly increased at 96 h p.i.	
	25 µM	DENV-infected MDMΦs	TNF-α	Significant reduction in secretion	[418]
			IFN-γ		
			IL-10		
			G-CSF		
			RANTES		
			MIP-1β	Significant increase in secretion	
			IL-6	No effect	
			IL-8		
			IL-17A		
			IP-10		
			MCP-1		
			MIF		
	120 mg/kg/ day	EBOV-infected Guinea pigs	TNF-α	No significant effect on mRNA levels in blood at necropsy	[359]
			TGF-β		
			IL-12		
2THO-DNJ	100 mg/kg TID	ADE-DENV infection of A129 mice	TNF-α	Significantly reduced at 72 and 96 h p.i.	[397]
			GM-CSF		
			MIP-1α		
			IL-1α		
			IL-1β		
			IL-2		
			IL-3		
			IL-12p40		
			IL-12p70		
			IL-17		
			IFN-γ	Significantly reduced at 72 h p.i.	
			MIP-1β	Significantly reduced at 96 h p.i.	
			RANTES		
			IL-10		
			MCP-1	No significant difference	
			Eotaxin		
			IL-9		
			KC	Significantly increased at 72 h p.i.	

DGJ-derivatives					
*N*B-DGJ	100 µM	DENV-infected MDMΦs	TNF-α	No effect	[418]
			IFN-γ		
			IL-10		
			G-CSF		
			RANTES		
			MIP-1β		
			IL-6		
			IL-8		
			IL-17A		
			IP-10		
			MCP-1		
			MIF		
Bicyclic iminosugars					
BuCAST	400 mg loading dose then 200 mg BID for 5 days	DENV patients (relative to placebo treatment) in CELADEN trial	TNF-α	Reduced circulating levels	[417]
			IFN-γ		
			IL-13	Increased circulating levels	

In addition to the effects observed on soluble inflammatory mediators, iminosugar treatment may be able to influence immune responses to infection in other ways. Immunosuppressive effects have been observed in several studies with bicyclic and DNJ-derivative iminosugars. Downregulation of class I and II major histocompatibility complex molecules, CD4 and CD8 on lymphoid cells and adhesion molecule ligand-receptor pairs on lymphoid and endothelial cells was seen with CAST treatment of rats receiving heart allografts, with the resulting immunosuppressive effect prolonging allograft survival [419]. Reduced T cell proliferation has also been observed with CAST treatment, while swainsonine, a mannosidase inhibitor, enhanced T cell proliferation in response to some but not all stimuli [420]. T cell activation was also reduced by CAST [421]. Observations of leukopaenia were also made in a clinical trial evaluating *N*B-DNJ efficacy in HIV-infected individuals, although this may not have been T cell-specific [422]. Conversely, immunostimulatory effects have also been observed with DNJ-derivative iminosugars. *N*B-DNJ treatment of the murine RAW264.7 macrophage cell line upregulated surface expression and functional capacity of scavenger receptor A, a receptor whose broad ligand profile includes low-density lipoprotein important in the pathogenesis of atherosclerosis

[423]. The modulation of the expression and function of further cytokine receptors by iminosugars is certainly possible: for example, N-glycosylation of the TNF-α receptor TNFR1 plays a functional role in ligand binding and signalling activation [424]. The unfolded protein response (UPR), primarily an adaptive mechanism to preserve protein folding and cell survival under conditions of ER stress, can also be activated by iminosugars [418]. While the relationship between pathogens and the UPR is complex, elements of UPR activation can have antiviral effects against viruses such as DENV, although this can also be exploited to proviral ends [425]. Thus, there are multiple ways in which iminosugars might influence responses to infection besides affecting soluble inflammatory mediators.

1.2.6 Clinical development of iminosugars as antivirals

As previously mentioned, iminosugars are licensed and well-tolerated in the treatment of several non-viral conditions, with *N*B-DNJ (Miglustat; Zavesca®) used to treat the lysosomal storage disorders Gaucher disease [338] and Niemann-Pick disease type C [339] and *N*-hydroxyethyldeoxynojirimycin (Miglitol; Glyset®) for non-insulin-dependent diabetes [329]. Clinical trials evaluating iminosugar treatment in HIV, HCV and DENV infections have been conducted (Table 5). Most studies have identified some gastrointestinal side effects due to off-target inhibition of intestinal disaccharidases, which can be ameliorated by dietary alteration [422] and may be improved further through the use of prodrugs and future structure-based drug design approaches [321, 334]. BuCAST (celgosivir) was evaluated in a Phase Ib trial against in DENV-infected individuals in Singapore, showing some non-significant trends towards efficacy in parameters including viral load, fever and NS1 clearance, although the study was underpowered to discriminate between effects in primary and secondary infection [403, 426]. Subsequent analysis demonstrated that BuCAST had antiviral efficacy against viruses amplified from patients enrolled in the study [403]. *In vivo* optimisation of dosing regimens has been

conducted [403] and implemented in the study design of a further clinical trial (ClinicalTrials.gov identifier NCT02569827). Safety, tolerability and pharmacokinetics of single- and multiple-ascending doses of M*O*N-DNJ were also evaluated in two clinical trials, but these have been discontinued for business reasons (Table 5).

Table 5. Clinical trials of iminosugars as antivirals (chronological where possible).

ClinicalTrials.gov identifiers for the studies are shown where appropriate.

Iminosugar	Condition	Clinical trial/use	Ref
*N*B-DNJ	HIV	Phase II trial (NCT00002079) of *N*B-DNJ with zidovudine (60 patients) or zidovudine plus placebo (58 patients). The *in vitro* inhibitory concentration of *N*B-DNJ was not achieved at the steady-state trough level. Increases in $CD4^+$ T cell counts were seen in both groups, although the combination was not significantly better. Gastrointestinal side effects were common for combination recipients.	[427]
*N*B-DNJ	Advanced HIV	Phase I dose-escalation trial (NCT00000692; 29 patients). Study discontinued due to cataract finding in long-range rat toxicology study, later shown to be transient and species-specific. Number of participants too small to determine trends in CD4 cell count or p24 antigen levels. Common gastrointestinal side effects, partially ameliorated by diet avoiding complex carbohydrates.	[422]
BuCAST	HIV	Phase I oral single or multiple dose-tolerance study (NCT00000692). Results unpublished.	
BuCAST	HIV	Phase II trial (NCT00002150 and NCT00002151) of celgosivir hydrochloride alone and in combination with zidovudine. Results unpublished.	
UT-231B	HCV genotype 1 non-responders to IFN	Phase II trial (NCT00069511). No reduction in HCV RNA levels with 12 weeks of treatment.	[428]
BuCAST	Chronic HCV genotype 1	Phase II trial (NCT00157534) for safety and efficacy of 12 weeks of treatment. Study results unpublished.	
BuCAST	Chronic HCV genotype 1 non-responders	Phase II trial (NCT00217139 and NCT00292084) of BuCAST and peginterferon α-2b ± ribavirin (57 patients highly resistant to prior peginterferon α-2b and ribavirin treatment). Clinically significant decrease in HCV RNA in the group with BuCAST. Well-tolerated with some gastrointestinal side effects.	[429]
BuCAST	Dengue	Phase Ib trial (NCT01619969; 50 patients) in Singapore. BuCAST administered as initial 400 mg loading dose followed by 200 mg every 12 hours for nine doses. Non-significant differences in mean virological log reduction (VLR) and area under the fever curve. However there were outliers in VLR in placebo group, and study was underpowered to discriminate between primary and secondary DENV infection. Similar incidence of adverse events as placebo.	[417, 426]

M*ON*-DNJ (UV-4B)	Dengue	Phase I trial (NCT02061358) for single-ascending dose safety, tolerability and pharmacokinetics, for 3-1000 mg UV-4B. Study completed with results available from ClinicalTrials.gov.
M*ON*-DNJ (UV-4B)	Viral infections	Phase I trial (NCT02696291) for multiple-ascending dose safety, tolerability and pharmacokinetics, for 30 mg, 75 mg, 150 mg and two higher doses administered thrice daily for 7 days. Study terminated (product development halted for business reasons).

1.2.7 Iminosugar antiviral efficacy in mosquitos

The potential impact of drugs used to treat arboviral infections on vector transmission should be evaluated. Insects possess N-glycosylation pathways that fulfil essential functions, with homologues of mammalian N-glycosylation pathway components including the ER α-glucosidases and calnexin [430, 431]. Indeed, DENV infection results in induction of the ER α-glucosidases in the midguts of mosquitos [432]. N-glycan processing enzymes in the Golgi differ however, leading to a predominance of high-mannose and paucimannose glycans in insect glycoproteins and very few complex glycans [430]. Iminosugar efficacy has been evaluated previously in *Aedes aegypti* mosquitos, where DNJ or CAST treatment [433] or silencing of one the α-glucosidases [434] did not impact DENV infection. However, the single iminosugar treatment used might not reflect potential iminosugar exposure with multiple doses administered per day, as envisaged by the current clinical outlook [403], combined with the potential for *Aedes* mosquitos to take multiple blood meals [435].

1.3 Iminosugars as immunomodulators beyond viral infection

Cytokines are important inflammatory mediators in a multitude of contexts beyond viral infection, including disease states such as sepsis and chronic inflammatory conditions. As mentioned in 1.2.5.3, the impact of iminosugars on aspects of the immune system is not restricted to viral infection, and iminosugar effects on cytokines elicited by non-viral stimuli are collated in Table 6. Effects vary between cytokines, with the secretion of IL-2 and MCP-1 often increased, but that of IL-4 and TNF-α most often decreased with iminosugar treatment.

Bidirectional effects on IFN-γ are reported in different systems. In addition, directionality of the effects on some cytokines differs depending on the iminosugar concentration [436, 437]. However, interpretation of these effects is complex in light of the variation in models and cytokines evaluated in each case.

Some mechanistic characterisation has been conducted. *N*-pentafluorobenzyl-1-deoxynojirimycin (5F-DNJ) reduced activation of the Janus kinase/signal transducers and activators of transcription (JAK/STAT) signalling pathway in peripheral blood mononuclear cells (PBMCs) stimulated with concanavalin A concomitant with reduced IL-4 secretion [438] while reduced activation of the NLRP3 inflammasome and NF-κB signalling was observed with 1-dodecylsulfonyl-5N,6O-oxomethylidenenojirimycin (DSO_2-ONJ) treatment of lipopolysaccharide (LPS)-stimulated Bv-2 mouse microglial cells [439]. *N*B-DNJ treatment of cystic fibrosis human bronchial epithelial cells did not affect overall binding of NF-κB and AP-1 to target oligonucleotides or protein/DNA complexes however [440]. Transcriptomics analysis of M*O*N-DNJ-treated unstimulated, DENV-infected and LPS-stimulated MDMΦs has also been conducted, identifying UPR activation as a potential mediator of the effects on cytokine responses [418].

Table 6. Effects of six-membered ring iminosugars on cytokine and chemokine production in contexts other than viral infection.

Studies included evaluated at least one cytokine in addition to chemokines.

Abbreviations: 5F-DNJ, N-pentafluorobenzyl-1-deoxynojirimycin; CF, cystic fibrosis; ConA, concanavalin A; CSF, cerebrospinal fluid; DSO_2-ONJ, 1-dodecylsulfonyl-5N,6O-oxomethylidenenojirimycin; G-CSF, granulocyte-colony stimulating factor; KC, keratinocyte chemoattractant (murine IL-8); MIF, macrophage migration inhibitory factor; MIP-1β, macrophage inflammatory protein-1β; PA, Pseudomonas aeruginosa*; PMA, phorbol 12-myristate-13-acetate;* R-*DS-ONJ, (1R)-1-dodecylsulfinyl- 5N,6O-oxomethylidenenojirimycin; SR1, 2-acetamido-1,4-imino-1,2,4-trideoxy-L-arabinitol; TGF-β, transforming growth factor β; TID, ter in die (thrice a day).*

Iminosugar	Conc.	System (stimulus)	Cytokine	Effect on cytokine	Ref.
DNJ derivatives					
DNJ	3 mM	Murine splenic T cells (anti-CD3)	IL-2	Doubled secretion	[441]
			IL-4	Reduced secretion	
			IL-5		
			IFN-γ		
				Total IFN-γ binding to CRT increased, but binding of newly synthesised IFN-γ decreased and cytokine degraded	[442]
		Human PBMCs (ConA)	IL-4	No effect	[438]
		Human CD4+ T cells (ConA)	IL-4	Minimal reduction in intracellular IL-4	
	10, 30, 90 μM	Human PBMCs	IL-4	Reduced secretion three-fold at 90 μM	[409]
			IFN-γ	Reduced secretion two-fold at 30 μM	
*N*M-DNJ	1 mM	Murine splenic T cells (anti-CD3)	IL-2	Doubled secretion	[441]
			IL-4	Reduced secretion	
			IL-5		
			IFN-γ		
	3 mM			Total IFN-γ binding to CRT increased, but binding of newly synthesised IFN-γ decreased and cytokine degraded.	[442]
*N*B-DNJ	100 μM	MDMΦs (LPS)	TNF-α	No effect	[418]
			IFN-γ		
			IL-6		
			IL-10		
			G-CSF		
			RANTES		
			MCP-1		
			IL-8		
			IL-17A		
			IP-10		
			MIF		
			MIP-1β		
	5, 50 or 500 μM (for 30 days)	RAW264.7 cells (untreated or SR1 pre-treated)	TNF-α	Untreated cells: 5 μM reduced secretion to below control levels. 500 μM increased secretion above control SR1 pre-treated cells: 5 μM reduced secretion to below control levels; 50-500 μM reduced cytokine secretion to below SR1-treated but not control levels	[436]
			MIP-1α		
			TGF-β		
	200 μM	CF and non-CF bronchial epithelial cells (PA)	IL-8	Reduced mRNA expression	[440]

	100 µM	CF primary respiratory epithelium (PA)	TNF-α	No effect	[443]
			IL-1α		
			IL-1β	Reduced mRNA expression	
			IL-8		
			IL-6		
			IP-10	No effect	
	100 mg/kg/ day for 3 days prior	C57BL/6 mice (LPS)	KC	Reduced mRNA expression (no other genes affected)	
	0.8 µg/g	Brain of mucopoly-saccharidosis IIIA mice	MIP-1α	Reduced mRNA expression	[444]
			IL-1β		
			TGF-β1		
			TNF-α	No effect	
			IFN-γ		
	Niemann-Pick disease type C1 patients treated with Miglustat		IL-3	Slight decrease in CSF levels	[445]
			IL-13		
			IL-10	Reduced levels in CSF samples taken post-treatment initiation	
M*O*N-DNJ	25 µM	MDMΦs (LPS)	TNF-α	Reduced secretion	[418]
			IFN-γ		
			IL-6		
			IL-10		
			G-CSF		
			RANTES		
			MCP-1	Increased secretion	
			IL-8	No effect	
			IL-17A		
			IP-10		
			MIF		
			MIP-1β		
5F-DNJ	10, 30, 90 µM	Human PBMCs (ConA)	IL-4	Reduced secretion 6-fold at 10 µM	[409]
			IFN-γ	Reduced secretion from 30 µM	
	90 µM	Human PBMCs (ConA)	IL-4	Reduced IL-4 secretion as well as phospho-STAT6, phospho-JAK1 and phospho-GATA3 expression	[438]
		Human CD4+ T cells (ConA)	IL-4	Reduced intracellular cytokine	
		Murine splenocytes (ConA)	IL-4	Reduced secretion	
	100 mM i/v	C57BL/6 mice (*Schistosoma japonicum* infection)	IL-4	Reduced spleen IL-4 to same as uninfected mice. No effect on liver IL-4. Protective effect (fewer schistosomes) and less granuloma pathology	

			IFN-γ	Increased IFN-γ in spleen of infected treated mice versus infected untreated. No effect on liver	
N-decyl-5-de(hydroxymethyl)-1-DNJ	30 µM	Murine splenocytes (ConA)	IL-4	Secretion reduced by 60.9%	[446]
			IFN-γ	Secretion reduced by 89.1%	
N-octyl-5-de(hydroxymethyl)-1-DNJ	30 µM	Murine splenocytes (ConA)	IL-4	Secretion reduced by 8.7%	[446]
			IFN-γ	Secretion reduced by 40.3%	
DGJ derivatives					
*N*B-DGJ	100 µM	MDMΦs (LPS)	TNF-α	No effect	[418]
			IFN-γ		
			IL-6		
			IL-10		
			G-CSF		
			RANTES		
			MCP-1		
			IL-8		
			IL-17A		
			IP-10		
			MIF		
			MIP-1β		
	5, 50 or 500 µM (for 30 days)	RAW264.7 cells (untreated or SR1 pre-treated)	TNF-α	Untreated cells or SR1 pre-treated cells: reduced cytokine secretion	[436]
			MIP-1α		
			TGF-β		
	200 µM	CF and non-CF bronchial epithelial cells (PA)	IL-8	Reduced mRNA accumulation	[440]
N-decyl-5-de(hydroxymethyl)-1-DGJ	30 µM	Murine splenocytes (ConA)	IL-4	Secretion reduced by 95.7%	[446]
			IFN-γ	Secretion reduced by 78.1%	
Compounds 1 and 4	25 µM	Murine splenocytes (ConA)	IL-4	Reduced secretion	[447]
			IFN- γ		
DMJ derivatives					
DMJ	3 mM	Murine splenic T cells (anti-CD3)	IL-2	Increased secretion and intracellular level	[441]
			IL-4	No effect on secretion	
			IL-5		
			IFN-γ		
				Did not increase degradation of newly synthesised IFN-γ	[442]
	90 µM	Human CD4+ T cells (PMA/ ionomycin)	IL-4	Minimal effect on intracellular IL-4	[438]
N-decyl-5-de(hydroxymethyl)-1-DMJ	30 µM	Murine splenocytes (ConA)	IL-4	Secretion reduced by 85.6%	[446]
			IFN-γ	Secretion reduced by 75.0%	
Other formulations					
Swainsonine	30 µM	Murine splenic T cells (anti-CD3)	IL-2	Increased secretion and intracellular level	[441]
			IL-4	No effect on secretion	

			IL-5		
			IFN-γ		
				Did not increase degradation of newly synthesised IFN-γ	[442]
Compounds 12f, 21b, 21h, 21k, 21n, 21t, 21x	50 µM	Murine splenocytes (ConA)	IL-4	Reduced secretion to varying degrees	[448]
			IFN-γ		
Compounds A5, A6, A16, A17, A45, A47, B3, B5, B8, B21, B30, B31, B33	60 µM	Murine splenocytes (ConA)	IFN-γ	Increased secretion	[449]
			IL-4	No effect	
4-*epi*-fagomine	10, 50, 100 µM	RAW264.7 cells (LPS)	TNF-α	Significant reduction	[437]
			IL-1β	Increase at 10 µM and reduction at 50 or 100 µM	
			IL-6	Significant reduction	
			IL-10		
Isofagomine	20, 600 mg/kg/ day	Midbrain of 4L;C* mice	TNF-α	Significantly reduced mRNA in treated midbrain	[450]
			IL-6	No significant effect on mRNA levels	
3,4-dihydroxypipecolic acid	10, 50, 100 µM	RAW264.7 cells (LPS)	TNF-α	Significant reduction	[437]
			IL-1β		
			IL-6	Significant reduction at 10 µM and increase at 50 or 100 µM	
			IL-10	Significant reduction	
Dihydroxy-indolizidine (Compound 18)	10, 50, 100 µM	RAW264.7 cells (LPS)	TNF-α	Significant reduction	[437]
			IL-1β	Significant reduction at 10 or 50 µM (below control at 10) and increase at 100 µM	
			IL-6	Significant reduction	
			IL-10		
Compounds 2, 3 and 5	25 µM	Murine splenocytes (ConA)	IL-4	Reduced secretion	[447]
			IFN-γ		
R-DS-ONJ	50 µM	Bv-2 mouse microglial cells (LPS)	IL-1β	Reduced mRNA levels	[451]
			IL-6		
			TNF-α	No effect on mRNA level	
DSO_2-ONJ	10 µM	Bv-2 mouse microglial cells (LPS)	IL-1β	Reduced mRNA levels and intracellular IL-1β protein	[439]
			IL-6	Reduced mRNA levels	
			TNF-α		

1.4 Aims of the thesis

Iminosugars have potential as broad-spectrum antivirals, with several mechanisms underlying their antiviral activity already identified for a range of viruses. This thesis aims to provide additional information about the mechanisms of action of iminosugars relevant to arbovirus infection and to a broader spectrum of infectious or inflammatory conditions where cytokines play a role in pathogenesis. Different aspects of the DENV infection cycle of MDMΦs which iminosugars might disrupt are investigated, with a focus on the iminosugar *N*-8'-2''-tetrahydrofuranyl-octyl-deoxynojirimycin (2THO-DNJ), in addition to considering how TNF-α and IFN-α/β responses to DENV infection are affected by iminosugar treatment. The potential application of iminosugars in the treatment of additional arbovirus infections is evaluated for ZIKV, for which no iminosugars had been tested at the outset of this project, and for CCHFV, through consideration of iminosugar effects against HAZV. Finally, the scope for iminosugar impacts on cytokine responses is extended by investigating the influence of iminosugar treatment on cytokine secretion elicited by stimulation of MDMΦs with a range of pathogen-associated molecular patterns (PAMPs). Potential effects of iminosugars on TLR signalling pathways are briefly addressed, aiming to obtain mechanistic insights into the immunomodulatory effects of iminosugars beyond the context of viral infection.

Chapter 2. Materials and Methods

2.1 Iminosugars and other compounds

2.1.1 Preparation of iminosugars and other antiviral compounds

The iminosugars utilised in this thesis comprise 2THO-DNJ (gift from Emergent BioSolutions, solubilised in acidified water), 2THO-DGJ (synthesised by JL Kiappes, Oxford Antiviral Drug Discovery Unit, solubilised in DMSO), *N*B-DNJ (gift from Oxford GlycoSciences Ltd, solubilised in phosphate buffered saline (PBS, Gibco) or water), *N*B-DGJ (Toronto Research Chemicals, solubilised in water), *N*N-DNJ (gift from Oxford GlycoSciences Ltd, solubilised in DMSO or acidified water), *N*N-DGJ (Toronto Research Chemicals, solubilised in DMSO or acidified water), M*O*N-DNJ (gift from United Therapeutics, solubilised in acidified water), DNJ (gift from Oxford GlycoSciences Ltd, solubilised in water) and CAST (Toronto Research Chemicals, solubilised in water). The non-iminosugar compounds ribavirin (Abcam) and ι-carrageenan (Sigma-Aldrich) were solubilised in water. *Clasto*-lactacystin β-lactone (Enzo Life Sciences) and baicalein (Sigma-Aldrich) were solubilised in dimethyl sulfoxide (DMSO). Compounds used for immunomodulation experiments or *in vivo* studies were assayed for pyrogen contamination and verified to contain less than 0.02 endotoxin units (EU)/ml.

2.1.2 Endotoxin detection assay

Iminosugar preparations were subjected to a recombinant Factor C-based endotoxin test using the EndoZyme® II assay (Hyglos) as per manufacturer's instructions. Briefly, samples were diluted in endotoxin-free water and added to a 96-well plate in duplicate alongside a standard curve prepared from LPS derived from *Escherichia coli* O55:B5, and warmed to 37°C. Recombinant enzyme, assay buffer and fluorogenic substrate were added 1:1 (v:v) of sample and fluorescence was measured for absorption at 380 nm and emission at 445 nm at time 0 and

following 1 hour of incubation at 37°C in the dark. Endotoxin concentrations in samples were interpolated from the standard curve produced by fitting a linear regression model to the $\log_{10}$ values of the difference in relative fluorescence. Spike controls were included for each sample and spike recovery determined to validate results.

2.1.3 Cytotoxicity assays

Cytotoxicity of compounds was assessed by a cell proliferation assay for mitochondrial metabolic activity using a CellTiter 96 AQ_{ueous} One Solution Cell Proliferation Assay (Promega), as per the manufacturer's instructions, except for experiments with DENV replicon cells. Briefly, cells were cultured with iminosugar in 200 µl culture medium in 96-well tissue culture plates for appropriate durations. After the incubation period, 100 µl of culture medium was removed and 20 µl of a solution containing a tetrazolium compound (3-(4,5-dimethyl-2-yl)-5-(3-carboxymethoxyphenyl)-2-(4-sulfophenyl)-2H-tetrazolium; MTS) and electron coupling reagent (phenazine ethosulfate) was added to the cells in the 100 µl remaining. Samples were incubated for approximately 1-2 hours (37°C, 5% CO_2), and the absorbance at 490 nm was measured on a SpectraMax M5 microplate reader (Molecular Devices). For experiments with DENV replicon cells, cytotoxicity of compounds was assessed using the WST-1 (4-[3-(4-iodophnyl)-2-(4-nitrophenyl)-2H-5-tetrazolio]-1,3-benzene disulfonate) assay (Sigma-Aldrich) according to manufacturer's instructions. Briefly, cells were cultured with iminosugar in 100 µl culture medium in 96-well tissue culture plates for appropriate durations. After the incubation period, 10 µl of solution containing the stable tetrazolium salt WST-1 and an electron coupling reagent was added to each well, and the plate incubated for approximately 1 hour (37°C, 5% CO_2). Absorbance at 450 nm was measured on a CLARIOstar microplate reader (BMG Labtech). Absorbance was normalised to untreated controls and visualised using GraphPad Prism. For 2THO-DNJ assays, CC_{10} and CC_{50} values (compound concentrations resulting in 10% or 50%

cytotoxicity, respectively) were interpolated using KaleidaGraph version 4.5.2 (Synergy Software).

2.2 Antiviral assays against DENV

2.2.1 DENV stocks

C6/36 *Aedes albopictus* cells (US Armed Forces Research Institute of Medical Sciences, Thailand (AFRIMS) or American Type Culture Collection (ATCC)) were cultured in C6/36 media (Leibovitz's L15 media (Gibco) supplemented with 10% heat-inactivated foetal bovine serum (HI-FBS; Gibco), 1x non-essential amino acids (NEAA, Gibco), 1 mM HEPES (Gibco), 0.1 mg/ml streptomycin and 100 U/ml penicillin (Sigma-Aldrich) at 28°C for the propagation of DENV-2 strain 16681 (a gift from Gavin Screaton, Oxford, UK). C6/36 flasks were infected at approximately 90% confluence at an MOI of 0.15 in 30 ml C6/36 media (with 1.5% HI-FBS, rather than 10% HI-FBS). Supernatant was collected and media replaced on day 4 post-infection and twice subsequently, depending on observed cytopathic effect (around days 7 and 10 post-infection). Cells were removed from harvested media by centrifugation (1500 x *g*, 15 minutes, 4°C) and virus was concentrated by precipitation with 10% weight per unit volume (w/v) poly(ethyleneglycol) M_r 6,000 (Sigma-Aldrich) with 0.6% sodium chloride (Sigma-Aldrich) at pH 7.2 overnight at 4°C. Following precipitation, virus was centrifuged at 2830 x *g* for 45 minutes at 4°C, resuspended in C6/36 media and stored at -80°C until use.

UV-inactivation of DENV was conducted by Joanna Miller. Briefly, concentrated DENV stock was irradiated for 10 minutes at a distance of 25 cm with a 254 nm lamp (UVS-18 EL Series, UVP Upland, CA, USA) to produce UV-inactivated DENV (UVi-DENV). UVi-DENV was confirmed to contain no detectable infectious DENV by plaque assay (as described in 2.2.6, but with a limit of detection of 3 plaque forming units (pfu)/ml).

2.2.2 Isolation and differentiation of monocyte-derived macrophages (MDMΦs)

Human PBMCs were isolated from buffy coats (National Health Service Blood and Transplant service (NHSBT), surplus to clinical requirements) by centrifugation over a Ficoll-Paque PLUS (Amersham) gradient. For utilisation of PBMCs, red blood cells were lysed and PBMCs resuspended in RPMI-1640 (Gibco) for infection with DENV. For isolation of monocytes from PBMCs, autologous plasma was collected, heat-inactivated (56°C, 30 minutes), and used to supplement (1%) X-VIVO10 (Lonza; hereafter X-VIVO) medium to produce MDMΦ growth medium. Adherent monocytes were isolated from PBMCs by incubation on 2% bovine gelatin (Sigma-Aldrich) coated tissue culture plates (37°C, 5% CO_2, 90 minutes). Non-adherent PBMCs were washed off using RPMI-1640, and remaining monocytes were incubated in MDMΦ growth medium (37°C, 5% CO_2). After 18 hours, supernatants containing monocytes were collected, and additional monocytes were collected by mechanical removal (vigorous pipetting) following incubation in ice-cold sterile PBS with 5 mM ethylenediaminetetraacetic acid (EDTA; Sigma-Aldrich) (4°C, 90 minutes) and combined with monocytes from the supernatant. Cells were seeded at 1 x 10^6 cells/ml in MDMΦ growth medium with 25 ng/ml recombinant human IL-4 (Peprotech) in 200 µl/well of a 96-well plate (for cytotoxicity assay), 1 ml/well of a 24-well plate (for antiviral assay) or 3 ml/well of a 6-well plate (for cell lysate preparation for free oligosaccharide assay or viral replication assay) and differentiated for 3 days (37°C, 5% CO_2) to generate MDMΦs. Cells generated in this manner are greater than 95% macrophages phenotypically ($CD14^+$, $CD16^-$, $CD86^+$, $HLA\text{-}DR^+$, $CD3^-$) by fluorescence activated cell sorting (FACS) as previously reported [7]. All donors were anonymous and isolations were assigned sequential two-character codes for processing and experimentation (i.e. donor 1 assigned AA). Donors utilised for individual experiments are indicated in figure legends. The use of human blood was approved by the NHS National Research Ethics Service (09/H0606/3).

2.2.3 Viral thermal stability assay

The stability of DENV infectivity over time was investigated by incubation of 1 x 10^6 pfu DENV-2 16681 in 1 ml of media at 4°C or 37°C. Media conditions were X-VIVO only, conditioned X-VIVO (day 4 MDMΦ supernatant from donor MT), or differentiation X-VIVO (MDMΦ growth medium for donor MT supplemented with 25 ng/ml recombinant human IL-4). After incubation for 1, 2, 24 or 48 hours, aliquots were taken for determination of viral titre (2.2.6).

2.2.4 Virucidal assay

The possibility of direct virucidal activity of iminosugars against DENV was investigated by incubation of 1 x 10^6 pfu DENV-2 16681 in 1 ml of X-VIVO supplemented with iminosugars, at 4°C or 37°C. After incubation for 2 or 24 hours, aliquots were taken for determination of viral titre (2.2.6).

2.2.5 *In vitro* DENV infection and iminosugar treatment for analysis of secreted virus

2.2.5.1 MDMΦ infection

MDMΦ were infected with DENV-2 16681 diluted to a multiplicity of infection (MOI) of 1 in X-VIVO10 without supplements for 90 minutes (room temperature, with rocking), in 150 µl/well of a 24-well tissue culture plate. Upon removal of virus, fresh MDMΦ growth medium (without IL-4), containing drug as indicated, was added to cells which were incubated for a further 46.5 hours for the 48 hour time point for a standard antiviral assay, or for other durations (calculated in the same fashion) as indicated (37°C, 5% CO_2). For collection of secreted virus, supernatant was harvested and centrifuged for 4 minutes (room temperature, 400 x *g*) to pellet any cells/debris, and supernatants were aliquoted and stored at -80°C until analysis. For some experiments to quantify cell-associated infectious virus, cells were washed in Hank's Balanced

Salt Solution (HBSS; Gibco), collected in HBSS using a cell scraper, and cells lysed by freeze-thawing to release any infectious virions retained in cells.

2.2.5.2 PBMC infection

PMBCs in suspension were infected with 1 or 5 million cells/ml at an MOI of 0.2 in the presence of relevant iminosugar. Cells were incubated (37°C, 5% CO_2) until 24 or 48 hours post-infection. Supernatant was harvested and centrifuged for 4 minutes (room temperature, 400 x *g*) to pellet any cells/debris, and supernatants were aliquoted and stored at -80°C until analysis.

2.2.5.3 C6/36 cell infection

C6/36 cells were seeded at 2.5 x 10^5 cells/ml in 1 ml/well of a 24-well plate in C6/36 media with 1.5% HI-FBS. The following day, cells were infected with DENV-2 16681 diluted to an MOI of 0.1 for 90 minutes (room temperature, with rocking). Upon removal of virus, media was replenished, containing drug as indicated. Cells were incubated for 48 hours (28°C) until supernatant was harvested, centrifuged for 4 minutes (room temperature, 400 x *g*) to pellet any cells/debris, aliquoted and stored at -80°C until analysis.

2.2.5.4 Vero cell infection

African Green Monkey (*Chlorocebus sabaeus*) kidney epithelial Vero E6 cells (ATCC) were utilised for some viral infection experiments. Wild-type (Vero-WT) cells were used alongside cells with ER α-glucosidase I (Vero-GluI) or II (Vero-GluII) knocked out using CRISPR/Cas9 technology. Knockout cells were generated by Johan Hill as described in [452], broadly following the protocol described by Bauer et al. [453]. Briefly, pairs of CRISPR plasmids were designed using a *Drosophila* target-finding CRISPR tool [454], the absence of off-target effects confirmed by National Center for Biotechnology Information (NCBI) Basic Local Alignment Search Tool (BLAST) search of the *Chlorocebus sabaeus* genome, and cloned into the pSpCas9(BB)-2A-Puro (PX459)

V2.0 plasmid (gift from Feng Zhang; Addgene plasmid #62988). Vero cells were transfected with appropriate pairs of CRISPR plasmids, and antibiotic selection pressure followed by clonal dilution used to select colonies of transfected cells. Successful knock-outs were confirmed by PCR and sequencing, and loss of functional ER α-glucosidase activity confirmed by free oligosaccharide assay (described in 2.2.11) [452].

All cell types were cultured in Vero media, comprising Dulbecco's Modified Eagle Medium (DMEM; Gibco) supplemented with 10% HI-FBS, 0.1 mg/ml streptomycin and 100 U/ml penicillin, at 37°C, 5% CO_2. For amplification, cells were washed twice with sterile PBS before incubation with trypsin-EDTA for 5 minutes at 37°C, then collected by media wash, centrifuged for 5 minutes at 500 x *g*, and the supernatant was discarded. Cells were resuspended in fresh media by pipetting. For antiviral assays, cells were seeded in Vero media with 2% HI-FBS at 2 x 10^5 cells/ml in 1 ml/well of a 24-well plate. The following day, cells were infected with DENV-2 16681 diluted to an MOI of 1 in Modified Eagle Medium (MEM; Gibco) media for 90 minutes (room temperature, with rocking). Upon removal of virus, media was replenished with Vero media with 2% HI-FBS containing drug as indicated, and cells were incubated for 4 days (37°C, 5% CO_2). Supernatant was harvested, centrifuged for 4 minutes (room temperature, 400 x *g*) to pellet any cells/debris, aliquoted and stored at -80°C until analysis.

2.2.6 Plaque assay

To determine infectious DENV titres, plaque assays on *Macaca mulatta* kidney cells (LLC-MK_2 cells) were used, as per previous descriptions [455]. LLC-MK_2 cells (AFRIMS) were propagated in Medium 199 (Gibco) supplemented with 10% HI-FBS, 0.1 mg/ml streptomycin and 100 U/ml penicillin at 37°C, 5% CO_2. For amplification, cells were washed twice with sterile PBS before incubation with trypsin-EDTA for 5 minutes at 37°C then collected by PBS wash, centrifuged for

5 minutes at 400 x *g*, and the supernatant was discarded. Cells were resuspended in fresh media either by pipetting or, for plaque assay seeding, with a 19-gauge needle (Terumo). LLC-MK_2s were seeded in confluent monolayers (typically at 1.7 x 10^5 cells/ml in 2 ml/well of a 12-well tissue culture plate) and allowed to adhere overnight. Media was removed and cells washed once with HBSS. Log_{10} serial dilution of cell supernatants was conducted in MEM supplemented with 10% HI-FBS, and virus was incubated on cells for 90 minutes (room temperature, with rocking). Upon removal of virus, first overlay (2.6.2), containing nutrients and low-melting point tissue culture-grade agarose (Sigma-Aldrich) was added and allowed to solidify at room temperature before incubation for 5 days (37°C, 5% CO_2), adapted from [455]. A second overlay (2.6.2) containing nutrients, low-melting point tissue culture-grade agarose, and neutral red stain [455] was then added and allowed to solidify at room temperature before further incubation for 1 day (37°C, 5% CO_2) after which plaques were counted by eye. The limit of detection for this assay is 33 plaque forming units per ml (pfu/ml). Plaque counts were converted to pfu/ml using Microsoft Excel and analysed routinely using GraphPad Prism version 7.01 (GraphPad Software, Inc).

For 2THO-DNJ titrations (section 3.3.1), KaleidaGraph version 4.5.2 (Synergy Software) was used to improve the precision of curve fitting, following methods modified from [398]. Drug-treated samples were normalised to untreated, technical replicates averaged and standard deviations determined (and presented as error bars). The drug concentration of untreated cells was adjusted to $2log_{10}$ steps lower than the minimum drug concentration tested (0.001 µM) to allow for plotting on a logarithmic axis ($log_{10}(0)$=undefined). Several logarithmic sigmoidal curve types were fitted to each data set, as described in the supplementary materials of [398], comprising:

Moddoseresplgst: $y = \frac{a+b}{1+\left(\frac{x}{c}\right)^d}$ with the initial values a=-70; b=186; c=5; d=0.2

Lgstsigmoid: $y = a + \frac{b-a}{1+\exp(-c*(x-d))}$ with the initial values a=100; b=0.01; c=0.05; d=20

Dosersplgst: $y = a + \frac{b-a}{1+\left(\frac{x}{c}\right)^d}$ with the initial values a=95.9; b=-0.86; c=0.04; d=-0.95.

The curve type with the lowest χ^2 value and R^2 value closest to 1 was used to interpolate IC_{50} and IC_{90} values. In each case, curve fit was weighted by precision of each data point as determined by coefficient of variance ($C_V = \frac{s}{\overline{x}}$) where *s* is the sample standard deviation and $\overline{x}$ is the sample mean. Relative C_V was subsequently determined by dividing each C_V by the minimum C_V for a given donor/drug experiment, setting the most precise C_V to 1 and less precise measures greater than 1.

2.2.7 Supernatant RNA extraction and DENV NS5 qRT-PCR

DENV RNA in cell culture supernatants was isolated according to the manufacturer's protocol for Direct-zol RNA MiniPrep Kit (Zymo Research) and assayed by reverse transcription-real time polymerase chain reaction (qRT-PCR) on an Applied Biosystems 7500 FAST real-time PCR system (Life Technologies). Thermo-Start DNA Taq polymerase was used to enable Taq-mediated release of fluorescently labelled dyes from a DENV2 NS5-specific probe adapted from a previously published protocol [456]. Probe and primer sequence and concentrations are listed in Table 11. The reaction mixture was prepared according to the manufacturer's instructions for Verso 1-Step RT-PCR Kit with Thermo-Start Taq (Thermo Scientific). Reactions were carried out in MicroAmp Fast 96-well reaction plates (ThermoFisher) sealed with MicroAmp optical adhesive film (ThermoFisher). Thermal cycling was conducted as follows. Synthesis of complementary DNA (cDNA) was performed for 30 minutes at 48°C, followed by a 15-minute activation of Thermo-Start Taq polymerase at 95°C. PCR thermocycling with fluorescence detection was executed for 40 cycles of 95°C for 15 seconds followed by 55°C for 60 seconds and a fluorescence read step at 60°C for 25 seconds. Samples were read in technical duplicate and compared to a standard curve generated from high-titre DENV viral RNA isolated from C6/36-grown DENV2, as previously described [337]. Genome equivalents (GEs)/reaction values

were converted to GE/ml using Microsoft Excel and analysed using GraphPad Prism version 7.01 (GraphPad Software, Inc).

2.2.8 Iminosugar effects on DENV adsorption to MDMΦs

To investigate whether iminosugars can impact DENV adsorption to MDMΦs, a protocol was adapted from [457]. MDMΦs were exposed to DENV-2 16681 for 1 hour at 4°C in the presence of iminosugar or baicalein (as indicated in figure legends), with virus diluted to MOI 1 in XVIVO-10 (in 150 µl/well of a 24-well tissue culture plate). After the incubation, the supernatant was removed and cells were washed vigorously and repeatedly with HBSS to remove any unbound virus. Cells were lysed and RNA extracted immediately using the RNeasy Mini Kit (Qiagen), according to manufacturer's instructions. DENV bound to cells was quantified by DENV NS5 qRT-PCR (described in 2.2.7).

2.2.9 Iminosugar effects on DENV entry to MDMΦs

To investigate whether iminosugars can affect DENV entry to MDMΦs, a protocol was adapted from [19, 457, 458]. DENV-2 16681 (diluted to MOI 1 in XVIVO-10) was allowed to bind to cells for 1 hour at 4°C (in 150 µl/well of a 24-well tissue culture plate). Unbound virus was then removed by repeated vigorous washing with HBSS. Iminosugars or baicalein (in 150 µl/well, diluted in XVIVO-10 to concentrations described in figure legends) were then applied to the cells, which were incubated for 1 hour (37°C, 5% CO_2) to allow viral entry. Media containing iminosugar was then removed, and cells washed with HBSS to ensure the removal of any virus that may have eluted off the cell surface. To further ensure that any virus remaining on the cell surface could not enter at a later time, cells were treated with 100 µl/well of 1 mg/ml proteinase K (in PBS; Invitrogen) for 45 minutes at 4°C to degrade exposed proteins. Proteinase K was then inactivated by treatment with 1 mM Pefabloc SC (Roche), a non-toxic and less hazardous

substitute for phenylmethylsulfonyl fluoride, for 15 minutes at 37°C. Following this incubation, cells were washed with HBSS, then lysed and RNA extracted immediately using the RNeasy Mini Kit (Qiagen), according to the manufacturer's instructions. DENV that had entered cells was quantified by DENV NS5 qRT-PCR (described in 2.2.7). Alternatively, washed cells were overlaid with MDMΦ growth media and incubated until 48 hours post-infection (37°C, 5% CO_2).

2.2.10 Analysing iminosugar effects on DENV replication

2.2.10.1 Replication effects in MDMΦs

For initial experiments, MDMΦs were infected with DENV-2 16681 and treated with iminosugars as described in 2.2.5. Supernatant was then discarded and cells washed with HBSS to remove any residual virus, before cell lysis and RNA extraction (described below).

For subsequent experiments, methods were employed to synchronise viral entry. DENV-2 16681 (diluted to MOI 1 in XVIVO-10) was allowed to bind to cells for 1 hour at 4°C (in 500 µl/well of a 6-well tissue culture plate). Unbound virus was then removed by repeated vigorous washing with HBSS, before 500 µl/well MDMΦ growth medium was added and cells incubated for 1 hour (37°C, 5% CO_2) to allow virus internalisation. MDMΦs were washed with HBSS to ensure removal of any virus that had eluted off the cells. Cells were then incubated (37°C, 5% CO_2) with MDMΦ growth media containing iminosugar or ribavirin as indicated for a further 11, 23 or 47 hours to generate time points of 12, 24 and 48 hours post-infection. At the end of the incubation period, supernatant was discarded and cells washed with HBSS to remove any residual virus, before cell lysis and RNA extraction (described below).

Additional methods for synchronisation of virus entry were also trialled (discussed in 8.5). For citrate buffer treatment, MDMΦs were treated with 500 µl/well of a citrate buffer (20 mM citric

acid, 10 mM potassium chloride, 135 mM sodium chloride (all Sigma-Aldrich) at pH 3) for 1 minute following the virus internalisation step, to degrade any surface-exposed virions, as described in [459]. MDMΦ growth media was then applied and the aforementioned protocol resumed. For ammonium chloride treatment, 20 mM ammonium chloride was added to the MDMΦ growth media containing iminosugar for the duration of the incubation, preventing further virion endocytosis, as described in [20]. At the end of the incubation period, supernatant was discarded and cells washed with HBSS to remove any residual virus, before cell lysis and RNA extraction (described below).

Cells were lysed in 350 µl Buffer RLT (supplemented with β-mercaptoethanol), and RNA extracted using the RNeasy Mini Kit (Qiagen), according to the manufacturer's instructions. For quantification of positive (+) and negative (-) sense DENV RNA, reverse transcription was conducted using SuperScript IV Reverse Transcriptase (Invitrogen) and residual RNA removed using RNase H (Invitrogen), according to the manufacturer's instructions. Primers specific to + or – sense DENV NS5 RNA were designed based on [58] (Table 10). No-template controls were included. qPCR was conducted using the DENV-2 NS5-specific probe and primers described in 2.2.7. The reaction mixture was prepared according to the manufacturer's instructions for TaqMan Fast Advanced Mastermix (Applied Biosystems). Reactions were carried out in MicroAmp Fast 96-well reaction plates (ThermoFisher) sealed with MicroAmp optical adhesive film (ThermoFisher). Thermal cycling was conducted as follows. Uracil-N-glycosylase was activated at 50°C for 2 minutes, to degrade carryover amplicons, and AmpliTaq Fast DNA Polymerase was activated at 95°C for 20 seconds. PCR thermocycling was conducted for 40 cycles of 95°C for 3 seconds followed by 60°C for 25 seconds, during which time the fluorescence was detected. Samples were analysed in technical duplicate. + and – sense RNA levels were normalised to *RPLP2* expression (quantified as described in 2.5.3) using the $2^{-\Delta\Delta CT}$ method [460]

to control for cell number, and analysed using GraphPad Prism version 7.01 (GraphPad Software, Inc).

2.2.10.2 Replication effects on DENV-2 replicon-expressing Huh7.5 cells

Huh7.5 cells stably expressing a DENV-2 New Guinea C replicon (Huh-DENV cells) were used (stable expression generated by Andrea Magri, McKeating Group, University of Oxford; replicon a gift of Andrew Davidson, University of Bristol). The replicon structure is as previously described [461], but with the green fluorescent protein gene replaced with a firefly luciferase reporter gene. Thus, DENV structural proteins are removed from the replicon while all non-structural proteins of DENV are retained for expression. Initially, Huh-DENV cells were seeded at $1x10^4$ cells/well in 96-well tissue culture plates and treated with titrations of drug for 48 hours. Cell viability was determined by WST-1 assay (as described in 2.1.3). Reagents were removed from cells, before washing with PBS and cell lysis using neutral lysis buffer. Cell lysates were transferred to white 96-well plates and luciferase activity determined using VivoGlo (Promega; final luciferin concentration 150 µg/ml) quantified using a GloMax Luminometer (Promega). For time course experiments, Huh-DENV cells were seeded at $1x10^4$ cells/well in white 96-well tissue culture plates in the presence of drug and luciferin (as previously). Plates were immediately transferred to a CLARIOstar microplate reader (BMG Labtech) and incubated (37°C, 5% CO_2) with luminescence measured every 30 minutes. Data were analysed using GraphPad Prism version 7.01 (GraphPad Software, Inc).

2.2.11 Free oligosaccharide (FOS) assay

MDMΦ were isolated and differentiated as described in 2.2.2. Media was replaced with X-VIVO containing appropriate drugs and cells were incubated for 48 hours (37°C, 5% CO_2). Cells were washed three times with sterile PBS and were removed from tissue culture plastic by mechanical

disruption (scraping) and transferred to microcentrifuge tubes for centrifugation (room temperature, 4000 x *g*, 5 minutes). Cells were lysed by three cycles of freeze-thawing (alternating room temperature and -80°C) in deionised H_2O and stored at -80°C for subsequent protein and FOS assay. FOS were detected as previously described by Alonzi et al. [462]. Briefly, cell lysates were subjected to mixed-bed ion exchange and then lyophilised. FOS were labelled with 2-aminobenzoic acid (2-AA) and purified using a DPA-6S column (Sigma-Aldrich). Unconjugated 2-AA was removed by phase splitting with ethyl acetate, and samples were lyophilised and resuspended in water and then purified using a concanavalin A column. Glycans were separated by normal phase-high performance liquid chromatography (NP-HPLC), and peak area was used to assess molar quantity in comparison to standards of known identity and quantity using Empower3 (Waters). FOS generation was normalised to protein concentration assessed using the absorbance at 280 nm (A_{280}) measured with a NanoDrop 1000 spectrophotometer (ThermoFisher Scientific).

2.3 Antiviral assays and *in vivo* efficacy testing against ZIKV

2.3.1 ZIKV stocks

For *in vitro* studies, Vero E6 cells (ATCC) were cultured as described in 2.2.5.4 for the propagation of ZIKV strain MR766 or MP1751 (a kind gift from Stuart Dowall, Public Health England). Glycosylation of the ZIKV strain obtained was confirmed in-house by mass spectrometry mass shift after peptide:N-glycosidase F (PNGase F) treatment and sequencing of the viral locus (Johan Hill, Stephen Woodhouse and Abhinav Kumar, data not shown). ZIKV stocks were prepared by Michelle Hill and Johan Hill. Briefly, confluent 175 cm^2 tissue culture flasks of Vero cells were infected at an MOI of 0.01 in 5 ml of MEM for 90 minutes, with gentle rocking. After this time, virus inoculum was removed and replaced with 25 ml of virus growth media (Vero cell media with 2% HI-FBS, rather than 10% HI-FBS), and flasks incubated for 4 days (37°C, 5% CO_2).

Cells/debris were removed from harvested media by centrifugation (1500 x *g*, 5 minutes, room temperature) and virus was concentrated by precipitation with 8% weight per unit volume (w/v) poly(ethyleneglycol) M_r 8000 (Sigma-Aldrich) overnight at 4°C. Following precipitation, virus was centrifuged at 10000 x *g* for 50 minutes at 4°C, resuspended in virus growth media and stored at -80°C until use.

2.3.2 *In vitro* infection and iminosugar treatment

Wild-type Vero cells (Vero-WT) and cells with ER α-glucosidase I (Vero-GluI) or II (Vero-GluII) knocked out were generated and cultured as described in 2.2.5.4. For antiviral assays, cells were seeded in Vero media with 2% HI-FBS at 2 x 10^5 cells/ml in 1 ml/well of a 24-well plate. The following day, additional wells for each cell type were counted to determine virus required for infection with an MOI of 1. Slight variations in cell number between cell types within confluent or near-confluent monolayers were previously demonstrated to have no effect on resulting virus secretion or titres (Johan Hill, unpublished data). Cells were infected with ZIKV MR766 diluted to an MOI of 1 in MEM media for 90 minutes (room temperature, with rocking). Upon removal of virus, media was replenished with Vero media with 2% HI-FBS containing drug as indicated, and cells were incubated for 48 hours (37°C, 5% CO_2). Supernatant was harvested, centrifuged for 4 minutes (room temperature, 400 x *g*) to pellet any cells/debris, aliquoted and stored at -80°C until analysis.

For antiviral assays in MDMΦs, cells were isolated and differentiated as described in 2.2.2. MDMΦs were infected with ZIKV (either the MR766 or MP1751 strain, as indicated) diluted to an MOI of 0.1 in X-VIVO for 90 minutes (room temperature, with rocking). Upon removal of virus, media was replenished with X-VIVO supplemented with 1% autologous serum containing iminosugars as indicated, and cells were incubated for 72 hours (37°C, 5% CO_2). Supernatant was

harvested, centrifuged for 4 minutes (room temperature, 400 x *g*) to pellet any cells/debris, aliquoted and stored at -80°C until analysis.

2.3.3 *In vivo* infection and iminosugar administration

For *in vivo* studies, the MP1751 ZIKV strain was used to infect A129 mice, deficient in the IFN-α/β receptor, as per the model established by Dowall et al. [463]. MP1751 stocks were produced by the Virology and Pathogenesis Group, Public Health England, using Vero cells as described in 2.3.1. A129 mice were obtained from an established breeding colony approved by the UK Home Office (B&K Universal). Equal numbers of male and female mice aged 5-6 weeks were used in each study group. Mice were inoculated with 100 pfu MP1751 diluted in PBS and administered subcutaneously in the hind legs. This dose was previously established to be 10-fold of the lethal dose in this model. In the first study, PBS only was used as a mock challenge alongside ZIKV infection. Animals were administered 100 mg/kg *N*N-DNJ or vehicle control diluted in endotoxin-free PBS twice a day (every 12 hours), beginning on the day of challenge. Doses were calculated based on cage average weights determined at the start of the study: male and female mice, accounting for the greatest difference in weights, were caged separately. In the first study, mice were administered 15 doses and 14 doses were administered in study two. Full study designs are shown in Figure 4 and Figure 5.

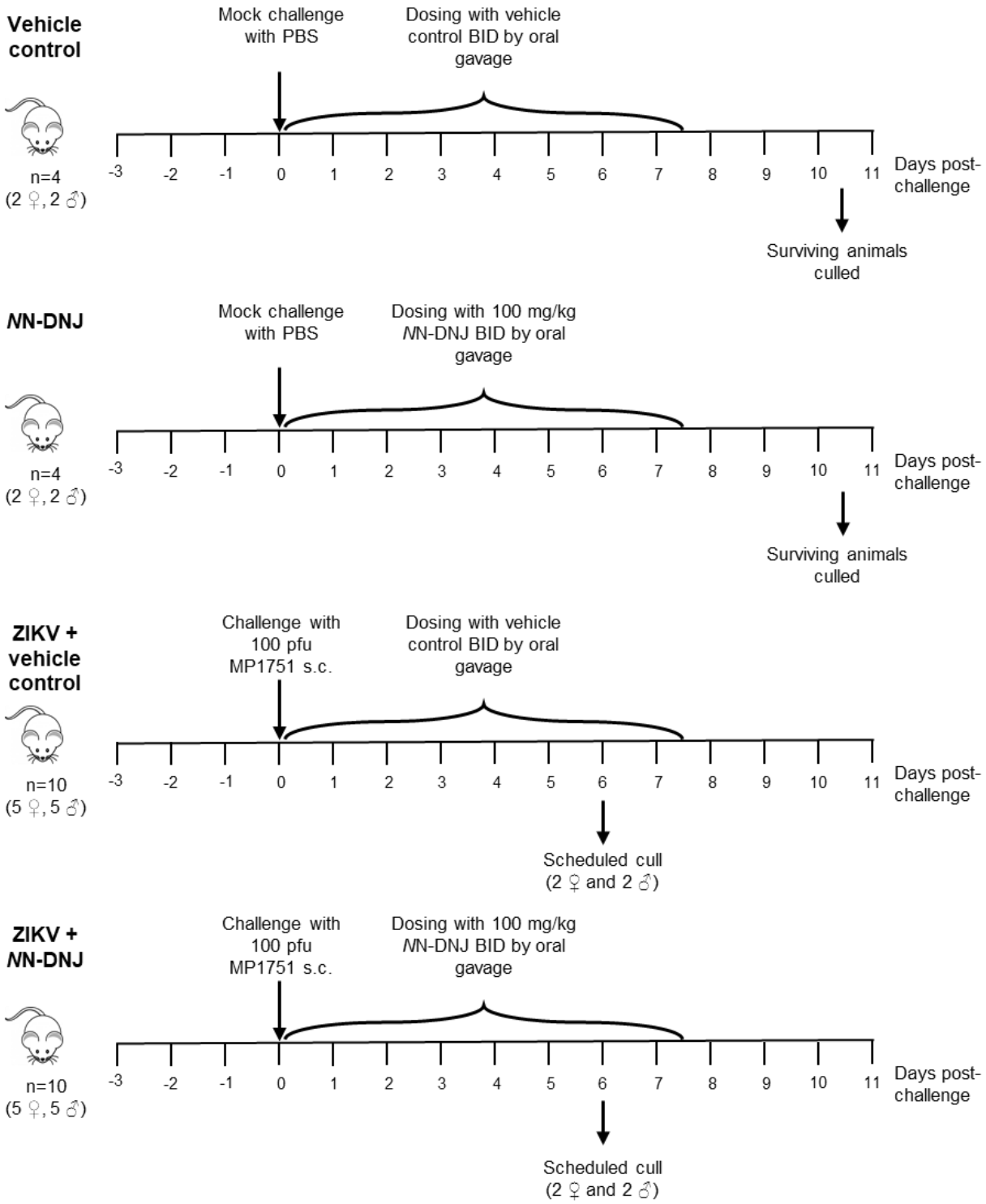

Figure 4. Study design for study one.

Abbreviations: BID, bis in die *(twice daily); pfu, plaque forming units; s.c., subcutaneous.*

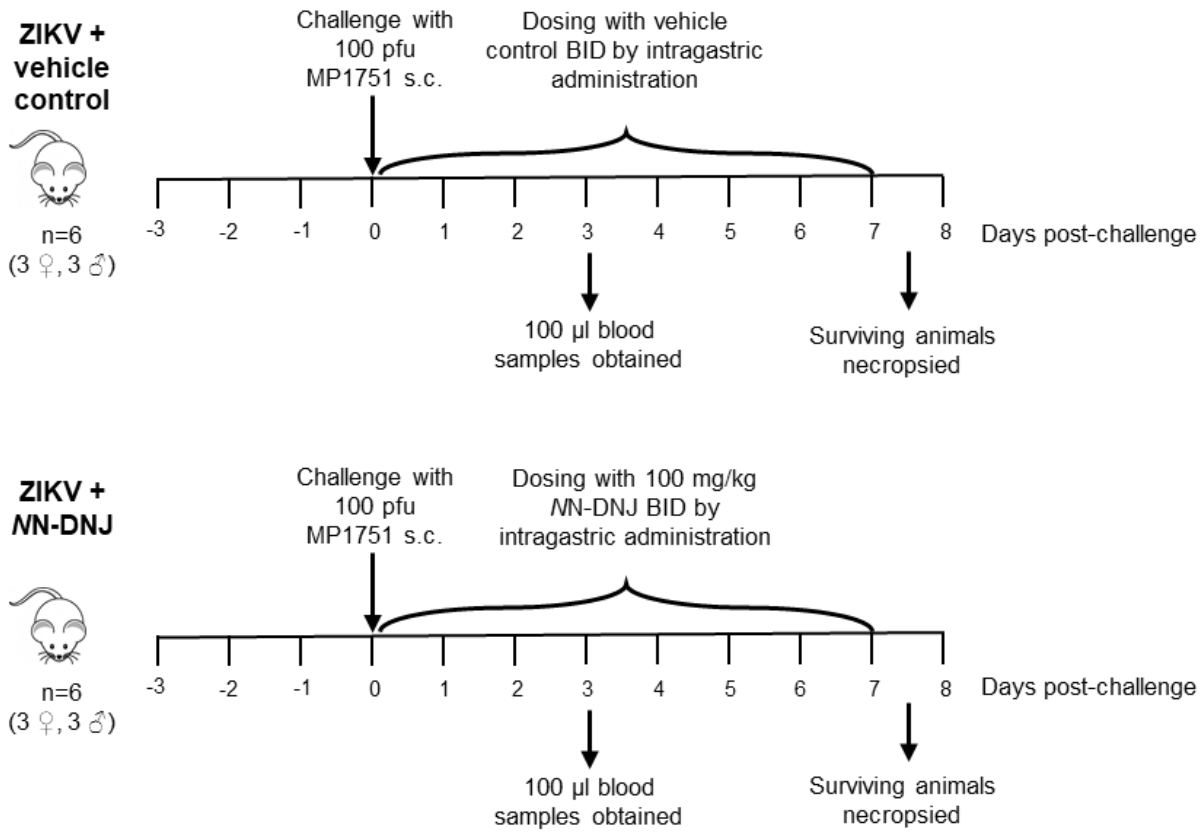

Figure 5. Study design for study two.

Abbreviations: BID, bis in die *(twice daily); pfu, plaque forming units; s.c., subcutaneous.*

Mice were monitored at least twice a day throughout the study and 4 times a day during the critical phase of infection, with clinical signs of disease recorded. Temperatures were recorded from an indwelling temperature chip, and weights were recorded once daily. Clinical signs were assigned a numerical score (0 normal; 2 ruffled fur; 3 eyes closed or sticky, photosensitive, hunched or lethargic; 5 laboured breathing or changes in breathing; 10 neurological signs, continual vocalisation or immobile). Humane clinical endpoints were pre-defined by veterinary staff as 20% weight loss, or 10% weight loss and clinical signs mandating euthanasia. In addition, in the first study, 4 animals from each ZIKV-challenged group were scheduled to be culled at 6 days post-challenge for virological assessment. In the second study, 100 µl of blood was extracted from all animals for virological analysis at 3 days post-challenge. Samples were collected at scheduled culls or necropsy, with 100 µl of blood transferred to RNAprotect Animal

Blood Tubes (Qiagen) and serum obtained using serum separation tubes. Sections of relevant tissues were also collected, comprising brain, liver and spleen in study one and brain, liver, spleen and ovary/testis in study two. All samples were stored at -80°C until analysis.

All procedures were undertaken according to the United Kingdom Animals (Scientific Procedures) Act 1986. These studies were approved by the ethical review process of Public Health England, Porton Down, UK and the Home Office, UK via an Establishment Licence (PEL PCD 70/1707) and project licence (30/3147). Infection and drug administration were conducted by members of the Virology and Pathogenesis Group and Biological Investigations Group at Public Health England, Porton Down. All virological assessment and clinical and virological data analysis was conducted by Beatrice Tyrrell.

2.3.4 RNA extraction and ZIKV E qRT-PCR from cell culture supernatants

RNA extractions from cell culture supernatants were conducted using the QIAamp Viral RNA Mini Kit (Qiagen), according to the manufacturer's instructions. ZIKV RNA was assayed by qRT-PCR using an Applied Biosystems 7500 FAST real-time PCR system. Thermo-Start DNA Taq polymerase was used to enable Taq-mediated release of fluorescently labelled dyes from a ZIKV E-specific probe. Probe and primer sequence and concentrations are listed in Table 11. The reaction mixture was prepared according to the manufacturer's instructions for the Luna Universal Probe One-Step RT-qPCR Kit (New England BioLabs). Reactions were carried out in MicroAmp Fast 96-well reaction plates (ThermoFisher) sealed with MicroAmp optical adhesive film (ThermoFisher). Samples were read in technical duplicate and compared to a standard curve generated from serial dilutions of an RNA oligonucleotide designed from the MR766 ZIKV strain E sequence (sequence: UCGUUGCCCAACACAAGGUGAAGCCUACCUUGACAAGCA AUCAGACACUCAAUAUGUCUGCAAAAGAACAUUAGUGG; Integrated DNA Technologies).

Genome equivalents (GEs)/reaction values were converted to GE/ml using Microsoft Excel and analysed using GraphPad Prism version 7.01 (GraphPad Software, Inc).

2.3.5 RNA extraction and ZIKV E qRT-PCR from *in vivo* samples

RNA was extracted from mouse blood stored in RNAprotect using the RNeasy Protect Animal Blood Kit (Qiagen), according to the manufacturer's instructions. ZIKV RNA was assayed by qRT-PCR using an Applied Biosystems 7500 FAST real-time PCR system. Thermo-Start DNA Taq polymerase was used to enable Taq-mediated release of fluorescently labelled dyes from a ZIKV E-specific probe. Probe and primer sequence and concentrations are given in Table 11. The reaction mixture was prepared according to the manufacturer's instructions for Verso 1-Step RT-PCR Kit with Thermo-Start Taq (Thermo Scientific). Thermal cycling was conducted as follows. Synthesis of complementary DNA (cDNA) was performed for 30 minutes at 48°C, followed by a 15-minute activation of Thermo-Start Taq polymerase at 95°C. PCR thermocycling with fluorescence detection was executed for 40 cycles of 95°C for 15 seconds followed by 55°C for 60 seconds and a fluorescence read step at 60°C for 25 seconds. Samples were read in technical duplicate and compared to a standard curve generated from serial dilutions of an RNA oligonucleotide designed from the sequence of E from Zika strain MR766 (sequence: UCGUUGCCCAACACAAGGUGAAGCCUACCUUGACAAGCAAUCAGACACUCAAUAUGUCUGCAAAA GAACAUUAGUGG; Integrated DNA Technologies). GEs/reaction were converted to GE/ml using Microsoft Excel and analysed using GraphPad Prism version 7.01 (GraphPad Software, Inc).

2.3.6 ZIKV plaque assay

To determine infectious ZIKV titres, plaque assays on Vero cells were used. Propagation was as described in 2.3.1, with resuspension by 19-gauge needle (Terumo). Vero cells were seeded in confluent monolayers (typically at 2 x 10^5 cells/ml in 2 ml/well of a 12-well tissue culture plate)

2 days prior to assay. Media was removed and cells washed once with HBSS. Log_{10} serial dilution of cell supernatants or murine serum was conducted in MEM, and virus was incubated on cells for 90 minutes (room temperature, with rocking). Upon removal of virus, 1 ml of overlay, containing nutrients (2.6.2) and low-melting point tissue culture-grade agarose, was added to each well and allowed to solidify at room temperature before incubation for 4 days (37°C, 5% CO_2). Cells were fixed and stained overnight at room temperature with 1 ml/well toluidine blue stain (0.1% toluidine blue (Sigma-Aldrich), 3.7% formaldehyde (Fisher Scientific), 1x PBS (Sigma-Aldrich)). The agarose plug was removed by washing and plates dried before plaques were counted by eye. Mock-infected supernatant samples were determined not to result in plaque formation. Plaque counts were converted to pfu/ml using Microsoft Excel and analysed using GraphPad Prism version 7.01 (GraphPad Software, Inc).

2.4 Antiviral assays against HAZV

2.4.1 HAZV stocks

HAZV stocks (strain JC280, passaged once in suckling mice at Porton Down and sequenced, GenBank accession numbers: L-DQ076419.1, M-DQ813514.1 and S-M86624.1) were generated by the Virology and Pathogenesis Group, Public Health England. Briefly, SW13 cells (European Collection of Authenticated Cell Cultures (ECACC) 87031801) were cultured in SW13 growth medium, comprised of DMEM supplemented with 10% HI-FBS, 0.1 mg/ml streptomycin and 100 U/ml penicillin, at 37°C, 5% CO_2. For amplification, cells were washed twice with sterile PBS before incubation with trypsin-EDTA for 5 minutes at 37°C, then collected by media wash, centrifuged for 5 minutes at 500 x *g* and the supernatant was discarded. Cells were resuspended in fresh media by pipetting. Subconfluent 75/175 cm^2 tissue culture flasks of SW13 cells were prepared for propagation of HAZV. Culture media was removed and replaced with HAZV stocks diluted in DMEM (1.5 ml DMEM with 50 µl virus for a 75 cm^2 tissue culture flask; 5 ml DMEM

with 100 µl virus for a 175 cm^2 tissue culture flask), and the flask incubated for 1 hour at 37°C. 15 ml or 25 ml DMEM supplemented with 2% HI-FBS was added to a 75 cm^2 or 175 cm^2 tissue culture flask, respectively, and cultures incubated at 37°C for 5-6 days. Flasks were frozen at -80°C to freeze the cells, before defrosting at 37°C. Flask contents were transferred to a 50 ml centrifuge tube and centrifuged to remove cell debris. Supernatant containing virus was then aliquoted into cryo-vials and stored at -80°C until use. For analysis of glycosylation, HAZV grown as described and further purified by 20% sucrose cushion gradient centrifugation (67000 x *g*, 4°C, 150 minutes) was used.

2.4.2 HAZV glycosylation analysis

For computational prediction of N-glycosylation sites, the NetNGlyc [464, 465] and GlycoEP [466] tools were used to analyse the JC280 strain glycoprotein sequence (UniProt Knowledge Base (UniProtKB) accession number A6XIP3). For glycosylation analysis by gel shift, HAZV and UGGT (a gift from Pietro Roversi) were digested according to the manufacturer's instructions using PNGase F (enzyme from Pietro Roversi and Dominic Alonzi, buffers from New England Biolabs) and endoglycosidase Hf (Endo Hf; New England Biolabs). Samples were denatured by heating with DTT and NuPAGE® LDS Sample Buffer, and run on a NuPAGE® Bis-Tris gel (200 V, 125 mA, 35 minutes) in NuPAGE® MES SDS Running Buffer (all Life Technologies). Protein was stained with InstantBlue (Expedeon) and molecular weights of sample bands were compared to Novex® Sharp Pre-stained Protein Standard (Invitrogen).

2.4.3 *In vitro* viral infection and drug treatment

Cytotoxicity of antiviral compounds on SW13 cells was determined following the protocol described in 2.1.3. For antiviral efficacy of iminosugars against HAZV, confluent monolayers of SW13 cells in 24-well plates (prepared by the ECACC facility at Public Health England, Porton

Down) were infected with HAZV diluted to an MOI of 0.01 in DMEM without supplements for 60 minutes (37°C). Upon removal of virus, fresh SW13 growth medium containing titrations of drug as indicated was added to cells, which were further incubated for 1, 3 or 6 days (37°C, 5% CO_2). For analysis of secreted virus, supernatant was harvested and diluted 1 in 5 in AVL buffer (Qiagen) and stored at 4°C until downstream RNA isolation. For analysis of infectious virus secretion, supernatant was harvested, aliquoted and stored at -80°C.

2.4.4 RNA extraction and HAZV S segment qRT-PCR

RNA extractions from cell culture supernatants were performed in 96-well plate format using a MagNA Pure 96 System (Roche) according to the manufacturer's instructions. HAZV RNA was assayed using an Applied Biosystems 7500 FAST real-time PCR system. Hot-start Taq DNA polymerase was used to enable Taq-mediated release of fluorescently labelled dyes from a HAZV S-specific probe, using an assay developed and optimised at Porton Down in line with the assay for CCHFV [467]. Probe and primer sequences and concentrations are given in Table 11. The reaction mixture was prepared according to the manufacturer's instructions for Superscript III Platinum One-Step Quantitative RT-PCR kit (Invitrogen). Thermal cycling was conducted as follows. Synthesis of cDNA was performed for 10 minutes at 50°C, followed by a 2 minute denaturation step at 95°C. PCR thermocycling with fluorescence detection was executed for 45 cycles of 95°C for 10 seconds followed by 60°C for 40 seconds. Samples were compared to a standard curve generated from serial dilutions of an RNA oligonucleotide designed from the sequence of the HAZV S segment (Integrated DNA Technologies). GEs/reaction were converted to GE/ml using Microsoft Excel and analysed using GraphPad Prism version 7.01 (GraphPad Software, Inc).

2.4.5 Settling plaque assay

To determine infectious HAZV titres in cell culture supernatants, SW13 cells were cultured as described in 2.4.1 for use in a settling plaque assay. A cell suspension containing 2 x 10^5 cells/ml in DMEM supplemented with 10% HI-FBS was prepared, with 500 µl required per well of a 24-well tissue culture plate used in the plaque assay. Serial 1:10 dilutions of supernatants were performed (undiluted to 10^{-5} dilution) and 100 µl of supernatant was added to a 24-well plate in duplicate. Media-only and virus stock controls were included. 500 µl of cell suspension was added to each well, and the plates mixed by rocking. Plates were incubated on a tray with wet tissue at 37^{o}C for 4 hours. During this time, plaque assay overlay was constituted by diluting one part 2% carboxmethyl-cellulose in one part 2xMEM media. The overlay was mixed vigorously and retained in the incubator at 37°C until required. 500 µl of overlay was added to each well by slow pipetting down the side of the well to minimise disruption to the cells, and plates were returned to the incubator for 5 days. Cells were fixed by the addition of 1 ml 20% formaldehyde in PBS per well, for at least 1 hour. The solution was removed by pipetting and plates washed with water. To stain the plates, 1 ml of 0.2% crystal violet solution was added to each well and left for around 30 minutes, until cells were stained. The dye was removed by pipetting and then plates were washed with water until the dye was removed. Plates were left to air dry, before plaques were counted by eye. Plaque counts were converted to pfu/ml using Microsoft Excel and analysed using GraphPad Prism version 7.01 (GraphPad Software, Inc).

2.4.6 Free oligosaccharide (FOS) assay

SW13 cells were infected with HAZV at MOI 0.01 as described in 2.4.3 or mock-infected (media-only) and incubated for indicated times. FOS were quantified as described in 2.2.11.

2.5 Immunological assays

2.5.1 MDMΦ stimulation with pathogen associated molecular patterns (PAMPs)

MDMΦs were isolated and differentiated as described in 2.2.2, with experiments conducted in 24-well plates. A range of canonical ligands for different pattern recognition receptors (PRRs) were utilised in order to probe the effect of iminosugars on cytokine responses elicited by different stimuli (

Table 7). The concentrations utilised were chosen based on a combination of laboratory experience and information in the literature pertaining to eliciting cytokine responses, as detailed, although often no publications utilising these stimuli in primary human macrophages were found. MDMΦs were stimulated with PAMPs for the durations described in figure legends, in 1 ml/well, for experiments without DENV. For experiments where PAMPs were compared directly with DENV infection, stimuli were added to the MDMΦ in the same volume as used for DENV infection, and after the 90 minute DENV infection period, stimuli were diluted to the final concentration shown in 1 ml/well (while DENV was removed and replaced with 1 ml/well iminosugar media as appropriate). After the stimulation period, supernatant was collected, aliquoted and stored at -80°C until analysis.

Table 7. PAMPs used in this study

PAMP (brief description)		
Routine concentration used (rationale)	Endotoxin level[a]	Catalogue number
PAM_3CSK_4 • Synthetic triacylated lipopeptide mimicking the proinflammatory component of bacterial (Gram-negative and Gram-positive) cell wall lipoproteins • TLR2/TLR1 heterodimer agonist		
100 ng/ml (based on 1 µg/ml for 18 hours' stimulation of MDMΦs from healthy human donors [468], and 50 ng/ml for 18 hours' stimulation of human monocytes or PBMCs [469], both investigating cytokine production, and Invivogen recommendation of 1-300 ng/ml)	<0.001 EU/µg	tlrl-pms (Invivogen)
FSL-1 ($Pam_2CGDPKHPKSF$) • Synthetic diacylated lipopeptide, mimicking the proinflammatory component of mycoplasmal lipoproteins • TLR2/TLR6 heterodimer agonist		

100 ng/ml (based on 50 ng/ml for 24 hours used to stimulate matrix metalloproteinase activity in THP-1-derived macrophages [470], 200 ng/ml for 8 hours used to stimulate TRIM expression in THP-1 cells [471], and Invivogen recommendation of 1-100 ng/ml)	<0.001 EU/µg	tlrl-fsl (Invivogen)
Polyinosinic-polycytidylic acid, high molecular weight (poly(I:C)) • Synthetic analog of double stranded RNA (dsRNA), a PAMP associated with viral infection • TLR3, RIG-I, and MDA5 agonist		
1 µg/ml (based on Invivogen recommendation of 30 ng/ml – 10 µg/ml, and routinely used laboratory concentration) or 10 ug/ml in experiments with peptide inhibitors	<0.001 EU/µg	tlrl-pic (Invivogen)
Polyadenylic–polyuridylic acid (poly(A:U)) • Synthetic dsRNA molecule • Pure TLR3 agonist		
10 µg/ml (based on Invivogen recommendation of 300 ng/ml – 100 µg/ml, and concentration matched to poly(I:C))	See [b]	tlrl-pau (Invivogen)
Lipopolysaccharide from *Salmonella enterica* serotype typhimurium (LPS-ST) • Principal proinflammatory component of Gram-negative bacteria, located in the outer membrane • TLR4 agonist, likely to also activate TLR2 due to lipopeptide contamination in a non-ultrapure preparation		
100 ng/ml (routinely used in the laboratory)	Not reported	L6143 (Sigma-Aldrich)
Lipopolysaccharide (ultrapure) from *Escherichia coli* O111:B4 (LPS-EB) • Principal proinflammatory component of Gram-negative bacteria, located in the outer membrane • TLR4 agonist, purified such that TLR2-activating contaminants are removed		
100 ng/ml (equal to that of LPS-ST)	1 x 10^6 EU/mg	tlrl-3pelps (Invivogen)
Flagellin (ultrapure) from *Bacillus subtilis* (FLA-BS) • Principal component of bacterial flagella, here from a Gram-positive bacterium • TLR5 agonist (surface) and NLRC4 and NAIP5 agonist (intracellular)		
100 ng/ml (based on Invivogen recommendations, and the use of the standard (not ultrapure) flagellin preparation at 50-500 ng/ml to stimulate Rhesus macaque PBMCs for 6 hours [472] or 0.1-10 µg/ml to stimulate vascular endothelial cells for 8 hours [473]; publications utilising flagellin in primary human macrophages were not identified)	<0.05 EU/µg	tlrl-pbsfla (Invivogen)
Imiquimod/R837 • Imidazoquinoline amine analog to guanosine; indirectly antiviral through IFN-α induction • TLR7 agonist		
5 µg/ml (based on Invivogen recommendation of 1-5 µg/ml, and 2.8 µg/ml used to stimulate murine macrophages for 24 hours [474])	See [b]	tlrl-imqs (Invivogen)
TL8-506 • Analog of TLR8 agonist VTX-2337 with enhanced water-solubility • TLR8 agonist (approximately 500-fold more potent activator of TLR8 than TLR7)		
100 ng/ml (based on Invivogen recommendation of 10-100 ng/ml, and publications using the analog VTX-2337 at 800 nM to elicit cytokine production from primary human monocytes (for TL8-506, 100 ng/ml = 302 µM, although analog potency will not be equivalent) [475] and 1 µM for granzyme B production from primary human monocytes [476])	Not reported	tlrl-tl8506 (Invivogen)

ODN-2006 • Synthetic 5'-tcgtcgttttgtcgttttgtcgtt-3' nucleotide sequence containing unmethylated CpG motifs that are hallmarks of bacterial DNA • Class B CpG oligonucleotide, therefore TLR9 agonist, with weak IFN-inducing ability		
5 µg/ml (utilised rather than more optimal 10 µg/ml due to availability, based on Invivogen recommendation of 1-5 µM (7.7-38.5 µg/ml) and use at 1 µM in B cell cytokine stimulation [477])	See [b]	tlrl-2006 (Invivogen)
Heat-killed *Candida albicans* (HKCA) • Contains β-glucans, present in the cell walls of fungi • Dectin-1 agonist, when extracellular, but can activate TLR2/TLR1 or TLR2/TLR6 if internalised to phagosomes		
1 x 10^6 cells/ml (based on stimulation of human PBMCs [478])	<0.001 EU/µg	tlrl-hkca (Invivogen)
Peptidoglycan (ultrapure), from *Staphylococcus aureus* (PGN-SAndi) • Major surface component of Gram-positive bacteria • NOD1 or NOD2 agonist (purified to remove lipophilic TLR2 agonists)		
5 µg/ml (based on Invivogen recommendation of 1-5 µg/ml, and stimulation of human primary monocytes or PBMCs with up to 10 µg/ml [479])	<0.001 EU/µg	tlrl-sipgn (Invivogen)
Bis-(3'-5')-cyclic dimeric guanosine monophosphate (c-di-GMP) • Bacterial second messenger • STING agonist		
25 µg/ml (based on Invivogen recommendation of 10-100 µg/ml for THP-1 reporter cell stimulation, and stimulation of THP-1 cells for 24 hours with 14 µg/ml [480], without transfection)	See [b]	tlrl-nacdg (Invivogen)
DENV-2 NS1 • Recombinant NS1 from DENV-2, produced in *Escherichia coli* • TLR4, TLR2, and TLR6 agonist[c]		
1 µg/ml (concentration used to stimulate PBMCs [481])	Not reported	ab64456 (Abcam)

[a]As reported by source.

[b]Absence of endotoxin contamination confirmed by lack of HEK-Blue TLR4 reporter cell response (Invivogen), validated by manufacturer.

[c]DENV NS1 (from this source) has previously been reported to activate TLR2 and TLR6 [481]. This activation was later attributed to bacterial contaminants in the NS1 preparation, and pure, endotoxin-free, NS1 to signal through TLR4 instead [75]. Consequently, this preparation of NS1 may activate a combination of TLRs.

Abbreviations: EU, endotoxin unit; NOD, nucleotide oligomerisation domain; MDA5, melanoma differentiation-associated protein 5; RIG-I, retinoic acid-inducible gene I; TLR, Toll-like receptor; TRIM, tripartite motif; STING, stimulator of interferon genes.

2.5.2 Peptide inhibitors of MyD88 and TRIF

In order to elucidate the dependence of iminosugar effects on TLR signalling adaptor proteins, peptide inhibitors of myeloid differentiation primary response 88 (MyD88; inhibitor Pepinh-MYD) or TIR-domain-containing adapter-inducing interferon-β (TRIF; inhibitor Pepinh-TRIF), and

the corresponding control peptide (Pepinh-Control; all Invivogen) were used. MDMΦs were pre-treated with peptide inhibitors at 50 µM for 6 hours, before the addition of PAMP stimulation (as described in 2.5.1) and iminosugar treatment. Stimulation occurred for 18 hours, during which time inhibitory peptides were present at 25 µM. Supernatant was collected, aliquoted and stored at -80°C until analysis.

2.5.3 Cytokine gene expression analysis

MDMΦs were infected with DENV and treated with iminosugars as described in 2.2.5. The supernatant was removed and cells washed once with HBSS. Cells were lysed in 350 µl Buffer RLT supplemented with β-mercaptoethanol and RNA extracted using the RNeasy Mini Kit (Qiagen), according to the manufacturer's instructions. qRT-PCR for cytokine (*TNFA* and *IFNA2*) and housekeeping (ribosomal protein lateral stalk subunit P2; *RPLP2*) genes was conducted using an Applied Biosystems 7500 FAST real-time PCR system. Primer/probe information is given in Table 12. The reaction mixture was prepared according to the manufacturer's instructions for Verso 1-Step RT-PCR Kit with Thermo-Start Taq. Thermal cycling was conducted as follows. Synthesis of cDNA was performed for 30 minutes at 50°C, followed by a 15-minute activation of Thermo-Start Taq polymerase at 95°C. PCR thermocycling was executed for 40 cycles of 95°C for 15 seconds followed by 60°C for 60 seconds, during which time the fluorescence was detected. Samples were analysed in technical duplicate. Cytokine gene expression was normalised to *RPLP2* expression using the $2^{-\Delta\Delta CT}$ method [460] to control for cell number, and analysed using GraphPad Prism version 7.01 (GraphPad Software, Inc).

2.5.4 Cytokine detection in supernatants

2.5.4.1 Cytokine ELISAs and LEGENDplex multiplex cytokine assay

High mobility group box protein 1 (HMGB1) secreted from MDMΦ was quantified by HMGB1 ELISA (ST51011, IBL International) according to the manufacturer's instructions (high sensitivity assay; limit of quantification 0.2 ng/ml). TNF-α was quantified by TNF-α ELISA (KHC3011, Invitrogen) according to the manufacturer's instructions. For multiplex analysis of cytokine secretion from PAMP-stimulated MDMΦs, the 13-plex LEGENDplex Human Inflammation Panel (740118, BioLegend) was used to quantify IL-1β, IFN-α2, IFN-γ, TNF-α, MCP-1, IL-6, IL-8, IL-10, IL-12p70, IL-17A, IL-18, IL-23 and IL-33. The assay was conducted according to the manufacturer's instructions and analysed using the accompanying LEGENDplex software. Limits of detection are assay-dependent and as such are detailed in appropriate figure legends.

2.5.4.2 HEK-Blue™ cytokine reporter cell functional cytokine assay

HEK-Blue™ TNF-α cells (TNF-α cells, catalogue #hkb-tnfdmyd, lot #X35-3501, Invivogen) and HEK-Blue™ IFN-α/β cells (IFN-α/β cells, catalogue #hkb-ifnab, lot #X12-3601) were cultured at 37°C, 5% CO_2. For 3 passages post-thawing and for assays, growth medium comprising DMEM with high glucose, L-glutamine, no pyruvate (Gibco), 10% HI-FBS, 50 U/ml penicillin, 50 µg/ml streptomycin and 100 µg/ml Normocin™ (Invivogen) was used. Selection medium was utilised for cell maintenance, and for the TNF-α cells comprised growth medium supplemented with 100 µg/ml Zeocin™ (Invivogen) and 1 µg/ml puromycin (Invivogen), whereas for the IFN-α/β cells, the supplements were 100 µg/ml Zeocin™ and 30 µg/ml blasticidin (Invivogen). Both reporter cell types were commercially produced by stably transfecting HEK293 cells such that cytokine binding to endogenously expressed TNF-α receptor or type I IFN receptor (for TNF-α or IFN-α/β cells respectively) results in secreted embryonic alkaline phosphatase (SEAP) release to the cell supernatant. In the TNF-α cells, the SEAP reporter gene is under the control of the IFN-β minimal promoter fused to 5 NF-κB and 5 AP-1 binding sites (Figure 6A). MyD88 is also knocked out to

render the cells unresponsive to IL-1β stimulation. In the IFN-α/β cells, human STAT2 and IRF9 genes are stably expressed to produce a fully functional type I IFN signalling pathway, and the SEAP reporter gene is under the control of the ISG54 promoter (Figure 6B).

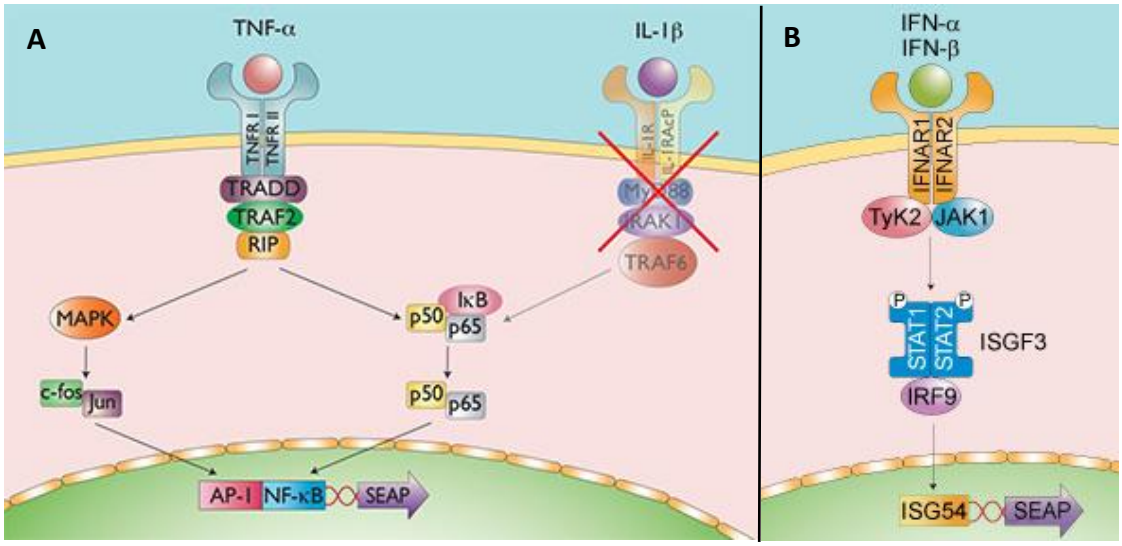

Figure 6. Signalling pathways for HEK-Blue™ TNF-α cells (A) and (B) HEK-Blue™ IFN-α/β cells (both reproduced from www.invivogen.com with permission for educational purposes).

Detection of biologically functional cytokine in cell supernatants was performed by adding 180 µl containing 5 x 10^5 cells of the appropriate type to 20 µl of standard or sample in a 96-well tissue culture plate, and incubating for 24 hours (37°C, 5% CO_2). 20 µl of induced cell supernatant was added to 180 µl of QUANTI-Blue™ (Invivogen) resuspended in endotoxin-free sterile water (Sigma-Aldrich). Plates were incubated (37°C, 5% CO_2) for 30 minutes-1 hour (TNF-α cells) or 1-3 hours (IFN-α/β cells) until the colorimetric change in the QUANTI-Blue™ of the standard curve wells was visible by eye. SEAP levels were quantified by measuring absorbance at 645 nm (A_{645}) using a NOVOstar microplate reader (BMG Labtech), for samples containing DENV, or a SpectraMax M5 microplate reader otherwise. Cytokine concentrations in samples were interpolated from a standard curve produced by serial dilution of recombinant human TNF-α (catalogue # 300-01A, Peprotech) for TNF-α cells or recombinant human IFN-2α (catalogue # 300-02AA) for IFN-α/β cells. Linear regression or sigmoidal four-point logarithmic curve fitting

of background-subtracted data was conducted using GraphPad Prism version 7.01 (GraphPad Software, Inc). Selected validation data is shown in 8.13.

2.5.5 HEK-Blue™ TLR reporter cells

To investigate the effects of iminosugars on TLR signalling, HEK-Blue™ hTLR2, hTLR3, hTLR4, hTLR9 and Null1 reporter cells (commercially available from Invivogen; kind gift of Natacha Zanin and Claudia Monaco, Kennedy Institute of Rheumatology, University of Oxford) were used. TLR reporter cells were cultured at 37°C, 5% CO_2. For 3 passages post-thawing and for assays, growth medium comprising DMEM with high glucose, L-glutamine, no pyruvate supplemented with 10% HI-FBS, 50 U/ml penicillin, 50 µg/ml streptomycin and 100 µg/ml Normocin™ was used. Selection medium was utilised for cell maintenance, comprising growth medium supplemented with antibiotics (Table 8).

Table 8. Composition of HEK-Blue™ TLR reporter cell selection media

Cell type	Selection antibiotic	Concentration
hTLR2	HEK-Blue Selection (Invivogen)	1x
hTLR3	Blasticidin	30 µg/ml
	Zeocin™	100 µg/ml
hTLR4	HEK-Blue Selection	1x
hTLR9	Blasticidin	10 µg/ml
	Zeocin™	100 µg/ml
Null1	Zeocin™	100 µg/ml

Similarly to the HEK-Blue™ cytokine reporter cells, the TLR reporter cells were commercially produced by stable transfection of HEK293 cells with relevant TLR genes (with the addition of CD14 for TLR2 and TLR4 cells, and MD-2 for TLR4 cells) and the SEAP reporter gene under the control of an NF-κB-responsive promoter. Consequently, TLR activation can be monitored through NF-κB activation, with the SEAP detected in cell supernatants. Activation of SEAP secretion through NF-κB activation directly or through endogenously-expressed TLRs on HEK293

cells was controlled for by inclusion of HEK-Null1 parental cells (transfected with the SEAP gene but no additional PRRs) in experiments, as indicated in figure legends.

To investigate the effects of iminosugars on TLR signalling, reporter cells were seeded at 5 x 10^4 cells/well of a 96-well tissue culture plate in 200 µl growth medium containing iminosugar (concentrations indicated in figure legends) and cultured in their presence for 3 days. After 3 days, media was exchanged for HEK-Blue Detection medium (Invivogen) containing canonical agonists (Table 9), or medium only, to stimulate the cells. HEK-Blue Detection medium contains the nutrients necessary for continued growth of the reporter cells, and a colorimetric substrate for SEAP, allowing the activity of SEAP secreted from the cells to be monitored in real-time. After an incubation period to allow SEAP secretion to be established, absorbance at 645 nm was read hourly using a SpectraMax M5 microplate reader.

Table 9. TLR reporter cell agonists

Cell type	Agonist	Concentration
hTLR2 or Null1	FSL-1	1 µg/ml
hTLR3 or Null1	Poly(I:C)	1 µg/ml
hTLR4 or Null 1	LPS-ST	100 ng/ml
hTLR9 or Null1	ODN-2006	10 µg/ml

2.6 Laboratory reagents

2.6.1 qRT-PCR primers and probes

Table 10. Viral RT primers used.

Target	DENV-2 nucleotides targeted	Sequence (5′ to 3′)	Reaction conc. (µM)	Source
DENV positive sense RNA	10723-10703	TCTTGGACAACTAAGTTGTCG	0.1	Custom (Thermo Fisher)
DENV negative sense RNA	9709-9729	GTACTCAATTAGTACTTTCTG	0.1	

Table 11. Viral qRT-PCR primers and probes used.

[a]Concentration for use with the Verso 1-Step RT-PCR Kit with Thermo-Start Taq (Thermo Scientific). [b]Concentration for use with Luna Universal Probe One-Step RT-qPCR Kit (New England BioLabs).

Target	Primer/ Probe	Label/ Quencher	Sequence (5′ to 3′)	Reaction conc. (µM)	Source
DENV NS5	Forward	N/A	ACAAGTCGAACAACCTGGTCC	0.8	Custom (Sigma-Aldrich)
	Reverse		GCCGCACCATTGGTCTTCTC	0.2	
	Probe	FAM/ TAMRA	CCAGTGGAATCATGGGAGGAAATCCCA	0.1	
HAZV S	Forward	N/A	CAAGGCAAGCATTGCACAAC	0.9	Custom (Integrated DNA Technologies)
	Reverse		GCTTTCTCTCACCCCTTTTAGGA	0.9	
	Probe	FAM/ MGB	TGAAGGATGGGTCAAAGA	1.25	
ZIKV E	Forward	N/A	TCGTTGCCCAACACAAG	0.8[a] or 0.4[b]	Custom (Sigma-Aldrich)
	Reverse		CCACTAATGTTCTTTTGCAGACAT	0.2[a] or 0.4[b]	
	Probe	FAM/ TAMRA	AGCCTACCTTGACAAGCAATCAGACACTCAA	0.1	

Table 12. Human qRT-PCR gene expression assays used.

Target	Probe Label/ Quencher	Source
TNFA	FAM/ MGB	Hs_00174128_m1 (ThermoFisher Scientific)
IFNA2	FAM/ MGB	Hs_00265051_s1 (ThermoFisher Scientific)
RPLP2	VIC/ MGB	Hs_01115128_gH (ThermoFisher Scientific)

2.6.2 Plaque assay reagents

Plaque assay reagents were formulated as described in the following tables. Hanks' solution A and B were filter-sterilised before use. DENV plaque assay first and second overlays were adjusted to pH 8.2 and 6.3, respectively, and filter-sterilised before use. The ZIKV plaque assay overlay was adjusted to pH 8.2 and filter-sterilised before use.

Table 13. Hanks' solution A (10x)

Reagent	Quantity
NaCl (all Sigma-Aldrich)	160 g
KCl	8 g
$MgSO_4 \cdot 7H_2O$	2 g
$MgCl_2 \cdot 6H_2O$	2 g
$CaCl_2 \cdot 2H_2O$	2.8 g
Double-distilled H_2O	To 1000 ml

Table 14. Hank's solution B (10x)

Reagent	Quantity
Na_2HPO_4 (all Sigma-Aldrich)	1.2 g
KH_2PO_4	1.2 g
D-glucose	20 g
Double-distilled H_2O	To 1000 ml

Table 15. DENV plaque assay first overlay

Reagent	Quantity
Hank's solution A	1x
Hank's solution B	1x
MEM vitamin solution (11120-037, Gibco)	1x
MEM amino acids solution (11130-036, Gibco)	2x
HI-FBS	10%
L-glutamine (25030-024, Gibco)	1.2 mM
Penicillin	100 U/ml
Streptomycin	0.1 mg/ml
7.5% $NaHCO_3$ pH 8.2 (25080-060, Gibco)	4%
Double-distilled H_2O	To volume

Table 16. DENV plaque assay second overlay

Reagent	Quantity
Hank's solution A	1x
Hank's solution B	1x
MEM vitamin solution	1x
MEM amino acid solution	2x
L-glutamine	1.2 mM
Penicillin	100 U/ml
Streptomycin	0.1 mg/ml
Double-distilled H_2O	To volume

Table 17. ZIKV plaque assay overlay

Reagent	Quantity
Hank's solution A	1x
Hank's solution B	1x
MEM vitamin solution	1x
MEM amino acid solution	2x
HI-FBS	2%
L-glutamine	1.2 mM
Penicillin	100 U/ml
Streptomycin	0.1 mg/ml
7.5% $NaHCO_3$ pH 8.2	3.6%
Double-distilled H_2O	To volume

Chapter 3. Antiviral mechanisms of action of 2THO-DNJ against DENV

3.1 Abstract

The antiviral efficacy of several glucose-stereochemistry iminosugars against DENV has previously been demonstrated and attributed to competitive inhibition of ER α-glucosidases, leading to a reduction in functional viral glycoprotein folding and infectious virion production. Here, the antiviral activity of the iminosugar 2THO-DNJ against DENV is characterised using primary human MDMΦs from healthy donors. 2THO-DNJ reduces virion assembly and secretion, in addition to impacting the infectivity of virions that are secreted, but does not appear to have virucidal activity against DENV, and does not reduce virion adsorption or entry to MDMΦs. 2THO-DNJ and *N*N-DNJ also inhibited DENV replication in MDMΦs and indications of the same activity were seen in a DENV-2 replicon system. Free oligosaccharide analysis and the lack of antiviral efficacy of the galactose-stereochemistry compound 2THO-DGJ support inhibition of ER α-glucosidases as the mechanism underlying 2THO-DNJ efficacy in MDMΦs. A panel of iminosugars were shown not to be antiviral against DENV in mosquito cells, indicating a lack of requirement for the calnexin cycle in mosquito cells.

3.2 Introduction

DENV is a virus of global public health concern, with the potential for infection to cause a fatal haemorrhagic fever and vascular shock. Despite some recent successes in vaccine development, the therapeutic landscape is sparse, with no licenced antivirals available. Instead, clinicians must rely on close monitoring and appropriate management of symptoms rather than targeting the aetiological agent – or agents, considering the combined role of virus and host immune response in dengue pathogenesis.

As discussed in Chapter 1, iminosugars have been in development as antivirals against DENV for several years, and have entered clinical trials for this indication (Table 5). 2THO-DNJ is a more recently-developed iminosugar. The antiviral efficacy of 2THO-DNJ has been demonstrated against DENV *in vivo* using the AG129 mouse model, where there was a beneficial effect on viral load and survival. However, previous *in vitro* studies of 2THO-DNJ efficacy are restricted to Vero cells [397]: a non-human continuous aneuploid cell line with an impaired immune response, with a homozygous deletion in chromosome 12 rendering IFN-α/β production impossible [482]. While this impairment makes the cell type ideal for virus propagation, they are less well-suited for modelling human DENV infection.

The mechanism of action of iminosugars against DENV has been the focus of several previous studies, with effects on viral glycoprotein folding demonstrated [51, 58, 352, 395] and the antiviral efficacy of DNJ-derivatives attributed to inhibition of ER α-glucosidases rather than effects on glycolipid processing [337, 394]. However, certain areas have been neglected, such as whether iminosugars inhibit DENV replication. In addition, some potential antiviral avenues have not been explored, including whether iminosugars can impact DENV binding and entry to cells, and whether they can directly impact virion infectivity. It must also be noted that much prior mechanistic analysis has been in non-relevant cell types: important since iminosugar

activity can be cell-type dependent, as exemplified by the impact of cell type on influenza virus susceptibility to iminosugar treatment [314]. Hence, to address mechanistic questions in a more physiologically-relevant cellular model, the antiviral efficacy and mechanisms of 2THO-DNJ were investigated in primary human partially-matured M2-type MDMΦs infected at a multiplicity of infection (MOI) of 1 [7].

As discussed previously, the involvement of the mosquito vector in the DENV transmission cycle necessitates consideration of any effects that a human dengue therapeutic might have on the vector, be those proviral or antiviral. Limited studies of iminosugar antiviral efficacy against DENV have been conducted in *Ae. aegypti* mosquitos, finding no evidence of an iminosugar effect on viral titres in the mosquito midgut [433]. However, the possibility remains that iminosugars could impact mosquito infection under different conditions, or treatment with different iminosugars might yield different results. While further exploration of these considerations in live mosquitos would be desirable, the C6/36 *Aedes albopictus* cell line was utilised as an amenable tool for screening the efficacy of a panel of iminosugars in this study.

Overall, this chapter aims to elucidate the antiviral mechanisms of action of 2THO-DNJ in the context of DENV infection of MDMΦs, with reference to other iminosugars. Specifically, the aims were:

1. To determine the antiviral efficacy profile of 2THO-DNJ against DENV in primary human MDMΦs, and whether this efficacy depends on inhibition of ER α-glucosidases;
2. To determine whether iminosugars have direct virucidal activity against DENV, or can affect the adsorption or entry of DENV to MDMΦs;
3. To determine whether iminosugars inhibit DENV replication in MDMΦs; and
4. To determine whether iminosugars have antiviral efficacy against DENV in C6/36 mosquito cells.

3.3 Results

3.3.1 Characterising the antiviral efficacy of 2THO-DNJ against DENV in MDMΦs

3.3.1.1 2THO-DNJ has potent antiviral efficacy against DENV in MDMΦs

Treating infected MDMΦs with titrations of 2THO-DNJ revealed that the drug potently inhibited the secretion of infectious DENV, with an IC_{50} (the concentration reducing infectious virus secretion by 50%) of 5.21 ± 2.5 μM and an IC_{90} (the concentration reducing infectious virus secretion by 90%) of 21.6 ± 11 μM, determined from analysis of eleven donors (Figure 7 and Table 19; both mean ± standard deviation). These concentrations are comparable to those for other iminosugars tested in this model [398], and the IC_{50} value is lower in MDMΦs than that reported for Vero cells [397]. All concentrations tested for antiviral efficacy were non-cytotoxic (see section 8.2.1 for cytotoxicity assays and selectivity indices).

While responses to 2THO-DNJ were broadly similar across the donors, there is an element of inter-donor variability, as expected for primary cells drawn from the outbred human population. Viral titres produced by MDMΦs derived from different donors vary significantly, but irrespective of donor, treatment with 100 μM 2THO-DNJ strikingly inhibits infectious virus secretion, with very little or no virus detectable (Figure 95); however, variation in untreated titres does not correlate with 2THO-DNJ efficacy when considering IC_{50} as a proxy (Figure 8).

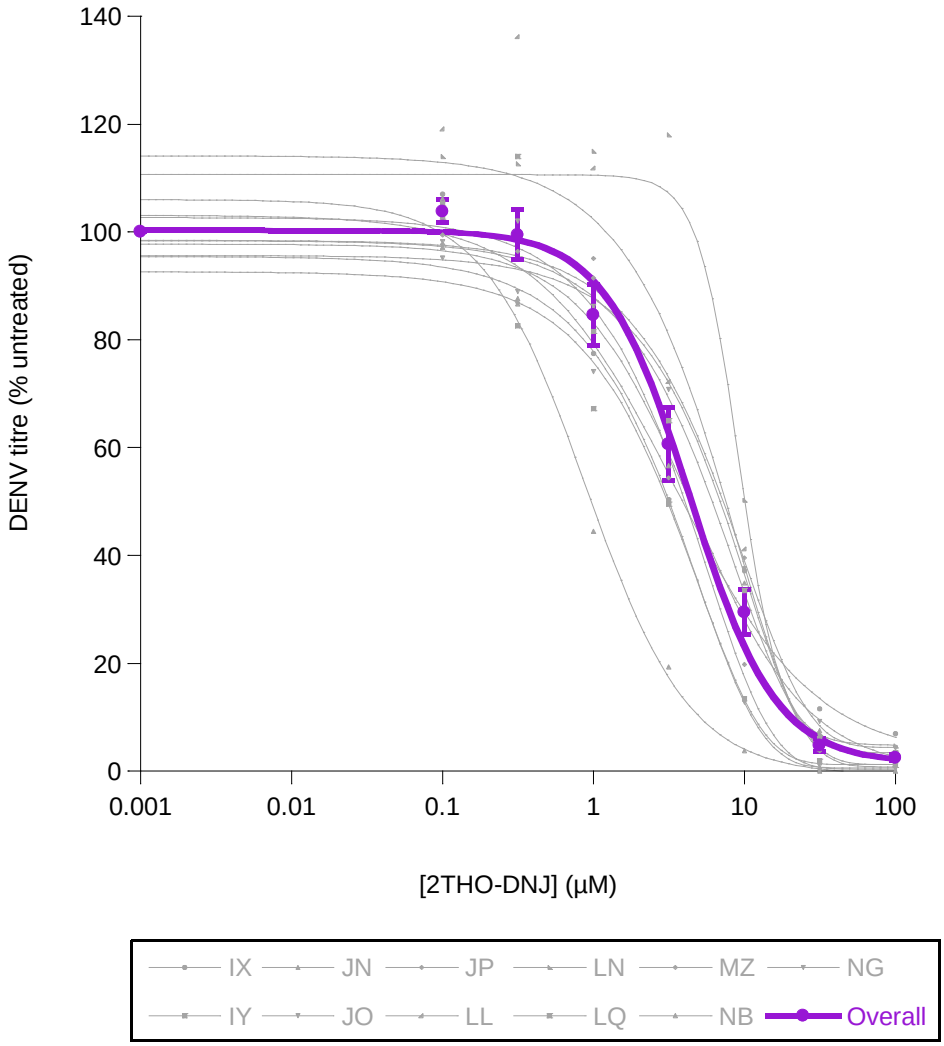

Figure 7. 2THO-DNJ reduces infectious DENV secretion from MDMΦs.

Primary MDMΦs (n=11 donors, as shown, assayed in technical triplicate) were infected with DENV and treated with a titration of 2THO-DNJ. Supernatant was collected at 48 hours post-infection and viral titres determined by plaque assay. Titres were normalised to untreated and the mean titre plotted for individual donors, with untreated represented as 0.001 µM to allow plotting on a logarithmic scale. Normalised data were pooled for all donors (overall; purple line) and plotted as mean ± standard error. Details of curve fitting and individual IC_{50} and IC_{90} values are given in 8.4.

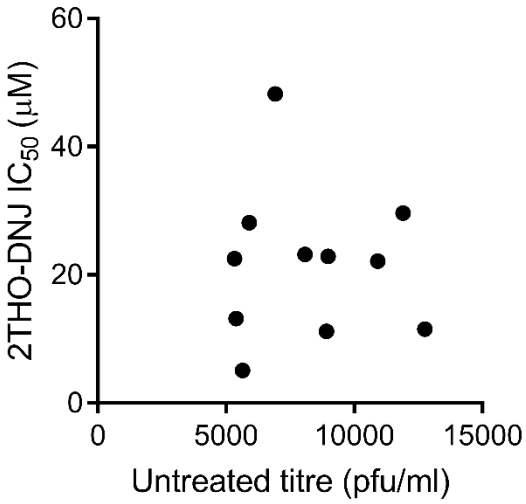

Figure 8. Baseline viral titres do not correlate with 2THO-DNJ efficacy.

Primary MDMΦs (n=11 donors, as shown in Figure 7, assayed in technical triplicate) were infected with DENV and treated with a titration of 2THO-DNJ. Supernatant was collected at 48 hours post-infection and viral titres determined by plaque assay. Mean titres of untreated samples were plotted against IC_{50} values for 2THO-DNJ for each donor. Pearson correlation was demonstrated no significant correlation between untreated titres and IC_{50} values (r= -0.02311, p= 0.9462 (two-tailed)).

3.3.1.2 2THO-DNJ antiviral activity is mediated by a combination of effects on virion secretion and infectivity

The reduction in viral titres with 2THO-DNJ treatment could be mediated by inhibition of virus secretion or by secretion of virions with impaired infectivity. Previous reports have indicated that *N*B-DNJ, BuCAST and M*O*N-DNJ primarily reduce virion secretion rather than infectivity [337, 394]. To investigate the effect of 2THO-DNJ, total secreted virus was quantified by qRT-PCR using primers directed against the NS5 gene, near the 3' end of the protein-coding region of the DENV genome. Since the DENV genome has a single open reading frame, detection using this qRT-PCR method should reflect the presence of complete DENV genomes in the supernatant. 2THO-DNJ substantially reduced the secretion of DENV from MDMΦs, occurring in proportion with the reduction in infectious virus secretion across much of the dose-titration (Figure 9). This indicates that 2THO-DNJ predominantly acts to reduce virus secretion.

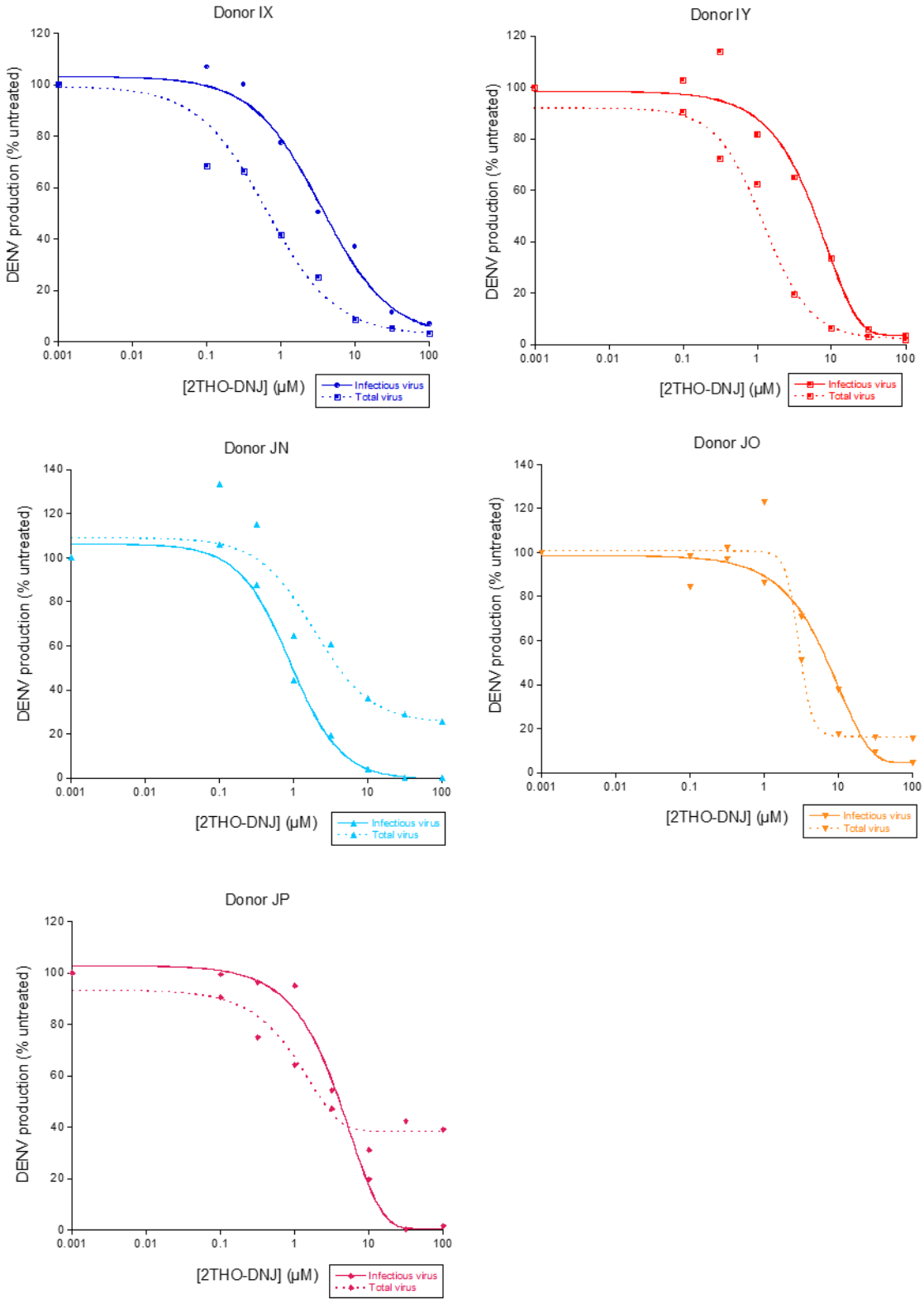

Figure 9. 2THO-DNJ inhibits a combination of virus secretion and infectivity.

Primary MDMΦs (n=5 donors, as shown, assayed in technical triplicate) were infected with DENV and treated with a titration of 2THO-DNJ. Supernatant was collected at 48 hours post-infection.

Viral titres were determined by plaque assay and total virus secretion by DENV NS5 qRT-PCR. Infectious virus (solid lines) and total virus (dotted lines) were normalised to untreated and mean values plotted (untreated values are represented as 0.001 µM to allow plotting on a logarithmic scale). Details of curve fitting are given in 8.4.

Across the five donors tested, the concentration required to reduce virus secretion to 50% untreated was 2.29 ± 1.3 µM (Table 20). This is similar to the calculated IC_{50} for 2THO-DNJ, particularly when considering the sensitivity of infectious virus detection. However, virus secretion was reduced by 90% from untreated levels in only two of the five donors tested, occurring at concentrations lower than 10 µM (Table 20). However in the other three donors, total virus secretion plateaued and this metric was not reached at 100 µM 2THO-DNJ, while infectious virus detection continued to decline. This suggests that alongside inhibiting virus secretion, higher concentrations of 2THO-DNJ can reduce the infectivity of the virions that are released.

To investigate this further, the specific infectivity of released virions was calculated by dividing infectious viral titres by genome equivalents for each replicate of each condition for five donors (Figure 10). The responses of these donors fall into two groups, where at lower concentrations, the specific infectivity for donors JN, JO, and JP remains similar to untreated, but at higher concentrations (above 1-10 µM), the specific infectivity falls and becomes lower than that of untreated samples. This indicates that the infectivity of individual virions is being reduced. In the case of donors IX and IY, however, the specific infectivity remains broadly consistent across the 2THO-DNJ titration. Since the specific infectivity is initially much lower in these two donors, relative to the other three, this might indicate that the infectivity of individual virions cannot be further reduced with high-concentration drug treatment without virion secretion being blocked by quality control mechanisms. However, there is a small spike in specific infectivity seen at 10 µM, which would indicate an enhancement in the infectivity of individual virions that are secreted. While many explanations for this observation might be possible, this effect occurs at

around the same concentration that 2THO-DNJ-mediated inhibition of ER α-glucosidase I becomes apparent, in addition to inhibition of α-glucosidase II (as discussed later; Figure 25). This might suggest that at the point of this gain of an additional target, there is a transient facilitation of viral glycoprotein folding, enabling better maturation rates and infectivity of the virions that are secreted. It is important to note that if there is any such effect, the reduction in virion secretion at this concentration is substantial enough to still correspond to significantly reduced infectious virus titres (Figure 9). The decrease in specific infectivity at higher concentrations of iminosugar was also seen with *N*B-DNJ and M*O*N-DNJ treatment (Figure 11), and with 2THO-DNJ treatment of DENV-infected monocyte-derived dendritic cells [483], indicating that iminosugar-mediated reductions in virion infectivity are not restricted to MDMΦs or to 2THO-DNJ.

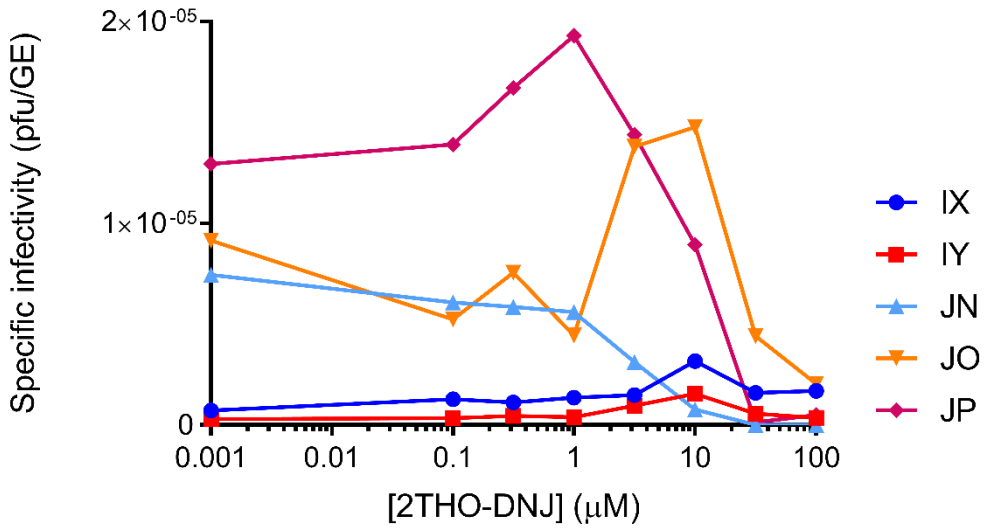

Figure 10. Specific infectivity of secreted virions is affected by 2THO-DNJ treatment.

Primary MDMΦs (n=5 donors, as shown, assayed in technical triplicate) were infected with DENV and treated with a titration of 2THO-DNJ. Supernatant was collected at 48 hours post-infection. Viral titres were determined by plaque assay and total virus secretion by DENV NS5 qRT-PCR. Infectious virus (pfu/ml) was divided by total virus (GE/ml) per well to give specific infectivity. Mean specific infectivity was plotted, with untreated values represented as 0.001 μM to allow plotting on a logarithmic scale.

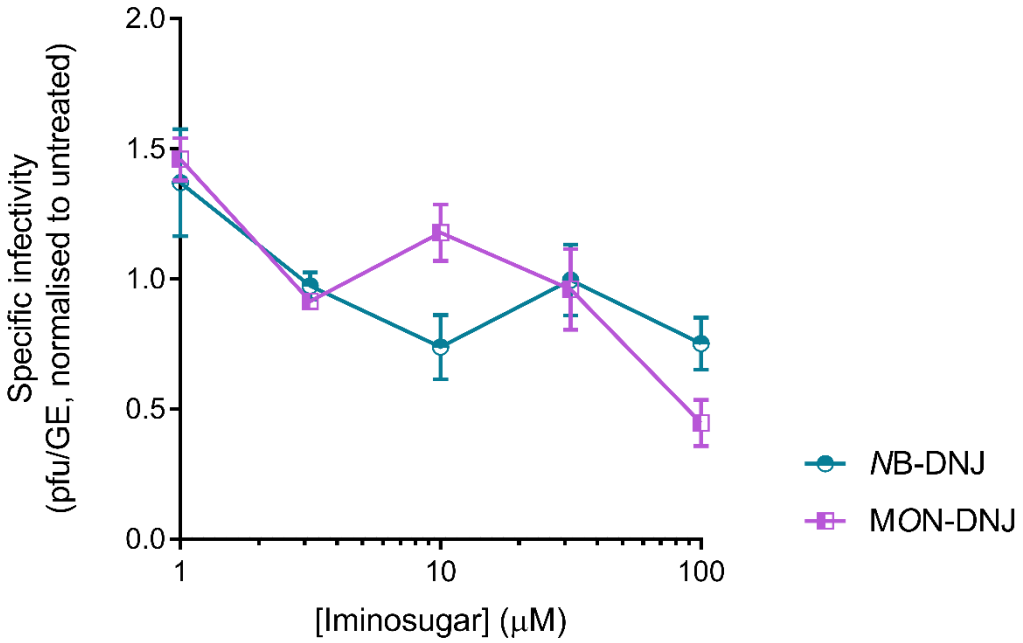

Figure 11. Specific infectivity of secreted virions is affected by N*B-DNJ and MON-DNJ treatment.*

Primary MDMΦs (n=3 donors (HF, HG, HH), assayed in technical triplicate) were infected with DENV and treated with a titration of N*B-DNJ or MON-DNJ. Supernatant was collected at 48 hours post-infection. Viral titres were determined by plaque assay and total virus secretion by DENV NS5 qRT-PCR. Infectious virus (pfu/ml) was divided by total virus (GE/ml) for each concentration to give specific infectivity, which was plotted as mean ± standard error. Data were collected by Beatrice Tyrrell and Andrew Sayce.*

3.3.1.3 Antiviral efficacy is sustained throughout the period of virus replication in MDMΦ cell culture

In order to gain a broader perspective on the antiviral effects of 2THO-DNJ, secretion of total (Figure 12) and infectious (Figure 13) virus was quantified over a time course up to 72 hours post-infection. Iminosugar concentrations used were non-cytotoxic at 72 hours post-infection (8.2.3). Despite inter-donor variability in virus production, responses to iminosugar treatment are broadly conserved, with *N*N-DGJ lacking efficacy, and the antiviral effects of *N*N-DNJ and 2THO-DNJ apparent from the 24 hour time point and persisting for the duration of culture. This indicates that this efficacy is not lost over longer periods in culture as might occur if the drug had degraded and virus production rebounded, or if iminosugar-mediated suppression of

antiviral immune responses had potentiated viral replication. M*O*N-DNJ also has sustained efficacy, up to 120 hours post-infection (Andrew Sayce, unpublished data).

The peak of virus secretion occurred at 48 hours post-infection, even in the untreated condition, which may indicate that the viral replication capacity of the cells has been exhausted and new virus is no longer being produced. The subtle drop in GEs detected at 72 hours post-infection might suggest that some degradation of secreted virions (including viral genome) or a combination of slowed virus production and re-uptake of virions from the culture media, perhaps clearance of degrading virions by phagocytosis, is occurring.

In the case of infectious virus, peak titres were observed at 36 hours post-infection, and a substantial drop in titre was seen thereafter, with little infectious virus detected at 72 hours post-infection. This suggests that the infectivity of the secreted virions is diminished over time in culture. To verify this, the retention of DENV infectivity in culture conditions was investigated by incubating DENV at 37°C, without cells, and determining the viral titre at various time points thereafter. Short time points were selected based on the thermal stability of DENV previously described [174], alongside longer time points relevant to the observations in Figure 13. DENV samples were incubated at 4°C in parallel for normalisation. At 4°C, most of the DENV infectivity was retained between 1 and 48 hours of incubation. In contrast, DENV titres were substantially reduced after 24 hours of incubation at 37°C, and were undetectable after 48 hours (Figure 14A). Although only one independent experiment was performed, the reduction in DENV titre was strongly apparent, in keeping with the known thermal lability of the virus. These findings demonstrate the reduction in virus infectivity for the LLC-MK_2 cells used for determining viral titre, using virus that was initially infectious in that system. It is possible that this could differ from DENV infectivity for MDMΦs, if the infectivity requirements for the cell types differ, if, for example, entry mechanisms vary.

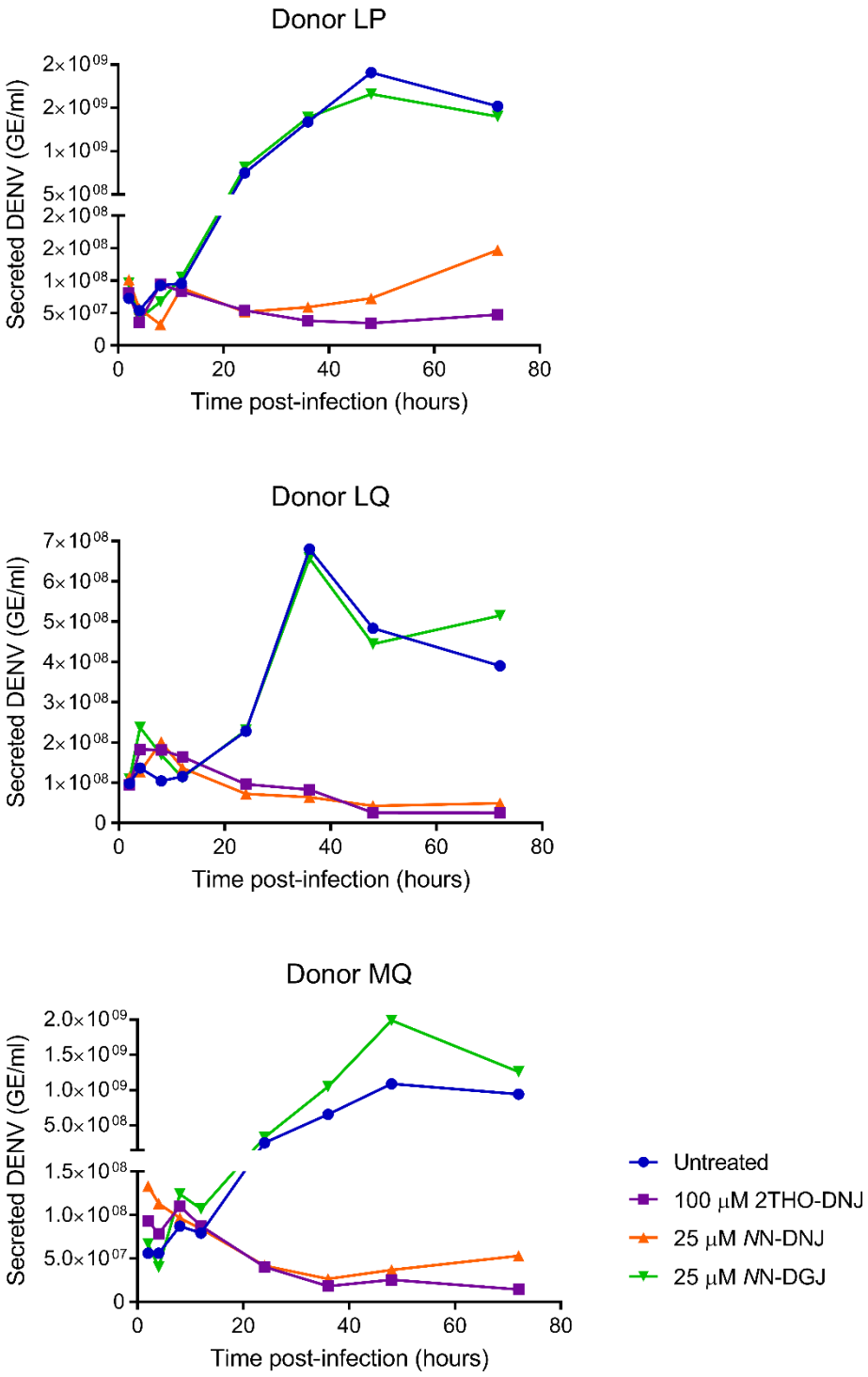

Figure 12. Antiviral efficacy of DNJ-derivative iminosugars is maintained throughout DENV infection (total secreted virus).

Primary MDMΦs (n=3 donors, as shown, assayed in technical triplicate) were DENV-infected then treated with 100 μM 2THO-DNJ, 25 μM NN*-DNJ, 25 μM* NN*-DGJ or media only. Supernatant was collected at the indicated time points and virus secretion determined by DENV NS5 qRT-PCR. Mean genome equivalents (GE)/ml are plotted.*

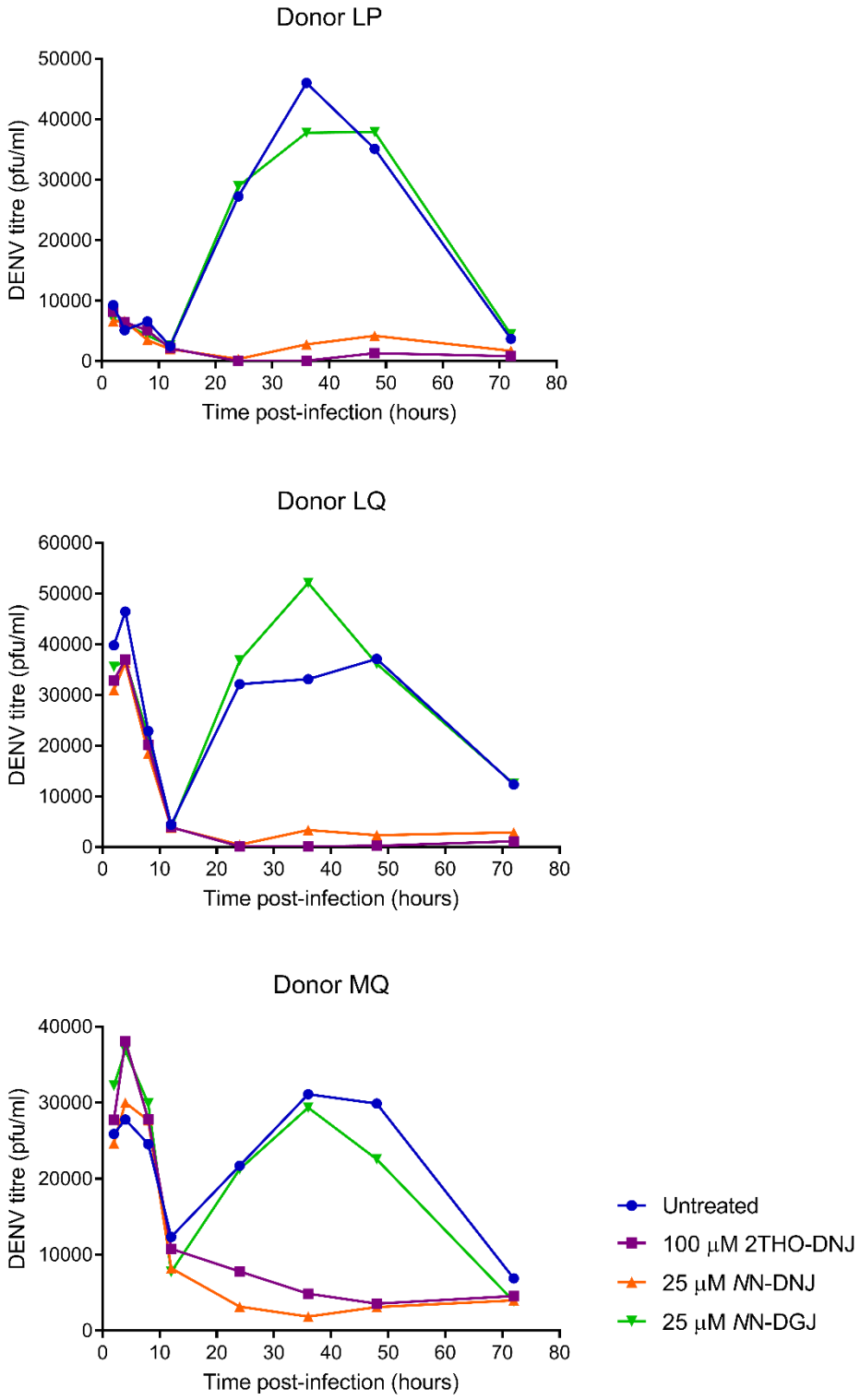

Figure 13. Antiviral efficacy of DNJ-derivative iminosugars is maintained throughout DENV infection (infectious virus).

Primary MDMΦs (n=3 donors, as shown, assayed in technical triplicate) were DENV-infected and treated with 100 μM 2THO-DNJ, 25 μM NN-DNJ, 25 μM NN-DGJ or media only. Supernatant was

collected at the indicated time points and viral titres determined by plaque assay. Mean viral titres (pfu/ml) were plotted.

DENV was incubated in different media conditions to assess whether the different media compositions that the virus is exposed to during the course of an experiment could significantly impact virion thermal stability. DENV was incubated with X-VIVO only (as used during initial MDMΦ infection), conditioned X-VIVO (day 4 MDMΦ supernatant from donor MT; representative of media containing any secreted factors produced by MDMΦs, in the absence of infection), or X-VIVO supplemented with 1% autologous serum and 25 ng/ml IL-4 (supplemented with serum from donor MT; as a control for the presence of IL-4 and serum in the conditioned X-VIVO). Although this experiment was performed only once, no striking differences were observed between incubation conditions, considering the sensitivity of the plaque assay detection method (Figure 14B), indicating that the presence of autologous serum or cellular secreted factors are unlikely to affect the stability of the virions during culture. However, this experiment would require repeating to confirm the results and does not examine the possibility that a host factor produced during infection could influence virion infectivity.

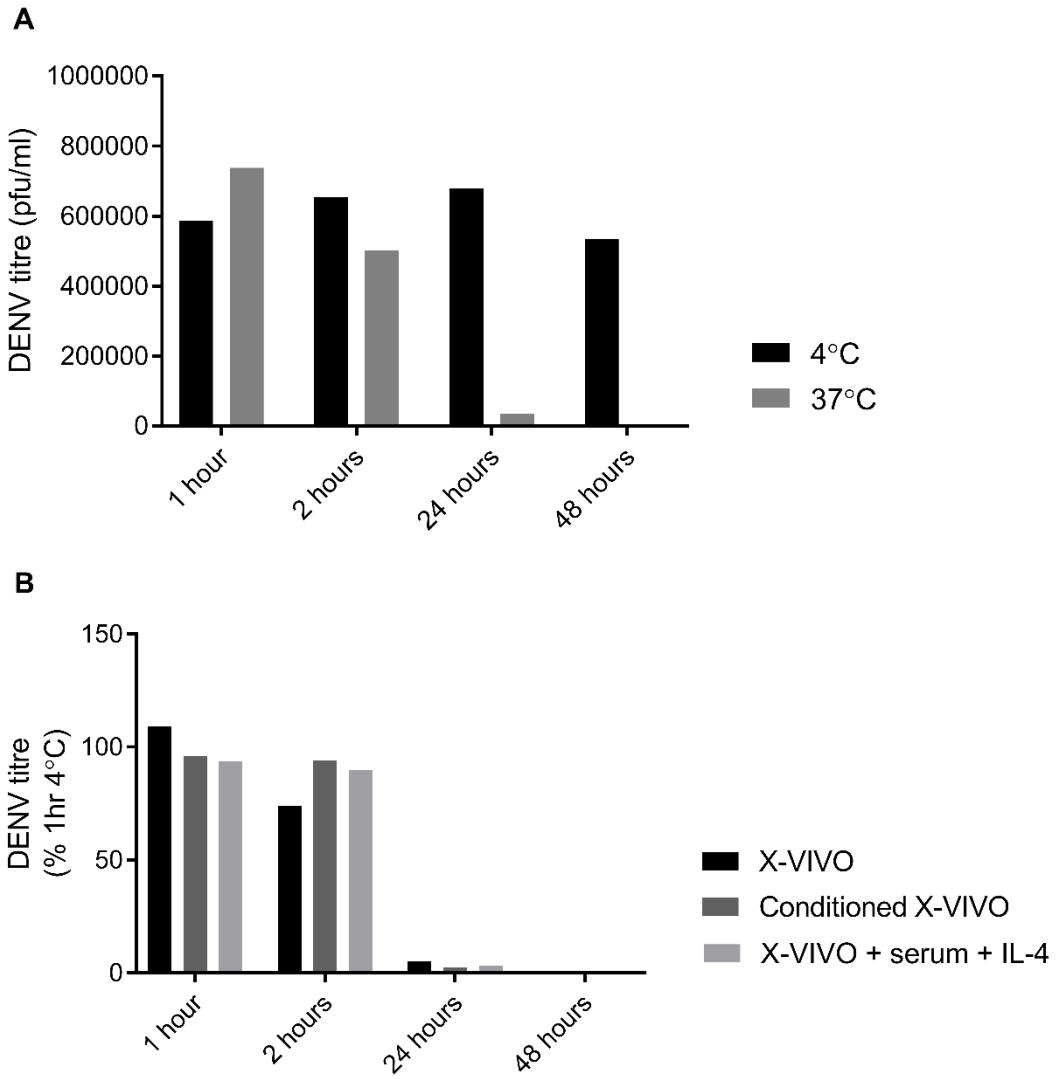

Figure 14. DENV infectivity is sensitive to temperature but not relevant media conditions.

(A) DENV (n=1, assayed in technical triplicate) was incubated at 4°C or 37°C in X-VIVO for indicated durations. Resulting mean viral titres are shown.

(B) DENV was incubated at 4°C or 37°C for indicated durations in X-VIVO, conditioned X-VIVO (day 4 MDMΦ supernatant from donor MT), or X-VIVO supplemented with autologous serum (from donor MT) and IL-4. Resulting viral titres for 37°C incubations were normalised to the average initial 4°C titre. The mean titre is displayed.

Since DENV infectivity is near-abrogated by 24 hours of incubation at 37°C (Figure 14), it is unlikely that the infectious virus measurable at later time points in the time course (Figure 13) derives from an initial round of infection with the C6/36 cell-derived virus inoculum, instead suggesting that it results from subsequent rounds of infection with MDMΦ-derived virus. While

primary macrophage and dendritic cell-derived DENV has been demonstrated to be infectious for the producing cell type [484], the intersection of MDMΦ-to-MDMΦ viral transmission and iminosugar antiviral activity has not been investigated. The anonymity of blood donors used here means that it is temporally impossible to test the infectivity of MDMΦ-derived virus derived from a certain donor for MDMΦs of that same donor. Therefore, MDMΦ-derived virus harvested from one donor (MT) 48 hours post-infection was titred, and used as the inoculum for MDMΦs from three subsequent donors, with C6/36-derived virus used in parallel. Although on average, matched MOI infections with C6/36- and MDMΦ-derived virus resulted in similar DENV titres after 48 hours (Figure 15A), donors varied in their response to infection with each virus source (Figure 15B). This confirms previous findings that MDMΦs are susceptible to infection by MDMΦ-derived virus [484]: at least that derived from a different donor, although the extent of this is somewhat donor-dependent. Reassuringly, only low viral titres were observed with 2THO-DNJ treatment of cells infected with virus from either source (Figure 15A).

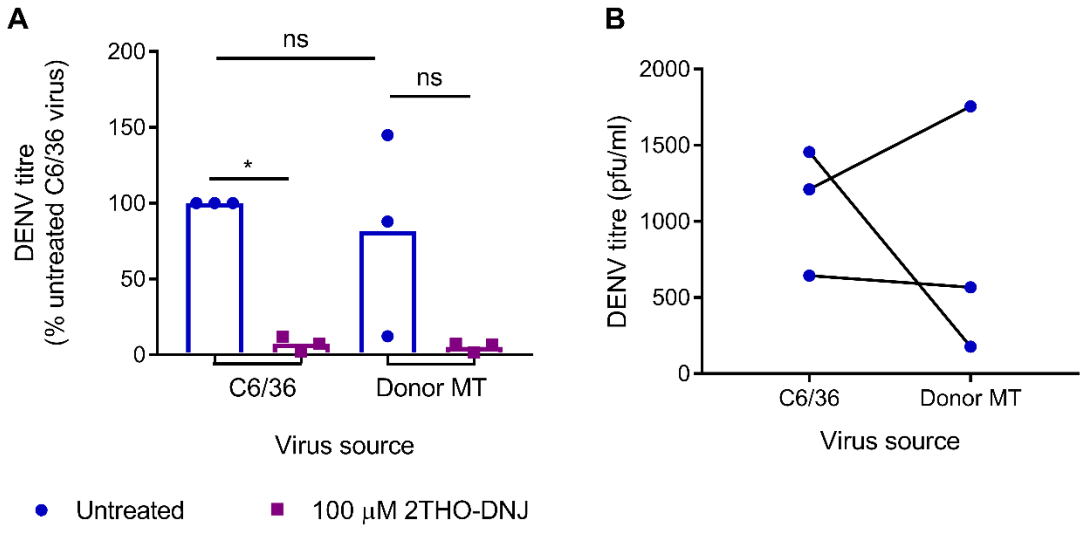

Figure 15. Virus derived from MDMΦs is infectious for MDMΦs, and the infection is susceptible to 2THO-DNJ treatment.

(A) Primary MDMΦs (n=3 donors (MZ, NB, NG), assayed in technical triplicate) were infected with the same MOI of DENV derived from C6/36 mosquito cells or from MDMΦs (donor MT) and treated with 100 μM 2THO-DNJ or media only. After 48 hours, supernatants were collected and infectious virus titres determined by plaque assay. The mean of titres normalised to untreated C6/36-derived virus are displayed (bars show the mean of the donors). Statistical analysis was

by one-way ANOVA with multiple comparisons, using Tukey's multiple comparisons test (, $p<0.05$).*

(B) Infectious virus titres were determined for media only-treated MDMΦs, infected as described for A. Corresponding mean viral titres resulting from infection with C6/36-derived and MDMΦ-derived DENV are shown for each donor.

3.3.1.4 Withdrawal of 2THO-DNJ treatment results in a rebound in virus secretion

Since continual treatment of MDMΦs with DNJ-derivative iminosugars persistently reduced infectious DENV production (Figure 13), the question arose as to whether this was due to continual iminosugar pressure or a lasting effect of initial iminosugar treatment. To investigate this, MDMΦs infected with DENV were treated with 100 µM 2THO-DNJ for 24 hours. After 24 hours of 2THO-DNJ treatment, comparably low levels of infectious virus were present in the supernatants of cells which went on to be treated with either fresh 2THO-DNJ media or media only for a further 24 hours. Viral titres were significantly higher when 2THO-DNJ treatment was removed than when it was replenished (Figure 16). Therefore, despite the very low levels of infectious virus present in the supernatant after 24 hours of 2THO-DNJ treatment, the majority of which will have been removed upon changing of the media, infectious virus production can rebound once the iminosugar is removed. This implies that a level of cellular infection and viral replication still occurs, at least during the first 24 hours of 2THO-DNJ treatment and indicates that the suppression of virus production achieved with 2THO-DNJ treatment is somewhat transient.

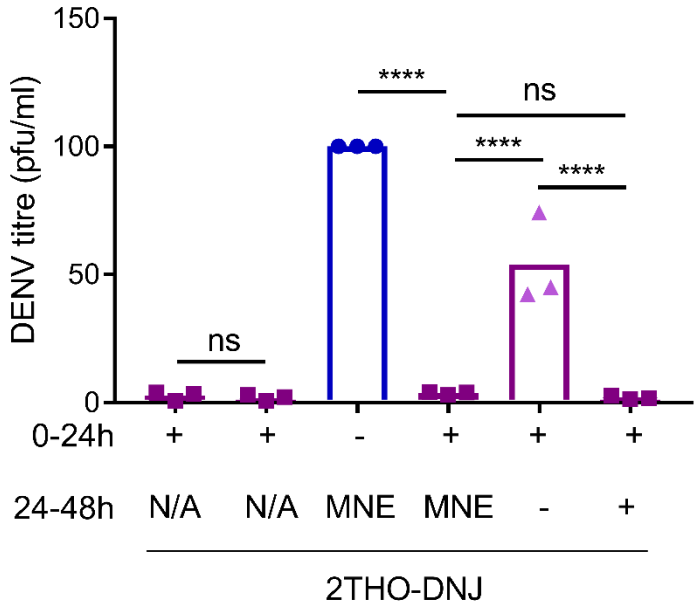

Figure 16. Withdrawal of 2THO-DNJ treatment results in a rebound in infectious virus production.

*Primary MDMΦs (n=3 donors (MZ, NB, NF), assayed in technical triplicate) were infected with DENV and treated with 100 μM 2THO-DNJ, media-only, or combinations for the indicated durations (MNE, media not exchanged). After 48 hours, supernatants were collected and infectious virus titres determined by plaque assay. Mean viral titres normalised to untreated (48h) are displayed (bars show the mean of the donors). Statistical analysis was by one-way ANOVA with multiple comparisons, using Tukey's multiple comparisons test (****, p<0.0001; ns, not significant).*

3.3.1.5 2THO-DNJ does not have direct virucidal activity against DENV

It is possible that the antiviral effect of iminosugars could be contributed to by direct virucidal activity, reducing virion infectivity in solution. Since the infectivity of DENV is stable at 4°C for 24 hours, the possibility for iminosugar virucidal activity was considered in both this infectivity-stable state, and during incubation at 37°C, where temperature alone leads to a significant reduction in infectious virus recovery (Figure 14). As such, DENV was incubated in X-VIVO with iminosugars at either 4 or 37°C for 2 or 24 hours, with the resulting DENV titres quantified by plaque assay (Figure 17). Although this experiment was conducted only once, no striking effects (a change in viral titre of over 50%) were observed at either incubation temperature for any iminosugar treatment. This suggests that iminosugars do not possess virucidal activity, although

this should be confirmed with further experiments. After 24 hours of incubation, there is some indication of a reduction in titre with *N*N-DNJ treatment, although this was only observed at 37°C, in the context of an overall reduction in viral titre, and not consistent with results after 2 hours of incubation. If this observation were borne out in further experiments, it should be noted that previous work has established that, as for other iminosugars, the presence of *N*N-DNJ does not interfere with the detection of DENV by plaque assay (data not shown). An alternative explanation to account for the observed virucidal activity would need to be established.

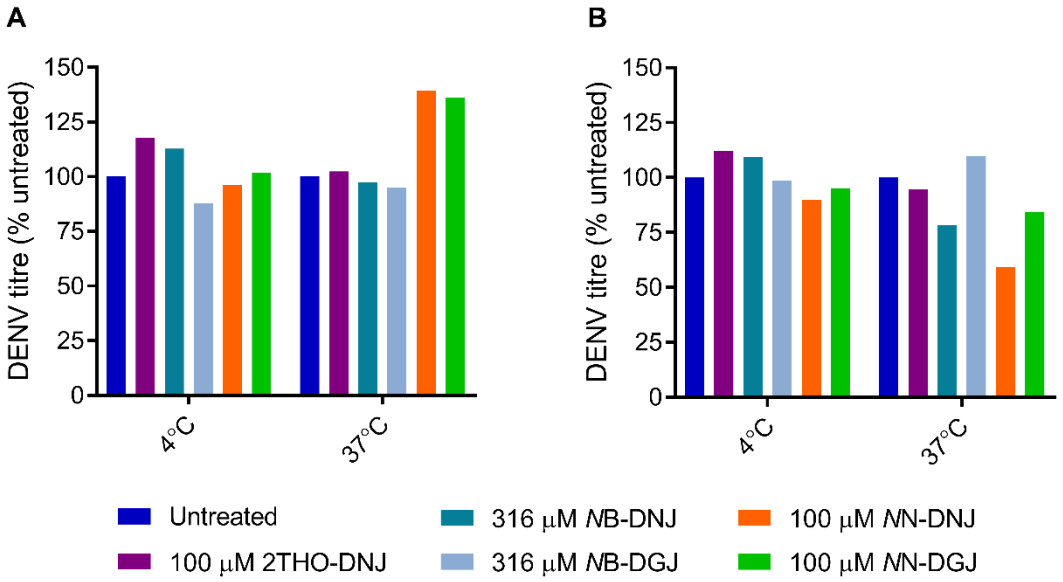

Figure 17. Virucidal activity of iminosugars against DENV after 2 hours (A) or 24 hours (B).

DENV (n=1, in technical triplicate) was incubated at 4 or 37°C in X-VIVO supplemented with iminosugars as indicated for 2 hours (A) or 24 hours (B), and viral titres post-incubation were quantified. Titres were normalised to untreated (for the appropriate incubation temperature), and the mean displayed.

3.3.1.6 Iminosugars do not affect DENV adsorption to MDMΦs

In order to determine whether iminosugars can impact the initial stages of cellular infection, DENV was allowed to bind to the surface of MDMΦs for 1 hour at 4°C, in the presence of iminosugar. Any unadsorbed DENV was then removed by repeated washing, and DENV RNA

that had bound to the cells was quantified. 2THO-DNJ, *N*N-DNJ and *N*N-DGJ did not affect DENV adsorption to MDMΦs (Figure 18A), indicating that reducing DENV attachment to MDMΦs does not contribute to the antiviral effect of DNJ-derivative iminosugars. However, it should be noted that the expression and function of DENV receptors may differ between 4°C and 37°C, which could impact the binding of DENV in this, and the following, experiment.

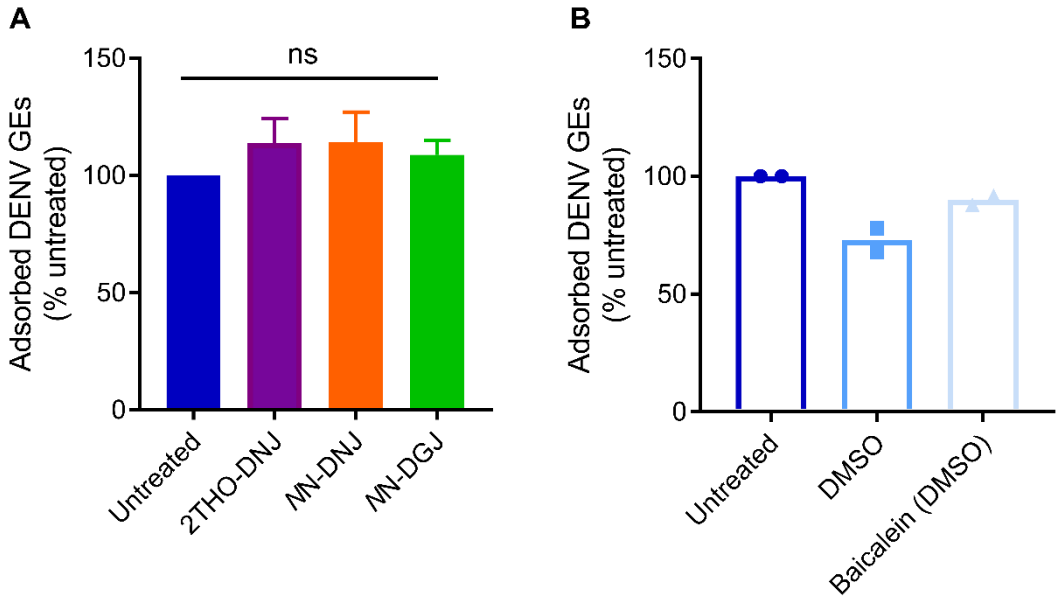

Figure 18. Iminosugars do not affect DENV adsorption to MDMΦs.

(A) Primary MDMΦs (n=4 donors (OE, OF, OI, OJ), assayed in technical triplicate) were incubated with DENV in the presence of 100 µM iminosugar or media only for 1 hour at 4°C. Unadsorbed DENV was removed by repeated washing, and DENV NS5 RNA extracted from cells quantified. Genome equivalents (GEs) were normalised to media only (untreated) for each donor, and displayed as mean ± standard error. Statistical analysis was by one-way ANOVA with multiple comparisons, using Dunnett's multiple comparisons test (ns, not significant).

(B) Primary MDMΦs (n=2 donors (OI, OJ), assayed in technical triplicate) were incubated with DENV in the presence of 25 µM baicalein, 25% DMSO (baicalein solvent control) or media only for 1 hour at 4°C. Unadsorbed DENV was removed by repeated washing, and DENV NS5 RNA extracted from cells quantified. GEs were normalised to media only or DMSO (for baicalein) and the mean displayed (bars show the mean of the donors).

Baicalein (5,6,7-trihydroxyflavone), a flavone compound derived from the root of the Chinese medicinal herb *Scutellaria baicalensis*, was included in the experimental design as an intended positive control, since it has previously been reported to have direct virucidal activity against

DENV, as well as an inhibitory effect on DENV entry to Vero cells (where baicalein was present for a 1 hour incubation at 37°C) [485]. Recently, molecular dynamics studies have suggested that baicalein can directly bind to the DENV-2 E protein at a site containing the fusion peptide, which could explain this activity [486]. However, in this experimental set-up, anti-adsorption effects of baicalein were not observed (Figure 18B). This is most likely due to the poor solubility of baicalein in aqueous solution, which has been referred to previously [487], resulting in DENV and MDMΦs being exposed to lower concentrations of baicalein than intended. Differences in experimental design in terms of temperature and cell type, where attachment factors and mechanisms may vary, could also contribute to the lack of efficacy. Furthermore, the readout for the previously-published effects of baicalein was foci formed by infectious virions or DENV RNA, 4 days post-infection. This time delay introduces the possibility that baicalein presence during cellular entry stages could have impacted downstream virus production through alternative pathways: for example, the antioxidant activity of even low concentrations of baicalein is rapidly apparent in human leukocytes (the IC_{50} for phorbol-12-myristate-13-acetate (PMA)-induced reactive oxygen species (ROS) around 2.5 µM) [487]. This antioxidant effect, combined with solubility issues and short treatment duration, may be reflected by the lack of cytotoxicity in MDMΦs (Figure 87).

3.3.1.7 DNJ-derivative iminosugars do not affect DENV entry to MDMΦs

Considering the lack of iminosugar effect on DENV adsorption to MDMΦs, the next step in the infection pathway that might be disrupted by iminosugars is cell entry. To examine this, DENV was allowed to bind to the surface of MDMΦs for 1 hour at 4°C, before removal of unadsorbed virus, and incubation at 37°C for 1 hour, allowing virus entry. Iminosugar was present for the final 37°C stage only. Any virus remaining on the surface of cells was degraded by proteinase K digestion, before DENV RNA that had entered the cells was quantified. 2THO-DNJ and *N*N-DNJ treatment tended to increase DENV entry to MDMΦs, although this was not statistically

significant (Figure 19A). However, *N*N-DGJ treatment led to a statistically significant increase in DENV entry, observed for all four donors tested. Understanding these effects is challenging considering the complexity of DENV entry. However, since effects are observed after a relatively short iminosugar treatment, it is unlikely to be explained by the established iminosugar mechanism of inhibiting cellular glycolipid processing, achieved to a similar extent by *N*N-DNJ and *N*N-DGJ in MDMΦs [337]. It is possible that the effects could be mediated by interactions of the long alkyl chain of *N*N-DGJ directly with the cell membrane, which might facilitate viral uptake, likely in an infectivity-independent manner. The discrepancy between *N*N-DNJ and *N*N-DGJ effects could be explained by the different stereochemistries, since steric differences might lead to *N*N-DGJ having a stronger detergent-like effect. Other alternative or additional interactions are possible: perhaps the DGJ headgroup could directly interact with, or activate, one or more entry receptors for DENV. To this end, it would be interesting to investigate whether the entry enhancement is replicated with other galactostereochemistry iminosugars. Regardless of mechanism, this enhancement of DENV entry by *N*N-DGJ did not correspond to increased virus secretion after 48 hours (data not shown). This is in agreement with previous reports of MDMΦ DENV titres being unaffected by *N*N-DGJ treatment for 48 hours [337]. This could occur if uptake of non-replication competent rather than infectious virions was promoted, which is not discerned by the qRT-PCR approach used here.

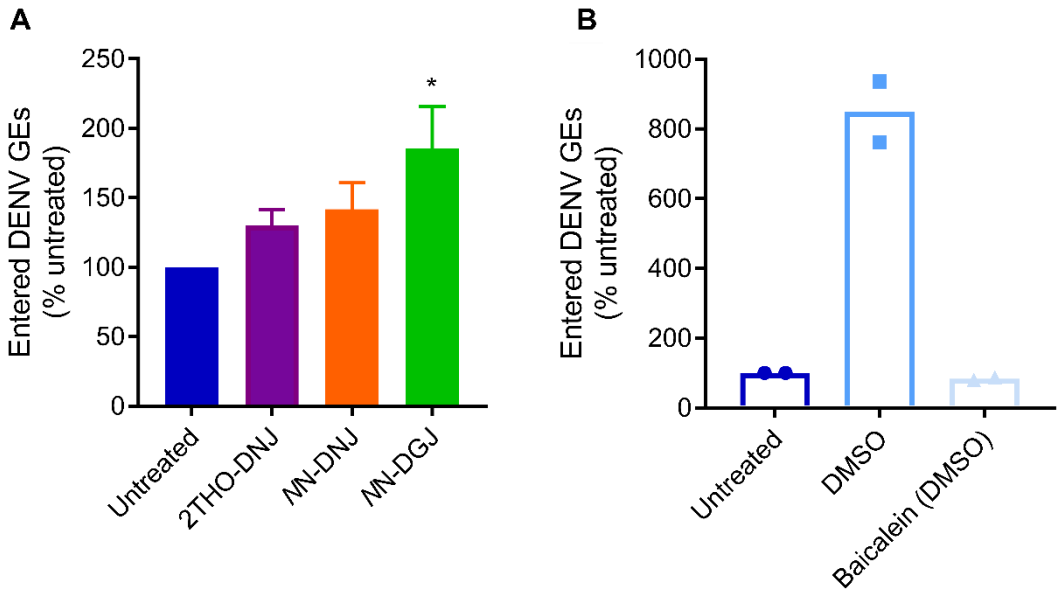

Figure 19. NN-DGJ *and DMSO treatment enhance DENV entry to MDMΦs.*

(A) DENV was allowed to adsorb to primary MDMΦs (n=4 donors (OE, OF, OI, OJ), assayed in technical triplicate) for 1 hour at 4°C. Adsorbed DENV was allowed to enter cells for 1 hour at 37°C in the presence of 100 µM iminosugar or media only. Remnant surface DENV was removed by proteinase K treatment, and DENV NS5 RNA extracted from cells was quantified. Genome equivalents (GEs) were normalised to media only, and displayed as mean ± standard error. Statistical analysis was by one-way ANOVA with multiple comparisons, using Dunnett's multiple comparisons test (, p<0.05).*

(B) DENV was allowed to adsorb to primary MDMΦs (n=2 donors (OI, OJ), assayed in technical triplicate) for 1 hour at 4°C. Adsorbed DENV was allowed to enter cells for 1 hour at 37°C in the presence of 25 µM baicalein, 25% DMSO (baicalein solvent control) or media only. Remnant surface DENV was removed by proteinase K treatment, and DENV NS5 RNA extracted from cells was quantified. GEs were normalised to media only or, for baicalein, DMSO, and mean values displayed (bars show the mean of the donors).

As discussed for DENV adsorption, baicalein treatment was included in this experimental design as an intended positive control for effects on DENV entry. However, in an effort to maintain the solubility of baicalein, an aqueous solution containing 25% v/v DMSO (with or without baicalein) was applied to the cells for the 1 hour internalisation period at 37°C. Although the n was 2 for this experiment, treatment with the DMSO control appeared to result in a substantial increase in DENV entry (Figure 19B). This may be due to the ability of DMSO to increase cell membrane permeability [488], which could facilitate entry of virions regardless of their infectivity.

Membrane permeability may be impacted despite the relatively high resistance of cell viability and function to high concentrations of DMSO for short exposure periods, such as PBMC exposure to 10% v/v DMSO for 1 hour [489]. Baicalein did not seem to significantly reduce DENV entry compared to the media-only condition (Figure 19B) in the context of the marked increase in DENV entry caused by DMSO exposure. This may be accounted for by a factor considered in 3.3.1.6, or could signify that any effect of baicalein was unable to overcome the potent and opposing effect of the DMSO solution.

3.3.1.8 2THO-DNJ and NN-DNJ inhibit DENV replication

3.3.1.8.1 Investigations in MDMΦs

Following DENV entry to the cell, iminosugars could interfere with DENV replication. This is a little-studied area for DENV, with one publication demonstrating that alongside disruption of viral glycoprotein folding, inhibition of DENV replication contributes to the antiviral activity of *N*N-DNJ against the DENV-2 strain PL046 [58], and CAST was shown to be active against a DENV replicon [352]. However, effects of iminosugars on DENV replication have not been investigated in primary human immune cells. Thus, the impact of 2THO-DNJ, *N*N-DNJ and *N*N-DNJ on DENV replication in MDMΦs was evaluated by quantifying both positive-sense DENV NS5 RNA, present in the virion and during replication, and negative-sense DENV NS5 RNA, present only as a replication intermediate, in infected MDMΦs using a protocol adapted from [58]. DENV RNA was normalised to the housekeeping gene *RPLP2*, which has a stable expression level on iminosugar treatment (8.6), to control for any subtle variations in cell number lysed. Initial investigations utilised our established DENV infection protocol. However, high variability in results meant that the protocol was optimised (see results and discussion in 8.5), resulting in the inclusion of an adsorption phase (1 hour at 4°C), extensive washing in HBSS to remove any unadsorbed virus, and an internalisation step (1 hour at 37°C). This enabled the effects of

iminosugars on DENV replication to be investigated, while avoiding the possibility that iminosugar effects on virus adsorption or cellular entry could influence the results.

Ribavirin was included as a positive control since it has been previously demonstrated to inhibit DENV replication in some cell culture models [490-493]. Mixed efficacy has also been reported in primary human immune cells, with no efficacy seen against DENV-2 16681 in human peripheral blood mononuclear leukocytes [490], while ribavirin was effective against DENV-2 NGC infection of MDMΦs [494]. However, in this assay, ribavirin was an effective inhibitor of DENV replication, significantly reducing the DENV RNA levels at all time points (Figure 20).

At 24 and 48 hours post-infection, the DNJ-derivative iminosugars tested significantly reduced the positive- and negative-sense DENV RNA detected (Figure 20). This would be anticipated for antivirals that act to inhibit virion secretion, since with virus secretion observed from approximately 12 hours post-infection [337, 495], by these time points multiple rounds of viral replication and cellular infection may have occurred. Thus, a reduction in intracellular DENV RNA might be explained by reduced viral secretion limiting the spread of viral infection to further permissive cells, since only 4-21% of the MDMΦ population are typically infected at 48 hours post-infection [7]. Indeed, the levels of intracellular DENV RNA detected increase over time, demonstrating that viral replication is occurring in the untreated conditions (Figure 102). Interestingly, at 12 hours post-infection, corresponding to a single round of replication, 2THO-DNJ and *N*N-DNJ treatment also significantly reduced positive-sense DENV RNA levels in the MDMΦs, and the same trends were seen for negative-sense RNA (Figure 20). *N*N-DGJ had no significant effect on intracellular DENV RNA (Figure 20). Negative/positive sense RNA ratios were consistent across time points and drug treatments (Figure 103) indicating that there was no specific block on *de novo* synthesis of negative-sense RNA for example. These findings indicate

that DNJ-derivative iminosugars can inhibit DENV replication in MDMΦs, contributing to their antiviral efficacy.

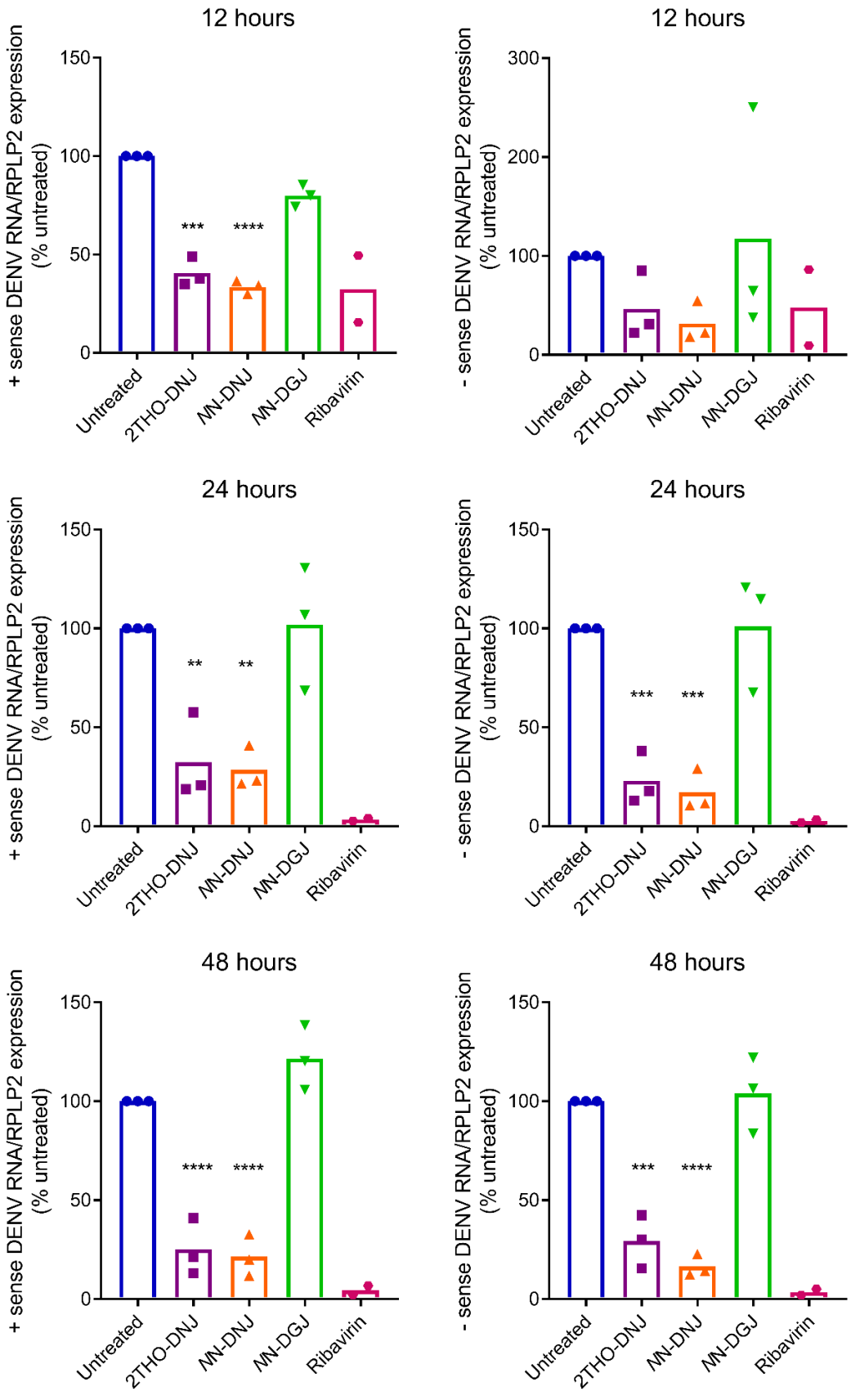

Figure 20. 2THO-DNJ and NN-DNJ inhibit DENV replication in MDMΦs.

Primary MDMΦs (n=3 (NZ, OI, OJ) or n=2 (OI, OJ) for ribavirin treatment, assayed in technical triplicate) were infected with DENV by an hour adsorption step at 4°C, followed by extensive washing in HBSS, and internalisation during a one hour incubation step at 37°C. Cells were then treated with 100 µM of iminosugar or ribavirin until indicated time points. Cellular RNA was extracted, positive- and negative-sense DENV RNA was reverse transcribed, quantified and normalised to RPLP2 *expression levels. Data were normalised to untreated and mean values displayed (bars show the mean of the donors). Statistical analysis was by one-way ANOVA with Dunnett's multiple comparisons test (***, p<0.001). Note that no p values were included for ribavirin since n=2.*

3.3.1.8.2 Investigations using a DENV-2 replicon

In concert with experiments in MDMΦs, a Huh7.5 cell line stably expressing a DENV-2 replicon (excluding E and prM, but containing a luciferase reporter gene; Huh-DENV cells) was utilised. The replicon is continuously replicating in the cells, therefore this system can only elucidate effects of iminosugars on established DENV replication, rather than any effects on *de novo* replication. However, due to the absence of genes encoding DENV structural proteins, virions cannot be produced: hence, the confounding factor of multiple rounds of virus infection is eliminated.

Initially, Huh-DENV cells were treated with titrations of iminosugars to quantify effects on cell viability and on DENV replication (indicated by luciferase activity). The effects on cell viability (Figure 21A) were more pronounced than those seen in the MDMΦs used routinely, but this could reflect the experimental protocol whereby cells were seeded directly in the presence of iminosugar, rather than allowing cell adherence prior to treatment. Note that while the cell viability tests used were different, this is unlikely to account for the discrepancy since both interrogate the same aspect of cellular respiration.

These preliminary data were suggestive of a dose-dependent reduction in DENV replication with *N*N-DNJ, *N*N-DGJ or 2THO-DNJ treatment (Figure 21B), with effects on replication substantially more pronounced than the impact on cell viability (Figure 21C). The short alkyl-chain

iminosugars *N*B-DNJ and *N*B-DGJ did not noticeably impact DENV replication, while the effects of ribavirin were as anticipated for a positive control (Figure 21C). The absence of iminosugar interference with luciferase activity was not confirmed in this assay; however, this possibility is unlikely since iminosugars have been used extensively in luciferase assays, including some of the iminosugars tested here [359, 410, 416], and concentrations up to 1 mM *N*B-DNJ, 240 µM *N*N-DNJ [496], 50 µM *N*N-DGJ [356] and 100 µM BuCAST [395] have previously been reported not to affect luciferase reporter activity.

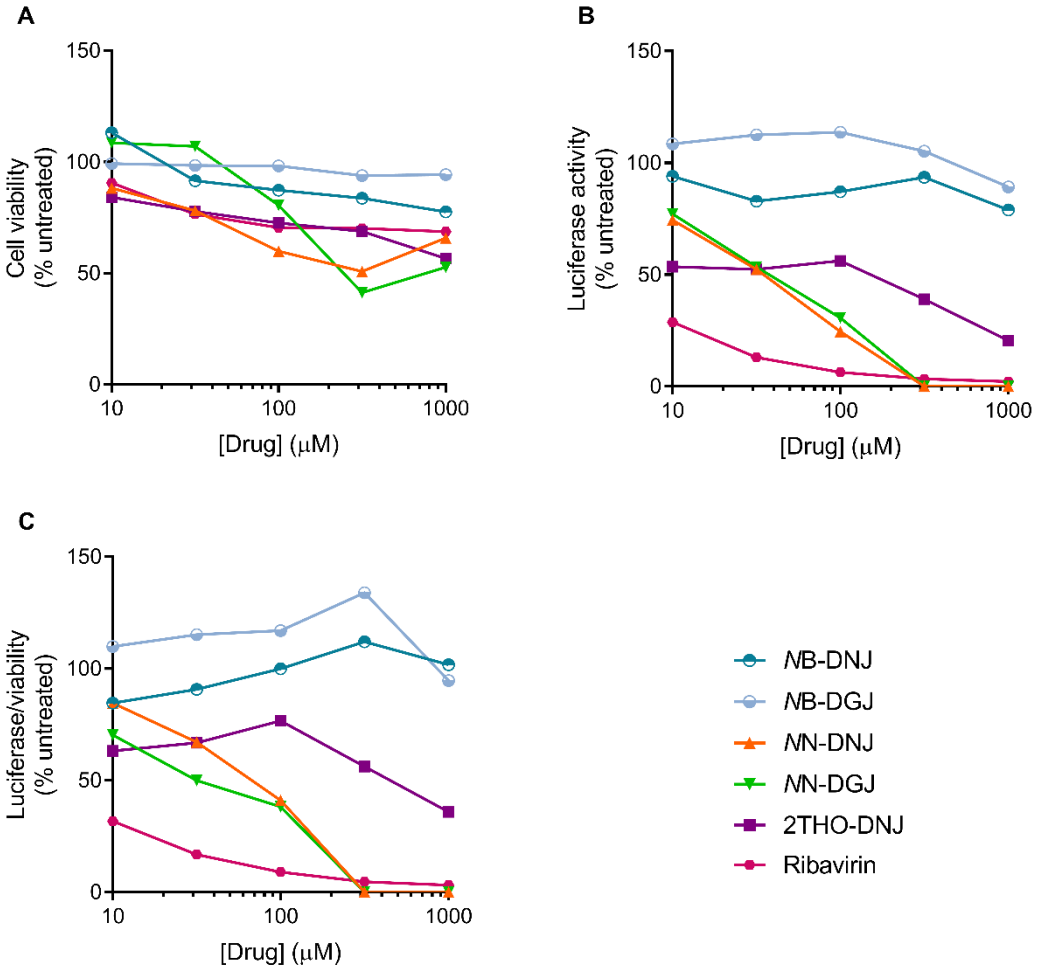

Figure 21. Iminosugars can inhibit replication of a DENV replicon.

Huh-DENV cells (n=1, assayed in technical triplicate) were cultured with iminosugars as indicated for 48 hours.

(A) Cell viability was determined by WST-1 assay, normalised to untreated and the mean displayed.

(B) Luciferase activity was quantified in the same cells, normalised to untreated and the mean displayed.

(C) Luciferase activity was normalised to cell viability for individual replicates and the mean displayed.

Data were collected with the assistance of Andrea Magri, McKeating Group, University of Oxford.

Since the primary aim of this experiment was to evaluate iminosugar impact on cell viability, high concentrations were utilised and consequently significant effects on cell viability were observed. Despite the marked replication of inhibition when normalised to cell viability (Figure 21C), concerns persisted about whether an effect on cell viability could have a disproportionately strong effect on replicon production.

Therefore, non-cytotoxic concentrations (i.e. up to 10% reduction in cell viability) of iminosugar were used in a preliminary experiment measuring the impact of iminosugars on DENV replication over time (Figure 22). As expected, ribavirin and sofosbuvir, a DENV NS5 inhibitor [497], inhibited DENV replication, with the effects of ribavirin observed from very early on compared to those of sofosbuvir, which took approximately 18 hours to become apparent. Effects of iminosugars also started to be observed at later time points and became more pronounced over time. 2THO-DNJ and *N*N-DNJ (both at 10 μM) appeared to inhibit DENV replication, although the impact of these iminosugars on replication was approximately half as strong as the effects of sofosbuvir or ribavirin after 48 hours. This is consistent with the major mechanism of action of ribavirin or sofosbuvir being targeting DENV replication, whereas effects on DENV replication may contribute to rather than constitute the antiviral effect of DNJ-derivative iminosugars. These results require confirmation in further experiments.

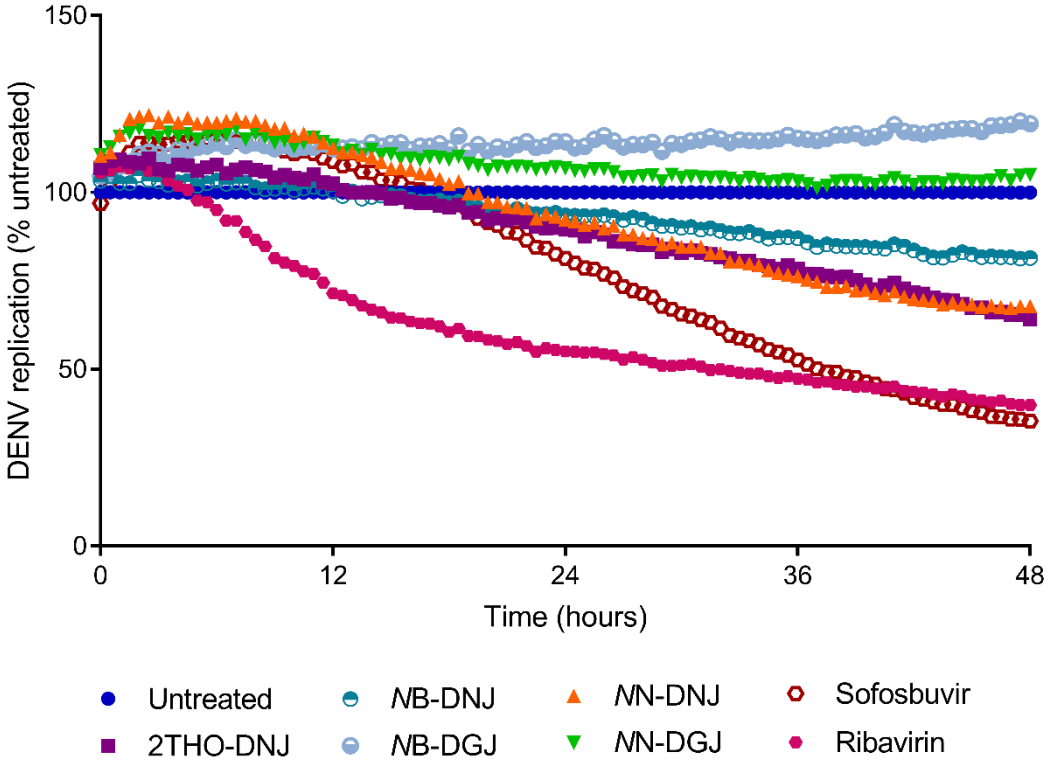

Figure 22. Non-cytotoxic concentrations of 2THO-DNJ and N*N-DNJ can inhibit DENV replication.*

Huh-DENV cells were cultured with 10 µM 2THO-DNJ, N*N-DNJ,* N*N-DGJ, ribavirin or sofosbuvir, or 100 µM* N*B-DNJ or* N*B-DGJ, or media-only (n=1, assayed in technical quintuplicate) for 48 hours in a CLARIOstar instrument. Every 30 minutes, luciferase activity, indicating DENV replication, was quantified and normalised to untreated, and the mean displayed. Data were collected with the assistance of Andrea Magri, McKeating Group, University of Oxford.*

In addition, iminosugars of particular interest (and ribavirin as a positive control) were assayed at higher concentrations, corresponding to approximately 25% reduction in cell viability (Figure 23). At these higher concentrations, an inhibitory effect of 2THO-DNJ and *N*N-DNJ remained apparent. Interestingly, at this concentration, *N*N-DGJ appeared to inhibit DENV replication to a similar extent as *N*N-DNJ. Considering the divergence of 2THO-DNJ and *N*N-DNJ efficacy at this concentration, and the appearance of an effect of *N*N-DGJ, perhaps at such high concentrations there is an additional effect linked to the *N*-nonyl alkyl chain. As previously discussed, perhaps this is mediated by disruption of cell membranes or ER-derived membranous structures required

for viral replication. However, as previously mentioned, these observations require confirmation in additional experiments.

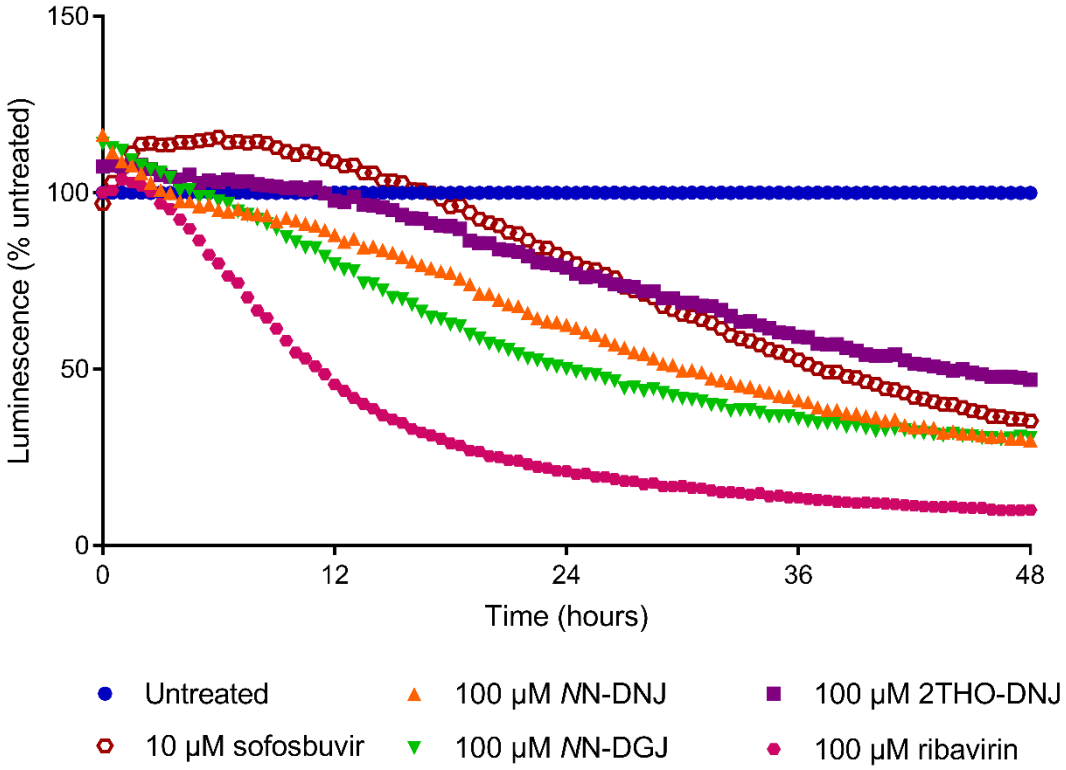

Figure 23. Iminosugar concentrations with <25% reduction in cell viability reduce DENV replication.

Huh-DENV cells were cultured with iminosugar, ribavirin or sofosbuvir (n=1, assayed in technical quintuplicate) as indicated for 48 hours in a CLARIOstar instrument. Every 30 minutes, luciferase activity was quantified, and mean values displayed. Data were collected with the assistance of Andrea Magri, McKeating Group, University of Oxford.

3.3.1.9 2THO-DNJ does not prevent release of assembled virions from cells

While evidence, both presented here and pre-existing, suggests that the direct antiviral activity of 2THO-DNJ is likely to be mediated by reducing viral replication and glycoprotein folding, it has not been demonstrated that the reduced viral secretion results from reduced virion formation, rather than an inhibition of virion release. In order to confirm that correctly assembled and matured virions are not retained within infected MDMΦs, infectious virions released to the supernatant or associated with cells were quantified by plaque assay. No positive control was

included since no inhibitors were identified in the literature that inhibited DENV virion release as their sole mechanism of action [498]. While 2THO-DNJ significantly reduced infectious virus secretion, no accumulation of infectious virions was observed in 2THO-DNJ-treated cell lysates (Figure 24). As anticipated, this demonstrates that 2THO-DNJ is not a virion release inhibitor for DENV.

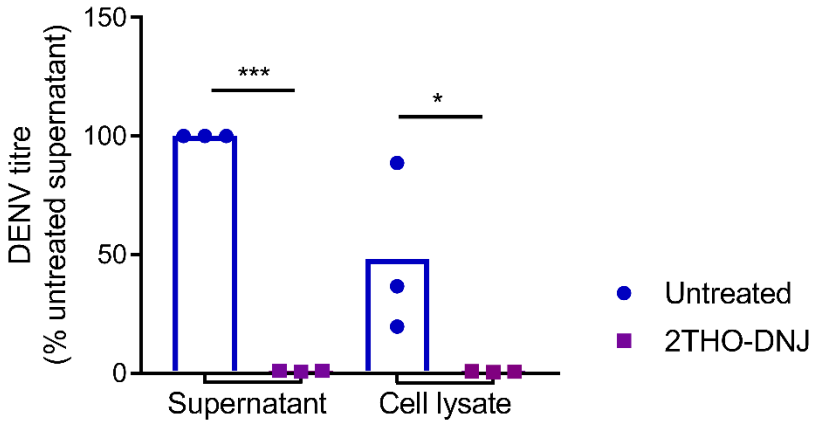

Figure 24. 2THO-DNJ treatment does not result in an accumulation of infectious virions inside MDMΦs.

Primary MDMΦs (n=3 donors (OC, OD, OF), assayed in technical triplicate) were infected with DENV and treated with 100 µM 2THO-DNJ or media only. After 48 hours, supernatants were collected and cell lysates prepared by freeze-thawing. Infectious virus titres were determined by plaque assay. Titres were normalised to untreated and the mean displayed (bars show the mean of the donors). Statistical analysis was by one-way ANOVA with multiple comparisons, using Tukey's multiple comparisons test (, p<0.05; ***, p<0.001).*

3.3.2 ER α-glucosidase inhibition is important for 2THO-DNJ antiviral activity

The antiviral efficacy of 2THO-DNJ against DENV infection of MDMΦs has been demonstrated in 3.3.1. In experiments described in 3.3.1, *N*N-DNJ and *N*N-DGJ were tested alongside 2THO-DNJ where possible. These two iminosugars differ only in the glucose- or galactose-stereochemistry of the headgroup. The inclusion of these iminosugars provided some insight into whether the effects of 2THO-DNJ are dependent on its glucostereochemistry, most significantly indicating that iminosugar effects on DENV replication are associated with this structural feature. In previous studies, the antiviral efficacy of *N*N-DNJ has been attributed to ER α-glucosidase

inhibition, rather than influencing glycolipid processing enzyme activity: a property shared by the long chain *N*N-DNJ and *N*N-DGJ iminosugars regardless of headgroup stereochemistry [337]. The antiviral activity of M*O*N-DNJ was also attributed to ER α-glucosidase inhibition by comparison with *N*-(9'-methoxynonyl)-1,6-dideoxygalactonojirimycin (MON-6d-DGJ) [394]. In the case of 2THO-DNJ, mechanistic investigations have shown inhibition of α-glucosidases using isolated rat liver enzymes and in HL60 and Madin-Darby bovine kidney (MDBK) cells by FOS assay [397]. However, the ability of 2THO-DNJ to inhibit ER α-glucosidases in MDMΦs, and any relationship of this with its antiviral efficacy, has not been demonstrated.

3.3.2.1 2THO-DNJ inhibits ER α-glucosidases in MDMΦs

Considering the previous findings, inhibition of ER α-glucosidases by 2THO-DNJ was characterised by FOS assay in MDMΦs (Figure 25). This technique is an established way of monitoring the induction of ERAD upon inhibition of ER α-glucosidases by iminosugars [499]. Inhibition of ER α-glucosidase II, indicated by accumulation of $Glc_1Man_4GlcNAc_1$ FOS species, was observed at all concentrations of 2THO-DNJ tested. The maximal accumulation of this FOS species was seen at 10 μM 2THO-DNJ, when inhibition of ER α-glucosidase I begins, indicated by accumulation of $Glc_3Man_5GlcNAc_1$ FOS species. At higher concentrations, increased α-glucosidase I inhibition was observed, with a linked reduction in α-glucosidase II inhibition as the supply of substrate glycoproteins to this downstream enzyme is reduced. This indicates that 2THO-DNJ does inhibit ER α-glucosidases in MDMΦs.

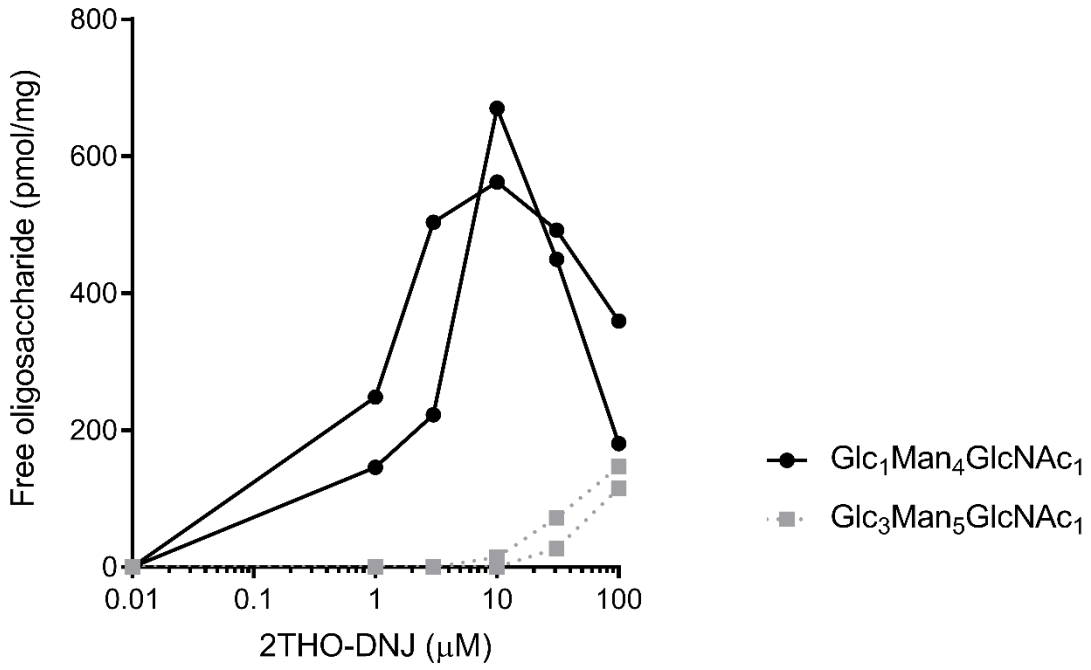

Figure 25. 2THO-DNJ inhibits ER α-glucosidases in MDMΦs.

Primary MDMΦs (n=2 donors (JO, JU), in technical duplicate) were treated with a titration of 2THO-DNJ for 48 hours. Cells were lysed and free oligosaccharide species purified and detected by NP-HPLC and normalised to total protein content. Mean values are presented for individual donors (untreated samples are shown at 0.01 μM to allow plotting on a logarithmic scale). Samples were generated by Beatrice Tyrrell and processed by Michelle Hill and Dominic Alonzi.

3.3.2.2 Lack of 2THO-DGJ antiviral efficacy suggests dependence of 2THO-DNJ efficacy on ER α-glucosidase inhibition

Further evidence that the antiviral activity of 2THO-DNJ is mediated through ER α-glucosidase inhibition was obtained by comparison of the antiviral efficacy of 2THO-DNJ with that of *N*-8'-(2''-tetrahydrofuranyl)-octyl-deoxygalactonojirimycin (2THO-DGJ), a compound with the same tail structure as 2THO-DNJ but with a galactostereochemistry headgroup (Figure 26A). This galactose stereochemistry means that the compound should not be able to competitively inhibit ER α-glucosidases. Since the compound was synthesised for the first time, to our knowledge, in-house (by J.L. Kiappes), this lack of inhibition was verified by FOS assay (Figure 26B). As expected, no significant ER α-glucosidase inhibition was observed. Subsequently, the antiviral efficacy of a titration of 2THO-DGJ was compared to 100 μM 2THO-DNJ (Figure 26C-D). Minimal, if any, effect

on viral secretion was seen at non-cytotoxic concentrations (Figure 85). This suggests that the primary antiviral mechanism of action of 2THO-DNJ is dependent on ER α-glucosidase inhibition.

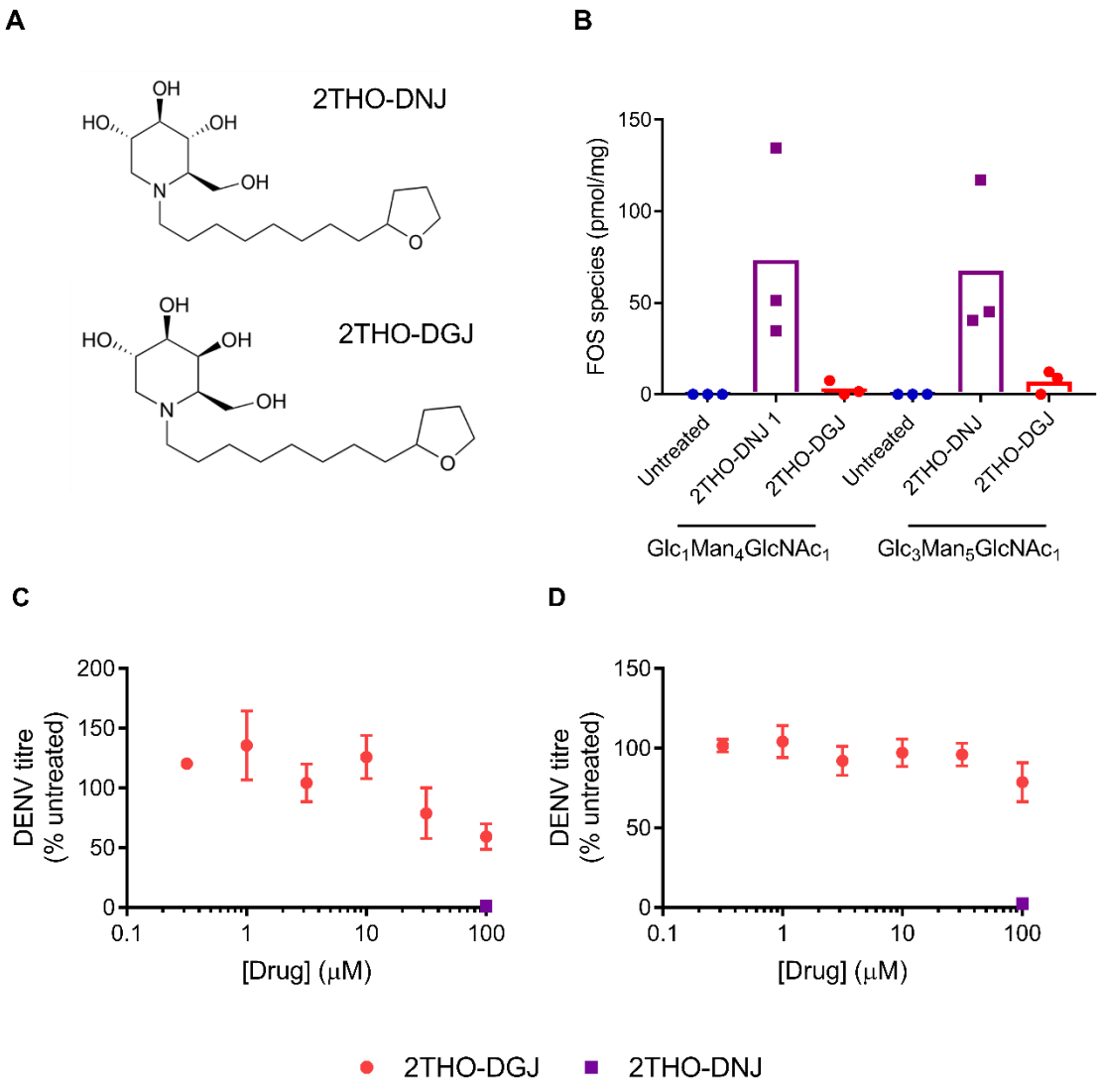

Figure 26. 2THO-DGJ does not have appreciable antiviral efficacy against DENV in MDMΦs.

(A) Chemical structures of 2THO-DNJ and 2THO-DGJ.

(B) For analysis of glucosidase inhibition by free oligosaccharide (FOS) assay, primary MDMΦs (n=3 donors (MB, MC, MD), assayed in technical duplicate) were treated with a titration of 2THO-DGJ or 100 μM 2THO-DNJ for 48 hours. Cells were lysed and FOS species purified and detected by NP-HPLC. The $Glc_3Man_5GlcNAc_1$ and $Glc_1Man_4GlcNAc_1$ FOS species detected, diagnostic for ER α-glucosidase I and II inhibition, respectively, were normalised to total protein content. The mean is displayed (bars shown the mean of the donors).

(C-D) The antiviral efficacy of 2THO-DNJ and 2THO-DGJ was compared by infection of primary MDMΦs (n=3 donors (MB, MC, MP), assayed in technical triplicate) with DENV and treatment as indicated. After 48 hours, supernatants were collected and total virus secretion determined by

DENV NS5 qRT-PCR (C) or infectious virus titres determined by plaque assay (D). DENV genome equivalents (C) or titres (D) were normalised to untreated and displayed as mean ± standard error.

Samples were generated with assistance from Stephen Early, and for (B) processed with assistance from Stephen Early, Juliane Brun, and Dominic Alonzi.

3.3.2.3 Dependence of DENV infection on α-glucosidases supports their selection as drug targets

While the antiviral efficacy of DNJ-derivative iminosugars in DENV infection has been attributed to ER α-glucosidase inhibition [337], it is possible that these compounds could have additional antiviral impact through pathways that are not dependent on an intact calnexin cycle. In order to explore this possibility, iminosugar treatment was used in concert with knockout of either of the ER α-glucosidases. Since it is technically very challenging to produce knockouts (or lasting knockdown) in primary MDMΦs, in part due to their non-replicating nature, Vero cells knocked-out for ER α-glucosidase I (Vero-GluI) or II (Vero-GluII) using CRISPR/Cas9 technology were utilised for this experiment alongside wild-type (Vero-WT) controls.

Ribavirin was included as a positive control, since it has previously been reported to be effective in Vero cells, with 50% inhibitory concentrations for DENV-2 reported in the order of 25-75 µM [164, 500, 501]. However, due to the cytotoxicity profile determined for these cells (Figure 89), 25 µM ribavirin was used, which had a slight but not significant antiviral effect (Figure 27). Treatment with a panel of iminosugars at non-cytotoxic concentrations (Figure 89) largely showed the expected pattern of efficacy in the Vero-WT cells, although in one experiment *N*N-DGJ had an antiviral effect leading to the higher error and statistical significance (Figure 27A). A dominant antiviral effect of either glucosidase knockout was seen, almost abrogating viral secretion. This rendered the evaluation of the contribution of potential off-target iminosugar effects to antiviral efficacy impossible, while providing further evidence of the importance of α-glucosidases for DENV infection.

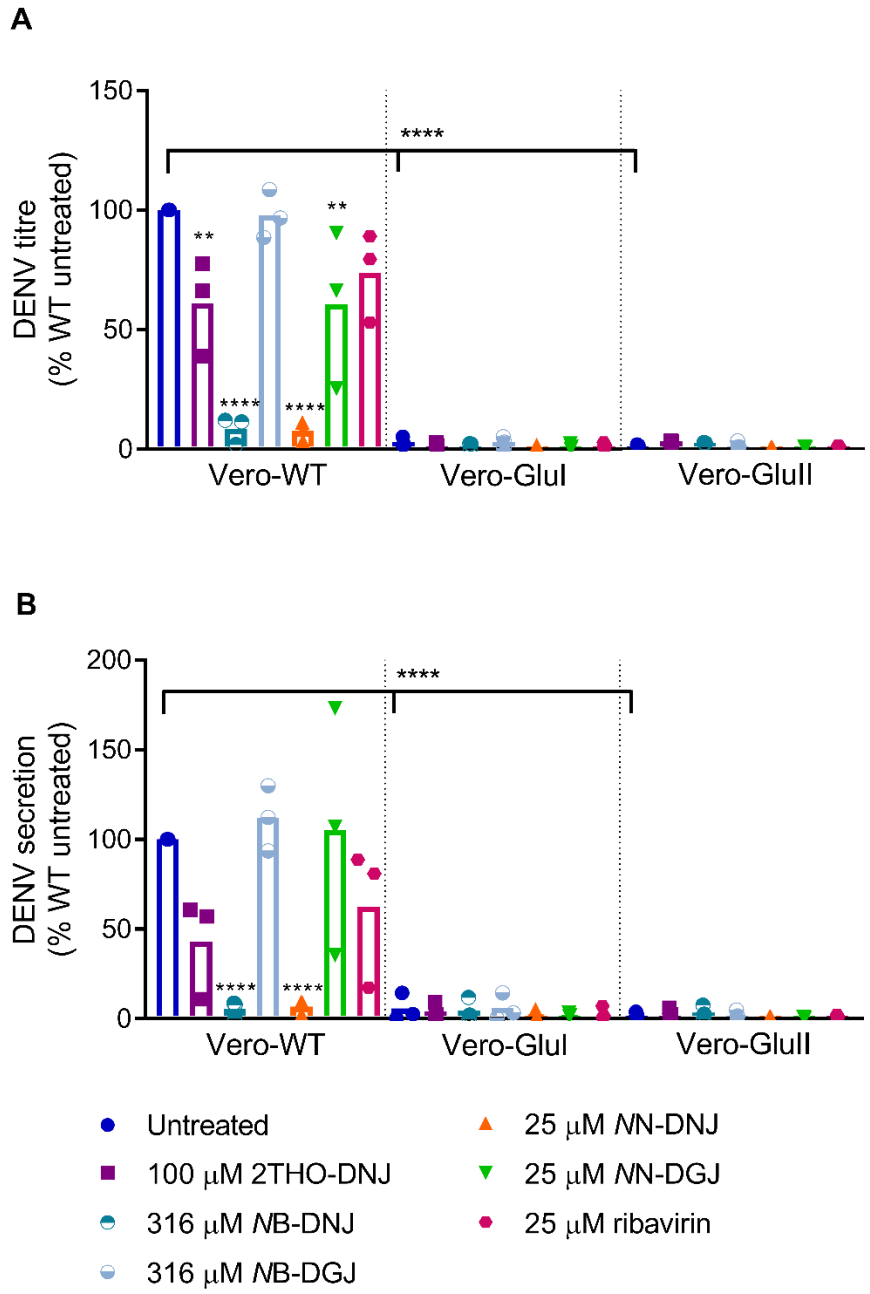

Figure 27. Glucosidase knockouts and DNJ-derivative iminosugars are antiviral against DENV in Vero cells.

*Vero-WT, Vero-GluI and Vero-GluII cells (n=3, assayed in technical triplicate) were infected with DENV and treated as indicated. After 4 days, supernatants were collected and total virus secretion determined by DENV NS5 qRT-PCR (A) or infectious virus titres determined by plaque assay (B). DENV genome equivalents (A) or titres (B) were normalised to untreated. Mean values are displayed. Statistical analysis was by one-way ANOVA with Tukey's multiple comparisons test (**, p<0.01; ****, p<0.0001). Asterisks shown directly above bars denote comparisons to the untreated condition within a cell type.*

3.3.3 Iminosugars are not antiviral against DENV in mosquito cells

While limited studies of iminosugar efficacy have been conducted in mosquitos and found no evidence of an effect, a broader panel of iminosugars was tested for efficacy in the C6/36 *Aedes albopictus* cell line. Positive controls were included alongside iminosugars. ι-carrageenan, a type of sulfated polysaccharide, has previously been reported to inhibit DENV infection of a high temperature (33°C)-adapted C6/36 cell line through a cell-dependent mechanism (in contrast to heparan sulfate structural mimicry-mediated inhibition of DENV entry in mammalian cells) [502]. While no studies were identified testing ribavirin in C6/36 cells, it was reported to inhibit DENV replication in *Aedes aegypti* infection [503]. Non-cytotoxic concentrations of these controls (Figure 90) were potently antiviral (Figure 28), likely demonstrating the antiviral efficacy of ribavirin in this system for the first time. In contrast, none of the iminosugars tested significantly inhibited DENV production. However, *N*N-DNJ treatment gave a slight but statistically significant increase in DENV titre. However, this is unlikely to be biologically significant considering the sensitivity of the plaque assay detection method. Taken together, this suggests that iminosugar treatment would not impact mosquito transmission of DENV once they were infected, were mosquitos to come into contact with the compounds.

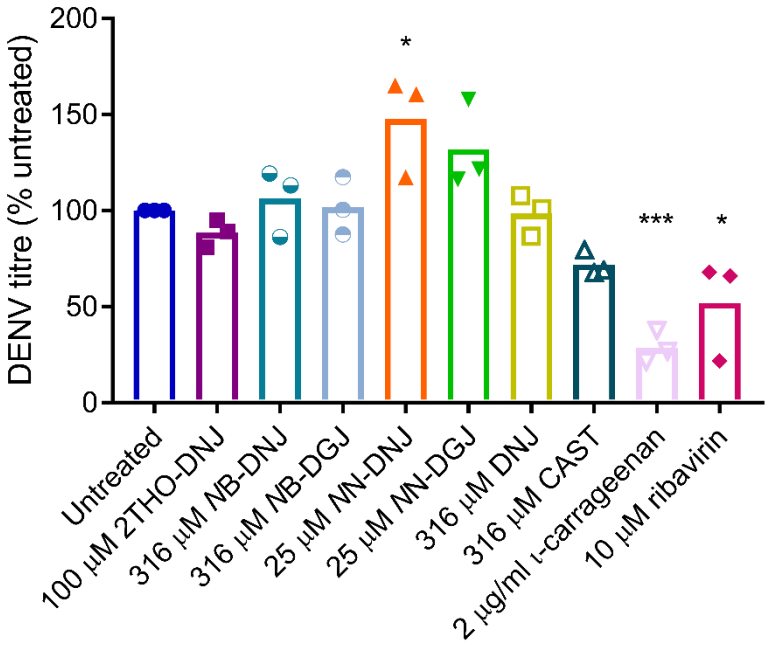

Figure 28. Iminosugars are not antiviral against DENV in C6/36 mosquito cells.

C6/36 cells (n=3, assayed in technical triplicate) were infected with DENV and drug-treated as indicated. After 48 hours, supernatants were collected and infectious virus titres determined by plaque assay. Titres were normalised to untreated and mean values displayed (bars show the mean of the experiments). Statistical analysis was by one way ANOVA with Dunnett's multiple comparisons test (, p<0.05; ***, p<0.001).*

3.4 Discussion

This chapter considered the antiviral mechanisms of 2THO-DNJ against DENV in MDMΦs, with reference to the activity of other iminosugars. MDMΦs were used in this study because of the natural tropism of DENV for these cells during human infection [112-114]. Here, MDMΦs were partially matured from monocytes derived from peripheral blood of healthy human donors, using IL-4. This is physiologically-relevant since murine studies provide evidence of significant IL-4 production and a shift from Th1 to Th2 cytokine responses at the site of mosquito bites, at least partially elicited by mosquito salivary proteins [107, 108]. This would promote macrophage differentiation towards an M2 phenotype, as conducted here. Differentiation of MDMΦs using IL-4 also increases the DENV infection rate, linked to upregulated surface expression of the

mannose receptor and DC-SIGN [7]. This effect is also seen with IL-4 treatment of CD14+ dermal DCs or dermal macrophages isolated from human skin [504], and facilitates the study of antivirals by increasing the range over which an antiviral effect might be observed.

In this model, viral titres produced by MDMΦs derived from different donors vary significantly. Multiple factors are likely to contribute to this variation. One possibility would be variation in DENV receptor expression, and variability in the impact of IL-4 treatment on this. Differences in mannose receptor expression between donors [7] might play a significant role, and the impact that receptor variation could have is compounded by the wide array of attachment and entry factors identified for DENV. Viral titres might also be influenced by the MDMΦ immune response to infection, particularly the IFN-α/β response which varies between donors (Figure 118B, for example). Serostatus might also contribute to variability, as although MDMΦ donors must meet NHSBT travel-related blood donation eligibility rules [505], it is possible that any circulating DENV IgG could be retained in the autologous serum used as they would be unlikely to aggregate and be removed following the 56°C heat-inactivation step [506, 507]. In addition, slight cell-type impurities in the monocytes isolated [7] might influence resulting viral titres, since there is patient-derived evidence for DENV replication in B cells [112, 116] and platelets [117].

2THO-DNJ reduces infectious virus production with a similar potency to other DNJ-derivatives tested in this model [398], with an IC_{50} of 5.21 ± 2.5 μM against DENV-2 strain 16681 determined from analysis of eleven MDMΦ donors. The IC_{50} of 2THO-DNJ against the DENV-2 NGC strain in Vero cells was previously reported to be 21.71 μM [397], and 100 μM 2THO-DNJ treatment was much less efficacious in Vero cells compared to MDMΦs in this study (Figure 7 versus Figure 27). This observation of enhanced efficacy in MDMΦs compared to Vero cells is in accordance with results for the iminosugar M*O*N-DNJ [394]. Efficacy data for bicyclic iminosugars indicates that cell type plays a role in iminosugar efficacy variation (Table 2), with the efficacy of CAST against

DENV-2 differing significantly in Huh7 human hepatoma and BHK-21 cells [352], and BuCAST efficacy varying between Vero, BHK-21 and Huh7 cell infection for multiple DENV serotypes [403]. This is in accordance with the cell type-dependent effects described for INFV [314]. In addition, significant variation in M*O*N-DNJ activity was seen in Vero cells infected with different strains of DENV, within each serotype, although all IC_{50}s were in the μM range [394]. Therefore it is likely that the observed differences in 2THO-DNJ efficacy are accounted for by a combination of within-serotype strain variation and cell type-dependence. Despite the long-standing dogma of protective serotype-wide antibody responses being elicited upon infection, there is increasing appreciation that variation in the E protein in different strains or genotypes within a serotype influences antibody binding and neutralisation [50, 508, 509], as well as E protein glycosylation [50], which might be pertinent to iminosugar efficacy. Multiple factors may explain cell type-dependent efficacy, including variation in plasma and ER membrane composition, determining iminosugar access to their ER targets [510], and potential transporters affecting cellular uptake of iminosugars [511]. Glycoprotein processing pathway components also vary between cell types [328, 512], which could affect the processing and dependence of viral glycoproteins on the calnexin cycle, and thus their susceptibility to iminosugar treatment.

The antiviral activity of 2THO-DNJ against DENV is associated with the inhibition of ER α-glucosidases. Here, this has been determined by the detection of FOS species characteristic of their inhibition, and comparison of the antiviral efficacy with the ineffective galactose-stereochemistry analogue 2THO-DGJ. FOS were detected in MDMΦs treated with 2THO-DNJ, with inhibition of ER α-glucosidase II observed at lower concentrations than ER α-glucosidase I. This is the inverse of the inhibitory activity seen against isolated rat liver glucosidases, where 2THO-DNJ was more inhibitory for α-glucosidase I, but is in accordance with the detection of diagnostic FOS in 2THO-DNJ-treated HL60 cells [397]. This suggests that in the context of the ER, it is more difficult for 2THO-DNJ to act on α-glucosidase I than II, which could possibly be

explained by the membrane-bound versus soluble enzyme localisations, or kinetic factors since initial glycan processing by α-glucosidase I occurs rapidly after the addition of the oligosaccharide precursor, while α-glucosidase II acts later [499, 513]. The ability of 2THO-DNJ to bind to α-glucosidases was also demonstrated by isothermal titration calorimetry, with the binding affinity (K_D) of 2THO-DNJ for recombinant *Mus musculus* α-glucosidase I predicted to be 126.9 nM (Johan Hill, unpublished data). The inhibition of α-glucosidases by 2THO-DNJ has been demonstrated to be transient in MDBK cells, with a half-life for ER α-glucosidase I inhibition of around 5 hours [397]. This transient inhibitory activity links to the finding that withdrawal of 2THO-DNJ treatment from infected MDMΦs leads to a loss of iminosugar-mediated suppression of virus titres. However, this transient suppression of virus production is unlike the finding of long-lasting efficacy of high dose *N*B-DNJ and M*O*N-DNJ treatment, sufficient to inhibit ER α-glucosidase I *in vivo*, in mouse models of DENV and INFV (Nicole Zitzmann, personal communication).

DENV secretion from Vero cells with ER α-glucosidase I or II knocked out was dramatically reduced, so much so that off-target effects of iminosugar treatment could not be evaluated. The effect of the knockouts was stronger than that reported in Huh7.5 cells, where a one-to-two log decrease in DENV titres was seen [226], indicating that there may be an element of cell-type specificity here. It is also important to recognise that Huh7.5 cells are not immunocompetent, thus it is possible that in a MDMΦ, the functional immune response might influence the infection and the response to iminosugar in the context of knockout or inhibition of ER α-glucosidases: an area explored in 0. In any case, achieving a similar reduction in viraemia in the clinic would be beneficial since patient studies have shown links between higher viraemia and disease severity [514]. The striking antiviral effect of the glucosidase knockouts indicates the importance of the calnexin cycle for DENV infection of mammalian cells and supports targeting ER α-glucosidases with iminosugars as an antiviral strategy.

Evidence suggests that 2THO-DNJ inhibits the formation of infectious virions. This is likely to be mediated by a combination of effects involving the misfolding of the N-glycosylated viral structural proteins prM and E, as shown previously for other antiviral iminosugars [51, 58, 352, 395], and the inhibition of DENV replication, perhaps via an effect on the N-glycosylated NS1 and NS4B, here demonstrated for the first time in MDMΦs.

While it is clear that 2THO-DNJ treatment reduces viral secretion, the lack of infectious virion accumulation inside treated MDMΦs does not differentiate between reduced virion formation, as a consequence of irretrievable misfolding of structural glycoproteins, or the possibility that virion formation occurs but virions are subsequently degraded intracellularly, perhaps being directed for proteasomal degradation by the ERAD pathway. A combination of these mechanisms is also possible, and this would likely depend on the extent to which prM and E are misfolded. The established observation that significantly more DENV virions are secreted than those quantified in infectious virus titres demonstrates that assembled virions with poor infectivity are secreted [484]. Indeed, under normal circumstances, virions are secreted at a range of maturation statuses, and thus infectivities (although interaction with anti-prM antibodies may render an otherwise non-infectious virion infectious through ADE). It is possible that any structural glycoproteins with iminosugar-induced misfolds that are incorporated into virions might be less accessible to the Golgi furin responsible for prM cleavage and virion maturation. This would lead to a reduction in specific infectivity, such as that seen with 2THO-DNJ treatment. Considering the distinctive appearance of mature, immature and partially-mature DENV virions using imaging techniques such as cryo-EM [515], it would be interesting to attempt to visualise virions secreted under the pressure of iminosugar treatment to determine the influence of iminosugars on virion maturation.

The reduction in virion specific infectivity observed with higher-concentration 2THO-DNJ treatment is also seen with other iminosugars (Figure 11 and [352]). The concentration-dependence of the effects observed may indicate that the reduction in specific infectivity is linked to the more complete, earlier-stage, blockade of glycoprotein processing resulting from inhibition of ER α-glucosidase I in addition to that of ER α-glucosidase II. Perhaps the halting of glycan processing at the triglucosylated stage enables the escape of misfolded viral glycoproteins from the ER before entering the calnexin cycle proper, avoiding the quality control oversight of UGGT that they would face as monoglucosylated glycans. These glycoproteins might then be incorporated into virions, consequently of reduced infectivity. Indeed, triglucosylated glycans have been detected on haemagglutinin molecules of INFV grown in the presence of *N*N-DNJ [324], indicating that there is a mechanism enabling incorporation of these unprocessed glycoproteins into virions. While the impact on specific infectivity has not been analysed for all viruses where iminosugar treatment is efficacious (Table 1), reductions in specific infectivity were seen for HIV-1 with CAST [346], DNJ [346] or *N*B-DNJ [347, 348] treatment, for cytomegalovirus with CAST treatment [349], and very substantially for Kunjin virus with *N*N-DNJ treatment [350]. In addition, for bovine viral diarrhoea virus (BVDV), the antiviral effect of *N*N-DGJ, which does not reduce virion secretion, was attributed to effects on the envelope proteins [341], although this could also be contributed to by disruption of the p7 viral ion channels as demonstrated for HCV [356, 414, 415]. However, CAST did not affect WNV specific infectivity [352], indicating that the effect is virus- rather than drug-specific.

Investigating the mechanism by which DENV secretion is reduced would require detailed examination of the effects of 2THO-DNJ on viral glycoprotein folding. However, this is non-trivial. One method of monitoring abundance and folding status of the viral glycoproteins, as extensively conducted for iminosugar-treated HIV [516], would require panels of well-defined antibodies that could detect viral glycoproteins in a range of folding statuses, including that

which might be induced by iminosugar treatment. Whether a linear epitope antibody, with the epitope spaced away from glycosylation sites, would satisfy this requirement is uncertain, precisely because we do not know what the misfolded glycoprotein looks like. Current evidence of iminosugar-induced viral glycoprotein misfolding is mostly concentrated around observations of altered molecular weight or electrophoretic mobility, related to impacts on glycan processing. There is also evidence of functional impacts on DENV glycoprotein folding including impaired prME dimer formation (Table 1 and Table 2). A better understanding of iminosugar-induced glycoprotein misfolding would enable analysis of the folding status of viral glycoproteins in infected cell extracts or potentially could be combined with imaging techniques to establish localisation and kinetic aspects of iminosugar effects. An additional difficulty with investigating effects on glycoproteins is that proteasome inhibitors are themselves antiviral against DENV. Multiple mechanisms have been described, including enhancing virion egress in ADE-infection of primary monocytes [517] and proteasomal degradation of the antiviral Sec3p being stimulated by DENV C, leading to increased viral RNA transcription and translation [518]. Proteasome inhibitor treatment also reduced viral load and pathology in murine infection [517]. Preliminary data indicated that the reduction in DENV titre with proteasome inhibitor treatment was also observed in the non-ADE primary MDMΦ model used here (Figure 104). This hampers determination of the role played by proteasomal degradation in processing of misfolded DENV glycoproteins.

Another interesting consideration is that it is currently assumed that the DENV RNA genomes detected in the supernatant represent secreted virions, which may or may not be infectious. However, while the DENV NS5 qRT-PCR is designed to detect complete viral genomes only, it is possible that some of the 'secreted virus' is actually secreted viral genome not contained within a virion, perhaps within exosomes. This is an intriguing possibility due to recent observations made with other viruses. The release of exosomes containing viral genomes with or without viral

proteins has been identified in cell culture models for other RNA viruses including Rift Valley fever virus (RVFV) [519] and human T-lymphotropic virus type 1 [520]. In the case of HCV, viral RNA-containing exosomes can mediate productive infection in target cells, potentially contributing to viral transmission, as well as activating innate immune responses [521-523]. Exosome production by MDMΦs infected with HIV-1 has also been observed [524]. There are currently no reports of DENV-infected mammalian cells producing exosomes containing viral RNA. However, exosomes containing immune response proteins have been identified in DENV-infected human cell lines [525]. Recently, DENV-infected mosquito cells have been reported to produce small extracellular vesicles (including, but not solely, exosomes) containing full-length DENV-2 RNA capable of mediating infection of mosquito and mammalian cells [526]. Furthermore, the mosquito glycoprotein Tsp29Fb, a putative orthologue of the mammalian exosome marker CD63, was found to directly interact with DENV E protein and contribute to the extracellular vesicle-mediated transmission of DENV [526]. If primary human cell-produced exosomes were shown to contribute to DENV infection, it would be interesting to study the effects of iminosugar treatment on this transmission mode, particularly if an interaction between E and the human N-linked glycoprotein CD63 is also demonstrated.

Besides effects on DENV structural proteins, it has been demonstrated here that *N*N-DNJ and 2THO-DNJ can inhibit DENV replication in MDMΦs. These observations are in accordance with the inhibitory effects of *N*N-DNJ on DENV replication in BHK-21 cells [58] and CAST against a DENV replicon [352], but extend such findings to a more physiologically-relevant cell type. This work also provides additional support for the phenomenon being linked to the glucose stereochemistry of these iminosugars. Inhibiting viral replication has been considered as a mechanism of action of iminosugars against a limited number of other viruses. However, an absence of a direct effect of *N*N-DNJ and *N*N-DGJ on viral replication was demonstrated for the bovine flavivirus BVDV, assessed by [5,6-^{3}H]uridine incorporation into BVDV genomic RNA [341].

For HCV, conflicting evidence exists, with no effect of *N*N-DNJ or *N*N-DGJ seen on replication of a subgenomic JFH-1 replicon [356], while the DNJ-derivative PBDNJ0804 reduced HCV intracellular viral RNA [354]. However, the latter analysis was conducted 4 days post-infection, thus this could be accounted for by reduced infectious virus production over multiple rounds of infection. These previous data indicate that iminosugar effects on viral replication certainly do not appear to be pan-flavivirus, and may be restricted to DENV. However, mechanistic analysis beyond the correlation of altered production, glycosylation or localisation of viral structural glycoproteins or virion infectivity with reduced infectious viral titres has not been conducted for most viruses where iminosugars have been found to be effective (Table 1). Thus, further interrogation of iminosugar mechanisms linked to inhibition of viral replication is warranted.

It is tempting to speculate that impacts on the glycoproteins NS1 or NS4B, implicated in viral replication, might unify the inhibition of DENV replication and ER α-glucosidases by DNJ-derivative iminosugars. Such an effect on NS1 has previously been proposed [58]. NS1 colocalises with the DENV-induced vesicle packets and replication complex [61], likely interacting with NS4A and NS4B: mutations in a 'greasy-finger' loop in the hydrophobic protrusion of NS1 inhibit viral replication [62]. In addition, DENV NS1 can interact with and remodel membranes [62], which might play a role in the formation of the ER-derived membranous structures critical for viral replication [21]. NS1 has also been reported to promote viral replication by interacting with vimentin and human heterogenous ribnocucleoprotein C1/C2, involved in mRNA production [63, 64], and by interacting with or relocalising the 60S ribosomal proteins RPL18, RPL18a and RPL17 to viral replication sites [65]. NS4B is also a component of the replication complex, and disrupts NS3 binding to DENV ssRNA which may increase NS3 productivity and thus viral replication [90]. Studies with WNV [91] and HCV [92] suggest that flaviviral NS4B may contribute to virus-induced membrane remodelling. Furthermore, N-linked glycosylation of both proteins has been shown to be important for their

roles in DENV replication, with the mutation of either or both glycosylation sites in NS4B reducing DENV replication [93]. For NS1, the impact of disrupting either glycosylation site on replication is somewhat contentious, with reports of impaired replication with mutation of N207 but not N130 in the DENV-2 TSV01 NS1 [85], and reduced growth in C6/36 cells for DENV-2 16681 mutated at either glycosylation site, but only some attenuation of replication in LLC-MK_2 cells for the N207 mutant [86], while more recently, glycosylation of N130 was found to be essential for replication of a recombinant DENV-1 derived from the NIID02-20 isolate in mammalian cells [87]. Although limited studies have been conducted, *N*N-DNJ and BuCAST have been shown to disrupt the production, folding and secretion of DENV NS1 (Table 2; [58, 395]). The inhibitory effect of BuCAST on a DENV-2 NGC replicon, lacking structural proteins, was attributed to effects on NS1 [395], although the subsequent report of NS4B glycosylation warrants consideration of altered NS4B production or function as a mediator of iminosugar effects. It would be interesting to pursue the possible link between NS1 and NS4B misfolding or degradation and the inhibition of DENV replication in MDMΦs. However, previous attempts in the laboratory to detect NS1 in or secreted by infected MDMΦs using commercially-available antibodies have met with limited success. Even with sufficient expression levels, the considerations discussed for antibody-mediated detection of structural proteins remain problematic. However, if identified, effects on NS1 or NS4B could play a significant role in reducing virion formation and secretion, and the relative contributions to iminosugar efficacy made by the disruption of structural and non-structural proteins would need to be evaluated. Due to the pleiotropic effects of NS1, iminosugar-induced changes in NS1 would likely have wide-ranging impacts on DENV pathogenesis beyond inhibiting viral replication which would also be important to evaluate.

Besides characterising the mechanism of action of 2THO-DNJ, interesting observations have also been made about the effects of *N*N-DNJ and *N*N-DGJ on DENV infection of MDMΦs, particularly

the ability of *N*N-DNJ to inhibit DENV replication, discussed previously, and the enhancement of DENV entry seen with *N*N-DGJ treatment. Previous investigations of iminosugar effects on viral entry are limited. *N*N-DNJ and *N*N-DGJ reportedly reduced entry of HCV [356], although while the iminosugars were only present for the 4 hour infection period, the readout for entry was 72 hours post-infection, during which period residual iminosugar or alternative iminosugar effects initiated during the infection period might influence the results. The reduced efficacy of CM-10-18 or PBDNJ0804 treatment in cells persistently infected with HCV compared to *de novo* infection was deemed suggestive of inhibition of viral entry [354], although this could be accounted for by effects on cellular remodelling required for viral replication. Iminosugar pre-treatment of MDBK cells for 24 hours has also been reported to reduce permissiveness for BVDV [354]. Pre-treatment of Huh7.5 cells with DNJ-derivative iminosugars for 3 days led to reduced entry of lentiviral particles pseudotyped with the envelope proteins of SARS-CoV, HCoV-NL63 or H1N1 IAV. SARS-CoV and HCoV-NL63 share the ACE2 entry receptor: iminosugar treatment affected ACE2 glycosylation and the ability of the receptor to trigger membrane fusion [410]. However, the entry of lentiviral particles pseudotyped for HCV, VSV, MLV, EBOV or LASV was unaffected [410], indicating that the effects on viral entry are not universal. Here, the effects of iminosugars present only during a single hour internalisation period were assessed, finding no effect of DNJ-derivative iminosugars but, surprisingly, a significant enhancement of DENV entry in the presence of *N*N-DGJ. However, this experiment quantified DENV genomes that had entered MDMΦs rather than the infectious potential of the entered virus. Considering the lack of enhancement in viral titre 48 hours post-infection seen here, or under continual *N*N-DGJ treatment [337], this enhancement of entry could be independent of virion infectivity and seems to be of limited importance in the context of longer duration infection. It is possible that the effects of *N*N-DGJ on DENV entry to cells could be accounted for by a detergent-like effect of *N*N-DGJ, disrupting the lipid membranes of the viral envelope or cell membrane. The different positions of the hydroxyl group in the *N*N-DNJ and *N*N-DGJ headgroups could explain why the

effect of *N*N-DGJ is more pronounced, as the grouping of hydroxyls could affect the interaction of the headgroup with the aqueous environment if the hydroxyl tail is embedded in a membrane. While some analysis of the critical micelle concentration of different iminosugars has been conducted [340], *N*N-DNJ and *N*N-DGJ have not been compared directly and limited technique sensitivity and the dominant effect of solvent composition might obscure subtle differences between the compounds. In the context of longer-duration iminosugar treatment of a viral infection, it seems more likely that any effects of iminosugars that alter DENV receptor expression or function would be more significant in determining DENV entry to MDMΦs. Indeed, iminosugars have previously been demonstrated to affect coronavirus entry through altering receptor function [410], and this matter has been the subject of recent investigation in the laboratory for DENV (Joanna Miller, personal communication).

The possibility for iminosugars to affect DENV production in the vector phase of the life cycle was also investigated using infected *Aedes albopictus*-derived C6/36 cells treated with a panel of iminosugars. No striking effects on DENV titre were seen on treatment of DENV-infected C6/36 cells with a panel of iminosugars (Figure 28), in accordance with previous studies finding that neither DNJ or CAST treatment [433] nor silencing one of the mosquito α-glucosidases [434] had an antiviral effect. Taken together, this indicates that iminosugars would be unlikely to influence mosquito transmission of DENV. Considering the applicability of DENV antivirals for mosquitos more broadly, differential efficacy in mammalian and mosquito cells is an established phenomenon. For example, chloroquine is an effective antiviral against DENV in Vero cells, likely through subverting virus fusion with the endosomal membrane, but is not antiviral in C6/36 cells [527]. Similarly, SDM25N, a δ-opioid receptor antagonist which targets NS4B, is effective in BHK-21 and HeLa cells, but not in C6/36 cells [528]. And, while ι-carrageenan, the positive control used here, is antiviral in both Vero and C6/36 cells, this is accounted for by reducing virion binding in Vero cells but through a cell-intrinsic mechanism reducing permissiveness in the

mosquito cells [502]. Thus, the infection mechanisms used by DENV in mammalian and mosquito cells differ. In the case of iminosugars, the lack of efficacy in mosquito cells is in line with the reduced requirement for N-glycosylation of E for functional DENV production in mosquito cell culture [36] or in *Aedes aegypti* mosquitos [37] relative to mammalian cells. Furthermore, this suggests that the production of DENV virions infectious for mammalian cells does not require interaction of viral glycoproteins with the calnexin cycle in mosquito cells. This is in stark contrast to the dependence of DENV on the ER α-glucosidases in mammalian cells, and this discrepancy should be a target of further research.

While taking a systematic approach to identifying 2THO-DNJ mechanisms of action in a physiologically-relevant cell type, many possibilities exist to extend the findings of this work. The scope of this investigation is restricted to a single DENV-2 strain, but it would be of interest to investigate the antiviral efficacy of 2THO-DNJ across different DENV serotypes and in clinical isolates, in order to better represent human infection. The findings are also restricted to the MDMΦ model. Concurrent work has confirmed the antiviral efficacy of 2THO-DNJ in primary human monocyte-derived dendritic cells [483], but exploring iminosugar efficacy in a mixed immune cell population would be interesting, allowing better representation of bloodstream infection in a human. It is possible that network interactions between the immune cells could influence the response to infection and iminosugar treatment. Preliminary experiments investigating the efficacy of iminosugars against DENV-infected PBMCs suggested that antiviral responses were consistent with those in MDMΦs, with 2THO-DNJ and *N*N-DNJ effective, and *N*N-DGJ and 2THO-DGJ lacking antiviral activity (Figure 96). It is encouraging that DNJ-derivative efficacy appears to be retained in this mixed immune cell context, and it would be interesting to optimise this infection model in order to establish which cell types are infected, and investigate the dynamics of the infection and response. Another facet of DENV infection of immune cells, ADE, has not been explored in this project. It would be interesting to investigate iminosugar

efficacy in ADE infection of MDMΦs [15], particularly with respect to the differing methods of cellular entry and the impact of iminosugars on the cytokine response to infection (considered in 0) via this route considering the phenomenon of intrinsic ADE.

In summary, iminosugar treatment impacts DENV infection of MDMΦs in multiple ways (Figure 29). 2THO-DNJ has antiviral efficacy in this system, which is related to the glucostereochemistry and inhibition of ER α-glucosidases. The DNJ-derivative iminosugars *N*N-DNJ and 2THO-DNJ inhibit DENV replication and reduce the secretion of virions from infected cells. Impacts on viral N-glycoprotein folding are likely to contribute to the reduced virion secretion through inhibiting virion formation, since there was no accumulation of infectious virions associated with cells treated with 2THO-DNJ. The specific infectivity of secreted virions was also reduced by 2THO-DNJ, also likely to be mediated by viral glycoprotein misfolding. DNJ-derivatives did not affect the binding or entry of virions to MDMΦs, and it is unlikely that any of the tested iminosugars have functionally important virucidal activity in solution. *N*N-DGJ treatment enhanced DENV entry over a short time period, as determined by quantification of genome equivalents, although the relevance of this observation is uncertain considering the lack of proviral activity of *N*N-DGJ over longer treatment periods. Moving away from mammalian cells, iminosugars lacked antiviral efficacy in DENV-infected C6/36 mosquito cells. This suggests that there is differential dependence on N-glycosylation pathways for the production of infectious virions in mammalian and mosquito cells. Further mechanistic analysis is warranted in both settings in order to enhance our understanding of how iminosugars interfere with DENV infection and to elucidate the factors involved.

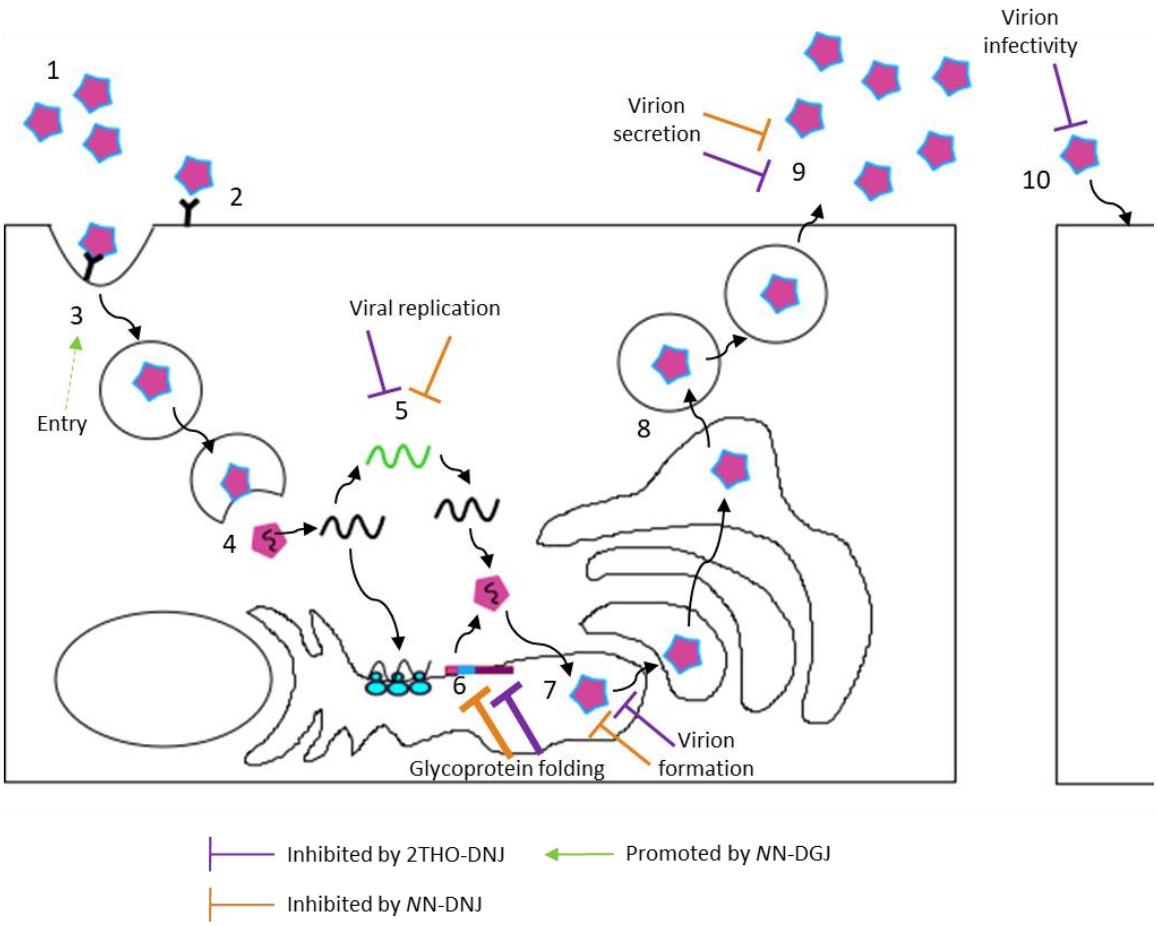

Figure 29. Summary of iminosugar antiviral effects against DENV infection of MDMΦs.

Infectivity of virions in solution is unlikely to be affected by iminosugars (1). Virion attachment to the cell (2) is unaffected by the iminosugars tested, while virion entry (3) was enhanced by NN-*DGJ (although this is of uncertain biological relevance; indicated by the dashed line). The nucleocapsid and DENV RNA are released from virions (4) and viral replication (5) occurs. DNJ-derivative iminosugars inhibited replication. Viral proteins are translated and glycoproteins undergo folding in the ER (6). Inhibition of this process by DNJ-derivative iminosugars, via inhibition of ER α-glucosidases, likely represents the major antiviral mechanism of action of these iminosugars against DENV (illustrated by the weighted arrows). Reduced functional glycoprotein folding leads to reduced virion assembly (7). Virions proceed through the secretory pathway (8), undergoing maturation prior to secretion (9). The overall effect of DNJ-derivative iminosugar treatment is reduced virion secretion from the infected cell. Subsequent infectivity of virions (10) is also reduced with DNJ-derivative iminosugar treatment.*

Chapter 4. *N*N-DNJ and *N*N-DGJ possess antiviral activity against ZIKV

4.1 Abstract

The recent ZIKV outbreak and the ensuing public health emergency catapulted the virus to the attention of virologists and antiviral drug developers. The apparent similarity of ZIKV and DENV in terms of overall structure and possession of structural and non-structural N-glycoproteins suggested that iminosugars might demonstrate antiviral efficacy against ZIKV. Preliminary experiments were conducted to test this hypothesis *in vitro*, finding evidence that *N*N-DNJ and *N*N-DGJ were effective against ZIKV infection of Vero cells and MDMΦs. 2THO-DNJ treatment appeared to be less effective. The lack of stereospecificity of the antiviral effect and the moderate rather than near-complete dependence of ZIKV infection on ER α-glucosidases demonstrate that inhibition of ER α-glucosidases alone cannot account for the antiviral activity of iminosugars against ZIKV. In addition, *N*N-DNJ administration in a murine ZIKV infection model showed some indications of therapeutic efficacy, reducing bloodstream viral loads.

4.2 Introduction

ZIKV infection during pregnancy is associated with CZS, including microcephaly in newborns, and Guillain-Barré syndrome in adults [2]. Although the first serological evidence for human infection came in 1952 [190, 191], and the first human virus isolate obtained soon after [192], ZIKV came to prominence during the recent outbreak beginning in Brazil in 2015. Intense research efforts following the outbreak lead to the development of multiple new animal models for ZIKV infection [224], some attempting to reproduce the effects of infection during pregnancy, and clinical trials of several vaccine candidates have since commenced. However, there are no specific therapeutics available and no clinical trials for antivirals registered with ClinicalTrials.gov.

Like DENV, ZIKV possesses N-glycosylated E, prM and NS1 proteins. However, glycoprotein structure and glycosylation differ between the viruses, as ZIKV E contains a loop encompassing the single N154 glycosylation site, or lacks glycosylation sites entirely, compared to the two sites in DENV [34, 174, 179, 180]. E glycosylation plays different roles between the viruses, such as in determination of cellular tropism [36, 37, 184] and receptor binding [35, 187]. ZIKV NS1 glycosylation is important for viral replication [189]. Thus, interference with N-glycosylation pathways has the potential to inhibit viral infection. This had not been investigated at the outset of this work, but recent support for this hypothesis has come from the antiviral effect of ER α-glucosidase I knockout in Huh7.5 cells on ZIKV infection and the efficacy of one DNJ-derivative iminosugar tested [226]. Therefore, investigation of iminosugars as potential antivirals against ZIKV is warranted.

Overall, this chapter aims to establish whether iminosugars have potential as antivirals against ZIKV. Specifically, the aims were:

1. To determine whether iminosugars have antiviral efficacy against ZIKV *in vitro*;

2. To investigate the dependence of ZIKV infection and iminosugar efficacy on ER α-glucosidases; and
3. To determine whether *N*N-DNJ has antiviral activity in a murine infection model.

4.3 Results

4.3.1 *N*N-DNJ has superior antiviral efficacy than 2THO-DNJ against ZIKV *in vitro*

The antiviral efficacy of iminosugars against ZIKV was determined by infecting Vero cells with ZIKV followed by treatment with titrations of 2THO-DNJ, *N*N-DNJ and *N*N-DGJ at concentrations established to be non-cytotoxic (Figure 89). All of the iminosugars tested had antiviral efficacy, reducing infectious ZIKV titres in a dose-dependent manner (Figure 30A). Iminosugar treatment also reduced the secretion of ZIKV from infected cells (Figure 30B). Calculated specific infectivity showed no clear dose-dependent response across iminosugar titrations (Figure 30C), indicating that iminosugar treatment predominantly restricts the formation or secretion of ZIKV virions, rather than reducing the infectivity of virions that are released. Previous data within the laboratory has confirmed the dose-dependent antiviral effect of both *N*N-DNJ and *N*N-DGJ against ZIKV in this infection model (Michelle Hill, unpublished data). The antiviral effect of *N*N-DGJ is notable considering the lack of antiviral efficacy of DGJ-derivatives against DENV [337], indicating discrepancies between iminosugar mechanisms of action against DENV and ZIKV. Comparing iminosugars, from this experiment it appears that *N*N-DNJ and *N*N-DGJ treatment resulted in a more substantial antiviral effect than 2THO-DNJ treatment, for which the antiviral effect plateaued at around a 40% reduction in total virus secretion. However, this experiment requires repeating to confirm these observations.

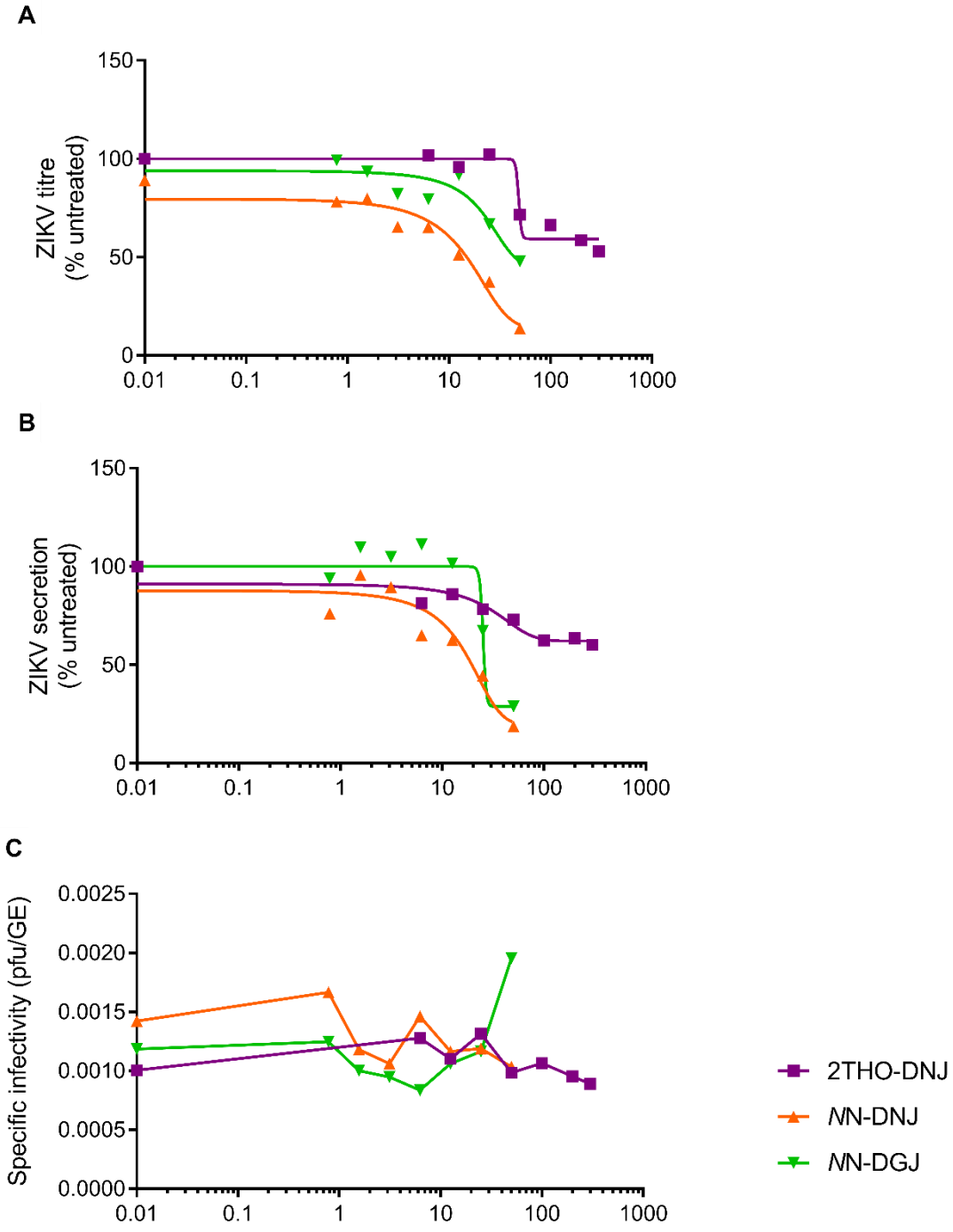

Figure 30. DNJ- and DGJ-derivative iminosugars have antiviral efficacy against ZIKV.

Vero cells were infected with ZIKV and treated with iminosugars or media only (n=1, assayed in technical triplicate). After 48 hours, supernatant was collected for analysis.

(A) Infectious virus was quantified by plaque assay, normalised to untreated and the mean displayed. Curve fits were generated using the 4-point logarithmic function. Untreated values are represented as 0.01 µM to allow plotting on a logarithmic scale.

(B) Secreted virus was quantified by ZIKV E qRT-PCR, normalised to untreated and the mean displayed. Curve fits were generated using the 4-point logarithmic function. Untreated values are represented as 0.01 µM to allow plotting on a logarithmic scale.

(C) Specific infectivity was calculated by dividing infectious virus (pfu/ml) by total virus (GE/ml) for each sample well and the mean was plotted. Untreated values are represented as 0.01 µM to allow plotting on a logarithmic scale.

4.3.2 *N*N-DNJ and *N*N-DGJ antiviral activity against ZIKV does not depend on an intact N-linked glycoprotein folding pathway

The antiviral efficacy of *N*N-DGJ against ZIKV cannot be mediated by inhibition of ER α-glucosidases, the established mechanism for iminosugar activity against DENV. Therefore, there must be additional or alternative mechanisms underlying iminosugar antiviral activity against ZIKV. The dependence of ZIKV on the N-glycoprotein folding pathway was investigated by studying infection of Vero cells knocked out for each of the ER α-glucosidases. While significant reductions in ZIKV titres were observed for infection of both knockout cell types, virus production was still evident at around 40% and 60% of wild-type levels for ER α-glucosidase I or II knockout, respectively (untreated bars in Figure 31). This indicates that there is only a partial dependence of ZIKV on the N-glycoprotein folding pathway, or more specifically the ER α-glucosidases, to produce infectious virions. This is in stark contrast to DENV (Figure 27), which is heavily dependent on ER α-glucosidase function for virus production. In both wild-type and ER α-glucosidase I knockout cells, the reduction in ZIKV titre is largely in keeping with the reductions in virion secretion. This supports the finding that the block on ZIKV production is at or prior to the level of virion release, rather than there being a reduction in specific infectivity of secreted virions (Figure 30C).

Infected wild-type and knockout cells were treated with a panel of iminosugars in order to better identify patterns of iminosugar efficacy, and to determine whether any iminosugar treatments gave antiviral effects beyond that of either glucosidase knockout (Figure 31). In Vero-WT cells,

2THO-DNJ had limited, if any, efficacy as previously demonstrated. As previously demonstrated, *N*N-DNJ and *N*N-DGJ both significantly reduced viral titres. Ribavirin was included in the experimental design as a positive control [529]; however, the impact of ribavirin on cell viability (Figure 89) limited the concentration that could be used to one that was not efficacious in this set-up. In the knockout cells, 2THO-DNJ, *N*B-DNJ and *N*B-DGJ did not have antiviral efficacy. In contrast, *N*N-DNJ and *N*N-DGJ appeared to have additional antiviral efficacy beyond that of the knockout (which was statistically significant for ER α-glucosidase II knockout cells only), supporting the hypothesis that their antiviral mechanism is not dependent on an intact ER α-glucosidase pathway. In addition, it seemed that *N*N-DNJ had a more pronounced effect than *N*N-DGJ on viral titres in Vero-WT cells, consistent with the dose-titration study (4.3.1), an efficacy gap which appeared to be lost in the knockout cell lines. Perhaps this could suggest that there is a component of ER α-glucosidase-dependent efficacy, acting in concert with a stereochemistry-independent mechanism that becomes more apparent when the N-glycosylation pathway is impaired. While similar trends were observed in secreted virus, differences were not statistically significant, likely linked to to the high variability observed between biological replicates in the ER α-glucosidase II knockout cells.

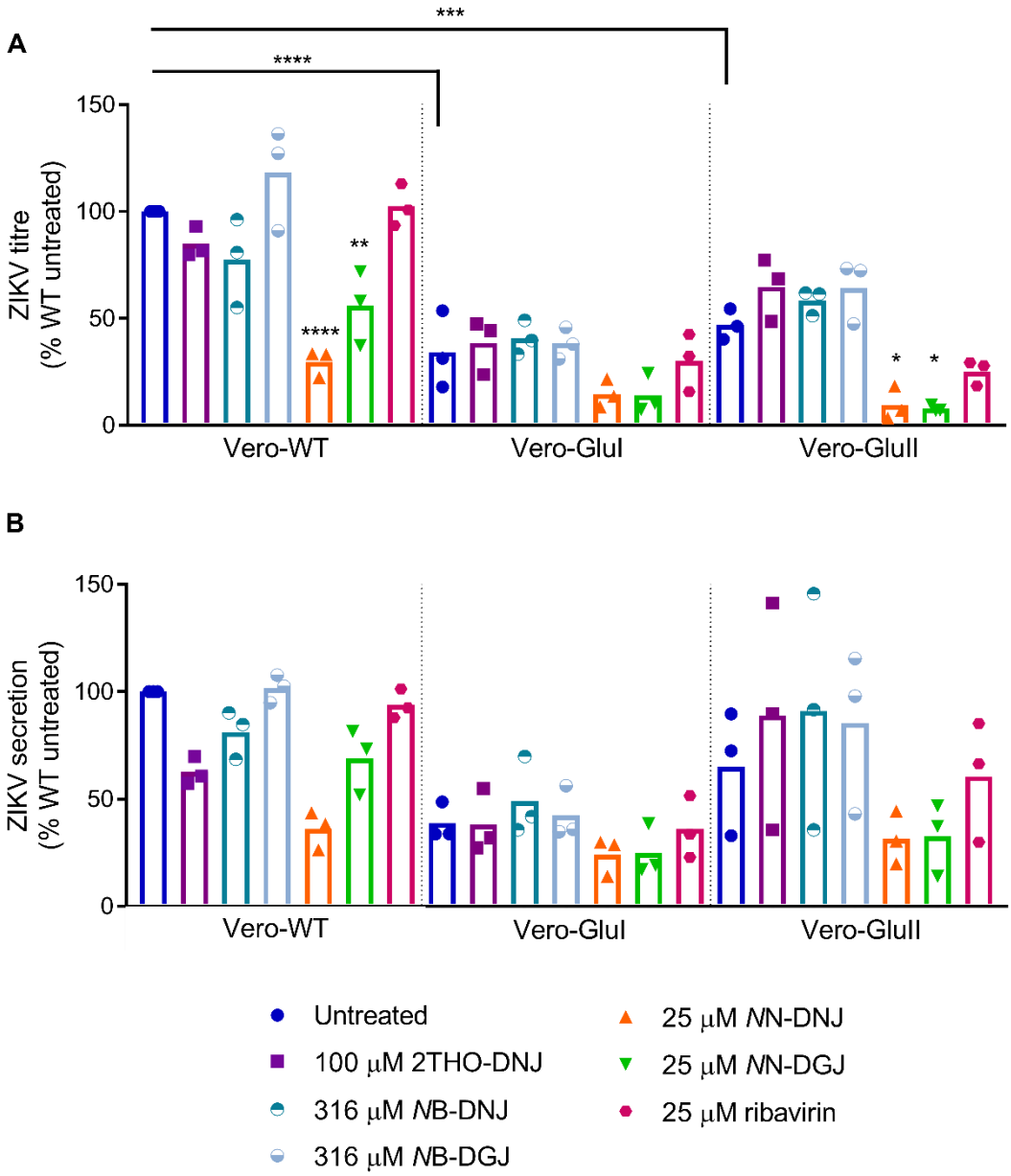

Figure 31. NN-DNJ and NN-DGJ *reduce ZIKV titres regardless of glucosidase knockout status.*

Vero-WT, Vero-GlcI or Vero-GlcII cells (n=3, assayed in technical triplicate) were infected with ZIKV and treated with iminosugars, ribavirin or media only. After 48 hours, supernatants were collected and infectious virus titres determined by plaque assay (A) or total virion secretion determined by ZIKV E qRT-PCR (B). Values were normalised to WT untreated and the mean displayed (bars shown the mean of biological replicates). Statistical analysis was by one-way ANOVA with multiple comparisons, using Tukey's multiple comparisons test (, p<0.05; **, p<0.01; ***, p<0.001; ****, p<0.0001). Asterisks shown directly above bars denote comparisons to the untreated condition within a cell type.*

4.3.3 ZIKV infection of MDMΦs

The antiviral efficacy of iminosugars against ZIKV infection of MDMΦs was also investigated. Two African ZIKV strains, namely MR766, used for the preceding *in vitro* experiments, and MP1751, the strain used for *in vivo* challenge (4.3.4), were utilised here. Due to limited virus stock availability and time constraints (due to the requirement to obtain additional ethical approvals), an MOI of 0.1 was used in this experiment, which is likely to have resulted in suboptimal infection levels for antiviral drug testing. It is worth noting that viral titres produced from infection with the MP1751 strain were approximately ten-fold lower than those resulting from MR766 infection (Figure 106). None of the tested iminosugars reduced ZIKV titres by more than 50%, a level that we can be certain represents a true change in viral titre given the sensitivity of plaque assays. However, there was an indication that some iminosugar conditions might have an antiviral effect, and this infection model should be optimised and antiviral assays repeated to investigate whether the antiviral effect of iminosugars against ZIKV extends to primary human immune cell infection.

Corresponding supernatant samples were also analysed for cytokine secretion using HEK-Blue™ TNF-α and IFN-α/β cytokine reporter cells (Invivogen; see 6.3.1 for assay development). Despite productive viral infection, neither significant TNF-α nor IFN-α/β secretion was induced on ZIKV infection (data not shown).

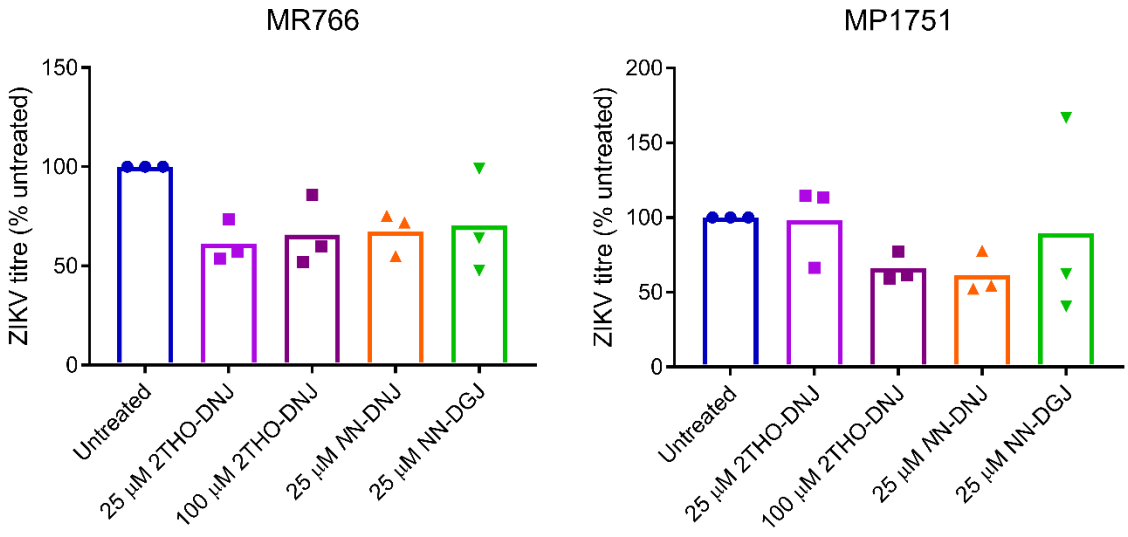

Figure 32. Iminosugars are antiviral against ZIKV infection of MDMΦs.

Primary MDMΦs (n=3 (donors OT, OU, OX), assayed in technical singlicate) were infected with indicated ZIKV strains and treated with iminosugars as indicated. After 72 hours, supernatant was harvested, infectious virus titres determined, normalised to untreated and the mean displayed (bars show the mean of the donors).

4.3.4 Reductions in viral load suggest antiviral efficacy of *N*N-DNJ against ZIKV *in vivo*

Whether the *in vitro* observations of the antiviral efficacy of *N*N-DNJ translated to an *in vivo* effect was investigated using the A129 murine ZIKV infection model in two studies. In both cases, mixed sex groups of mice were challenged with 100 pfu of the MP1751 ZIKV strain as per Dowall et al. [463] and subsequently administered 100 mg/kg *N*N-DNJ or vehicle control twice a day by oral gavage or intragastric administration (full study designs are described in 2.3.3). This iminosugar dosing regimen was previously shown to be well-tolerated in an antiviral study against DENV infection of AG129 mice [399], as was 200 mg/kg *N*N-DNJ administered by oral feeding tube once daily for 3 weeks as an antiviral against JEV infection of ICR mice [58]. In addition, C57BL/6 mice have been maintained on 250 mg/kg/day *N*N-DNJ administered in powdered food for up to 120 days for biochemical characterisation of glycogen metabolism [530].

The aim of the first study was to establish whether *N*N-DNJ treatment improved survival or reduced viral load in ZIKV-infected mice. Therefore mice were infected with ZIKV and treated with *N*N-DNJ or vehicle control and clinical signs and survival recorded. Four mice per group were scheduled to be culled at 6 days post-challenge to allow analysis of any effect on viral load at a consistent time point, rather than at the variable time points of necropsy (Figure 4). ZIKV infection resulted in significant weight loss, in keeping with previous studies [463]. This occurred regardless of treatment group (Figure 33). Mean temperatures remained broadly consistent across the study, with significant temperature drops in some animals reaching humane endpoints contributing to the high variation seen at some time points (Figure 34). In terms of overall survival, *N*N-DNJ treatment had no significant effect, with a median survival of 8.31 days for both groups calculated by Kaplan-Meier survival analysis (Figure 35). However, clinical signs appeared to be improved slightly in the treated group, although the different numbers of animals surviving in each group at a given time, discussed later, complicates this analysis (Figure 36). Virological analysis was conducted for blood and serum samples derived from four mice in each group, two of each sex, scheduled to be culled 6 days post-challenge as well as necropsy samples from all mice. Blood viral load was quantified by qRT-PCR directed against ZIKV E and infectious virus in the serum by plaque assay. While the most detailed coverage of any time point was for the scheduled cull, it appeared that viral loads and titres declined following the scheduled cull (Figure 37A and Figure 38A). *N*N-DNJ treatment significantly reduced viral load at 6 days post-infection (Figure 37B), although only a non-significant trend towards reduction was seen for the considerably lower infectious virus titre quantified from serum at this time point (Figure 38B). It is possible that a more prominent effect could be identified in murine tissues collected at 6 days post-infection, although this analysis has not been conducted.

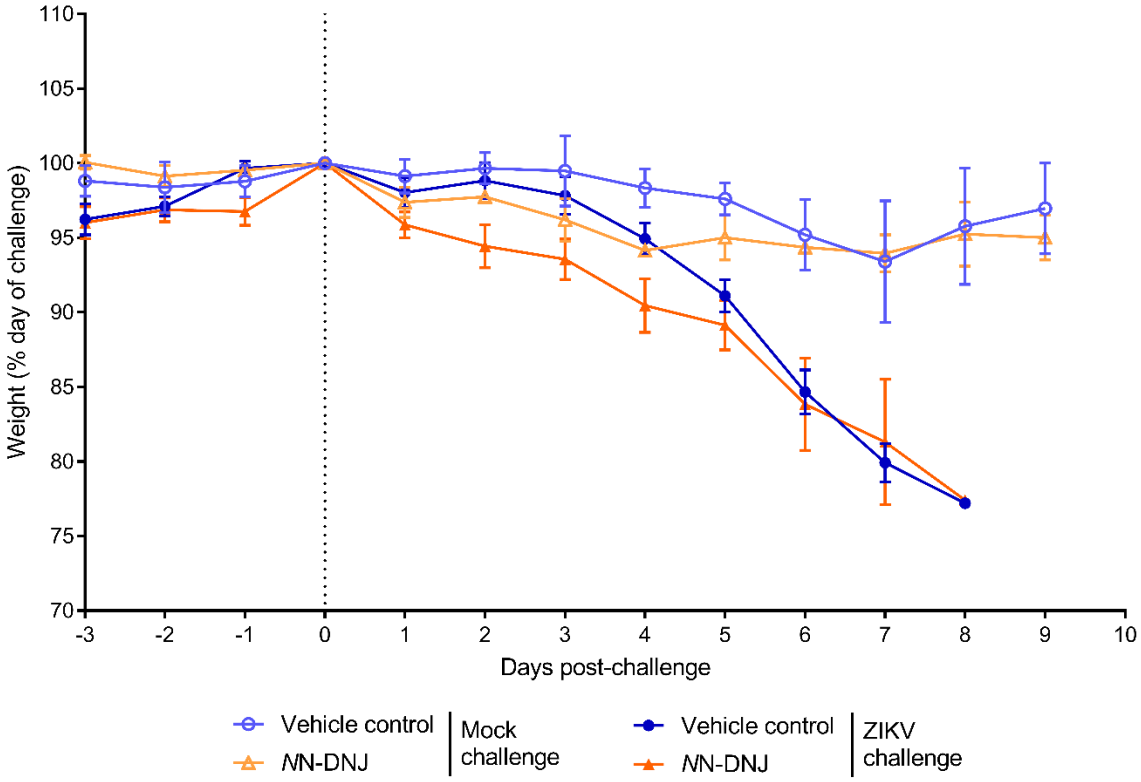

Figure 33. ZIKV infection leads to significant weight loss in A129 mice regardless of iminosugar treatment.

A129 mice were ZIKV-infected (n=10/group) or mock-challenged (n=4/group) and treated with NN*-DNJ or vehicle control as per 2.3.3. Weights were recorded each day and plotted as mean ± standard error for each group. The vertical dotted line indicates the time of challenge.*

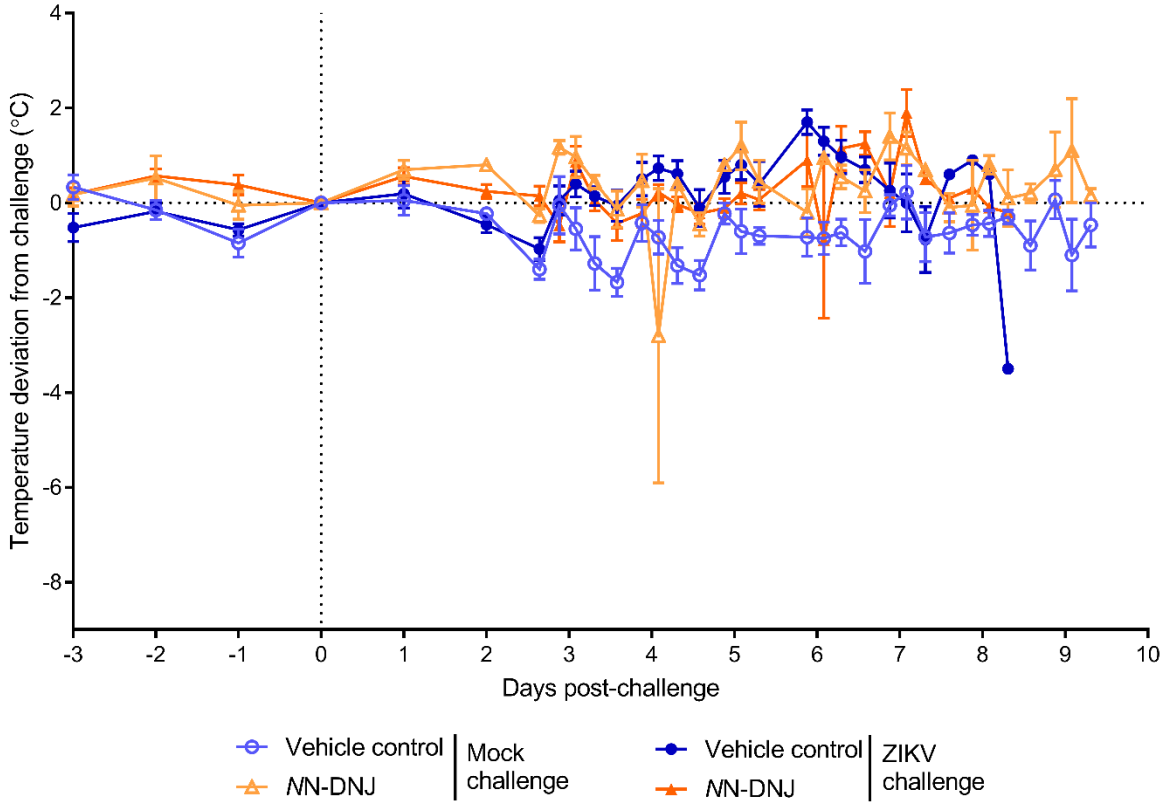

Figure 34. ZIKV infection did not significantly affect the temperature of A129 mice regardless of iminosugar treatment.

A129 mice were ZIKV-challenged (n=10/group) or mock-challenged (n=4/group) and treated with N*N-DNJ or vehicle control as per 2.3.3. Temperatures were recorded each day and plotted as mean ± standard error for each group. The vertical dotted line indicates the time of challenge.*

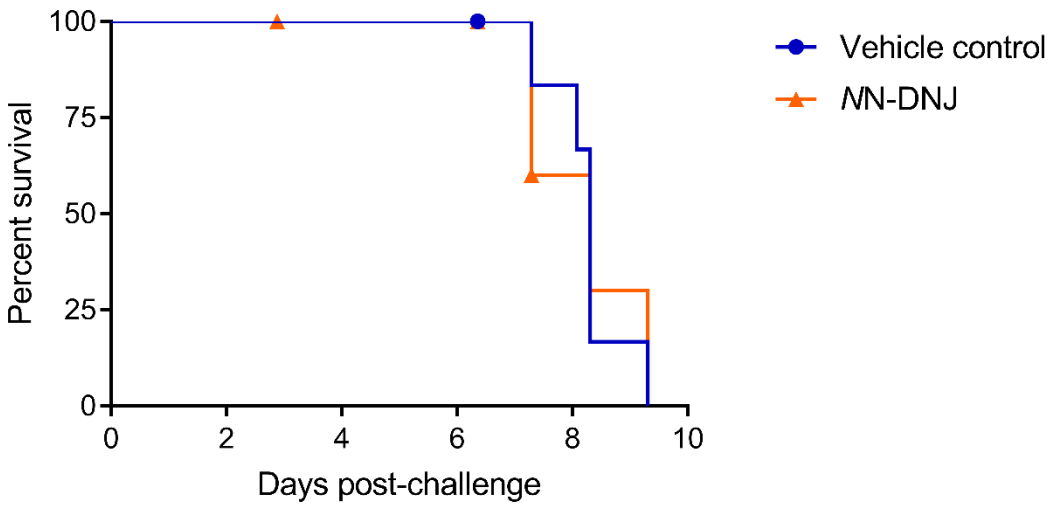

Figure 35. N*N-DNJ treatment had no significant effect on survival of ZIKV-infected A129 mice.*

A129 mice (n=10/group) were ZIKV-infected and treated with NN-DNJ *or vehicle control as per 2.3.3. A Kaplan-Meier survival curve generated in accordance with animals meeting humane endpoints as a result of ZIKV infection. Statistical analysis of differences between survival curves was by Log-rank (Mantel-Cox) test.*

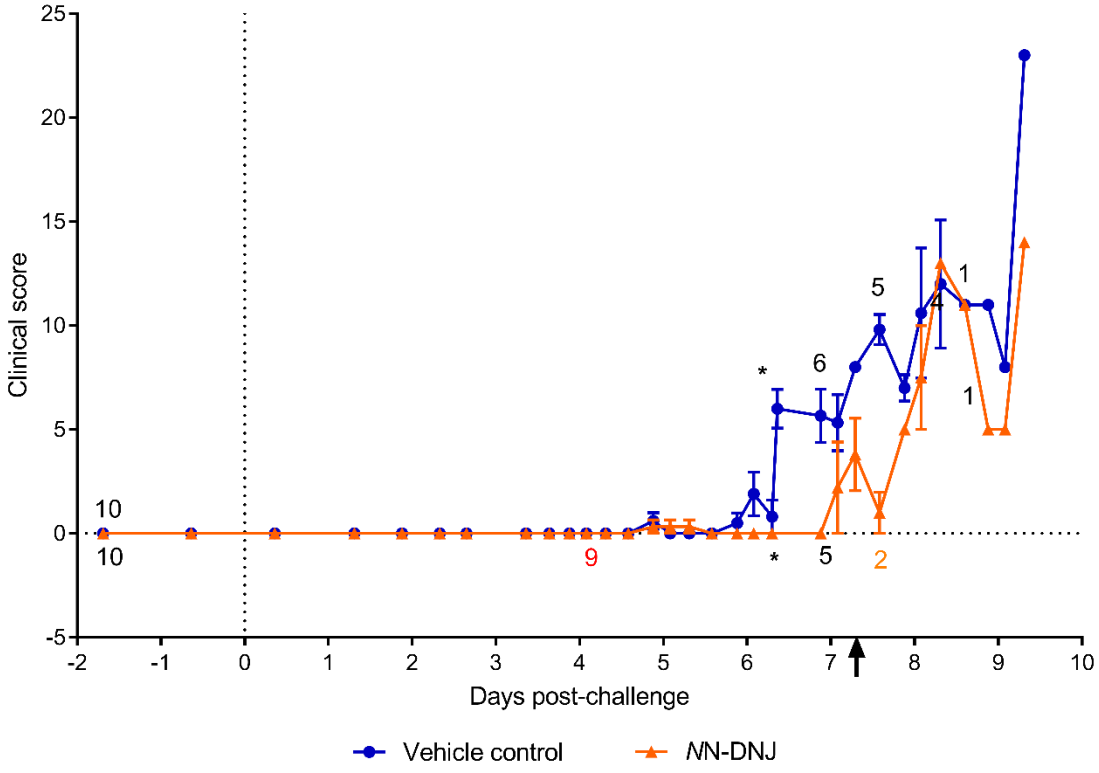

Figure 36. NN-DNJ *slightly improves clinical signs in ZIKV-infected mice.*

A129 mice (n=10/group) were ZIKV-infected and treated with NN-DNJ *or vehicle control as per 2.3.3. Clinical signs were recorded, assigned numerical values and plotted as mean ± standard error for each group. Asterisks indicate a scheduled cull of 4 animals. Numbers given indicate the surviving number of animals per group from that time point; those given above and below lines refer to the vehicle control and* NN-DNJ*, respectively. Numbers in red indicate animal deaths attributed to be as a result of the dosing procedure following veterinary examination, and orange indicates that this occurred in 1 of 3 animals meeting humane end-points at that time point. The arrow denotes the end of dosing and the vertical dotted line indicates the time of challenge.*

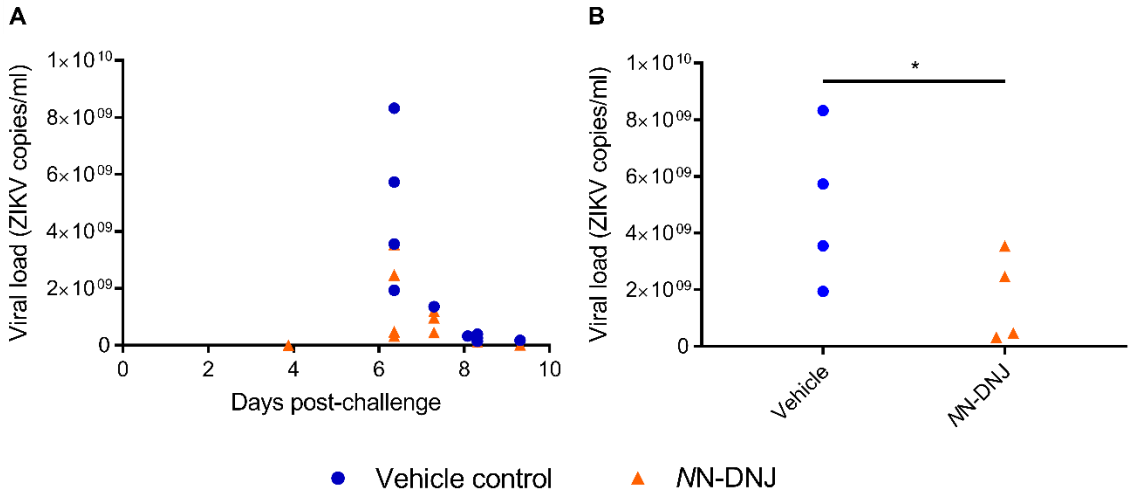

Figure 37. N*N-DNJ treatment significantly reduces blood viral loads in ZIKV-infected A129 mice.*

A129 mice (n=10/group) were ZIKV-infected and treated with N*N-DNJ or vehicle control as per 2.3.3. At necropsy (A) and at day 6 (B), blood was collected and stored in RNAprotect. RNA was extracted and ZIKV viral load determined by ZIKV E qRT-PCR.*

(A) Mean viral loads for individual animals were plotted against time of sampling.

(B) Mean viral loads at day 6 are displayed. Statistical analysis was by one-tailed t-test (, p<0.05).*

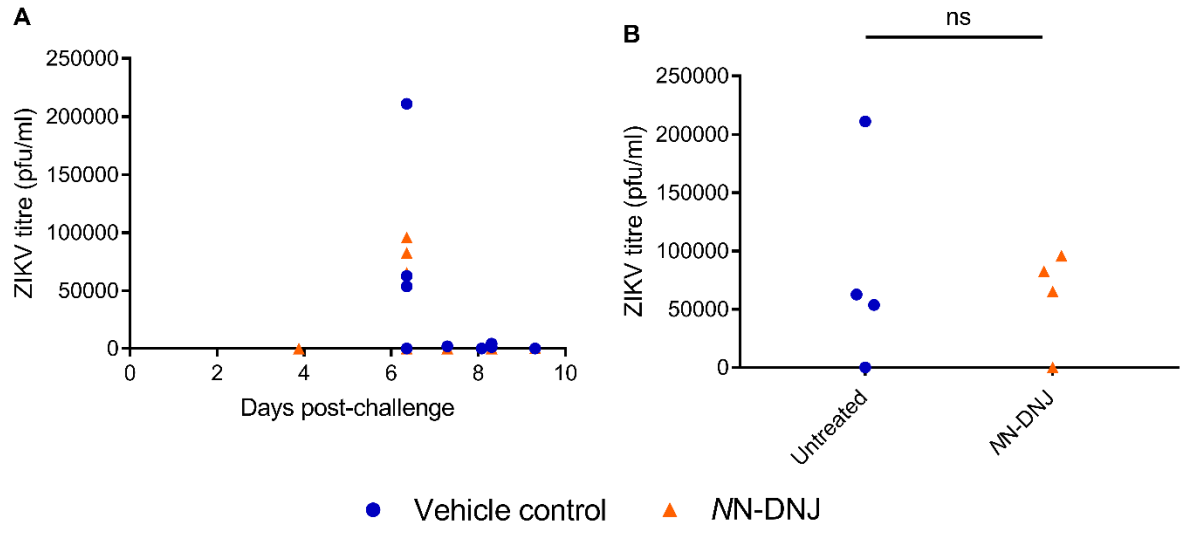

Figure 38. N*N-DNJ treatment has no significant effect on detected serum infectious virus in ZIKV-infected A129 mice.*

A129 mice (n=10/group) were ZIKV-infected and treated with N*N-DNJ or vehicle control as per 2.3.3. At necropsy (A) and at day 6 (B), serum was obtained from blood and infectious virus quantified by plaque assay.*

(A) Mean viral titres for individual animals were plotted against time of sampling.

(B) Mean viral titres at day 6 are displayed. Statistical analysis was by one-tailed t-test (ns, not significant).

In study one, the tolerability of dosing was assessed by the inclusion of two groups of unchallenged animals administered either the acidified water vehicle control or the *N*N-DNJ solubilised in acidified water (Figure 4). Both groups contained animals that displayed some clinical signs, indicating poor tolerability of the dosing procedure. In the mock-challenged groups, one death was determined to have occurred as a result of the procedure since it occurred immediately post-procedure (Figure 107). On necropsy, oesophageal pathology was identified. These animals were dosed by oral gavage, using flexible plastic needles to administer doses to the oesophagus, proximal to the mouth. We hypothesised that repeated dosing using this method with the acidified compound lead to tolerability issues. Therefore, in the second study, we attempted to overcome these issues by solubilising *N*N-DNJ in DMSO then further diluting the solution in endotoxin-free water at a neutral pH to result in a solution with a low percentage of DMSO. In addition, intragastric dosing was conducted, demonstrated in an interim trial to alleviate the oesophageal irritation previously observed.

The aim of the second study was to determine whether the reduction in viral load observed with *N*N-DNJ treatment in the first study was repeatable, with the improved dosing protocol. As seen in the first study, ZIKV infection resulted in significant weight loss regardless of treatment group (Figure 39), and mean temperatures remained broadly consistent across the study (Figure 40). In this case, clinical signs did not differ between treatment groups (Figure 41). Unfortunately two of the female mice in the *N*N-DNJ treatment group died post-dosing, and their deaths were attributed to the procedure. Virological analysis was conducted for samples taken from animals 3 days post-challenge; these animals were not sacrificed at this time. Blood viral loads in untreated animals were around 2 logs lower in these day 3 samples compared to the samples

taken at day 6 in study one (Figure 42 versus Figure 37B), in keeping with previous characterisation of this model [463]. Once again, *N*N-DNJ treatment reduced bloodstream viral loads (Figure 42). Analysis of serum taken at necropsy was also conducted but viral titres were below the limit of detection (in this case 333 pfu/ml; data not shown). Taken together, the two studies suggest that *N*N-DNJ treatment can significantly reduce ZIKV viral loads *in vivo*, although further analysis of tissue samples should be conducted and the results reproduced in further studies.

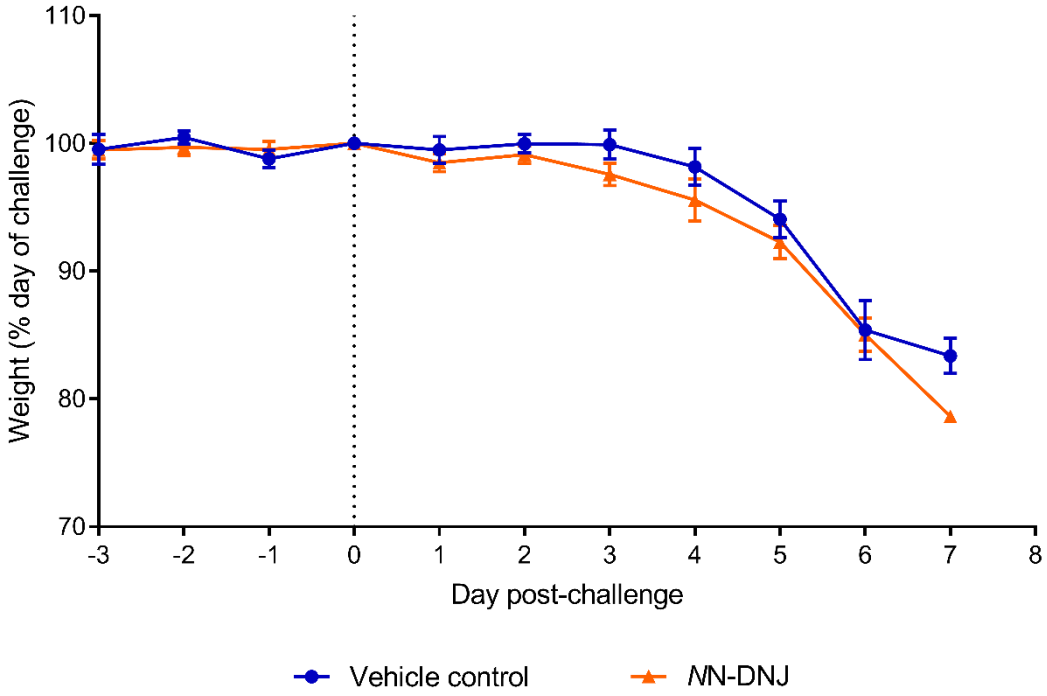

Figure 39. ZIKV infection leads to significant weight loss in A129 mice regardless of iminosugar treatment.

A129 mice (n=6/group) were ZIKV-infected and treated with NN-DNJ *or vehicle control as per 2.3.3. Weights were recorded each day and plotted as mean ± standard error for each group. The vertical dotted line indicates the time of challenge.*

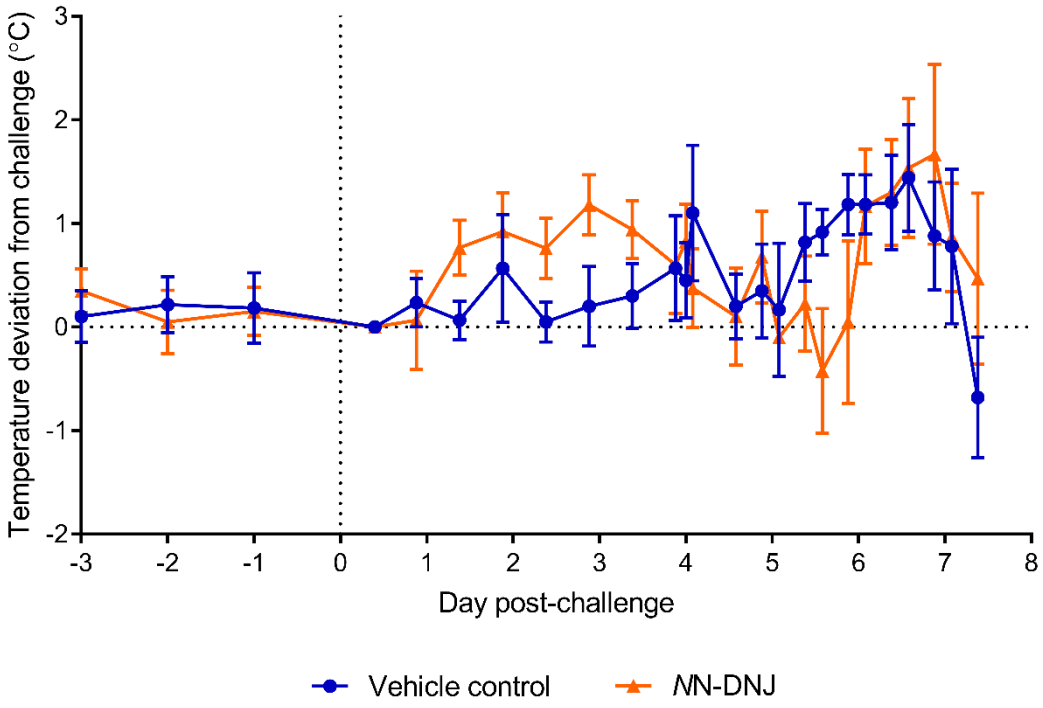

Figure 40. ZIKV infection did not significantly affect the temperature of A129 mice regardless of iminosugar treatment.

A129 mice (n=6/group) were ZIKV-infected and treated with NN-DNJ *or vehicle control as per 2.3.3. Temperatures were recorded each day and plotted as mean ± standard error for each group. The vertical dotted line indicates the time of challenge.*

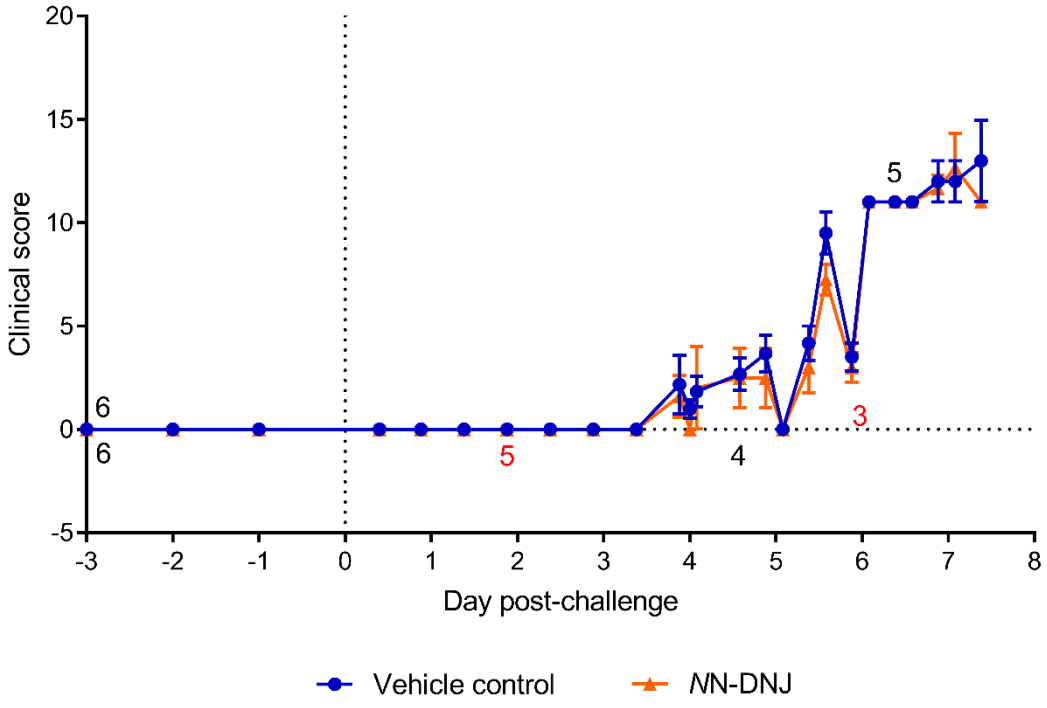

Figure 41. NN-DNJ *treatment did not affect clinical signs in ZIKV-infected mice.*

A129 mice (n=6/group) were ZIKV-infected and treated with NN-DNJ *or vehicle control as per 2.3.3. Clinical signs were recorded, assigned numerical values and plotted as mean ± standard error for each group. Numbers given indicate the surviving number of animals per group from that time point; those given above and below lines refer to the vehicle control and* NN-DNJ*, respectively. Numbers in red indicate animal deaths attributed to occur as a result of the dosing procedure following veterinary examination. The vertical dotted line indicates the time of challenge.*

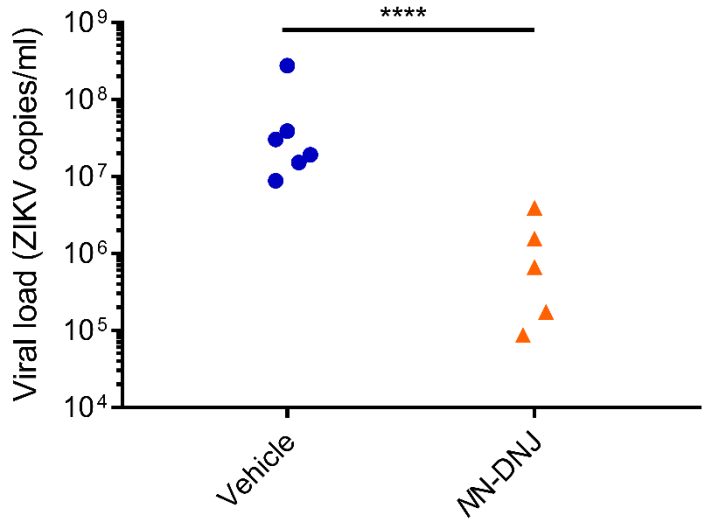

Figure 42. NN-DNJ *treatment significantly reduces viral loads in ZIKV-infected A129 mice.*

A129 mice (n=10/group) were ZIKV-infected and treated with N*N-DNJ or vehicle control as per 2.3.3. 3 days post-challenge, blood was collected and stored in RNAprotect. RNA was extracted and ZIKV viral load determined by ZIKV E qRT-PCR. Statistical analysis was by two-tailed t-test (****, p<0.0001).*

4.4 Discussion

While the antiviral efficacy of iminosugars against DENV is well-established, here efficacy of DNJ-derivative iminosugars against ZIKV is demonstrated for only the second time [226], and efficacy of a DGJ-derivative is indicated for the first time. Considered in combination with existing unpublished data in the laboratory (Michelle Hill), *N*N-DNJ and *N*N-DGJ have a reproducible antiviral effect against ZIKV, while any effect of 2THO-DNJ appeared to be limited (Figure 30). Thus, the structure-activity relationship differs from that identified for DENV, where DNJ-derivative iminosugars mediate antiviral efficacy through inhibition of ER α-glucosidases [337]. In addition, knocking out either ER α-glucosidase had only a moderate antiviral effect against ZIKV, with the greater effect of ER α-glucosidase I knockout in accordance with previous findings [226]. This is in stark contrast to the effect of ER α-glucosidase knockout on DENV, where infection is near-abrogated (Figure 27). In the context of the α-glucosidase knockouts, treatment with *N*N-DNJ or *N*N-DGJ appeared to have an additional antiviral effect beyond that of the knockout (Figure 31). Taken together, this indicates that a component of the antiviral mechanism of action is independent of effects on ER α-glucosidases and suggests that this is related to the shared *N*-nonyl alkyl chain.

Previous work characterising the effects of *N*-alkylated iminosugars has established two mechanisms of action occurring irrespective of headgroup stereochemistry, namely inhibition of glycosphingolipid generation and of viral ion channels. Firstly, *N*-alkylated DNJ and DGJ iminosugars inhibit GCS, the enzyme catalysing glucosylation of ceramide in the generation of

glycosphingolipids [335, 336]. Flaviviruses interact with cellular lipids for attachment, entry, fusion, replication and assembly, and are increasingly understood to make wide-ranging alterations to the cellular lipid environment [531]. These modulations include changes in sphingolipid biosynthesis as well as catabolism of glucosylceramide leading to increased ceramide levels, although the importance of ceramide for viral replication differs between WNV and DENV [532]. For ZIKV, ceramide levels are increased in infected microglial cells [533] and the transcriptome of infected human primary retinal pigmented epithelial cells identified upregulation of genes involved in ceramide metabolism [534]. Perhaps modulation of ceramide metabolism might contribute to the antiviral effect of *N*N-DNJ and *N*N-DGJ, although conflicting data exist about the effects of *N*B-DNJ and *N*B-DGJ on cellular ceramide levels in different models [340, 443]. Indeed, antiviral efficacy of some strategies interfering with cellular lipid metabolism has been demonstrated against ZIKV [229, 535, 536], supporting the importance of lipid modulation for ZIKV, although none of these approaches have targeted ceramide. Analysis of lipid metabolism upon ZIKV infection in Vero cells as well as any effect of iminosugar treatment would be required to further pursue this hypothesis.

A second antiviral avenue through which the long alkyl chain iminosugars *N*N-DNJ and *N*N-DGJ operate is disruption of viral ion channel function. The HCV p7 protein forms a proton channel that acts to prevent acidification of intracellular compartments, and is required for productive infection [537]. While DNJ-derivative iminosugars promote degradation of the E2-p7 protein in HCV-infected cells [354], both DNJ- and DGJ-derivative iminosugars with long alkyl chains can inhibit p7 ion channel activity. *N*N-DNJ, *N*N-DGJ and *N*-7-oxanonyl-6-deoxy-DGJ dose-dependently reduced the conductance of p7 ion channels reconstituted in black lipid membranes, while *N*B-DNJ and *N*B-DGJ had no effect [414]. The inhibitory activity was also demonstrated for *N*N-DNJ and *N*N-DGJ in lipid bilayers [356], and for UT-231B, another DGJ-derivative [538]. Blocking of the channel pore and disrupting p7 ion channel formation have

been suggested as potential underlying mechanisms of action [356, 414, 415], while intercalation of the long alkyl chain of *N*N-DNJ between protomers of the human papillomavirus E5 viroproin leading to channel disruption has also been proposed [416]. Furthermore, the antiviral efficacy of long alkyl chain iminosugars against BVDV [341, 539, 540], the HCV model pestivirus, could also be contributed to by disruption of ion channels formed by BVDV p7, since similar pestivirus p7 proteins form viroporins [541] and non-iminosugar inhibitors of HCV p7 ion channels also have antiviral efficacy against BVDV [542]. The issue of whether ZIKV possesses a viral ion channel that might be targeted by iminosugars is yet to be discussed in the literature. However, this is a contentious topic for the related DENV, since a C-terminal portion of DENV M was shown to have ion channel activity in lipid bilayers [543] but this was not replicated in studies expressing prM or M in *Xenopus laevis* oocytes [544]. Thus investigation of ZIKV proteins for ion channel activity might uncover a target which could explain the efficacy of *N*N-DNJ and *N*N-DGJ against ZIKV.

Viral ion channels notwithstanding, ZIKV has been shown to interact with cellular ion channels. The voltage-dependent anion-selective channel, mediating mitochondrial metabolite transport across the outer mitochondrial membrane [545], was upregulated on ZIKV infection of A549 cells [546]. The endosomal cation channel mucolipin-2 enhanced ZIKV infection of $STAT1^{-/-}$ fibroblasts, presumably via enhancing virion trafficking through endosomes [547]. Thirdly, the activation of the calcium-permeable nonselective cation channel transient receptor potential vanilloid 4, leading to nuclear translocation of DEAD-box RNA helicase DDX3X, has been implicated in ZIKV infection of Huh7 cells [548]. Interactions of iminosugars with cellular ion channels have not been described save for misfolded cystic fibrosis transmembrane conductance regulator chloride channels: however, in this case, inhibition of ER α-glucosidases by *N*B-DNJ rescues secretion and function of the protein otherwise destined for ERAD [549, 550]. Thus whether *N*N-DNJ and *N*N-DGJ could interact with relevant organelle membranes and

disrupt the function of cellular ion channels important for viral infection remains to be evaluated.

Nevertheless, it remains likely that the inhibition of N-glycosylation plays a role in the antiviral efficacy of DNJ-derivative iminosugars against ZIKV. Glycosylation of ZIKV E is important for its secretion when expressed in mammalian cells alone or in the context of a flaviviral replicon, and contributes to virion infectivity [183], although it did not impact infection of mammalian cell lines [184, 186]. E glycosylation is implicated in ZIKV pathogenicity in mouse models, although reports of the contribution to lethality and neurovirulence differ [184, 185]. One study found that mutation of the E glycosylation site enhanced ZIKV attachment, entry, assembly and infectivity of secreted virions from C6/36 cells [184], although another found no effect on peak titres derived from C6/36 cell infection [186]. Abolishing E glycosylation inhibited ZIKV crossing the midgut barrier in experimental infection of *Aedes aegypti* mosquitos. Interestingly, this was linked to the N-glycosylated E protein inhibiting the antiviral ROS response in the midgut [186]. Glycosylation of E in the MR766 strain used here was confirmed by sequencing and mass spectrometry (Johan Hill, Stephen Woodhouse and Abhinav Kumar, data not shown), in light of the fact that variation in the number of E glycosylation sites between ZIKV strains is also evident within the extensively-passaged MR766 strain [174, 179, 180]. Multiple glycosylation sites are also predicted across the established ZIKV glycoproteins in the MP1751 strain by analysis of the published genome (GenBank: KY288905.1) using the NetNGlyc server [464, 465]. Glycosylation of ZIKV NS1 has also been shown to be important for viral replication in Vero cells [189]. Analysis of the E, prM and NS1 proteins in ZIKV-infected cells should be conducted to determine whether their trafficking and secretion is disrupted in the context of iminosugar treatment.

In addition to direct effects on the virion, interfering with N-glycosylation could indirectly affect ZIKV infection by modulating cellular receptor expression or function. One receptor identified

for ZIKV, TIM1 [208], is N-glycosylated thus could potentially be affected by iminosugar treatment; although its N-glycosylation is dispensable for the selectin binding important for its role in T cell adhesion [551]. It follows that the permanent alteration of N-glycosylation pathway function in the glucosidase knockout Vero cells employed here could also affect this receptor. However, even if this is the case, the ability of ZIKV infection to be established in the knockout cells is unaffected as there were no significant differences in percentage infection of knockout and wild-type Vero cells at 48 hours post-infection as determined by immunofluorescence [452].

It would be of interest to conduct further mechanistic analysis into how the antiviral effect against ZIKV is mediated, as the data presented here solely indicate that the restriction point is prior to or at virion secretion. This is particularly important in light of the finding that iminosugar efficacy is not tied to the glucostereochemistry of the DNJ-derivatives as it is for DENV [337], indicating that while misfolding of viral structural proteins downstream of ER α-glucosidases may contribute to reduced virion secretion, this cannot be the sole mechanism. In Chapter 3, various aspects of the DENV infection cycle which could be perturbed by iminosugar treatment were investigated. Similar analyses could be conducted for ZIKV, including assessment of whether iminosugars affect virion attachment or entry to cells, or viral replication.

Both the Vero cells used in this study and the previously reported α-glucosidase knockout Huh7.5 cells [226] are immunocompromised cell lines, differing considerably from the physiological scenario involving viral infection of monocytes and macrophages in bloodstream and tissues, respectively [200, 206, 207, 552]. Thus, any contribution of iminosugar modulation of cytokine responses to infection (see 0) to the antiviral effect would be missed in this model. Preliminary investigations were conducted into the antiviral efficacy of iminosugar treatment in MDMΦs infected with the MR766 and MP1751 ZIKV strains (Figure 32). However, this model requires optimisation regarding the MOI and time point for antiviral assay, and further study is

necessary before conclusions can be drawn. While productive viral infection was established, a lack of TNF-α secretion was identified from infected MDMΦs, in agreement with other studies using primary blood monocytes and placental macrophages [200, 206, 552]. The lack of TNF-α induction in ZIKV-infected MDMΦs differs from the responses of DENV-infected MDMΦs (Figure 49, for example), and while differences in donors, time points, and MOI used are likely to be contributing factors, this in combination with clinical and other experimental evidence is suggestive of a difference in MDMΦ cytokine responses to ZIKV and DENV infections. Indeed, a recent study comparing DENV and ZIKV infection of primary MDMΦs and macrophages derived from either human embryonic stem cells or human induced pluripotent stem cells found that while all cell types supported productive infection with both viruses, DENV infection induced significant levels of TNF-α secretion whereas two strains of ZIKV did not [553].

Technical challenges notwithstanding, it would be interesting to establish the dependence of ZIKV infection and iminosugar efficacy on the ER α-glucosidases in MDMΦs. While two ZIKV strains were studied here, and some iminosugar efficacy identified against both, the investigation could be further extended by assessing the dependence of different ZIKV strains on ER α-glucosidases and their responses to iminosugar treatment. While the antiviral efficacy of ER α-glucosidase-targeted iminosugars is relatively consistent across DENV serotypes [394], strain-dependent iminosugar efficacy has been identified against other viruses [314, 388]. The variation in E glycosylation across ZIKV strains makes this assessment particularly interesting and could provide further insight into the relationship between ZIKV and the N-glycoprotein folding pathway.

The investigation of iminosugar antiviral efficacy against ZIKV was extended *in vivo* to the A129 murine ZIKV infection model described by Dowall et al. [463]. While some experimental difficulties were experienced in the first study, complicating the survival analysis, statistically

significant reductions in viral load from blood samples taken during the course of ZIKV infection were observed with *N*N-DNJ treatment in both studies (Figure 37 and Figure 42). This provides further support for the potential benefit of iminosugars against ZIKV infection, although this requires validation through further studies. Considering the pathological significance of ZIKV infection during pregnancy, *in vivo* testing of iminosugars could subsequently be conducted in relevant mouse models [224]. However, while *N*B-DNJ is licensed for the treatment of Gaucher and Niemann-Pick type C diseases, it is contraindicated in pregnancy [554]. Therefore, extensive safety evaluation and significant differences in the drug safety profile during pregnancy from that of *N*B-DNJ would have to be established for any candidate iminosugar treatment for ZIKV in pregnant women. That said, an antiviral for treatment of ZIKV infection in non-pregnant individuals would still be of clinical benefit if protective against Guillain-Barré syndrome. Nevertheless, neither the reductions in viral secretion nor infectious virus on iminosugar treatment were so significant that they approached the limit of detection in tissue culture models or *in vivo*. This lack of potency suggests that iminosugars, at least those in the tested panel, are unlikely to be successful as standalone therapeutics against ZIKV. However, they might have potential as part of a combination therapy, a concept proven for BVDV, DENV, YFV and EBOV [226, 400, 540]. Alternatively, better mechanistic understanding would facilitate rational design of new iminosugars, which could yield an iminosugar effective as monotherapy.

In summary, this chapter presents preliminary evidence demonstrating that both DNJ- and DGJ-derivative iminosugars can have antiviral effects against ZIKV, hinting at a surprising structure-activity relationship in comparison to the effects of iminosugars against DENV. Although only some findings were statistically significant, a reduction in viral titre of at least two-fold was observed with both *N*N-DNJ and *N*N-DGJ treatment in the context of Vero cells knockouts for either ER α-glucosidase I or II, implying that the long, non-oxygen-containing alkyl chain is the major determinant of antiviral efficacy, rather than glucostereochemistry. Significant reductions

in viral loads were also observed with *N*N-DNJ treatment in a mouse model of ZIKV infection, although these findings should be confirmed in tissue samples, and additional studies should be conducted to investigate whether *N*N-DNJ treatment confers a survival benefit. Further mechanistic analysis is required to understand the basis of iminosugar antiviral efficacy against ZIKV, which might yield opportunities to develop more effective compounds.

Chapter 5. Do iminosugars have potential as antivirals for CCHFV?

5.1 Abstract

CCHFV is a pathogen of increasing public health concern, being the second most widely distributed arbovirus, recently emergent in Europe, and the causative agent of the potentially fatal CCHF. HAZV is a genetically and serologically related virus that has been proposed as a surrogate for antiviral and vaccine testing for CCHFV. Glycosylation analysis of HAZV has been limited, thus firstly, occupation of N-glycosylation sites in the HAZV glycoprotein was confirmed. Despite this, there was no apparent antiviral efficacy of a panel of iminosugars against HAZV, determined by quantification of total secretion and infectious virus titres produced following infection of SW13 cells. This lack of efficacy was not due to an inability of DNJ-derivative iminosugars to access and inhibit ER α-glucosidases, as demonstrated by free oligosaccharide assays in uninfected and infected SW13 cells. Even so, iminosugars may yet have potential as antivirals for CCHFV since the positions and importance of N-linked glycans may differ between the viruses: a hypothesis requiring further evaluation.

5.2 Introduction

CCHF is a severe and often fatal disease caused by infection with the tick-borne nairovirus, CCHFV. CCHFV is one of the most widely distributed arboviruses, and is recently emergent in Europe [245]. This, combined with the lack of therapeutics with proven efficacy [295-297], renders CCHFV a pathogen of increasing public health concern. In order to consider the potential applicability of iminosugar treatment for CCHF patients, at least two mechanistic angles should be considered. The first is whether the virus possesses N-glycoproteins which might be misfolded upon iminosugar inhibition of ER α-glucosidases, a mechanism of action of iminosugars demonstrated against multiple viruses of different families (Table 1 and Table 2). Indeed, the Gn and Gc surface glycoproteins of CCHFV both possess occupied N-glycosylation sites, which are conserved across known CCHFV strains [240, 241]. Furthermore, the N-glycosylation of Gn is functionally important since it is required for transport of both Gn and Gc to the Golgi apparatus for virion assembly [240, 555]. Secondly, the importance of cytokines such as TNF-α in the pathogenesis of the disease should be considered, since iminosugar treatment has been shown to modulate a broad range of cytokine responses (Table 4 and Table 6). These effects include reducing production of a key mediator of DENV pathogenesis, TNF-α, both in terms of secretion from DENV-infected MDMΦs [337] (see also 0) and circulating levels in murine DENV infection [397, 399]. While the pathogenesis of CCHF is not well characterised, certain studies have implicated TNF-α in disease severity [252, 261, 263-265], although this finding is not universal [266, 267]. Thus, there is a promising case for testing iminosugars as antivirals against CCHFV.

However, the severity of CCHF poses a considerable risk to laboratory study. Therefore the related nairovirus HAZV was utilised as a surrogate for antiviral testing in this study, since a lack of reports of pathogenic human infection means that the virus can safely be manipulated at BSL2, rather than the BSL4 required for CCHFV [286, 287]. HAZV is both genetically [281, 282]

and serologically [280, 283-285] closely related to CCHFV. Furthermore, infection with HAZV was reported to provide cross-protection against CCHFV in mice [286], and intradermal inoculation of A129 mice with HAZV gave similar clinical signs, pathology and mortality to those reported in murine CCHFV infection models [291]. Consequently, the HAZV murine infection model was proposed as a surrogate for the development of antivirals and vaccines for CCHFV [291] and *in vitro* HAZV infection was proposed to act as a surrogate for testing of small interfering RNA and ribavirin as antiviral strategies against CCHFV [287]. However, no studies have validated antivirals against HAZV and CCHFV in parallel *in vitro* or in mouse models.

Despite the isolation of HAZV in 1964 [279, 280] and subsequent postulation of HAZV as a model for CCHFV infection, the virus is relatively little-studied. Particularly relevant for investigation of iminosugars as antivirals is the N-glycosylation status of HAZV glycoproteins. Early analysis of radiolabelled virus preparations suggested that HAZV possessed three envelope-associated glycoproteins, although this was determined by radiolabelled glucosamine incorporation [286] so could be accounted for by O- rather than N-glycosylation. Analysis of the singular JC280 strain glycoprotein sequence since deposited (UniProtKB accession number A6XIP3) using the NetOGlyc4.0 server [556] indicates several regions of potential O-glycosylation in the HAZV M segment; CCHFV glycoproteins have predicted O-glycosylation most heavily in the mucin-like domain of M but also in Gn and Gc sequences [239]. Computational analysis has determined regions corresponding to the Gn and Gc of CCHFV in the HAZV M segment [281], indicating the presence of at least two potential glycoprotein sequences. However, multiple additional glycoprotein fragments produced from the CCHFV M segment have been identified [235], thus HAZV might possess further glycoproteins fulfilling either structural or non-structural roles. Very recently, visualisation of surface glycoprotein spikes on HAZV virions has been achieved using cryo-EM, although the precise glycoprotein composition and arrangement was unable to be determined [292]. However, the N-glycosylation status of HAZV glycoproteins has not been

confirmed: an important factor in determining its suitability as a surrogate for CCHFV for iminosugar antiviral efficacy testing.

Overall, this chapter aims to establish whether iminosugars have antiviral efficacy against HAZV, and thus potential for treating CCHFV. Specifically, the aims were:

1. To confirm whether HAZV expresses N-linked glycoproteins with occupied glycosylation sites;
2. To identify whether iminosugars have antiviral efficacy against HAZV infection in SW13 cells; and
3. To investigate the interactions of HAZV infection and iminosugar treatment of SW13 cells with the N-glycosylation pathway, using free oligosaccharide analysis.

5.3 Results

5.3.1 HAZV possesses N-glycosylated glycoprotein(s)

Prior to iminosugar testing in HAZV infection, the presence of N-glycosylated proteins was confirmed, since the best understood antiviral mechanism of action of iminosugars involves disruption of viral N-linked glycoprotein folding. Analysis of the JC280 strain glycoprotein sequence (UniProtKB accession number A6XIP3) using the NetNGlyc server [464, 465] identified 8 potential N-glycosylation sites, 3 of which were predicted to be N-glycosylated when sequons containing proline were excluded (Figure 108), while analysis with GlycoEP [466] predicted that 5 sites would be N-glycosylated when sequons containing proline were excluded (Table 21).

To investigate whether the predicted N-glycosylation was borne out experimentally, sucrose-cushion purified HAZV was digested with PNGase F, an endoglycosidase which cleaves the bond

between the asparagine residue and the GlcNAc of N-linked oligosaccharides, or Endo Hf, which cleaves the bond between the two GlcNAc residues of the chitobiose core of high mannose and certain complex N-linked oligosaccharides. PNGase F- and Endo Hf-treated HAZV samples were run on a gel alongside HAZV that was not enzymatically treated. UGGT, a known N-glycosylated protein [557], was included as a positive control, for which a gel shift was seen with PNGase F treatment (Figure 43). Strong gel bands at predicted molecular weights were seen corresponding to the enzymes. Unfortunately, the band corresponding to Endo Hf obscured the major band seen in the HAZV sample, thus gel shift could not be assessed for this treatment. However, on PNGase F treatment, a gel shift was observed for the major HAZV band, indicative of N-glycosylation (arrow in Figure 43).

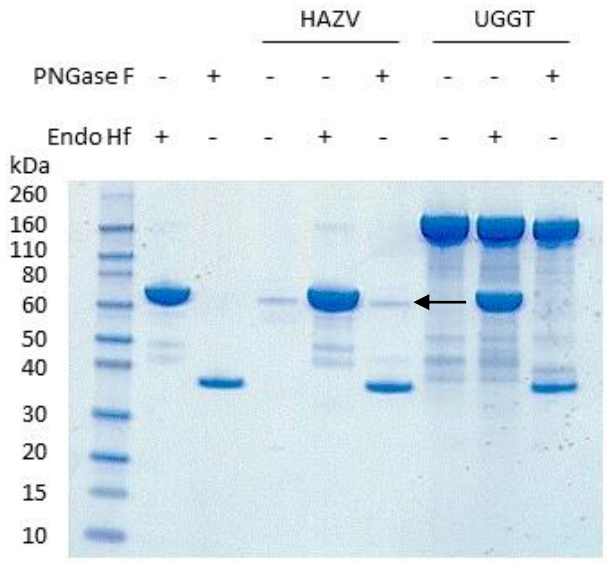

Figure 43. A gel shift is observed on PNGase F digestion of purified HAZV, suggesting N-glycans are present.

HAZV and UGGT, a known N-glycosylated protein, were digested with PNGase F or Endo Hf and the samples run on a 4-12% Bis-Tris gel alongside untreated samples and enzymes. An arrow indicates the HAZV band having undergone gel shift after PNGase F digestion.

Mass spectrometry analysis of the gel band indicated that it contained a partial sequence corresponding to the JC280 glycoprotein, suggesting that the band was a cleavage fragment

(Abhinav Kumar and Bevin Gangadharan, data not shown). For further analysis, purified HAZV was left untreated or digested with PNGase F in-solution, followed by in-solution trypsin digestion and sample analysis by parallel reaction monitoring targeted mass spectrometry. The detection of a peptide containing an aspartic acid where an asparagine residue appears in the sequence is indicative of an occupied N-glycosylation site when detected in PNGase F-treated samples but not untreated samples. This analysis identified two occupied N-glycosylation sites at the N97 (peptide sequence LADFFIDT**N**SSQCYDEILVK) and N346 (peptide sequence NDGPGDHITFC**N**GSVVTK) residues, while two other peptides containing potential N-glycosylation sites that were expected to be produced upon tryptic digest were not detected in either treatment condition (Abhinav Kumar and Bevin Gangadharan, data not shown). Taken together, these data confirmed that HAZV expresses N-linked glycoproteins and therefore was potentially susceptible to iminosugar-mediated ER α-glucosidase inhibition.

5.3.2 Iminosugars lack antiviral efficacy against HAZV

In line with established methods for culturing HAZV, the SW13 human adrenal adenocarcinoma cell line was utilised for *in vitro* antiviral efficacy testing in this study. To assess the antiviral activity of a panel of iminosugars, SW13 cells were infected with HAZV and immediately treated with titrations of compound at non-cytotoxic concentrations (Figure 91). Ribavirin was included as a positive control, since this compound was previously shown to inhibit the release of infectious HAZV from A549 human lung adenocarcinoma cells [287]. Supernatant was collected from cells at 1, 3 and 6 days post-infection to measure total virus secretion by qRT-PCR detecting S (nucleoprotein) segment RNA. Since iminosugars might impact the infectivity of virions rather than their secretion, infectious virus released to the supernatant was also quantified by plaque assay for day 3 supernatant samples. Although the experiment was conducted only once, by both measures, ribavirin demonstrated potent antiviral efficacy, whereas neither 2THO-DNJ,

*N*N-DNJ or *N*N-DGJ at concentrations of up to 100 µM nor *N*B-DNJ or *N*B-DGJ at concentrations of up to 316 µM possessed notable antiviral efficacy in terms of reducing total HAZV secretion (Figure 44) or release of infectious HAZV (Figure 45), suggesting that iminosugars do not have antiviral potential against HAZV.

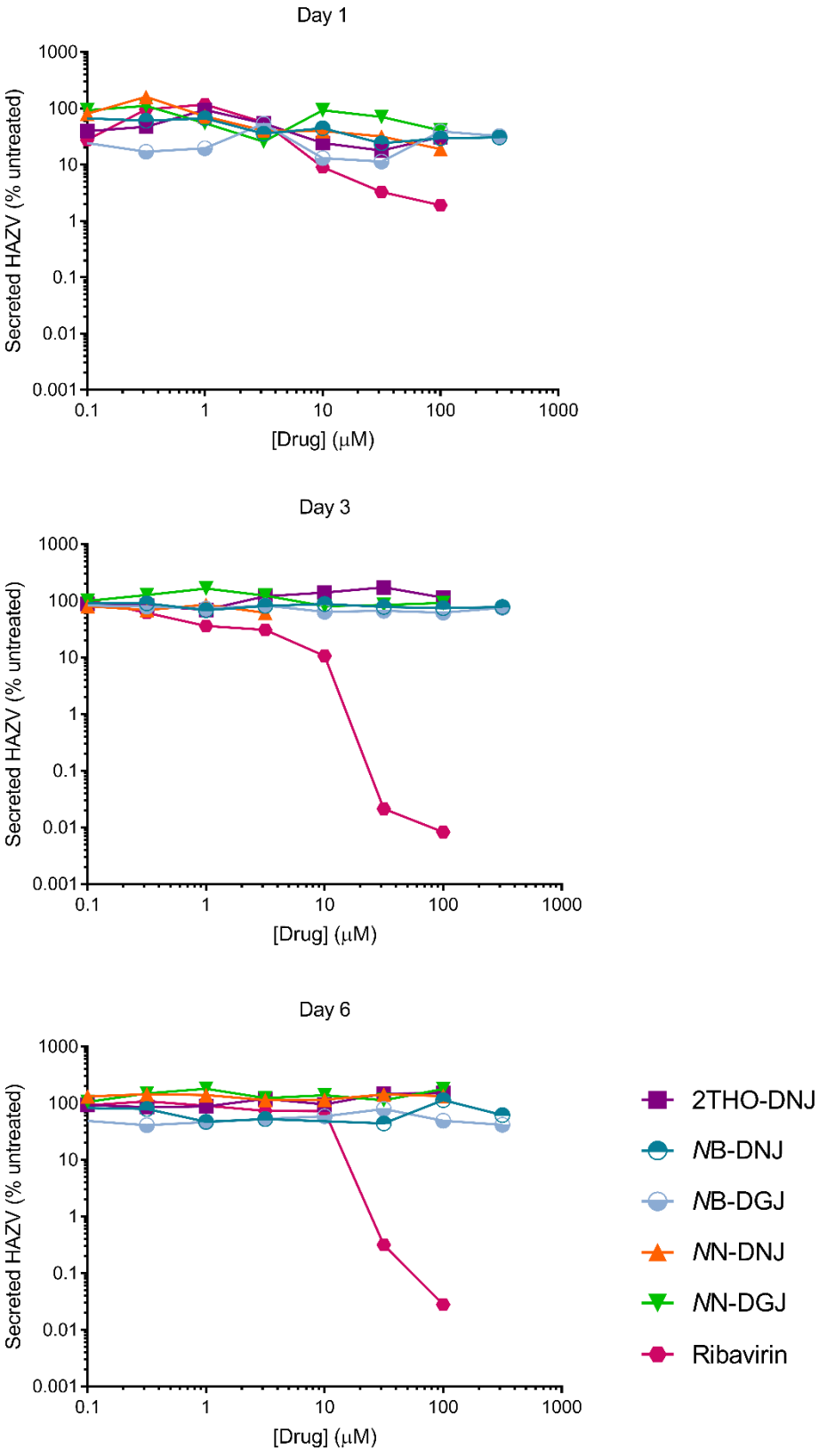

Figure 44. Iminosugars do not have any significant antiviral effect on HAZV secretion.

SW13 cells (n=1, assayed in technical triplicate) were infected with HAZV and treated with drug and for durations as indicated. Cell supernatants were collected and HAZV genome equivalents quantified by HAZV S (nucleoprotein) segment qRT-PCR. Data were normalised to untreated samples for each drug and the mean displayed. Data were collected in collaboration with Andrew Bosworth, Virology and Pathogenesis Group, Public Health England (Porton Down).

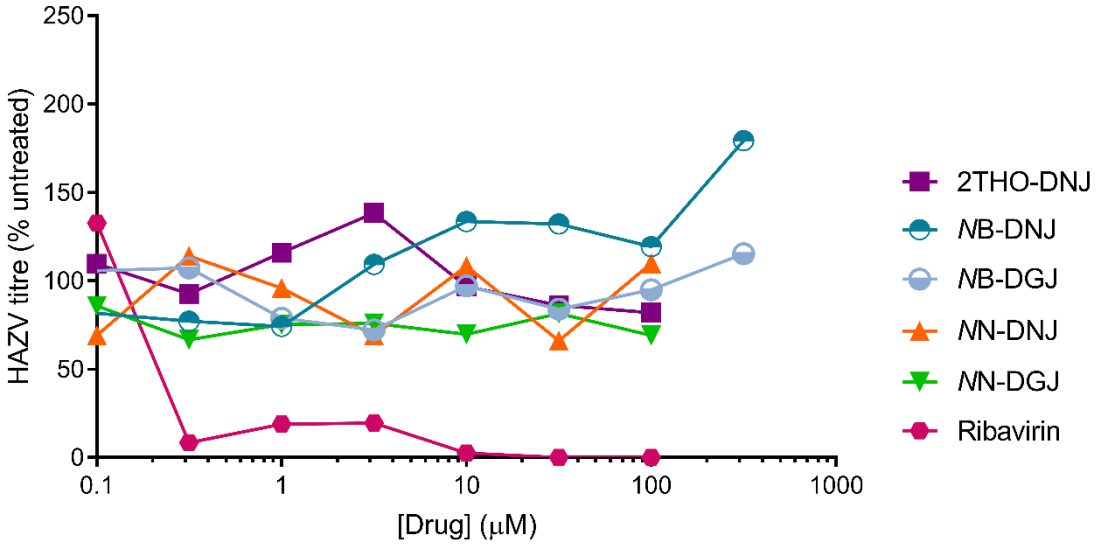

Figure 45. Iminosugars do not reduce infectious HAZV secretion from SW13 cells.

SW13 cells (n=1, assayed in technical triplicate) were infected with HAZV and treated with drug as indicated. Cell supernatants were collected after 3 days and HAZV titres quantified by plaque assay. Data were normalised to untreated samples for each drug and the mean displayed. Data were collected with the assistance of Victoria Graham, Virology and Pathogenesis Group, Public Health England (Porton Down).

5.3.3 FOS assay confirms that SW13 cells are susceptible to iminosugar treatment

Since the antiviral assays indicated that iminosugars lacked efficacy against HAZV, confirmation was sought that this was not due to a lack of susceptibility of the SW13 cells to iminosugar treatment. As such, both uninfected and HAZV-infected SW13 cells were treated with iminosugars under conditions reflecting the antiviral assay. Subsequently, cell lysates were subjected to FOS assay, involving the purification and HPLC-mediated identification of diagnostic oligosaccharide species generated upon inhibition of ER α-glucosidases, namely $Glc_3Man_5GlcNAc_1$ and $Glc_1Man_4GlcNAc_1$, indicative of ER α-glucosidase I and II inhibition,

respectively. Detection of FOS is dependent on activity of the N-linked glycosylation pathway, such that there is a flux of ER α-glucosidase substrates that will lead to FOS generation upon enzyme inhibition, and on the accessibility of the glucosidases to iminosugars. This may vary between cell types due to variable membrane compositions imposing different permeability barriers to iminosugar entry [314, 510], as well as potential roles of transporters in iminosugar uptake [511].

Analysis of both uninfected and HAZV-infected SW13 cells identified the accumulation of FOS species diagnostic for inhibition of both ER α-glucosidases upon treatment with DNJ-derivative iminosugars (Figure 46; representative HPLC profiles in Figure 110). As expected, ER α-glucosidase inhibition was not seen for treatment with ribavirin or DGJ-derivative iminosugars, although there was some background for the $Glc_3Man_7GlcNAc_2$ detected, particularly in the samples taken after 3 days (Figure 46B). The detection of these FOS species in DNJ-derivative iminosugar-treated cells indicates that the ER α-glucosidases in SW13 cells are accessible and susceptible to inhibition by iminosugars, although these results represent one biological replicate. However, the amount of FOS accumulation seen in uninfected SW13 cells appeared to be considerably lower than that generated upon iminosugar treatment of MDMΦs (approximately ten-fold lower in Figure 111), although this observation is not based on directly comparable experiments. This might indicate that there is greater throughput for the N-glycosylation pathway in MDMΦs relative to SW13 cells, or that iminosugars are better able to access the ER α-glucosidases in MDMΦs.

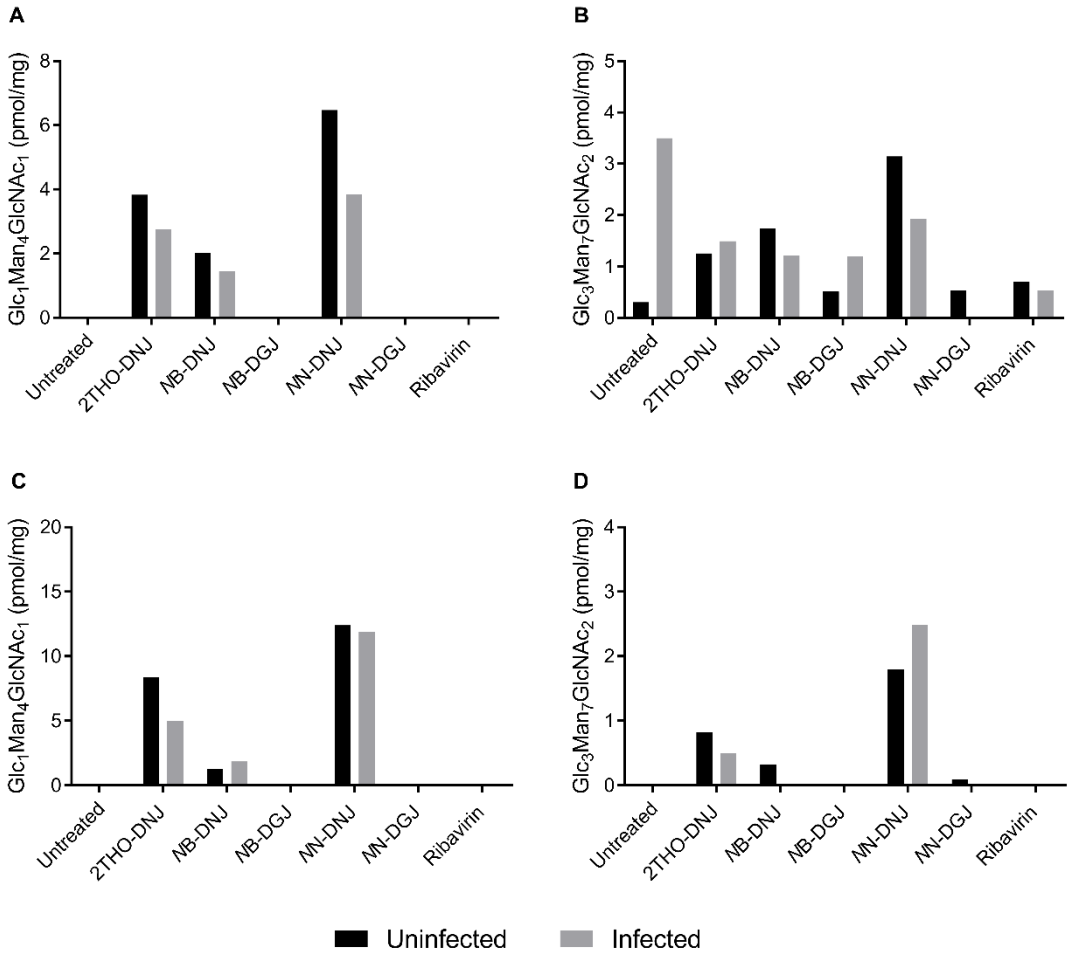

Figure 46. Uninfected and HAZV-infected SW13 cells are susceptible to iminosugar-mediated ER α-glucosidase inhibition.

SW13 cells (n=1, assayed in technical duplicate) were left untreated or treated with 100 µM 2THO-DNJ, N*N-DNJ,* N*N-DGJ or ribavirin, or 316 µM* N*B-DNJ or* N*B-DGJ for 3 days (A-B) or 6 days (C-D). In (A-B), cells were either mock- or HAZV-infected on day 0, immediately prior to drug treatment. In (C-D), cells were drug-treated for 3 days prior to mock- or HAZV-infection, after which the same drug treatment was continued for 3 days. At the end of the culture period, cells were lysed and FOS species purified and detected by NP-HPLC. The $Glc_3Man_7GlcNAc_2$ and $Glc_1Man_4GlcNAc_1$ FOS species detected, diagnostic for ER α-glucosidase I and II inhibition, respectively, were normalised to total protein content and the mean plotted. Samples were prepared and analysed with the assistance of Juliane Brun and Dominic Alonzi.*

Interestingly, ER α-glucosidase II inhibition mediated by some iminosugar treatments appeared to be reduced in the context of HAZV-infection compared to uninfected cells (Figure 46). This was unexpected, since increased glycoprotein turnover upon infection with an N-linked glycoprotein-expressing virus, like HAZV, might be expected to result in increased FOS

generation on iminosugar treatment. To explore one possible reason for this, SW13 cells were pre-treated with iminosugar for 3 days, prior to infection with HAZV or mock-infection and treatment continuation for a further 3 days. Cell lysates were collected and FOS assays performed. As expected, diagnostic FOS species for ER α-glucosidase I and II inhibition were detected with DNJ-derivative treatment, although a surprising peak indicative of ER α-glucosidase I inhibition was observed at Day 3 with *N*B-DGJ treatment (Figure 47), which was not consistent with previous analyses. In this single experiment, a reduction in the $Glc_1Man_4GlcNAc_1$ FOS species accumulated in response to 2THO-DNJ-mediated ER α-glucosidase II inhibition was again observed (Figure 47B as in Figure 46C). This suggests that the accumulation of FOS indicative of iminosugar-mediated ER α-glucosidase II inhibition may be reduced in the context of HAZV infection, although this experiment should be repeated to confirm these findings.

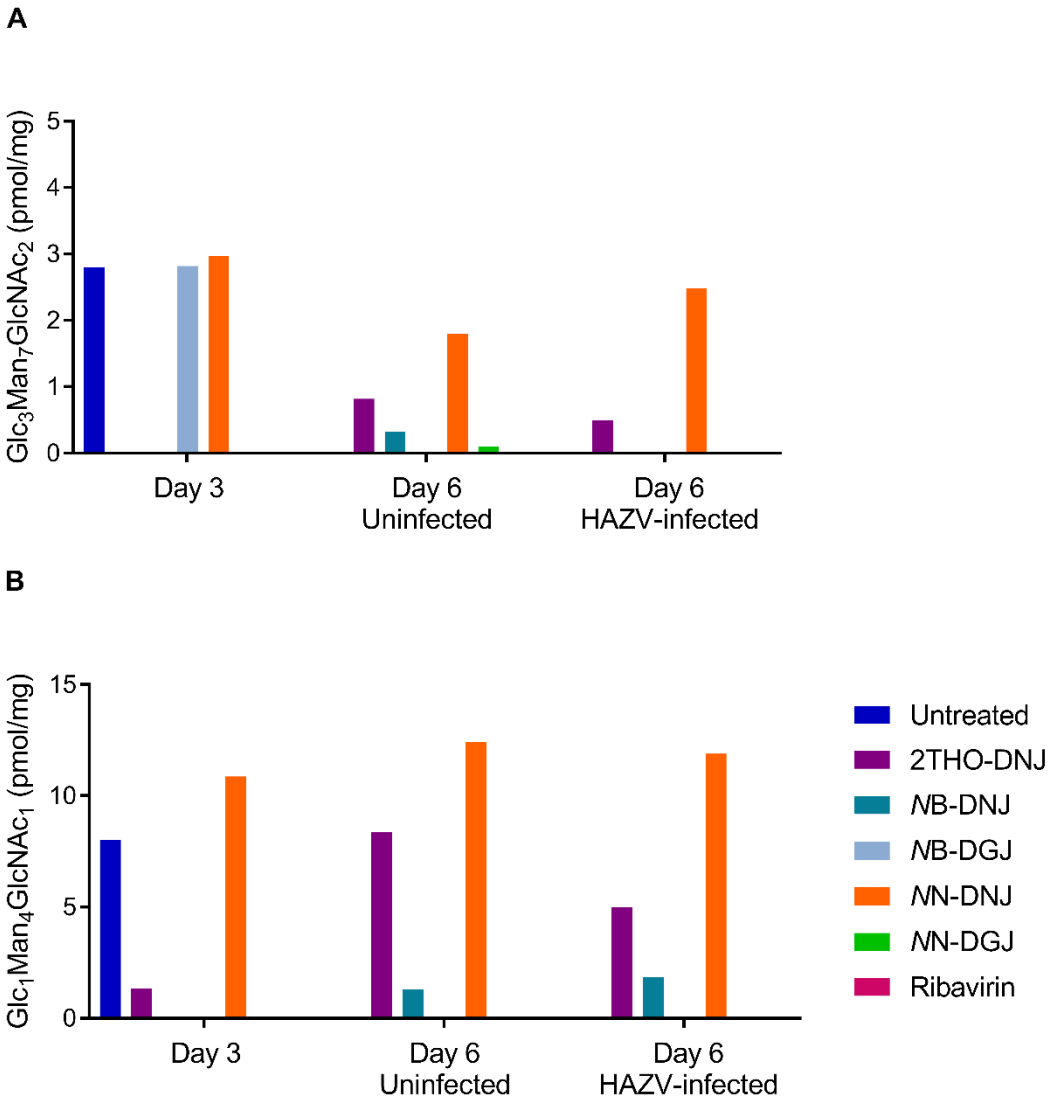

Figure 47. HAZV infection reduces some iminosugar-induced FOS accumulation.

SW13 cells (assayed in technical duplicate) were left untreated or treated with 100 µM 2THO-DNJ, NN-DNJ, NN-DGJ or ribavirin, or 316 µM NB-DNJ or NB-DGJ for 3 days (Day 3 samples) prior to mock- or HAZV-infection, after which the same drug treatment was continued for 3 days (Day 6 Uninfected or Day 6 HAZV-infected samples). Cells were lysed and FOS species purified and detected by NP-HPLC. The $Glc_3Man_7GlcNAc_2$ (A) and $Glc_1Man_4GlcNAc_1$ (B) FOS species detected, diagnostic for ER α-glucosidase I and II inhibition, respectively, were normalised to total protein content and the mean plotted. Samples were prepared and analysed with the assistance of Juliane Brun.

5.3.4 IFN-α/β secretion from HAZV-infected SW13 cells is modulated by drug treatment

Supernatants from infected SW13 cells were analysed for cytokine secretion using HEK-Blue™ TNF-α and IFN-α/β cytokine reporter cells (Invivogen; see 6.3.1 for assay development). No TNF-α secretion was detected (data not shown). While SW13 cells have been demonstrated to respond to TNF-α stimulation by increasing cell death [558], vasoactive peptide secretion [559] or NF-κB activation [560], the lack of detectable TNF-α secretion is in keeping with a lack of reports of TNF-α secretion by SW13 cells in the literature.

On the contrary, HAZV infection promoted a significant type I interferon (IFN-α/β) response. The cytokine response to *in vitro* HAZV infection has not previously been described, and IFN-α/β induction in SW13 cells has only been reported at the mRNA level thus far [561, 562]. Unfortunately, the response was greatly in excess of 850 pg/ml, the highest concentration of the standard curve used to attempt quantification in these samples. Limited sample volumes precluded reanalysis with a broader standard curve, meaning that absolute quantification of IFN-α/β secretion was not possible. However, since the SEAP secretion response to IFN-α stimulation of the reporter cell type is generally well described by linear regression, the relative secretion of IFN-α/β secretion was analysed by comparison to untreated HAZV-infected samples (Figure 48). This indicated that ribavirin treatment, the only drug in the panel to notably reduce virus production, also appeared to reduce IFN-α/β secretion from the SW13 cells as might be expected with less viral stimulus present. Higher concentrations of 2THO-DNJ and *N*N-DNJ also appeared to have some suppressive effect on IFN-α/β production, despite the lack of apparent antiviral efficacy, although this cannot be certain as IFN-α/β secretion was not quantified directly. This could be accounted for by an immunomodulatory property of iminosugars in the absence of an antiviral effect, a mechanism revisited in 0.

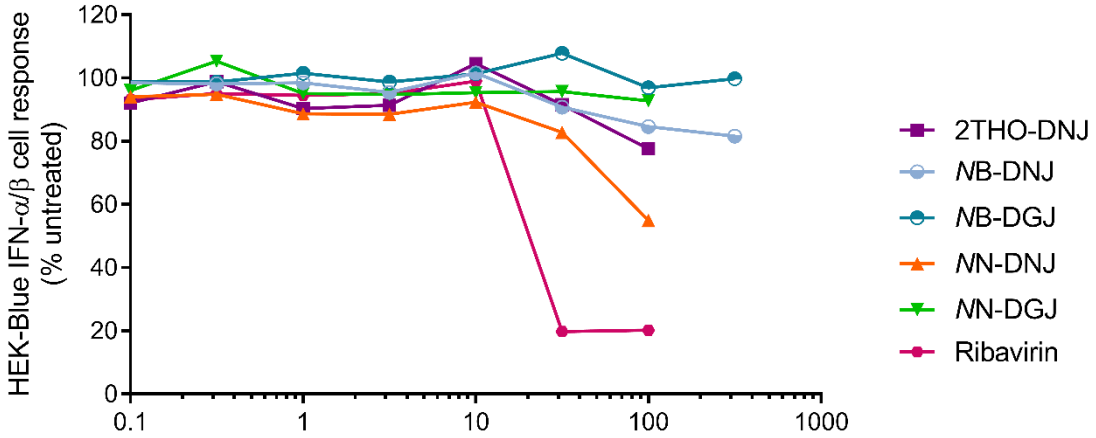

Figure 48. Supernatants from HAZV-infected SW13 cells treated with ribavirin or high concentrations of iminosugar show reduced activation of IFN-α/β reporter cell responses relative to infected, untreated cell supernatants.

SW13 cells (n=1, assayed in technical triplicate) were infected with HAZV and treated with iminosugar and ribavirin titrations as indicated. Supernatant was collected 6 days post-infection and analysed for secreted IFN-α/β by functional cytokine assay. Since SEAP secretion values were above the standard curve used in this assay, cytokine concentrations were not interpolated. Instead, SEAP secretion responses of the reporter cells normalised to untreated and the mean displayed to provide an indication of IFN-α/β secretion.

5.4 Discussion

CCHF represents a disease of increasing public health concern, with no vaccine and no effective antivirals available against CCHFV [295, 296, 563]. The conserved N-glycosylation of the structural Gn and Gc glycoproteins of CCHFV, known to be of functional importance for virion assembly [240, 241, 555], renders CCHFV a promising target for DNJ-derivative iminosugars that inhibit ER α-glucosidases. Consequential viral glycoprotein misfolding has demonstrated antiviral efficacy against diverse viruses (Table 1 and Table 2). However, the severity of CCHF warrants handling at BSL4, whereas the genetically and serologically related HAZV can be handled at BSL2, and has been proposed as a surrogate for testing antivirals and vaccines against CCHFV *in vitro* and in an A129 mouse model [287, 291]. Consequently, HAZV infection of SW13 cells was used for iminosugar antiviral efficacy testing in this study, as a putative surrogate for CCHFV.

Initially, the N-glycosylation of the HAZV glycoprotein sequence was confirmed by gel shift following endoglycosidase treatment (Figure 43) and by mass spectrometry, confirming the presence of N-glycosylation at two of the putative sites (Abhinav Kumar and Bevin Gangadharan; data not shown). Alignment and annotation of the HAZV and CCHFV glycoprotein sequences indicates that some, but not all, of the putative HAZV N-glycosylation sites align with those found in the CCHFV sequence (Figure 109). Of the HAZV sites confirmed to be N-glycosylated (5.3.1), N97 is not aligned with an N-glycosylation site for CCHFV, falling within the GP38 region of the CCHFV glycoprotein, while the HAZV N346 site aligns with a CCHFV N-glycosylation site within the Gn glycoprotein sequence. However, the presence of different processed glycoproteins derived from the HAZV M segment and their structural or non-structural roles remain to be elucidated. Thus, while the presence of N-glycans on the HAZV glycoprotein confirms the potential suitability of iminosugar-induced N-glycoprotein misfolding as an antiviral strategy for HAZV, the apparent differences between the N-glycosylation sites of HAZV and CCHFV glycoproteins suggest that the functional significance of N-glycosylation could differ between the viruses.

Following confirmation of HAZV N-glycosylation, a panel of iminosugars was tested for antiviral efficacy against HAZV. Ribavirin was used as a positive control and had a potent effect in the one experiment conducted (Figure 44 and Figure 45). The antiviral efficacy of ribavirin against HAZV has previously been demonstrated in a tissue culture model [287], with this efficacy translating to *in vitro* CCHFV infection [564, 565] and mixed efficacy in murine infection models for CCHFV [566-569]. In accordance with the mixed pre-clinical efficacy profile, the use of ribavirin in the treatment of CCHF patients is controversial and systematic reviews conclude that there is a lack of evidence for its clinical benefit, confounded by a paucity of well controlled clinical trials [296-298]. Undoubtedly, further antiviral drug development is required. However, in contrast to ribavirin, the tested iminosugars lacked any substantial antiviral effect on HAZV virion secretion

or infectious virus titres (Figure 44 and Figure 45), leading us to pause antiviral testing in order to confirm that the observed lack of efficacy was not because of a lack of susceptibility of the SW13 cell type to iminosugar treatment. To do this, a FOS assay was conducted on uninfected and HAZV-infected cells treated with iminosugars, finding that ER α-glucosidase inhibition was evident under both conditions (Figure 46). Thus, it seems that the lack of antiviral effect cannot be accounted for by enzyme inaccessibility. However, the levels of FOS induced by DNJ-derivative iminosugars in uninfected SW13 cells appeared to be significantly lower than those induced on treatment of uninfected MDMΦs (Figure 111), although this observation is drawn from experimental designs that are not directly comparable. This could potentially indicate reduced iminosugar uptake in the SW13 cells or a lower rate of N-glycoprotein processing. Cell type-dependent iminosugar efficacy has previously been described for INFV [314] and DENV [352, 394, 403], and may be related to variations in membrane composition determining access to the ER [510], the presence of putative iminosugar transporters [511], or differences in glycoprotein processing pathways between cell types [328, 512]. In order to confirm that the lack of antiviral efficacy against HAZV is not cell type-specific, antiviral efficacy testing could be repeated in A549 or Vero cells which are also susceptible to HAZV infection, although not the best established or highest-yielding cell types for HAZV (Stuart Dowall, personal communication).

If one considers the lack of iminosugar efficacy against HAZV to be established, however, this implies that the N-glycosylation of the viral glycoproteins does not render HAZV susceptible to the effects of iminosugars. While a single N-linked glycan can be sufficient to endow susceptibility to iminosugar treatment [323], the lack of efficacy of iminosugars against N-glycosylated viruses is not without precedent. Despite the N-glycosylation of INFV glycoproteins, virus strain-specific efficacy is seen, reviewed in [314], and while secretion and infectious titres of the VSV San Juan strain were reduced by DNJ or CAST treatment, the Orsay strain was

unaffected [388]. This illustrates that N-glycosylation of a glycoprotein does not necessitate reliance on the calnexin cycle, entry to which is controlled by ER α-glucosidase II. Alternative chaperones such as BiP may aid the folding of N-glycosylated viral glycoproteins [570], or N-glycosylation may be dispensable for the folding or function of a glycoprotein. Thus virion formation and infectivity may be preserved regardless of iminosugar treatment. The recent development of Vero cells with each of the ER α-glucosidases knocked out using CRISPR/Cas9 technology [452] presents an opportunity for future study of the dependence of HAZV on these enzymes for productive viral infection (as conducted for DENV and ZIKV in 3.3.2.3 and 4.3.2, respectively), with a lack of effect of DNJ-derivative iminosugars rationalised if virus production was unaffected in the knockout cell lines. Interestingly, despite the lack of efficacy against HAZV, multiple DNJ-derivative iminosugars are antiviral against the related bunyavirus RVFV *in vitro* [357, 358]. This emphasises the importance of investigating iminosugar efficacy against viruses and virus strains individually, using physiologically-relevant cell types.

The suitability of HAZV as a surrogate for the antiviral efficacy testing of iminosugars against CCHFV is called into question by the differences in N-glycosylation of their viral glycoproteins (Figure 109). Therefore, iminosugar efficacy might still be assessed directly against CCHFV infection, although the requirement for BSL4 facilities [291] and experimental challenges in accurate quantification of infectious virus (Stuart Dowall and Victoria Graham, personal communication) remain barriers to this line of enquiry. Unlike for therapeutics targeting viral replication for example, the CCHFV minigenome or viral-like particle (VLP) systems that have been developed [571] lack the M segment and are therefore unsuitable for assessment of iminosugar efficacy since, if efficacious, impacts on viral glycoprotein folding are likely to be instrumental. Future development of a reverse genetics system for HAZV could provide a valuable resource for iminosugar efficacy testing against a recombinant virus possessing CCHFV glycoproteins, if the CCHFV M segment were incorporated into VLPs with a HAZV background.

Using this system, the infectivity of VLPs resulting from iminosugar-treated cells could be determined as a measure of iminosugar efficacy. Such a system would also enable comparison of antiviral efficacy between HAZV and CCHFV glycoprotein-containing VLPs, identifying whether any differences in iminosugar efficacy could be attributed to the respective viral glycoproteins. If efficacy was identified *in vitro*, efficacy testing could progress to one of the CCHFV murine infection models [306, 567, 572, 573]. Considering possible clinical use of iminosugars against CCHFV, the involvement of hepatocyte [253, 258-260] and immune cell infection [253-255] in disease pathogenesis means that iminosugars with such tropisms might be beneficial. Recently, 5'-tocopheroxypentyl-DNJ has been described as a liver- and myeloid immune cell-targeted iminosugar with antiviral efficacy against DENV and HCV *in vitro* [355]. Testing such targeted iminosugars might prove valuable in the pursuit of these candidate antivirals against CCHFV.

In summary, the antiviral efficacy of iminosugars against HAZV was explored, as a proposed surrogate virus for CCHFV antiviral drug development. Occupation of N-glycosylation sites in the HAZV glycoprotein was confirmed, supporting the possibility for iminosugar-mediated glycoprotein misfolding as a mechanism of action against the virus. However, treatment of HAZV-infected SW13 cells with a panel of iminosugars failed to have an antiviral effect, while ribavirin was potently efficacious in the one experiment conducted. This lack of iminosugar efficacy did not appear to be due to an absence of ER α-glucosidase inhibition by DNJ-derivative iminosugars. Since the glycosylation of CCHFV and HAZV glycoproteins appears to differ, and CCHFV the N-glycosylation of CCHFV glycoproteins is of functional importance, iminosugars may yet hold potential as antivirals against CCHFV. However, this requires evaluation against CCHFV directly *in vitro* and *in vivo*, since HAZV may not be an appropriate surrogate for CCHFV for the study of antivirals targeting N-linked glycosylation.

Chapter 6. Iminosugar effects on cytokines induced by viral and non-viral stimuli

6.1 Abstract

Evaluating the impact of antiviral drugs on cytokine responses is important since this may significantly influence disease pathogenesis and the outcome of infection. Previous studies have suggested that diverse iminosugars may have immunomodulatory properties, and that these extend beyond viral infection. However, there has been little mechanistic analysis with regards to how cytokine production is affected or the structure-activity relationship. Here, the effect of 2THO-DNJ treatment on TNF-α and IFN-α/β responses to DENV infection of MDMΦs is characterised, finding a dose-dependent reduction in functional TNF-α and IFN-α/β secretion which was significantly correlated with antiviral efficacy. While other iminosugars influenced *TNFA* transcription, 2THO-DNJ did not, indicating a post-transcriptional regulatory mechanism is involved. Consideration of the cytokine-modulatory effects of iminosugars is extended beyond viral infection, to evaluate the effects of 2THO-DNJ, *N*N-DNJ and *N*N-DGJ on cytokine production elicited by MDMΦ stimulation with a panel of non-replicative pathogen-associated molecular patterns targeting a range of pattern recognition receptors. While the DNJ-derivatives had a widespread suppressive effect on TNF-α secretion, *N*N-DNJ and *N*N-DGJ had differential effects, requiring further mechanistic analysis. Multiplex cytokine analysis also indicated that iminosugars could affect IFN-γ, IL-1β and MCP-1 secretion in response to LPS-EB and TL8-506 stimulation. Ultimately, the wide-ranging ability of iminosugars to modulate cytokine production suggests potential clinical utility of iminosugars in settings beyond viral infection.

6.2 Introduction

Cytokines play a critical role in viral infection. Type I interferons (IFN-α/β) are crucial for initiating the antiviral state through induction of interferon-stimulated genes and are a cornerstone of the innate antiviral immune responses. On the other hand, pro-inflammatory cytokines such as TNF-α can contribute to disease pathogenesis, particularly in haemorrhagic fevers such as DHF and CCHF. Thus, it is important to evaluate the effect of antiviral drugs on the cytokine response to infection, as this may have a significant impact on the efficacy and treatment outcome in the context of an infected patient.

Many cytokines are implicated in DENV infection, as discussed in 1.1.1. TNF-α, however, has a central role in the pathogenesis of disease, increasing endothelial cell permeability leading to vascular leakage [574], and is proposed as a key mediator of disease severity [138, 575]. In contrast, cellular [130], murine [131] and clinical [118] data suggest a protective role for IFN-α/β in DENV infection. Studies in various systems have implicated multiple pattern recognition receptors (PRRs) in TNF-α production downstream of DENV recognition, namely CLEC5A recognition of DENV virions [141], RIG-I and MDA5 recognition of viral RNA [146], and TLR4 recognition of NS1 [75]. The viral NS2B3 protease can also directly promote TNF-α production by activating NF-κB [147, 148]. IFN-α/β production is mediated by recognition of viral RNA by TLR7 [141, 149-151], TLR3 [152-154], RIG-I [152, 153, 155-157] and MDA5 [152, 157], and by TLR4 recognition of NS1 [75]. In DENV infection of human monocytes and macrophages, secretion of IFN-α/β and TNF-α has previously been identified [15, 129, 576], enabling study of the influence of iminosugars on the production of these cytokines in the MDMΦ system.

In addition to viral infection, cytokines are critical mediators in other infectious disease states such as sepsis as well as chronic inflammatory conditions. Sepsis is defined as “a life threatening condition that arises when the body's response to an infection injures its own tissues and

organs" [577], and can result from infection with diverse viral, bacterial and fungal pathogens. While controversial, sepsis is usually characterised by early dysregulated pro-inflammatory responses, which can correlate with mortality. Many sepsis-related deaths occur later, however, in a phase of disease defined by immunosuppression when there may be increased rates of opportunistic infection [578-580]. The heterogeneity of patients poses significant problems for therapeutic evaluation in clinical trials [578]; however, a meta-analysis found that anti-TNF-α therapies may improve survival in patients with severe sepsis or those experiencing septic shock [581]. Therefore, the evaluation of iminosugar activities against TNF-α production elicited by a range of PAMPs could provide insights of therapeutic relevance.

Six-membered ring iminosugars of various stereochemistries have been demonstrated to affect the production of various cytokines. A range of effects on different cytokines have been identified in a limited number of *in vitro* studies of primary human immune cells and cell lines, *ex vivo* murine splenocytes and tissues, and *in vivo* in murine DENV infection models (Table 4 and Table 6). M*O*N-DNJ treatment has previously been shown to reduce TNF-α secretion, quantified by ELISA, elicited by DENV infection or LPS-stimulation of MDMΦs [418]. In the same study, *N*B-DNJ and *N*B-DGJ were compared, with neither compound having a significant effect on TNF-α secretion [418]. However, two studies comparing the effects of *N*B-DNJ and *N*B-DGJ on cytokine responses [418, 436], there has been a lack of side-by-side evaluation of iminosugars differing only in stereochemistry. In addition, the number of PAMPs for which cytokine-modulatory effects of iminosugars have been investigated is limited. Here, the effects of iminosugars on cytokines elicited by DENV-infection or PAMP stimulation of MDMΦs were evaluated by consideration of TNF-α and IFN-α/β production. The principal iminosugar studied was 2THO-DNJ, for which effects on cytokines have only been described in a murine DENV infection model to date. In addition, the effects of *N*N-DNJ and *N*N-DGJ were compared with respect to MDMΦ cytokine production elicited by stimulation with a panel of PAMPs.

Overall, this chapter aims to elucidate the effects that iminosugars have on cytokine production in response to DENV infection and PAMP stimulation of MDMΦs. Specifically, the aims were:

1. To investigate the effects of 2THO-DNJ on MDMΦ cytokine production in response to DENV infection and PAMP stimulation;
2. To investigate the relationship between the antiviral efficacy of DNJ-derivative iminosugars and their effects on cytokine production in DENV-infected MDMΦs, and to investigate potential underlying mechanisms including effects on cytokine transcription and secretion;
3. To compare the effects of 2THO-DNJ, *N*N-DNJ and *N*N-DGJ on MDMΦ cytokine production in response to stimulation with a broad spectrum of PAMPs; and
4. To compare the effects of 2THO-DNJ, *N*N-DNJ and *N*N-DGJ pre-treatment on TLR signalling using reporter cells for TLR2, TLR3, TLR4 and TLR9 signalling.

6.3 Results

6.3.1 Development of functional cytokine assays for TNF-α and type I interferon

Previous work has established that iminosugars can modulate the secretion of cytokines from cell culture systems and circulating cytokine levels *in vivo* in murine viral infection models (Table 4 and Table 6). However, these studies have not considered the biological functional activity of these cytokines, often using antibody-based techniques such as ELISA for their detection, which do not necessarily discriminate between a functional and a misfolded signalling-defective molecule. For N-glycosylated cytokines, it is possible that the competitive inhibition of ER α-glucosidases by DNJ-derivative iminosugars could lead to the misfolding of the cytokine, and subsequent degradation or continued secretion of cytokine molecules with altered functionality. Interestingly, murine TNF-α is N-glycosylated, but human TNF-α is not [582], which could

underlie any species-specificity in TNF-α responses to DNJ-derivative iminosugar treatment. Considering type I interferon, IFN-α subtypes vary in N-glycosylation [583-585], while human IFN-β is N-glycosylated [586]. While reduced secretion of an N-glycosylated cytokine could derive from a direct effect on the cytokine itself, modulation of an N-glycosylated upstream regulator could occur alternatively or in addition. This might also explain effects on cytokines that are not themselves N-glycosylated, although alternative iminosugar mechanisms of action might be responsible.

In order to pursue this area further, assays based on commercially available HEK-Blue™ TNF-α and IFN-α/β cytokine reporter cells (Invivogen) were developed to quantify the levels of functional cytokine (able to bind and signal through the relevant cytokine receptor) in supernatant samples, with reference to standard curves of recombinant cytokine (see 2.5.4.2). The presence of DENV or relevant stimuli in the supernatant was demonstrated not to induce reporter cell responses, and the presence of iminosugars or other antivirals used in this study was demonstrated not to affect reporter cell responses (see 8.13).

6.3.2 Iminosugar treatment affects cytokine production in DENV infection

6.3.2.1 2THO-DNJ reduces functional TNF-α production from DENV-infected MDMΦs

In order to establish whether 2THO-DNJ treatment impacts the cytokine response to DENV infection, biologically functional TNF-α secreted from DENV-infected MDMΦs was quantified 48 hours post-infection, corresponding to the routinely used time point for antiviral assays. 2THO-DNJ treatment dose-dependently reduced TNF-α secretion (Figure 49A). Overall, this reduction correlated with the antiviral effect of 2THO-DNJ (Figure 49B). For each donor, linear regression and Pearson correlation were used to determine the relationship between TNF-α secretion and DENV titre. A statistically significant positive correlation between viral titre and TNF-α secretion

was found for four of five donors tested, indicating that the antiviral effect of 2THO-DNJ is associated with reduced TNF-α production. For donor JO, the slope of the line of best-fit was greater than 0.5 indicating that TNF-α secretion changed more for a given change in viral titre. For donors IX, IY and JP, the slope was positive but less than 0.5, indicating that there was a greater effect of 2THO-DNJ treatment on viral titre than TNF-α production. For donor JN, for which there was no significant correlation, little TNF-α was induced upon infection, allowing little drug-mediated downmodulation (10 pg/ml TNF-α induced in DENV-infected untreated samples compared to over 100 pg/ml from donor IX; Figure 116). Reduced production of TNF-α in the context of the antiviral effect of iminosugars can be rationalised by the presence of less viral stimulus for pro-inflammatory cytokine production, be that viral genome or viral proteins, both of which are reduced by iminosugar treatment.

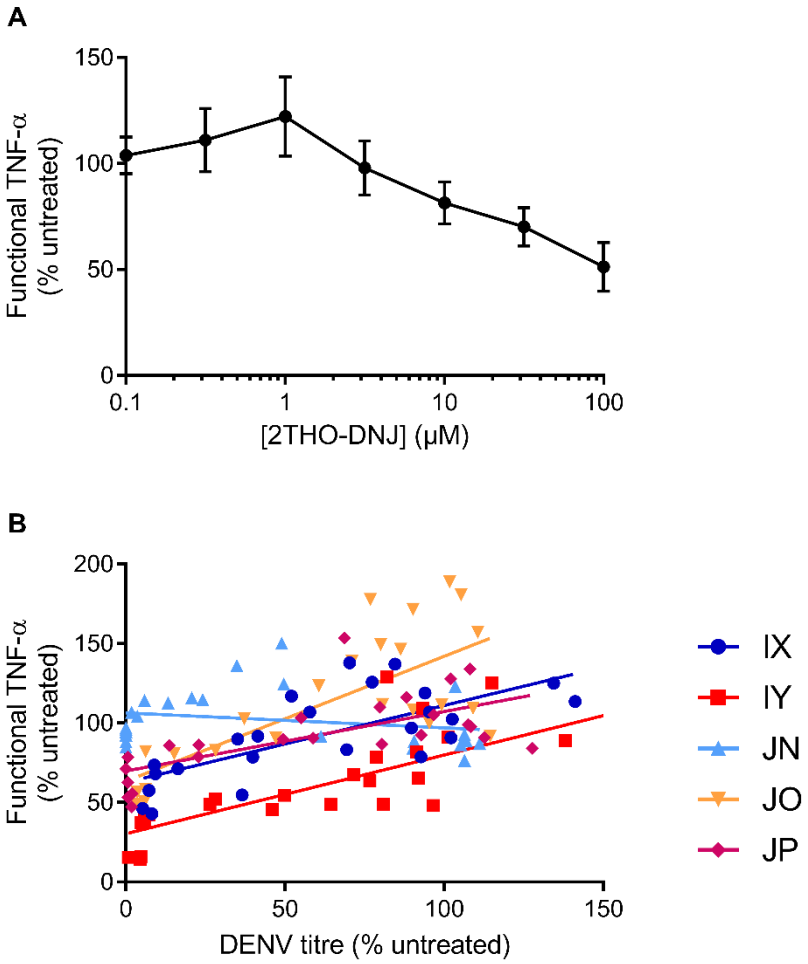

Figure 49. 2THO-DNJ reduces functional TNF-α secretion from DENV-infected MDMΦs.

Primary MDMΦs (n=5 donors, as shown, assayed in technical triplicate) were infected with DENV and treated with a titration of 2THO-DNJ. Supernatant was collected at 48 hours post-infection, and secreted TNF-α was quantified by functional assay.

(A) Functional TNF-α was normalised to untreated for each donor and plotted as mean ±standard error.

(B) Viral titres, determined by plaque assay (see Figure 95), were normalised to untreated and mean titres plotted against mean normalised functional TNF-α for each sample. Linear regression was used to describe the data with lines of best fit and Pearson correlation used to assess correlation between the measures (Table 22).

Further support for the antiviral efficacy of 2THO-DNJ being the principal mediator of the reduction in TNF-α secretion is the lack of effect of 2THO-DGJ treatment on TNF-α production (Figure 50). This demonstrates that the TNF-α-modulating effect is linked to the glucose

stereochemistry of the compound. However, this does not discriminate between this effect being due to the antiviral nature of 2THO-DNJ associated with ER α-glucosidase inhibition, or an alternative mechanism linked to the headgroup stereochemistry that might directly affect cytokine production, for which the tail structure might be important or dispensable, but not sufficient.

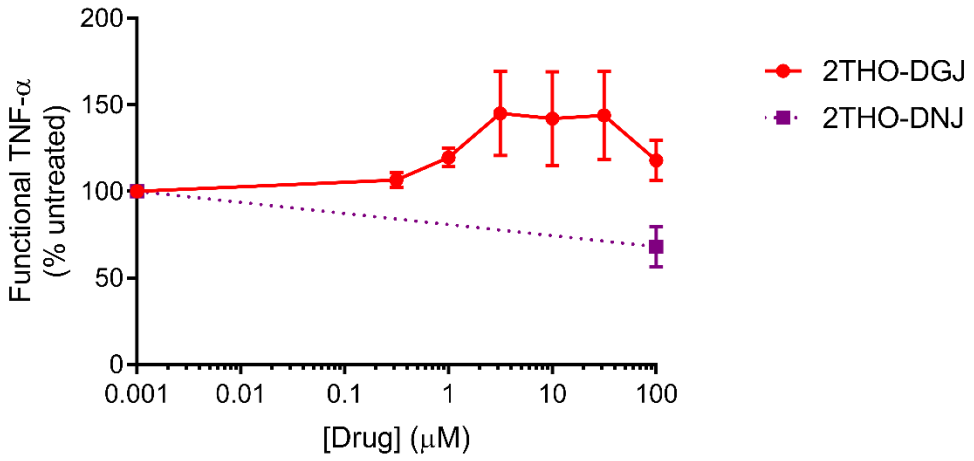

Figure 50. 2THO-DGJ does not reduce DENV-induced TNF-α production.

Primary MDMΦs (n=3 donors (MB, MC, MP), assayed in technical triplicate) were infected with DENV and treated as indicated. After 48 hours, supernatant was collected and TNF-α secretion determined by functional assay. Data were normalised to untreated for each donor and plotted as mean ± standard error (untreated is displayed at 0.001 μM to allow visualisation on a logarithmic axis).

To further investigate whether the cytokine-modulating effect of 2THO-DNJ is due purely to its antiviral effect, or whether an additional mechanism is at play, the effects of 2THO-DNJ were compared to those of ribavirin, which does not inhibit ER α-glucosidases. Multiple mechanisms have been proposed to underpin the antiviral activity of ribavirin against DENV, principally reducing transcription, translation and viral replication by depletion of cellular guanosine triphosphate pools [493], and ribavirin triphosphate inhibiting NS5 methyltransferase activity [587]. Ribavirin incorporation as a lethal mutagen into viral genomes has been demonstrated for other viruses [588]. In addition to antiviral effects, ribavirin has also been described to suppress cytokine and chemokine production in response to DENV infection, with IL-6, TNF-α,

IP-10 and RANTES production suppressed in A549 cells [491] and IL-6 and IL-8 secretion reduced in human umbilical vein endothelial cells [492], although this has not been investigated in human immune cells. Conflicting evidence exists regarding the ability of ribavirin to influence cytokine production elicited by non-infectious stimuli in immune cells, with data showing that ribavirin can promote Th1 but suppress Th2 cytokine responses in human peripheral blood T cells [589] and promote IL-12 production from PBMCs [590], although ribavirin did not affect cytokine transcription in response to LPS stimulation of murine peritoneal macrophages [591]. Consequently, the antiviral and immunomodulatory properties of ribavirin and 2THO-DNJ in DENV-infected MDMΦs were compared.

While the antiviral efficacy of ribavirin against DENV is well documented in cell lines, demonstration of activity in MDMΦs is restricted to DENV-2 NGC [494]. Therefore, dose-dependent antiviral efficacy of ribavirin was first validated in our model (Figure 51) using concentrations determined to be non-toxic (Figure 88).

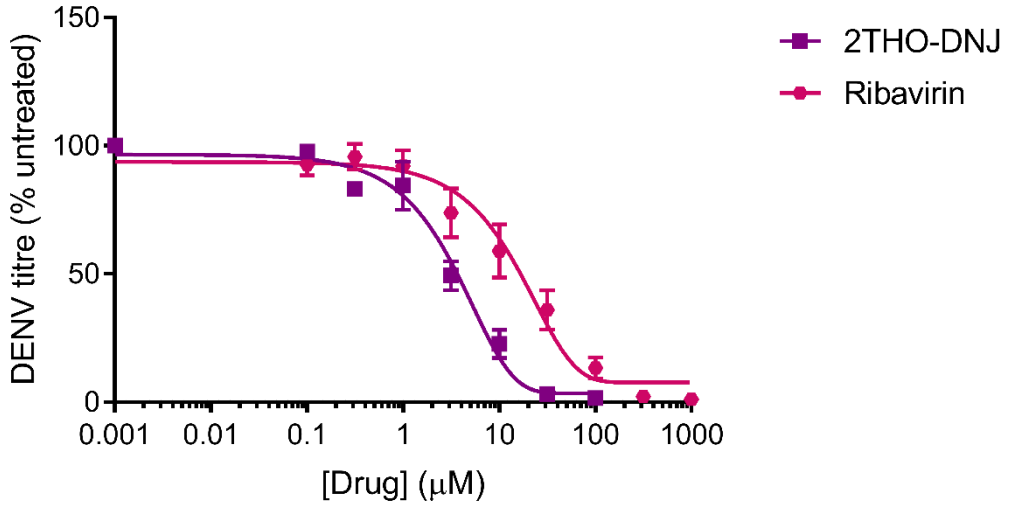

Figure 51. Ribavirin is antiviral against DENV in MDMΦs.

Primary MDMΦs (n=6 donors (MZ, NB, NG, NY, OC, OD), or n=3 for ribavirin 0.1 and 0.316 μM (MZ, NB, NG) and 316 and 1000 μM (NY, OC, OD), assayed in technical triplicate) were infected with DENV and treated with a titration of 2THO-DNJ or ribavirin. Supernatant was collected at 48 hours post-infection and viral titres determined by plaque assay. Titres were normalised to

untreated and plotted as mean ± standard error, with untreated represented as 0.001 µM to allow plotting on a logarithmic scale and curves fit using the sigmoidal 4-point log function.

Both 2THO-DNJ and ribavirin dose-dependently reduced functional TNF-α secretion (Figure 52). However, unlike with viral titres, a residual level of DENV-induced TNF-α secretion was observed even at the highest drug concentrations used, exceeding that produced at baseline from mock-infected MDMΦs (historical controls, data not shown). This highlights a disconnect between both viral secretion and stimulation of TNF-α production, and the antiviral and immunomodulatory capacities of the compounds, although it does not rule out the possibility for a complete dampening of TNF-α secretion were higher concentrations to be used.

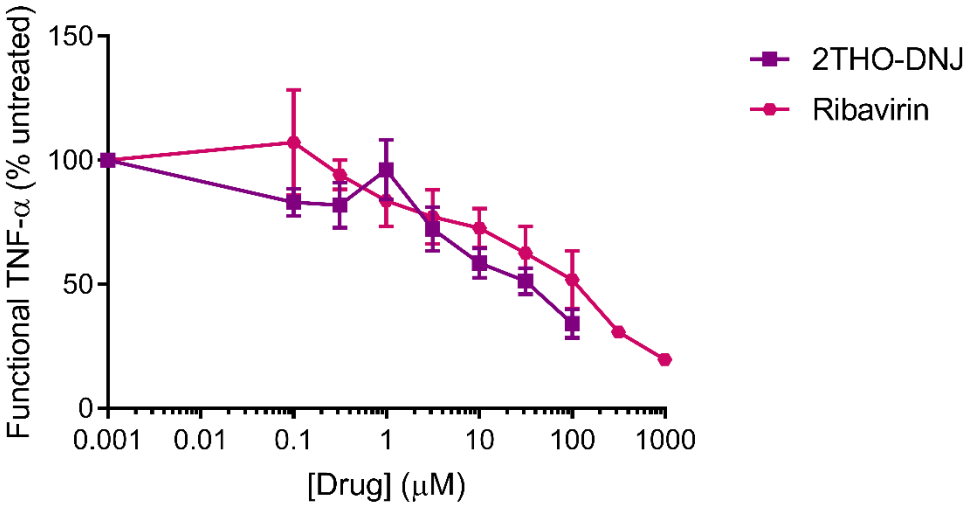

Figure 52. 2THO-DNJ and ribavirin treatment both reduce TNF-α secretion from DENV-infected MDMΦs.

Primary MDMΦs (n=6 donors (MZ, NB, NG, NY, OC, OD), or n=3 for ribavirin 0.1 and 0.316 µM (MZ, NB, NG) and 316 and 1000 µM (NY, OC, OD), assayed in technical triplicate) were infected with DENV and treated with a titration of 2THO-DNJ or ribavirin. Supernatant was collected at 48 hours post-infection and secreted TNF-α quantified. Values were normalised to untreated and plotted as mean ± standard error, with untreated represented as 0.001 µM to allow plotting on a logarithmic scale.

To ascertain the relationship between antiviral effect and cytokine production, DENV titres and TNF-α secretion were normalised to untreated for each donor and plotted against each other for each compound (Figure 53). In both cases, reduced DENV titres were associated with

reduced TNF-α secretion. Despite the high variability derived from analysis of multiple MDMΦ donors, the correlation was highly significant as determined by Pearson's correlation ($p<0.0001$ for both compounds; Table 23). For ribavirin, the gradient indicates that for a given percentage change in DENV titre, cytokine secretion is affected more, whereas for 2THO-DNJ, the dominant effect appears to be on viral titre. It is interesting to note that even with potent reductions in viral titres, for example to below 10% of untreated, a broad range of TNF-α responses are observed, particularly for 2THO-DNJ treatment (Figure 53), reflecting inter-donor variability in cytokine responses (Figure 117). Therefore, it appears that in the context of DENV infection of MDMΦs, for a given antiviral effect, ribavirin has a stronger dampening effect on TNF-α secretion than 2THO-DNJ. However, while ribavirin appears to have the stronger suppressive effect on TNF-α yet lacks efficacy *in vivo* [400, 404, 592], the mechanisms underlying the antiviral effect and cytokine modulatory ability likely differ between the two compounds, indicating that cytokine-modulation by 2THO-DNJ might still be therapeutically useful.

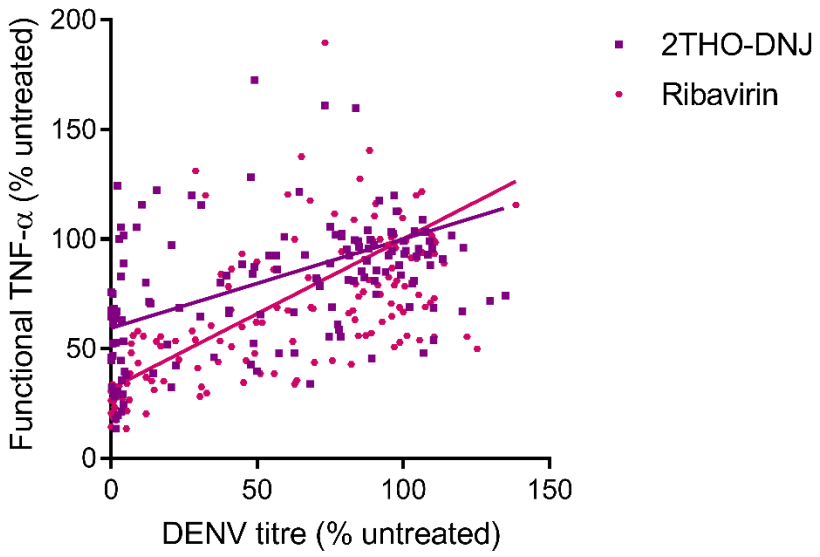

Figure 53. 2THO-DNJ and ribavirin treatment both reduce TNF-α secretion from DENV-infected MDMΦs.

Primary MDMΦs (n=6 donors (MZ, NB, NG, NY, OC, OD), assayed in technical triplicate) were infected with DENV and treated with a titration of 2THO-DNJ or ribavirin. Supernatant was collected at 48 hours post-infection, and viral titres assay and functional TNF-α secretion quantified. Values derived from individual samples were normalised to untreated for each donor

and mean antiviral efficacy plotted against mean cytokine response. Linear regression was used to find lines of best fit, with associations assessed by Pearson correlation (see Table 23).

6.3.2.2 The influence of 2THO-DNJ and ribavirin treatment on IFN-α/β responses of DENV-infected MDMΦs is donor-dependent

In addition to quantifying functional TNF-α secretion from DENV-infected MDMΦs, functional type I interferon (IFN-α/β) secretion was investigated. Despite the antiviral efficacy of both ribavirin and 2THO-DNJ in all of the donors (Figure 51), the effect of the compounds on IFN-α/β responses was variable (Figure 54). In donors MZ and NB, higher concentrations of 2THO-DNJ enhanced IFN-α/β production, corresponding to high levels of IFN-α/β secretion when viral titres were substantially reduced (Figure 55). In contrast, in donors NY, OC and OD, ribavirin treatment dose-dependently enhanced IFN-α/β secretion, while 2THO-DNJ treatment was associated with reduced IFN-α/β release. Meanwhile, donor NG made a poor IFN-α/β response to infection (around 50 pg/ml in untreated samples, compared to over 1500 pg/ml for most other donors), and neither compound affected IFN-α/β secretion. Therefore, despite antiviral efficacy being apparent in all of these scenarios, the influence of 2THO-DNJ or ribavirin treatment on the IFN-α/β response of MDMΦs to DENV infection is highly donor-dependent. Since the reduced virus secretion pursuant to treatment with either compound reduces the viral agonist stimulating IFN-α/β production, it is interesting that enhanced secretion is sometimes observed, and could correspond to reduced production of viral proteins responsible for evading interferon production [134] outweighing the effect of a reduced stimulus. This promotion of IFN-α/β secretion in the context of infection might be beneficial for the host, since cellular [130], murine [131] and clinical [118] data suggest a protective role for IFN-α/β in DENV infection. The interferon receptor deficiency in many of the mouse models commonly used to evaluate DENV antivirals [593] might have been a limitation for assessing any contribution that this mechanism might have *in vivo*. However, the inter-donor variability of this response requires further investigation, and careful consideration should be given to this issue in a clinical context.

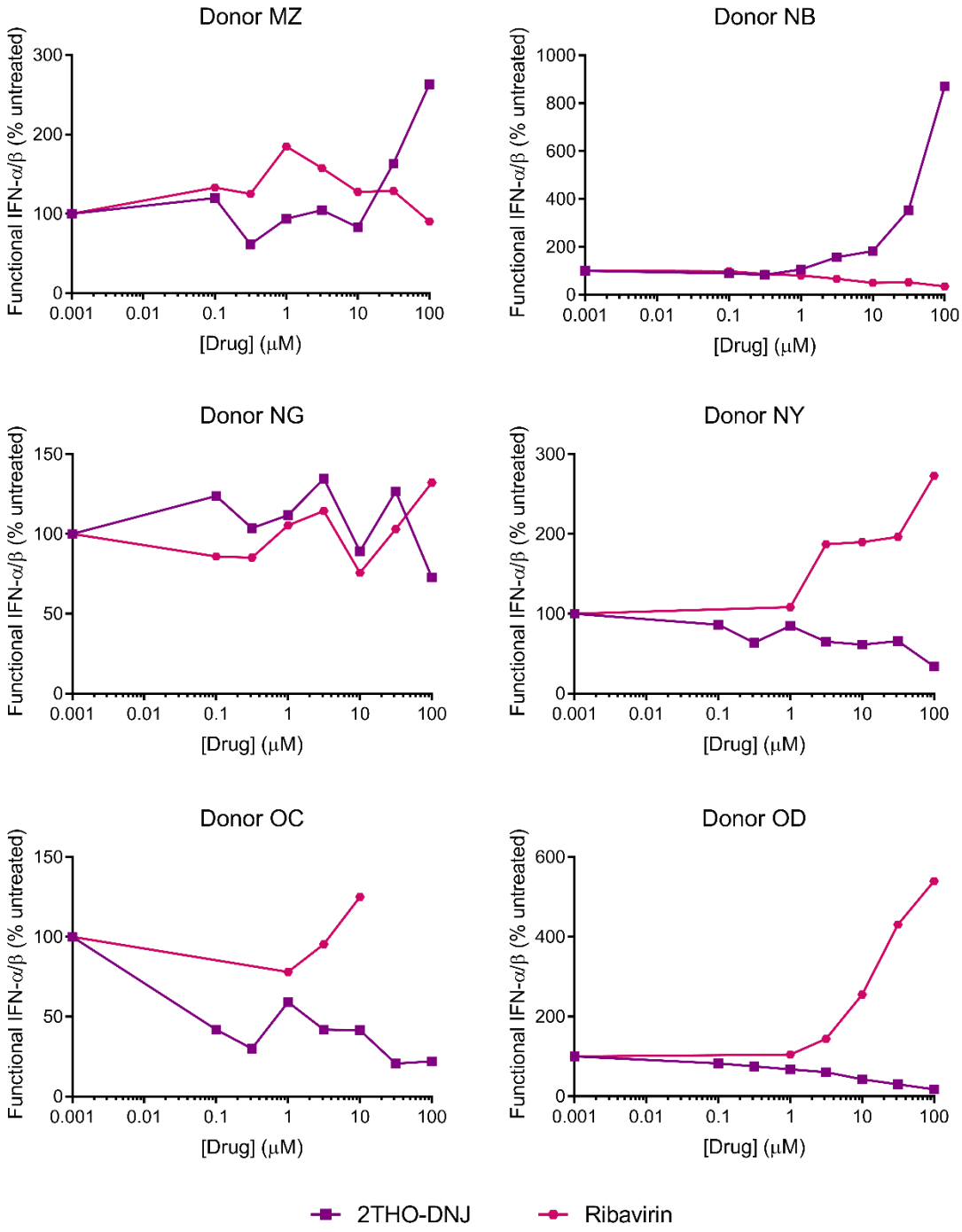

Figure 54. 2THO-DNJ and ribavirin have variable effects on the IFN-α/β response to DENV infection of MDMΦs.

Primary MDMΦs (n=6 donors, as shown, assayed in technical triplicate) were infected with DENV and treated with a titration of 2THO-DNJ or ribavirin. Supernatant was collected at 48 hours post-infection, and IFN-α/β secretion quantified by functional assay. Values were normalised to untreated and the mean plotted, with untreated represented as 0.001 μM to allow plotting on a logarithmic scale. For donors NY, OC, and OD, peak values for ribavirin represent the top of the standard curve used in the assay (5000 pg/ml).

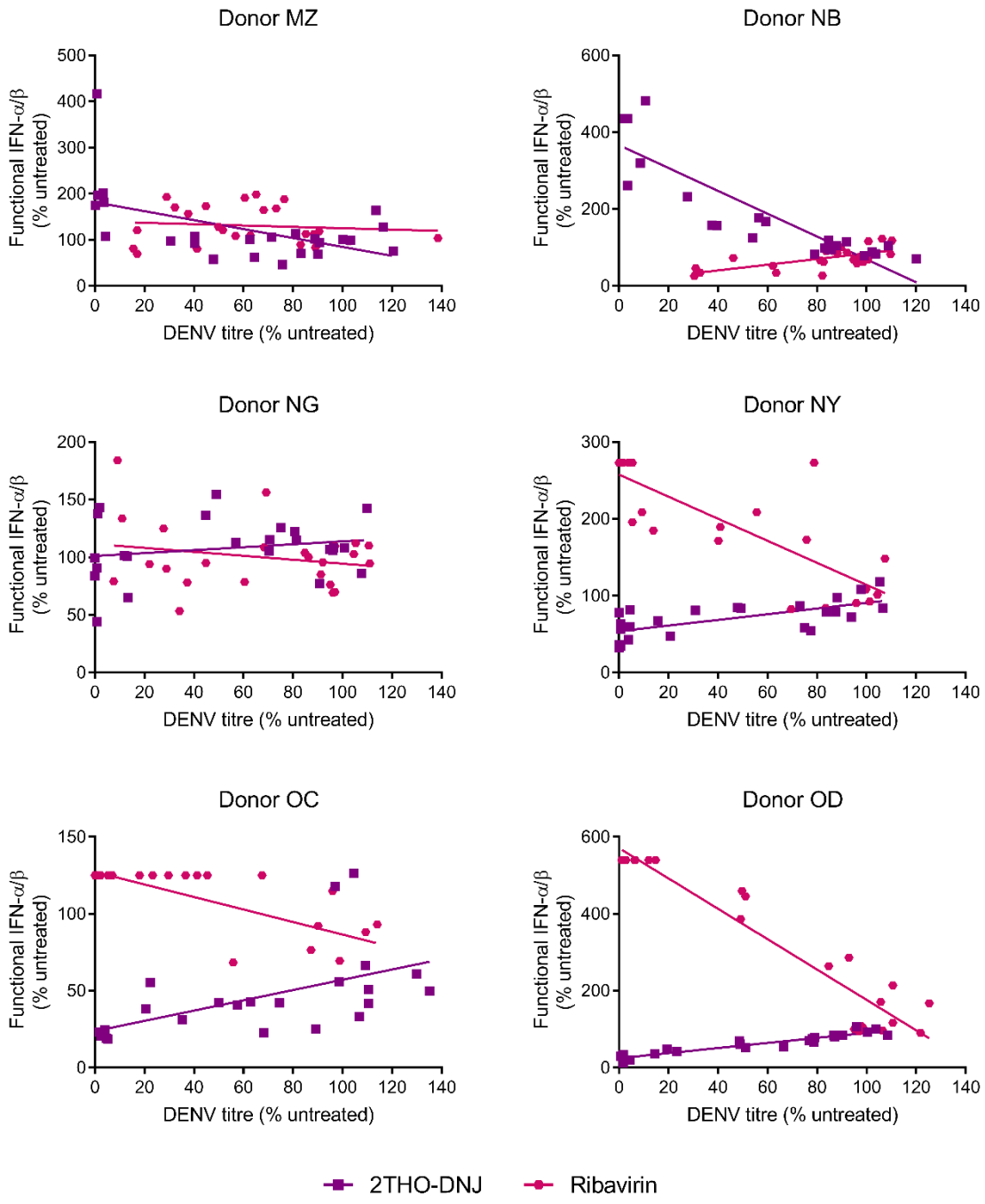

Figure 55. The relationship between functional IFN-α/β secretion and DENV titre varies between MDMΦ donors treated with 2THO-DNJ or ribavirin.

Primary MDMΦs (n=6 donors, as shown, assayed in technical triplicate) were infected with DENV and treated with a titration of 2THO-DNJ or ribavirin. Supernatant was collected at 48 hours post-infection for quantification of viral titre and functional IFN-α/β secretion. Values derived from individual samples were normalised to untreated for each donor and mean antiviral efficacy plotted against mean cytokine response. For donors NY, OC, and OD, peak values for ribavirin represent the top of the standard curve used in the assay (5000 pg/ml). Linear regression was used to find lines of best fit, with associations assessed by Pearson correlation (Table 24).

6.3.2.3 2THO-DNJ, NN-DNJ and NN-DGJ reduce TNF-α and IFN-α/β secretion from DENV-infected MDMΦs

In addition to considering the influence of iminosugars on the cytokine response at 48 hours post-infection, functional cytokine secretion from DENV-infected MDMΦs was analysed over time. The kinetics of cytokine production varied significantly between donors for both TNF-α and IFN-α/β (Figure 56 and Figure 57). However, in all cases, 2THO-DNJ treatment had the greatest suppressive effect on TNF-α and IFN-α/β production of the compounds tested, although 100 µM 2THO-DNJ was compared with 25 µM *N*N-DNJ or *N*N-DGJ treatment since these concentrations of DNJ-derivatives have a comparable degree of antiviral efficacy (exemplified by Figure 12). In all three donors, *N*N-DNJ reduced TNF-α secretion to a numerically greater extent than *N*N-DGJ. In contrast, for IFN-α/β, *N*N-DNJ was consistently suppressive, while the effects were more subtle and variable with *N*N-DGJ. Interestingly, while 100 µM 2THO-DNJ and 25 µM *N*N-DNJ have a very similar antiviral effect against DENV (Figure 12 and Figure 13 demonstrate this for the same donors), the higher concentration of 2THO-DNJ used appears to have more of a suppressive effect on cytokine secretion. *N*N-DGJ, despite the lack of antiviral efficacy, also appeared to have some effects on cytokine secretion. Taken together, this illustrates the disconnect between the antiviral and immunomodulatory activities of iminosugars.

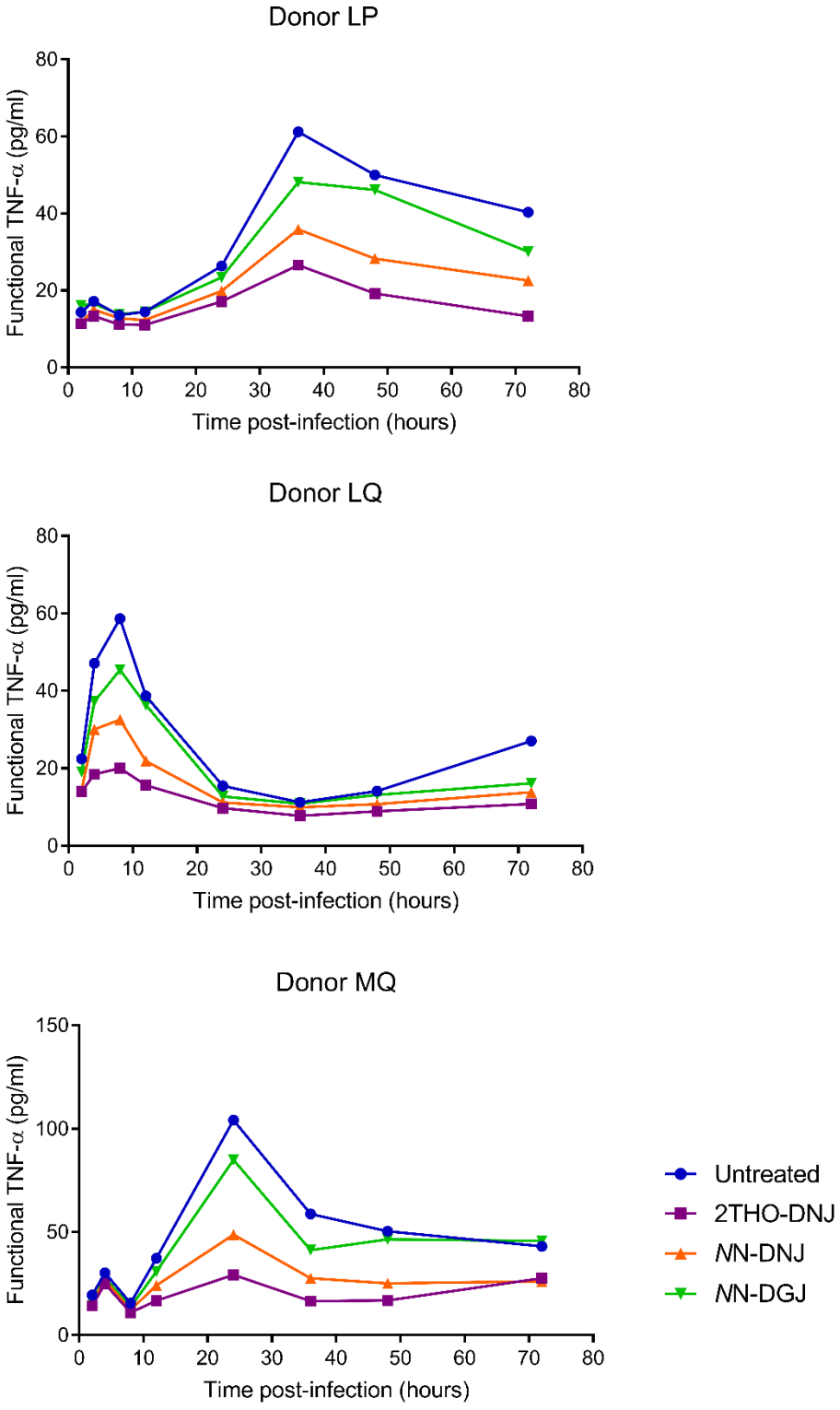

Figure 56. Iminosugars reduce TNF-α secretion from DENV-infected MDMΦs over time.

Primary MDMΦs (n=3 donors, as shown, assayed in technical triplicate) were infected with DENV and treated with 100 µM 2THO-DNJ, 25 µM NN-DNJ or 25 µM NN-DGJ. Supernatant was collected at the indicated time points, functional TNF-α quantified and the mean plotted.

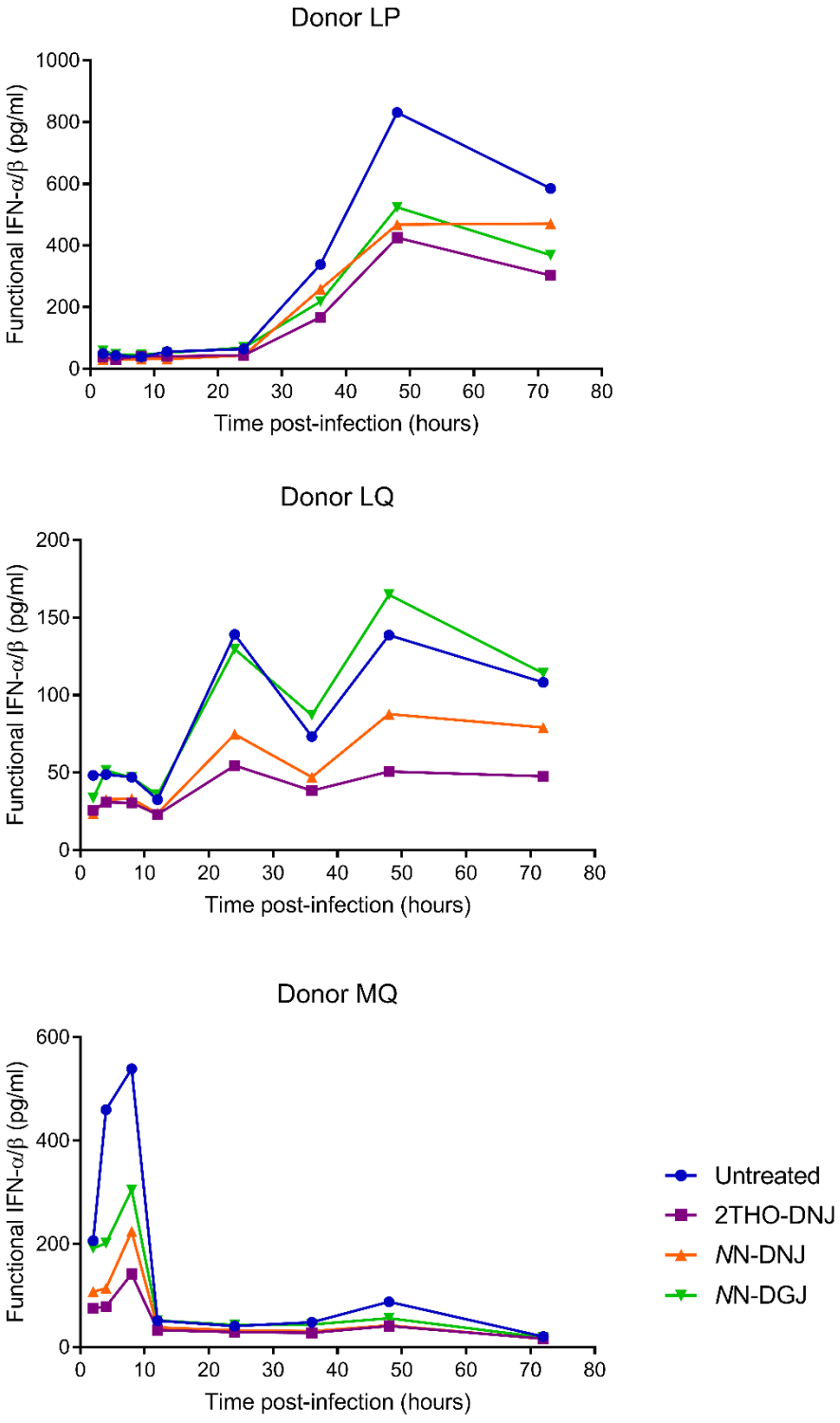

Figure 57. Iminosugars reduce IFN-α/β secretion from DENV-infected MDMΦs over time.

Primary MDMΦs (n=3 donors, as shown, assayed in technical triplicate) were infected with DENV and treated with 100 μM 2THO-DNJ, 25 μM NN-DNJ or 25 μM NN-DGJ. Supernatant was collected at the indicated time points, functional IFN-α/β quantified and the mean plotted.

6.3.2.4 MON-DNJ reduces functional TNF-α and IFN-α/β secretion from DENV-infected MDMΦs

MON-DNJ is an iminosugar previously described to affect cytokine secretion, quantified by ELISA and investigated by transcriptomic analysis, in the context of DENV-infection or LPS-stimulation of MDMΦs (Table 4 and Table 6; [418]). Here, MON-DNJ treatment also gave a dose-dependent reduction in functional TNF-α and IFN-α/β secretion from DENV-infected MDMΦs (Figure 58). As anticipated, donors varied in their strength of cytokine response to DENV infection (Figure 118), and the cytokine-modulatory effect of iminosugar treatment was more evident in donors with a stronger cytokine response.

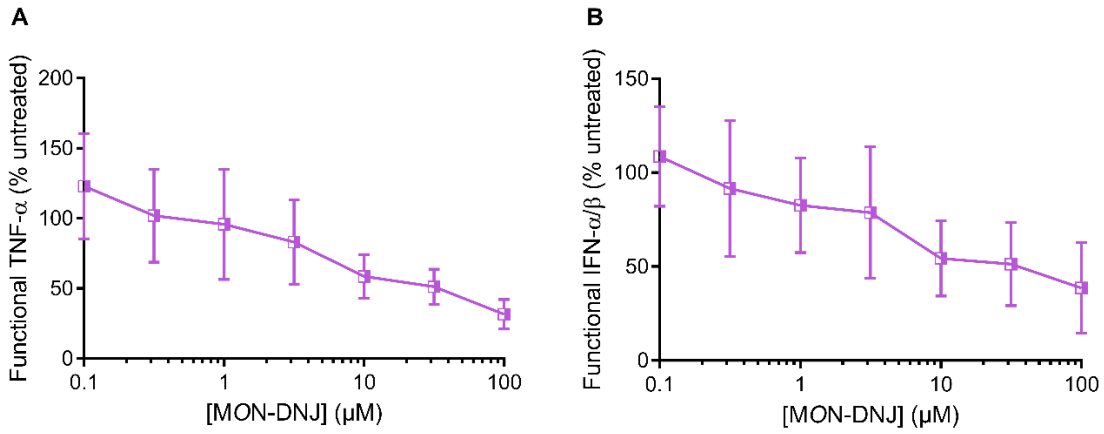

Figure 58. MON-DNJ reduces functional TNF-α and IFN-α/β secretion from DENV-infected MDMΦs.

Primary MDMΦs (n=4 donors (KR, KS, LL, MQ), assayed in technical triplicate) were infected with DENV and treated with a titration of MON-DNJ. Supernatant was collected at 48 hours post-infection, secreted TNF-α (A) or IFN-α/β (B) quantified by functional assay, normalised to untreated for each donor and plotted as mean ± standard error.

The tendency for MON-DNJ treatment to suppress TNF-α production was also seen in an experiment treating DENV-infected MDMΦs with a single concentration (25 μM) of MON-DNJ, although no effects were statistically significant (Figure 59). On the contrary, the effects of MON-DNJ on IFN-α/β production seem not to be so clear-cut. In this case, IFN-α/β production tended to be enhanced by iminosugar treatment in the context of DENV infection. While virus secretion from these MDMΦs was not quantified, it is unlikely that this enhanced IFN-α/β production is

related to increased virus production as reproducible antiviral efficacy has been seen with this concentration of MON-DNJ in the MDMΦ system [394]. It is possible that this discrepancy is related to the strength of IFN-α/β response made by the donors: the average IFN-α/β response made upon DENV-infection in these donors was almost 20-fold lower than that of the donors used in Figure 58 (Figure 118 versus Figure 119), and there was little enhancement of IFN-α/β secretion upon infection. Perhaps in the context of a weak antiviral IFN-α/β response being induced, MON-DNJ can enhance this response, whereas it suppresses stronger IFN-α/β responses. Further experimentation would be required to confirm whether these observations hold true across additional donors and to test this hypothesis. In any case, a previous transcriptomics analysis of MON-DNJ-treated DENV-infected MDMΦs (Andrew Sayce, unpublished data) predicted that such treatment would enhance IFN-α/β secretion, matching the effect seen here.

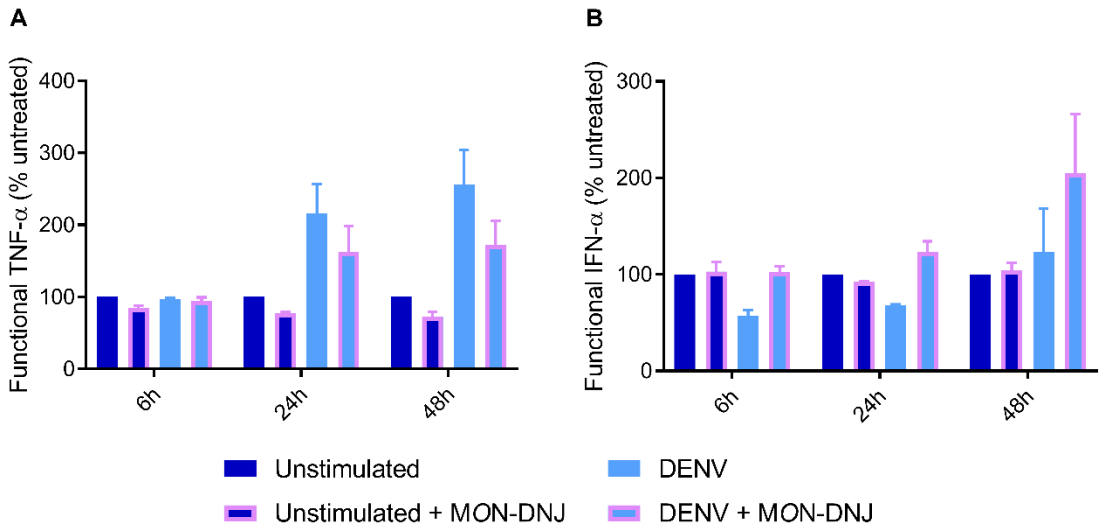

Figure 59. MON-DNJ reduces functional TNF-α and enhances IFN-α/β secretion from DENV-infected MDMΦs.

Primary MDMΦs (n=3 donors (MQ, MR, MS), assayed in technical triplicate) were infected with DENV and treated with 25 μM MON-DNJ. Supernatant was collected at indicated times post-infection, secreted TNF-α (A) or IFN-α/β (B) quantified by functional assay, normalised to unstimulated for each donor within each time points and plotted as mean ± standard error. Statistical analysis was by two-way ANOVA with Tukey's multiple comparisons test (no comparisons between unstimulated ± MON-DNJ or DENV ± MON-DNJ were statistically significant).

6.3.2.5 *The association between TNF-α secretion and viral titre following 2THO-DNJ treatment holds true in DENV-infected monocyte-derived dendritic cells*

Preliminary analysis of DENV-infected iminosugar-treated immature monocyte-derived dendritic cell (imDCs; differentiated from monocytes isolated as for MDMΦs using IL-4 and GM-CSF, and samples prepared as for MDMΦs by Nilanka Perera) supernatants was conducted. Iminosugar treatment of infected imDCs appeared to give a dose-dependent reduction in functional TNF-α secretion for all of the iminosugars tested (Figure 60A), recapitulating the findings with 2THO-DNJ treatment of DENV-infected MDMΦs. Similarly, the reduction in DENV titre upon 2THO-DNJ treatment correlated with the reduction in functional TNF-α secretion, and this was also found to be the case for *N*N-DNJ treatment (Figure 60B). In both cases, the slope of the line of best-fit was greater than 0.5, indicating that TNF-α secretion changed more for a given percentage change in viral titre. Any conclusions drawn from this are limited by the restricted analysis of samples derived from only one donor, although these effects have been reproduced subsequently in further donors in concurrent work [483]. This suggests that the glucostereochemistry headgroup is not the sole determinant of the effect of DNJ-derivative iminosugars on TNF-α secretion.

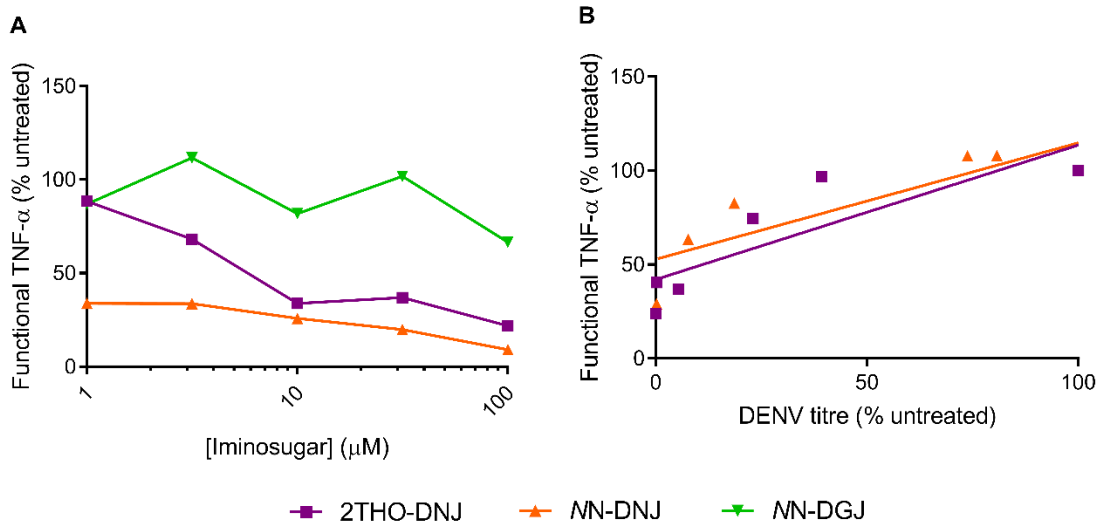

Figure 60. Iminosugars reduce TNF-α secretion from DENV-infected imDCs.

imDCs (donor KR or donor KM for NN-DNJ, assayed in technical triplicate) were infected with DENV and treated with iminosugar titrations as shown. Supernatant was collected at 48 hours post-infection and secreted TNF-α quantified by functional assay.

(A) Functional TNF-α was normalised to untreated and the mean plotted.

(B) Viral titres were determined by plaque assay, normalised to untreated and mean titres plotted against mean normalised functional TNF-α for each condition. Linear regression was used describe the data with lines of best fit and Pearson correlation used to assess correlation between the measures (Table 25).

Samples were generated and viral titres quantified by Nilanka Perera. Cytokine assay and data analysis were by Beatrice Tyrrell.

6.3.2.6 Other DENV-infected cell types did not make measurable cytokine responses to infection

Supernatant samples from other DENV-infected iminosugar-treated cell types were also analysed by functional cytokine assay. However, DENV infection lead to no or minimal measurable cytokine responses in these cell types.

Firstly, in an attempt to better represent human bloodstream DENV infection, a mixed immune cell population (PBMCs) was isolated rather than selecting for monocytes and differentiation to MDMΦs, as routinely used in this project. PBMCs were infected with DENV and treated with a panel of iminosugars in order to identify whether the antiviral and cytokine-modulatory effects of iminosugars in PBMCs, where multiple cell types are present and interacting, were consistent with the findings in MDMΦs. However, only very low levels of TNF-α and IFN-α/β production were detected from analysis of two donors at 24 and 48 hours post-infection (8.17).

Supernatants from DENV-infected Vero cells, utilised for studies of the effects of ER α-glucosidase knockout, were also analysed. DENV infection did not elicit cytokine responses above background (data not shown). For IFN-α/β, this is unsurprising considering the 9Mb deletion in chromosome 12 resulting in the loss of the type I IFN gene cluster, likely responsible for their susceptibility to diverse viral infections [482]. Therefore, the lack of detectable reporter

cell response is anticipated and reassuringly supports the reporter pathway specificity. For TNF-α, searches of UniProtKB and BLASTp search using the human TNF-α protein sequence (P01375 TNFA_HUMAN) identified the existence of the *TNFA* gene (GenBank: ACI28908.1; UniProtKB: B6E118_CHLSB) in the *Chlorocebus sabaeus* genome, the origin of Vero cells, with 95.7% protein sequence identity to human TNF-α. However, references to the production of TNF-α by Vero cells could not be identified in the literature, although TNF gene polymorphisms have been identified and linked to obesity phenotypes in a different *Chlorocebus* species [594]. The lack of detectable functional TNF-α on DENV infection of Vero cells identified here likely indicates that TNF-α production was not stimulated by infection, although it could also be explained by a lack of cross-reactivity between the human TNF-α receptor and the *Chlorocebus sabaeus* cytokine.

Supernatants from DENV-infected C6/36 *Aedes albopictus* mosquito cells were also analysed. Mosquito innate immune defence pathways activated during infection are fairly well understood, with the Toll and JAK/STAT pathways important in controlling DENV infection of *Aedes aegypti* mosquitos [595, 596]. RNA interference also constitutes an important defence against infection of mosquitos with arboviruses, although pathways differ between species and cell lines [597]. Interestingly, cytokine-like activity of small polypeptides secreted from DENV-infected C6/36 cells has also been reported [598]. Thus, DENV-infected untreated and iminosugar-treated C6/36 cell supernatants generated during this project were subjected to exploratory functional cytokine assay, looking for any cross-reactivity of cytokine-like molecules that might be produced from these cells. No activation of the TNF-α or IFN-α/β cells was identified (data not shown), indicating that this was not the case.

6.3.3 The effects of iminosugars on virus-induced cytokine production does not depend on viral replication

6.3.3.1 UV-inactivated DENV does not elicit a MDMΦ cytokine response

Analysing the effect of iminosugar treatment on cytokine production in the context of viral infection is confounded by their antiviral efficacy. One way to determine whether iminosugar effects on DENV-elicited cytokines depend on the antiviral effect is to compare the responses to replicating and non-replicating forms of the virus. To this end, UV-inactivated DENV (UVi-DENV) was used to stimulate MDMΦs alongside DENV infection. However, when matched genome equivalents of infectious and inactivated DENV genome equivalents were used (based on equal volumes of a virus stock that was either UV-inactivated or left untreated), minimal TNF-α or IFN-α/β responses to UVi-DENV were detected in a donor strongly responsive to DENV stimulation (Figure 61), precluding analysis of iminosugar effects. This suggests that cellular entry and either protein synthesis or genome replication are critical for these cytokine responses, although it is possible that any virion surface epitopes, that might be required for CLEC5A recognition for example [141], may have been disrupted by the inactivation protocol. The reduced cytokine response to inactivated virus is in keeping with previous studies with heat-inactivated DENV stimulation of RAW264.7 macrophages [147], UVi-DENV stimulation of myeloid DCs [149] or human brain microvascular endothelial cells [156]. However, IFN-α production from plasmacytoid DCs was mostly unaffected by UV inactivation [149]; this cell type has been demonstrated to make IFN-α/β responses to viral glycoproteins derived from IFNV, HIV-1 and SARS-CoV [599].

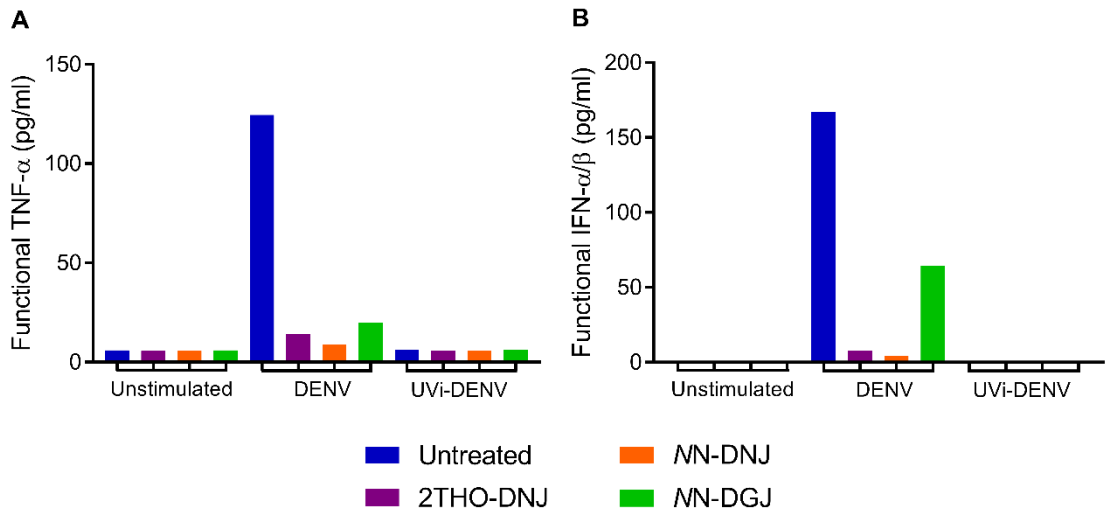

Figure 61. UVi-DENV is a poor inducer of TNF-α (A) and IFN-α/β (B) relative to DENV.

Primary MDMΦs (n=1 donor (OI), assayed in technical triplicate) were mock-infected or infected with DENV, or stimulated with the equivalent number of UVi-DENV virions, and treated with 100 μM of the indicated iminosugar after 90 minutes. Functional cytokine secretion after 24 hours was quantified and the mean displayed.

6.3.3.2 DNJ-derivatives reduce TNF-α secretion stimulated by poly(I:C)

In lieu of investigating iminosugar effects on the cytokine response to inactivated virus, the response to stimulation with the synthetic dsRNA analogue poly(I:C) was studied. Poly(I:C) is a canonical PRR agonist often used to mimic the dsRNA stimulus present, although concealed, during infection with an RNA virus such as DENV [600]. Importantly, poly(I:C) has no potential to replicate, thus allowing determination of whether iminosugar-mediated cytokine effects are dependent on active viral replication or viral protein production in the context of viral infection. The effects of iminosugars on cytokine production in response to poly(I:C) stimulation of MDMΦs was investigated over a time course. DNJ-derivatives appeared to consistently reduce functional TNF-α secretion (Figure 62), an effect which was reproduced in experiments using a broader panel of PAMP stimuli (Figure 70). On the contrary, in these experiments, the modulation of IFN-α/β secretion was less consistent, but at time points when there was a considerable cytokine response to treatment, there was also some indication that DNJ-

derivatives could reduce IFN-α/β secretion (Figure 63), which was confirmed in a later experiment (Figure 71).

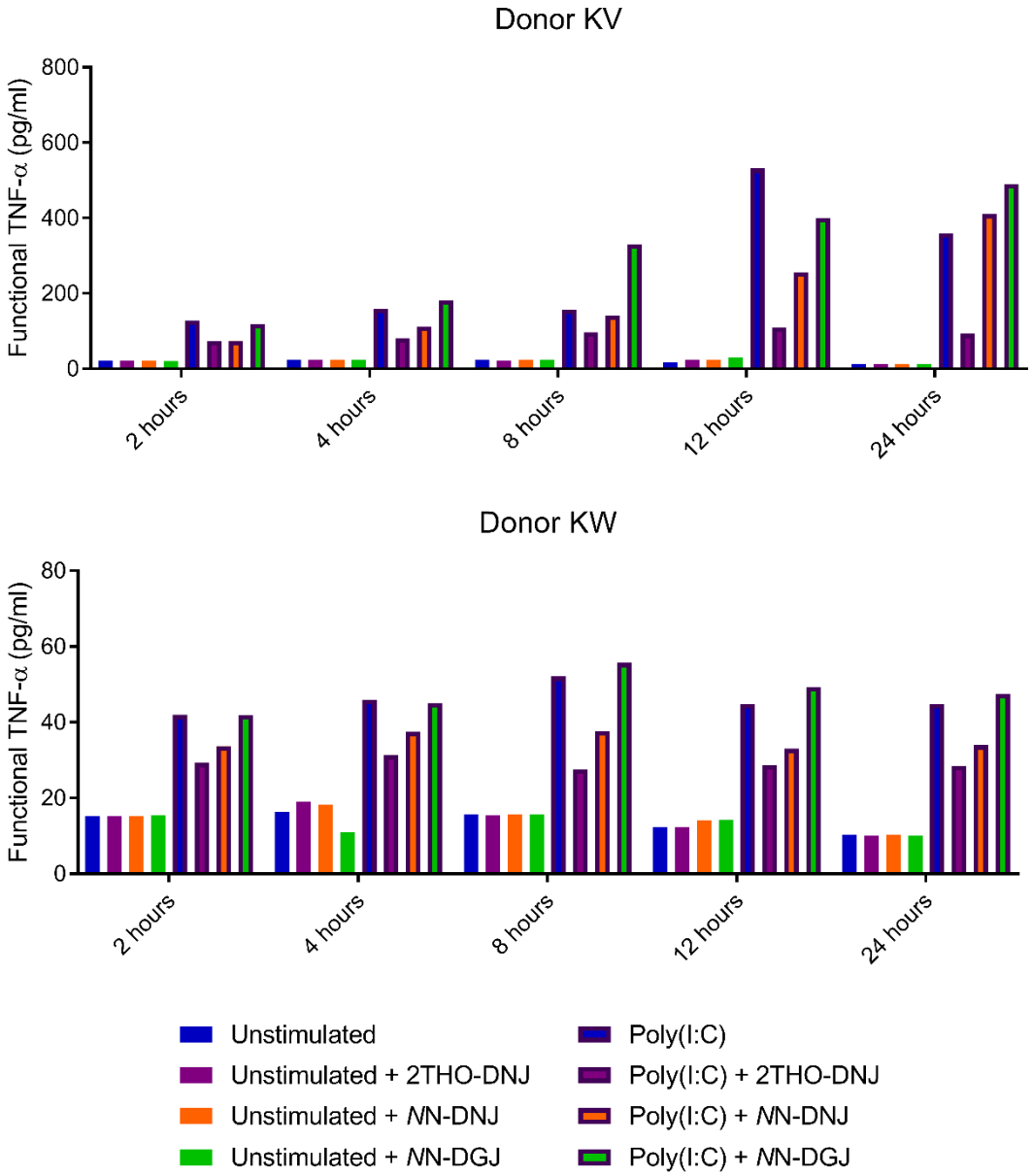

Figure 62. DNJ-derivatives reduce TNF-α secretion in response to poly(I:C) stimulation of MDMΦs.

Primary MDMΦs (donors as shown, assayed in technical triplicate) were unstimulated or stimulated with 10 µg/ml poly(I:C) (outlined bars; catalogue #27-4729-01, Amersham Biosciences, for this experiment only) and treated with 80 µM 2THO-DNJ, 25 µM NN*-DNJ or 25 µM* NN*-DGJ. After incubations of indicated duration, supernatant was harvested, TNF-α secretion quantified by functional assay and the mean plotted.*

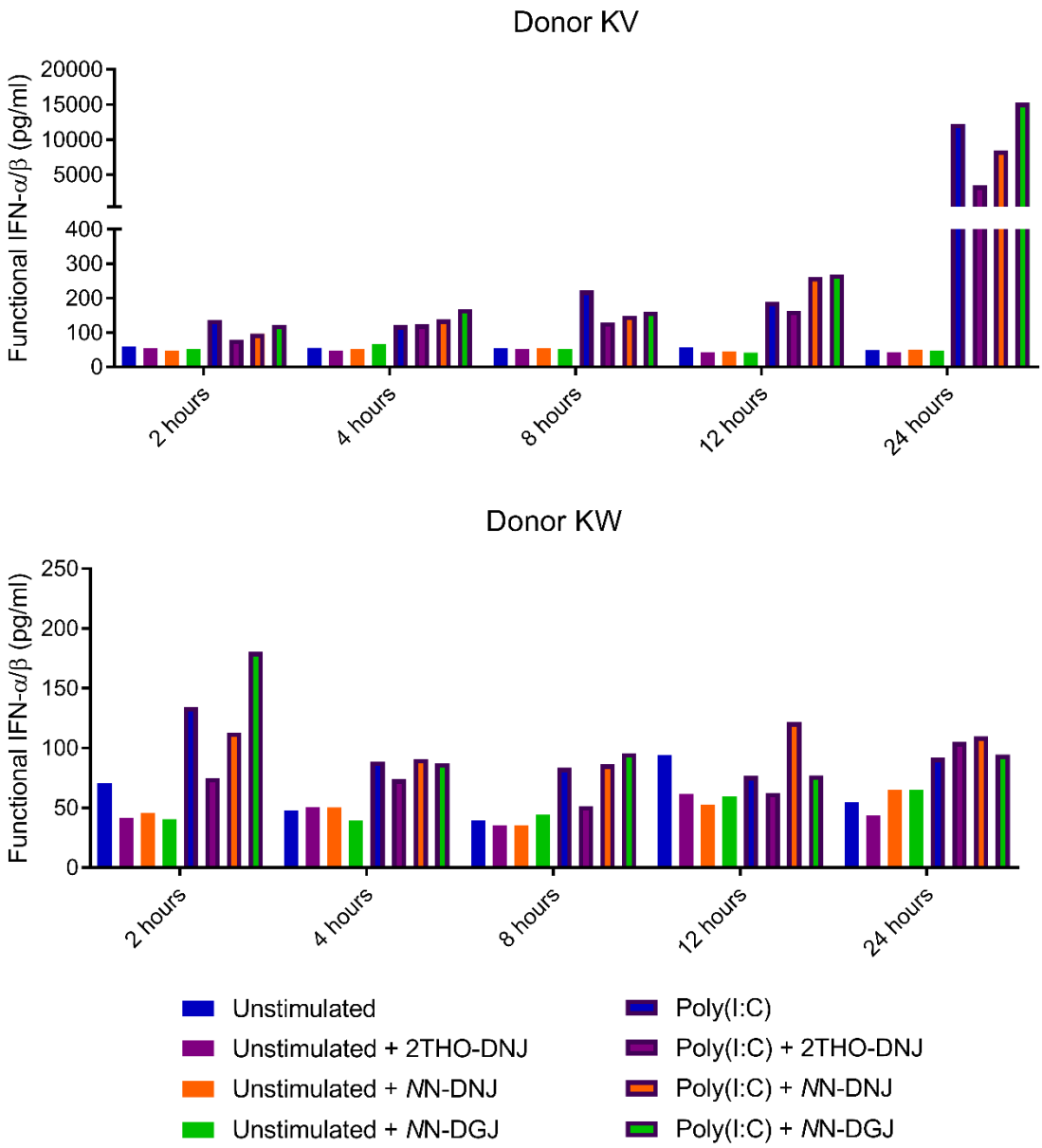

Figure 63. DNJ-derivatives show some modulation of IFN-α/β secretion in response to poly(I:C) stimulation of MDMΦs.

Primary MDMΦs (donors as shown, assayed in technical triplicate) were unstimulated or stimulated with 10 µg/ml poly(I:C) (outlined bars; catalogue #27-4729-01, Amersham Biosciences, for this experiment only) and treated with 80 µM 2THO-DNJ, 25 µM NN*-DNJ or 25 µM* NN*-DGJ. After incubations of indicated duration, supernatant was harvested, IFN-α/β secretion quantified by functional assay and the mean plotted.*

6.3.4 Iminosugar modulation of DENV-elicited cytokine production occurs at pre- and post-transcriptional levels

6.3.4.1 Iminosugars can modulate cytokine gene transcription

Alongside determination of the effects of iminosugars on DENV replication (3.3.1.8.1), RNA was extracted from DENV-infected iminosugar- or ribavirin-treated MDMΦ lysates and transcription of the *TNFA* and *IFNA2* genes, encoding TNF-α and IFN-α2 respectively, determined. *IFNA2* was selected as a representative of type I IFN genes, since it is commonly studied as the first IFN-α subtype identified. Expression levels were normalised to the housekeeping gene *RPLP2*, which is expressed stably on iminosugar treatment (8.6). At 12 and 24 hours post-infection, there was a statistically significant reduction in *TNFA* transcription with *N*N-DNJ and *N*N-DGJ treatment, and the same trend was observed for ribavirin (where n=2), whereas 2THO-DNJ had no effect (Figure 64A). At 48 hours post-infection, there was no significant difference from untreated transcription levels with any of the iminosugars, which may relate to the decline in transcript levels at 48 hours post-infection after increases from 12 to 24 hours (data not shown). For ribavirin and DNJ-derivative iminosugars, reduced *TNFA* transcription could be rationalised by the antiviral effect reducing the viral stimulus for pro-inflammatory cytokine production. This also translates to a reduction in functional TNF-α secretion for the DNJ-derivative iminosugars (Figure 56). However, the antiviral effect cannot be the sole factor in determining iminosugar effects on *TNFA* transcription since *N*N-DGJ treatment also reduced transcription and secretion (Figure 56), and yet is not antiviral (Figure 12). Furthermore, 2THO-DNJ treatment is antiviral (Figure 12) and reduces functional TNF-α secretion (Figure 49), but did not affect *TNFA* transcription. While it is possible that 2THO-DNJ treatment might only impact *TNFA* transcription early in the response to infection, since here 12 hours post-infection was the first time point analysed, this may indicate that the modulation of TNF-α production by 2THO-DNJ occurs at a post-transcriptional stage. Although not assessed in the same experimental set-up, M*O*N-DNJ treatment did not affect *TNF* transcription in DENV-infected or LPS-treated MDMΦs, quantified

as part of a transcriptomics experiment (data generated by Andrew Sayce; Figure 65A). In any case, the variation in responses observed suggests that a combination of mechanisms is responsible for the downstream reduction in TNF-α secretion seen with iminosugar treatment.

In contrast to *TNFA*, no statistically significant changes in *IFNA2* transcription were seen with iminosugar treatment (Figure 64B and Figure 65B). Since the transcription of only one IFN-α subtype was analysed, this does not exclude the possibility that transcription of other type I interferon genes is affected by iminosugar treatment, or it could indicate that iminosugars modulate IFN-α/β production at a post-transcriptional level, or that transcriptional changes might be observed only at an earlier time point.

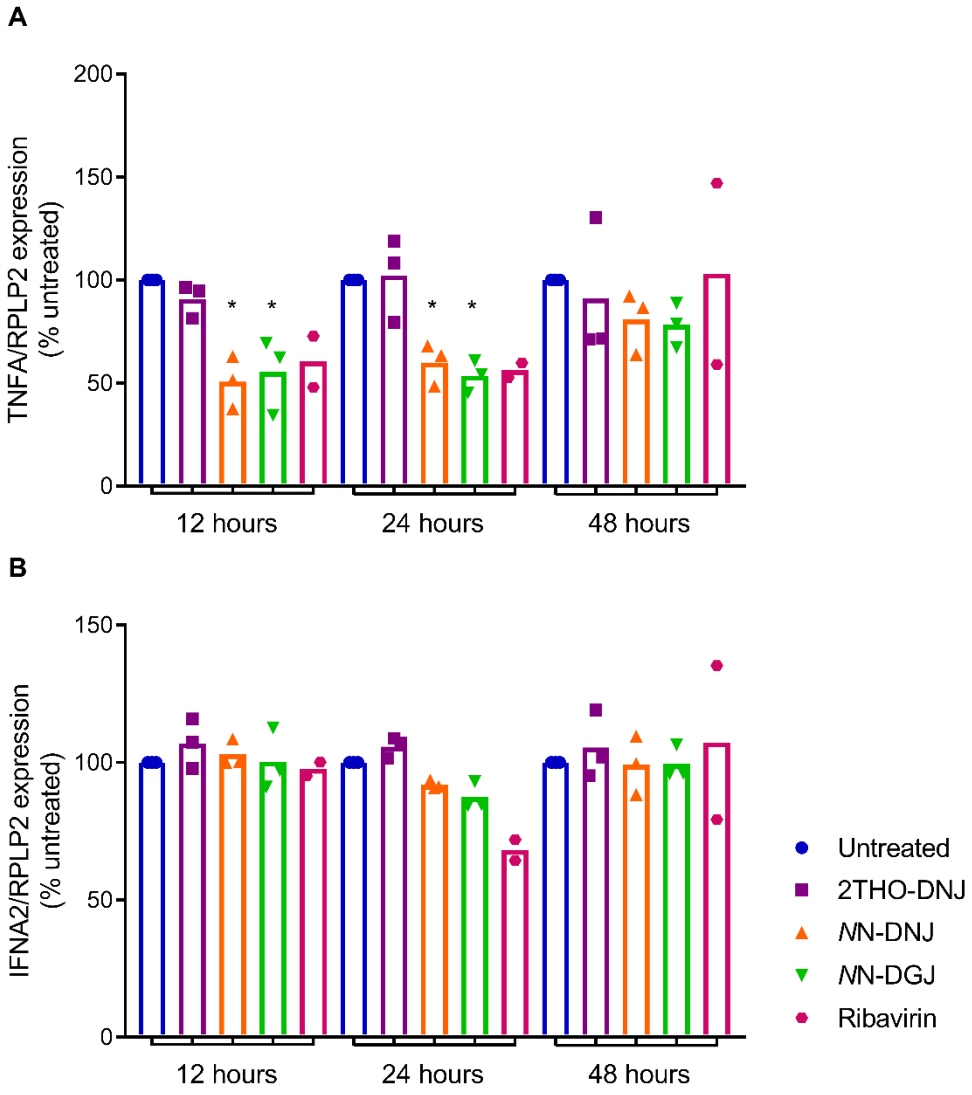

Figure 64. Iminosugar treatment can impact cytokine gene transcription.

Primary MDMΦs (n=3 donors (NZ, OI, OJ) or n=2 donors for ribavirin (OI, OJ), assayed in technical triplicate) were infected with DENV and treated with 100 µM iminosugar or ribavirin. After incubations of indicated durations, cellular RNA was extracted and TNFA *(A) and* IFNA2 *(B) gene transcription quantified. Cytokine gene transcription was normalised to* RPLP2 *transcripts. Values were normalised to untreated for each time point, and the mean plotted (bars show the mean of the donors). Statistical analysis was by two-way ANOVA with Dunnett's multiple comparisons test was used to compare treatments within time points (*, p<0.05). Note that statistics are not shown for ribavirin since n=2.*

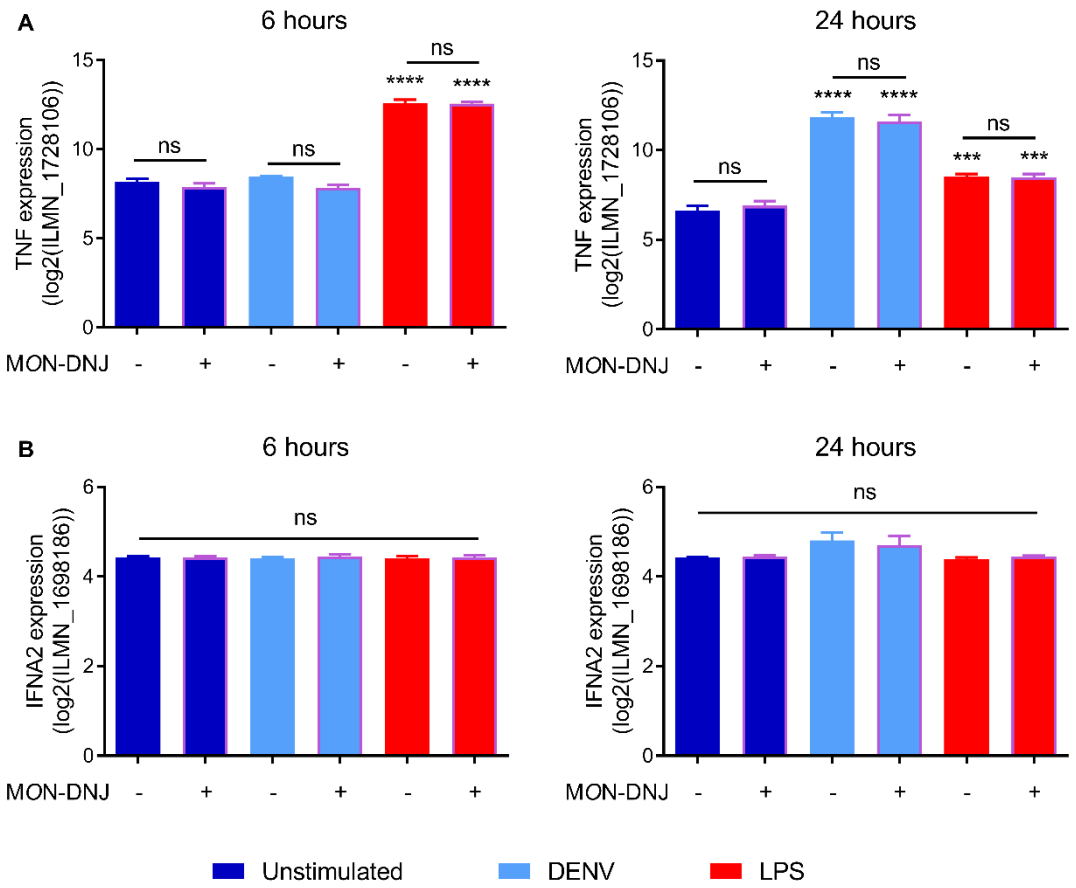

Figure 65. MON-DNJ treatment does not affect TNF *or* IFNA2 *transcription.*

Primary MDMΦs (n=4 donors (FY, FZ, GA, GB)) were infected with DENV or stimulated with 100 ng/ml LPS-ST and untreated or treated with 25 µM MON-DNJ. After 6 or 24 hours, cellular RNA was extracted and the transcriptome profiled and data analysed as described in [418]. Sample generation and transcriptome processing were conducted by Andrew Sayce. The log2 quantification of probes corresponding to TNF *(A) or* IFNA2 *(B) genes was plotted as mean ± standard error. Statistical analysis was by one-way ANOVA with Tukey's multiple comparisons test (ns, not significant; ***, p<0.001; ****, p<0.0001).*

6.3.4.2 *MON-DNJ treatment does not impair the functionality of secreted TNF-α, but reduces secretion overall*

Since the secretion of functional TNF-α is dose-dependently reduced by MON-DNJ treatment (Figure 58), it was investigated whether this was due to an overall reduction in cytokine secretion or maintained secretion of increasingly signalling-defective TNF-α on treatment with increasing concentrations of iminosugar. The impact of MON-DNJ treatment on TNF-α secretion was quantified by functional assay and ELISA, which would detect cytokine regardless of

biological activity, provided antibody binding was maintained. The reduction in TNF-α secretion with M*O*N-DNJ treatment was very similar as measured by both methods (Figure 66), indicating that the inhibition of TNF-α production occurs at or prior to the secretion stage, rather than there being a facilitation of defective cytokine secretion upon iminosugar treatment. This is as anticipated, since as human TNF-α is not N-glycosylated [582] the inhibition of ER α-glucosidases by M*O*N-DNJ should not directly impact the folding and function of TNF-α. It is possible however that M*O*N-DNJ treatment leads to the misfolding and degradation of a signalling pathway member or regulator upstream of TNF-α production. However, as previously discussed in 3.4, this is difficult to interrogate since interference with proteasomal degradation pathways can have antiviral and cytokine-modulatory consequences (exemplified for 2THO-DNJ, *N*N-DNJ and *N*N-DGJ treatment in 8.7). Thus M*O*N-DNJ treatment impacts TNF-α production at a post-transcriptional level, either at or prior to cytokine secretion.

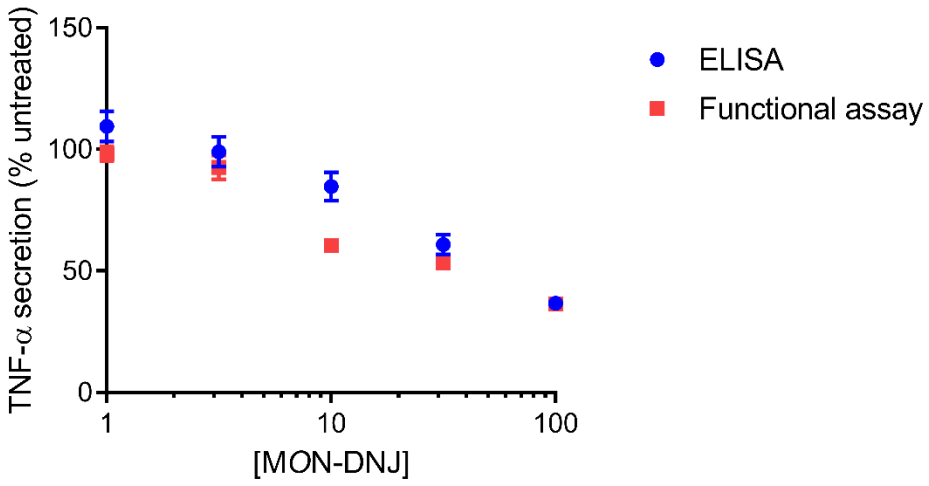

Figure 66. Equivalent impacts of MON-DNJ treatment are seen on secreted TNF-α quantified by ELISA or functional assay.

Primary MDMΦs (n=3 donors (HE, HF, HG for ELISA and KR, KS, MQ for functional assay), assayed in technical triplicate) were infected with DENV and treated with a titration of MON-DNJ. After 48 hours, supernatant was collected and TNF-α secretion quantified by ELISA or functional assay. TNF-α secretion was normalised to untreated and plotted as mean ± standard error.

6.3.5 The effects of iminosugars on cytokine production extend beyond viral stimuli

6.3.5.1 MON-DNJ modulates TNF-α production following MDMΦs stimulation with LPS and heat-killed Candida albicans

Since the effects of DNJ-derivative iminosugars on TNF-α secretion are not restricted to replicating virus, this suggests that iminosugars could be employed therapeutically to modulate the cytokine response to other stimuli. This might be relevant for the treatment of a range of infections and consequences such as sepsis. The effects of M*O*N-DNJ on MDMΦ cytokine production elicited by LPS or heat-killed *Candida albicans* (HKCA) stimulation, representative of bacterial and fungal agonists, respectively, was assessed. M*O*N-DNJ treatment seemed to substantially reduce TNF-α secretion in response to LPS stimulation, although this was assessed in only 2 donors, with a seemingly more subtle effect observed with HKCA and DENV stimulation (Figure 67). IFN-α/β responses to stimulation were lower than TNF-α responses, and no response above baseline was seen for LPS or HKCA stimulation across time points. However, M*O*N-DNJ treatment seemed to enhance the low level of IFN-α/β production in response to DENV stimulation (Figure 68), as previously observed (Figure 59). While better understanding of the clinical aspects of sepsis is certainly required, the suppressive effect of M*O*N-DNJ treatment on TNF-α secretion induced by multiple stimuli might have clinical utility.

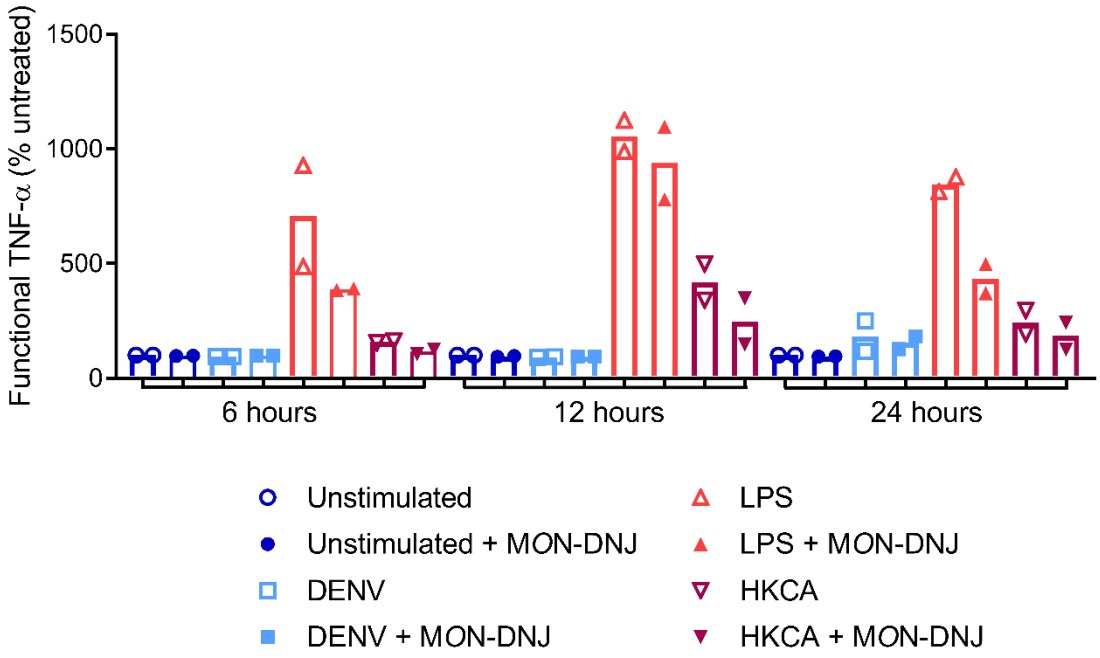

Figure 67. MON-DNJ reduces TNF-α secretion from LPS-stimulated MDMΦs.

Primary MDMΦs (n=2 donors (NF, NG), assayed in technical triplicate) were infected with DENV or stimulated with LPS-ST or HKCA, with or without 25 μM MON-DNJ. After incubations of indicated duration, supernatant was harvested and TNF-α secretion quantified by functional assay. Functional TNF-α was normalised to untreated and the mean plotted (bars show the mean of the donors).

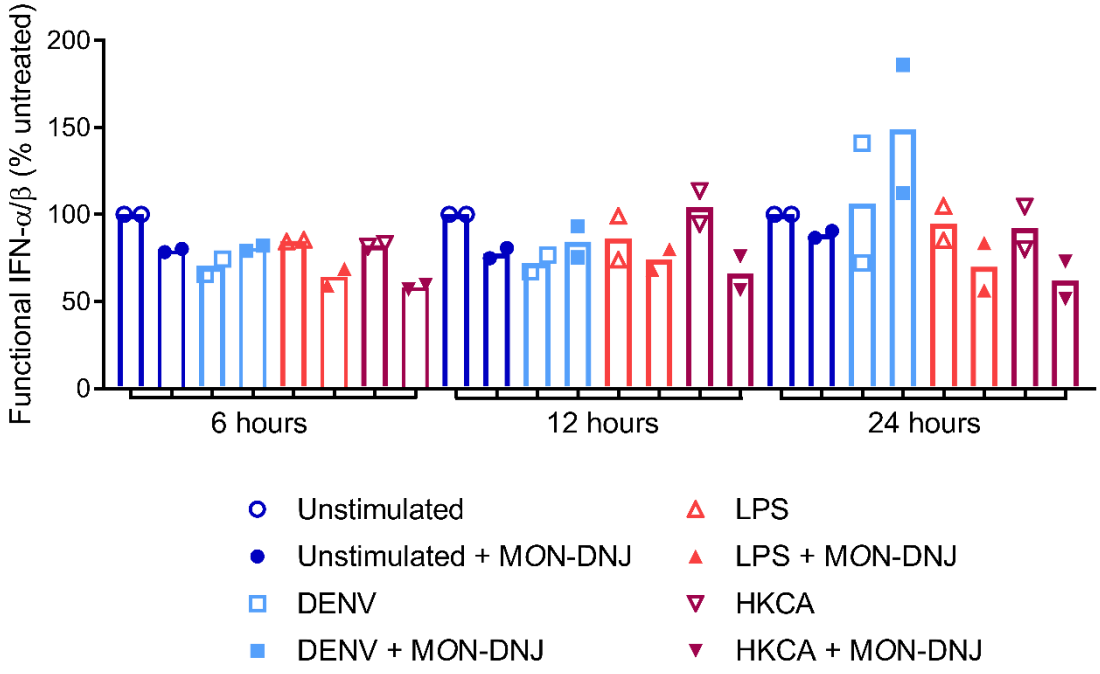

Figure 68. MON-DNJ reduces IFN-α/β secretion from MDMΦs stimulated with HKCA but enhances the response to DENV infection.

Primary MDMΦs (n=2 donors (NF, NG), assayed in technical triplicate) were infected with DENV or stimulated with LPS-ST or HKCA, with or without 25 μM MON-DNJ. After incubations of indicated duration, supernatant was harvested and IFN-α/β secretion quantified by functional assay. Functional IFN-α/β was normalised to untreated and the mean plotted (bars show the mean of the donors).

6.3.5.2 HMGB1 secretion is unaffected by MON-DNJ treatment

One possible mechanism underlying the reduction in TNF-α secretion on M*O*N-DNJ would be iminosugar treatment reducing the secretion of HMGB1 from MDMΦs. HMGB1 is a multi-functional protein, residing in the nucleus as a DNA-binding protein regulating transcription at baseline. However, it can be released passively on cellular necrosis [601] or actively secreted to the extracellular environment, classically demonstrated to occur on stimulation with LPS [602]. Phosphorylation and hyperacetylation have both been implicated in the nuclear export of HMGB1 in monocytes [603-605]. In turn, HMGB1 can induce the production of pro-inflammatory cytokines, including TNF-α by monocytes [606], with the receptor for advanced glycation end products [607], TLR2 and TLR4 [608] implicated in signalling. In the context of DENV infection, HMGB1 translocates out of the nucleus and is secreted from primary human monocytes [609]. HMGB1 can also be secreted from DENV-infected primary DCs and T cells [607, 610], and is linked to necrosis of A549 epithelial cells when infected at the high MOI of 10 [611]. In addition, in DENV-infected patients, HMGB1 levels are significantly increased compared to healthy controls, peaking the day after the onset of symptoms [612], implying that it may be important in the early pathogenesis of human infection.

Previous network analysis of the transcriptome of DENV-infected MDMΦs treated with 25 μM M*O*N-DNJ suggested that iminosugar treatment would lead to the downmodulation of HMGB1 expression [418]. Consequently, the effect of M*O*N-DNJ on HMGB1 secretion from MDMΦs that were DENV-infected or stimulated with LPS or HKCA was quantified by ELISA. Stimulation, particularly with LPS or HKCA, induced HMGB1 secretion, with different response patterns in

each donor. However, HMGB1 secretion did not appear to be affected by M*O*N-DNJ treatment (Figure 69). *HMGB1* transcription, quantified in cell lysates corresponding to the supernatant samples analysed by ELISA, was also found to be unaffected by treatment (Nilanka Perera, unpublished data). Therefore, altered *HMGB1* transcription or secretion of HMGB1 is unlikely to explain the reduction in TNF-α secretion in iminosugar-treated DENV-infected or PAMP-stimulated MDMΦs, although an influence on M*O*N-DNJ on the shuttling of HMGB1 between the nucleus and cytoplasmic organelles has not been ruled out.

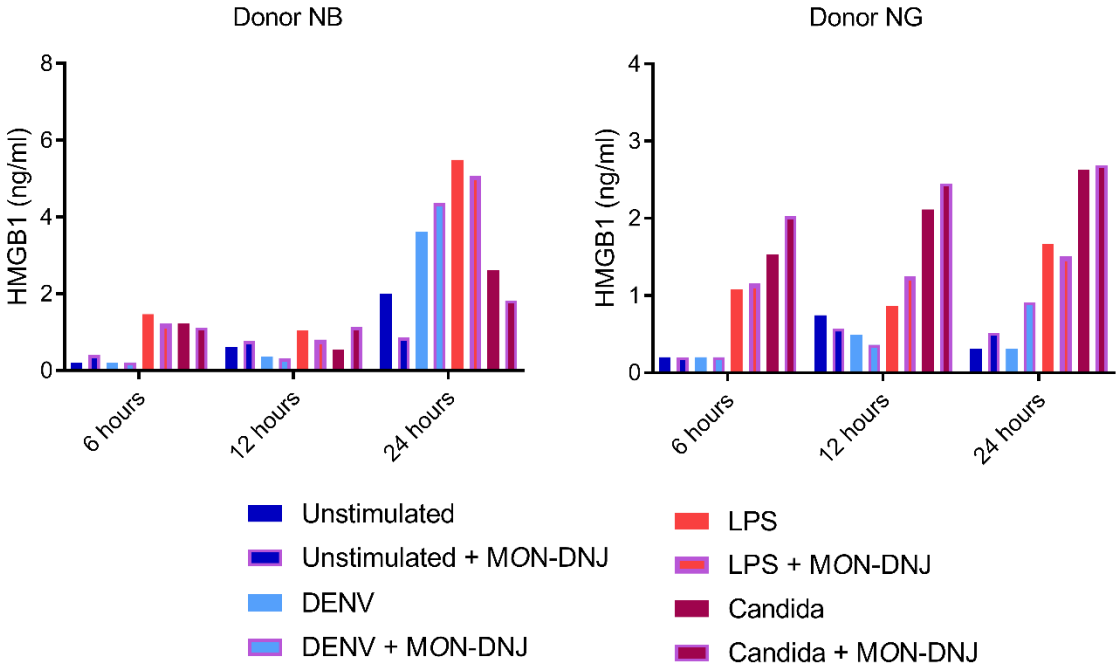

Figure 69. HMGB1 secretion is not influenced by MON-DNJ treatment.

Primary MDMΦs (n=2 donors, as shown, assayed in technical triplicate) were infected with DENV or stimulated with LPS-ST or HKCA and left untreated or treated with 25 μM MON-DNJ. After incubations of indicated durations, supernatant was harvested and HMGB1 secretion quantified by ELISA and the mean plotted. Samples for donor NB were prepared by Andrew Sayce.

6.3.5.3 DNJ-derivatives consistently reduce TNF-α secretion elicited by PAMP stimulation of MDMΦs, while NN-DGJ effects bifurcate

Since DNJ-derivative iminosugars had an inhibitory effect on TNF-α secretion elicited by a limited panel of non-viral stimuli, this effect was investigated further using 2THO-DNJ and *N*N-DNJ

treatment of MDMΦs stimulated with a broader panel of PAMPs. *N*N-DGJ was used alongside the DNJ-derivatives to examine the effects of a DGJ-derivative iminosugar on the cytokine response. Selected PAMPs were canonical agonists of TLRs 1-9, RIG-I/MDA5, NOD1/NOD2, Dectin-1 and STING, as described in 2.5.1.

With the stimulation protocol used, not all stimuli elicited significant TNF-α or IFN-α/β responses (considered here to be at least a two-fold induction from unstimulated levels), namely the TLR9 agonist ODN-2006, the TLR7 agonist imiquimod, and the STING agonist c-di-GMP (Figure 121 and Figure 122). This likely indicates that the concentration, time point or route of stimulation was suboptimal: in none of these cases could reports of stimulation of MDMΦs with these agonists be identified in the literature, and transfection of the stimuli might be required to enhance their accessibility to the cell and thus effect, as suggested for c-di-GMP stimulation [613]. The lack of IFN-α/β response to imiquimod, largely responsible for its clinical utility as an antiviral for herpes simplex virus [614], again indicates the requirement to optimise some of the stimulation conditions, although effects of certain PAMPs may be cell-type specific.

However, most of the stimuli induced significant TNF-α responses in all three donors analysed, although there was some variation between donors in their relative responsiveness to different stimuli (Figure 121 for individual donor TNF-α concentrations). Regardless, 2THO-DNJ and *N*N-DNJ treatment significantly reduced TNF-α secretion, in a consistent way between donors as well as across stimuli (Figure 70). The extent of the suppression did vary between stimuli, with the TNF-α response to PAM_3CSK_4 stimulation reduced by about 80% while the response to poly(I:C) stimulation only by 30-40%. There appears to be no clear relationship between the impact iminosugar treatment has on the response and the strength of the TNF-α response elicited by individual stimuli (by comparison with Figure 121). This indicates that while the effect

of the DNJ-derivatives is conserved across stimuli, the mechanism for this does not appear to be a broad non-specific suppression of TNF-α production, but is influenced by the stimulus.

In contrast, the effects of *N*N-DGJ treatment on TNF-α secretion were more selective, with significant reductions in TNF-α secretion elicited by some, but not all, of the stimuli. The effects of *N*N-DGJ on the response to PAM_3CSK_4 and FLA-BS were particularly potent and similar in degree to the effects of the DNJ-derivatives. Notably, the response to poly(I:C) stimulation in particular was unaffected by *N*N-DGJ. This suggests that the effects of *N*N-DGJ on TNF-α production may be mediated by impacts on particular PRR signalling pathways, revisited later.

Fewer stimuli elicited an IFN-α/β than a TNF-α response from the MDMΦs (Figure 71; concentrations for individual donors are shown in Figure 122). However, DNJ derivatives reduced the IFN-α/β responses to poly(I:C) and FSL-1 stimulation, while *N*N-DGJ had no significant effect. While *N*N-DGJ had no effect on TNF-α secretion in response to poly(I:C) stimulation, it did significantly reduce the TNF-α response to FSL-1, indicating that as well as being stimulus-dependent, the immunomodulatory effect of *N*N-DGJ is also cytokine-specific.

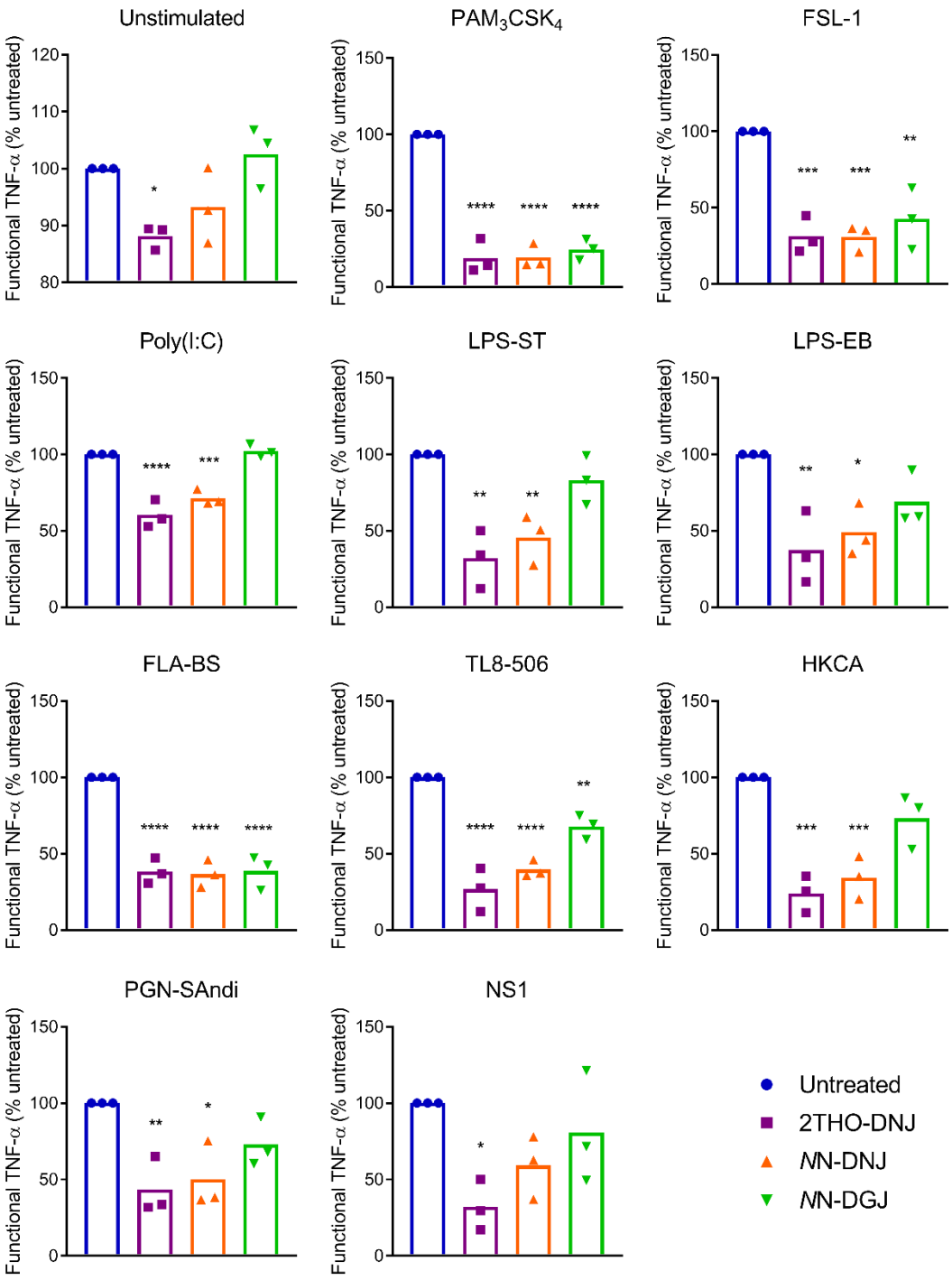

Figure 70. Iminosugars influence TNF-α secretion from MDMΦs elicited by a broad spectrum of PAMPs.

Primary MDMΦs (n=3 donors (NR, NS, OI), assayed in technical duplicate) were stimulated with PAMPs (2.5.1) and left untreated or treated with 100 µM 2THO-DNJ, 25 µM NN*-DNJ or 25 µM* NN*-DGJ. After 18 hours, supernatant was harvested and TNF-α secretion quantified by functional assay. Functional TNF-α was normalised to untreated for each donor and the mean plotted (bars show the mean of the donors). One-way ANOVA with Dunnett's multiple comparisons test was*

used to compare drug treatments to untreated for each stimulus (, p<0.05; **, p<0.01; ***, p<0.001; ****, p<0.0001).*

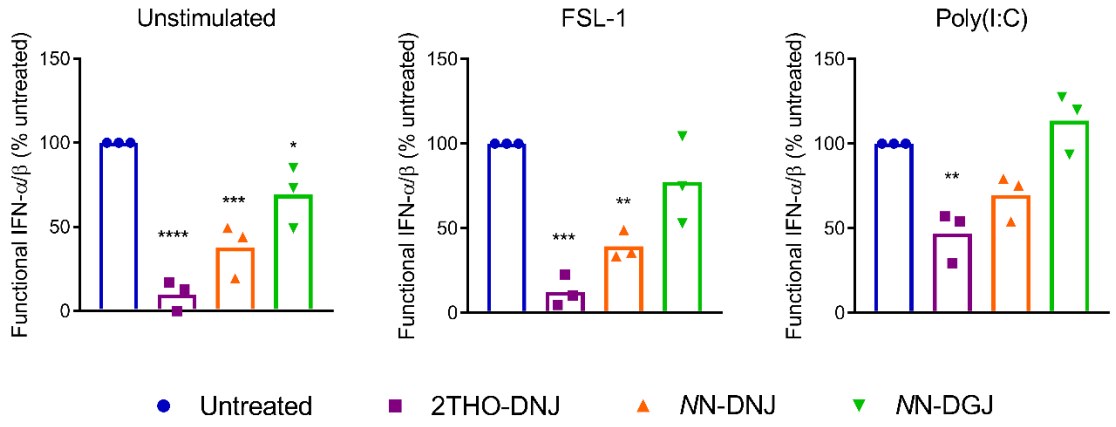

Figure 71. DNJ-derivate iminosugars influence IFN-α/β secretion from MDMΦs elicited by FSL-1 and poly(I:C).

Primary MDMΦs (n=3 donors (NR, NS, OI), assayed in technical duplicate) were stimulated with PAMPs (2.5.1) and left untreated or treated with 100 μM 2THO-DNJ, 25 μM N*N-DNJ or 25 μM* N*N-DGJ. After 18 hours, supernatant was harvested and IFN-α/β secretion quantified by functional assay. Functional IFN-α/β was normalised to untreated for each donor and plotted as mean ± standard deviation. One-way ANOVA with Dunnett's multiple comparisons test was used to compare drug treatments to untreated for each stimulus (*, p<0.05; **, p<0.01; ***, p<0.001; ****, p<0.0001).*

The differential effects of *N*N-DGJ treatment on TNF-α production elicited by different stimuli raised an interesting possibility for mechanistic analysis. Significant suppression of the TNF-α response was observed for PAM_3CSK_4, FSL-1, FLA-BS and TL8-506, agonists of TLR1/2, TLR2/6, TLR5 and TLR8, respectively (Figure 70). These TLRs all require the adaptor protein MyD88 for signalling. In contrast, among the TLR agonists which induced significant TNF-α responses, poly(I:C) was the only stimulus for which no effect of *N*N-DGJ was seen. Poly(I:C) detection can be mediated by TLR3, as well as RIG-I and MDA5. TLR3 signalling is dependent on the adaptor protein TRIF, not MyD88 [615]. The other PAMPs for which there was a TNF-α response but no effect of *N*N-DGJ treatment stimulate PRRs whose signalling pathways utilise neither the MyD88 nor TRIF adaptor proteins. Interestingly, and uniquely among TLRs, the TLR4 response to LPS can

be mediated by both MyD88- and TRIF-dependent signalling pathways. The MyD88-dependent pathway has traditionally been seen as critical for LPS-induced pro-inflammatory cytokine production in murine macrophages and dendritic cells, while MyD88- and the TRIF-dependent pathways influence macrophage and dendritic cell maturation [616-618]. However, more recently, cooperative roles for TRIF- and MyD88-dependent signalling have been identified in LPS-induced pro-inflammatory cytokine production [615]. While the TNF-α response to LPS-ST or LPS-EB stimulation was not statistically significantly affected by *N*N-DGJ treatment, there was a trend towards a reduction in TNF-α secretion. Thus, the hypothesis that the TNF-α-modulatory effects of *N*N-DGJ require MyD88 was investigated.

To this end, preliminary investigations were conducted using peptide inhibitors of TRIF and MyD88, which inhibit signalling by preventing adaptor protein homodimerisation, alongside a control peptide inhibitor. MDMΦs were pre-treated with the relevant inhibitor before stimulation with LPS, poly(I:C) or poly(A:U) and iminosugar treatments were added. The rationale was that the dual adaptor use of the TLR4 response to LPS would enable investigation of the MyD88-dependence. If the suppressive effect of *N*N-DGJ on TNF-α production required MyD88, directing the TLR4-mediated LPS response solely through the MyD88-dependent pathway would result in the response pattern matching that of PAM_3CSK_4, FSL-1, FLA-BS and TL8-506. In other words, a significant reduction in TNF-α secretion on *N*N-DGJ treatment would be expected, comparable with the DNJ-derivatives.

Poly(A:U) was introduced as a stimulus alongside poly(I:C) since detection of poly(A:U) is mediated solely by TLR3, compared to poly(I:C) which can signal through TLR3, RIG-I and MDA5. Interestingly, neither of the donors assayed made any TNF-α or IFN-α/β response to poly(A:U) stimulation, contrasting with the poly(I:C) response (Figure 72 and Figure 73), although it is possible that the poly(A:U) stimulation protocol was suboptimal. The TRIF inhibitor appeared to

have a small impact on cytokine responses to poly(I:C) stimulation, but a moderate cytotoxic effect of the TRIF inhibitor (not seen with the other inhibitors; Figure 123) is likely to have contributed to this. In any case, the cytokine response to poly(I:C) was not abolished on TRIF inhibition and was less affected than the response to LPS stimulation. Taken together, this suggests that the cytokine response to poly(I:C) stimulation is not mediated by TLR3, but by RIG-I and/or MDA5, under these conditions. This may be unsurprising considering the variation in reports of whether human monocytes and macrophages express TLR3 at baseline [619-621]: indeed, in a transcriptomic analysis of MDMΦs prepared according to our protocol, expression of TLR3 along with TLR9 did not reach the detection threshold, implying low abundance (Andrew Sayce, unpublished data). However, TLR3 expression can be induced in human macrophages by IFN-α/β [622, 623], suggesting that the response to poly(I:C) treatment might become TRIF-dependent if a later time point was considered.

Considering the effects of MyD88 and TRIF inhibition on the cytokine response to LPS stimulation, unfortunately a significant TNF-α response was made in only one of the donors tested (Figure 72). This response was reduced to baseline by application of the TRIF inhibitor, regardless of the iminosugar treatment. The MyD88 inhibitor, by contrast, had little effect. The discrepancy in the effects of the MyD88 and TRIF inhibitors in the no iminosugar condition indicates that under these stimulation conditions, the LPS-elicited TNF-α response is TRIF-dependent but MyD88-independent. Due to the lack of MyD88 inhibitor effect, it is unsurprising that the combination of MyD88 inhibitor and *N*N-DGJ retains the intermediate, slight TNF-α suppression phenotype observed previously (Figure 70), rather than reducing TNF-α secretion in line with the effect of *N*N-DNJ. Overall, these data neither support nor refute the hypothesis that *N*N-DGJ can influence TNF-α secretion elicited by MyD88-dependent TLR signalling. The findings require confirmation in additional MDMΦ donors, particularly considering the variable levels of cytokine response between donors. Biasing the TLR4-mediated LPS response towards

the MyD88- or TRIF-dependent pathways using peptide inhibitors might yet be an elegant way to interrogate the MyD88-dependence of the effects of *N*N-DGJ. Since the prevailing view is that MyD88 may be important for early signalling, and TRIF later [624], investigation of the effects of adaptor protein inhibition and consequently iminosugar treatment on the TNF-α response over time might prove worthwhile. It would be interesting to establish how variable or consistent this response pattern might be between human donors.

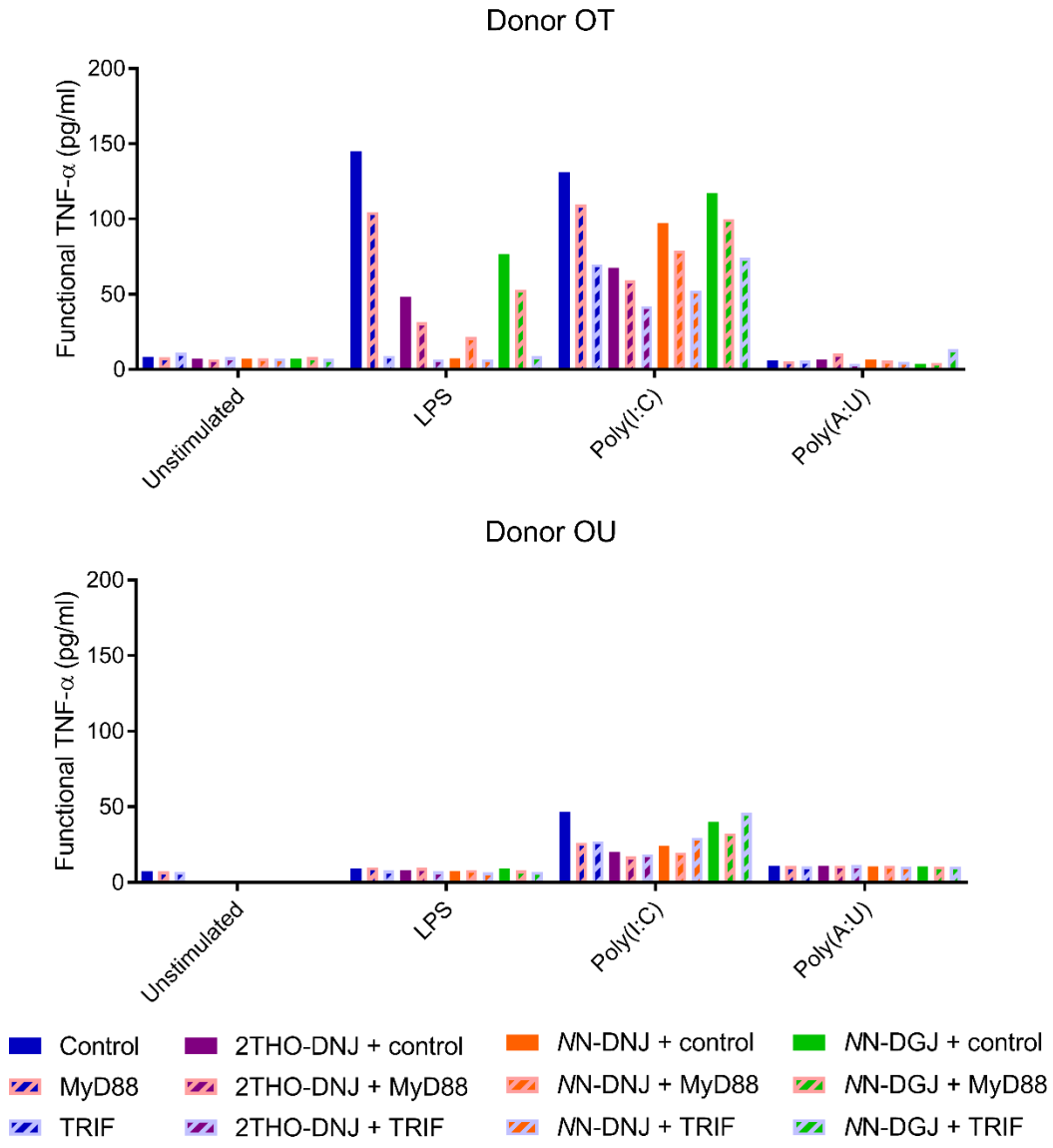

Figure 72. LPS-induced TNF-α production is TRIF-dependent whilst the response to poly(I:C) does not appear to be TLR3-mediated.

Primary MDMΦs (donors as shown, assayed in technical singlicate) were pre-treated with peptide inhibitors of MyD88 or TRIF, or a control peptide for 6 hours. Inhibitor-treated MDMΦs

were then left unstimulated or stimulated with LPS-EB, poly(I:C) or poly(A:U) (2.5.1) and left untreated or treated with 100 µM 2THO-DNJ, 25 µM NN*-DNJ or 25 µM* NN*-DGJ. After a further 18 hours, supernatant was harvested and TNF-α secretion quantified by functional assay.*

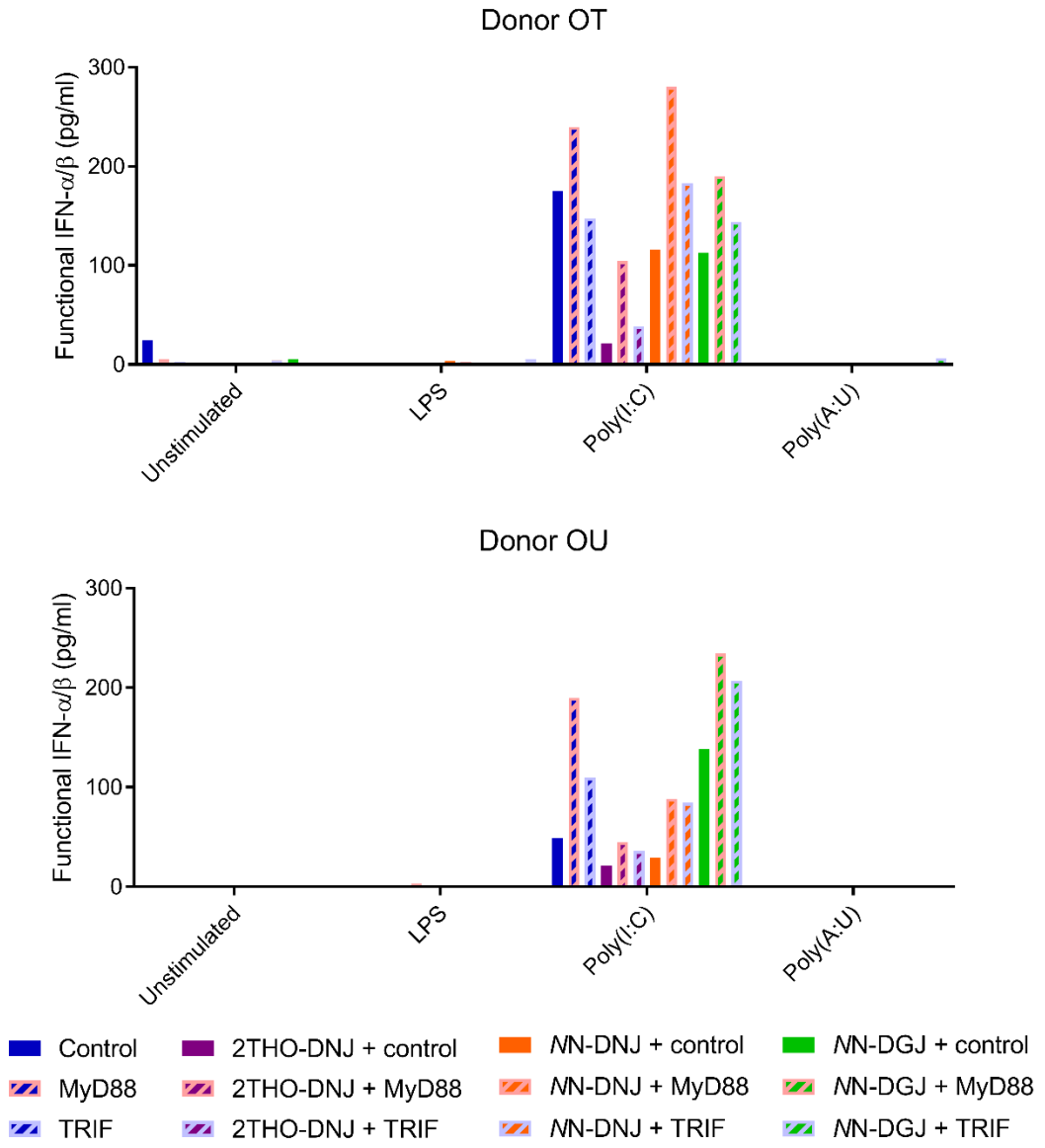

Figure 73. The IFN-α/β response to poly(I:C) does not appear to be TLR3-mediated.

Primary MDMΦs (donors as shown, assayed in technical singlicate) were pre-treated with peptide inhibitors of MyD88 or TRIF, or a control peptide for 6 hours. Inhibitor-treated MDMΦs were then left unstimulated or stimulated with LPS-EB, poly(I:C) or poly(A:U) (2.5.1) and left untreated or treated with 100 µM 2THO-DNJ, 25 µM NN*-DNJ or 25 µM* NN*-DGJ. After a further 18 hours, supernatant was harvested and IFN-α/β secretion quantified by functional assay.*

6.3.5.4 Multiplex cytokine assay reveals that 2THO-DNJ, NN-DNJ and NN-DGJ can modulate secretion of IFN-γ, IL-1β and MCP-1

In order to gain a broader perspective on how 2THO-DNJ, *N*N-DNJ and *N*N-DGJ treatment can affect cytokine secretion from MDMΦs, an antibody-based assay, the LEGENDplex human inflammation panel, was used to quantify 13 cytokines in parallel in supernatants derived from MDMΦs stimulated with the PAMP panel previously described. Here, data is presented for the cytokines where at least one stimulation induced substantial cytokine secretion relative to the unstimulated condition and a similar response pattern to iminosugar treatment was seen for two of the donors (results for IL-6, IL-8, IL-10, IL-12p70, IL-17A, IL-18, and IL-23 can be found in 8.19; results for IL-33 are not presented due to high technical variability). Across the cytokines measured, LPS-EB and TL8-506 stimulations led to cytokine responses most frequently. However, there was a significant degree of inter-donor variability in the three donors tested in terms of responsiveness to different stimuli and the effects of iminosugars, and combining data from the donors for analysis lost sensitivity to these differences (exemplified for LPS-EB and TL8-506 responses in Figure 131 and Figure 132, respectively). Thus, in the following figures, the donors are presented separately.

The effects of iminosugars on TNF-α and IFN-α/β responses were previously analysed by functional cytokine assay (6.3.5.3). For TNF-α, the effects of iminosugar treatment assessed by LEGENDplex assay (Figure 74) were broadly in keeping with those seen by functional TNF-α assay (Figure 70). For IFN-α/β, the LEGENDplex assay is specific to the IFN-α2 subtype unlike the functional cytokine assay which detects any IFN-α/β subtype. Here, LPS-EB and TL8-506 stimulations led to substantial cytokine responses (Figure 75), unlike in the functional assay where poly(I:C) was consistently the most potent stimulus (Figure 122), implying that the majority of the response to poly(I:C) comprises other IFN-α subtypes or IFN-β at this time point.

2THO-DNJ, *N*N-DNJ and *N*N-DGJ treatment all appeared to have the ability to significantly reduce IFN-α2 secretion, although this was donor-dependent (Figure 75).

Considering other cytokines not previously investigated in this chapter, significant inductions of IFN-γ, IL-1β and MCP-1 secretion were observed with LPS-EB and TL8-506 stimulation. For IFN-γ, 2THO-DNJ, *N*N-DNJ and *N*N-DGJ treatment all appeared to be able to reduce secretion of the cytokine, although this was donor-dependent, particularly for the response to LPS-EB (Figure 76). Reduced IFN-γ secretion has previously been observed from MDMΦs stimulated with LPS-ST or infected with DENV and treated with M*O*N-DNJ [418], as well as in M*O*N-DNJ and 2THO-DNJ-treated DENV-infected mice and by a range of iminosugars in diverse *in vitro* settings (Table 4 and Table 6). The presence of two occupied N-glycosylation sites in IFN-γ [625, 626] indicates that inhibition of ER α-glucosidases by DNJ-derivatives could directly suppress IFN-γ secretion.

IL-1β secretion could be suppressed by DNJ-derivative iminosugars, while *N*N-DGJ treatment had a range of effects in different donors (Figure 77), in accordance with significantly reduced circulating IL-1β levels in a DENV-infected mouse model treated with 2THO-DNJ [397]. However, despite the presence of an N-glycosylation site, IL-1β does not enter the ER and is secreted in a non-glycosylated form by human monocytes [627]. Thus DNJ-derivative inhibition of ER α-glucosidases would not be able to directly impact the secretion of this cytokine.

In contrast, while MCP-1 secretion in response to TL8-506 stimulation seemed to be reduced by iminosugar treatment, in two of the three donors, iminosugar treatment seemed to enhance MCP-1 secretion in response to LPS-EB stimulation (Figure 78). This is in agreement with the previous finding that M*O*N-DNJ treatment significantly increased MCP-1 secretion from LPS-ST-stimulated MDMΦs and a trend towards this was observed at day 5 post-DENV infection [418], although in DENV-infected mouse models, MCP-1 secretion was unaffected by 2THO-DNJ

treatment [397] and the increase in secretion was delayed by MON-DNJ [399]. These differences may reflect the lack of occupied N-glycosylation sites reported in human MCP-1, compared to the N- and O-glycosylation of murine MCP-1, meaning that DNJ-derivative iminosugars might be able to directly inhibit the folding and thus secretion of murine but not human MCP-1 [628].

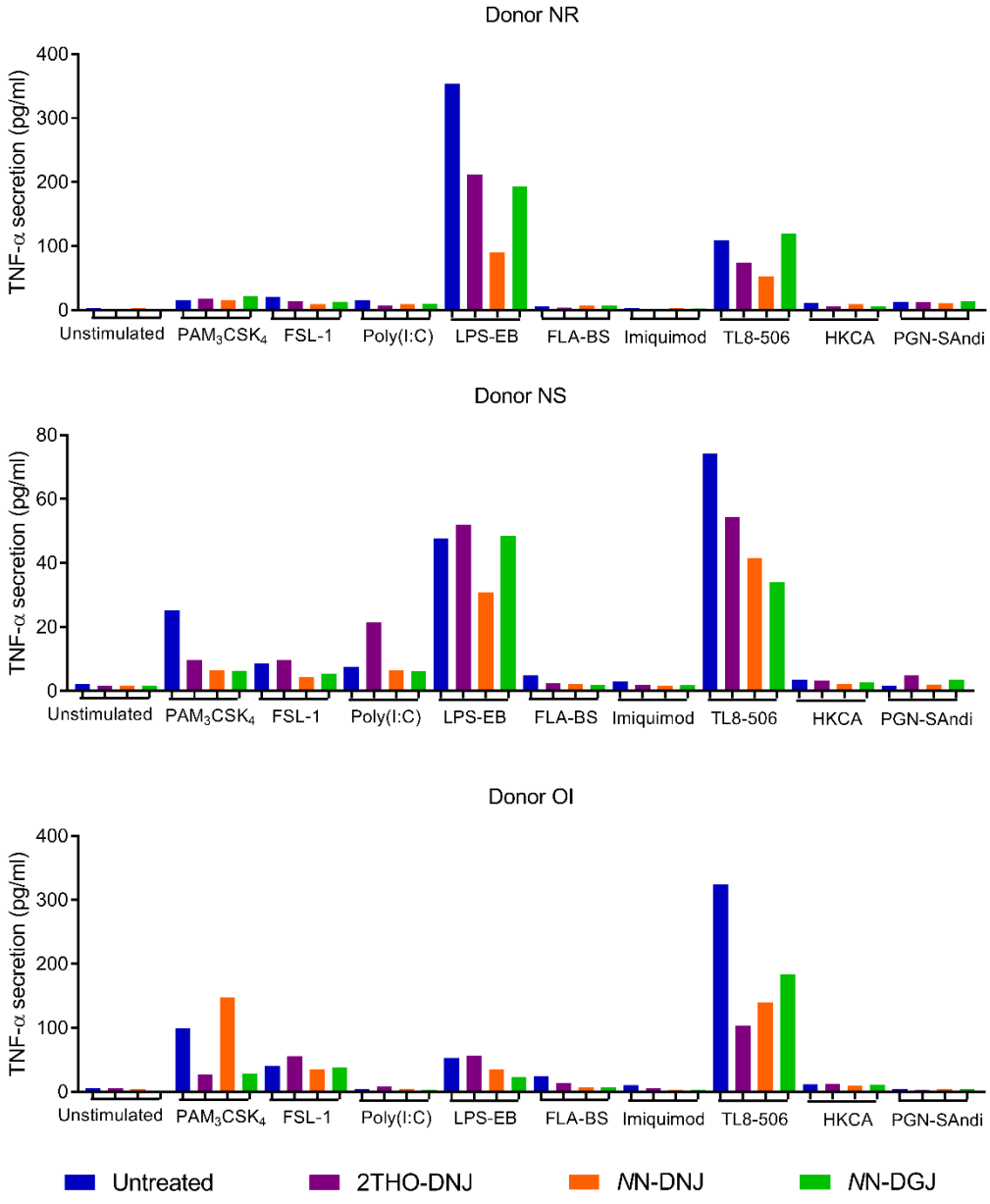

Figure 74. Iminosugar treatment can affect TNF-α secretion in response to PAMP stimulation of MDMΦs.

Primary MDMΦs (donors as shown) were stimulated with PAMPs (2.5.1) and left untreated or treated with 100 µM 2THO-DNJ, 25 µM NN*-DNJ or 25 µM* NN*-DGJ. After 18 hours, supernatant was harvested. TNF-α secretion was quantified by LEGENDplex assay and the mean plotted. Samples below the LOD are shown as 0.71 and 1.65 pg/ml for donors NR and NS, respectively.*

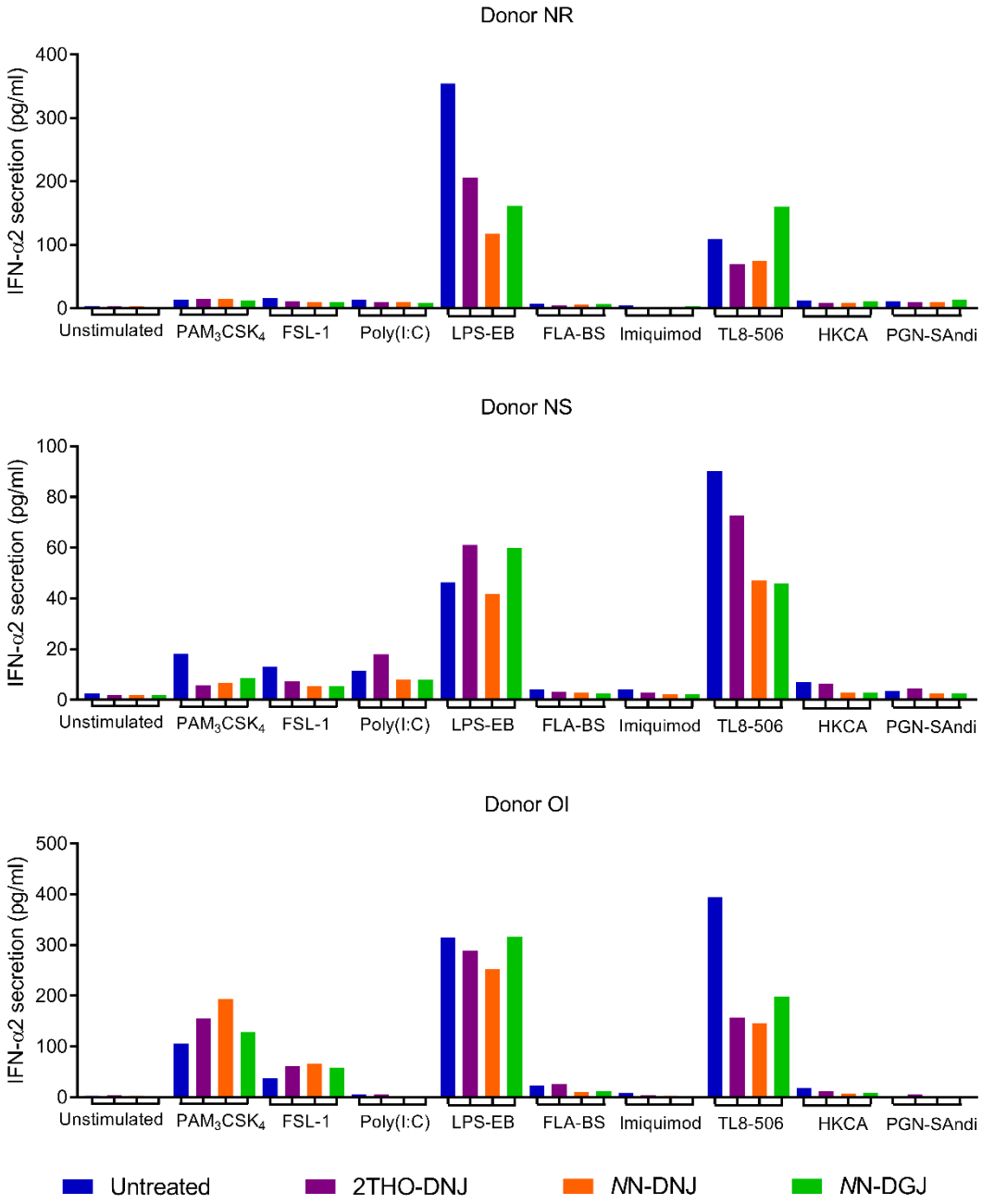

Figure 75. Iminosugar treatment can affect IFN-α2 secretion in response to PAMP stimulation of MDMΦs.

Primary MDMΦs (donors as shown) were stimulated with PAMPs (2.5.1) and left untreated or treated with 100 µM 2THO-DNJ, 25 µM NN*-DNJ or 25 µM* NN*-DGJ. After 18 hours, supernatant was harvested. IFN-α2 secretion was quantified by LEGENDplex assay and the mean plotted. Samples below the LOD are shown as 1.89 and 0.45 pg/ml for donors NR and OI, respectively.*

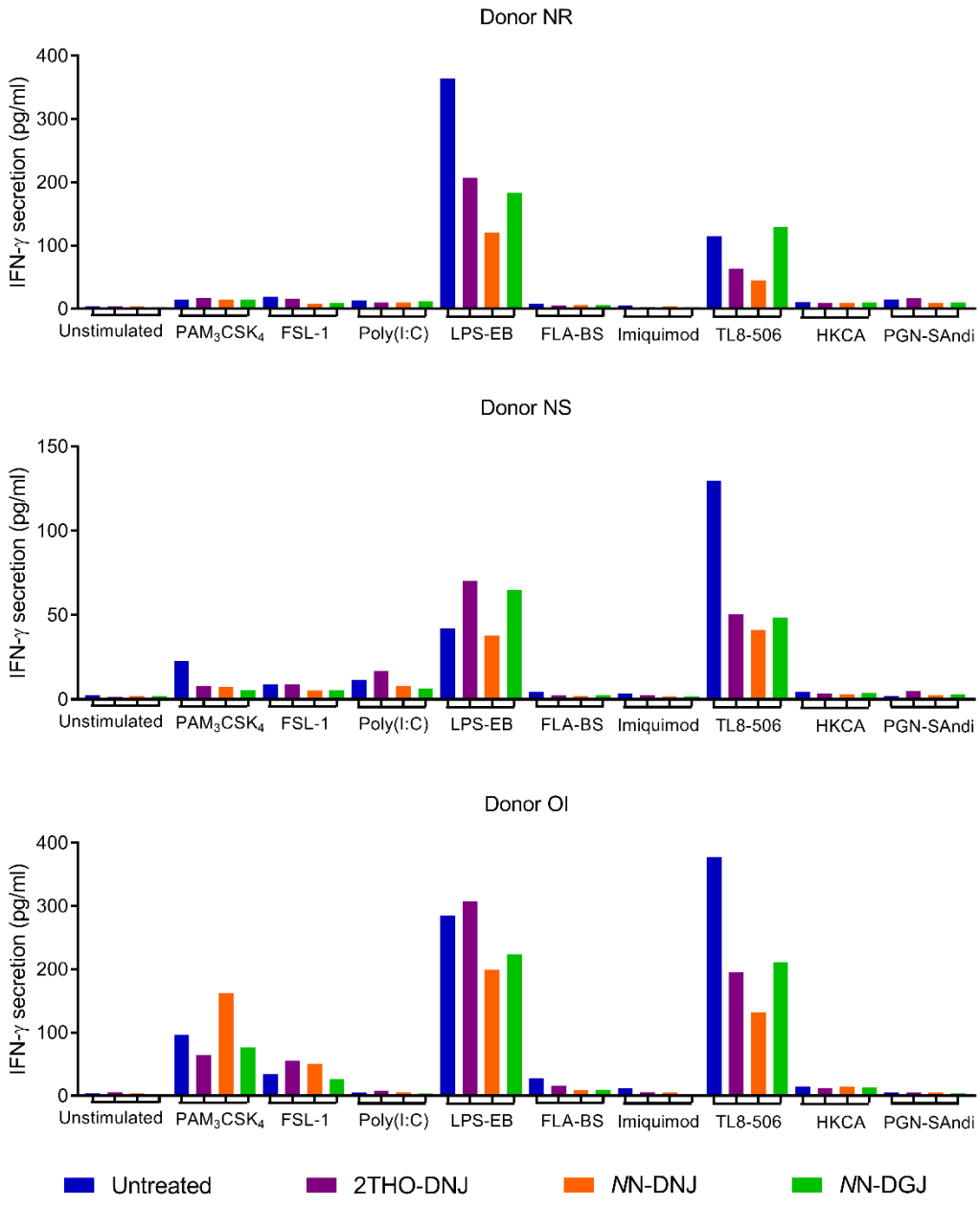

Figure 76. Iminosugar treatment can affect IFN-γ secretion in response to PAMP stimulation of MDMΦs.

Primary MDMΦs (donors as shown) were stimulated with PAMPs (2.5.1) and left untreated or treated with 100 µM 2THO-DNJ, 25 µM NN-DNJ or 25 µM NN-DGJ. After 18 hours, supernatant was harvested. IFN-γ secretion was quantified by LEGENDplex assay and the mean plotted. Samples below the LOD are shown as 1.73 pg/ml for donor NS.

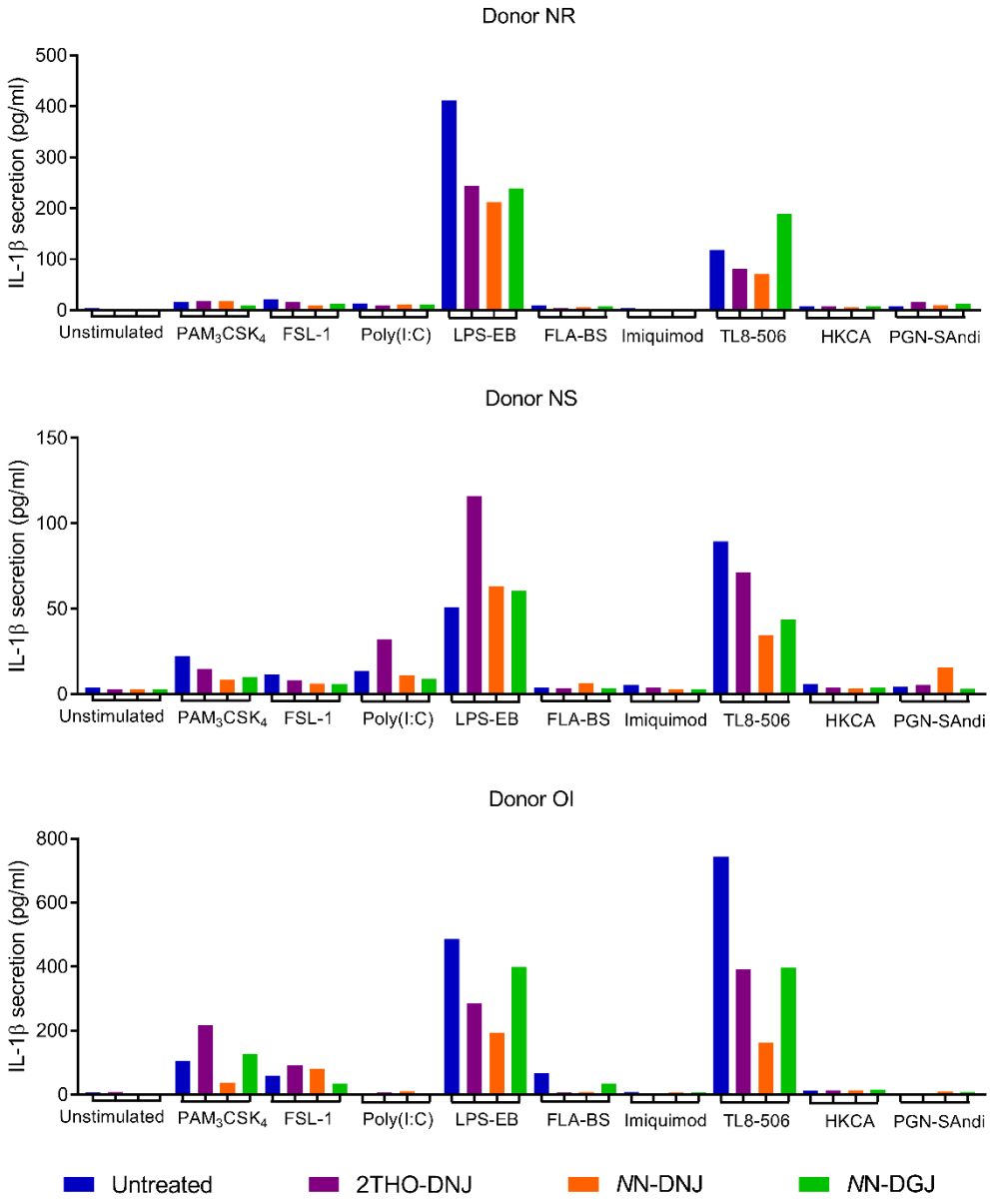

Figure 77. Iminosugar treatment can affect IL-1β secretion in response to PAMP stimulation of MDMΦs.

Primary MDMΦs (donors as shown) were stimulated with PAMPs (2.5.1) and left untreated or treated with 100 µM 2THO-DNJ, 25 µM NN-DNJ *or 25 µM* NN-DGJ*. After 18 hours, supernatant was harvested. IL-1β secretion was quantified by LEGENDplex assay and the mean plotted. Samples below the LOD are shown as 2.65 and 1.62 pg/ml for donors NR and OI, respectively.*

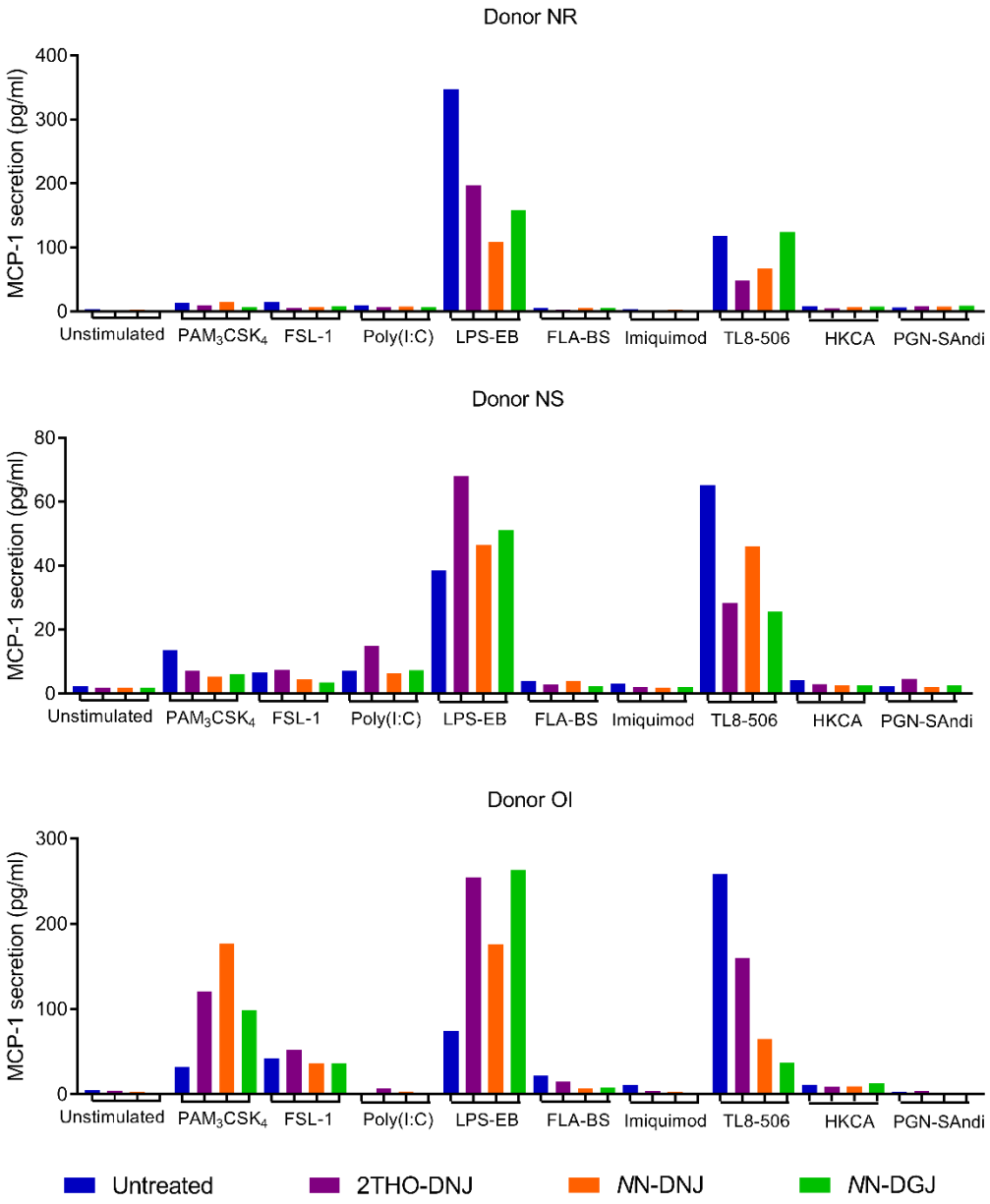

Figure 78. Iminosugar treatment can affect MCP-1 secretion in response to PAMP stimulation of MDMΦs.

Primary MDMΦs (donors as shown) were stimulated with PAMPs (2.5.1) and left untreated or treated with 100 µM 2THO-DNJ, 25 µM NN*-DNJ or 25 µM* NN*-DGJ. After 18 hours, supernatant was harvested. MCP-1 secretion was quantified by LEGENDplex assay and the mean plotted. Samples below the LOD are shown as 1.89 pg/ml for donor NS.*

6.3.6 Iminosugars modulate TLR signalling in a reporter cell system

As established in 6.3.5, iminosugars can impact cytokine production in response to multiple non-infectious stimuli, including a broad range of TLR agonists. Therefore, the potential for iminosugars to affect TLR signalling was investigated.

6.3.6.1 Transcriptomic analysis suggests that iminosugar treatment has little effect on TLR expression level

Initially, potential effects on TLR expression were interrogated by analysis of TLR gene transcripts quantified as part of a transcriptomics experiment (sample generation and transcriptomics data processing by Andrew Sayce). In DENV-infected or LPS-stimulated MDMΦs, TLR gene expression was largely unaffected by M*O*N-DNJ treatment, with the exception of TLR4, which was significantly upregulated upon M*O*N-DNJ treatment in the context of DENV infection only (Figure 79). However, the effect on TLR4 expression requires validation at the mRNA level relative to housekeeping gene expression. Furthermore, the lack of a consistent effect across the TLRs indicates that modulation of TLR expression is unlikely to account for the effects of iminosugars on TNF-α responses to TLR stimulation.

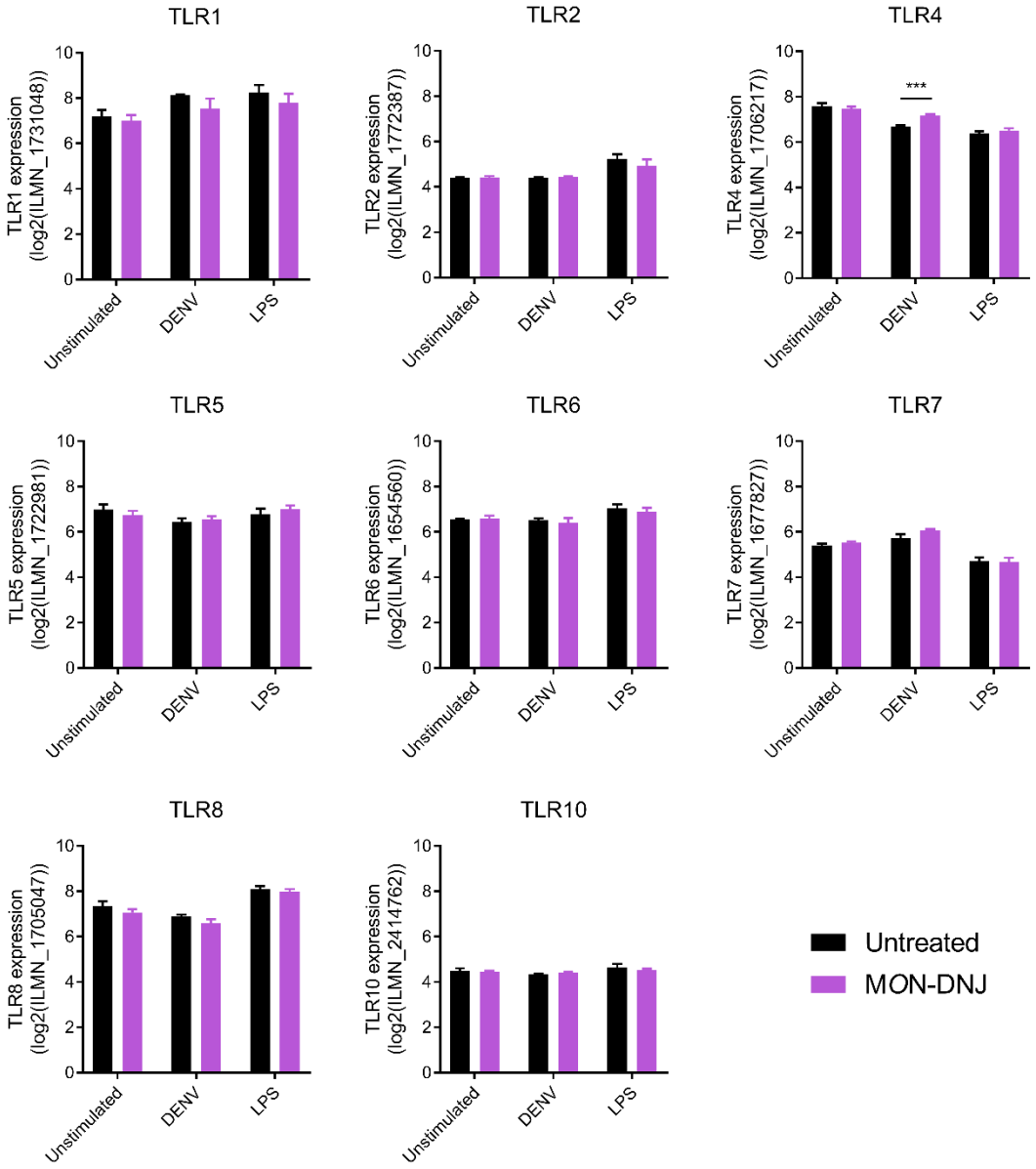

Figure 79. MON-DNJ has little effect on TLR gene expression.

*Primary MDMΦs (n=4 donors (FY, FZ, GA, GB)) were infected with DENV or stimulated with 100 ng/ml LPS-ST and untreated or treated with 25 µM MON-DNJ. After 24 hours, cellular RNA was extracted, the transcriptome profiled and data analysed as described in [418]. Sample generation and transcriptome processing were conducted by Andrew Sayce. The average log2 quantification of probes detected corresponding to TLR genes was displayed as mean ± standard error. Quantifications were compared across stimulation and treatment conditions, with statistical analysis by multiple t-test with False Discovery Rate (two-stage set-up) approach (***, p<0.001).*

6.3.6.2 NN-DGJ enhances TLR signalling in a TLR reporter cell system

To investigate whether TLR signalling is affected by iminosugar treatment, commercially available TLR reporter cell lines (2.5.5) were utilised, representing a subset of the TLR responses previously investigated. Cells were pre-treated with iminosugars for 3 days, aiming to allow turnover of TLR signalling pathway components in the presence of iminosugar. TLRs are N-glycosylated proteins [629], thus new TLR synthesis during the pre-treatment period might be susceptible to misfolding and degradation as a consequence of iminosugar pressure, alongside other components of the signalling pathway. This 3 day treatment at 25 µM iminosugar did not impact cell viability in any of the TLR reporter cells (Figure 92). Following iminosugar treatment, cells were stimulated with canonical agonists (FSL-1, poly(I:C), LPS-ST, and ODN-2006 for TLR2, TLR3, TLR4, and TLR9 reporter cells, respectively; Table 9). In the reporter cells, TLR stimulation results in SEAP secretion. Here, resulting SEAP secretion was quantified directly in colorimetric detection media, allowing sequential readings without removal of media from wells.

Since the HEK293 cells used as the background for the TLR reporter cell system express certain TLRs at a basal level, the non-specific responses of HEK-Null cells were subtracted from the responses of the reporter cells to enable assessment of iminosugar effects on the signalling pathways of particular TLRs. Interestingly, iminosugar treatment appeared to affect the background SEAP secretion of the HEK-Null cells, with this suppressed by DNJ-derivative treatment and possibly enhanced by *N*N-DGJ (Figure 80 for LPS-ST stimulation; same effect seen for other stimuli, data not shown). The background SEAP secretion was unaffected by stimulation of the cells with the TLR agonists tested. In contrast, when SEAP secretion from the TLR reporter cells is considered in isolation, a response is seen when the TLR agonist is present, while SEAP secretion from unstimulated cells remains very stable over time (Figure 81 for HEK-TLR4 reporter cells; same effect seen for other reporter cells, data not shown). The amplitude of the SEAP response in the reporter cell was much greater than the background level of

secretion in the stimulated HEK-Null cells. As observed for the HEK-Null cells, there appeared to be a trend towards a suppressive effect of DNJ-derivatives and a stronger enhancing effect of *N*N-DGJ on SEAP responses.

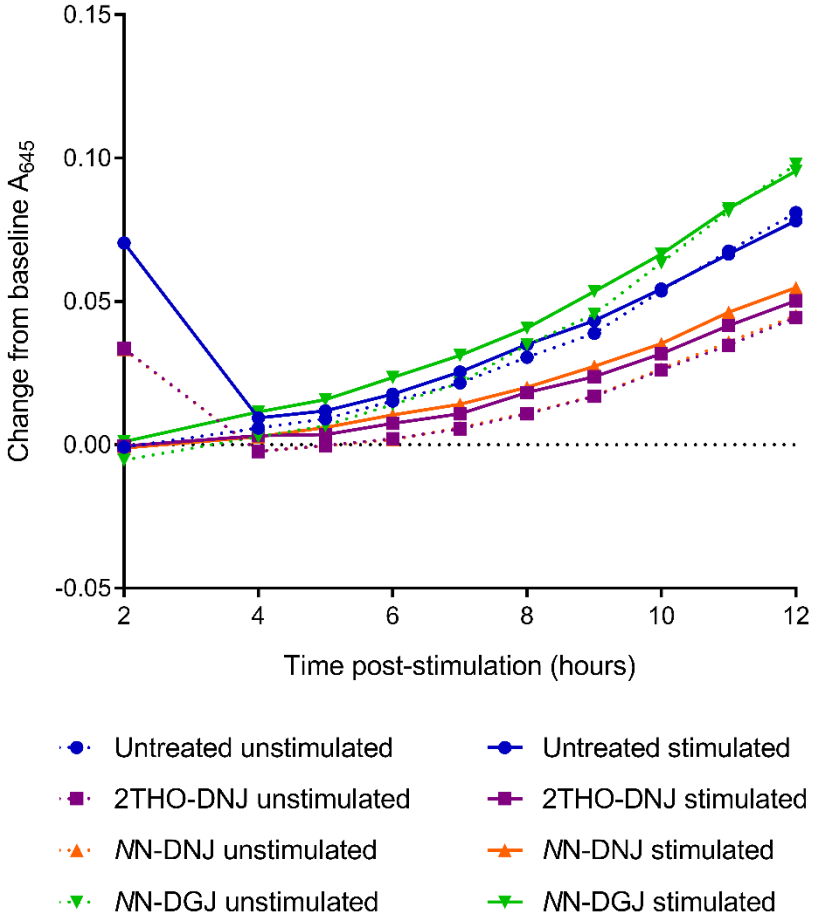

Figure 80. Iminosugar treatment affects baseline SEAP secretion in HEK-Null cells.

HEK-Null cells (assayed in triplicate, representative of 2 experiments) were untreated or pre-treated with 25 µM iminosugar for 3 days before stimulation with LPS-ST, or no stimulation. Resulting SEAP secretion was quantified over time and the mean change in A_{645} from baseline plotted.

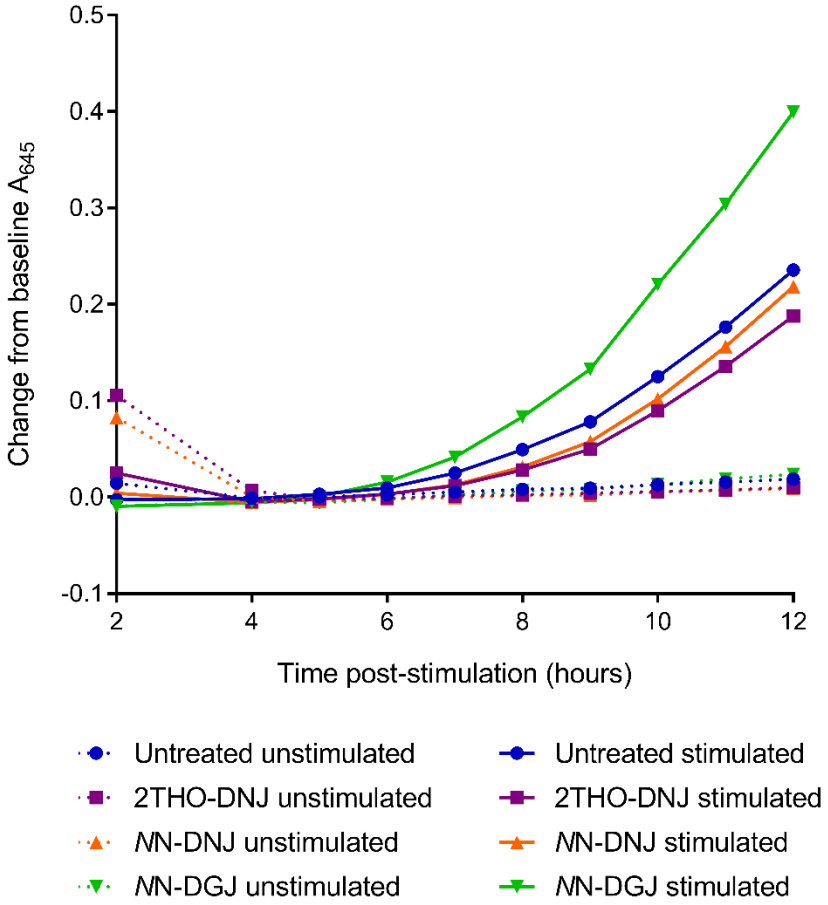

Figure 81. HEK-TLR4 reporter cells have very low background SEAP secretion when unstimulated.

HEK-TLR4 reporter cells (assayed in triplicate, representative of 2 experiments) were untreated or pre-treated with 25 µM iminosugar for 3 days before stimulation with LPS-ST, or no stimulation. Resulting SEAP secretion was quantified over time and the mean change in A_{645} from baseline plotted.

To enable assessment of the impact of iminosugar pre-treatment on TLR signalling pathway function, corresponding responses of the HEK-Null cells were subtracted from those of the TLR reporter cells (Figure 82). While response amplitudes varied between reporter cell types, possibly reflecting different stimulation efficiencies, *N*N-DGJ treatment consistently enhanced TLR reporter cell responses to stimulation. In contrast, *N*N-DNJ and 2THO-DNJ treatment had little if any effect on responses.

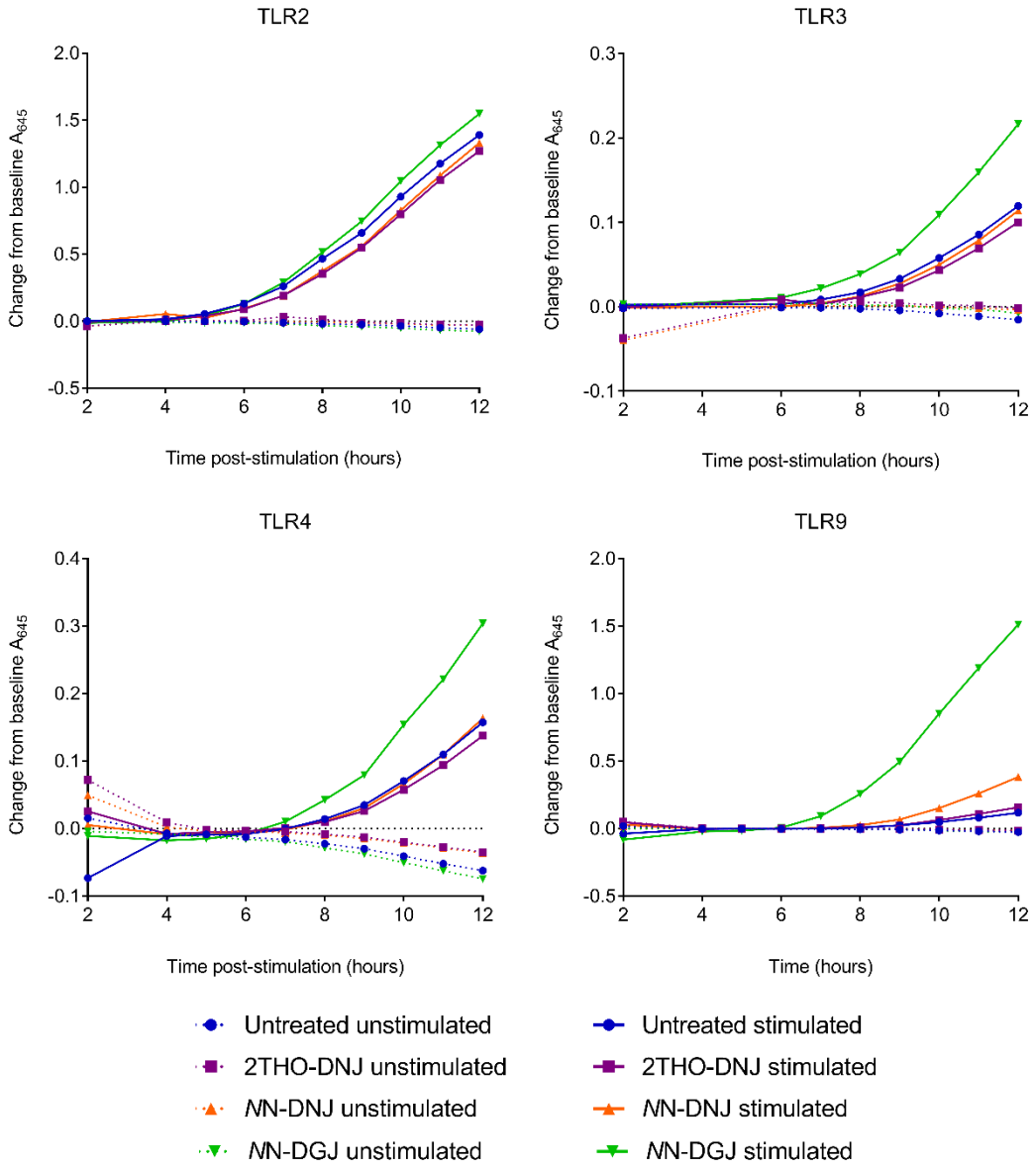

Figure 82. N*N-DGJ pre-treatment of HEK-TLR reporter cells enhances TLR signalling pathway activation.*

HEK-TLR reporter cells and HEK-Null cells (assayed in triplicate, representative of 2 experiments) were untreated or pre-treated with 25 µM iminosugar for 3 days. Reporter cells were then left unstimulated or stimulated with canonical TLR agonists (2.5.5). Resulting SEAP secretion was quantified over time. Non-specific stimulation, as determined by the background responses of HEK-Null cells stimulated with the same stimulus, was subtracted from the responses of the HEK-TLR reporter cells. The mean change in A_{645} from baseline was plotted.

6.4 Discussion

DNJ-derivative iminosugars may represent a 'double threat' to the pathogenesis of viral haemorrhagic fevers, with both antiviral efficacy and the ability to reduce secretion of the pro-inflammatory, pathogenic TNF-α in the context of DENV infection of primary human MDMΦs. These effects are shared by 2THO-DNJ, *N*N-DNJ and M*O*N-DNJ. The antiviral effect of 2THO-DNJ appears to be the driving force for the reduction in TNF-α secretion. Since 2THO-DNJ inhibits DENV replication (3.3.1.8.1), treatment would result in a reduced viral RNA stimulus for TLR3, TLR7, RIG-I and MDA5 activation [141, 146, 149-153, 155-157]. It is also likely that, as an N-linked glycoprotein, NS1 production and/or function would be inhibited by 2THO-DNJ treatment, as seen with *N*N-DNJ and BuCAST [58, 395], which could reduce NS1-mediated TLR4 stimulation [75]. It would be interesting to investigate whether and how TLR signalling and cytokine responses made by MDMΦs are affected by stimulation with equal genome equivalents of MDMΦ-derived DENV produced in the presence or absence of iminosugar. This would encompass effects on any NS1 secreted from the infected cells as well as perturbations in the virion structure as a result of the increased incorporation of misfolded structural glycoproteins inferred from the reduced specific infectivity with high-dose iminosugar treatment (3.3.1.2). This could affect virion recognition by CLEC5A [141] and could potentially affect any TLR7-depedent signalling since TLR7-mediated IFN-α/β responses were shown to be modulated by the maturity of DENV virions used to stimulate plasmacytoid DCs [150].

While the antiviral effect of 2THO-DNJ appears to be the driving force in the reduction of TNF-α secretion in the context of DENV infection of MDMΦs, this alone cannot account for the effects of iminosugars on cytokine secretion. Firstly, non-antiviral iminosugars (*N*N-DGJ) can affect the cytokine response to DENV infection, and secondly, cytokine responses elicited by non-viral agonists are susceptible to modulation. Both of these observations have support in the literature (1.2.5.3), however, immunomodulatory effects on cytokine responses elicited by diverse PAMPs

have not been considered, and widespread evaluation of DNJ- and DGJ-derivative iminosugars in parallel is lacking.

Cytokine secretion occurs downstream of PAMP detection and signalling pathways, modulation of which could account for the effects of iminosugars on cytokines. To investigate this, MDMΦs were stimulated with a range of PAMPs targeting TLRs, RIG-I/MDA5, NOD1/NOD2 and Dectin-1 with iminosugar treatment, allowing interrogation of iminosugar effects on cytokine responses to a broad range of stimuli and in the absence of the confounding factor of antiviral effects. 2THO-DNJ and *N*N-DNJ treatment reduced resulting TNF-α secretion measured 18 hours post-stimulation. These effects could be mediated by the established mechanism of inhibition of ER α-glucosidases, impacting the folding and function of N-linked glycoproteins. Indeed, many PRRs are N-glycosylated, with multiple N-glycosylation sites predicted for each TLR and present in crystal structures obtained to date [629]. Functional studies have demonstrated the importance of N-glycosylation for the signalling of multiple TLRs [630]. For TLR4, cell surface expression requires N-linked glycosylation, and LPS-responsiveness requires MD-2 N-glycosylation and core fucosylation of CD14, and is regulated by sialylation of TLR4 and MD-2 [631-636]. The importance of N-linked glycosylation for expression or signalling of TLR2 [637], TLR3 [638], TLR5 [639] and bovine TLR8 [640] has also been demonstrated. In addition, N-glycosylation of Dectin-1 is essential for recognition of fungal β-glucans and downstream signalling [641]. Thus, DNJ-derivative treatment could directly inhibit the generation of some new PRR molecules. However, the 18 hour iminosugar treatment window might not provide sufficient opportunity for this to occur. Alternatively, NF-κB is a downstream regulator of pro-inflammatory cytokine production shared by these PRR pathways, but it is not N-glycosylated. Perhaps this might instead be targeted by a different iminosugar mechanism of action.

Another potential mechanism by which iminosugars could influence pro-inflammatory cytokine production is through the ER stress induced by the accumulation of misfolded proteins upon DNJ-derivative-mediated inhibition of ER α-glucosidases. Indeed, transcriptomic analysis, validated by qRT-PCR, of DENV-infected or LPS-stimulated MDMΦs indicated that M*O*N-DNJ treatment induced UPR genes at 6 hours post-stimulation, while downstream TNF-α secretion and ROS production were reduced ([418], Figure 58, and Andrew Sayce, Beatrice Tyrrell and Nilanka Perera, unpublished data). The ER stress-induced UPR conventionally involves activation of the inositol-requiring enzyme 1α (IRE1α), protein kinase R-like ER kinase (PERK) and activating transcription factor 6 (ATF6) pathways and, overall, acts to enhance protein folding capacity and misfolded protein degradation capabilities to maintain cellular survival, as well as intersecting with cytokine production on multiple levels, reviewed in [642]. UPR activation leads to a low level of pro-inflammatory cytokine production, with all three pathways impacting NF-κB activation, and IFN-α/β secretion, although the mechanism for this induction varies depending on the type of ER stress [643]. UPR transcription factors of all three arms (X-box binding protein 1 (XBP1), CCAAT-enhancer-binding protein homologous protein (CHOP) and ATF4 for the IRE1α, PERK and ATF6 pathways, respectively) can also directly activate the transcription of certain cytokine genes, including *TNF*, *IFNB1*, *IL6* and *IL23A* [644-647]. Upstream of this, the UPR also affects PRR responses. It is generally accepted that PRR stimulation of an ER-stressed cell enhances the cytokine response, in an XBP1-dependent fashion for TNF-α and IFN-β [644, 645]. However, this is not always clear-cut as pre-conditioning of cells to ER stress by depletion of BiP [648] and treatment with the classical ER stress-inducer tunicamycin [632, 649, 650] can result in impaired NF-κB activation, although this effect of tunicamycin may be independent of ER stress [650]. In addition, PRR stimulation in the absence of ER stress can selectively activate aspects of the UPR, exemplified by stimulation of TLR2 and TLR4 activating the IRE1α pathway, leading to pro-inflammatory cytokine transcription without transcription of characteristic ER stress response target genes [644]. To complicate matters further, in the context of an infection

additional considerations must be made due to the dynamic nature of virus interactions with different arms of the UPR, as discussed for DENV [425]. The complex and interconnected nature of the UPR makes the analysis of the impacts of iminosugars on the pathways challenging. However, this has been the subject of a concurrent doctoral project which has found further support for the modulation of UPR pathways by iminosugars including 2THO-DNJ, concurrent with downstream reductions in DENV-elicited TNF-α secretion [483].

Besides the effects of DNJ-derivatives, *N*N-DGJ selectively inhibited the TNF-α response made to MDMΦ stimulation with certain PAMPs. *N*-alkylated DNJ and DGJ iminosugars both inhibit GCS, the enzyme catalysing glucosylation of ceramide in the generation of glycosphingolipids [335, 336]. This activity underpins the clinical use of *N*B-DNJ as a substrate-reduction therapy for the lysosomal storage disorders Gaucher disease [338] and Niemann-Pick disease type C [339]. Since ceramide has been implicated in the macrophage inflammatory response [651] and macrophages bear the brunt of glucosylceramide storage in Gaucher disease, it is unsurprising that immune responses are affected, with increased TNF-α, IL-1β, IL-6 and IL-10 reported in patient serum [652]. In Niemann-Pick disease type C1 patients, transcription of some cytokine genes was altered in post-mortem frontal cortex and cerebellar tissues, and cerebrospinal fluid cytokine secretion was also impacted, with increased IL-3, C-X-C motif chemokine 5, IL-15 and MIP-1α and decreased IL-4, IL-10, IL-13 and IL-12p40 detected relative to patients undergoing lumbar puncture for different clinical indications. Interestingly, there were also indications that *N*B-DNJ treatment reduced IL-3, IL-10 and IL-13 levels [445]. Thus, iminosugars could impact cytokine responses through modulation of glycosphingolipids. Indeed, TLR signalling involves and affects cellular lipids, including ceramides and glucosylceramides. TLR4 and TLR9 signalling modulated transcription of genes involved in synthesis and processing of these lipids, including that encoding GCS, with different patterns seen for different TLRs in RAW264.7 macrophages. Changes in sphingolipid metabolism and addition of different ceramides also modulated TLR4

trafficking and pro-inflammatory cytokine production following LPS stimulation [653]. LPS stimulation increases cellular ceramide levels, which in turn inhibits TNF-α production [654, 655]. Poly(I:C) stimulation of keratinocytes increased ceramide levels and decreased glucosylceramides, although this occurred independently of TLR3 [656]. Perhaps RIG-I or MDA5 recognition of poly(I:C) is responsible, broadening the impact of perturbing levels of ceramides to other PRRs. However, while increasing alkyl chain length enhances the inhibitory capacity of monocyclic iminosugars for glycolipid processing enzymes, stereochemistry is unimportant as *N*N-DNJ and *N*N-DGJ inhibit glycolipid processing to equivalent levels in MDMΦs [337]. Therefore, iminosugar effects on glycolipid processing alone cannot explain the inhibition of TNF-α production in response to PRR stimulation, as the effects of *N*N-DNJ and *N*N-DGJ differ significantly. The ability of 2THO-DNJ to inhibit glycolipid processing has yet to be evaluated, although M*O*N-DNJ and *N*-(9'-methoxynonyl)-1-DGJ, which have oxygenated alkyl chains, effectively inhibit this in MDMΦs [394]. Thus, it is possible that a combination of glycolipid- and glucosidase-inhibitory effects, that vary depending on the stimulus, are involved in determining the outcome of iminosugar treatment for cytokine production. Comparing the effects of bicyclic iminosugars, which do not inhibit glycolipid processing in MDMΦs [337], with the monocyclic iminosugars utilised here, could also provide interesting mechanistic insights.

In addition to effects of iminosugars on PRR signalling pathways, their modulatory effects could be mediated by direct effects on cytokine production. In the case of TNF-α, the long alkyl chain iminosugars *N*N-DNJ and *N*N-DGJ reduced *TNFA* transcription in the context of DENV infection, which has been shown to induce *TNFA* expression [146, 657]. While early effects on transcription may have been missed here, no effect was seen with 2THO-DNJ treatment, indicating that the suppressive effect of iminosugars on TNF-α secretion is unlikely to be solely mediated by impacting transcription. The equivalence of TNF-α secretion quantified by techniques sensitive and insensitive to the functional activity of TNF-α following M*O*N-DNJ treatment indicates that

iminosugars likely interfere with TNF-α production at or prior to secretion, rather than allowing continued secretion of increasingly signalling-impaired cytokine molecules under increasing iminosugar pressure. This scenario might have been mediated by DNJ-derivatives inhibiting ER α-glucosidases, leading to misfolding of N-glycosylated proteins: however, human TNF-α is not N-glycosylated, lacking N-glycosylation sequons [464]. Thus, this is not a plausible explanation for effects observed in humans. In contrast, murine TNF-α is N-glycosylated at position 86 (UniProtKB: P06804), hence this direct mechanism could contribute to the reduction in serum TNF-α levels observed in iminosugar-treated DENV-infected mouse models (Table 4; [397, 399]).

TNF-α production is regulated post-translationally, with the full length transmembrane precursor TNF-α cleaved to release the mature soluble form, involving tumour necrosis factor converting enzyme (TACE) [658-660], proteinase-3 [661, 662], and matrix metalloproteinase 13 [663]. Inhibition or elimination of these enzymes reduces LPS-induced TNF-α secretion [660, 661, 664, 665]. TACE has multiple N-glycosylation sites and changes in N-glycosylation have been shown to affect its catalytic activity [666]. Recently, the ability of azidothymidine to inhibit N-glycosylation [667] has been linked to reduced TACE glycosylation, surface expression and function in THP-1 cells. Furthermore, *ex vivo* CD14+ monocytes from HIV-patients treated with azidothymidine-based versus tenofovir disoproxil fumarate-based regimens showed reduced TACE function in terms of monocyte activation (CD163 secretion) and TNF-α secretion [668]. It is therefore possible that DNJ-derivative iminosugars could inhibit TNF-α secretion through inhibiting the glycosylation and function of TACE, an interesting hypothesis for future investigation. Intriguingly, azidothymidine treatment can affect glycosphingolipid synthesis as well as impacting protein N-glycosylation [667], an effect which was not considered by Chen et al. [668]. Since this is a property shared by N-alkylated iminosugars, this represents another potential mechanism requiring future evaluation.

In contrast to TNF-α production, secretion of IFN-α/β from MDMΦs was less frequently observed in response to DENV infection or PAMP stimulation. The limited and donor-specific nature of IFN-α/β responses to DENV infection of MDMΦs has previously been described [15] and may be explained by NS2B3-mediated STING cleavage inhibiting the IFN-α/β response as reported in primary monocyte-derived DCs [134]. Nevertheless, DNJ- and DGJ-derivative iminosugars were able to inhibit IFN-α/β secretion under certain conditions. Limited mechanistic analysis was conducted, with iminosugars having no significant effect on *IFNA2* transcription in response to DENV infection, at the relatively late time points analysed. However, transcription of genes encoding other IFN-α subtypes or IFN-β, shown to be induced by DENV infection [155-157, 669-671], was not investigated. In addition, the potential for iminosugars to modulate post-transcriptional regulation of IFN-α/β, such as through miRNAs and adenylate uridylate-rich element-mediated decay affecting IFN-β mRNA stability [672], was not considered. These factors could be targets of future research.

Multiplex cytokine analysis also found that 2THO-DNJ, *N*N-DNJ and *N*N-DGJ treatment could affect the secretion of IFN-γ, IL-1β and MCP-1. However, there was a significant degree of inter-donor variability in responses: varied host genetic background and immunological memory may play significant roles in cytokine responses to PAMP stimulation. Thus, these cytokines should be considered as targets for future investigation. IFN-γ, a major macrophage activator, possesses two occupied N-glycosylation sites, mutation of which can inhibit secretion and activity [625, 626], indicating that inhibition of ER α-glucosidases by DNJ-derivatives could account for the reduced cytokine secretion, or detection in this antibody-based assay. IFN-γ secretion has previously been observed from MDMΦs prepared according to the same protocol and stimulated with LPS-ST or infected with DENV, with both responses reduced by M*O*N-DNJ treatment [418]. Furthermore, in murine T cells stimulated with anti-CD3, DNJ-derivative iminosugars reduced IFN-γ secretion by inhibiting the interaction of newly-synthesised cytokine

with calreticulin, thus enhancing its degradation [441, 442]. However, the production of IFN-γ by macrophages is controversial, and the possibility that a low frequency of contaminating lymphoid cells in the MDMΦ preparation could account for this cannot be ruled out without further profiling of the response at a single-cell level [673]. Interestingly, IFN-γ stimulation has been shown to increase the transcription or secretion of TNF-α [674, 675], including in the context of LPS-stimulation of human MDMΦs [676]. Thus, reduction of IFN-γ production by iminosugars could represent another mechanism through which TNF-α secretion is affected.

There were significant differences in the pictures painted by the responses of the TLR reporter cells and PAMP stimulation of MDMΦs. While DNJ-derivative iminosugars consistently reduced TNF-α secretion in response to stimulation of MDMΦs with PAMPs, they had little if any effect on TLR signalling pathways in the reporter cell system. This could indicate that the effect on TNF-α secretion is regulated after the activation of NF-κB, which determines reporter cell responses. In fact, the lack of a consistent reduction in *TNFA* gene transcription in DENV-infected iminosugar-treated MDMΦs supports this observation, indicating that a later stage might be affected by iminosugars instead. In the case of *N*N-DGJ treatment, in the reporter cell system, this consistently enhanced TLR signalling, while in PAMP-stimulated or DENV-infected MDMΦs, TNF-α secretion was either unaffected or dampened. This could either indicate an initial stimulation of TLR signalling that is then inhibited by *N*N-DGJ prior to TNF-α secretion, a discrepancy resulting from differences in the iminosugar treatment protocols (18 hours co-treatment in MDMΦs compared to a 3 day pre-treatment in the TLR reporter cells), or cell-type dependence in the response to iminosugar treatment. Discriminating between these possibilities would require further experimentation in MDMΦs, where the effects of different iminosugar treatment durations could be investigated and NF-κB nuclear translocation could be analysed downstream of TLR activation.

There are many angles from which iminosugars might interfere with PRR signalling and cytokine responses that have not been considered here. At the PRR level, TLR activation intensity and duration are tightly controlled to prevent pathogenic over-activation of pro-inflammatory responses, subject to multiple regulatory mechanisms that are TLR-dependent [630]. For example, TLR4 signalling is regulated by endosomal trafficking, lysosomal degradation and proteasomal degradation [677-679]. In addition, downstream signalling pathway components are subject to regulation by a host of mechanisms [630], which could be influenced by iminosugars. In the context of an infected patient, iminosugar treatment might also influence the response to cytokine signalling through influencing the expression of cytokine receptors: the type I IFN receptor and the TNF type 1 and type 2 receptors are N-glycosylated [424, 680, 681]. Indeed, *N*B-DNJ and M*O*N-DNJ upregulate total IFN-γ receptor and TNF-α receptor expression in uninfected and DENV-infected MDMΦs, but reduce downstream signalling (Joanna Miller, unpublished data), indicating complex modulation of cytokine detection by iminosugars.

In summary, the effects of iminosugars on cytokine responses appear to be complex and are likely mediated at multiple levels. Antiviral efficacy almost certainly contributes to reduced TNF-α secretion on iminosugar treatment of DENV-infected MDMΦs. However, this cannot account for all of the cytokine-modulatory effects of iminosugars since non-antiviral iminosugars can modulate cytokines and modulation is evident in the absence of a replicating viral stimulus. Evidence is presented that iminosugars reduce TNF-α secretion in response to MDMΦ stimulation with a wide range of PAMPs, and that they can affect TLR signalling in reporter cell lines. Some effects on pro-inflammatory cytokine transcription are observed; however, this cannot account for all of the observed iminosugar effects on TNF-α production. Perhaps TNF-α release might be affected by iminosugars, with effects on TACE a promising candidate for future investigation, or reduced secretion of the stimulatory N-glycosylated IFN-γ. The differential effects of *N*N-DNJ and *N*N-DGJ treatment on TNF-α secretion in response to MDMΦ stimulation

with different PAMPs is intriguing and provides opportunities for future mechanistic analysis. Ultimately, the ability of iminosugars to modulate cytokine production elicited by such a broad range of stimuli opens new doors for therapeutic investigation. Perhaps iminosugars might have clinical utility in settings beyond viral infection where the modulation of cytokine production were beneficial, such as certain non-viral infectious diseases, chronic low level inflammatory and autoimmune conditions. Better mechanistic understanding is required to determine the viability of this approach, which might ultimately enable the development of more specific immunomodulatory iminosugars and consequent tailoring to particular disease states.

Chapter 7. Final discussion

This thesis comprises an in-depth investigation into the mechanisms of iminosugar antiviral activity against DENV in MDMΦs, as well as exploring the potential for iminosugar treatment to be extended to new viruses, ZIKV and CCHFV, and inflammatory disease states. The findings open up many avenues for future research, as discussed in detail throughout the thesis.

In terms of mechanisms of action against DENV, the ability of the DNJ-derivative iminosugars 2THO-DNJ and *N*N-DNJ, but not *N*N-DGJ, to inhibit DENV replication was demonstrated for the first time in primary human immune cells, with supporting observations made in a DENV replicon system. This replicates findings made in DENV-infected BHK-21 cells [58] in a more physiological model and indicates that it is related to the glucostereochemistry of the DNJ-derivatives. The underlying mechanism remains to be established, including whether this is related to misfolding of the viral glycoprotein components of the replication complex, NS1 and/or NS4B. The potential for iminosugar antiviral activity in the C6/36 mosquito cell line was also considered. The lack of efficacy requires further investigation since insect cells possess homologues of the mammalian ER α-glucosidase iminosugar targets [430, 431], inhibition of which underlies the potent efficacy of DNJ-derivative iminosugars in MDMΦs [337, 394].

The antiviral efficacy of iminosugars was also explored in ZIKV infection. Very recently, a DNJ-derivative iminosugar IHVR19029 was demonstrated to be effective against ZIKV infection *in vitro* [226]. In this thesis and accompanying work in the laboratory, both *N*N-DNJ and *N*N-DGJ were found to possess antiviral efficacy against ZIKV infection of Vero cells. This, combined with the moderate antiviral effect of ER α-glucosidase knockout that was enhanced by co-treatment with these iminosugars, indicates that the iminosugar efficacy against ZIKV is not solely reliant on ER α-glucosidase inhibition. This is in stark contrast with DENV, where DNJ-derivative

iminosugars alone have antiviral efficacy [337, 394], and virus production has near complete dependence on functional ER α-glucosidases. The striking differences between these two viruses with respect to calnexin cycle utilisation is further supported by their differential dependence on UGGT [452]. Differences in glycosylation sites and the significance of viral glycoprotein glycosylation in DENV and ZIKV, as described in 1.1.1.2 and 1.1.2.2, might underlie this discrepancy, although this remains to be investigated. If ZIKV were to possess an ion channel, this could contribute to the efficacy of *N*N-DNJ and *N*N-DGJ, as seen for HCV p7 [356, 414, 415]. Considering these apparent differences between the two viruses, it would be interesting to evaluate their interaction with the N-glycosylation pathway and the antiviral and immunomodulatory effects of iminosugars in co-infected primary human immune cell cultures. Recent analysis of DENV/Chikungunya virus (CHIKV) co-infected PBMCs identified effects on viral replication dynamics and significantly increased TNF-α production compared to mono-infection [682], indicating that interesting observations might also be obtained with DENV/ZIKV co-infection. Such a co-infection model may be of therapeutic relevance in light of the recent shift in ZIKV distribution into DENV endemic areas and the demonstration that mosquitos can be co-infected and transmit these viruses simultaneously [683-685]. Multiple reports of DENV/ZIKV co-infection in patients [686-691] support this line of enquiry, and triple co-infections with CHIKV [692-695], a virus for which iminosugar efficacy has been demonstrated [357] but not pursued, adds further dimension to the clinical context.

HAZV infection of SW13 cells seemed not to be susceptible to iminosugar treatment, despite indications that the ER α-glucosidases were inhibited. This emphasises the importance of evaluating iminosugar efficacy against individual viruses, since N-glycosylation of viral proteins does not necessitate calnexin cycle dependence and thus susceptibility to the effects of DNJ-derivative iminosugars, as previously observed with some strains of INFV and VSV [314, 388]. The possibility of cell type-dependent iminosugar efficacy is also important to consider, as has

previously been described for INFV and DENV [314, 352, 394, 403], and future research exploring the antiviral efficacy of iminosugars should be mindful of these two factors.

Finally, the effects of 2THO-DNJ, *N*N-DNJ and *N*N-DGJ on cytokine responses was investigated in the context of MDMΦ stimulation with a broad panel of non-infectious PAMPs. This found that the effects of DNJ-derivative iminosugars on TNF-α secretion were broadly conserved across different stimuli, while the effects of *N*N-DGJ were more selective. The mechanisms underlying the suppressive effect of DNJ-derivatives on TNF-α secretion remain to be elucidated specifically, but this effect is likely to be explained by a combination of effects on PRR signalling pathways culminating in transcriptional changes as well as regulation at a post-transcriptional level. Differential dependence on the MyD88 and TRIF signalling adaptors was briefly considered as a determinant of the effects of *N*N-DGJ, a hypothesis requiring further attention. Taken together, these observations accentuate the fact that iminosugars can modulate immune responses independently of their antiviral effects, and provides support for extending the scope of iminosugar research into non-viral infections and inflammatory disease states.

The therapeutic purview of iminosugars is broad, already represented in the clinic as treatments for lysosomal storage disorders and non-insulin-dependent diabetes. Pre-clinical efficacy against a broad-spectrum of viruses is well-established, and furthered here with additional iminosugar stereochemistries shown to possess antiviral activity against ZIKV. Iminosugars can influence viruses in multiple ways, and this may be mediated by different mechanisms of action even against related viruses such as DENV and ZIKV. Furthermore, evidence provided here supports future research into the untapped potential of iminosugars for modulating inflammatory responses in contexts beyond viral infection.

Chapter 8. Appendices

8.1 Publications arising during this degree

Miller, JL, **Tyrrell, BE** and Zitzmann, N. *Mechanisms of antiviral activity of iminosugars against dengue virus*, in Dengue and Zika: Control and Antiviral Treatment Strategies, R. Hilgenfeld and S.G. Vasudevan, Editors. 2018, Springer Singapore: Singapore. p. 277-301.

Tyrrell, BE, Sayce, AC, Warfield, KL, Miller, JL and Zitzmann, N. *Iminosugars: Promising therapeutics for influenza infection*. Critical Reviews in Microbiology, 2017. 43(5): p. 521-545.

Sayce, AC, Alonzi, DS, Killingbeck, SS, **Tyrrell, BE**, Hill, ML, Caputo, AT, Iwaki, R, Kinami, K, Ide, D, Kiappes, JL, Beatty, PR, Kato, A, Harris, E, Dwek, RA, Miller, JL and Zitzmann, N. *Iminosugars inhibit dengue virus production via inhibition of ER alpha-glucosidases—not glycolipid processing enzymes*, PLoS Neglected Tropical Diseases, 2016. 10(3):e0004524.

Warfield, KL, Plummer, EM, Sayce, AC, Alonzi, DS, Tang, W, **Tyrrell, BE**, Hill, ML, Caputo, AT, Killingbeck, SS, Beatty, PR, Harris, E, Iwaki, R, Kinami, K, Ide, D, Kiappes, JL, Kato, A, Buck, MD, King, K, Eddy, W, Khaliq, M, Sampath, A, Treston, AM, Dwek, RA, Enterlein, SG, Miller, JL, Zitzmann, N, Ramstedt, U and Shresta, S. *Inhibition of endoplasmic reticulum glucosidases is required for in vitro and in vivo dengue antiviral activity by the iminosugar UV-4*, Antiviral Research, 2016. 129:93-98.

Manuscripts in preparation:

Sayce, AC, Martinez, FO, **Tyrrell, BE**, Perera, N, Hill, ML, Dwek, RA, Miller, JL and Zitzmann, N. *Glycotherapy of human macrophages with the iminosugar MON-DNJ induces the unfolded*

protein response and attenuates dengue virus and TLR ligand inflammatory signatures. (submitted)

Tyrrell, BE*, **Hill, JC***, Hill, ML, Alonzi, DS, Roversi, P and Zitzmann, N. *Dengue and Zika viruses have different dependencies on endoplasmic reticulum α-glucosidases and the quality control mediators UGGT1 and UGGT2.* *Contributed equally

8.2 Cytotoxicity assays

8.2.1 Cytotoxicity of 2THO-DNJ for primary MDMΦs

The cytotoxicity of two stocks of 2THO-DNJ in primary MDMΦs, with low pH (Figure 83) and with neutral pH (Figure 84), was evaluated by MTS assay. Both showed dose-dependent cytotoxicity, with the acidic stock more cytotoxic as expected. However, even with the low pH formulation that was used in initial investigations, the average concentration at which there was a 10% reduction in cell viability (CC_{10}) was in excess of 100 µM and the average stringent selectivity index 2 (SI2 = CC_{10}/IC_{90}) was 10.1 (Table 18). While matched donors were not evaluated for cytotoxicity and antiviral efficacy of the neutral pH stock, the average selectivity index (SI2) in this case was 21.5, indicating an improved toxicity-efficacy window (Table 18).

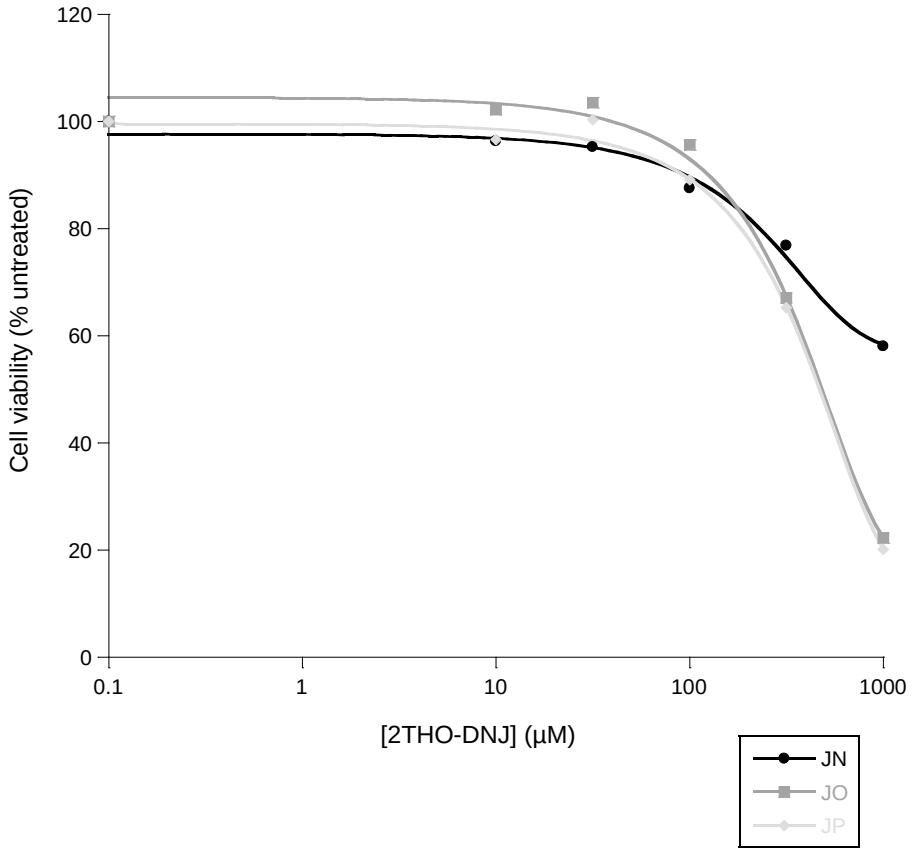

Figure 83. Cytotoxicity of low pH 2THO-DNJ stock in MDMΦs.

Primary MDMΦs (donors as shown, assayed in technical triplicate) were treated with drug as indicated for 48 hours prior to cell viability assessment by MTS assay. Data were normalised to untreated and the mean displayed.

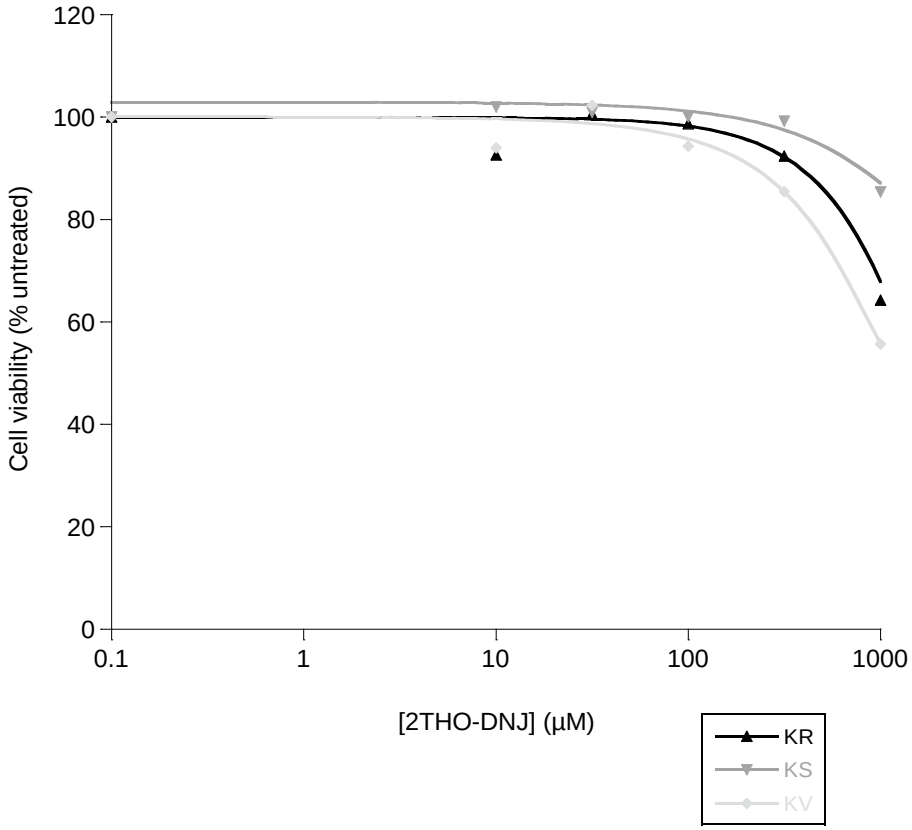

Figure 84. Cytotoxicity of neutral pH 2THO-DNJ stock in MDMΦs.

Primary MDMΦs (donors as shown, assayed in technical triplicate) were treated with drug as indicated for 48 hours prior to cell viability assessment by MTS assay. Data were normalised to untreated and the mean displayed.

Table 18. Cytotoxicity summary for 2THO-DNJ in primary MDMΦs.

[a]Selectivity index (SI) 1 = CC_{50}/IC_{50}. [b]SI2 = CC_{10}/IC_{90}. IC values are taken from Table 19.

Donor	Curve fit used	R^2	CC_{10} (µM)	CC_{50} (µM)	SI1[a]	SI2[b]
JN	Lgstsigmoid	0.99272	95.6	> 1000	> 1034	18.9
JO	Lgstsigmoid	0.99865	125	483	66.8	4.45
JP	Lgstsigmoid	0.99774	93.0	470	116	7.05
KR	Dosersplgst	0.97682	384	>1000		
KS	Lgstsigmoid	0.93658	790	>1000		
KV	Lgstsigmoid	0.99033	222	>1000		

8.2.2 Cytotoxicity of 2THO-DGJ for MDMΦs

The cytotoxicity of 2THO-DGJ in MDMΦs was evaluated by MTS assay (Figure 85). In two of the three donors tested, cell viability was seen to increase above that of the solvent control treatment at higher concentrations. Past laboratory experience indicates that this may be indicative of the iminosugar concentration approaching cytotoxicity as there may be a transient increase in metabolic activity observed in a stressed cell.

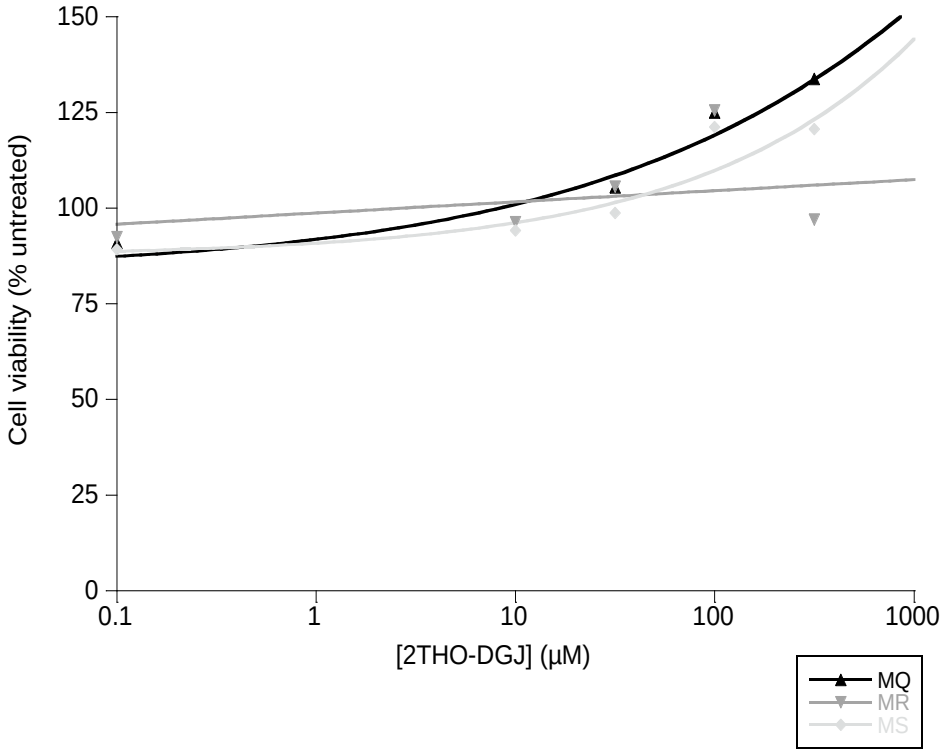

Figure 85. Cytotoxicity of 2THO-DGJ in MDMΦs.

Primary MDMΦs (donors as shown, assayed in technical triplicate) were treated with drug as indicated for 48 hours prior to cell viability assessment by MTS assay. Data were normalised to the solvent control (untreated) and the mean displayed.

8.2.3 Cytotoxicity of iminosugars for MDMΦs at 72 hours

Due to iminosugar treatments being extended in this study beyond the standard 48 hours used for antiviral assays, cell viability after 72 hours of iminosugar treatment was evaluated in MDMΦs (Figure 86). After 72 hours, the cytotoxicity profile of the iminosugars tested remained

similar to that observed after 48 hours of treatment (8.2.1; [398]; Andrew Sayce, unpublished data).

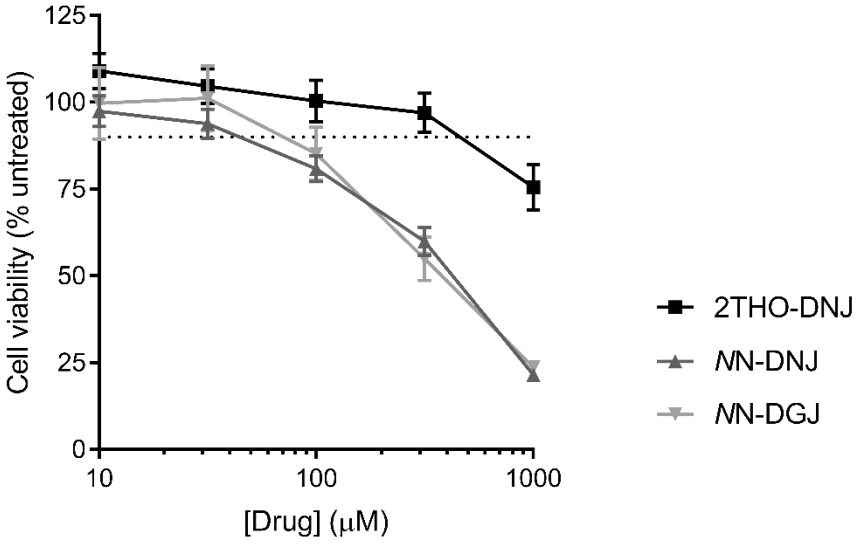

Figure 86. Cytotoxicity of iminosugars for MDMΦs after prolonged treatment.

Primary MDMΦs (n=3 donors (NY, OB, OC), assayed in technical triplicate) were treated with drug as indicated for 72 hours prior to cell viability assessment by MTS assay. Data were normalised to untreated and represented as mean ± standard error. The dotted line indicates a reduction in cell viability of 10%.

8.2.4 Cytotoxicity of baicalein in MDMΦs

Baicalein was used in experiments investigating drug effects on adsorption or entry of DENV to MDMΦs and the cell viability impact of the drug was tested accordingly. 25 μM baicalein, the concentration ultimately selected, did not impact cell viability (Figure 87).

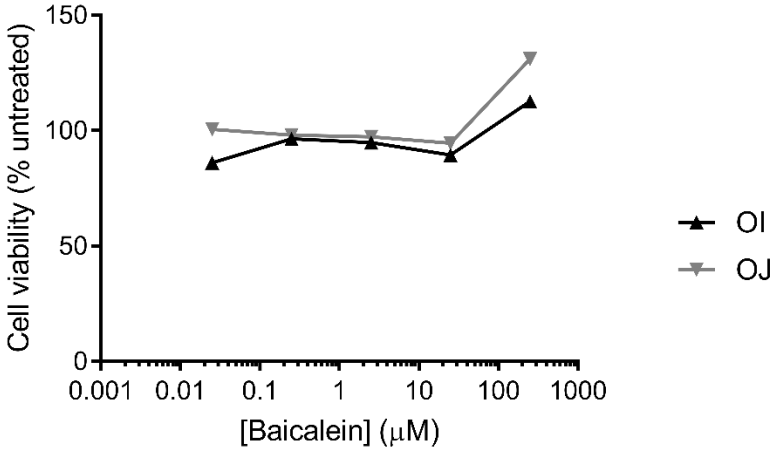

Figure 87. Cytotoxicity of baicalein in MDMΦs.

Primary MDMΦs (donors as shown, assayed in technical triplicate) were treated with drug as indicated for 1 hour before replacement with media-only and incubation for a further 47 hours prior to cell viability assessment by MTS assay. Data were normalised to untreated and the mean displayed.

8.2.5 Cytotoxicity of ribavirin in MDMΦs

The cytotoxicity of ribavirin was evaluated in MDMΦs. No significant cytotoxicity was observed at 1000 μM, the maximum concentration tested (Figure 88).

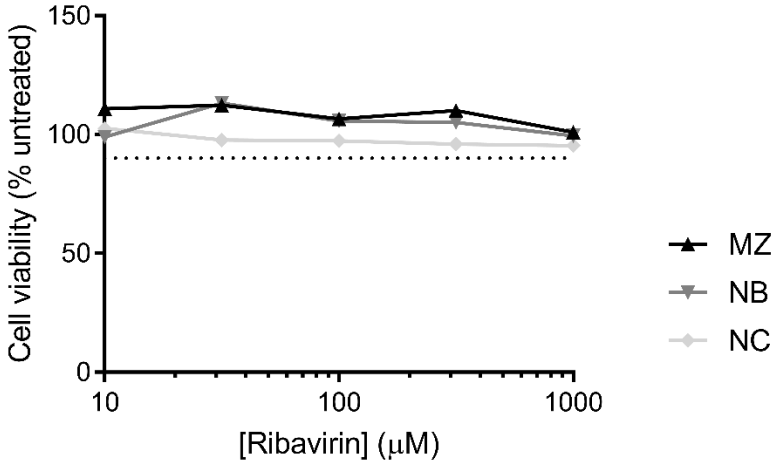

Figure 88. Cytotoxicity of ribavirin in MDMΦs.

Primary MDMΦs (donors as shown, assayed in technical triplicate) were treated with drug as indicated for 48 hours prior to cell viability assessment by MTS assay. Data were normalised to untreated and the mean displayed. The dotted line indicates a reduction in cell viability of 10%.

8.2.6 Cytotoxicity of iminosugars and ribavirin in WT and glucosidase knockout Vero cells

In order to use drug treatments in combination with glucosidase knockout, the cytotoxicity of iminosugars and ribavirin was evaluated in Vero-WT, Vero-GluI and Vero-GluII cells in parallel (Figure 89). No cytotoxicity was observed with *N*B-DNJ, *N*B-DGJ or 2THO-DNJ treatment up to 316 µM. Significant reductions in cell viability were seen with *N*N-DNJ or *N*N-DGJ treatment, with 100 µM treatment generally exceeding the CC_{10}. The cytotoxicity of iminosugars was very similar between the different cell types, excluding 1000 µM 2THO-DNJ treatment where the Vero-WT cells appeared to be more susceptible to drug toxicity than the knockouts. There was a slight observed improvement in ribavirin tolerability in the Vero-GluI cells compared to the Vero-WT cells, in which 100 µM ribavirin exceeded the CC_{10}, demonstrating increased susceptibility to ribavirin toxicity than that in some previous reports [696, 697].

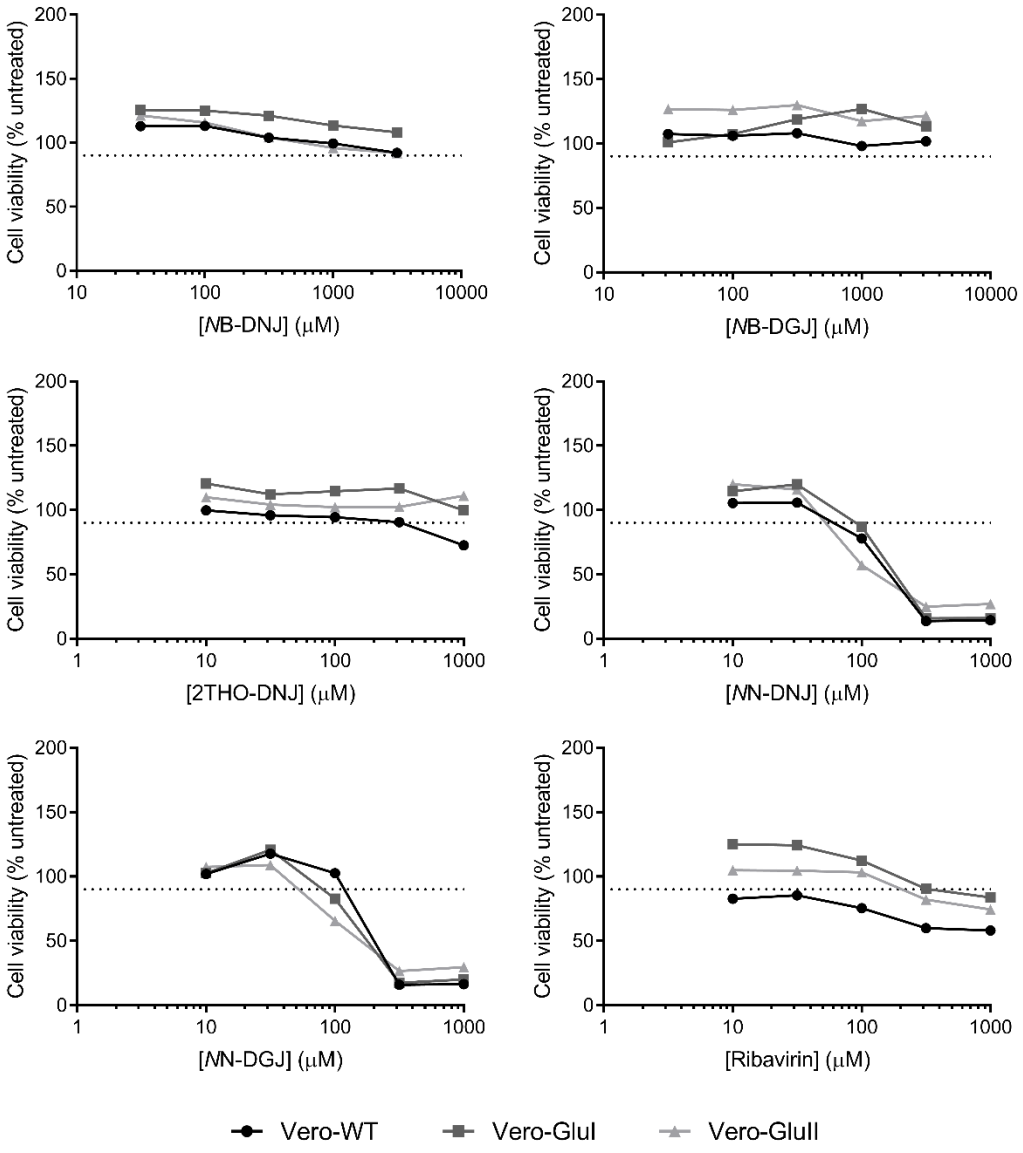

Figure 89. Cytotoxicity of iminosugars and ribavirin for Vero-WT, Vero-GluI and Vero-GluII cells.

Vero cells (n=1, assayed in technical triplicate) were cultured with drug as indicated for 4 days prior to cell viability assessment by MTS assay. Data were normalised to untreated, for each cell type, and the mean displayed. The dotted line indicates a reduction in cell viability of 10%. Data were collected by Johan C Hill and analysed myself.

8.2.7 Cytotoxicity of drugs in C6/36 cells

Cytotoxicity of iminosugar or selected non-iminosugar drug treatment for 48 hours was determined in C6/36 mosquito cells (Figure 90). Iminosugar cytotoxicity was broadly similar to that seen in MDMΦs (8.2; [398]; Andrew Sayce, unpublished data). C6/36 cells were more

susceptible to ribavirin-mediated cytotoxicity than MDMΦs (8.2.5); reports of previous ribavirin efficacy or cytotoxicity testing in C6/36 cells were not identified in the literature. The cytotoxicity of ι-carrageenan was similar to that previously reported [502]: consequently, 2 μg/ml was used in this study rather than the 10 μg/ml used previously, since this reduced cell viability by slightly more than 10%.

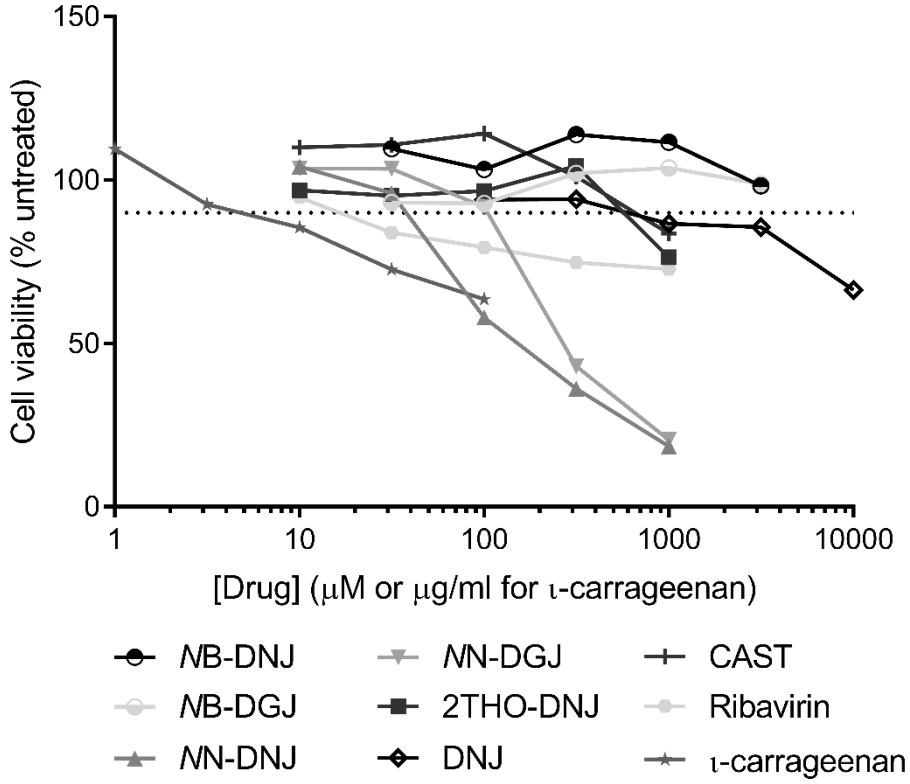

Figure 90. Cytotoxicity of iminosugars, ribavirin and ι-carrageenan in C6/36 mosquito cells.

C6/36 cells (n=1, assayed in technical triplicate) were treated with drug as indicated for 48 hours prior to cell viability assessment by MTS assay. Data were normalised to untreated and the mean displayed. The dotted line indicates a reduction in cell viability of 10%.

8.2.8 Cytotoxicity of iminosugars and ribavirin in SW13 cells

The effect of iminosugar or ribavirin treatment on the viability of SW13 cells was determined for the time points used for antiviral assay (data for 3 days of treatment is shown in Figure 91).

Accordingly, maximum concentrations used in antiviral assays against HAZV were selected to be 316 µM for *N*B-DNJ and *N*B-DGJ and 100 µM for *N*N-DNJ, *N*N-DGJ, 2THO-DNJ and ribavirin.

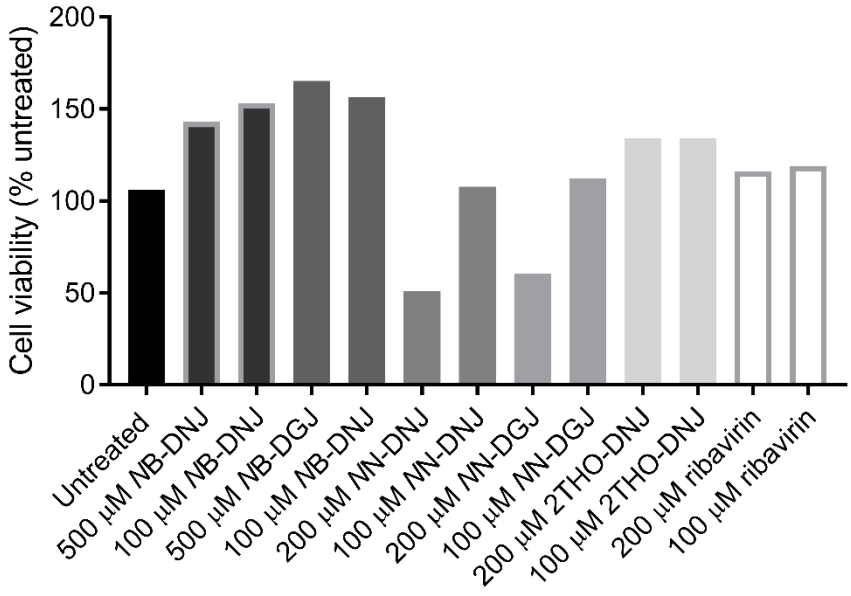

Figure 91. Cytotoxicity of iminosugars and ribavirin in SW13 cells.

SW13 cells (n=1, assayed in technical quadruplicate) were treated with drug as indicated for 3 days prior to cell viability assessment by MTS assay. Data were normalised to untreated and the mean displayed.

8.2.9 Cytotoxicity of iminosugars in TLR reporter cells

In order to determine the effects of iminosugars on TLR signalling, TLR reporter cells were pre-treated with iminosugars for 3 days prior to stimulation. 2THO-DNJ, *N*N-DNJ and *N*N-DGJ had similar effects on cell viability, although HEK-Null cells appeared less sensitive to iminosugar treatment while HEK-TLR2 and HEK-TLR4 reporter cells were more so (Figure 92).

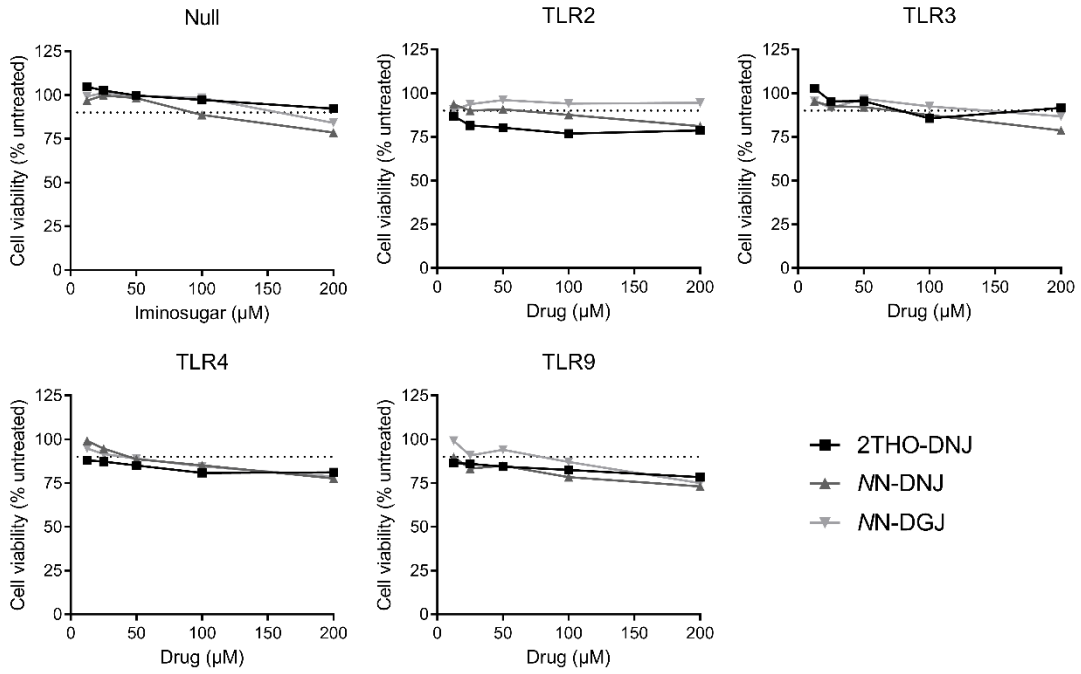

Figure 92. Cytotoxicity of iminosugars in HEK-TLR reporter cells.

TLR reporter cells (n=1, assayed in technical triplicate) were treated with drug as indicated for 3 days prior to cell viability assessment by MTS assay. Data were normalised to untreated and the mean displayed. The dotted line indicates a reduction in cell viability of 10%.

8.3 Testing antivirals for interference in plaque assay detection of DENV

Since 2THO-DNJ had not previously been utilised in the laboratory, it was confirmed that the presence of 2THO-DNJ in cell supernatant samples could not interfere with the detection of DENV virions by plaque assay. The lack of interference of other iminosugars used has previously been demonstrated, and thus it was deemed unlikely for different results to be found with this compound. 2THO-DNJ at a concentration reflecting the maximum concentration present in samples, 100 μM, was added to DENV stock samples and subjected to plaque assay. Since it is generally recognised that a two-fold change in detected titres indicates of a true difference in titre, considering the sensitivity of the plaque assay technique, the presence of 2THO-DNJ did not affect the titre detected (Figure 93), supporting the validity of this technique for assaying these samples.

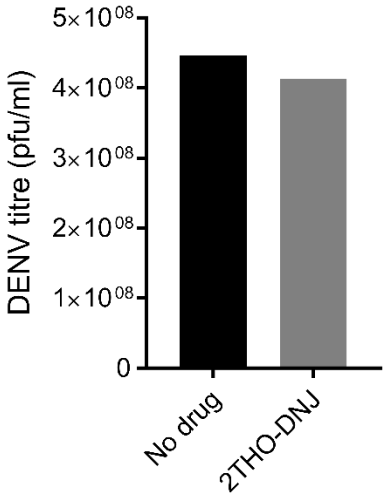

Figure 93. 2THO-DNJ does not interfere with plaque assay detection of DENV.

DENV stock was diluted in MEM to a detectable titre for plaque assay and was added to LLC-MK_2 cells (n=1, assayed in technical triplicate) with media-only or with 2THO-DNJ at a concentration to reflect 100 µM in a cell supernatant being added to a plaque assay. The usual plaque assay protocol was then followed and mean titres displayed.

Ribavirin has also not previously been used in the laboratory as a DENV antiviral. In addition, ribavirin has previously been reported to have antiviral efficacy against DENV in infection of LLC-MK_2 cells [490, 493], although these studies used culture periods of 3-5 days in the presence of ribavirin: significantly different from the 90 minute infection period for a plaque assay. Ribavirin at a range of concentrations up to 1000 µM, reflecting the maximum concentration that might be present in samples, was added to DENV stock samples and subjected to plaque assay. Ribavirin did not impact the titre detected (Figure 94), again supporting the validity of this technique for assaying these samples.

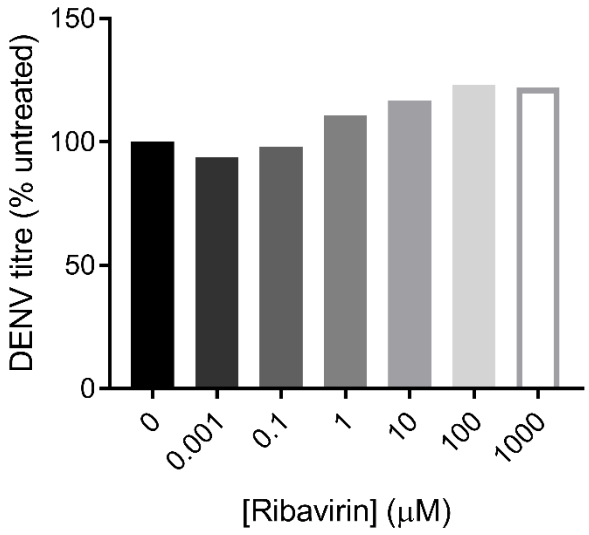

Figure 94. Ribavirin does not interfere with plaque assay detection of DENV.

DENV stock was diluted in MEM to a detectable titre for plaque assay and was added to LLC-MK$_2$ cells (n=1, assayed in technical triplicate) with media-only or with ribavirin, with the concentrations indicated reflecting the concentration in a cell supernatant being added to a plaque assay. The usual plaque assay protocol was then followed and mean titres displayed.

8.4 Supplementary information for 2THO-DNJ anti-DENV efficacy

8.4.1 Raw DENV titres for 2THO-DNJ titrations

In 3.3.1.1, the antiviral efficacy of 2THO-DNJ in MDMΦs is presented with DENV titres normalised to untreated. The raw values for DENV titre are shown in Figure 95.

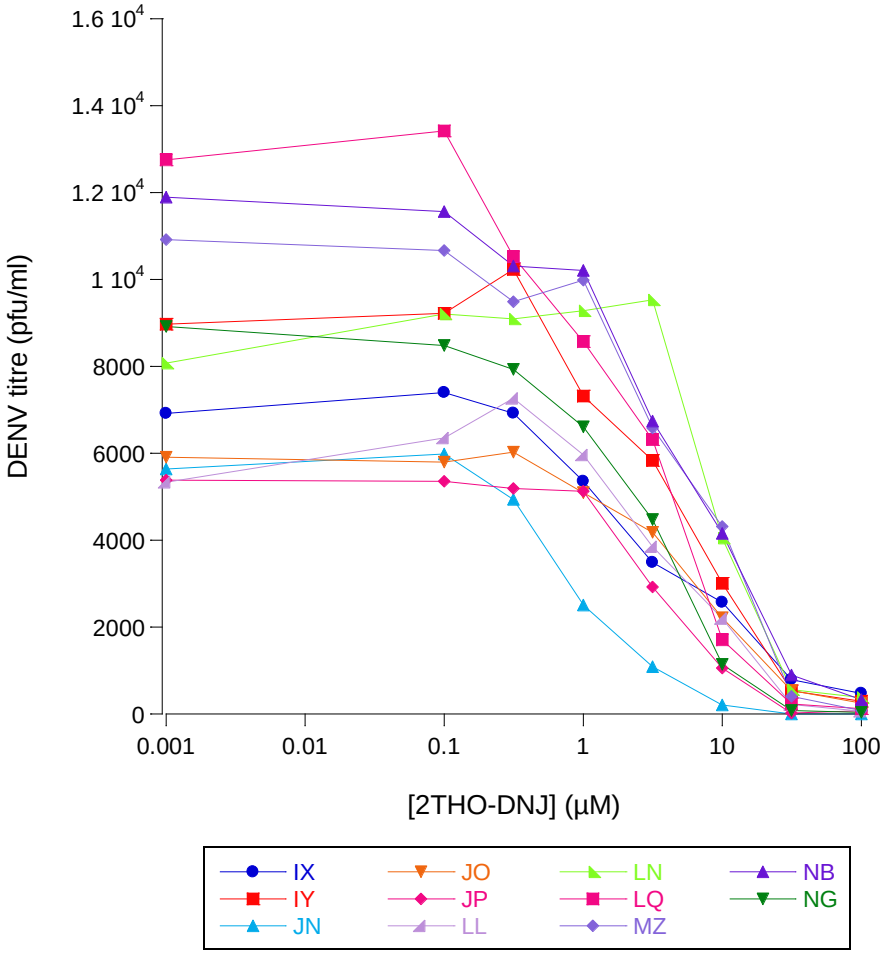

Figure 95. DENV titres vary between donors.

Primary MDMΦs (n=11 donors, as shown, assayed in technical triplicate) were DENV-infected and treated with a titration of 2THO-DNJ. Supernatant was collected at 48 hours post-infection and viral titres determined by plaque assay. Mean titres were plotted, with untreated represented as 0.001 µM to allow plotting on a logarithmic scale.

8.4.2 Curve fitting for quantification of antiviral efficacy of 2THO-DNJ in MDMΦs

As detailed in 2.2.6, KaleidaGraph was used for precise curve fitting for DENV titres in response to treatment with titrations of 2THO-DNJ, allowing interpolation of IC_{50} and IC_{90} values for 2THO-DNJ treatment (Table 19). The same methods were applied to total DENV secretion (Table 20).

Table 19. 2THO-DNJ antiviral effect on infectious DENV secretion from primary MDMΦs. Abbreviations: ND, not determined.

Donor	Curve fit used	R^2	IC_{50} (µM)	IC_{90} (µM)
Overall	Moddoseresplgst	0.99944	ND	ND
IX	Moddoseresplgst	0.98244	3.89	48.2
IY	Lgstsigmoid	0.99339	6.11	22.9
JN	Moddoseresplgst	0.99348	0.967	5.06
JO	Lgstsigmoid	0.99785	7.23	28.1
JP	Lgstsigmoid	0.98516	4.04	13.2
LL	Lgstsigmoid	0.98259	7.52	22.5
LN	Dosersplgst	0.99584	10.1	23.2
LQ	Lgstsigmoid	0.98887	3.09	11.5
MZ	Lgstsigmoid	0.99321	6.90	22.1
NB	Moddoseresplgst	0.9949	4.33	29.6
NG	Lgstsigmoid	0.99827	3.17	11.2

Table 20. 2THO-DNJ antiviral effect on total DENV secretion from primary MDMΦs.

Donor	Curve fit used	R^2	50% reduction in virus secretion (µM)	90% reduction in virus secretion µM)
IX	Moddoseresplgst	0.9931	0.680	9.15
IY	Moddoseresplgst	0.98832	1.11	6.74
JN	Moddoseresplgst	0.95589	4.04	> 100
JO	Moddoseresplgst	0.9751	3.21	> 100
JP	Lgstsigmoid	0.94684	2.41	> 100

8.4.3 Antiviral efficacy of iminosugars in PBMCs

As a preliminary experiment, the antiviral efficacy of a panel of iminosugars was evaluated in PBMCs from a single donor (Figure 96). The efficacy of DNJ-derivative iminosugars and lack of efficacy of DGJ-derivative iminosugars was observed, as expected from infection of isolated MDMΦs. DMSO had no effect on viral titre. Resulting viral titres were within the range seen with infection of MDMΦs (Figure 95), although the number of cells and MOI used differed (MDMΦs:

1 million cells/well infected at MOI 1 compared to PBMCs: 5 million cells/well infected at MOI 0.2).

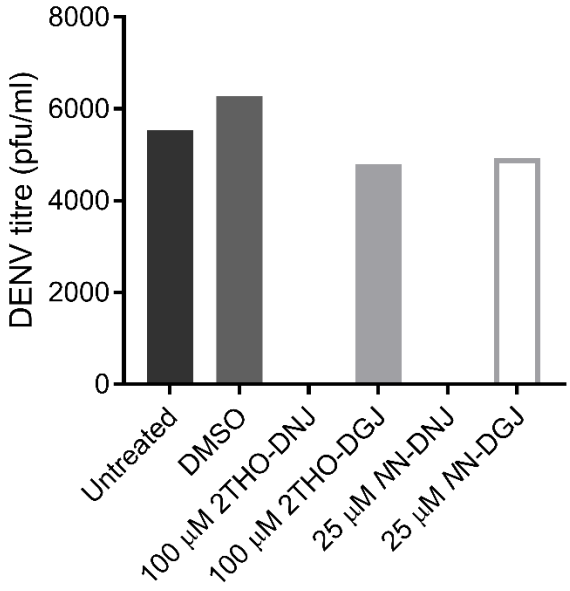

Figure 96. Iminosugar antiviral efficacy in PBMCs is in concordance with MDMΦ data.

Primary PBMCs (donor MM, assayed in technical triplicate) were infected with DENV in the presence of iminosugar as indicated. Supernatant was collected 48 hours post-infection and viral titres determined by plaque assay. Mean titres were plotted.

8.5 Optimisation of iminosugar effects on DENV replication protocols

In order to investigate whether iminosugars affect DENV replication, the general protocol previously published in [58] had to be adapted for primary MDMΦ infection. Final results are presented in 3.3.1.8.1, with discussion of prior experiments and optimisation below.

Initially, this experiment was conducted using the laboratory's established DENV infection protocol, where MDMΦs are infected with DENV for 90 minutes at room temperature, before virus is removed (without extensive washing) and iminosugar treatment commences (2.2.5.1). At 24 and 48 hours post-infection, by which point multiple rounds of infection may have taken place, treatment with DNJ-derivative iminosugars consistently tended to reduce both positive-

and negative-sense DENV RNA (Figure 97), as would be expected for an iminosugar known to reduce the secretion of infectious virus, and thus the potential for subsequent rounds of infection. However, there was problematically high variability between biological replicates, particularly for *N*N-DGJ treatment conditions. One possibility was that this was related to asynchronous virion entry during the relatively prolonged infection period, which could correspond to a large disparity in the progress of virion replication in different cells. Perhaps the ability of *N*N-DGJ treatment to enhance DENV entry to MDMΦs described in 3.3.1.7 might contribute to the particularly high variability seen with this treatment.

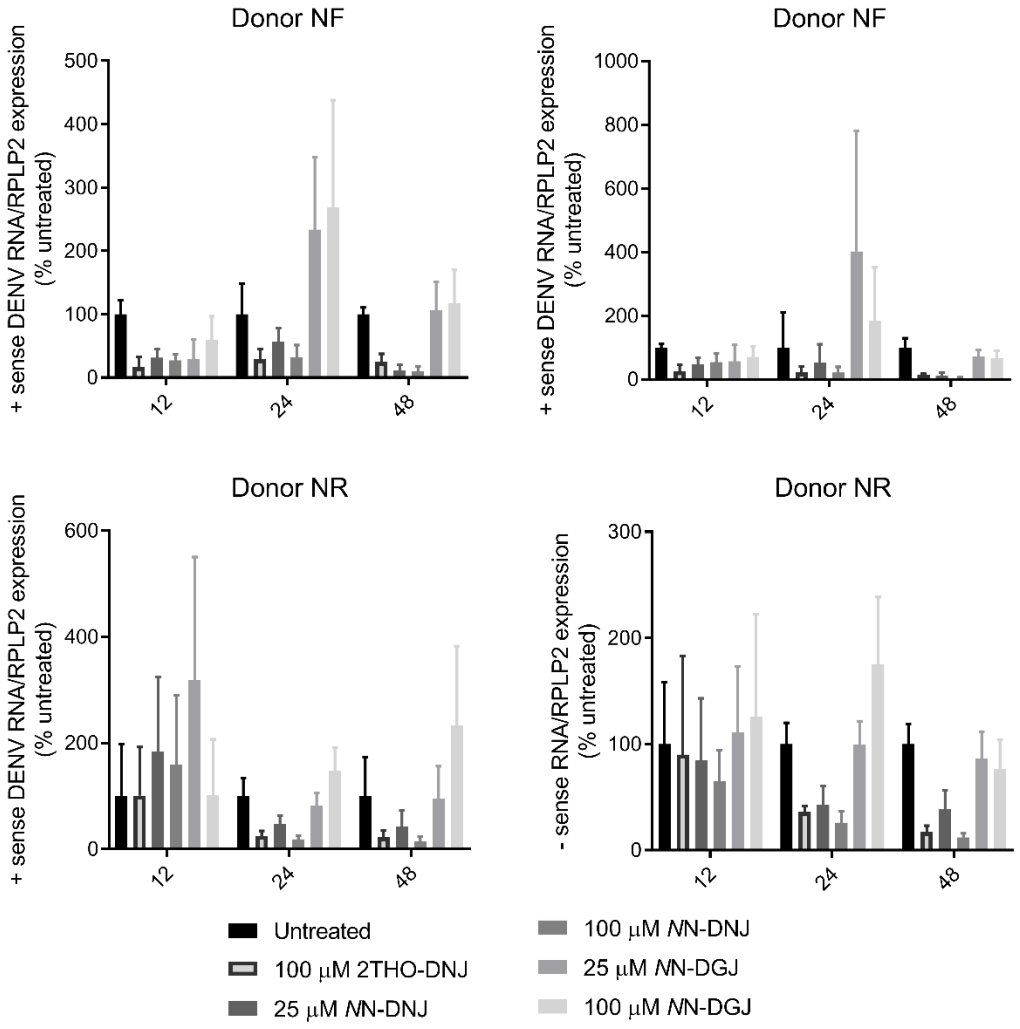

Figure 97. DNJ-derivative iminosugars tend to reduce intracellular DENV RNA, but high variability obfuscates the data.

Primary MDMΦs (donors as indicated, assayed in technical triplicate) were infected with DENV. At the indicated time points, cellular RNA was extracted. Positive- and negative-sense DENV RNA was reverse transcribed, quantified and normalised to RPLP2 *expression levels. For each time point, data were normalised to untreated and the mean displayed. In this case alone, error bars display the standard deviation of the technical replicates, in order to illustrate the extent of technical variability observed.*

In an attempt to ameliorate this high variability, different methods for synchronising virion entry were trialled using MDMΦs from a single donor at a single time point. A 1 hour adsorption step at 4°C was added for all treatments, followed by extensive washing in HBSS to remove any unadsorbed virus. Internalisation then occurred during an hour-long incubation at 37°C before drug treatment commenced, thereby avoiding the possibility that iminosugar effects on virus adsorption or cellular entry could influence the results. In addition, post-internalisation, a pH 3 citrate buffer treatment was utilised to degrade surface-exposed virions [459] or 20 mM ammonium chloride was added concurrently with drug treatment to prevent further virion endocytosis [20].

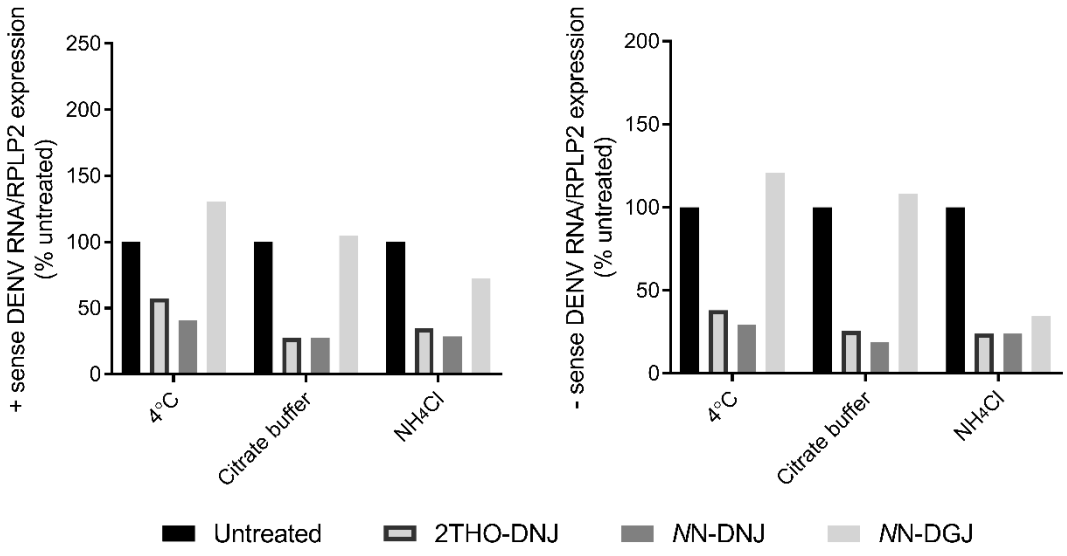

Figure 98. Citrate buffer and ammonium chloride treatment do not influence iminosugar effects on DENV replication.

Primary MDMΦs (donor NZ, assayed in technical triplicate) were infected with DENV by an hour adsorption step at 4°C, followed by extensive washing in HBSS, and internalisation during an hour-long incubation at 37°C. Cells were then treated with 100 µM of indicated iminosugars (4°C bars). In addition, some cells were treated with a pH 3 citrate buffer for 1 minute to degrade

exposed virions (citrate buffer bars) or iminosugar-containing media was supplemented with 20 mM ammonium chloride (NH_4Cl bars) to prevent further virion endocytosis. Cells were incubated until 24 hours post-infection, when cellular RNA was extracted. Positive- and negative-sense DENV RNA was reverse transcribed, quantified and normalised to RPLP2 *expression levels. For each synchronisation condition, data were normalised to untreated and the mean displayed.*

The protocol modification to include adsorption and entry steps appeared to reduce variability (technical variability not shown), while the additional treatments did not seem to consistently change the effects of iminosugars (Figure 98). This, combined with the moderate cytotoxicity of the treatments (Figure 99A), meant that the experiment was repeated using the adsorption/entry steps modification alone. Despite not affecting the response pattern to iminosugars, the citrate buffer seemed to increase the abundance of DENV RNA recovered from treated MDMΦs, whereas ammonium chloride treatment had no effect (Figure 99B-D). This might suggest that while the citrate buffer treatment was reported to inactivate surface-bound but non-internalised DENV on Vero cells [459], it is ineffective at this in MDMΦs. The low pH, although present for only a short exposure, might in fact promote DENV entry or facilitate exposure of the fusion loop and endosomal fusion of virions, leading to greater DENV RNA recovery downstream.

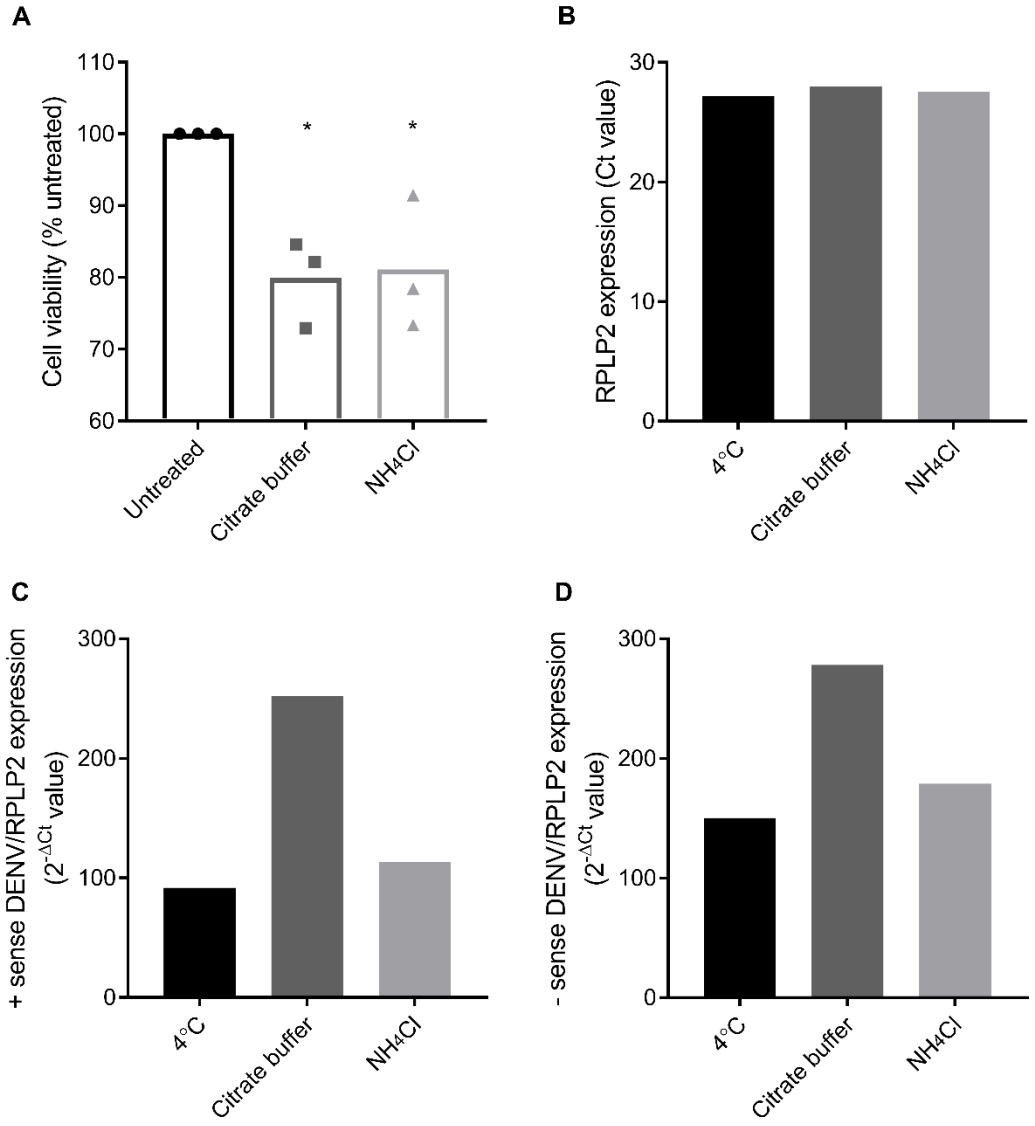

Figure 99. Citrate buffer treatment enhances DENV RNA yield obtained from MDMΦs.

(A) Cytotoxicity of pH 3 citrate buffer (citrate buffer) and 20 mM ammonium chloride (NH_4Cl) treatment on MDMΦs (n=3 donors (NY, OE, OF), assayed in technical triplicate) was determined by MTS assay. Cell viability was normalised to untreated and the mean plotted (bars show the mean of the donors). Statistical analysis was by one-way ANOVA with Dunnett's multiple comparisons test (, p<0.05).*

(B-D) Primary MDMΦs (donor NZ, assayed in technical triplicate) were treated as described for Figure 98. RPLP2 *expression (B) or the relative expression of positive-sense (C) or negative-sense (D) to* RPLP2 *expression was determined in samples that were not iminosugar-treated, and the mean displayed.*

8.6 Assessment of iminosugar effects on DENV replication

Iminosugars and DENV infection have previously been demonstrated to affect the expression level of certain housekeeping genes. Expression of GAPDH in murine tissues was modulated by DENV infection and M*O*N-DNJ or BuCAST treatment [418] and thus was not a suitable housekeeping gene. Transcriptomics data derived from DENV-infected or LPS-stimulated MDMΦs with or without M*O*N-DNJ treatment (generated and analysed by Andrew Sayce, Zitzmann group) suggested that the expression levels of the ribosomal housekeeping gene *RPLP2* remained the most stable across these conditions, which was subsequently validated by qRT-PCR. *RPLP2* was used as a housekeeping gene in this study: the expression level was consistent with 2THO-DNJ, *N*N-DNJ or *N*N-DGJ treatment in DENV-infected MDMΦs (Figure 100 shows this for a representative donor).

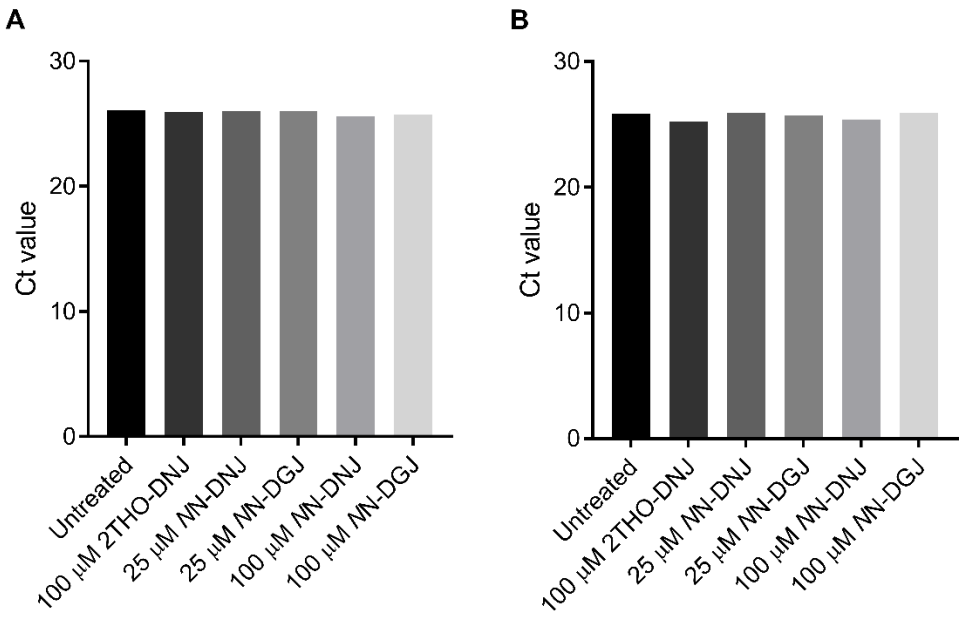

Figure 100. RPLP*2 expression levels remain consistent across iminosugar treatments.*

RNA was extracted from DENV-infected, iminosugar-treated MDMΦs (data for one donor (NF) are shown, conditions assayed in technical triplicate; qRT-PCR in technical duplicate). qRT-PCR for RPLP2, multiplexed with TNFA *(A) or* IFNA2 *(B), was conducted and mean* RPLP2 *Ct values displayed.*

Efficiency calculations were performed for the qRT-PCR of positive- or negative-sense RNA, as this had not previously been used in the laboratory. The efficiency was in the optimal 90-100% range (Figure 101). Multiplex qRT-PCRs for a range of cytokine genes combined with *RPLP2* have previously been conducted in the laboratory; efficiency was also within the acceptable range.

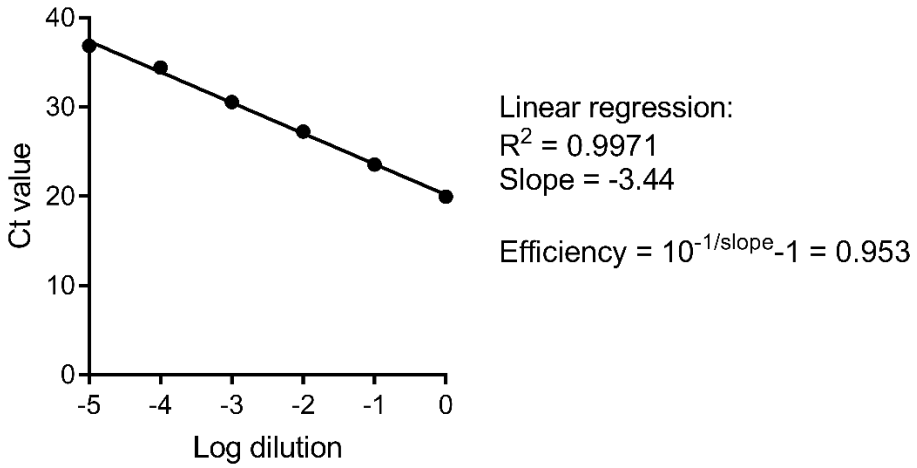

Figure 101. Sample DENV positive-sense qRT-PCR efficiency calculation.

RNA was extracted and reverse transcription conducted for positive-sense DENV RNA in a DENV-infected MDMΦ sample (n=1, donor NF). 10-fold dilutions of cDNA were prepared and positive-sense DENV RNA quantified by qRT-PCR. Mean Ct values were plotted and linear regression was performed. The efficiency of the qRT-PCR was calculated according to the formula shown.

While positive- and negative-sense DENV RNA quantification is normalised within time points in Figure 20 to facilitate comparison of iminosugar treatments, Figure 102 confirms that DENV replication is occurring in the infected cells as detectable RNA levels increase over time. Ratios of positive- and negative- sense RNA also remain consistent across time points and drug treatments (Figure 103).

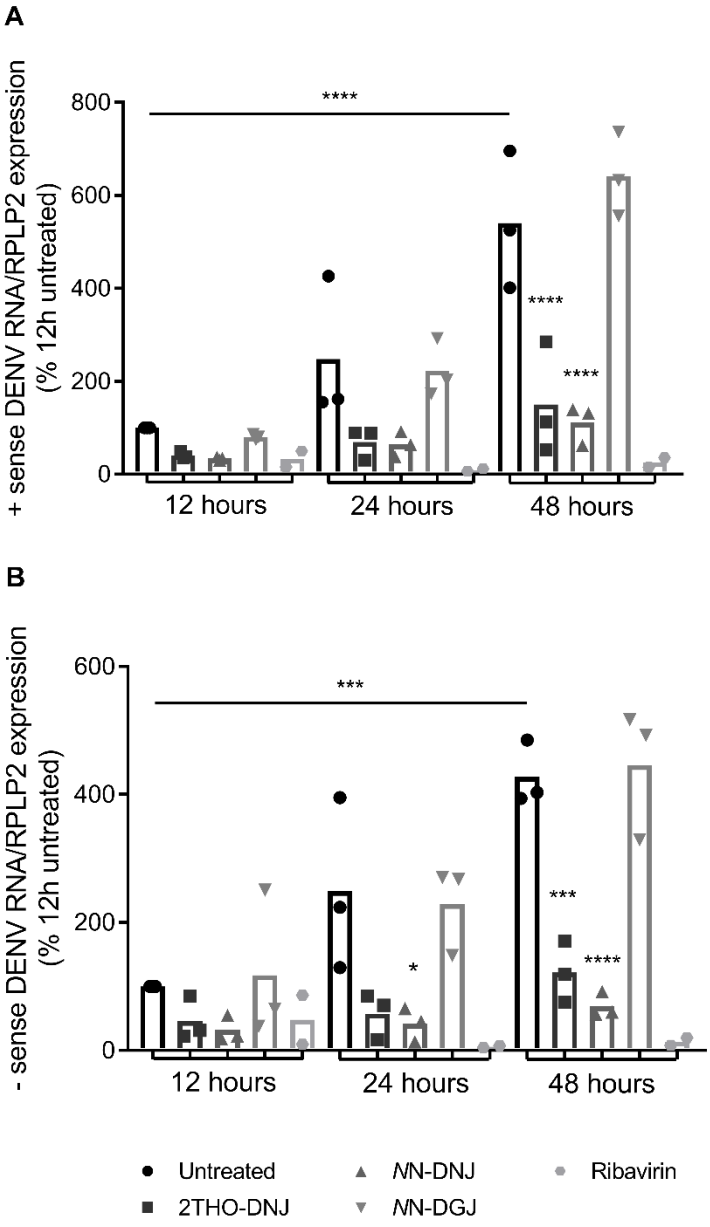

Figure 102. DENV replication over time is reflected in increases in detectable positive- and negative-sense DENV RNA.

Primary MDMΦs (n=3 (NZ, OI, OJ) or n=2 (OI, OJ) for ribavirin treatment, assayed in technical triplicate) were infected with DENV by an hour adsorption step at 4°C, followed by extensive washing in HBSS, and internalisation during an hour's incubation at 37°C. Cells were then treated with media only or 100 µM drug until indicated time points. Cellular RNA was extracted, positive-sense DENV RNA (A) and negative-sense DENV RNA (B) was reverse transcribed, quantified and normalised to RPLP2 *expression levels. For each donor, data were normalised to the 12 hour untreated values and the mean displayed (bars show the mean of the donors). Statistical analysis was by two-way ANOVA with Tukey's multiple comparisons test, with comparisons to untreated for each time point shown directly above bars (*, p<0.05; ***, p<0.001, ****, p<0.0001). Note that statistics are not shown for ribavirin since n=2.*

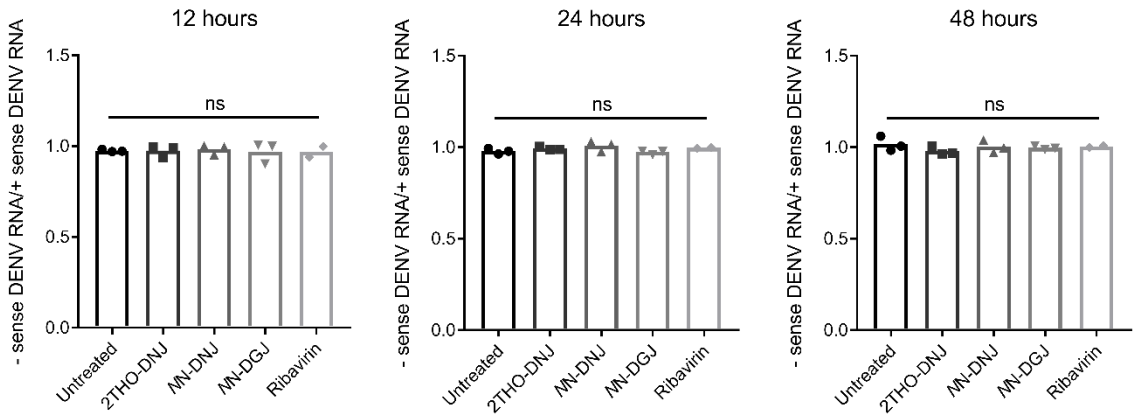

Figure 103. Ratios of negative- to positive-sense DENV RNA are unaffected across time points and drug treatments.

Primary MDMΦs (n=3 (NZ, OI, OJ) or n=2 (OI, OJ) for ribavirin treatment, assayed in technical triplicate) were infected with DENV by an hour adsorption step at 4°C, followed by extensive washing in HBSS, and internalisation during an hour's incubation at 37°C. Cells were then treated with 100 µM of iminosugar or ribavirin until indicated time points. Positive- and negative-sense DENV RNA extracted from cells was reverse transcribed and quantified. Negative-sense RNA was normalised to positive-sense RNA and the mean displayed (bars show the mean of the donors). Statistical analysis was by one-way ANOVA with Dunnett's multiple comparisons test (ns, not significant). Note that statistics for ribavirin are not shown since n=2.

8.7 Effects of proteasome inhibitor treatment on DENV infection

DENV-infected MDMΦs were treated with iminosugars and the proteasome inhibitor *clasto*-lactacystin β-lactone. The proteasome inhibitor treatment was previously determined to be non-cytotoxic at concentrations <31 µM for 48 hour treatment of MDMΦs (Michelle Hill, unpublished data). Although determined in only one donor, proteasome inhibitor treatment alone or in combination with *N*N-DGJ was potently antiviral (Figure 104). It also substantially reduced TNF-α secretion from DENV-infected or LPS-stimulated MDMΦs, seeming to have an additional effect beyond that of *N*N-DNJ or *N*N-DGJ treatment in the context of DENV infection (Figure 105).

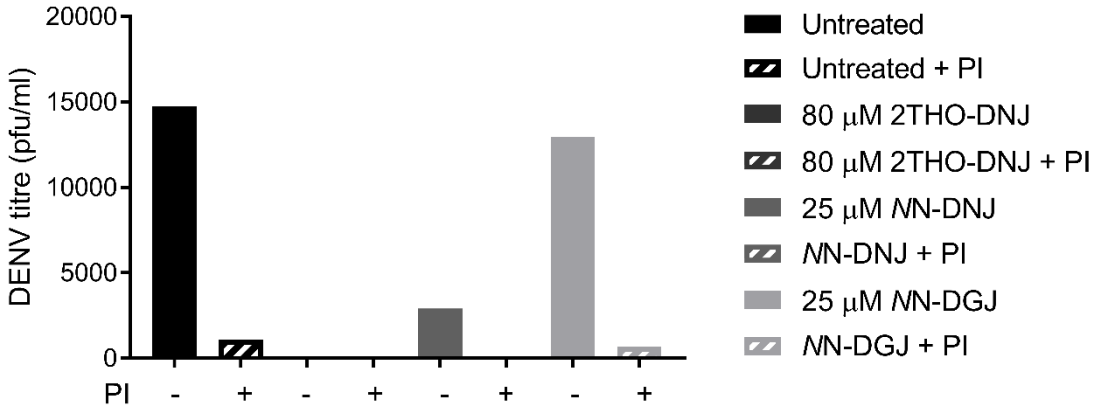

Figure 104. Clasto-lactacystin β-lactone is antiviral against DENV in MDMΦs.

Primary MDMΦs (donor JO, assayed in technical triplicate) were infected with DENV before treatment with iminosugars as indicated, with (hashed bars) or without (full bars) 10 μM clasto-lactacystin β-lactone (PI). Supernatant was collected at 24 hours post-infection, viral titres determined by plaque assay and mean titres displayed.

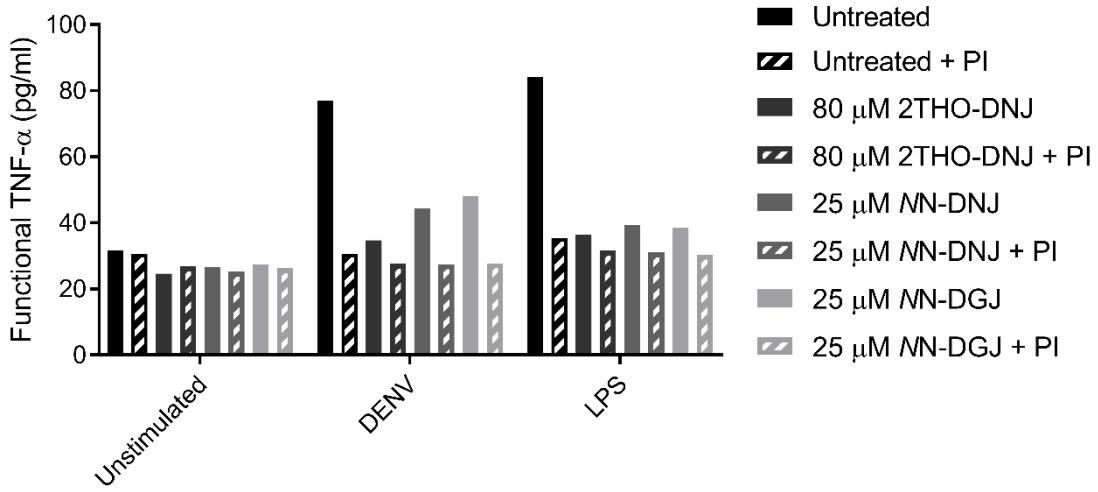

Figure 105. Clasto-lactacystin β-lactone reduces DENV-elicited TNF-α secretion from MDMΦs.

Primary MDMΦs (donor JO, assayed in technical triplicate) were infected with DENV before treatment with iminosugars as indicated, with (hashed bars) or without (full bars) 10 μM clasto-lactacystin β-lactone (PI). Supernatant was collected at 24 hours post-infection, TNF-α secretion determined by functional assay and the mean displayed.

8.8 Antiviral efficacy of iminosugars against ZIKV

Preliminary experiments were conducted to investigate whether the antiviral efficacy of iminosugars against ZIKV observed in Vero cells (Figure 30 and Figure 31) translated to MDMΦs (Figure 32; titres for individual donors are shown in Figure 106).

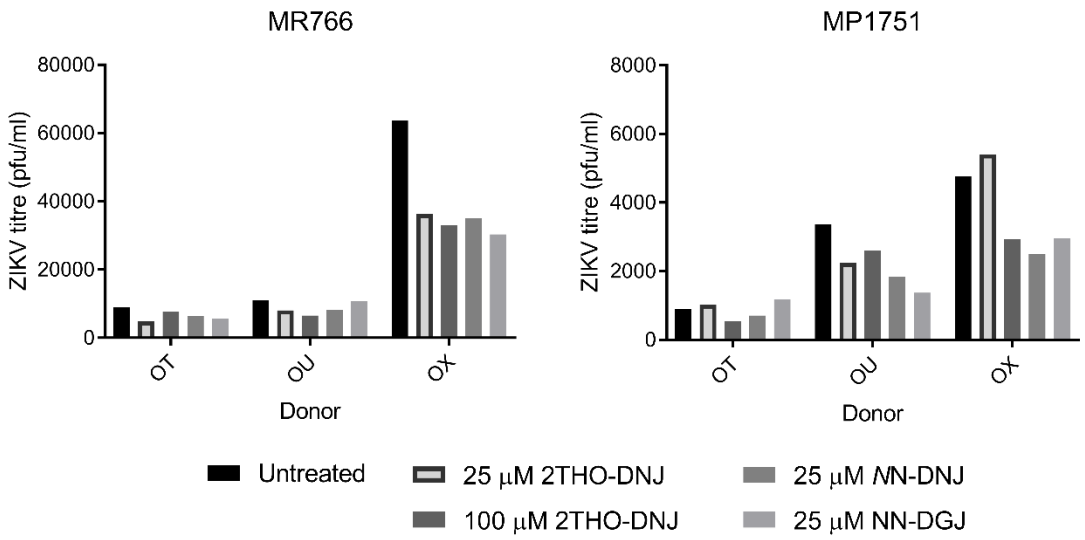

Figure 106. Iminosugars are antiviral against ZIKV infection of MDMΦs.

Primary MDMΦs (n=3, donors as shown, assayed in technical singlicate) were infected with indicated ZIKV strains and treated with iminosugars as indicated. After 72 hours, supernatant was harvested, infectious virus titres determined, and the mean displayed.

8.9 Antiviral efficacy of *N*N-DNJ against ZIKV *in vivo*

The first *in vivo* study testing the antiviral efficacy of *N*N-DNJ also assessed the tolerability of the dosing strategy, twice-daily oral gavage with drug solubilised in acidified water, in mock-challenged mice. Some issues with the tolerability of dosing were identified, including a death attributed to drug administration with oesophageal trauma identified on necropsy. The resulting clinical scores are shown in Figure 107.

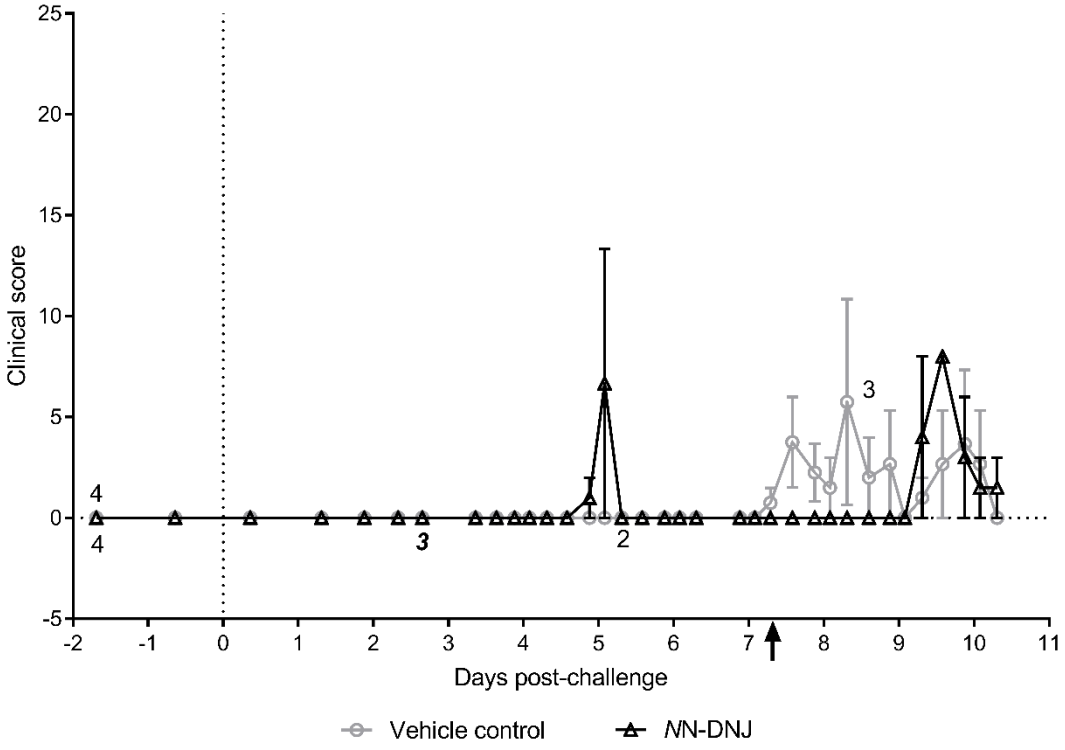

Figure 107. Uninfected A129 mice treated with acidified water experience some clinical signs.

A129 mice (n=4/group) were mock-infected and treated with NN*-DNJ or vehicle control as per 2.3.3. Clinical signs were recorded, assigned numerical values and plotted as mean ± standard error for each group. Numbers given indicate the surviving number of animals per group from that time point; those given above and below lines refer to the vehicle control and* NN*-DNJ, respectively. The bold, italicised number indicates an animal death as a result of the dosing procedure. The arrow denotes the end of dosing.*

8.10 N-glycosylation predictions for HAZV glycoproteins

Computational N-glycosylation prediction tools were used to investigate the glycosylation status of the HAZV glycoprotein, using the published JC280 strain glycoprotein sequence (UniProtKB accession number A6XIP3). NetNGlyc identified three sites likely to be N-glycosylated after disregarding sequons containing proline (Figure 108) while GlycoEP identified five sites with the same consideration (Table 21).

Asn-Xaa-Ser/Thr sequons in the sequence output below are highlighted in blue.
Asparagines predicted to be N-glycosylated are highlighted in red.

Output for 'tr_A6XIP3_A6XIP3_9VIRU'

```
Name:  tr_A6XIP3_A6XIP3_9VIRU   Length:  1421
MEGSYWWLSLLALLAWGANGESTSPAETSPAPTTPNPPVVNPSLRRKIVNQRILSAMGMDSDPSNEALNGVCQSIHSNGC      80
NANELKLRLADFFIDTNSSQCYDEILVKKPCSSLTPAHNSHWVPRGLDKSEVDKIFDTKLKLFFSQSRKVTCLSASALNP     160
SQFVKHFQVKIQETSGPAKQSLRSLHCVNLVWSHSHKGEKEVVHVLQSAVPVKLKNCLAMLNFRQCYYNQQSEGPVVVPS     240
YQHNGEKWVTGAYTMTVEVDKHADGPCEISTTCITEGSEIKPGVHSLRGFKTTLVIHGKRNTGRRLLSSSNARQECSSGT     320
FLGEGGSAQVVGPKNDGPGDHITFCNGSVVTKIRLGQEHGCYTVRRIKTYRNCRPEEGSSACEVDDELKPCGAQKCMNVH     400
LSVKGLVKTSRGSNVQVHSCDKDCLIQIPEGFGDIQIDCPGGTQHYLESNVLDVDCPMYNRLGGLMLYFCRMSHRPRTCL     480
ALFIWLGAGYGITCIAGYMVYYAILALSMLTRCLKRKYMVKGDFCLKCEQKCVTSLDQTLHDESCSYNICPYCGNRLPEE     560
GLRRHVPSCPKRKQRLEEIDLYLDYLLVPCPLHFALSTAVKLGTLLKRLSWVTVFLCLFLTAIAPVQGQVTTSPVLPSNQ     640
STECTLLPPPVFLIFSAVLMSKTLKRMGPVNKVGAAGHSARRTNSPKNLYKSKQIANTKSGPREPRRRVVVKALLILTAS     720
SALQSIHLAQAFDSGSLPEGAWEEEMQLVQGCNQECSLEEDECSCPDGQSMTRKLLFFKGLNSAASKMASSHRLLTSVSI     800
DTPWGAIKVESTYKPRLASSNIQLAWNSIEEQGDKVILSGKSTSIIKLEEKTGMQWSLGSESAAEEKRLLVSILDYTQVY     880
SSTFQYITGDRTVSEWPKATCTGDCPDRCGCSTSSCLYKSWPHSRNWRCNPTWCWGVGTGCTCCGVDILRPFNKYFVTKW     960
TTEYVRTDVLVCVELTDQERHCDVVEAGSQFVIGPVRVVVSDPQNVQTKLPSEILTIQKLEGNQVVDIMHATSIVSAKNA    1040
CKLQSCTHGSPGDMQILHTDNLIQHSHDGGLNLADLNPLVNSTWMSWEGCDLDYYCTTGSWPSCTYTGINSENTESFDNL    1120
LNTESNLCERFHFHSKRISASGSTLQMDLKGRPNSGGGELSVLVDVKGLELHSKKISLKGLSFKTLSCSGCYACSSGLSC    1200
TVEVRIERPDEFTVHLRSVSPDIAVAEGSIIARRMTGGPLSRLRAFAVRKVKKICFEIVEKSYCKDCKNEDTTKCIEVEL    1280
QPPKDILLEHKGTIIKRQNETCVSGLQCWTESASSFVSGVGSFFRNYLGSITLGIVLTLLPVAVVLLFFCYGDKLFKLCS    1360
CFRCCRGLSRGKVRKELDEDELRNKLKKFSKEGELFGKEKKDARTIALLLSGKGKNYKELV
.....................................N.....................................      80
.............N.....................................................N.     160
................................................................................     240
................................................................................     320
.......................N.....................................................     400
................................................................................     480
................................................................................     560
................................................................................     640
................................................................................     720
................................................................................     800
................................................................................     880
.................................................N..............................     960
................................................................................    1040
.....................................N......................................     1120
................................................................................    1200
................................................................................    1280
................................................................................    1360
.........................................................                       1440

(Threshold=0.5)
--------------------------------------------------------------------
SeqName      Position  Potential   Jury    N-Glyc
                                 agreement result
--------------------------------------------------------------------
tr_A6XIP3_A6XIP3_9VIRU   41 NPSL   0.6857     (9/9)   ++   WARNING: PRO-X1.
tr_A6XIP3_A6XIP3_9VIRU   97 NSSQ   0.6163     (8/9)   +
tr_A6XIP3_A6XIP3_9VIRU  159 NPSQ   0.7756     (9/9)   +++  WARNING: PRO-X1.
tr_A6XIP3_A6XIP3_9VIRU  346 NGSV   0.5580     (7/9)   +
tr_A6XIP3_A6XIP3_9VIRU  639 NQST   0.4717     (7/9)   -
tr_A6XIP3_A6XIP3_9VIRU  930 NPTW   0.5820     (8/9)   +    WARNING: PRO-X1.
tr_A6XIP3_A6XIP3_9VIRU 1081 NSTW   0.5839     (8/9)   +
tr_A6XIP3_A6XIP3_9VIRU 1299 NETC   0.4993     (5/9)   -
--------------------------------------------------------------------
```

Figure 108. Prediction of N-glycosylation sites in HAZV glycoprotein (UniProtKB accession number A6XIP3) using NetNGlyc [464, 465].

Table 21. Sites predicted to be N-glycosylated in the HAZV glycoprotein (UniProtKB accession number A6XIP3) using GlycoEP (N-linked glycosylation prediction based on binary profile of patterns using default 0.0 threshold) [466].

Position	Sequon	Score
41	NPS	0.18850765
97	NSS	1.0690017
159	NPS	0.32975269
346	NGS	0.63686428
639	NQS	1.2295097
1081	NST	0.91890507
1299	NET	0.80099642

8.11 Comparison of CCHFV and HAZV glycoprotein N-glycosylation

CCHFV and HAZV glycoprotein sequences were aligned and annotated for N-glycosylation sites (Figure 109). Some, but not all, of the putative HAZV glycosylation sites are aligned with those found in the CCHFV sequence, and there are differences in N-glycosylation sites falling within the CCHFV structural glycoprotein (Gn and Gc) regions. For the two sites where N-glycosylation was confirmed by mass spectrometry (5.3.1), N97 of HAZV is not aligned with a site in the CCHFV glycoprotein sequence. This residue falls within the GP38 region of the CCHFV glycoprotein. Conversely, the N346 site in HAZV aligns with an N-glycosylation site for CCHFV in the Gn glycoprotein sequence. Thus, there may be differences in N-glycosylation and its functional significance between the glycoproteins of HAZV and CCHFV.

```
TR|A6XIP3|A6XIP3_9VIRU ------------------------------------------------------------
SP|Q8JSZ3|GP_CCHFI     MHISLMYAILCLQLCGLGETHGSHNETRHNKTDTMTTPGDNPSSEPPVSTALSITLDPST  60

TR|A6XIP3|A6XIP3_9VIRU ------------------------------------------------------------
SP|Q8JSZ3|GP_CCHFI     VTPTTPASGLEGSGEVYTSPPITTGSLPLSETTPELPVTTGTDTLSAGDVDPSTQTAGGT 120

TR|A6XIP3|A6XIP3_9VIRU --------------------MEGSYWWLSLLALLAWGANGES-------TSPAETSPAPTT  34
SP|Q8JSZ3|GP_CCHFI     SAPTVRTSLPNSPSTPSTPQDTHHPVRNLLSVTSPGPDETSTPSGTGKESSATSSPHPVS 180

TR|A6XIP3|A6XIP3_9VIRU PNPPVV----------------------------------------NPSL------------  44
SP|Q8JSZ3|GP_CCHFI     NRPPTPPATAQGPTENDSHNATEHPESLTQSATPGLMTSPTQIVHPQSATPITVQDTHPS 240

TR|A6XIP3|A6XIP3_9VIRU -----RR--------------KIVNQRILSAMGMDSDPSNEALNGVCQSIHSNGCNANEL  85
SP|Q8JSZ3|GP_CCHFI     PTNRSKRNLKMEIILTLSQGLKKYYGKILRLLQLTLEEDTEGLLEWCKRNLGLDCDDTFF 300

TR|A6XIP3|A6XIP3_9VIRU KLRLADFFIDTNSSQCYDEILVKKPCSSLTPAHNSHWVPRGLDKSEVDKIF-DTKLKLFF 144
SP|Q8JSZ3|GP_CCHFI     QKRIEEFFITGEG--HFNEVLQFRTPGTLS---TTESTPAGLPTAEPFKSYFAKGFLSID 355

TR|A6XIP3|A6XIP3_9VIRU SQSRKVTCLSASALNPSQF--VKHFQVKIQETSGPAKQSLRSLHCVNLVWSHSHKGEKEV 202
SP|Q8JSZ3|GP_CCHFI     SGYYSAKCYSGTSNSGLQLINITRHSTRIVDTPGPKITNLKTINCINLKASIFKEHREVE 415

TR|A6XIP3|A6XIP3_9VIRU VHVLQSAVPVKLKNCLAMLNFRQCYYNQQSEGPVVVPSYQHNGEKWVTGAYTMTVEVDKH 262
SP|Q8JSZ3|GP_CCHFI     INVLLPQVAVNLSNCHVVIKSHVCDYSLDIDGAVRLPHIYHEG-VFIPGTYKIVIDKKNK 474

TR|A6XIP3|A6XIP3_9VIRU ADGPCEISTTCITEGSEIKPGVHSLRGFKTTLVIHGKRNTGRRLLSSSNARQECSSGTFL 322
SP|Q8JSZ3|GP_CCHFI     LNDRCTLFTDCVIKGREVRKGQSVLRQYKTEIRIGK-ASTGSRRLLSEEPSDDCISRTQL 533

TR|A6XIP3|A6XIP3_9VIRU GEGGSAQVVGPKNDGPGDHITFCNGSVVTKIRLGQEHGCYTVRRIKTYRNCRPEEGSSAC 382
SP|Q8JSZ3|GP_CCHFI     LRTETAEIHGDNYGGPGDKITICNGSTIVDQRLGSELGCYTINRVRSFKLCENSATGKNC 593

TR|A6XIP3|A6XIP3_9VIRU EVDDELKPCGAQKCMNVHLSVKGLVKTSRGSNVQVHSCDKDCLIQIPEGFGDIQIDCPGG 442
SP|Q8JSZ3|GP_CCHFI     EIDSVPVKCRQGYCLRITQEGRGHVKLSRGSEVVLDACDTSCEIMIPKGTGDILVDCSGG 653

TR|A6XIP3|A6XIP3_9VIRU TQHYLESNVLDVDCPMYNRLGGLMLYFCRMSHRPRTCLALFIWLGAGYGITCIAGYMVYY 502
SP|Q8JSZ3|GP_CCHFI     QQHFLKDNLIDLGCPKIPLLGKMAIYICRMSNHPKTTMAFLFWFSFGYVITCILCKAIFY 713

TR|A6XIP3|A6XIP3_9VIRU AILALSMLTRCLKRKYMVKGDFCLKCEQKCVTSLDQTLHDESCSYNICPYCGNRLPEEGL 562
SP|Q8JSZ3|GP_CCHFI     LLIIVGTLGKRLKQYRELKPQTCTICETTPVNAIDAEMHDLNCSYNICPYCASRLTSDGL 773

TR|A6XIP3|A6XIP3_9VIRU RRHVPSCPKRKQRLEEIDLYLDYLLVPCPLHFALSTAVKLGTLLKRLSWVTVFLCLFLTA 622
SP|Q8JSZ3|GP_CCHFI     ARHVIQCPKRKEKVEETELYLNLERIPWVVRKLLQVSESTGVALKRSSWLIVLLVLFTVS 833

TR|A6XIP3|A6XIP3_9VIRU IAPVQGQVTTSPVL------PSNQSTECTLLPPPVFLIFSAVLMSKTLKRMGPVNKVG-- 674
SP|Q8JSZ3|GP_CCHFI     LSPVQSAPIGQGKTIEAYRAREGYTSICLFVLGSILFIVSC-LMKGLVDSVGNSFFPGLS 892

TR|A6XIP3|A6XIP3_9VIRU ---------------AAGHSA----------RRTNSPKNLYKSKQ-I-ANTKSGP------ 702
SP|Q8JSZ3|GP_CCHFI     ICKTCSISSINGFEIESHKCYCSLFCCPYCRHCSTDKEIHKLHLSICKRRKKGSNVMLAV 952

TR|A6XIP3|A6XIP3_9VIRU ----------REPRRRVVVK----ALLILTASSALQSIHLAQAFDSGSLPEGAWEEEMQL 748
SP|Q8JSZ3|GP_CCHFI     CKLMCFRATMEVSNRALFIRSIINTTFVLCILILAVCVVSTSAVEMENLPAGTWEREEDL 1012

TR|A6XIP3|A6XIP3_9VIRU VQGCNQECSLEEDECSCPDGQSMTRKLLFFKGLNSAASKMASSHRLLTSVSIDTPWGAIK 808
SP|Q8JSZ3|GP_CCHFI     TNFCHQECQVTETECLCPYEALVLRKPLFLDSTAKGMKNLLNSTSLETSLSIEAPWGAIN 1072

TR|A6XIP3|A6XIP3_9VIRU VESTYKPRLASSNIQLAWNSIEEQGDKVILSGKSTSIIKLEEKTGMQWSLGSESAAEEKR 868
SP|Q8JSZ3|GP_CCHFI     VQSTYKPTVSTANIALSWSSVEHRGNKILVSGRSESIMKLEERTGISWDLGVEDASESKL 1132

TR|A6XIP3|A6XIP3_9VIRU LLVSILDYTQVYSSTFQYITGDRTVSEWPKATCTGDCPDRCGCSTSSCLYKSWPHSRNWR 928
SP|Q8JSZ3|GP_CCHFI     LTVSVMDLSQMYSPVFEYLSGDRQVGEWPKATCTGDCPERCGCTSSTCLHKEWPHSRNWR 1192

TR|A6XIP3|A6XIP3_9VIRU CNPTWCWGVGTGCTCCGVDILRPFNKYFVTKWTTEYVRTDVLVCVELTDQERHCDVVEAG 988
SP|Q8JSZ3|GP_CCHFI     CNPTWCWGVGTGCTCCGLDVKDLFTDYMFVKWKVEYIKTEAIVCVELTSQERQCSLIEAG 1252
```

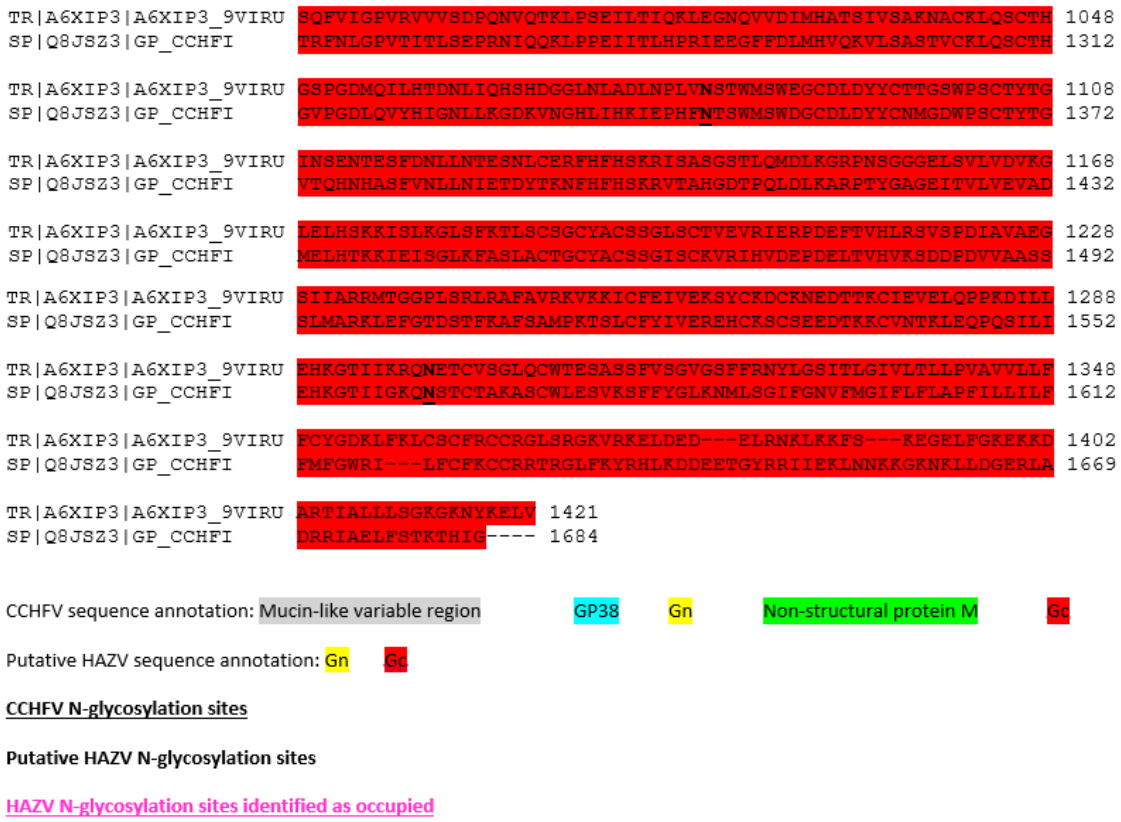

Figure 109. Comparison of CCHFV and HAZV glycoprotein N-glycosylation.

CCHFV and HAZV glycoprotein sequences (UniProtKB Q8JSZ3 and A6XIP3, respectively) were aligned using CLUSTAL Omega (1.2.4) multiple sequence alignment. CCHFV domains and N-glycosylation sites were annotated according to the UniProtKB record. Putative Gn and Gc proteins in the HAZV sequence, as determined by analysis of nairovirus proteolytic cleavage sites in [281], were also included. Putative HAZV N-glycosylation sites, as determined in 8.10, and sites for which N-glycosylation was confirmed in 5.3.1 were also annotated.

8.12 SW13 cells are susceptible to iminosugar-mediated ER α-glucosidase inhibition

As a result of the lack of antiviral efficacy of iminosugars against HAZV, FOS analysis was performed for SW13 cells treated with the iminosugar panel used to confirm that iminosugars were able to access the ER α-glucosidases to inhibit them. The expected inhibition of these enzymes was identified in mock- and HAZV-infected SW13 cells (Figure 46) and representative FOS profiles indicating the effect of 2THO-DNJ treatment, shown as an example iminosugar, are presented in Figure 110. Note that these traces are not normalised to cell lysate protein

concentration and thus are not quantitative, although initial cell numbers were the same for each treatment condition and protein concentrations were broadly consistent between samples (data not shown).

Although SW13 cells were found to be susceptible to iminosugar-mediated ER α-glucosidase inhibition, comparison of typical FOS profiles between SW13 cells and MDMΦs, either untreated or treated with 2THO-DNJ, reveals that the amount of FOS accumulation seen in uninfected SW13 cells appears to be considerably lower than that generated upon iminosugar treatment of MDMΦs (Figure 111). This effect may be contributed to by the different time points used here, but it could indicate greater levels of N-linked glycosylation occurring in MDMΦs, or greater accessibility of iminosugars to the ER α-glucosidases in MDMΦs relative to SW13 cells.

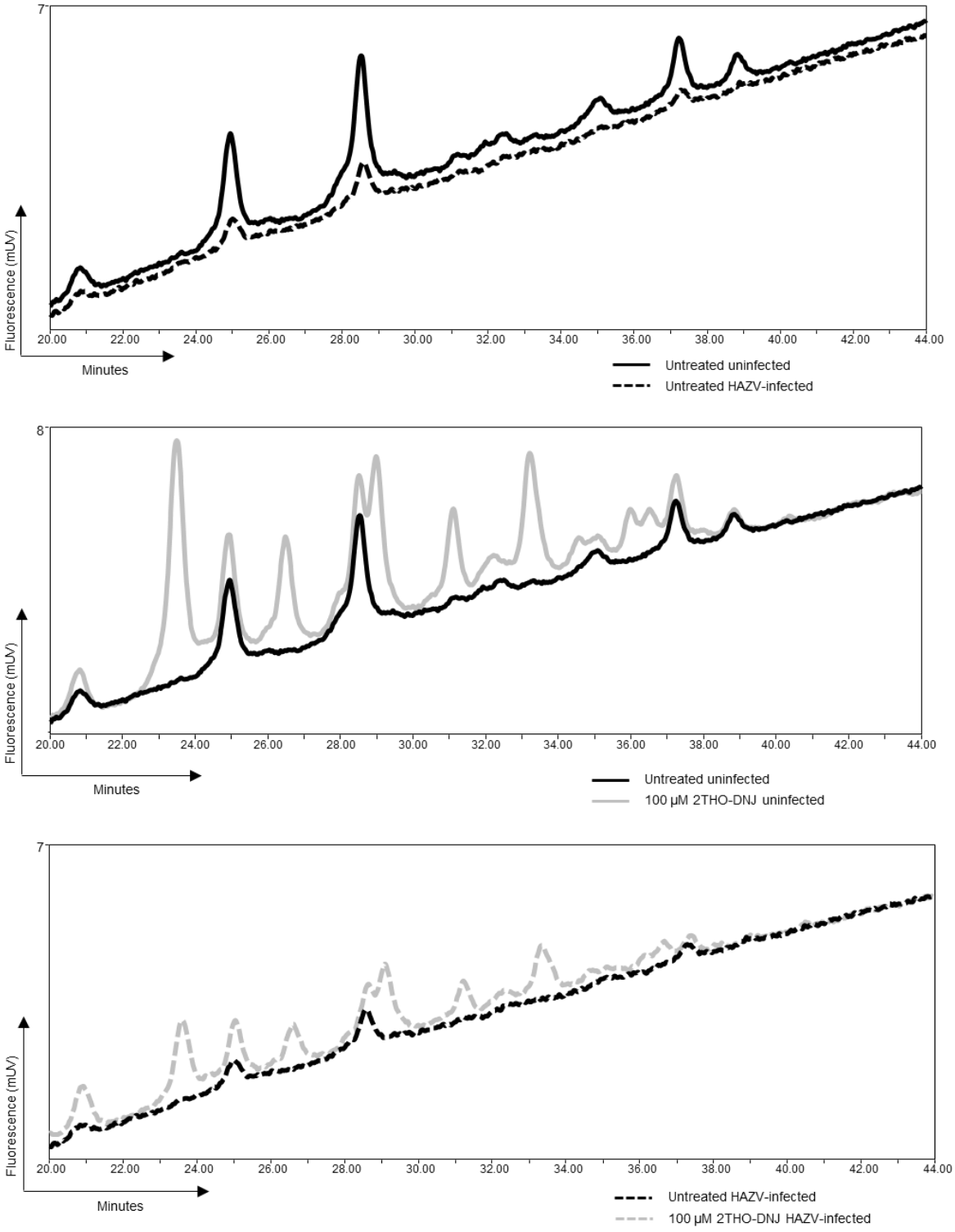

Figure 110. Representative FOS profiles for HAZV-infected and 2THO-DNJ treated SW13 cells.

SW13 cells (assayed in technical duplicate) were left untreated or treated with 100 µM 2THO-DNJ for 3 days prior to mock- or HAZV-infection. After infection, media was replenished with media only or iminosugar as prior to infection and treatment continued for 3 further days. FOS were purified from cell lysates and run on NP-HPLC. Representative FOS profiles (not normalised for protein concentration) for conditions indicated in legends are shown to illustrate changes upon infection or iminosugar treatment. Samples were prepared and analysed with the assistance of Juliane Brun and Dominic Alonzi.

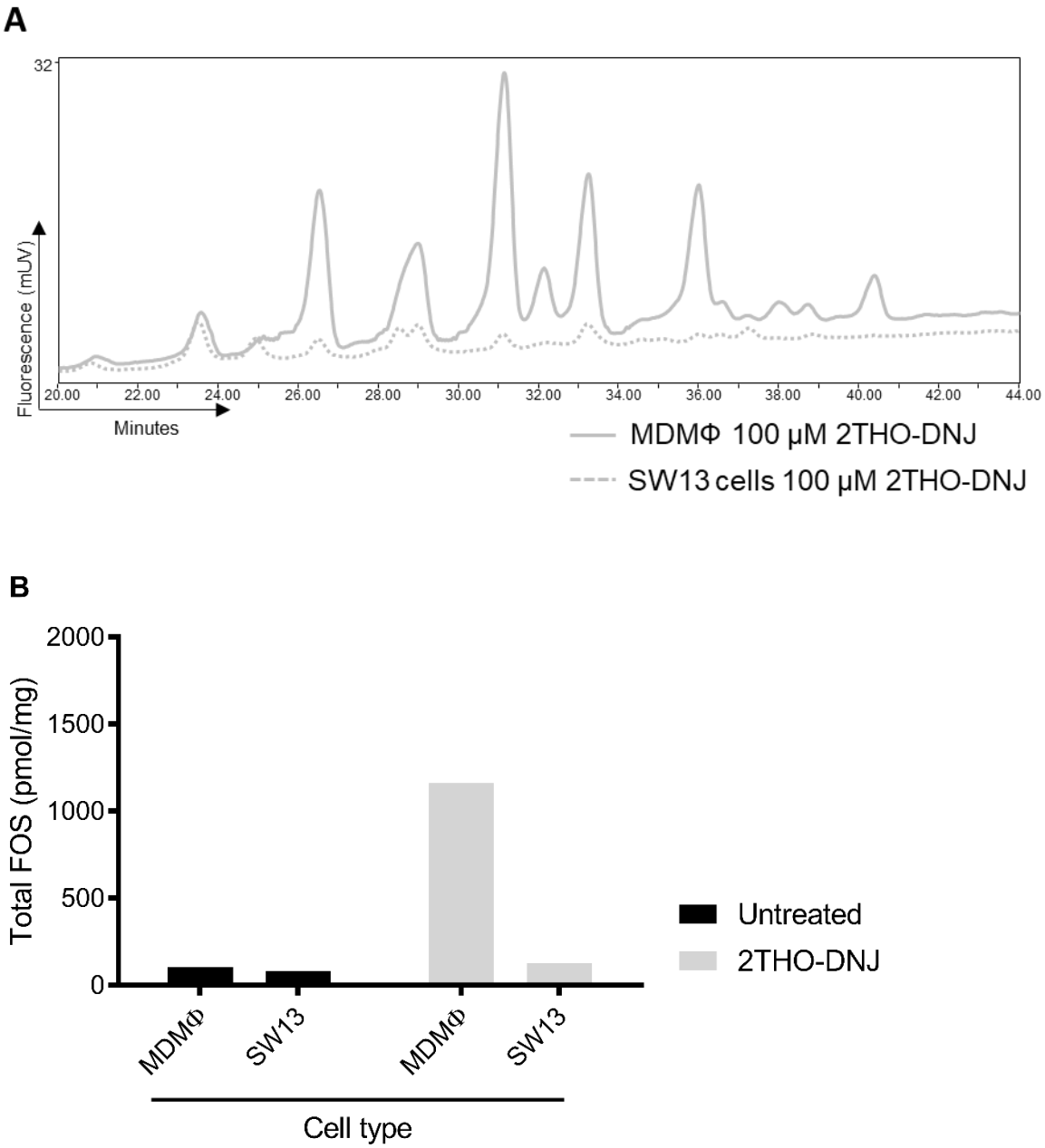

Figure 111. Iminosugar treatment of MDMΦs appears to induce greater FOS accumulation than in SW13 cells.

Primary MDMΦs (n=3 donors (MB, MC, MD), assayed in technical duplicate) were left untreated or treated with 100 µM 2THO-DNJ for 48 hours and SW13 cells (n=1, assayed in technical duplicate) were left untreated or treated with 100 µM 2THO-DNJ for 3 days. Total FOS accumulation in cell lysates was determined.

(A) A representative HPLC trace (non-normalised for total protein concentration) for a 2THO-DNJ-treated MDMΦ and SW13 cell trace is shown.

(B) Mean total FOS generation (normalised for protein concentration) is shown for 2THO-DNJ-treated MDMΦs and SW13 cells.

Samples were prepared and analysed with the assistance of Juliane Brun, Stephen Early and Dominic Alonzi.

8.13 Validation of HEK-Blue cytokine reporter cell responses

8.13.1 Relevant PAMPs and viruses do not stimulate reporter cell responses

In order to determine that the presence of PAMPs did not erroneously stimulate cytokine reporter cells used for the detection of functional cytokine in cell supernatants, TNF-α and IFN-α/β reporter cells were assayed with media samples containing LPS or heat-killed *Candida albicans* (HKCA) at concentrations routinely used for cell stimulations, as per the functional cytokine assay protocol (2.5.4.2). The presence of these PAMPs did not induce responses from the reporter cells (Figure 112).

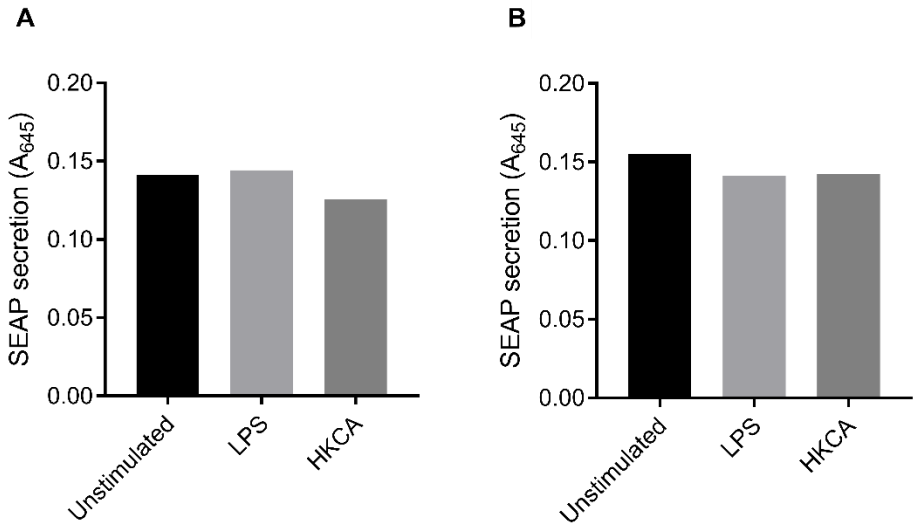

Figure 112. Representative non-infectious stimuli do not induce reporter cell responses.

TNF-α reporter cells (A) and IFN-α/β reporter cells (B) were seeded for functional cytokine assay in 180 µl and stimulated with a 20 µl media 'sample' containing LPS-ST (100 ng/ml) or HKCA (1 x 10^6 cells/ml) to reflect concentrations routinely used for stimulating MDMΦs for 24 hours (n=1, assayed in technical triplicate). SEAP secretion was then quantified by absorbance at 645 nm and the mean displayed.

The presence of DENV in supernatants for analysis was also determined not to induce reporter cell responses. In order to represent a situation assessing cytokine responses to DENV infection

in the presence of iminosugars, viral titres produced by MDMΦs infected with DENV and treated with a titration of 2THO-DNJ were quantified. The same supernatants were then analysed for functional TNF-α alongside samples of a matched DENV titre prepared from DENV stocks in MDMΦ media. The presence of DENV did not induce a response from the cytokine reporter cells, while the dose-dependent reduction in secreted TNF-α with 2THO-DNJ treatment was evident (Figure 113). The stimulation of TNF-α and IFN-α/β cytokine reporter cells with a range of ZIKV titres also did not induce any reporter cell response (data not shown).

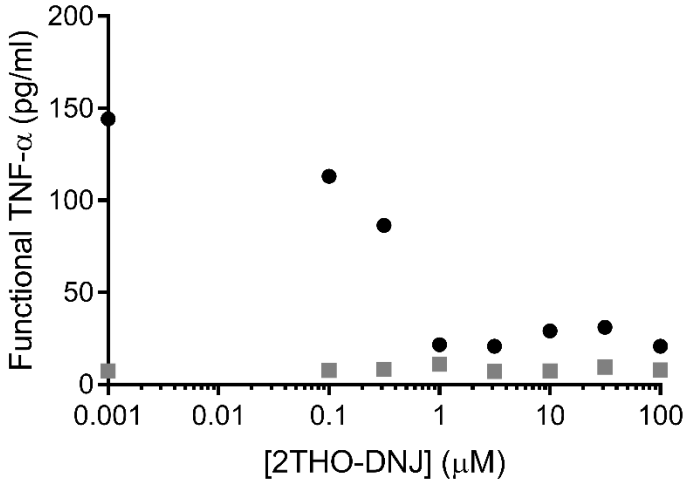

Figure 113. The presence of DENV in supernatants does not induce a reporter cell response.

Primary MDMΦs (donor IX, assayed in technical triplicate) were infected with DENV and treated with a titration of 2THO-DNJ. Supernatant was collected after 48 hours and viral titres determined by plaque assay. TNF-α in the supernatant was quantified by functional assay. Samples of a matched DENV titre were prepared in MDMΦ media from DENV stocks, and subjected to functional TNF-α assay alongside the MDMΦ supernatants. Mean functional TNF-α values were displayed for the MDMΦ supernatant samples (black circles) and DENV samples (grey squares).

8.13.2 Antiviral compounds do not consistently impact cytokine reporter cell responses

Since cytokine reporter cells were used to quantify TNF-α and IFN-α/β in supernatant samples from cells treated with a range of iminosugars and other antiviral compounds, the effects of stimulation with these drugs on the cell viability (Figure 114) and SEAP secretion (Figure 115)

was assessed. There were no significant effects on cell viability, and no consistent effects on the TNF-α reporter cells.

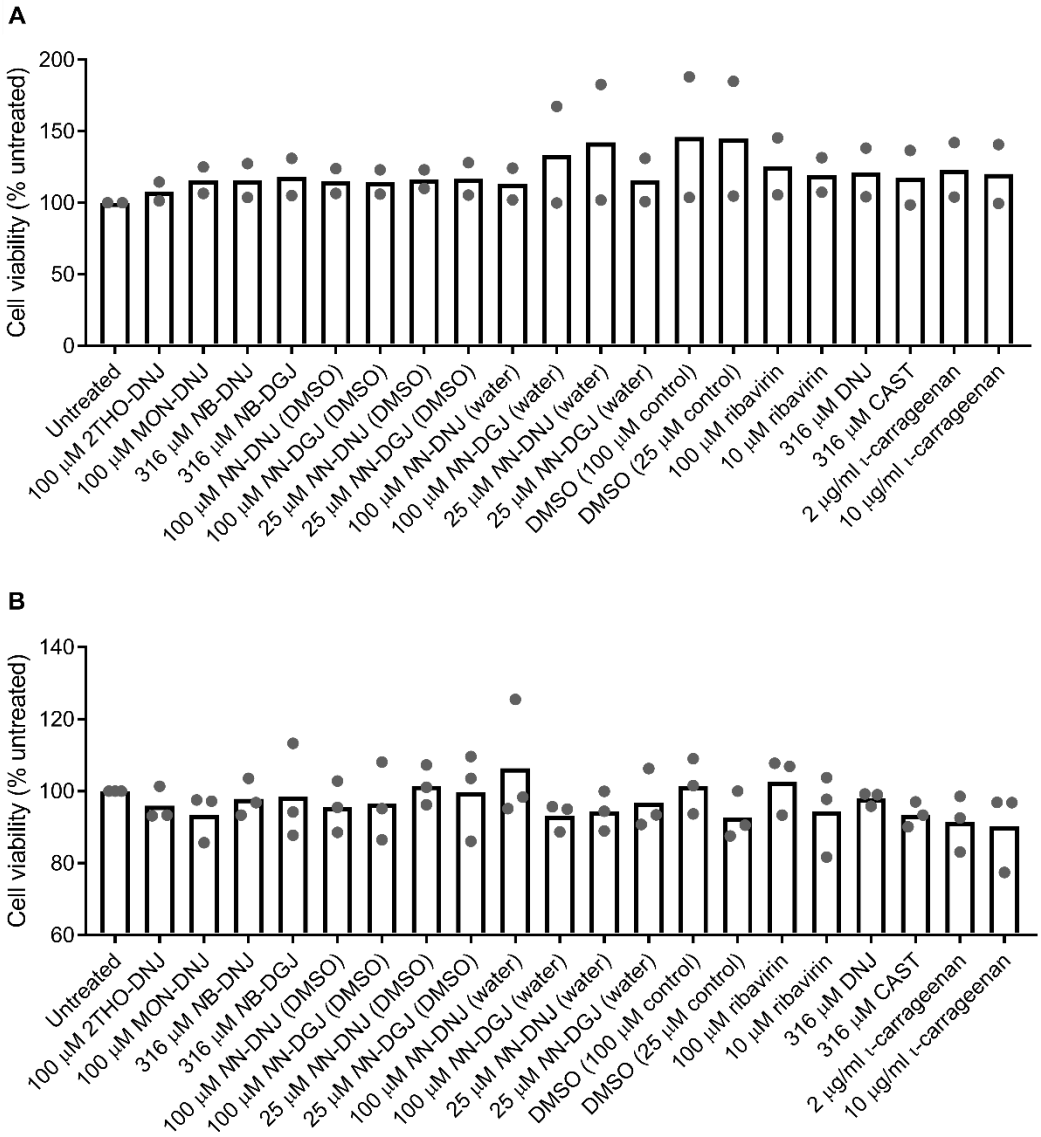

Figure 114. Antiviral drug treatment does not affect cytokine reporter cell viability.

TNF-α reporter cells (A) and IFN-α/β reporter cells (B) were seeded for functional cytokine assay in 180 µl and stimulated with a 20 µl media 'sample' containing the concentration of drug indicated. After 24 hours, cell viability was assessed by MTS assay. Data were normalised to untreated and the mean displayed (n=2 for TNF-α reported cells; n=3 for IFN-α/β reporter cells). Statistical analysis (conducted for B only) was by one-way ANOVA with Dunnett's multiple comparisons test, and identified no statistically significant differences.

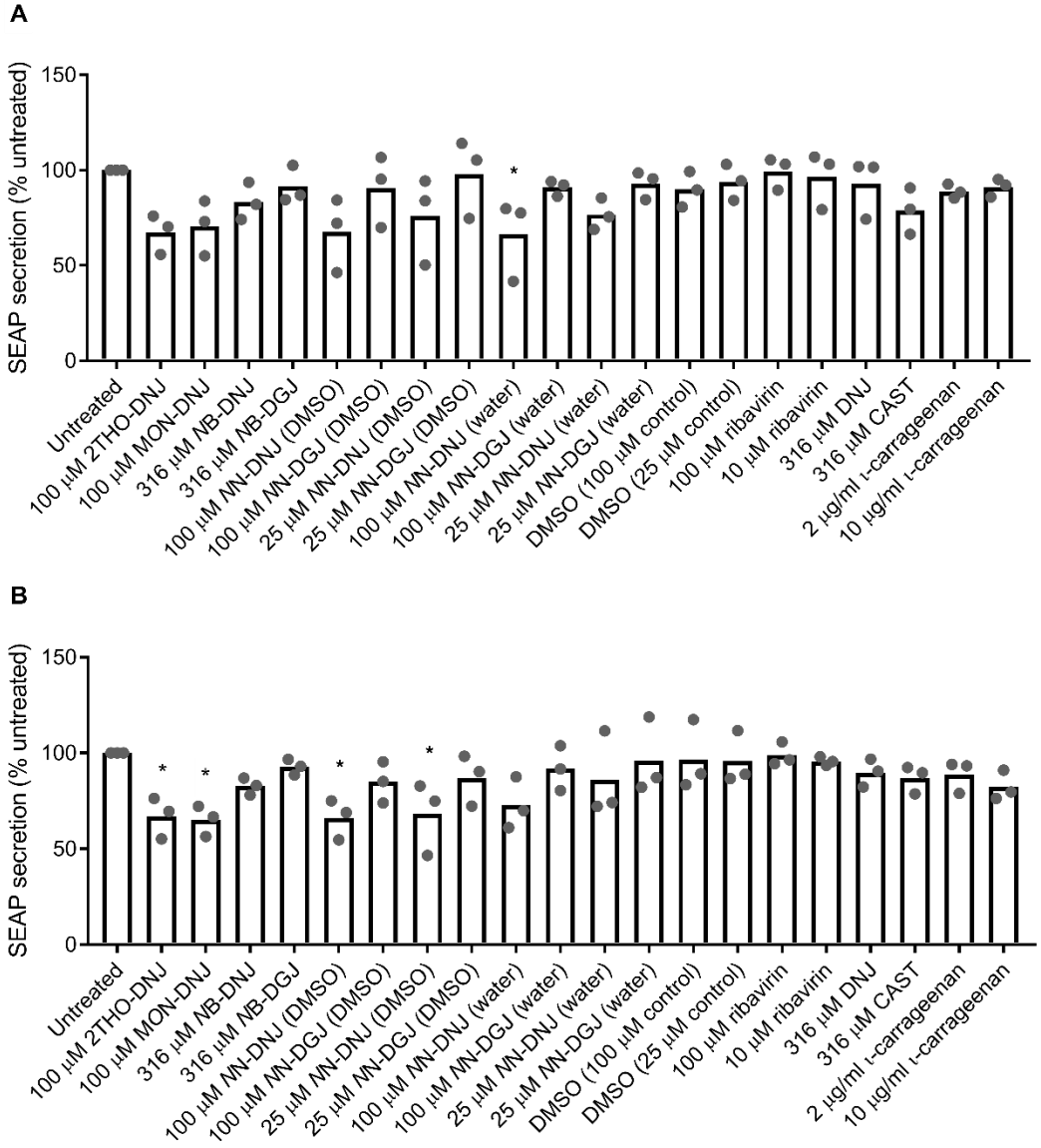

Figure 115. Antiviral drug treatments do not consistently impact cytokine reporter cell responses.

TNF-α reporter cells (A) and IFN-α/β reporter cells (B) were seeded for functional cytokine assay in 180 µl and stimulated with a 20 µl media 'sample' containing the concentration of drug indicated. After 24 hours, reporter cell responses were assessed by determining SEAP secretion and the mean displayed (n=3 in both cases). Statistical analysis was by one-way ANOVA with Dunnett's multiple comparisons test (, p<0.05).*

8.14 2THO-DNJ effects on cytokine production from DENV-infected MDMΦs

2THO-DNJ treatment dose-dependently reduced functional TNF-α secretion from DENV-infected MDMΦs (6.3.2.1). Supporting information follows.

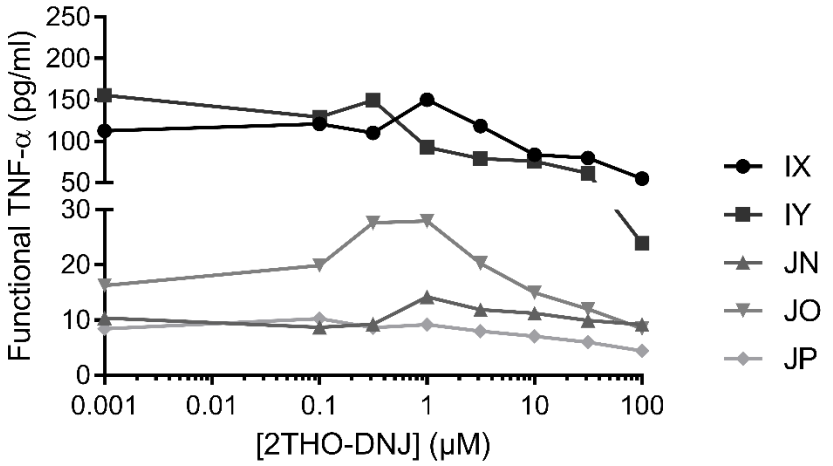

Figure 116. 2THO-DNJ reduces functional TNF-α secretion from DENV-infected MDMΦs.

Primary MDMΦs (n=5 donors, as shown, assayed in technical triplicate) were infected with DENV and treated with a titration of 2THO-DNJ. Supernatant was collected at 48 hours post-infection, secreted TNF-α quantified by functional assay and the mean plotted.

Table 22. Linear regression details for functional TNF-α response to 2THO-DNJ titrations (Figure 49B).

Primary MDMΦs (n=5 donors, as shown, assayed in technical triplicate) were infected with DENV and treated with a titration of 2THO-DNJ. Supernatant was collected at 48 hours post-infection for determination of viral titre and functional TNF-α secretion. Values were normalised to untreated for each donor and corresponding points plotted against each other. Linear regression was used to find lines of best fit, with associations assessed by Pearson correlation.

Donor	Equation	R^2 value	Pearson r	P value
IX	y = 0.4847x + 62.61	0.5151	0.7177	<0.0001
IY	y = 0.4957x + 30.33	0.5218	0.7223	<0.0001
JN	y = -0.09398x + 106.4	0.053	-0.2302	0.2792
JO	y = 0.7862x + 63.39	0.5474	0.7398	<0.0001
JP	y = 0.3745x + 69.83	0.4372	0.6612	0.0004

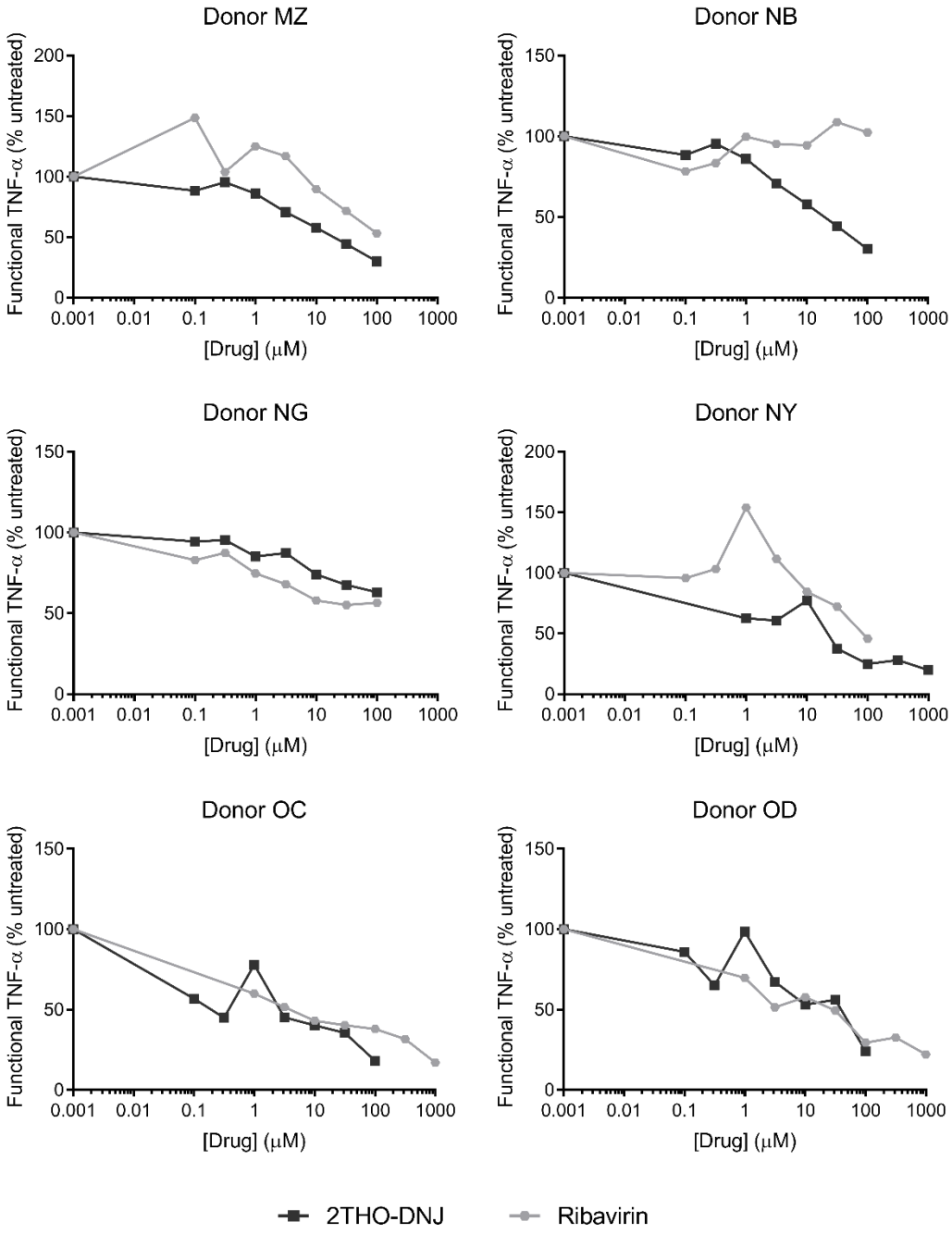

Figure 117. 2THO-DNJ and ribavirin treatment reduce TNF-α secretion from DENV-infected MDMΦs.

Primary MDMΦs (assayed in technical triplicate) were infected with DENV and treated with a titration of 2THO-DNJ or ribavirin. Supernatant was collected at 48 hours post-infection and secreted TNF-α quantified. Values were normalised to untreated and the mean plotted, with untreated represented as 0.001 μM to allow plotting on a logarithmic scale.

Table 23. Linear regression details for Figure 53.

Primary MDMΦs (n=6 donors (MZ, NB, NG, NY, OC, OD), assayed in technical triplicate) were infected with DENV and treated with a titration of 2THO-DNJ or ribavirin. Supernatant was collected at 48 hours post-infection for quantification of viral titre and functional TNF-α secretion. Values were normalised to untreated for each donor and antiviral efficacy plotted against cytokine response. Linear regression was used to find lines of best fit, with associations assessed by Pearson correlation.

Drug	Equation	R^2 value	Pearson r	P value
2THO-DNJ	y = 0.4059x + 59.41	0.3821	0.6181	<0.0001
Ribavirin	y = 0.6819x + 31.81	0.4451	0.6672	<0.0001

Table 24. Linear regression details for Figure 55.

Primary MDMΦs (n=6 donors, as shown, assayed in technical triplicate) were infected with DENV and treated with a titration of 2THO-DNJ or ribavirin. Supernatant was collected at 48 hours post-infection, and IFN-α/β secretion quantified. Values were normalised to untreated and plotted as mean ± standard deviation, with untreated represented as 0.001 µM to allow plotting on a logarithmic scale. For donors NY, OC, and OD, peak values for ribavirin represent the top of the standard curve used in the assay (5000 pg/ml). Linear regression was used to find lines of best fit, with associations assessed by Pearson correlation.

[a]Slope not significantly non-zero.

Donor	Drug	Equation	R^2 value	Pearson r	P value
MZ	2THO-DNJ	y = -0.9689x + 181.7	0.2756	-0.5249	0.0084
	Ribavirin	y = -0.1472x + 140[a]	0.0118	-0.1086	0.6134
NB	2THO-DNJ	y = -2.971x + 366.5	0.7791	-0.8827	<0.0001
	Ribavirin	y = 0.7423x + 10.91	0.4480	0.6693	0.0003
NG	2THO-DNJ	y = 0.1274x + 101.1[a]	0.04167	0.2041	0.3387
	Ribavirin	y = -0.1711x + 111.6[a]	0.04612	-0.2148	0.3136
NY	2THO-DNJ	y = 0.3696x + 53.79	0.4541	0.6738	0.0003
	Ribavirin	y = -1.435x + 257.6	0.6660	-0.8161	<0.0001
OC	2THO-DNJ	y = 0.3341x + 23.74	0.3097	0.5565	0.0047
	Ribavirin	y = -0.3589x + 122.6[a]	0.1242	-0.3524	0.2612
OD	2THO-DNJ	y = 0.6616x + 24.61	0.905	0.9513	<0.0001
	Ribavirin	y = -3.949x + 571	0.916	-0.9571	<0.0001

8.15 M*O*N-DNJ effects on cytokine secretion from DENV-infected MDMΦs

M*O*N-DNJ treatment dose-dependently reduced functional cytokine production from DENV-infected MDMΦs (Figure 58; non-normalised values in Figure 118). However, in some situations, potentially corresponding to low baseline induction of IFN-α/β, M*O*N-DNJ treatment was observed to enhance cytokine secretion (Figure 59; non-normalised values in Figure 119).

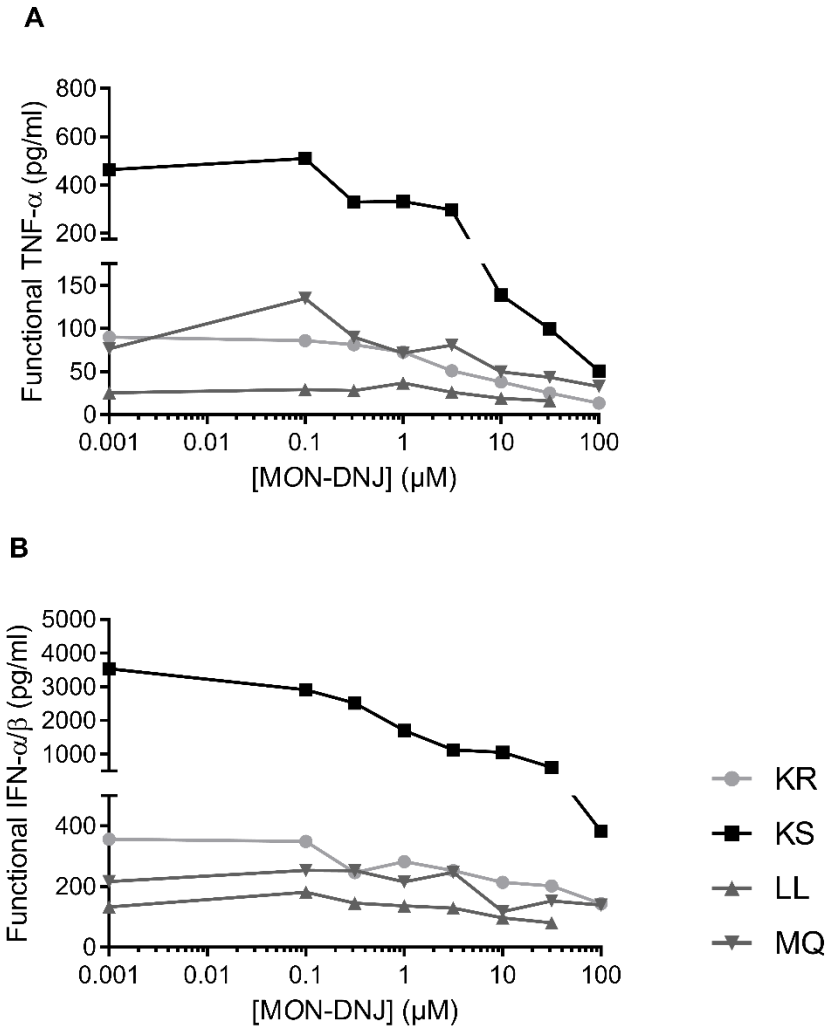

Figure 118. MON-DNJ reduces functional TNF-α and IFN-α/β secretion from DENV-infected MDMΦs.

Primary MDMΦs (n=4 donors (KR, KS, LL, MQ), assayed in technical triplicate) were infected with DENV and treated with a titration of MON-DNJ. Supernatant was collected at 48 hours post-infection, secreted TNF-α (A) or IFN-α/β (B) quantified by functional assay and the mean displayed.

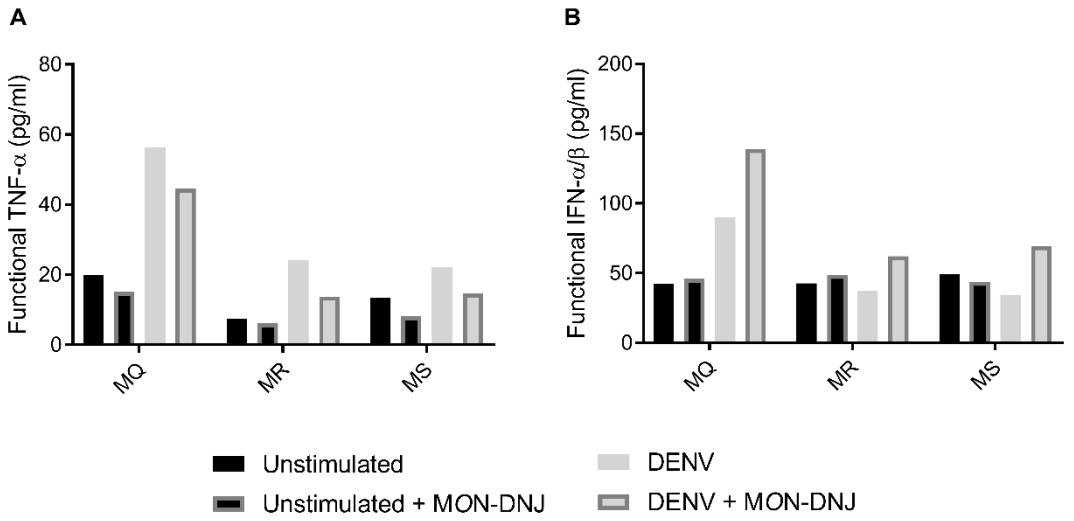

Figure 119. MON-DNJ reduces functional TNF-α and enhances IFN-α/β secretion from DENV-infected MDMΦs.

Primary MDMΦs (n=3 donors (MQ, MR, MS), assayed in technical triplicate) were infected with DENV and treated with 25 µM MON-DNJ. Supernatant was collected at indicated times post-infection, secreted TNF-α (A) or IFN-α/β (B) quantified by functional assay and the mean displayed.

8.16 Assessment of iminosugar effects on cytokine secretion from dendritic cells

Immature dendritic cells were DENV-infected and treated with iminosugars. The relationship between antiviral efficacy and effect on TNF-α secretion (Figure 60B) was assessed (Table 25).

Table 25. Linear regression details for dendritic cell TNF-α and viral titre data (Figure 60B).

Primary monocyte-derived dendritic cells (donors as shown, assayed in technical triplicate) were infected with DENV and treated with iminosugar titrations. Supernatant was collected at 48 hours post-infection, and TNF-α secretion and viral titre quantified. Values were normalised to untreated for each donor and corresponding points plotted against each other. Linear regression was used to find lines of best-fit, with associations assessed by Pearson correlation. Samples were generated and viral titres quantified by Nilanka Perera. Cytokine assay and data analysis were by Beatrice Tyrrell.

Donor	Iminosugar	Equation	R^2 value	Pearson r	P value
KR	2THO-DNJ	y = 0.7162x + 42.01	0.7088	0.8419	0.0355
KM	*N*N-DNJ	y = 0.6201x + 52.77	0.7355	0.8576	0.0290

8.17 PBMC cytokine production following DENV infection

In an effort to determine whether iminosugar treatment could impact the secretion of cytokines from a mixed population of immune cells, this was assessed in DENV-infected PBMCs. However, a very low level of TNF-α production was seen (Figure 120), with similarly low levels observed for IFN-α/β (data not shown), meaning that the effects of iminosugar treatment could not be assessed in this system.

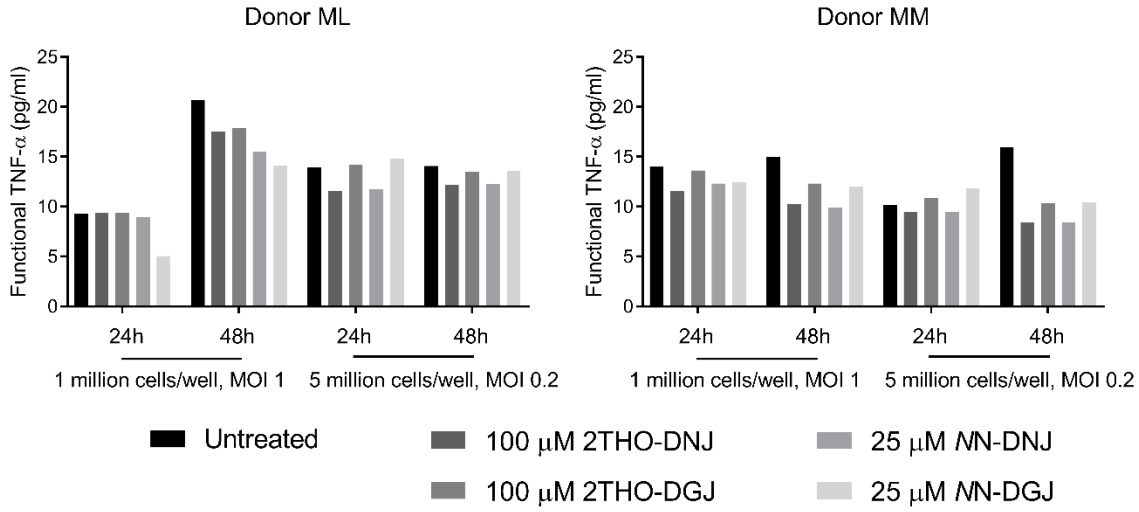

Figure 120. PBMCs make little TNF-α response to DENV infection.

PBMCs (donors as shown, assayed in technical triplicate) were infected with DENV using the protocol as shown, treated with iminosugar and supernatant collected after 24 or 48 hours as indicated. Functional TNF-α secretion was determined and the mean displayed.

8.18 Non-normalised cytokine secretion following MDMΦ stimulation with PAMPs

The effects of 2THO-DNJ, *N*N-DNJ and *N*N-DGJ on cytokine production elicited by stimulation of MDMΦs with a panel of PAMPs were assessed (Figure 70 and Figure 71). Few stimuli induced an IFN-α/β response (Figure 122), whereas most induced TNF-α production (Figure 121). DNJ-derivative iminosugars reduced production of both cytokines in response to all stimuli whereas *N*N-DGJ had more selective effects.

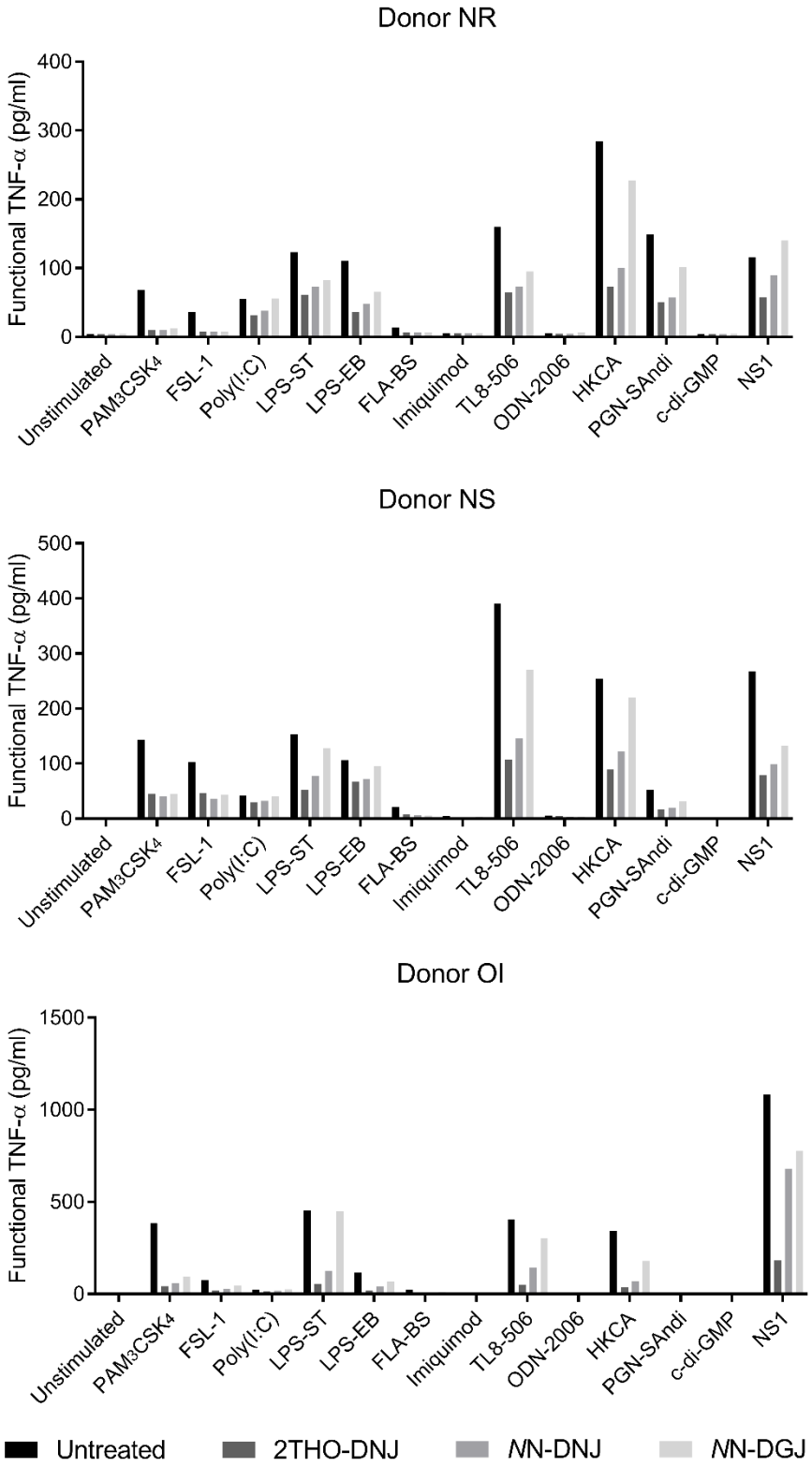

Figure 121. Iminosugars influence TNF-α secretion from MDMΦs elicited by a broad spectrum of PAMPs.

Primary MDMΦs (donors as shown, assayed in technical duplicate) were stimulated with PAMPs (2.5.1) and left untreated or treated with 100 µM 2THO-DNJ, 25 µM N*N-DNJ or 25 µM* N*N-DGJ.*

After 18 hours, supernatant was harvested and TNF-α secretion quantified by functional assay and the mean displayed.

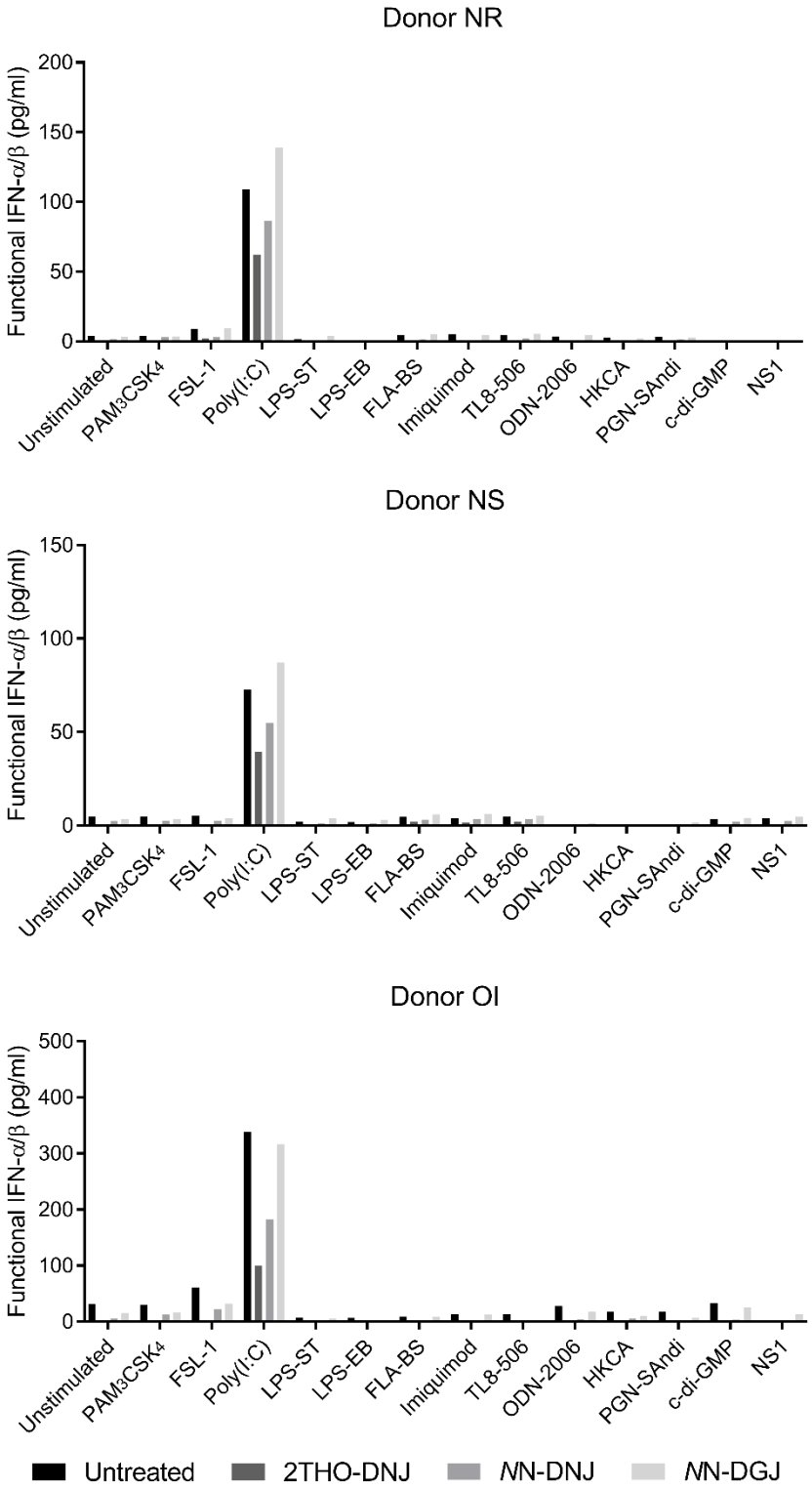

Figure 122. Iminosugars influence IFN-α/β secretion from MDMΦs elicited by a broad spectrum of PAMPs.

Primary MDMΦs (donors as shown, assayed in technical duplicate) were stimulated with PAMPs (2.5.1) and left untreated or treated with 100 µM 2THO-DNJ, 25 µM N*N-DNJ or 25 µM* N*N-DGJ. After 18 hours, supernatant was harvested and IFN-α/β secretion quantified by functional assay and the mean displayed.*

In order to explore the dependence of the effects of *N*N-DGJ on the TLR signalling adaptor molecules, peptide inhibitors of MyD88 and TRIF were used (Figure 72 and Figure 73). Cell viability after treatment with the peptide inhibitors was assessed: while there was no effect of the control peptide or the MyD88 inhibitor, the TRIF inhibitory peptide seemed to have a marked effect, reducing cell viability to approximately 70% of untreated (Figure 123).

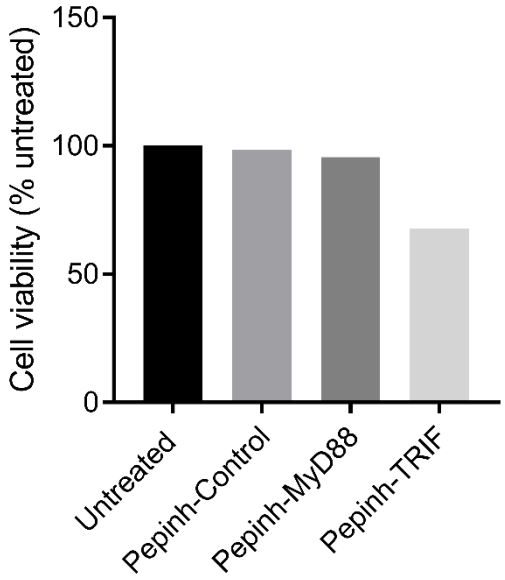

Figure 123. Pepinh-TRIF treatment significantly reduces MDMΦ cell viability.

Primary MDMΦs (donor OT, assayed in technical triplicate) were untreated or treated with peptide inhibitors of MyD88 (Pepinh-MyD88), TRIF (Pepinh-TRIF) or a control peptide (Pepinh-Control) at 50 µM for 6 hours, before dilution to 25 µM in X-VIVO for a further 18 hours. Cell viability was assessed by MTS assay and the mean displayed.

8.19 Supplementary information for multiplex cytokine analysis of PAMP-stimulated iminosugar-treated MDMΦs

The effects of iminosugar treatment on TNF-α, IFN-α2, IFN-γ and MCP-1 quantified by LEGENDplex assay were discussed in 6.3.5.4, as cytokines where at least one stimulation lead to a statistically significant increase in cytokine secretion in all three donors and a similar response pattern to iminosugar treatment was seen for at least two of the donors tested. Data for the remaining cytokines assayed are presented here. Significant cytokine secretion was induced by at least one stimulation, but a lack of consistent iminosugar effects was found for IL-8 (Figure 124), IL-10 (Figure 125), IL-12p70 (Figure 126) and IL-17A (Figure 127). For IL-6 (Figure 128), IL-18 (Figure 129) and IL-23 (Figure 130), consistent statistically significant responses to stimulations were lacking. Data obtained for IL-33 were highly variable, which may reflect a technical issue since the number of beads recovered in the assay representing IL-33 were lower than desirable (data not shown).

The significant degree of inter-donor variability meant that normalising and combining data from the donors for analysis obscured the response patterns to iminosugar treatment that could often be observed in two but not all three of the donors. Examples of this combined analysis are shown for LPS-EB (Figure 131) and TL8-506 (Figure 132) stimulation, since these stimuli lead to cytokine responses most frequently across all of the cytokines measured.

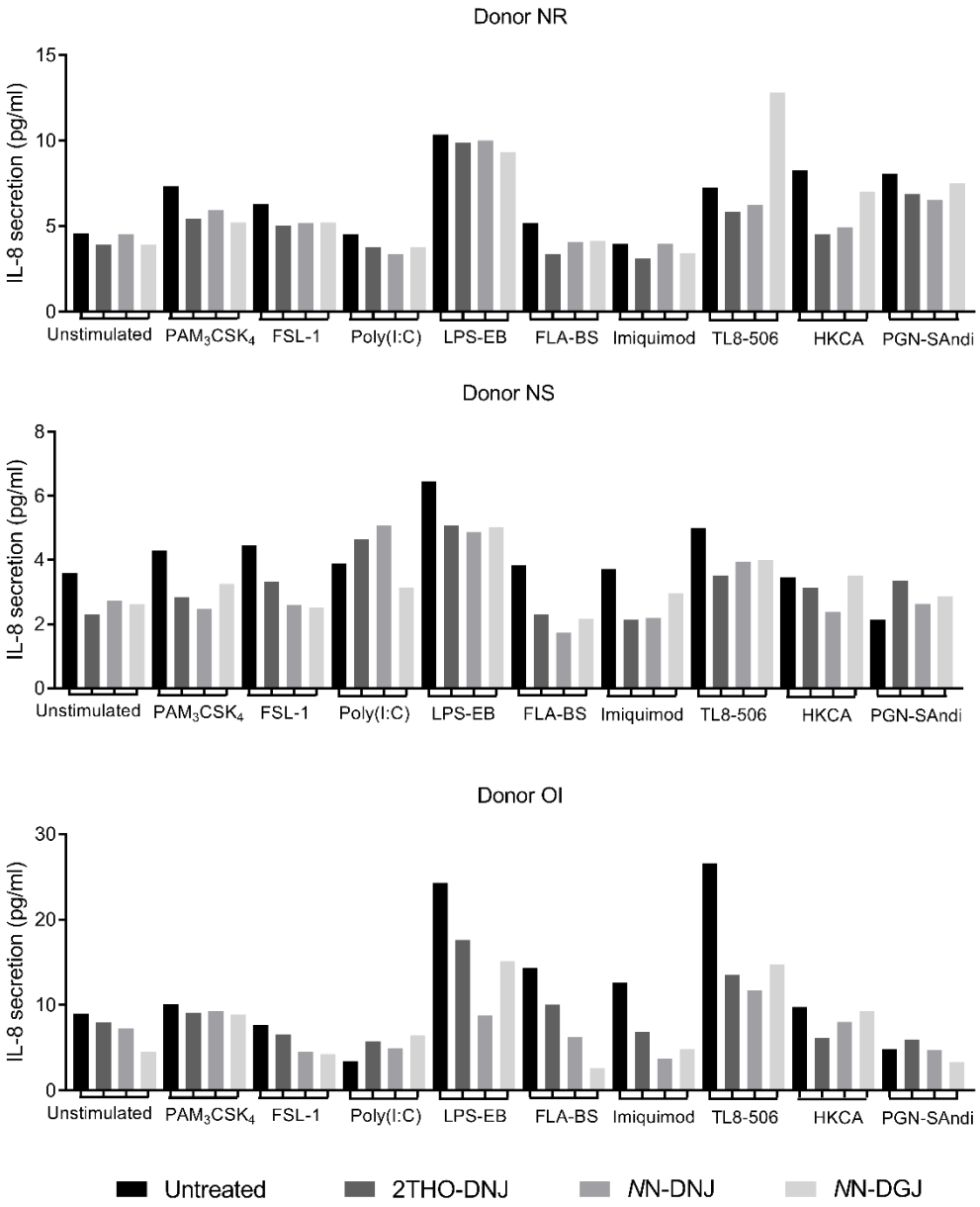

Figure 124. Iminosugar treatment can affect IL-8 secretion in response to PAMP stimulation of MDMΦs.

Primary MDMΦs (donors as shown) were stimulated with PAMPs (2.5.1) and left untreated or treated with 100 µM 2THO-DNJ, 25 µM N*N-DNJ or 25 µM* N*N-DGJ. After 18 hours, supernatant was harvested. IL-8 secretion was quantified by LEGENDplex assay and the mean plotted. Samples below the LOD are shown as 1.59 pg/ml for donor NS.*

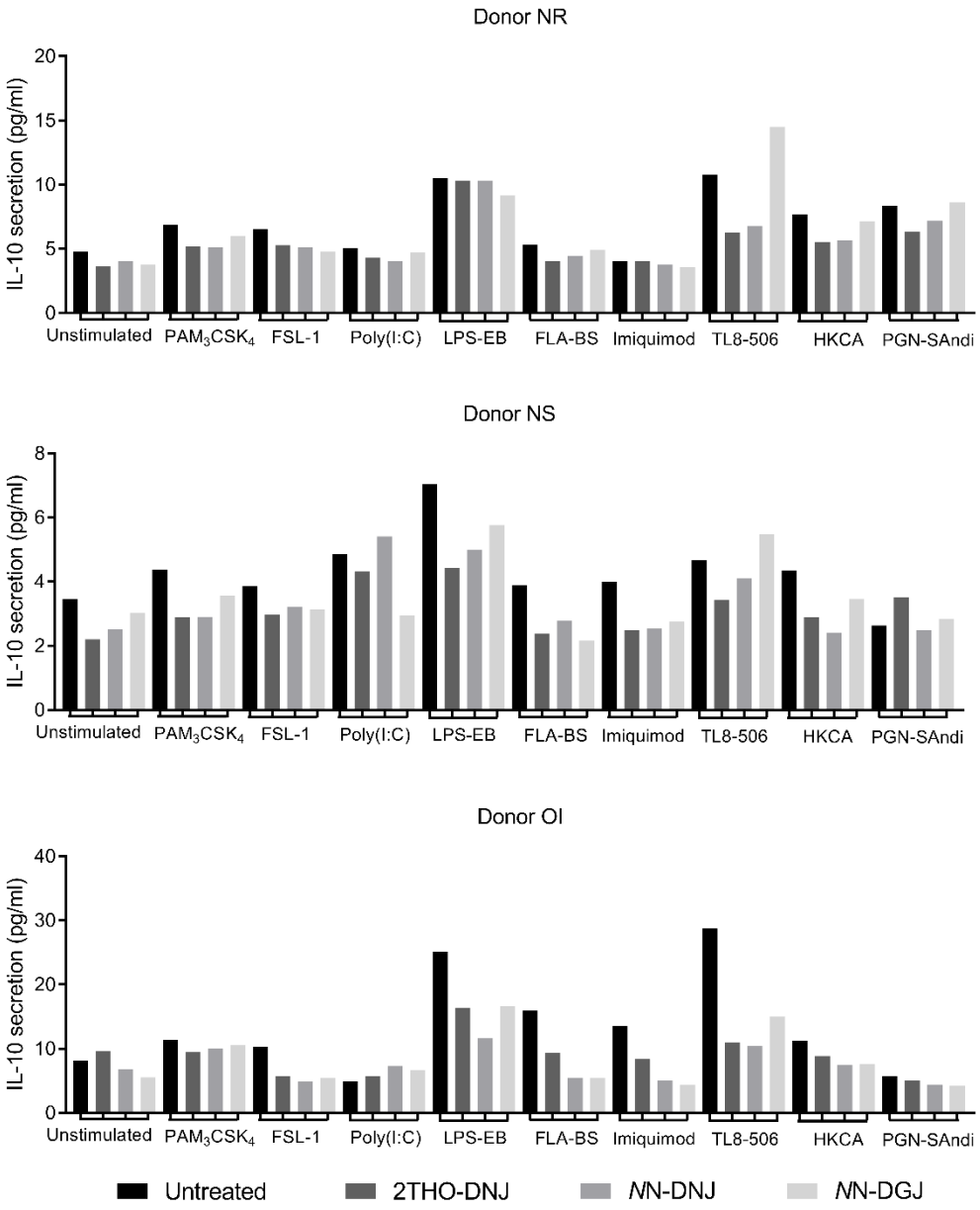

Figure 125. Iminosugar treatment can affect IL-10 secretion in response to PAMP stimulation of MDMΦs.

Primary MDMΦs (donors as shown) were stimulated with PAMPs (2.5.1) and left untreated or treated with 100 µM 2THO-DNJ, 25 µM N*N-DNJ or 25 µM* N*N-DGJ. After 18 hours, supernatant was harvested. IL-10 secretion was quantified by LEGENDplex assay and the mean plotted*

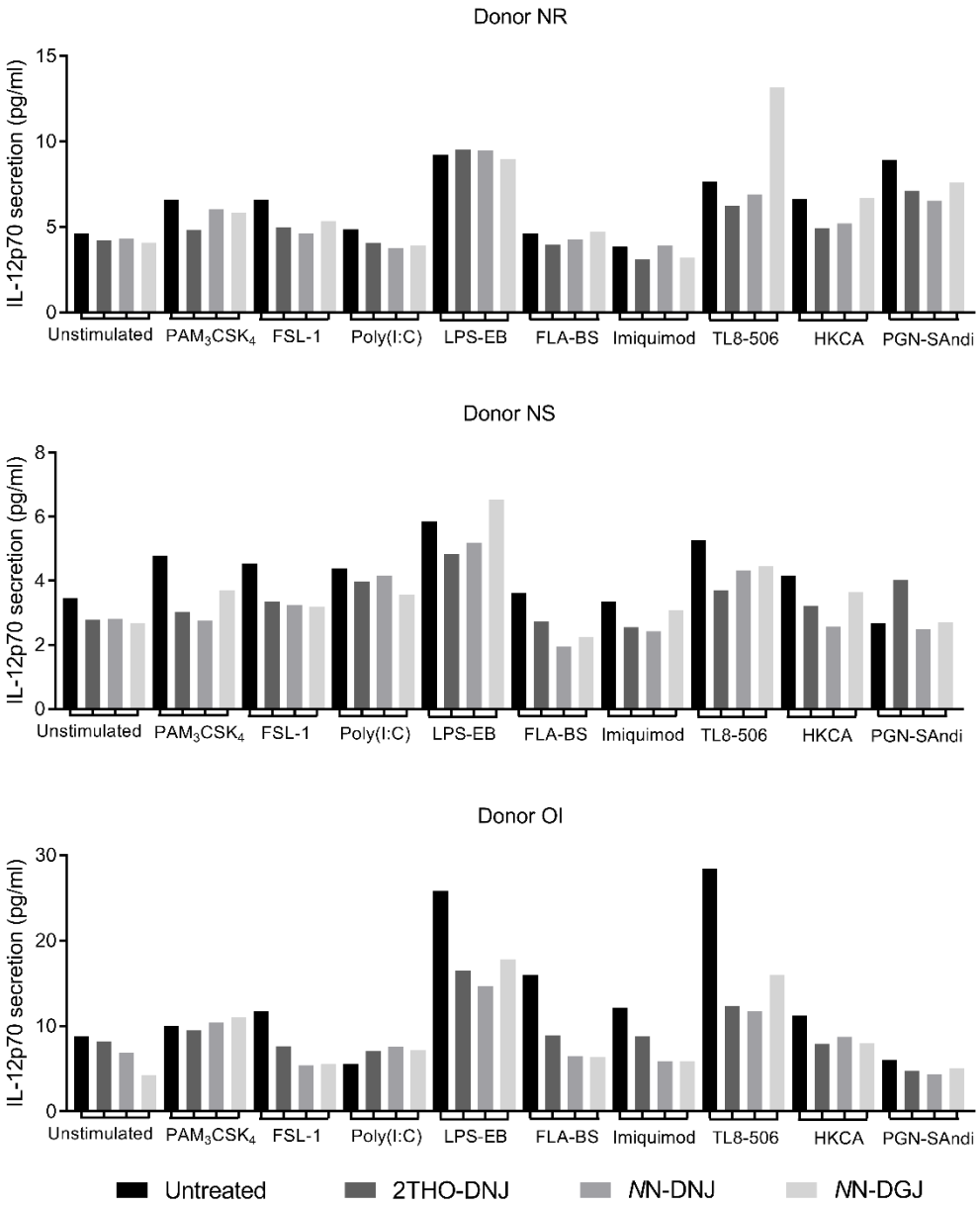

Figure 126. Iminosugar treatment can affect IL-12p70 secretion in response to PAMP stimulation of MDMΦs.

Primary MDMΦs (donors as shown) were stimulated with PAMPs (2.5.1) and left untreated or treated with 100 µM 2THO-DNJ, 25 µM NN*-DNJ or 25 µM* NN*-DGJ. After 18 hours, supernatant was harvested. IL-12p70 secretion was quantified by LEGENDplex assay and the mean plotted.*

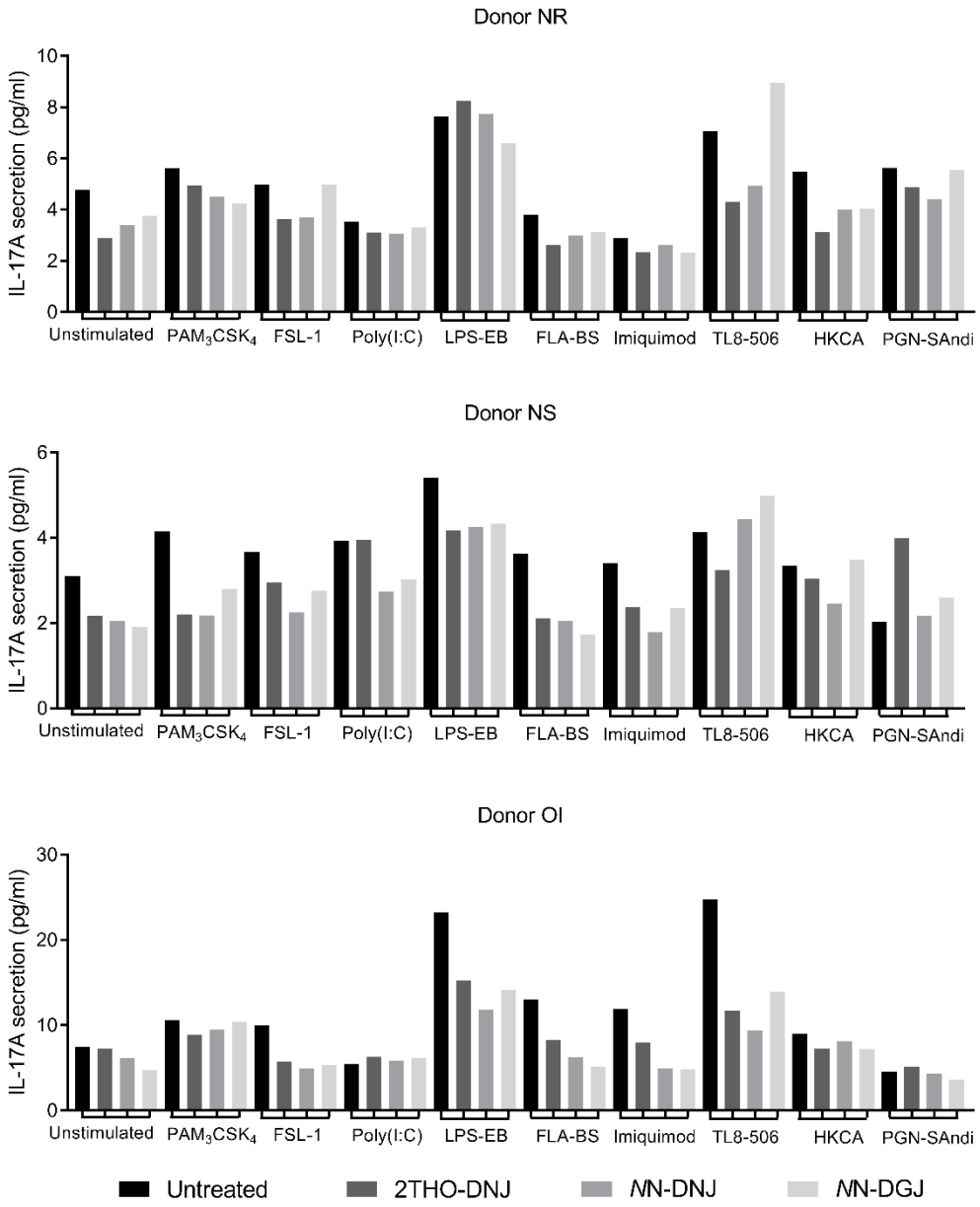

Figure 127. Iminosugar treatment can affect IL-17A secretion in response to PAMP stimulation of MDMΦs.

Primary MDMΦs (donors as shown) were stimulated with PAMPs (2.5.1) and left untreated or treated with 100 µM 2THO-DNJ, 25 µM NN*-DNJ or 25 µM* NN*-DGJ. After 18 hours, supernatant was harvested. IL-17A secretion was quantified by LEGENDplex assay and the mean plotted. Samples below the LOD are shown as 1.58 pg/ml for donor NS.*

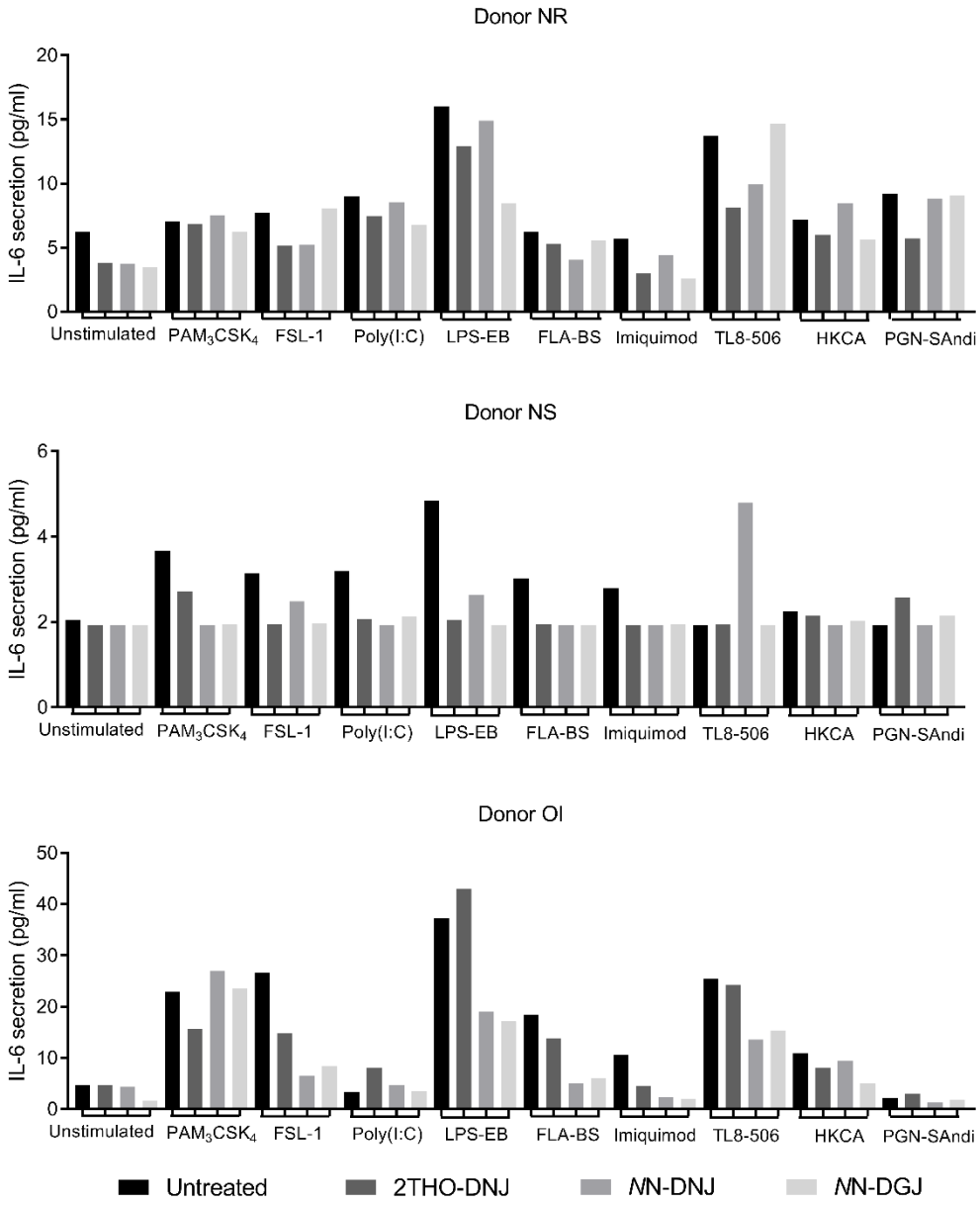

Figure 128. Iminosugar treatment can affect IL-6 secretion in response to PAMP stimulation of MDMΦs.

Primary MDMΦs (donors as shown) were stimulated with PAMPs (2.5.1) and left untreated or treated with 100 µM 2THO-DNJ, 25 µM NN*-DNJ or 25 µM* NN*-DGJ. After 18 hours, supernatant was harvested. IL-6 secretion was quantified by LEGENDplex assay and the mean plotted. Samples below the LOD are shown as 1.93 pg/ml for donor NS.*

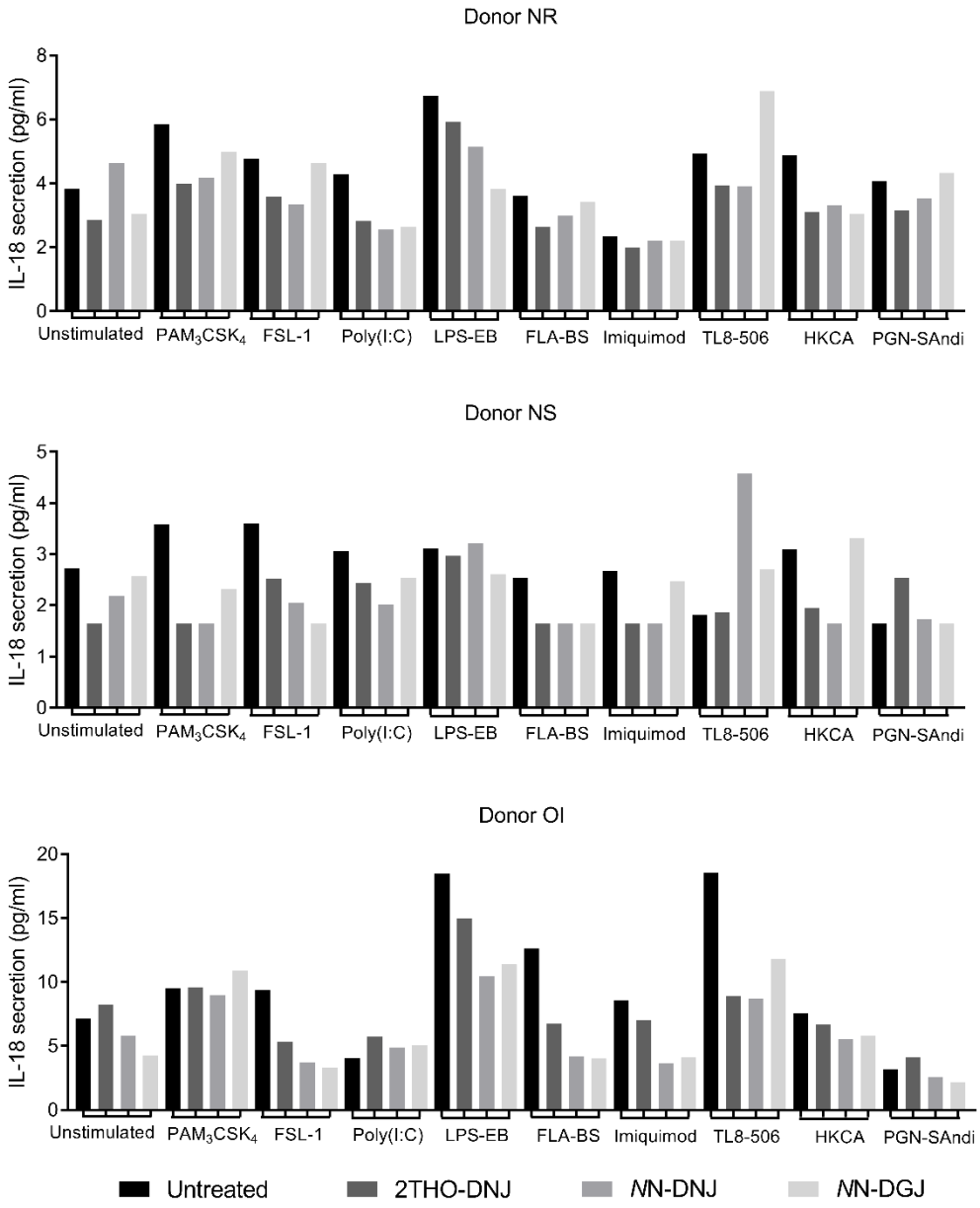

Figure 129. Iminosugar treatment can affect IL-18 secretion in response to PAMP stimulation of MDMΦs.

Primary MDMΦs (donors as shown) were stimulated with PAMPs (2.5.1) and left untreated or treated with 100 µM 2THO-DNJ, 25 µM N*N-DNJ or 25 µM* N*N-DGJ. After 18 hours, supernatant was harvested. IL-18 secretion was quantified by LEGENDplex assay and the mean plotted. Samples below the LOD are shown as 1.65 pg/ml for donor NS.*

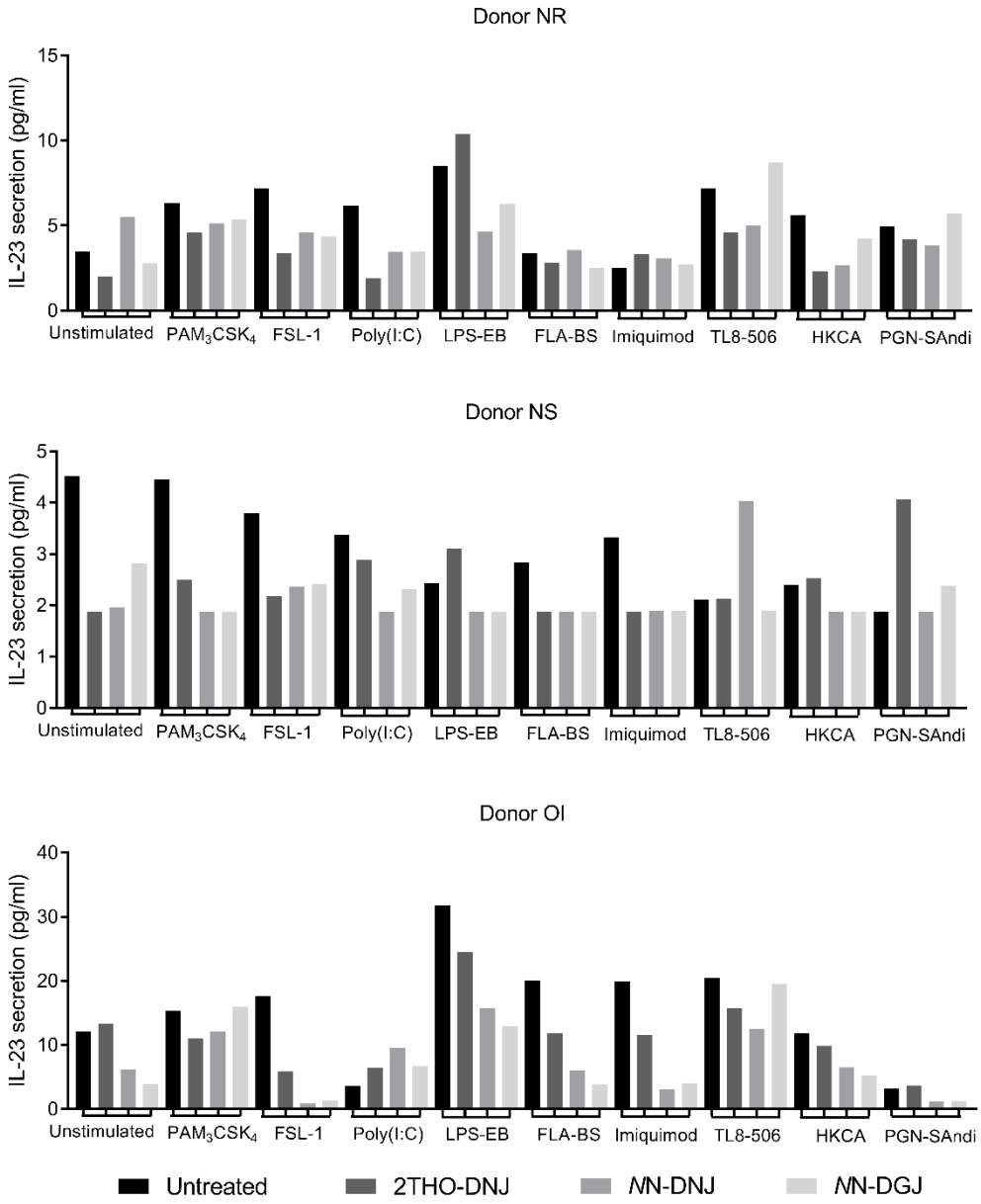

Figure 130. Iminosugar treatment can affect IL-23 secretion in response to PAMP stimulation of MDMΦs.

Primary MDMΦs (donors as shown) were stimulated with PAMPs (2.5.1) and left untreated or treated with 100 µM 2THO-DNJ, 25 µM NN*-DNJ or 25 µM* NN*-DGJ. After 18 hours, supernatant was harvested. IL-23 secretion was quantified by LEGENDplex assay and the mean plotted. Samples below the LOD are shown as 1.88 and 0.29 pg/ml for donors NS and OI, respectively.*

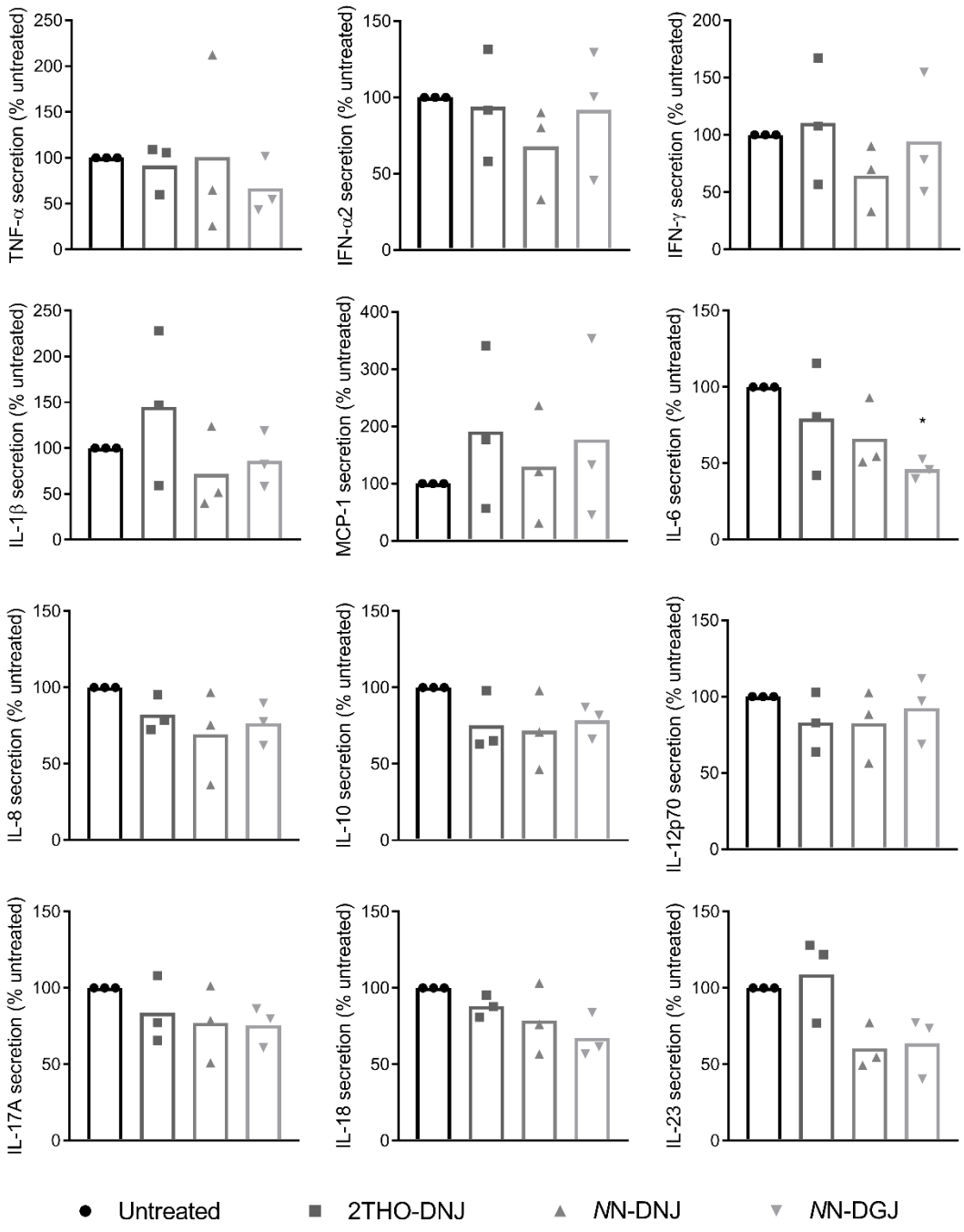

Figure 131. Inter-donor variation obscures iminosugar effects on cytokine secretion in response to LPS-EB stimulation of MDMΦs.

Primary MDMΦs (n=3 donors (NR, NS, OI)) were stimulated with 100 ng/ml LPS-EB (2.5.1) and left untreated or treated with 100 µM 2THO-DNJ, 25 µM NN*-DNJ or 25 µM* NN*-DGJ. After 18 hours, supernatant was harvested. Secretion of cytokines as shown was quantified by LEGENDplex assay, normalised to the no iminosugar (untreated) condition for each donor, and the mean displayed (bars show the mean of the donors). Statistical analysis is by one-way ANOVA with Dunnett's multiple comparisons test (*, p<0.05).*

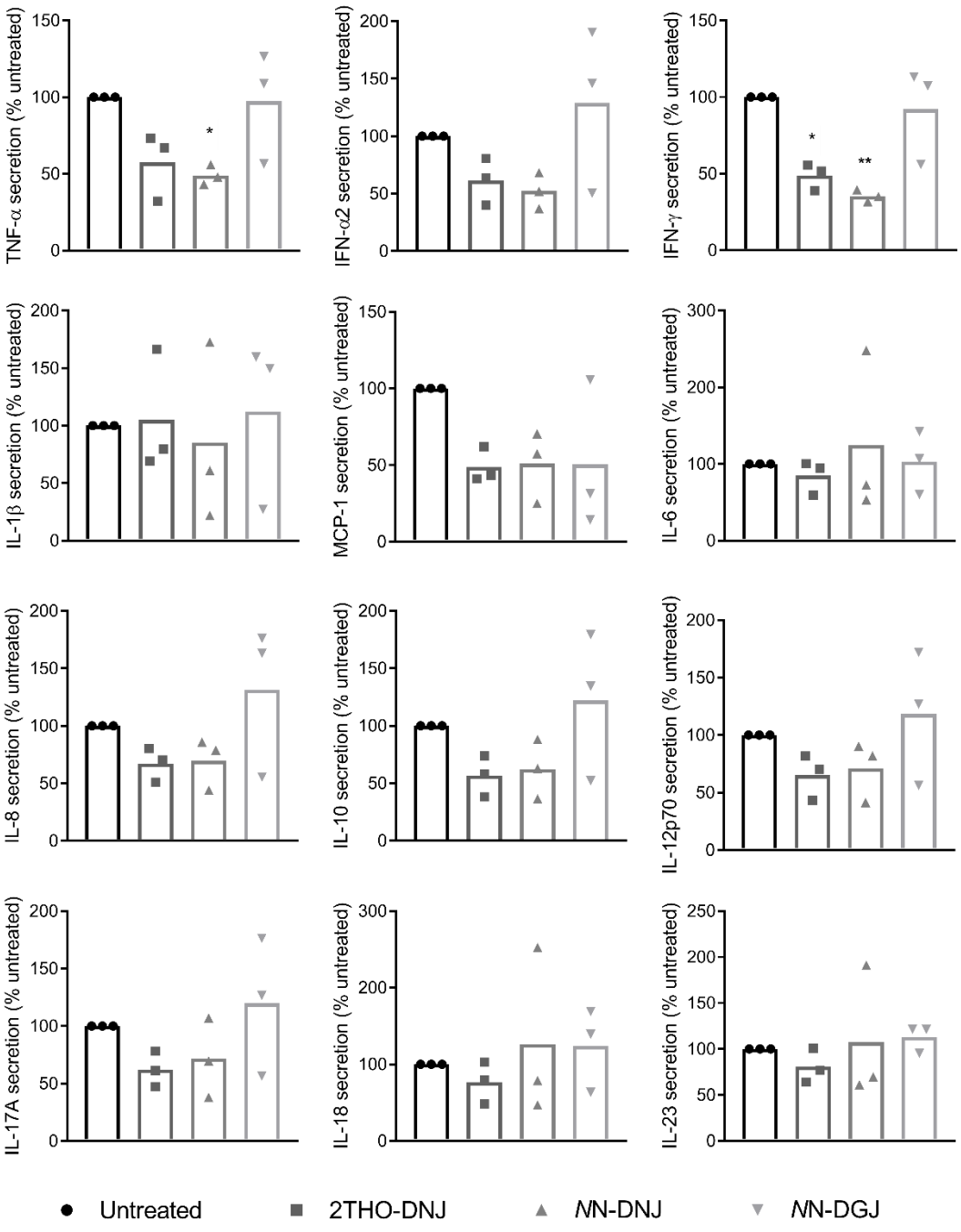

Figure 132. Inter-donor variation obscures iminosugar effects on cytokine secretion in response to TL8-506 stimulation of MDMΦs.

Primary MDMΦs (n=3 donors (NR, NS, OI)) were stimulated with TL8-506 (2.5.1) and left untreated or treated with 100 µM 2THO-DNJ, 25 µM N*N-DNJ or 25 µM* N*N-DGJ. After 18 hours, supernatant was harvested. Secretion of cytokines as shown was quantified by LEGENDplex assay, normalised to the no iminosugar (untreated) condition for each donor, and the mean displayed (bars show the mean of the donors). Statistical analysis is by one-way ANOVA with Dunnett's multiple comparisons test (*, p<0.05).*

Chapter 9. References

1. Centers for Disease Control and Prevention. *Viral hemorrhagic fevers fact sheet.* 2013; Available from: http://www.cdc.gov/ncidod/dvrd/spb/mnpages/dispages/Fact_Sheets/Viral_Hemorrhagic_Fevers_Fact_Sheet.pdf.
2. Krauer, F., et al., *Zika virus infection as a cause of congenital brain abnormalities and Guillain–Barré syndrome: systematic review.* PLoS Medicine, 2017. **14**(1): p. e1002203.
3. World Health Organization. *2018 Annual review of diseases prioritized under the Research and Development Blueprint*. WHO Research and Development Blueprint 2018; Available from: https://www.who.int/blueprint/priority-diseases/en/.
4. Gubler, D.J., Kuno, G. and Markoff, L., *Flaviviruses*, in *Fields Virology*, D.M. Knipe and P.M. Howley, Editors. 2007, Wolters Kluwer Health / Lippincott Williams & Wilkins: London. p. 1154-252.
5. Calisher, C.H., et al., *Antigenic relationships between flaviviruses as determined by cross-neutralization tests with polyclonal antisera.* Journal of General Virology, 1989. **70**(1): p. 37-43.
6. Mustafa, M.S., et al., *Discovery of fifth serotype of dengue virus (DENV-5): a new public health dilemma in dengue control.* Medical Journal Armed Forces India, 2015. **71**(1): p. 67-70.
7. Miller, J.L., et al., *The mannose receptor mediates dengue virus infection of macrophages.* PLoS Pathogens, 2008. **4**(2): p. e17.
8. Tassaneetrithep, B., et al., *DC-SIGN (CD209) mediates dengue virus infection of human dendritic cells.* The Journal of Experimental Medicine, 2003. **197**(7): p. 823-9.
9. Navarro-Sanchez, E., et al., *Dendritic-cell-specific ICAM3-grabbing non-integrin is essential for the productive infection of human dendritic cells by mosquito-cell-derived dengue viruses.* EMBO Reports, 2003. **4**(7): p. 723-8.
10. Lo, Y.L., et al., *Dengue virus infection is through a cooperative interaction between a mannose receptor and CLEC5A on macrophage as a multivalent hetero-complex.* PLoS ONE, 2016. **11**(11): p. e0166474.
11. Chen, Y., et al., *Dengue virus infectivity depends on envelope protein binding to target cell heparan sulfate.* Nature Medicine, 1997. **3**(8): p. 866-71.
12. Reyes-del Valle, J., et al., *Heat shock protein 90 and heat shock protein 70 are components of dengue virus receptor complex in human cells.* Journal of Virology, 2005. **79**(8): p. 4557-67.
13. Meertens, L., et al., *The TIM and TAM families of phosphatidylserine receptors mediate dengue virus entry.* Cell Host & Microbe, 2012. **12**(4): p. 544-57.
14. Ayala-Nunez, N.V., et al., *How antibodies alter the cell entry pathway of dengue virus particles in macrophages.* Scientific Reports, 2016. **6**: p. 28768.
15. Flipse, J., et al., *Antibody-dependent enhancement of dengue virus infection in primary human macrophages; balancing higher fusion against antiviral responses.* Scientific Reports, 2016. **6**: p. 29201.
16. Flipse, J., Wilschut, J. and Smit, J.M., *Molecular mechanisms involved in antibody-dependent enhancement of dengue virus infection in humans.* Traffic, 2013. **14**(1): p. 25-35.
17. Cruz-Oliveira, C., et al., *Receptors and routes of dengue virus entry into the host cells.* FEMS Microbiology Reviews, 2015. **39**(2): p. 155-70.
18. van der Schaar, H.M., et al., *Dissecting the cell entry pathway of dengue virus by single-particle tracking in living cells.* PLoS Pathogens, 2008. **4**(12): p. e1000244.

19. Acosta Eliana, G., Castilla, V. and Damonte Elsa, B., *Alternative infectious entry pathways for dengue virus serotypes into mammalian cells.* Cellular Microbiology, 2009. **11**(10): p. 1533-49.
20. van der Schaar, H.M., et al., *Characterization of the early events in dengue virus cell entry by biochemical assays and single-virus tracking.* Journal of Virology, 2007. **81**(21): p. 12019-28.
21. Welsch, S., Miller, S. and Romero-Brey, I., *Composition and three-dimensional architecture of the dengue virus replication and assembly sites.* Cell Host & Microbe, 2009. **5**(4): p. 365-75.
22. Kuhn, R.J., et al., *Structure of dengue virus: implications for flavivirus organization, maturation, and fusion.* Cell, 2002. **108**(5): p. 717-25.
23. Zhang, W., et al., *Visualization of membrane protein domains by cryo-electron microscopy of dengue virus.* Nature Structural Biology, 2003. **10**: p. 907.
24. Yu, I.M., et al., *Structure of the immature dengue virus at low pH primes proteolytic maturation.* Science, 2008. **319**(5871): p. 1834-7.
25. Zhang, Y., et al., *Structures of immature flavivirus particles.* The EMBO Journal, 2003. **22**(11): p. 2604-13.
26. Richter, M.K.S., et al., *Immature dengue virus is infectious in human immature dendritic cells via interaction with the receptor molecule DC-SIGN.* PLoS ONE, 2014. **9**(6): p. e98785.
27. Rodenhuis-Zybert, I.A., et al., *Immature dengue virus: a veiled pathogen?* PLoS Pathogens, 2010. **6**(1): p. e1000718.
28. Dejnirattisai, W., et al., *Cross-reacting antibodies enhance dengue virus infection in humans.* Science, 2010. **328**(5979): p. 745-8.
29. Wirawan, M., et al., *Mechanism of enhanced immature dengue virus attachment to endosomal membrane induced by prM antibody.* Structure, 2018. **27**(2): p. 253-67.
30. Rodenhuis-Zybert, I.A., et al., *A fusion-loop antibody enhances the infectious properties of immature flavivirus particles.* Journal of Virology, 2011. **85**(22): p. 11800-8.
31. da Silva Voorham, J.M., et al., *Antibodies against the envelope glycoprotein promote infectivity of immature dengue virus serotype 2.* PLoS ONE, 2012. **7**(3): p. e29957.
32. Yap, S.S.L., et al., *Dengue virus glycosylation: what do we know?* Frontiers in Microbiology, 2017. **8**: p. 1415.
33. Kuhn, R.J., et al., *Structure of dengue virus: implications for flavivirus organization, maturation, and fusion.* Cell, 2002. **108**(5): p. 717-25.
34. Zhang, X., et al., *Cryo-EM structure of the mature dengue virus at 3.5-Å resolution.* Nature Structural & Molecular Biology, 2012. **20**: p. 105-10.
35. Pokidysheva, E., et al., *Cryo-EM reconstruction of dengue virus in complex with the carbohydrate recognition domain of DC-SIGN.* Cell, 2006. **124**(3): p. 485-93.
36. Mondotte, J.A., et al., *Essential role of dengue virus envelope protein N glycosylation at asparagine-67 during viral propagation.* Journal of Virology, 2007. **81**(13): p. 7136-48.
37. Bryant, J.E., et al., *Glycosylation of the dengue 2 virus E protein at N67 is critical for virus growth in vitro but not for growth in intrathoracically inoculated Aedes aegypti mosquitoes.* Virology, 2007. **366**(2): p. 415-23.
38. Lee, E., et al., *Both E protein glycans adversely affect dengue virus infectivity but are beneficial for virion release.* Journal of Virology, 2010. **84**(10): p. 5171-80.
39. Beasley, D.W.C., et al., *Envelope protein glycosylation status influences mouse neuroinvasion phenotype of genetic lineage 1 West Nile virus strains.* Journal of Virology, 2005. **79**(13): p. 8339-47.
40. Miagostovich, M.P., et al., *Retrospective study on dengue fatal cases.* Clinical Neuropathology, 1997. **16**(4): p. 204-8.

41. Ramos, C., et al., *Dengue virus in the brain of a fatal case of hemorrhagic dengue fever.* Journal of Neurovirology, 1998. **4**(4): p. 465-8.
42. Johnson, A.J., Guirakhoo, F. and Roehrig, J.T., *The envelope glycoproteins of dengue 1 and dengue 2 viruses grown in mosquito cells differ in their utilization of potential glycosylation sites.* Virology, 1994. **203**(2): p. 241-9.
43. Smith, G.W. and P.J. Wright, *Synthesis of proteins and glycoproteins in dengue type 2 virus-infected vero and Aedes albopictus cells.* Journal of General Virology, 1985. **66**: p. 559-71.
44. Lei, Y., et al., *Characterization of N-glycan structures on the surface of mature dengue 2 virus derived from insect cells.* PLoS ONE, 2015. **10**(7): p. e0132122.
45. Hacker, K., White, L., and de Silva, A.M., *N-linked glycans on dengue viruses grown in mammalian and insect cells.* Journal of General Virology, 2009. **90**(9): p. 2097-106.
46. Jarvis, D.L., *Developing baculovirus-insect cell expression systems for humanized recombinant glycoprotein production.* Virology, 2003. **310**(1): p. 1-7.
47. Feinberg, H., et al., *Structural basis for selective recognition of oligosaccharides by DC-SIGN and DC-SIGNR.* Science, 2001. **294**(5549): p. 2163-6.
48. Mitchell, D.A., Fadden, A.J. and Drickamer, K., *A novel mechanism of carbohydrate recognition by the C-type lectins DC-SIGN and DC-SIGNR: subunit organization and binding to multivalent ligands.* Journal of Biological Chemistry, 2001. **276**(31): p. 28939-45.
49. Dubayle, J., et al., *Site-specific characterization of envelope protein N-glycosylation on Sanofi Pasteur's tetravalent CYD dengue vaccine.* Vaccine, 2015. **33**(11): p. 1360-8.
50. Gallichotte, E.N., et al., *Genetic variation between dengue virus type 4 strains impacts human antibody binding and neutralization.* Cell Reports, 2018. **25**(5): p. 1214-24.
51. Courageot, M.P., et al., *α-Glucosidase inhibitors reduce dengue virus production by affecting the initial steps of virion morphogenesis in the endoplasmic reticulum.* Journal of Virology, 2000. **74**(1): p. 564-72.
52. Lorenz, I.C., et al., *Folding and dimerization of tick-borne encephalitis virus envelope proteins prM and E in the endoplasmic reticulum.* Journal of Virology, 2002. **76**(11): p. 5480-91.
53. Zai, J., et al., *N-glycosylation of the premembrane protein of Japanese encephalitis virus is critical for folding of the envelope protein and assembly of virus-like particles.* Acta Virologica, 2013. **57**(1): p. 27-33.
54. Yu, I.M., et al., *Structure of the immature dengue virus at low pH primes proteolytic maturation.* Science, 2008. **319**(5871): p. 1834-7.
55. Slon Campos, J.L., Mongkolsapaya, J. and Screaton, G.R., *The immune response against flaviviruses.* Nature Immunology, 2018. **19**(11): p. 1189-98.
56. Després, P., Frenkiel, M.P., and Deubel, V., *Differences between cell membrane fusion activities of two dengue type-1 isolates reflect modifications of viral structure.* Virology, 1993. **196**(1): p. 209-19.
57. Markoff, L., *In vitro processing of dengue virus structural proteins: cleavage of the pre-membrane protein.* Journal of Virology, 1989. **63**(8): p. 3345-52.
58. Wu, S.F., et al., *Antiviral effects of an iminosugar derivative on flavivirus infections.* Journal of Virology, 2002. **76**(8): p. 3596-604.
59. Muller, D.A. and Young, P.R., *The flavivirus NS1 protein: molecular and structural biology, immunology, role in pathogenesis and application as a diagnostic biomarker.* Antiviral Research, 2013. **98**(2): p. 192-208.
60. Glasner, D.R., et al., *The good, the bad, and the shocking: the multiple roles of dengue virus nonstructural protein 1 in protection and pathogenesis.* Annual Review of Virology, 2018. **5**(1): p. 227-53.

61. Mackenzie, J.M., Jones, M.K. and Young, P.R., *Immunolocalization of the dengue virus nonstructural glycoprotein NS1 suggests a role in viral RNA replication.* Virology, 1996. **220**(1): p. 232-40.
62. Akey, D.L., Brown, W.C. and Dutta, S., *Flavivirus NS1 structures reveal surfaces for associations with membranes and the immune system.* Science, 2014. **343**(6173): p. 881-5.
63. Noisakran, S., et al., *Identification of human hnRNP C1/C2 as a dengue virus NS1-interacting protein.* Biochemical and Biophysical Research Communications, 2008. **372**(1): p. 67-72.
64. Kanlaya, R., et al., *Vimentin interacts with heterogeneous nuclear ribonucleoproteins and dengue nonstructural protein 1 and is important for viral replication and release.* Molecular BioSystems, 2010. **6**(5): p. 795-806.
65. Cervantes-Salazar, M., et al., *Dengue virus NS1 protein interacts with the ribosomal protein RPL18: This interaction is required for viral translation and replication in Huh-7 cells.* Virology, 2015. **484**: p. 113-26.
66. Alcon, S., et al., *Enzyme-linked immunosorbent assay specific to dengue virus type 1 nonstructural protein NS1 reveals circulation of the antigen in the blood during the acute phase of disease in patients experiencing primary or secondary infections.* Journal of Clinical Microbiology, 2002. **40**(2): p. 376-81.
67. Libraty, D.H., et al., *High circulating levels of the dengue virus nonstructural protein NS1 early in dengue illness correlate with the development of dengue hemorrhagic fever.* Journal of Infectious Diseases, 2002. **186**(8): p. 1165-8.
68. Falconar, A.K., *The dengue virus nonstructural-1 protein (NS1) generates antibodies to common epitopes on human blood clotting, integrin/adhesin proteins and binds to human endothelial cells: potential implications in haemorrhagic fever pathogenesis.* Archives of Virology, 1997. **142**(5): p. 897-916.
69. Avirutnan, P., et al., *Vascular leakage in severe dengue virus infections: a potential role for the nonstructural viral protein NS1 and complement.* The Journal of Infectious Diseases, 2006. **193**(8): p. 1078-88.
70. Cheng, H.J., et al., *Anti-dengue virus nonstructural protein 1 antibodies recognize protein disulfide isomerase on platelets and inhibit platelet aggregation.* Molecular Immunology, 2009. **47**(2): p. 398-406.
71. Lien, T.S., et al., *Dengue virus and antiplatelet autoantibodies synergistically induce haemorrhage through Nlrp3-inflammasome and FcgammaRIII.* Journal of Thrombosis and Haemostasis, 2015. **113**(5): p. 1060-70.
72. Sun, D.S., et al., *Antiplatelet autoantibodies elicited by dengue virus non-structural protein 1 cause thrombocytopenia and mortality in mice.* Journal of Thrombosis and Haemostasis, 2007. **5**(11): p. 2291-9.
73. Lin, C.F., et al., *Antibodies from dengue patient sera cross-react with endothelial cells and induce damage.* Journal of Medical Virology, 2003. **69**(1): p. 82-90.
74. Beatty, P.R., et al., *Dengue virus NS1 triggers endothelial permeability and vascular leak that is prevented by NS1 vaccination.* Science Translational Medicine, 2015. **7**(304): p. 304ra141.
75. Modhiran, N., Watterson, D. and Muller, D.A., *Dengue virus NS1 protein activates cells via Toll-like receptor 4 and disrupts endothelial cell monolayer integrity.* Science Translational Medicine, 2015. **7**(304): p. 304ra142.
76. Adikari, T.N., et al., *Dengue NS1 antigen contributes to disease severity by inducing interleukin (IL)-10 by monocytes.* Clinical & Experimental Immunology, 2016. **184**(1): p. 90-100.
77. Malavige, G.N., et al., *Suppression of virus specific immune responses by IL-10 in acute dengue infection.* PLoS Neglected Tropical Diseases, 2013. **7**(9): p. e2409.

78. Puerta-Guardo, H., Glasner, D.R., and Harris, E., *Dengue virus NS1 disrupts the endothelial glycocalyx, leading to hyperpermeability.* PLoS Pathogens, 2016. **12**(7): p. e1005738.
79. Malavige, G.N. and Ogg, G.S., *Pathogenesis of vascular leak in dengue virus infection.* Immunology, 2017. **151**(3): p. 261-9.
80. Jayathilaka, D., et al., *Role of NS1 antibodies in the pathogenesis of acute secondary dengue infection.* Nature Communications, 2018. **9**(1): p. 5242.
81. Winkler, G., et al., *Evidence that the mature form of the flavivirus nonstructural protein NS1 is a dimer.* Virology, 1988. **162**(1): p. 187-96.
82. Putnak, J.R., et al., *Functional and antigenic domains of the dengue-2 virus nonstructural glycoprotein NS-1.* Virology, 1988. **163**(1): p. 93-103.
83. Flamand, M., et al., *Dengue virus type 1 nonstructural glycoprotein NS1 is secreted from mammalian cells as a soluble hexamer in a glycosylation-dependent fashion.* Journal of Virology, 1999. **73**(7): p. 6104.
84. Pryor, M.J. and Wright, P.J., *Glycosylation mutants of dengue virus NS1 protein.* Journal of General Virology, 1994. **75**: p. 1183-7.
85. Fan, J., Liu, Y. and Yuan, Z., *Critical role of dengue virus NS1 protein in viral replication.* Virologica Sinica, 2014. **29**(3): p. 162-9.
86. Crabtree, M.B., Kinney, R.M. and Miller, B.R., *Deglycosylation of the NS1 protein of dengue 2 virus, strain 16681: construction and characterization of mutant viruses.* Archives of Virology, 2005. **150**(4): p. 771-86.
87. Tajima, S., Takasaki, T. and Kurane, I., *Characterization of Asn130-to-Ala mutant of dengue type 1 virus NS1 protein.* Virus Genes, 2008. **36**(2): p. 323-9.
88. Pryor, M.J., et al., *Growth restriction of dengue virus type 2 by site-specific mutagenesis of virus-encoded glycoproteins.* Journal of General Virology, 1998. **79**(11): p. 2631-9.
89. Somnuke, P., et al., *N-linked glycosylation of dengue virus NS1 protein modulates secretion, cell-surface expression, hexamer stability, and interactions with human complement.* Virology, 2011. **413**(2): p. 253-64.
90. Umareddy, I., et al., *Dengue virus NS4B interacts with NS3 and dissociates it from single-stranded RNA.* Journal of General Virology, 2006. **87**(9): p. 2605-14.
91. Kaufusi, P.H., et al., *Induction of endoplasmic reticulum-derived replication-competent membrane structures by West Nile virus non-structural protein 4B.* PLoS ONE, 2014. **9**(1): p. e84040.
92. Egger, D., et al., *Expression of hepatitis C virus proteins induces distinct membrane alterations including a candidate viral replication complex.* Journal of Virology, 2002. **76**(12): p. 5974-84.
93. Naik, N.G. and Wu, H.N., *Mutation of putative N-glycosylation sites on dengue virus NS4B decreases RNA replication.* Journal of Virology, 2015. **89**(13): p. 6746-60.
94. Brady, O.J., et al., *Refining the global spatial limits of dengue virus transmission by evidence-based consensus.* PLoS Neglected Tropical Diseases, 2012. **6**(8): p. e1760.
95. Bhatt, S., et al., *The global distribution and burden of dengue.* Nature, 2013. **496**(7446): p. 504-7.
96. Basurko, C., et al., *Estimating the risk of vertical transmission of dengue: a prospective study.* American Journal of Tropical Medicine and Hygiene, 2018. **98**(6): p. 1826-32.
97. World Health Organization. *Dengue: guidelines for diagnosis, treatment, prevention and control*. 2009; Available from: http://apps.who.int/iris/bitstream/10665/44188/1/9789241547871_eng.pdf.
98. Katzelnick, L.C., Coloma, J. and Harris, E., *Dengue: knowledge gaps, unmet needs, and research priorities.* The Lancet Infectious Diseases, 2017. **17**(3): p. e88-100.

99. Mongkolsapaya, J., et al., *Original antigenic sin and apoptosis in the pathogenesis of dengue hemorrhagic fever.* Nature Medicine, 2003. **9**: p. 921-7.
100. Midgley, C.M., et al., *An in-depth analysis of original antigenic sin in dengue virus infection.* Journal of Virology, 2011. **85**(1): p. 410-21.
101. Schmid, M.A. and Harris, E., *Monocyte recruitment to the dermis and differentiation to dendritic cells increases the targets for dengue virus replication.* PLoS Pathogens, 2014. **10**(12): p. e1004541.
102. Wu, S.J.L., et al., *Human skin Langerhans cells are targets of dengue virus infection.* Nature Medicine, 2000. **6**: p. 816-20.
103. Cerny, D., et al., *Selective susceptibility of human skin antigen presenting cells to productive dengue virus infection.* PLoS Pathogens, 2014. **10**(12): p. e1004548.
104. Duangkhae, P., et al., *Interplay between keratinocytes and myeloid cells drives dengue virus spread in human skin.* Journal of Investigative Dermatology, 2018. **138**(3): p. 618-26.
105. Schmid, M.A., et al., *Mosquito saliva increases endothelial permeability in the skin, immune cell migration, and dengue pathogenesis during antibody-dependent enhancement.* PLoS Pathogens, 2016. **12**(6): p. e1005676.
106. Rathore, A.P.S. and St John, A.L., *Immune responses to dengue virus in the skin.* Open Biology, 2018. **8**(8): p. 180087.
107. Boppana, V.D., et al., *SAAG-4 is a novel mosquito salivary protein that programmes host CD4+ T cells to express IL-4.* Parasite Immunology, 2009. **31**(6): p. 287-95.
108. Zeidner, N.S., et al., *Mosquito feeding modulates Th1 and Th2 cytokines in flavivirus susceptible mice: an effect mimicked by injection of sialokinins, but not demonstrated in flavivirus resistant mice.* Parasite Immunology, 1999. **21**(1): p. 35-44.
109. Halstead, S.B., *Antibody, macrophages, dengue virus infection, shock, and hemorrhage: a pathogenetic cascade.* Reviews of Infectious Diseases, 1989. **11**(S4): p. S830-9.
110. Couvelard, A., et al., *Report of a fatal case of dengue infection with hepatitis: Demonstration of dengue antigens in hepatocytes and liver apoptosis.* Human Pathology, 1999. **30**(9): p. 1106-10.
111. Huerre, M.R., et al., *Liver histopathology and biological correlates in five cases of fatal dengue fever in Vietnamese children.* Virchows Arch: European Journal of Pathology, 2001. **438**(2): p. 107-15.
112. Jessie, K., et al., *Localization of dengue virus in naturally infected human tissues, by immunohistochemistry and in situ hybridization.* Journal of Infectious Diseases, 2004. **189**(8): p. 1411-8.
113. Aye, K.S., et al., *Pathologic highlights of dengue hemorrhagic fever in 13 autopsy cases from Myanmar.* Human Pathology, 2014. **45**(6): p. 1221-33.
114. Balsitis, S.J., et al., *Tropism of dengue virus in mice and humans defined by viral nonstructural protein 3-specific immunostaining.* The American Journal of Tropical Medicine and Hygiene, 2009. **80**(3): p. 416-24.
115. Seneviratne, S.L., Malavige, G.N. and de Silva, H.J., *Pathogenesis of liver involvement during dengue viral infections.* Transactions of The Royal Society of Tropical Medicine and Hygiene, 2006. **100**(7): p. 608-14.
116. King, A.D., et al., *B cells are the principal circulating mononuclear cells infected by dengue virus.* Southeast Asian Journal of Tropical Medicine and Public Health, 1999. **30**(4): p. 718-28.
117. Noisakran, S., et al., *Detection of dengue virus in platelets isolated from dengue patients.* Southeast Asian Journal of Tropical Medicine and Public Health, 2009. **40**(2): p. 253-62.
118. De La Cruz Hernández, S.I., et al., *A strong interferon response correlates with a milder dengue clinical condition.* Journal of Clinical Virology, 2014. **60**(3): p. 196-9.

119. Fagundes, C.T., et al., *IFN-γ production depends on IL-12 and IL-18 combined action and mediates host resistance to dengue virus infection in a nitric oxide-dependent manner.* PLoS Neglected Tropical Diseases, 2011. **5**(12): p. e1449.
120. Kurane, I., et al., *High levels of interferon alpha in the sera of children with dengue virus infection.* The American Journal of Tropical Medicine and Hygiene, 1993. **48**(2): p. 222-9.
121. Azeredo, E.L., et al., *Characterisation of lymphocyte response and cytokine patterns in patients with dengue fever.* Immunobiology, 2001. **204**(4): p. 494-507.
122. Libraty, D.H., et al., *Differing influences of virus burden and immune activation on disease severity in secondary dengue-3 virus infections.* The Journal of Infectious Diseases, 2002. **185**(9): p. 1213-21.
123. Malavige, G.N., et al., *Serum IL-10 as a marker of severe dengue infection.* BMC Infectious Diseases, 2013. **13**(1): p. 341.
124. Kumar, Y., et al., *Serum proteome and cytokine analysis in a longitudinal cohort of adults with primary dengue infection reveals predictive markers of DHF.* PLoS Neglected Tropical Diseases, 2012. **6**(11): p. e1887.
125. Mustafa, A.S., et al., *Elevated levels of interleukin-13 and IL-18 in patients with dengue hemorrhagic fever.* FEMS Immunology & Medical Microbiology, 2001. **30**(3): p. 229-33.
126. Hober, D., et al., *High levels of sTNFR p75 and TNFα in dengue-infected patients.* Microbiology and Immunology, 1996. **40**(8): p. 569-73.
127. Malavige, G.N., et al., *Cellular and cytokine correlates of severe dengue infection.* PLoS ONE, 2012. **7**(11): p. e50387.
128. de la Cruz Hernández, S.I., et al., *Primary dengue virus infections induce differential cytokine production in Mexican patients.* Memórias do Instituto Oswaldo Cruz, 2016. **111**: p. 161-7.
129. Valero, N., et al., *Differential induction of cytokines by human neonatal, adult, and elderly monocyte/macrophages infected with dengue virus.* Viral Immunology, 2014. **27**(4): p. 151-9.
130. Diamond, M.S., et al., *Modulation of dengue virus infection in human cells by alpha, beta, and gamma interferons.* Journal of Virology, 2000. **74**(11): p. 4957-66.
131. Shresta, S., et al., *Interferon-dependent immunity is essential for resistance to primary dengue virus infection in mice, whereas T- and B-cell-dependent immunity are less critical.* Journal of Virology, 2004. **78**(6): p. 2701-10.
132. Gomez, D. and Reich, N.C., *Stimulation of primary human endothelial cell proliferation by IFN.* The Journal of Immunology, 2003. **170**(11): p. 5373-81.
133. Liu, P., et al., *Dengue virus infection differentially regulates endothelial barrier function over time through type I interferon effects.* The Journal of Infectious Diseases, 2009. **200**(2): p. 191-201.
134. Aguirre, S., et al., *DENV inhibits type I IFN production in infected cells by cleaving human STING.* PLoS Pathogens, 2012. **8**(10): p. e1002934.
135. Morrison, J., Aguirre, S. and Fernandez-Sesma, A., *Innate immunity evasion by dengue virus.* Viruses, 2012. **4**(3): p. 397-413.
136. Royall, J.A., et al., *Tumor necrosis factor and interleukin 1 alpha increase vascular endothelial permeability.* American Journal of Physiology, 1989. **257**(6): p. 399-410.
137. Shresta, S., et al., *Murine model for dengue virus-induced lethal disease with increased vascular permeability.* Journal of Virology, 2006. **80**(20): p. 10208-17.
138. Fernandez-Mestre, M.T., et al., *TNF-alpha-308A allele, a possible severity risk factor of hemorrhagic manifestation in dengue fever patients.* Tissue Antigens, 2004. **64**(4): p. 469-72.

139. Perez, A.B., et al., *Tumor necrosis factor–alpha, transforming growth factor–β1, and interleukin-10 gene polymorphisms: implication in protection or susceptibility to dengue hemorrhagic fever.* Human Immunology, 2010. **71**(11): p. 1135-40.
140. Naing, C., et al., *Association of tumour necrosis factor-α (TNF-α) gene polymorphisms (-308 G>A and -238 G>A) and the risk of severe dengue: A meta-analysis and trial sequential analysis.* PLoS ONE, 2018. **13**(10): p. e0205413.
141. Chen, S.T., et al., *CLEC5A is critical for dengue-virus-induced lethal disease.* Nature, 2008. **453**(7195): p. 672-6.
142. Watson, A.A., et al., *Structural flexibility of the macrophage dengue virus receptor CLEC5A: implications for ligand binding and signaling.* Journal of Biological Chemistry, 2011. **286**(27): p. 24208-18.
143. Cheng, Y.L., et al., *Activation of Nrf2 by the dengue virus causes an increase in CLEC5A, which enhances TNF-α production by mononuclear phagocytes.* Scientific Reports, 2016. **6**: p. 32000.
144. Wu, M.F., et al., *CLEC5A is critical for dengue virus–induced inflammasome activation in human macrophages.* Blood, 2013. **121**(1): p. 95-106.
145. Xavier-Carvalho, C., et al., *Association of rs1285933 single nucleotide polymorphism in CLEC5A gene with dengue severity and its functional effects.* Human Immunology, 2017. **78**(10): p. 649-56.
146. Sprokholt, J.K., et al., *RIG-I–like receptor triggering by dengue virus drives dendritic cell immune activation and Th1 differentiation.* The Journal of Immunology, 2017. **198**(12): p. 4764-771.
147. Cheng, Y.L., et al., *Dengue virus infection causes the activation of distinct NF-KB pathways for inducible nitric oxide synthase and TNF-a expression in RAW264.7 cells.* Mediators of Inflammation, 2015. **2015**: p. 274025.
148. Lin, J.C., et al., *Dengue viral protease interaction with NF-κB inhibitor α/β results in endothelial cell apoptosis and hemorrhage development.* The Journal of Immunology, 2014. **193**(3): p. 1258-67.
149. Sun, P., et al., *Functional characterization of ex vivo blood myeloid and plasmacytoid dendritic cells after infection with dengue virus.* Virology, 2009. **383**(2): p. 207-15.
150. Décembre, E., et al., *Sensing of immature particles produced by dengue virus infected cells induces an antiviral response by plasmacytoid dendritic cells.* PLoS Pathogens, 2014. **10**(10): p. e1004434.
151. Wang, J.P., et al., *Flavivirus activation of plasmacytoid dendritic cells delineates key elements of TLR7 signaling beyond endosomal recognition.* The Journal of Immunology, 2006. **177**(10): p. 7114-21.
152. Nasirudeen, A.M.A., et al. *RIG-I, MDA5 and TLR3 synergistically play an important role in restriction of dengue virus infection*. PLoS Neglected Tropical Diseases, 2011. **5**, e926.
153. Bustos-Arriaga, J., et al., *Activation of the innate immune response against DENV in normal non-transformed human fibroblasts.* PLoS Neglected Tropical Diseases, 2011. **5**(12): p. e1420.
154. Tsai, Y.T., et al., *Human TLR3 recognizes dengue virus and modulates viral replication in vitro.* Cellular Microbiology, 2009. **11**(4): p. 604-15.
155. Loo, Y.M., et al., *Distinct RIG-I and MDA5 signaling by RNA viruses in innate immunity.* Journal of Virology, 2008. **82**(1): p. 335-45.
156. da Conceição, T.M., et al., *Essential role of RIG-I in the activation of endothelial cells by dengue virus.* Virology, 2013. **435**(2): p. 281-92.
157. Sprokholt, J.K., et al., *RIG-I-like receptor activation by dengue virus drives follicular T helper cell formation and antibody production.* PLoS Pathogens, 2017. **13**(11): p. e1006738.

158. Torres, S., et al., *Differential expression of Toll-like receptors in dendritic cells of patients with dengue during early and late acute phases of the disease.* PLoS Neglected Tropical Diseases, 2013. **7**(2): p. e2060.
159. Sprokholt, J., Helgers, L.C. and Geijtenbeek, T.B., *Innate immune receptors drive dengue virus immune activation and disease.* Future Virology, 2017. **13**(4): p. 287-305.
160. Halstead, S.B., et al., *Intrinsic antibody-dependent enhancement of microbial infection in macrophages: disease regulation by immune complexes.* The Lancet Infectious Diseases, 2010. **10**(10): p. 712-22.
161. Low, J.G.H., Ooi, E.E. and Vasudevan, S.G., *Current status of dengue therapeutics research and development.* The Journal of Infectious Diseases, 2017. **215**(S2): p. S96-102.
162. Malavige, G.N., et al., *A preliminary study on efficacy of rupatadine for the treatment of acute dengue infection.* Scientific Reports, 2018. **8**(1): p. 3857.
163. Botta, L., et al. *Drug repurposing approaches to fight dengue virus infection and related diseases*. Frontiers in Bioscience (Landmark edition), 2018. **23**: p. 997-1019.
164. Mohan, S., et al., *Antiviral activities of sulfonium-ion glucosidase inhibitors and 5-thiomannosylamine disaccharide derivatives against dengue virus.* International Journal of Antimicrobial Agents, 2012. **40**(3): p. 273-6.
165. Shashidhara, K.C., et al., *Effect of high dose of steroid on plateletcount in acute stage of dengue Fever with thrombocytopenia.* Journal of Clinical and Diagnostic Research, 2013. **7**(7): p. 1397-400.
166. Terry, M.F., et al., *Dengue patients treated with doxycycline showed lower mortality associated to a reduction in IL-6 and TNF levels.* Recent Patents on Anti-Infective Drug Discovery, 2015. **10**(1): p. 51-8.
167. World Health Organization. *Immunization, vaccines and biologicals: dengue*. 2016; Available from: http://www.who.int/immunization/diseases/dengue/en/.
168. World Health Organization, *Dengue vaccine: WHO position paper, July 2016 – recommendations.* Vaccine, 2017. **35**(9): p. 1200-1.
169. Hadinegoro, S.R., et al., *Efficacy and long-term safety of a dengue vaccine in regions of endemic disease.* New England Journal of Medicine, 2015. **373**(13): p. 1195-206.
170. Malisheni, M., et al., *Clinical efficacy, safety, and immunogenicity of a live attenuated tetravalent dengue vaccine (CYD-TDV) in children: a systematic review with meta-analysis.* Frontiers in Immunology, 2017. **8**: p. 863.
171. Gailhardou, S., et al., *Safety overview of a recombinant live-attenuated tetravalent dengue vaccine: pooled analysis of data from 18 clinical trials.* PLoS Neglected Tropical Diseases, 2016. **10**(7): p. e0004821.
172. Tripathi, N.K. and Shrivastava, A., *Recent developments in recombinant protein–based dengue vaccines.* Frontiers in Immunology, 2018. **9**: p. 1919.
173. Sirohi, D., et al., *The 3.8 Å resolution cryo-EM structure of Zika virus.* Science, 2016. **352**(6284): p. 467-70.
174. Kostyuchenko, V.A., et al., *Structure of the thermally stable Zika virus.* Nature, 2016. **533**: p. 425-8.
175. Beaver, J.T., et al., *Evolution of two major Zika virus lineages: implications for pathology, immune response, and vaccine development.* Frontiers in Immunology, 2018. **9**: p. 1640.
176. Hamel, R., et al., *Biology of Zika virus infection in human skin cells.* Journal of Virology, 2015. **89**(17): p. 8880-96.
177. Meertens, L., et al., *Axl mediates Zika virus entry in human glial cells and modulates innate immune responses.* Cell Reports, 2017. **18**(2): p. 324-33.
178. Bagasra, O., et al., *Cellular targets and receptor of sexual transmission of Zika virus.* Applied Immunohistochemistry & Molecular Morphology, 2017. **25**(10): p. 679-86.

179. Dai, L., et al., *Structures of the Zika virus envelope protein and its complex with a flavivirus broadly protective antibody.* Cell Host & Microbe, 2016. **19**(5): p. 696-704.
180. Widman, D.G., et al., *A reverse genetics platform that spans the Zika virus family tree.* mBio, 2017. **8**(2): p. e02014-16.
181. Goo, L., et al., *Zika virus is not uniquely stable at physiological temperatures compared to other flaviviruses.* mBio, 2016. **7**(5): p. e01396-16.
182. May, M. and Relich, R.F., *A comprehensive systems biology approach to studying Zika virus.* PLoS ONE, 2016. **11**(9): p. e0161355.
183. Mossenta, M., et al., *Role of N-glycosylation on Zika virus E protein secretion, viral assembly and infectivity.* Biochemical and Biophysical Research Communications, 2017. **492**(4): p. 579-86.
184. Fontes-Garfias, C.R., et al., *Functional analysis of glycosylation of Zika virus envelope protein.* Cell Reports, 2017. **21**(5): p. 1180-90.
185. Annamalai, A.S., et al., *Zika virus encoding nonglycosylated envelope protein is attenuated and defective in neuroinvasion.* Journal of Virology, 2017. **91**(23): p. e01348-17.
186. Wen, D., et al., *N-glycosylation of viral E protein is the determinant for vector midgut invasion by flaviviruses.* mBio, 2018. **9**(1): p. e00046-18.
187. Goo, L., et al., *The Zika virus envelope protein glycan loop regulates virion antigenicity.* Virology, 2018. **515**: p. 191-202.
188. Brown, W.C., et al., *Extended surface for membrane association in Zika virus NS1 structure.* Nature Structural & Molecular Biology, 2016. **23**: p. 865-7.
189. Richner, J.M., et al., *Vaccine mediated protection against Zika virus-induced congenital disease.* Cell, 2017. **170**(2): p. 273-283.
190. Smithburn, K.C., *Neutralizing antibodies against certain recently isolated viruses in the sera of human beings residing in East Africa.* The Journal of Immunology, 1952. **69**(2): p. 223-34.
191. Dick, G.W.A., *Zika virus (II). Pathogenicity and physical properties.* Transactions of the Royal Society of Tropical Medicine and Hygiene, 1952. **46**(5): p. 521-34.
192. MacNamara, F.N., *Zika virus: A report on three cases of human infection during an epidemic of jaundice in Nigeria.* Transactions of the Royal Society of Tropical Medicine and Hygiene, 1954. **48**(2): p. 139-45.
193. Kindhauser, M.K., et al., *Zika: the origin and spread of a mosquito-borne virus.* Bulletin of the World Health Organization, 2016. **94**(9): p. 675-86.
194. Guedes, D.R.D., et al., *Zika virus replication in the mosquito Culex quinquefasciatus in Brazil.* Emerging Microbes & Infections, 2017. **6**: p. e69.
195. Hills, S., et al., *Transmission of Zika virus through sexual contact with travelers to areas of ongoing transmission — continental United States, 2016.* Morbidity and Mortality Weekly Report, 2016. **65**: p. 215–6.
196. Venturi, G., et al., *An autochthonous case of Zika due to possible sexual transmission, Florence, Italy, 2014.* Eurosurveillance, 2016. **21**(8): p. 30148.
197. Paz-Bailey, G., et al., *Persistence of Zika virus in body fluids - final report.* New England Journal of Medicine, 2018. **379**(13): p. 1234-43.
198. Mead, P.S., et al., *Zika virus shedding in semen of symptomatic infected men.* New England Journal of Medicine, 2018. **378**(15): p. 1377-85.
199. Londono-Renteria, B., et al., *A relevant in vitro human model for the study of Zika virus antibody-dependent enhancement.* Journal of General Virology, 2017. **98**(7): p. 1702-12.
200. Zimmerman, M.G., et al., *Cross-reactive dengue virus antibodies augment Zika virus infection of human placental macrophages.* Cell Host & Microbe, 2018. **24**(5): p. 731-42.

201. Pantoja, P., et al., *Zika virus pathogenesis in rhesus macaques is unaffected by pre-existing immunity to dengue virus.* Nature Communications, 2017. **8**: p. 15674.
202. Terzian, A.C.B., et al., *Viral load and cytokine response profile does not support antibody-dependent enhancement in dengue-primed Zika virus–infected patients.* Clinical Infectious Diseases, 2017. **65**(8): p. 1260-5.
203. Gordon, A., et al., *Prior dengue virus infection and risk of Zika: a pediatric cohort in Nicaragua.* PLoS Medicine, 2019. **16**(1): p. e1002726.
204. George, J., et al., *Prior exposure to Zika virus significantly enhances peak dengue-2 viremia in Rhesus macaques.* Scientific Reports, 2017. **7**(1): p. 10498.
205. Fowler, A.M., et al., *Maternally acquired Zika antibodies enhance dengue disease severity in mice.* Cell Host & Microbe, 2018. **24**(5): p. 743-50.
206. Foo, S.S., et al., *Asian Zika virus strains target CD14+ blood monocytes and induce M2-skewed immunosuppression during pregnancy.* Nature Microbiology, 2017. **2**(11): p. 1558-70.
207. Michlmayr, D., et al., *CD14+CD16+ monocytes are the main target of Zika virus infection in peripheral blood mononuclear cells in a paediatric study in Nicaragua.* Nature Microbiology, 2017. **2**(11): p. 1462-70.
208. Tabata, T., et al., *Zika virus targets different primary human placental cells, suggesting two routes for vertical transmission.* Cell Host & Microbe, 2016. **20**(2): p. 155-66.
209. Tang, H., et al., *Zika virus infects human cortical neural progenitors and attenuates their growth.* Cell Stem Cell, 2016. **18**(5): p. 587-90.
210. Retallack, H., et al., *Zika virus cell tropism in the developing human brain and inhibition by azithromycin.* Proceedings of the National Academy of Sciences, 2016. **113**(50): p. 14408-13.
211. Roach, T. and Alcendor, D.J., *Zika virus infection of cellular components of the blood-retinal barriers: implications for viral associated congenital ocular disease.* Journal of Neuroinflammation, 2017. **14**(1): p. 43.
212. Tappe, D., et al., *Cytokine kinetics of Zika virus-infected patients from acute to reconvalescent phase.* Medical Microbiology and Immunology, 2016. **205**(3): p. 269-73.
213. Kam, Y.W., et al., *Specific biomarkers associated with neurological complications and congenital central nervous system abnormalities from Zika virus–infected patients in Brazil.* The Journal of Infectious Diseases, 2017. **216**(2): p. 172-81.
214. Lum, F.M., et al., *Longitudinal study of cellular and systemic cytokine signatures to define the dynamics of a balanced immune environment during disease manifestation in Zika virus–infected patients.* The Journal of Infectious Diseases, 2018. **218**(5): p. 814-24.
215. Naveca, F.G., et al., *Analysis of the immunological biomarker profile during acute Zika virus infection reveals the overexpression of CXCL10, a chemokine linked to neuronal damage.* Memórias do Instituto Oswaldo Cruz, 2018. **113**(6): p. e170542.
216. Foo, S.S., et al., *Biomarkers and immunoprofiles associated with fetal abnormalities of ZIKV-positive pregnancies.* JCI Insight, 2018. **3**(21): p. 124152.
217. Wang, W., et al., *Zika virus infection induces host inflammatory responses by facilitating NLRP3 inflammasome assembly and interleukin-1β secretion.* Nature Communications, 2018. **9**(1): p. 106.
218. Dang, J., et al., *Zika virus depletes neural progenitors in human cerebral organoids through activation of the innate immune receptor TLR3.* Cell Stem Cell, 2016. **19**(2): p. 258-65.
219. Donald, C.L., et al., *Full genome sequence and sfRNA interferon antagonist activity of Zika virus from Recife, Brazil.* PLoS Neglected Tropical Diseases, 2016. **10**(10): p. e0005048.

220. Bowen, J.R., et al., *Zika virus antagonizes type I interferon responses during infection of human dendritic cells.* PLOS Pathogens, 2017. **13**(2): p. e1006164.
221. Xia, H., et al., *An evolutionary NS1 mutation enhances Zika virus evasion of host interferon induction.* Nature Communications, 2018. **9**(1): p. 414.
222. Chazal, M., et al., *RIG-I recognizes the 5' region of dengue and Zika virus genomes.* Cell Reports, 2018. **24**(2): p. 320-8.
223. Hertzog, J., et al., *Infection with a Brazilian isolate of Zika virus generates RIG-I stimulatory RNA and the viral NS5 protein blocks type I IFN induction and signaling.* European Journal of Immunology, 2018. **48**(7): p. 1120-36.
224. Morrison, T.E. and Diamond, M.S., *Animal models of Zika virus infection, pathogenesis, and immunity.* Journal of Virology, 2017. **91**(8): p. e00009-17.
225. Saiz, J.C. and Martín-Acebes, M.A., *The race to find antivirals for Zika virus.* Antimicrobial Agents and Chemotherapy, 2017. **61**(6): p. e00411-17.
226. Ma, J., et al., *Enhancing the antiviral potency of ER α-glucosidase inhibitor IHVR-19029 against hemorrhagic fever viruses in vitro and in vivo.* Antiviral Research, 2018. **150**: p. 112-22.
227. Albulescu, I.C., et al., *Suramin inhibits Zika virus replication by interfering with virus attachment and release of infectious particles.* Antiviral Research, 2017. **143**: p. 230-6.
228. Estoppey, D., et al., *The natural product cavinafungin selectively interferes with Zika and dengue virus replication by inhibition of the host signal peptidase.* Cell Reports, 2017. **19**(3): p. 451-60.
229. Jiménez de Oya, N., et al., *Direct activation of adenosine monophosphate-activated protein kinase (AMPK) by PF-06409577 inhibits flavivirus infection through modification of host cell lipid metabolism.* Antimicrobial Agents and Chemotherapy, 2018. **62**(7): p. e00360-18.
230. Merino-Ramos, T., et al., *Antiviral activity of nordihydroguaiaretic acid and its derivative tetra-O-methyl nordihydroguaiaretic acid against West Nile virus and Zika virus.* Antimicrobial Agents and Chemotherapy, 2017. **61**(8): p. e00376-17.
231. Donets, M.A., et al., *Physicochemical characteristics, morphology and morphogenesis of virions of the causative agent of Crimean hemorrhagic fever.* Intervirology, 1977. **8**(5): p. 294-308.
232. Martin, M.L., et al., *Distinction between Bunyaviridae genera by surface structure and comparison with Hantaan virus using negative stain electron microscopy.* Archives of Virology, 1985. **86**(1): p. 17-28.
233. Whitehouse, C.A., *Crimean–Congo hemorrhagic fever.* Antiviral Research, 2004. **64**(3): p. 145-60.
234. Guu, T.S.Y., Zheng, W., and Tao, Y.J., *Bunyavirus: structure and replication*, in *Viral Molecular Machines*, M.G. Rossmann and V.B. Rao, Editors. 2012, Springer New York. p. 245-66.
235. Sanchez, A.J., et al., *Crimean-Congo hemorrhagic fever virus glycoprotein precursor is cleaved by furin-like and SKI-1 proteases to generate a novel 38-kilodalton glycoprotein.* Journal of Virology, 2006. **80**(1): p. 514-25.
236. Barnwal, B., et al., *The non-structural protein of Crimean-Congo hemorrhagic fever virus disrupts the mitochondrial membrane potential and induces apoptosis.* Journal of Biological Chemistry, 2016. **291**(2): p. 582-92.
237. Xiao, X., et al., *Identification of a putative Crimean-Congo hemorrhagic fever virus entry factor.* Biochemical and Biophysical Research Communications, 2011. **411**(2): p. 253-8.
238. Estrada, D.F. and De Guzman, R.N., *Structural characterization of the Crimean-Congo hemorrhagic fever virus Gn tail provides insight into virus assembly.* Journal of Biological Chemistry, 2011. **286**(24): p. 21678-86.

239. Sanchez, A.J., Vincent, M.J., and Nichol, S.T., *Characterization of the Glycoproteins of Crimean-Congo Hemorrhagic Fever Virus.* Journal of Virology, 2002. **76**(14): p. 7263-75.
240. Erickson, B.R., et al., *N-linked glycosylation of Gn (but not Gc) is important for Crimean Congo hemorrhagic fever virus glycoprotein localization and transport.* Virology, 2007. **361**(2): p. 348-55.
241. Deyde, V.M., et al., *Crimean-Congo hemorrhagic fever virus genomics and global diversity.* Journal of Virology, 2006. **80**(17): p. 8834-42.
242. Shi, X., Brauburger, K., and Elliott, R.M., *Role of N-linked glycans on Bunyamwera virus glycoproteins in intracellular trafficking, protein folding, and virus infectivity.* Journal of Virology, 2005. **79**(21): p. 13725-34.
243. Ergönül, Ö., *Crimean-Congo haemorrhagic fever.* Lancet Infectious Diseases, 2006. **6**(4): p. 203-14.
244. Yu-Chen, Y., Ling-Xiong, K. and Ling, L., *Characteristics of Crimean-Congo hemorrhagic fever virus (Xinjiang strain) in China.* American Journal of Tropical Medicine and Hygiene, 1985. **34**(6): p. 1179-82.
245. Papa, A., et al., *Meeting report: first international conference on Crimean-Congo hemorrhagic fever.* Antiviral Research, 2015. **120**: p. 57-65.
246. Spengler, J.R., et al., *Second international conference on Crimean-Congo hemorrhagic fever.* Antiviral Research, 2018. **150**: p. 137-47.
247. Gargili, A., et al., *The role of ticks in the maintenance and transmission of Crimean-Congo hemorrhagic fever virus: a review of published field and laboratory studies.* Antiviral Research, 2017. **144**: p. 93-119.
248. Leblebicioglu, H., et al., *Consensus report: preventive measures for Crimean-Congo hemorrhagic fever during Eid-al-Adha festival.* International Journal of Infectious Diseases, 2015. **38**: p. 9-15.
249. Swanepoel, R., et al., *Epidemiologic and clinical features of Crimean-Congo hemorrhagic fever in southern Africa.* American Journal of Tropical Medicine and Hygiene, 1987. **36**(1): p. 120-32.
250. Hoogstraal, H., *Review Article: The epidemiology of tick-borne Crimean-Congo hemorrhagic fever in Asia, Europe, and Africa.* Journal of Medical Entomology, 1979. **15**(4): p. 307-417.
251. Akinci, E., et al., *Prognostic factors, pathophysiology and novel biomarkers in Crimean-Congo hemorrhagic fever.* Antiviral Research, 2016. **132**: p. 233-43.
252. Saksida, A., et al., *Interacting roles of immune mechanisms and viral load in the pathogenesis of Crimean-Congo hemorrhagic fever.* Clinical and Vaccine Immunology, 2010. **17**(7): p. 1086-93.
253. Burt, F.J., et al., *Immunohistochemical and in situ localization of Crimean-Congo hemorrhagic fever (CCHF) virus in human tissues and implications for CCHF pathogenesis.* Archives of Pathololgy & Laboratory Medicine, 1997. **121**(8): p. 839-46.
254. Connolly-Andersen, A.M., et al., *Crimean Congo hemorrhagic fever virus infects human monocyte-derived dendritic cells.* Virology, 2009. **390**(2): p. 157-62.
255. Peyrefitte, C.N., et al., *Differential activation profiles of Crimean–Congo hemorrhagic fever virus- and Dugbe virus-infected antigen-presenting cells.* Journal of General Virology, 2010. **91**(1): p. 189-98.
256. Connolly-Andersen, A.M., et al., *Crimean-Congo hemorrhagic fever virus activates endothelial cells.* Journal of Virology, 2011. **85**(15): p. 7766-74.
257. Rodrigues, R., et al., *Crimean-Congo hemorrhagic fever virus-infected hepatocytes induce ER-stress and apoptosis crosstalk.* PLoS ONE, 2012. **7**(1): p. e29712.
258. Swanepoel, R., et al., *The clinical pathology of Crimean-Congo hemorrhagic fever.* Reviews of Infectious Diseases, 1989. **11**(S4: p. S794-800.

259. Negredo, A., et al., *Autochthonous Crimean–Congo hemorrhagic fever in Spain.* New England Journal of Medicine, 2017. **377**(2): p. 154-61.
260. Muco, E., et al., *Crimean-Congo hemorrhagic fever with hepatic impairment and vaginal hemorrhage: a case report.* Journal of Medical Case Reports, 2018. **12**(1): p. 118.
261. Papa, A., et al., *Cytokines as biomarkers of Crimean-Congo hemorrhagic fever.* Journal of Medical Virology, 2016. **88**(1): p. 21-7.
262. Ergönül, Ö., et al., *Cytokine response in crimean-congo hemorrhagic fever virus infection.* Journal of Medical Virology, 2017. **89**(10): p. 1707-13.
263. Ergonul, O., et al., *Evaluation of serum levels of interleukin (IL)–6, IL-10, and tumor necrosis factor–α in patients with Crimean-Congo hemorrhagic fever.* Journal of Infectious Diseases, 2006. **193**(7): p. 941-4.
264. Papa, A., et al., *Cytokine levels in Crimean-Congo hemorrhagic fever.* Journal of Clinical Virology, 2006. **36**(4): p. 272-6.
265. Kaya, S., et al., *Sequential determination of serum viral titers, virus-specific IgG antibodies, and TNF-α, IL-6, IL-10, and IFN-γ levels in patients with Crimean-Congo hemorrhagic fever.* BMC Infectious Diseases, 2014. **14**(1): p. 1-8.
266. Tezer, H., et al., *Cytokine concentrations in pediatric patients with Crimean-Congo hemorrhagic fever.* The Paediatric Infectious Diseases Journal, 2014. **33**(11): p. 1185-7.
267. Sancakdar, E., et al., *Evaluation of cytokines as Th1/Th2 markers in pathogenesis of children with Crimean-Congo hemorrhagic fever.* International Journal of Clinical and Experimental Medicine, 2014. **7**(3): p. 751-7.
268. Parlak, E., et al., *The effect of inflammatory cytokines and the level of vitamin D on prognosis in Crimean-Congo hemorrhagic fever.* International Journal of Clinical and Experimental Medicine, 2015. **8**(10): p. 18302-10.
269. Arasli, M., et al., *Elevated chemokine levels during adult but not pediatric Crimean–Congo hemorrhagic fever.* Journal of Clinical Virology, 2015. **66**: p. 76-82.
270. Papa, A., et al., *Crimean-Congo hemorrhagic fever: CXCL10 correlates with the viral load.* Journal of Medical Virology, 2015. **87**(6): p. 899-903.
271. Spengler, J.R., et al., *RIG-I mediates an antiviral response to Crimean-Congo hemorrhagic fever virus.* Journal of Virology, 2015. **89**(20): p. 10219-29.
272. Habjan, M., et al., *Processing of genome 5′ termini as a strategy of negative-strand RNA viruses to avoid RIG-I-dependent interferon induction.* PLoS ONE, 2008. **3**(4): p. e2032.
273. Andersson, I., et al., *Crimean-Congo hemorrhagic fever virus delays activation of the innate immune response.* Journal of Medical Virology, 2008. **80**(8): p. 1397-404.
274. Frias-Staheli, N., et al., *Ovarian tumor domain-containing viral proteases evade ubiquitin- and ISG15-dependent innate immune responses.* Cell Host & Microbe, 2007. **2**(6): p. 404-16.
275. van Kasteren, P.B., et al., *Arterivirus and nairovirus ovarian tumor domain-containing deubiquitinases target activated RIG-I to control innate immune signaling.* Journal of Virology, 2012. **86**(2): p. 773-85.
276. Arslan, S., et al., *Toll-like receptor 7 Gln11Leu, c.4-151A/G, and +1817G/T polymorphisms in Crimean Congo hemorrhagic fever.* Journal of Medical Virology, 2015. **87**(7): p. 1090-5.
277. Engin, A., et al., *Toll-like receptor 8 and 9 polymorphisms in Crimean-Congo hemorrhagic fever.* Microbes and Infection, 2010. **12**(12): p. 1071-8.
278. Kızıldağ, S., et al., *Effect of TLR10 (2322A/G, 720A/C, and 992T/A) polymorphisms on the pathogenesis of Crimean Congo hemorrhagic fever disease.* Journal of Medical Virology, 2018. **90**(1): p. 19-25.

279. Begum, F., Wisseman, Jr., C.L., and Casals, J., *Tick-borne viruses of West Pakistan. II. Hazara virus, a new agent isolated from Ixodes redikorzevi ticks from the Kaghan Valley, W. Pakistan.* American Journal of Epidemiology, 1970. **92**(3): p. 192-4.
280. Begum, F., Wisseman, Jr., C.L., and Traub, R., *Tick-borne viruses of West Pakistan. I. Isolation and general characteristics.* American Journal of Epidemiology, 1970. **92**(3): p. 180-91.
281. Shimada, S., et al., *Tofla virus: a newly identified nairovirus of the Crimean-Congo hemorrhagic fever group isolated from ticks in Japan.* Scientific Reports, 2016. **6**: p. 20213.
282. Kuhn, H.J., et al., *Genomic characterization of the genus nairovirus (family Bunyaviridae).* Viruses, 2016. **8**(6): p. e164.
283. Buckley, S.M., *Cross plaque neutralization tests with cloned Crimean hemorrhagic fever-Congo (CHF-C) and Hazara viruses.* Proceedings of the Society for Experimental Biology and Medicine, 1974. **146**(2): p. 594-600.
284. Casals, J. and Tignor, G.H., *Neutralization and hemagglutination-inhibition tests with Crimean hemorrhagic fever-Congo virus.* Proceedings of the Society for Experimental Biology and Medicine, 1974. **145**(3): p. 960-6.
285. Casals, J. and Tignor, G.H., *The nairovirus genus: serological relationships.* Intervirology, 1980. **14**(3-4): p. 144-7.
286. Foulke, R.S., Rosato, R.R. and French, G.R., *Structural polypeptides of Hazara virus.* Journal of General Virology, 1981. **53**(1): p. 169-72.
287. Flusin, O., et al., *Inhibition of Hazara nairovirus replication by small interfering RNAs and their combination with ribavirin.* Virology Journal, 2011. **8**: p. 249.
288. Darwish, M.A., et al., *A sero-epidemiological survey for Bunyaviridae and certain other arboviruses in Pakistan.* Transactions of the Royal Society of Tropical Medicine and Hygiene, 1983. **77**(4): p. 446-50.
289. Molinas, A., et al., *Protective role of host aquaporin 6 against Hazara virus, a model for Crimean–Congo hemorrhagic fever virus infection.* FEMS Microbiology Letters, 2016. **363**(8): p. fnw058.
290. Molinas, A., et al., *Perturbation of wound healing, cytoskeletal organization and cellular protein networks during Hazara virus infection.* Frontiers in Cell and Developmental Biology, 2017. **5**: p. 98.
291. Dowall, S.D., et al., *Hazara virus infection is lethal for adult type I interferon receptor-knockout mice and may act as a surrogate for infection with the human-pathogenic Crimean–Congo hemorrhagic fever virus.* Journal of General Virology, 2012. **93**(3): p. 560-4.
292. Punch, E.K., et al., *Potassium is a trigger for conformational change in the fusion spike of an enveloped RNA virus.* Journal of Biological Chemistry, 2018. **293**(26): p. 9937-44.
293. World Health Organization. *19th WHO model list of essential medicines*. 2015; Available from: https://www.who.int/medicines/publications/essentialmedicines/EML2015_8-May-15.pdf.
294. Ergonul, O., *Treatment of Crimean-Congo hemorrhagic fever.* Antiviral Research, 2008. **78**(1): p. 125-31.
295. Koksal, I., et al., *The efficacy of ribavirin in the treatment of Crimean-Congo hemorrhagic fever in Eastern Black Sea region in Turkey.* Journal of Clinical Virology, 2010. **47**(1): p. 65-8.
296. Ascioglu, S., et al., *Ribavirin for patients with Crimean–Congo haemorrhagic fever: a systematic review and meta-analysis.* Journal of Antimicrobial Chemotherapy, 2011. **66**(6): p. 1215-22.

297. Johnson, S., et al., *Ribavirin for treating Crimean Congo haemorrhagic fever.* Cochrane Database of Systematic Reviews, 2018. **6**: CD012713.
298. Soares-Weiser, K., et al., *Ribavirin for Crimean-Congo hemorrhagic fever: systematic review and meta-analysis.* BMC Infectious Diseases, 2010. **10**(1): p. 207.
299. Dilber, E., et al., *High-dose methylprednisolone in children with Crimean-Congo haemorrhagic fever.* Tropical Doctor, 2010. **40**(1): p. 27-30.
300. Sharifi-Mood, B., et al., *Efficacy of high-dose methylprednisolone in patients with Crimean-Congo haemorrhagic fever and severe thrombocytopenia.* Tropical Doctor, 2013. **43**(2): p. 49-53.
301. van Eeden, P.J., et al., *A nosocomial outbreak of Crimean-Congo haemorrhagic fever at Tygerberg Hospital. Part II. Management of patients.* South African Medical Journal, 1985. **68**(10): p. 718-21.
302. Vassilenko, S., et al., *Specific intravenous immunoglobulin for Crimean-Congo haemorrhagic fever.* The Lancet, 1990. **335**(8692): p. 791-2.
303. Kubar, A., et al., *Prompt administration of Crimean-Congo hemorrhagic fever (CCHF) virus hyperimmunoglobulin in patients diagnosed with CCHF and viral load monitorization by reverse transcriptase-PCR.* Japanese Journal of Infectious Diseases, 2011. **64**(5): p. 439-43.
304. Mendoza, E.J., et al., *Crimean–Congo haemorrhagic fever virus: Past, present and future insights for animal modelling and medical countermeasures.* Zoonoses and Public Health, 2018. **65**(5): p. 465-80.
305. Dowall, S.D., Carroll, M.W. and Hewson, R., *Development of vaccines against Crimean-Congo haemorrhagic fever virus.* Vaccine, 2017. **35**(44): p. 6015-23.
306. Buttigieg, K.R., et al., *A novel vaccine against Crimean-Congo haemorrhagic fever protects 100% of animals against lethal challenge in a mouse model.* PLoS One, 2014. **9**(3): p. e91516.
307. Apweiler, R., Hermjakob, H. and Sharon, N., *On the frequency of protein glycosylation, as deduced from analysis of the SWISS-PROT database.* Biochimica et Biophysica Acta, 1999. **1473**(1): p. 4-8.
308. Kornfeld, R. and Kornfeld, S., *Assembly of asparagine-linked oligosaccharides.* Annual Review of Biochemistry, 1985. **54**(1): p. 631-64.
309. Kasturi, L., Chen, H. and Shakin-Eshleman, S.H., *Regulation of N-linked core glycosylation: use of a site-directed mutagenesis approach to identify Asn-Xaa-Ser/Thr sequons that are poor oligosaccharide acceptors.* Biochemical Journal, 1997. **323**(2): p. 415-9.
310. Moremen, K.W., Tiemeyer, M., and Nairn, A.V., *Vertebrate protein glycosylation: diversity, synthesis and function.* Nature Reviews Molecular Cell Biology, 2012. **13**: p. 448-62.
311. Hammond, C., Braakman, I., and Helenius, A., *Role of N-linked oligosaccharide recognition, glucose trimming, and calnexin in glycoprotein folding and quality-control.* Proceedings of the National Academy of Sciences of the United States of America, 1994. **91**(3): p. 913-7.
312. Hebert, D.N., et al., *Calnexin, calreticulin, and Bip/Kar2p in protein folding*, in *Cold Spring Harbor Symposia on Quantitative Biology*. 1995. p. 405-15.
313. Molinari, M. and Helenius, A., *Glycoproteins form mixed disulphides with oxidoreductases during folding in living cells.* Nature, 1999. **402**(6757): p. 90-3.
314. Tyrrell, B.E., et al., *Iminosugars: promising therapeutics for influenza infection.* Critical Reviews in Microbiology, 2017. **43**(5): p. 521-45.
315. De Praeter, C.M., et al., *A novel disorder caused by defective biosynthesis of N-linked oligosaccharides due to glucosidase I deficiency.* The American Journal of Human Genetics, 2000. **66**(6): p. 1744-56.

316. Sadat, M.A., et al., *Glycosylation, hypogammaglobulinemia, and resistance to viral infections.* New England Journal of Medicine, 2014. **370**(17): p. 1615-25.
317. Kim, Y.M., et al., *Characteristic dysmorphic features in congenital disorders of glycosylation type IIb.* Journal of Human Genetics, 2018. **63**(3): p. 383-6.
318. Li, M., et al., *Compound heterozygous variants in MOGS inducing congenital disorders of glycosylation (CDG) IIb.* Journal of Human Genetics, 2019. **64**: p. 265-8.
319. Nash, R.J., et al., *Iminosugars as therapeutic agents: recent advances and promising trends.* Future Medicinal Chemistry, 2011. **3**(12): p. 1513-21.
320. Datema, R., et al., *On the role of oligosaccharide trimming in the maturation of Sindbis and influenza virus.* Archives of Virology, 1984. **81**(1-2): p. 25-39.
321. Caputo, A.T., et al., *Structures of mammalian ER α-glucosidase II capture the binding modes of broad-spectrum iminosugar antivirals.* Proceedings of the National Academy of Sciences of the United States of America, 2016. **113**(32): p. e4630-8.
322. Norton, P.A., Gu, B., and Block, T.M., *Iminosugars as antiviral agents*, in *Iminosugars: From Synthesis to Therapeutic Applications*. 2008, John Wiley & Sons, Ltd. p. 209-24.
323. Block, T.M., et al., *Secretion of human hepatitis B virus is inhibited by the imino sugar N-butyldeoxynojirimycin.* Proceedings of the National Academy of Sciences of the United States of America, 1994. **91**(6): p. 2235-9.
324. Hussain, S., et al., *Strain-specific antiviral activity of iminosugars against human influenza A viruses.* Journal of Antimicrobial Chemotherapy, 2015. **70**(1): p. 136-52.
325. Block, T.M., et al., *Treatment of chronic hepadnavirus infection in a woodchuck animal model with an inhibitor of protein folding and trafficking.* Nature Medicine, 1998. **4**(5): p. 610-4.
326. Marcus, N.Y. and Perlmutter, D.H., *Glucosidase and mannosidase inhibitors mediate increased secretion of mutant α1 antitrypsin Z.* Journal of Biological Chemistry, 2000. **275**(3): p. 1987-92.
327. Moore, S.E. and Spiro, R.G., *Demonstration that Golgi endo-alpha-D-mannosidase provides a glucosidase-independent pathway for the formation of complex N-linked oligosaccharides of glycoproteins.* Journal of Biological Chemistry, 1990. **265**(22): p. 13104-12.
328. Karaivanova, V.K., Luan, P., and Spiro, R.G., *Processing of viral envelope glycoprotein by the endomannosidase pathway: evaluation of host cell specificity.* Glycobiology, 1998. **8**(7): p. 725-30.
329. Campbell, L.K., Baker, D.E., and Campbell, R.K., *Miglitol: assessment of its role in the treatment of patients with diabetes mellitus.* Annals of Pharmacotherapy, 2000. **34**(11): p. 1291-301.
330. Kiappes, J.L., *Synthesis and biological characterization of natural and designed sugars*. 2014, The Scripps Research Institute and University of Oxford.
331. Zitzmann, N., et al., *Imino sugars inhibit the formation and secretion of bovine viral diarrhea virus, a pestivirus model of hepatitis C virus: implications for the development of broad spectrum anti-hepatitis virus agents.* Proceedings of the National Academy of Sciences of the United States of America, 1999. **96**(21): p. 11878-82.
332. Tan, A., et al., *Chemical modification of the glucosidase inhibitor 1-deoxynojirimycin. Structure-activity relationships.* Journal of Biological Chemistry, 1991. **266**(22): p. 14504-10.
333. Mellor, H.R., et al., *Preparation, biochemical characterization and biological properties of radiolabelled N-alkylated deoxynojirimycins.* Biochemical Journal, 2002. **366**(1): p. 225-33.
334. Chang, J., Block, T.M. and Guo, J.T., *Antiviral therapies targeting host ER alpha-glucosidases: current status and future directions.* Antiviral Research, 2013. **99**(3): p. 251-60.

335. Butters, T.D., Dwek, R.A., and Platt, F.M., *Inhibition of glycosphingolipid biosynthesis: application to lysosomal storage disorders.* Chemical Reviews, 2000. **100**(12): p. 4683-96.
336. Butters, T.D., et al., *Small-molecule therapeutics for the treatment of glycolipid lysosomal storage disorders.* Philosophical Transactions of the Royal Society of London. Series B, Biological sciences, 2003. **358**(1433): p. 927-45.
337. Sayce, A.C., et al., *Iminosugars inhibit dengue virus production via inhibition of ER alpha-glucosidases—not glycolipid processing enzymes.* PLoS Neglected Tropical Diseases, 2016. **10**(3): p. e0004524.
338. Cox, T., et al., *Novel oral treatment of Gaucher's disease with N-butyldeoxynojirimycin (OGT 918) to decrease substrate biosynthesis.* The Lancet, 2000. **355**(9214): p. 1481-5.
339. Lyseng-Williamson, K.A., *Miglustat: a review of its use in Niemann-Pick disease type C.* Drugs, 2014. **74**(1): p. 61-74.
340. Mellor, H.R., et al., *Membrane disruption and cytotoxicity of hydrophobic N-alkylated imino sugars is independent of the inhibition of protein and lipid glycosylation.* The Biochemical Journal, 2003. **374**(Pt 2): p. 307-14.
341. Durantel, D., et al., *Study of the mechanism of antiviral action of iminosugar derivatives against bovine viral diarrhea virus.* Journal of Virology, 2001. **75**(19): p. 8987-98.
342. Pollock, S., et al., *N-Butyldeoxynojirimycin is a broadly effective anti-HIV therapy significantly enhanced by targeted liposome delivery.* AIDS, 2008. **22**(15): p. 1961-9.
343. Plummer, E., et al., *Dengue virus evolution under a host-targeted antiviral.* Journal of Virology, 2015. **89**(10): p. 5592-601.
344. Aggarwal, S., et al., *Biochemical characterization of enzyme fidelity of influenza A virus RNA polymerase complex.* PLoS ONE, 2010. **5**(4): p. e10372.
345. Miller, J.L., Tyrrell, B.E. and Zitzmann, N., *Mechanisms of antiviral activity of iminosugars against dengue virus*, in *Dengue and Zika: control and antiviral treatment strategies*, R. Hilgenfeld and S.G. Vasudevan, Editors. 2018, Springer Singapore: Singapore. p. 277-301.
346. Gruters, R.A., et al., *Interference with HIV-induced syncytium formation and viral infectivity by inhibitors of trimming glucosidase.* Nature, 1987. **330**(6143): p. 74-7.
347. Dedera, D., Vander Heyden, N., and Ratner, L.E.E., *Attenuation of HIV-1 infectivity by an inhibitor of oligosaccharide processing.* AIDS Research and Human Retroviruses, 1990. **6**(6): p. 785-94.
348. Taylor, D.L., et al., *6-0-Butanoylcastanospermine (MDL 28,574) inhibits glycoprotein processing and the growth of HIVs.* AIDS, 1991. **5**(6): p. 693-8.
349. Taylor, D.L., et al., *Loss of cytomegalovirus infectivity after treatment with castanospermine or related plant alkaloids correlates with aberrant glycoprotein synthesis.* Antiviral Research, 1988. **10**(1): p. 11-26.
350. Mackenzie, J.M. and Westaway, E.G., *Assembly and maturation of the flavivirus Kunjin virus appear to cccur in the rough endoplasmic reticulum and along the secretory pathway, respectively.* Journal of Virology, 2001. **75**(22): p. 10787-99.
351. Gu, B., et al., *Antiviral profiles of novel iminocyclitol compounds against bovine viral diarrhea virus, West Nile virus, dengue virus and hepatitis B virus.* Antiviral Chemistry and Chemotherapy, 2007. **18**(1): p. 49-59.
352. Whitby, K., et al., *Castanospermine, a potent inhibitor of dengue virus infection in vitro and in vivo.* Journal of Virology, 2005. **79**(14): p. 8698-706.
353. Chang, J., et al., *Novel imino sugar derivatives demonstrate potent antiviral activity against flaviviruses.* Antimicrobial Agents and Chemotherapy, 2009. **53**(4): p. 1501-8.

354. Qu, X., et al., *Inhibitors of endoplasmic reticulum α-glucosidases potently suppress hepatitis C virus virion assembly and release.* Antimicrobial Agents and Chemotherapy, 2011. **55**(3): p. 1036-44.
355. Kiappes, J.L., et al., *ToP-DNJ, a selective inhibitor of endoplasmic reticulum α-glucosidase II exhibiting antiflaviviral activity.* ACS Chemical Biology, 2018. **13**(1): p. 60-5.
356. Steinmann, E., et al., *Antiviral effects of amantadine and iminosugar derivatives against hepatitis C virus.* Hepatology, 2007. **46**(2): p. 330-8.
357. Ramstedt, U., et al., *Iminosugars and methods of treating bunyaviral and togaviral diseases (US20100317696A1)*, United States Patent and Trademark Office, Editor. 2013, United Therapeutics Corporation, The Chancellor, Masters and Scholars of the University of Oxford.
358. Chang, J., et al., *Small molecule inhibitors of ER alpha-glucosidases are active against multiple hemorrhagic fever viruses.* Antiviral Research, 2013. **98**(3): p. 432-40.
359. Miller, J.L., et al., *Minimal in vivo efficacy of iminosugars in a lethal Ebola virus guinea pig model.* PLoS ONE, 2016. **11**(11): p. e0167018.
360. Warfield, K.L., et al., *Assessment of the potential for host-targeted iminosugars UV-4 and UV-5 activity against filovirus infections in vitro and in vivo.* Antiviral Research, 2017. **138**: p. 22-31.
361. Schlesinger, S., et al., *The effects of inhibitors of glucosidase I on the formation of Sindbis virus.* Virus Research, 1985. **2**(2): p. 139-49.
362. McDowell, W., et al., *Glucose trimming and mannose trimming affect different phases of the maturation of Sindbis virus in infected BHK cells.* Virology, 1987. **161**(1): p. 37-44.
363. Boehme, K.W., et al., *Linkage of an alphavirus host-range restriction to the carbohydrate-processing phenotypes of the host cell.* Journal of General Virology, 2000. **81**(1): p. 161-70.
364. Naim, H.Y. and Koblet, H., *Investigation of the role of glycans for the biological activity of Semliki Forest virus grown in Aedes albopictus cells using inhibitors of asparagine-linked oligosaccharides trimming.* Archives of Virology, 1988. **102**(1): p. 73-89.
365. Kaluza, G., Repges, S., and McDowell, W., *The significance of carbohydrate trimming for the antigenicity of the Semliki Forest virus glycoprotein E2.* Virology, 1990. **176**(2): p. 369-78.
366. Bolt, G., Rode Pedersen, I., and Blixenkrone-Møller, M., *Processing of N-linked oligosaccharides on the measles virus glycoproteins: importance for antigenicity and for production of infectious virus particles.* Virus Research, 1999. **61**(1): p. 43-51.
367. Tsujii, E., et al., *Nectrisine is a potent inhibitor of α-glucosidases, demonstrating activities similarly at enzyme and cellular levels.* Biochemical and Biophysical Research Communications, 1996. **220**(2): p. 459-66.
368. Bridges, C.G., et al., *The effect of oral treatment with 6-O-butanoyl castanospermine (MDL 28,574) in the murine zosteriform model of HSV-1 infection.* Glycobiology, 1995. **5**(2): p. 249-53.
369. Jacob, G.S., et al., *Method of treating herpesviruses (US4957926 (A))* United States Patent Office, Editor. 1990, Monsanto Company.
370. Ahmed, S.P., et al., *Antiviral activity and metabolism of the castanospermine derivative MDL 28,574, in cells infected with herpes simplex virus type 2.* Biochemical and Biophysical Research Communications, 1995. **208**(1): p. 267-73.
371. Karpas, A., et al., *Aminosugar derivatives as potential anti-human immunodeficiency virus agents.* Proceedings of the National Academy of Sciences of the United States of America, 1988. **85**(23): p. 9229-33.
372. Tyms, A.S., et al., *Castanospermine and other plant alkaloid inhibitors of glucosidase activity block the growth of HIV.* The Lancet, 1987. **330**(8566): p. 1025-6.

373. Fleet, G.W.J., et al., *Inhibition of HIV replication by amino-sugar derivatives.* FEBS Letters, 1988. **237**(1-2): p. 128-32.
374. Asano, N., et al., *N-alkylated nitrogen-in-the-ring sugars: conformational basis of inhibition of glycosidases and HIV-1 replication.* Journal of Medicinal Chemistry, 1995. **38**(13): p. 2349-56.
375. Shimizu, H., et al., *Inhibitory effect of novel 1-deoxynojirimycin derivatives on HIV-1 replication.* AIDS, 1990. **4**(10): p. 975-80.
376. Montefiori, D.C., Robinson, W.E., and Mitchell, W.M., *Antibody-independent, complement-mediated enhancement of HIV-1 infection by mannosidase I and II inhibitors.* Antiviral Research, 1989. **11**(3): p. 137-46.
377. Pal, R., et al., *Processing and secretion of envelope glycoproteins of human immunodeficiency virus type 1 in the presence of trimming glucosidase inhibitor deoxynojirimycin.* Intervirology, 1989. **30**(1): p. 27-35.
378. Ratner, L., Heyden, N.V., and Dedera, D., *Inhibition of HIV and SIV infectivity by blockade of α-glucosidase activity.* Virology, 1991. **181**(1): p. 180-92.
379. Ratner, L.E.E. and Heyden, N.V., *Mechanism of action of N-butyl deoxynojirimycin in inhibiting HIV-1 infection and activity in combination with nucleoside analogs.* AIDS Research and Human Retroviruses, 1993. **9**(4): p. 291-7.
380. Shimizu, H., et al., *Effect of N-(3-phenyl-2-propenyl)-1-deoxynojirimycin on the lectin binding to HIV-1 glycoproteins* Japanese Journal of Medical Science and Biology, 1990. **43**(3): p. 75-87.
381. Walker, B.D., et al., *Inhibition of human immunodeficiency virus syncytium formation and virus replication by castanospermine.* Proceedings of the National Academy of Sciences of the United States of America, 1987. **84**(22): p. 8120-4.
382. Johnson, V.A., et al., *Synergistic inhibition of human immunodeficiency virus type 1 and type 2 replication in vitro by castanospermine and 3'-azido-3'-deoxythymidine.* Antimicrobial Agents and Chemotherapy, 1989. **33**(1): p. 53-7.
383. Sunkara, P.S., et al., *Anti-HIV activity of castanospermine analogues.* The Lancet, 1989. **333**(8648): p. 1206.
384. Asano, N., et al., *Homonojirimycin isomers and N-alkylated homonojirimycins: structural and conformational basis of inhibition of glycosidases.* Journal of Medicinal Chemistry, 1998. **41**(14): p. 2565-71.
385. Wright, K.E., et al., *Post-translational processing of the glycoproteins of lymphocytic choriomeningitis virus.* Virology, 1990. **177**(1): p. 175-83.
386. Silber, A.M., Candurra, N.A., and Damonte, E.B., *The effects of oligosaccharide trimming inhibitors on glycoprotein expression and infectivity of Junin virus.* FEMS Microbiology Letters, 1993. **109**(1): p. 39-43.
387. Block, T.M., et al., *Secretion of human hepatitis B virus is inhibited by the imino sugar N-butyldeoxynojirimycin.* Proc Natl Acad Sci U S A, 1994. **91**(6): p. 2235-9.
388. Schlesinger, S., Malfer, C., and Schlesinger, M.J., *The formation of vesicular stomatitis virus (San Juan strain) becomes temperature-sensitive when glucose residues are retained on the oligosaccharides of the glycoprotein.* Journal of Biological Chemistry, 1984. **259**(12): p. 7597-601.
389. Burke, B., et al., *Inhibition of N-linked oligosaccharide trimming does not interfere with surface expression of certain integral membrane proteins.* EMBO Journal, 1984. **3**(3): p. 551-6.
390. Blatt, L.M., Tan, H., and Seiwert, S., *Use of alpha-glucosidase inhibitors to treat alphavirus infections* United States Patent and Trademark Office, Editor. 2011, Intermune, Inc.

391. Fukushi, M., et al., *Monitoring of S protein maturation in the endoplasmic reticulum by calnexin is important for the infectivity of severe acute respiratory syndrome coronavirus.* Journal of Virology, 2012. **86**(21): p. 11745-53.
392. Ritchie, G., et al., *Identification of N-linked carbohydrates from severe acute respiratory syndrome (SARS) spike glycoprotein.* Virology, 2010. **399**(2): p. 257-69.
393. Wu, C.Y., et al., *Small molecules targeting severe acute respiratory syndrome human coronavirus.* Proceedings of the National Academy of Sciences of the United States of America, 2004. **101**(27): p. 10012-7.
394. Warfield, K.L., et al., *Inhibition of endoplasmic reticulum glucosidases is required for in vitro and in vivo dengue antiviral activity by the iminosugar UV-4.* Antiviral Research, 2016. **129**: p. 93-8.
395. Rathore, A.P.S., et al., *Celgosivir treatment misfolds dengue virus NS1 protein, induces cellular pro-survival genes and protects against lethal challenge mouse model.* Antiviral Research, 2011. **92**(3): p. 453-60.
396. Rathore, A.P., et al., *Celgosivir treatment misfolds dengue virus NS1 protein, induces cellular pro-survival genes and protects against lethal challenge mouse model.* Antiviral Research, 2011. **92**(3): p. 453-60.
397. Warfield, K.L., et al., *A novel iminosugar UV-12 with activity against the diverse viruses influenza and dengue (Novel iminosugar antiviral for influenza and dengue).* Viruses, 2015. **7**(5): p. 2404-27.
398. Miller, J.L., et al., *Liposome-mediated delivery of iminosugars enhances efficacy against dengue virus in vivo.* Antimicrobial Agents and Chemotherapy, 2012. **56**(12): p. 6379-86.
399. Perry, S.T., et al., *An iminosugar with potent inhibition of dengue virus infection in vivo.* Antiviral Research, 2013. **98**(1): p. 35-43.
400. Chang, J., et al., *Combination of α-glucosidase inhibitor and ribavirin for the treatment of dengue virus infection in vitro and in vivo.* Antiviral Research, 2011. **89**(1): p. 26-34.
401. Yu, W., et al., *Design, synthesis, and biological evaluation of N-alkylated deoxynojirimycin (DNJ) derivatives for the treatment of dengue virus infection.* Journal of Medicinal Chemistry, 2012. **55**(13): p. 6061-75.
402. Du, Y., et al., *N-Alkyldeoxynojirimycin derivatives with novel terminal tertiary amide substitution for treatment of bovine viral diarrhea virus (BVDV), dengue, and Tacaribe virus infections.* Bioorganic & Medicinal Chemistry Letters, 2013. **23**(7): p. 2172-6.
403. Watanabe, S., et al., *Optimizing celgosivir therapy in mouse models of dengue virus infection of serotypes 1 and 2: The search for a window for potential therapeutic efficacy.* Antiviral Research, 2016. **127**: p. 10-9.
404. Schul, W., et al., *A dengue fever viremia model in mice shows reduction in viral replication and suppression of the inflammatory response after treatment with antiviral drugs.* Journal of Infectious Diseases, 2007. **195**(5): p. 665-74.
405. Watanabe, S., et al., *Dose- and schedule-dependent protective efficacy of celgosivir in a lethal mouse model for dengue virus infection informs dosing regimen for a proof of concept clinical trial.* Antiviral Research, 2012. **96**(1): p. 32-5.
406. Chang, J., et al., *Competitive inhibitor of cellular alpha-glucosidases protects mice from lethal dengue virus infection.* Antiviral Research, 2011. **92**(2): p. 369-71.
407. Fischer, P.B., et al., *The alpha-glucosidase inhibitor N-butyldeoxynojirimycin inhibits human immunodeficiency virus entry at the level of post-CD4 binding.* Journal of Virology, 1995. **69**(9): p. 5791-7.
408. Fischer, P.B., et al., *N-butyldeoxynojirimycin-mediated inhibition of human immunodeficiency virus entry correlates with impaired gp120 shedding and gp41 exposure.* Journal of Virology, 1996. **70**(10): p. 7153-60.

409. Zhang, X.L., et al., *Specific inhibition effects of N-pentafluorobenzyl-1-deoxynojirimycin on human CD4+ T cells.* Bioorganic & Medicinal Chemistry Letters, 2004. **14**(14): p. 3789-92.
410. Zhao, X., et al., *Inhibition of endoplasmic reticulum-resident glucosidases impairs severe acute respiratory syndrome coronavirus and human coronavirus NL63 spike protein-mediated entry by altering the glycan processing of angiotensin I-converting enzyme 2.* Antimicrobial Agents and Chemotherapy, 2015. **59**(1): p. 206-16.
411. Griffin, S.D.C., et al., *The p7 protein of hepatitis C virus forms an ion channel that is blocked by the antiviral drug, Amantadine.* FEBS Letters, 2003. **535**(1-3): p. 34-8.
412. Sakai, A., et al., *The p7 polypeptide of hepatitis C virus is critical for infectivity and contains functionally important genotype-specific sequences.* Proceedings of the National Academy of Sciences, 2003. **100**(20): p. 11646-51.
413. Steinmann, E., et al., *Hepatitis C virus p7 protein is crucial for assembly and release of infectious virions.* PLoS Pathogens, 2007. **3**(7): p. e103.
414. Pavlović, D., et al., *The hepatitis C virus p7 protein forms an ion channel that is inhibited by long-alkyl-chain iminosugar derivatives.* Proceedings of the National Academy of Sciences of the United States of America, 2003. **100**(10): p. 6104-8.
415. Foster, T.L., et al., *Resistance mutations define specific antiviral effects for inhibitors of the hepatitis C virus p7 ion channel.* Hepatology, 2011. **54**(1): p. 79-90.
416. Wetherill, L.F., et al., *Alkyl-imino sugars inhibit the pro-oncogenic ion channel function of human papillomavirus (HPV) E5.* Antiviral Research, 2018. **158**: p. 113-21.
417. Sung, C., et al., *Extended evaluation of virological, immunological and pharmacokinetic endpoints of CELADEN: a randomized, placebo-controlled trial of celgosivir in dengue fever patients.* PLoS Neglected Tropical Diseases, 2016. **10**(8): p. e0004851.
418. Sayce, A.C., *Iminosugars as dengue virus therapeutics: molecular mechanisms of action of a drug entering clinical trials*, in *Department of Biochemistry*. 2014, University of Oxford.
419. Grochowicz, P.M., et al., *Castanospermine, an oligosaccharide processing inhibitor, reduces membrane expression of adhesion molecules and prolongs heart allograft survival in rats.* Transplant Immunology, 1996. **4**(4): p. 275-85.
420. Wall, K.A., Pierce, J.D., and Elbein, A.D., *Inhibitors of glycoprotein processing alter T-cell proliferative responses to antigen and to interleukin 2.* Proceedings of the National Academy of Sciences of the United States of America, 1988. **85**(15): p. 5644-8.
421. van Kemenade, F.J., et al., *Glucosidase trimming inhibitors preferentially perturb T cell activation induced by CD2 mAb.* Journal of Leukocyte Biology, 1994. **56**(2): p. 159-65.
422. Tierney, M., et al., *The tolerability and pharmacokinetics of N-butyl-deoxynojirimycin in patients with advanced HIV disease (ACTG 100).* Journal of Acquired Immune Deficiency Syndromes, 1995. **10**(5): p. 549-53.
423. Tian, G., et al., *Inhibition of α-glucosidases I and II increases the cell surface expression of functional class A macrophage scavenger receptor (SR-A) by extending its half-life.* Journal of Biological Chemistry, 2004. **279**(38): p. 39303-9.
424. Han, L., et al., *The role of N-glycan modification of TNFR1 in inflammatory microglia activation.* Glycoconjugate Journal, 2015. **32**(9): p. 685-93.
425. Perera, N., Miller, J.L., and Zitzmann, N., *The role of the unfolded protein response in dengue virus pathogenesis.* Cellular Microbiology, 2017. **19**(5): p. e12734.
426. Low, J.G., et al., *Efficacy and safety of celgosivir in patients with dengue fever (CELADEN): a phase 1b, randomised, double-blind, placebo-controlled, proof-of-concept trial.* Lancet Infectious Diseases, 2014. **14**(8): p. 706-15.
427. Fischl, M.A., et al., *The safety and efficacy of combination N-butyl-deoxynojirimycin (SC-48334) and zidovudine in patients with HIV-1 infection and 200-500 CD4 cells/mm.* Journal of Acquired Immune Deficiency Syndromes, 1994. **7**(2): p. 139-47.

428. McHutchison, J.G., et al., *The face of future hepatitis C antiviral drug development: Recent biological and virologic advances and their translation to drug development and clinical practice.* Journal of Hepatology, 2006. **44**(2): p. 411-21.
429. Kaita, K., et al., *Proof of concept study of celgosivir in combination with peginterferon alpha-2b and ribavirin in chronic hepatitis C genotype-1 non-responder patients* Journal of Hepatology, 2007. **46**: p. S56-7.
430. Walski, T., et al., *Diversity and functions of protein glycosylation in insects.* Insect Biochemistry and Molecular Biology, 2017. **83**: p. 21-34.
431. Pelletier, M.F., et al., *The heterodimeric structure of glucosidase II is required for its activity, solubility, and localization in vivo.* Glycobiology, 2000. **10**(8): p. 815-27.
432. Tchankouo-Nguetcheu, S., et al., *Differential protein modulation in midguts of Aedes aegypti infected with chikungunya and dengue 2 viruses.* PLoS ONE, 2010. **5**(10): p. e13149.
433. Kang, S., et al., *Suppressing dengue-2 infection by chemical inhibition of Aedes aegypti host factors.* PLOS Neglected Tropical Diseases, 2014. **8**(8): p. e3084.
434. Sim, S., et al., *Transcriptomic profiling of diverse Aedes aegypti strains reveals increased basal-level immune activation in dengue virus-refractory populations and identifies novel virus-vector molecular interactions.* PLOS Neglected Tropical Diseases, 2013. **7**(7): p. e2295.
435. Farjana, T. and Tuno, N., *Multiple blood feeding and host-seeking behavior in Aedes aegypti and Aedes albopictus (Diptera: Culicidae).* Journal of Medical Entomology, 2013. **50**(4): p. 838-46.
436. Boomkamp, S.D., et al., *Lysosomal storage of oligosaccharide and glycosphingolipid in imino sugar treated cells.* Glycoconjugate Journal, 2010. **27**(3): p. 297-308.
437. Kumar, K.S.A., et al., *Divergent synthesis of 4-epi-fagomine, 3,4-dihydroxypipecolic acid, and a dihydroxyindolizidine and their β-galactosidase inhibitory and immunomodulatory activities.* Journal of Organic Chemistry, 2013. **78**(15): p. 7406-13.
438. Liu, M., et al., *An iminosugar N-pentafluorobenzyl-1-deoxynojirimycin as a novel potential immunosuppressant for the treatment of Th2-related diseases.* Bioorganic & Medicinal Chemistry Letters, 2012. **22**(1): p. 564-70.
439. Alcalde-Estévez, E., et al., *The sp2-iminosugar glycolipid 1-dodecylsulfonyl-5N,6O-oxomethylidenenojirimycin (DSO2-ONJ) as selective anti-inflammatory agent by modulation of hemeoxygenase-1 in Bv.2 microglial cells and retinal explants.* Food and Chemical Toxicology, 2018. **111**: p. 454-66.
440. Dechecchi, M.C., et al., *Anti-inflammatory effect of miglustat in bronchial epithelial cells.* Journal of Cystic Fibrosis, 2008. **7**(6): p. 555-65.
441. Kosuge, T., et al., *Effect of inhibitors of glycoprotein processing on cytokine secretion and production in anti CD3-stimulated T cells.* Biological & Pharmaceutical Bulletin, 2000. **23**(1): p. 1-5.
442. Kosuge, T. and Toyoshima, S., *Increased degradation of newly synthesized interferon-gamma; (IFN-gamma;) in anti CD3-stimulated lymphocytes treated with glycoprotein processing inhibitors.* Biological & Pharmaceutical Bulletin, 2000. **23**(5): p. 545-8.
443. Dechecchi, M.C., et al., *Modulators of sphingolipid metabolism reduce lung inflammation.* American Journal of Respiratory Cell and Molecular Biology, 2011. **45**(4): p. 825-33.
444. Kaidonis, X., et al., *N-butyldeoxynojirimycin treatment restores the innate fear response and improves learning in mucopolysaccharidosis IIIA mice.* Molecular Genetics and Metabolism, 2016. **118**(2): p. 100-10.
445. Cologna, S.M., et al., *Human and mouse neuroinflammation markers in Niemann-Pick disease, type C1.* Journal of Inherited Metabolic Disease, 2014. **37**(1): p. 83-92.

446. Wang, G.-N., et al., *Synthetic N-alkylated iminosugars as new potential immunosuppressive agents.* ACS Medicinal Chemistry Letters, 2011. **2**(9): p. 682-6.
447. Ye, X.S., et al., *Synthetic iminosugar derivatives as new potential immunosuppressive agents.* Journal of Medicinal Chemistry, 2005. **48**(11): p. 3688-91.
448. Wu, X., et al., *N-arylated-lactam-type iminosugars as new immunosuppressive agents: discovery, optimization, and biological evaluation.* Chemistry – An Asian Journal, 2014. **9**(8): p. 2260-71.
449. Zhang, L., et al., *Discovery of iminosugar derivatives with strong IFN-γ inducing activity.* ChemMedChem, 2009. **4**(5): p. 756-60.
450. Sun, Y., et al., *Isofagomine in vivo effects in a neuronopathic Gaucher disease mouse.* PLoS ONE, 2011. **6**(4): p. e19037.
451. Arroba, A.I., et al., *Modulation of microglia polarization dynamics during diabetic retinopathy in db/db mice.* Biochimica et Biophysica Acta (BBA) - Molecular Basis of Disease, 2016. **1862**(9): p. 1663-74.
452. Hill, J.C., *Structural characterisation of calnexin cycle components and assessment as antiviral targets*, in *Department of Biochemistry*. 2018, University of Oxford: Oxford.
453. Bauer, D.E., Canver, M.C., and Orkin, S.H., *Generation of genomic deletions in mammalian cell lines via CRISPR/Cas9.* JoVE, 2015(95): p. e52118.
454. Gratz, S.J., et al., *Highly specific and efficient CRISPR/Cas9-catalyzed homology-directed repair in Drosophila.* Genetics, 2014. **196**(4): p. 961-71.
455. Russell, P.K., et al., *A plaque reduction test for dengue virus neutralizing antibodies.* The Journal of Immunology, 1967. **99**(2): p. 285-90.
456. Laue, T., Emmerich, P., and Schmitz, H., *Detection of dengue virus RNA in patients after primary or secondary dengue infection by using the TaqMan automated amplification system.* Journal of Clinical Microbiology, 1999. **37**(8): p. 2543-7.
457. Talarico, L.B. and Damonte, E.B., *Interference in dengue virus adsorption and uncoating by carrageenans.* Virology, 2007. **363**(2): p. 473-85.
458. Piccini, L.E., Castilla, V., and Damonte, E.B., *Dengue-3 virus entry into Vero cells: role of clathrin-mediated endocytosis in the outcome of infection.* PLoS ONE, 2015. **10**(10): p. e0140824.
459. Talarico, L.B., et al., *The antiviral activity of sulfated polysaccharides against dengue virus is dependent on virus serotype and host cell.* Antiviral Research, 2005. **66**(2-3): p. 103-10.
460. Applied Biosystems, *Relative quantitation of gene expression: ABI PRISM 7700 sequence detection system: user bulletin #2*. 1997.
461. Massé, N., et al., *Dengue virus replicons: production of an interserotypic chimera and cell lines from different species, and establishment of a cell-based fluorescent assay to screen inhibitors, validated by the evaluation of ribavirin's activity.* Antiviral Research, 2010. **86**(3): p. 296-305.
462. Alonzi, D., et al., *Glucosylated free oligosaccharides are biomarkers of endoplasmic-reticulum α-glucosidase inhibition.* Biochemical Journal, 2008. **409**(2): p. 571-80.
463. Dowall, S.D., et al., *A susceptible mouse model for Zika virus infection.* PLoS Neglected Tropical Diseases, 2016. **10**(5): p. e0004658.
464. Gupta, R., Jung, E., and Brunak, S.. *Prediction of N-glycosylation sites in human proteins*. 2004; Available from: http://www.cbs.dtu.dk/services/NetNGlyc/.
465. Gupta, R. and Brunak, S., *Prediction of glycosylation across the human proteome and the correlation to protein function.* Pacific Symposium on Biocomputing, 2002: p. 310-22.
466. Chauhan, J.S., Rao, A. and Raghava, G.P.S., *In silico platform for prediction of N-, O- and C-glycosites in eukaryotic protein sequences.* PLoS ONE, 2013. **8**(6): p. e67008.

467. Atkinson, B., et al., *Development of a real-time RT-PCR assay for the detection of Crimean-Congo hemorrhagic fever virus.* Vector-Borne and Zoonotic Diseases, 2012. **12**(9): p. 786-93.
468. Victoria, S., et al., *Activation of Toll-like receptor 2 increases macrophage resistance to HIV-1 infection.* Immunobiology, 2013. **218**(12): p. 1529-36.
469. Funderburg, N.T., et al., *The Toll-like receptor 1/2 agonists Pam(3)CSK(4) and human β-defensin-3 differentially induce interleukin-10 and nuclear factor-κB signalling patterns in human monocytes.* Immunology, 2011. **134**(2): p. 151-60.
470. Ahmad, R., et al., *FSL-1 induces MMP-9 production through TLR-2 and NF-KB/AP-1 signaling pathways in monocytic THP-1 cells.* Cellular Physiology and Biochemistry, 2014. **34**(3): p. 929-42.
471. Jiang, M.X., et al., *Expression profiling of TRIM protein family in THP1-derived macrophages following TLR stimulation.* Scientific Reports, 2017. **7**: p. 42781.
472. Black, C., et al., *Early life wildfire smoke exposure is associated with immune dysregulation and lung function decrements in adolescence.* American Journal of Respiratory Cell and Molecular Biology, 2017. **56**(5): p. 657-66.
473. Hilbert, T., et al., *Pulmonary vascular inflammation: effect of TLR signalling on angiopoietin/TIE regulation.* Clinical and Experimental Pharmacology and Physiology, 2016. **44**(1): p. 123-31.
474. Hemmi, H., et al., *Small anti-viral compounds activate immune cells via the TLR7 MyD88–dependent signaling pathway.* Nature Immunology, 2002. **3**: p. 196-200.
475. Lu, H., et al., *VTX-2337 is a novel TLR8 agonist that activates NK cells and augments ADCC.* Clinical Cancer Research, 2012. **18**(2): p. 499-509.
476. Elavazhagan, S., et al., *Granzyme B expression is enhanced in human monocytes by TLR8 agonists and contributes to antibody-dependent cellular cytotoxicity.* The Journal of Immunology, 2015. **194**(6): p. 2786-95.
477. Li, R., et al., *Antibody-independent function of human B cells contributes to antifungal T cell responses.* The Journal of Immunology, 2017. **198**(8): p. 3245-54.
478. Gow, N.A.R., et al., *Immune recognition of Candida albicans β-glucan by dectin-1.* The Journal of Infectious Diseases, 2007. **196**(10): p. 1565-71.
479. Frodermann, V., et al., *A modulatory interleukin-10 response to staphylococcal peptidoglycan prevents Th1/Th17 adaptive immunity to Staphylococcus aureus.* The Journal of Infectious Diseases, 2011. **204**(2): p. 253-62.
480. York, A.G., et al., *Limiting cholesterol biosynthetic flux spontaneously engages type I IFN signaling.* Cell, 2015. **163**(7): p. 1716-29.
481. Chen, J., Ng, M.M. and Chu, J.J., *Activation of TLR2 and TLR6 by dengue NS1 protein and its implications in the immunopathogenesis of dengue virus infection.* PLoS Pathogens, 2015. **11**(7): p. e1005053.
482. Osada, N., et al., *The genome landscape of the African green monkey kidney-derived Vero cell line.* DNA Research, 2014. **21**(6): p. 673-83.
483. Perera, N., *Evaluating the effects of dengue virus and iminosugar treatment on cellular unfolded protein response and redox homeostasis*, in *Department of Biochemistry*. 2019, University of Oxford: Oxford.
484. Flipse, J., et al., *Dengue tropism for macrophages and dendritic cells: the host cell effect.* Journal of General Virology, 2016. **97**(7): p. 1531-6.
485. Zandi, K., et al., *Novel antiviral activity of baicalein against dengue virus.* BMC Complementary and Alternative Medicine, 2012. **12**(1): p. 214.
486. Ismail, N.A. and Jusoh, S.A., *Molecular docking and molecular dynamics simulation studies to predict flavonoid binding on the surface of DENV2 E protein.* Interdisciplinary Sciences: Computational Life Sciences, 2017. **9**(4): p. 499-511.

487. Shen, Y.C., et al., *Mechanisms in mediating the anti-inflammatory effects of baicalin and baicalein in human leukocytes.* European Journal of Pharmacology, 2003. **465**(1): p. 171-81.
488. Notman, R., et al., *Molecular basis for dimethylsulfoxide (DMSO) action on lipid membranes.* Journal of the American Chemical Society, 2006. **128**(43): p. 13982-3.
489. Kloverpris, H., et al., *Dimethyl sulfoxide (DMSO) exposure to human peripheral blood mononuclear cells (PBMCs) abolish T cell responses only in high concentrations and following coincubation for more than two hours.* Journal of Immunological Methods, 2010. **356**(1): p. 70-8.
490. Koff, W.C., Elm, J.L., and Halstead, S.B., *Antiviral effects of ribavirin and 6-mercapto-9-tetrahydro-2-furylpurine against dengue viruses in vitro.* Antiviral Research, 1982. **2**(1): p. 69-79.
491. Rattanaburee, T., et al., *Inhibition of dengue virus production and cytokine/chemokine expression by ribavirin and compound A.* Antiviral Research, 2015. **124**: p. 83-92.
492. Huang, Y.H., et al., *Dengue virus infects human endothelial cells and induces IL-6 and IL-8 production.* American Journal of Tropical Medicine and Hygiene, 2000. **63**(1-2): p. 71-5.
493. Takhampunya, R., et al., *Inhibition of dengue virus replication by mycophenolic acid and ribavirin.* Journal of General Virology, 2006. **87**(7): p. 1947-52.
494. Jain, M., et al., *Effect of Hippophae rhamnoides leaf extract against Dengue virus infection in human blood-derived macrophages.* Phytomedicine, 2008. **15**(10): p. 793-9.
495. Knipe, D.M., *Fields Virology p 2456*. 2013, Philadelphia, PA, USA: Lippincott Williams and Wilkins.
496. Chapel, C., et al., *Reduction of the infectivity of hepatitis C virus pseudoparticles by incorporation of misfolded glycoproteins induced by glucosidase inhibitors.* Journal of General Virology, 2007. **88**(4): p. 1133-43.
497. Xu, H.T., et al., *Evaluation of sofosbuvir (β-D-2'-deoxy-2'-α-fluoro-2'-β-C-methyluridine) as an inhibitor of dengue virus replication.* Scientific Reports, 2017. **7**(1): p. 6345.
498. Scaturro, P., et al., *Characterization of the mode of action of a potent dengue virus capsid inhibitor.* Journal of Virology, 2014. **88**(19): p. 11540-55.
499. Alonzi, D.S., et al., *Iminosugar antivirals: the therapeutic sweet spot.* Biochemical Society Transactions, 2017. **45**(2): p. 571-82.
500. Crance, J.M., et al., *Interferon, ribavirin, 6-azauridine and glycyrrhizin: antiviral compounds active against pathogenic flaviviruses.* Antiviral Research, 2003. **58**(1): p. 73-9.
501. McDowell, M., et al., *A novel nucleoside analog, 1-β-d-ribofuranosyl-3-ethynyl-[1,2,4]triazole (ETAR), exhibits efficacy against a broad range of flaviviruses in vitro.* Antiviral Research, 2010. **87**(1): p. 78-80.
502. Talarico, L.B., et al., *Differential inhibition of dengue virus infection in mammalian and mosquito cells by iota-carrageenan.* Journal of General Virology, 2011. **92**(6): p. 1332-42.
503. Lee, H.L., Phong, T.V., and Rohani, A., *Effects of ribavirin and hydroxyurea on oral infection of Aedes aegypti (L.) with dengue virus [abstract only].* Southeast Asian Journal of Tropical Medicine and Public Health, 2012. **43**(6): p. 1358-64.
504. Schaeffer, E., et al., *Dermal CD14+ dendritic cell and macrophage infection by dengue virus is stimulated by interleukin-4.* Journal of Investigative Dermatology, 2015. **135**(7): p. 1743-51.
505. NHS Blood and Transplant. *Health, Eligibility and Travel*. [cited 20/10/18; Available from: https://my.blood.co.uk/knowledgebase/travel].

506. Schaefer, J.V. and Plückthun, A., *Transfer of engineered biophysical properties between different antibody formats and expression systems.* Protein Engineering, Design and Selection, 2012. **25**(10): p. 485-506.
507. Vermeer, A.W. and Norde, W., *The thermal stability of immunoglobulin: unfolding and aggregation of a multi-domain protein.* Biophysical Journal, 2000. **78**(1): p. 394-404.
508. Wahala, W.M.P.B., et al., *Natural strain variation and antibody neutralization of dengue serotype 3 viruses.* PLoS Pathogens, 2010. **6**(3): p. e1000821.
509. Sukupolvi-Petty, S., et al., *Functional analysis of antibodies against Dengue virus type 4 reveals strain-dependent epitope exposure that impacts neutralization and protection.* Journal of Virology, 2013. **87**(16): p. 8826-42.
510. Tan, A., et al., *Introduction of oxygen into the alkyl chain of N-decyl-dNM decreases lipophilicity and results in increased retention of glucose residues on N-linked oligosaccharides.* Glycobiology, 1994. **4**(2): p. 141-9.
511. Mellor, H.R., et al., *Cellular effects of deoxynojirimycin analogues: uptake, retention and inhibition of glycosphingolipid biosynthesis.* Biochemical Journal, 2004. **381**(3): p. 861-6.
512. Zurzolo, C., et al., *Opposite polarity of virus budding and of viral envelope glycoprotein distribution in epithelial cells derived from different tissues.* Journal of Cell Biology, 1992. **117**(3): p. 551-64.
513. Hubbard, S.C. and Ivatt, R.J., *Synthesis and processing of asparagine-linked oligosaccharides.* Annual Review of Biochemistry, 1981. **50**(1): p. 555-83.
514. Vaughn, D.W., et al., *Dengue viremia titer, antibody response pattern, and virus serotype correlate with disease severity.* The Journal of Infectious Diseases, 2000. **181**(1): p. 2-9.
515. Kostyuchenko, V.A., et al., *Immature and mature dengue serotype 1 virus structures provide insight into the maturation process.* Journal of Virology, 2013. **87**(13): p. 7700-7.
516. Fischer, P.B., et al., *N-butyldeoxynojirimycin-mediated inhibition of human immunodeficiency virus entry correlates with changes in antibody recognition of the V1/V2 region of gp120.* Journal of Virology, 1996. **70**(10): p. 7143-52.
517. Choy, M.M., et al., *Proteasome inhibition suppresses dengue virus egress in antibody dependent infection.* PLoS Neglected Tropical Diseases, 2015. **9**(11): p. e0004058.
518. Bhuvanakantham, R. and Ng, M.L., *West Nile virus and dengue virus capsid protein negates the antiviral activity of human Sec3 protein through the proteasome pathway.* Cellular Microbiology, 2013. **15**(10): p. 1688-706.
519. Ahsan, N.A., et al., *Presence of viral RNA and proteins in exosomes from cellular clones resistant to Rift Valley fever virus infection.* Frontiers in Microbiology, 2016. **7**: p. 139.
520. Jaworski, E., et al., *Human T-lymphotropic virus type 1 infected cells secrete exosomes that contain Tax protein.* Journal of Biological Chemistry, 2014. **289**(32): p. 22284-305.
521. Dreux, M., et al., *Short-range exosomal transfer of viral RNA from infected cells to plasmacytoid dendritic cells triggers innate immunity.* Cell Host & Microbe, 2012. **12**(4): p. 558-70.
522. Ramakrishnaiah, V., et al., *Exosome-mediated transmission of hepatitis C virus between human hepatoma Huh7.5 cells.* Proceedings of the National Academy of Sciences, 2013. **110**(32): p. 13109-13.
523. Longatti, A., Boyd, B. and Chisari, F.V., *Virion-independent transfer of replication-competent hepatitis C virus RNA between permissive cells.* Journal of Virology, 2015. **89**(5): p. 2956-61.
524. Kadiu, I., et al., *Biochemical and biologic characterization of exosomes and microvesicles as facilitators of HIV-1 infection in macrophages.* The Journal of Immunology, 2012. **189**(2): p. 744-54.

525. Zhu, X., et al., *IFITM3-containing exosome as a novel mediator for anti-viral response in dengue virus infection.* Cellular Microbiology, 2015. **17**(1): p. 105-18.
526. Vora, A., et al., *Arthropod EVs mediate dengue virus transmission through interaction with a tetraspanin domain containing glycoprotein Tsp29Fb.* Proceedings of the National Academy of Sciences, 2018. **115**(28): p. e6604-13.
527. Farias, K.J.S., et al., *Chloroquine inhibits dengue virus type 2 replication in Vero cells but not in C6/36 cells.* The Scientific World Journal, 2013. **2013**: p. 282734.
528. van Cleef, K.W.R., et al., *Identification of a new dengue virus inhibitor that targets the viral NS4B protein and restricts genomic RNA replication.* Antiviral Research, 2013. **99**(2): p. 165-71.
529. Kim, J.A., et al., *Favipiravir and ribavirin inhibit replication of Asian and African strains of Zika virus in different cell models.* Viruses, 2018. **10**(2): p. e72.
530. Andersson, U., et al., *Inhibition of glycogen breakdown by imino sugars in vitro and in vivo.* Biochemical Pharmacology, 2004. **67**(4): p. 697-705.
531. Martín-Acebes, M.A., Vázquez-Calvo, Á., and Saiz, J.C., *Lipids and flaviviruses, present and future perspectives for the control of dengue, Zika, and West Nile viruses.* Progress in Lipid Research, 2016. **64**: p. 123-37.
532. Aktepe, T.E., Pham, H. and Mackenzie, J.M., *Differential utilisation of ceramide during replication of the flaviviruses West Nile and dengue virus.* Virology, 2015. **484**: p. 241-50.
533. Diop, F., et al., *Zika virus infection modulates the metabolomic profile of microglial cells.* PLoS ONE, 2018. **13**(10): p. e0206093.
534. Singh, P.K., et al., *Determination of system level alterations in host transcriptome due to Zika virus (ZIKV) Infection in retinal pigment epithelium.* Scientific Reports, 2018. **8**(1): p. 11209.
535. Li, C., et al., *25-hydroxycholesterol protects host against Zika virus infection and its associated microcephaly in a mouse model.* Immunity, 2017. **46**(3): p. 446-56.
536. Gaudry, A., et al., *The flavonoid isoquercitrin precludes initiation of Zika virus infection in human cells.* International Journal of Molecular Sciences, 2018. **19**(4): p. e1093.
537. Wozniak, A.L., et al., *Intracellular proton conductance of the hepatitis C virus p7 protein and its contribution to infectious virus production.* PLoS Pathogens, 2010. **6**(9): p. e1001087.
538. Razonable, R. and McGill, J., *Investigational drugs in clinical development for the treatment of chronic hepatitis*, in *Hepatitis prevention and treatment*, J. Colacino and B. Heinz, Editors. 2004, Springer Basel AG: Basel. p. 192.
539. Durantel, D., et al., *Effects of interferon, ribavirin, and iminosugar derivatives on cells persistently infected with noncytopathic bovine viral diarrhea virus.* Antimicrobial Agents and Chemotherapy, 2004. **48**(2): p. 497-504.
540. Woodhouse, S.D., et al., *Iminosugars in combination with interferon and ribavirin permanently eradicate noncytopathic bovine viral diarrhea virus from persistently infected cells.* Antimicrobial Agents and Chemotherapy, 2008. **52**(5): p. 1820-8.
541. Largo, E., et al., *Pore-forming activity of pestivirus p7 in a minimal model system supports genus-specific viroporin function.* Antiviral Research, 2014. **101**: p. 30-6.
542. Luscombe, C.A., et al., *A novel hepatitis C virus p7 ion channel inhibitor, BIT225, inhibits bovine viral diarrhea virus in vitro and shows synergism with recombinant interferon-α-2b and nucleoside analogues.* Antiviral Research, 2010. **86**(2): p. 144-53.
543. Premkumar, A., Horan, C.R., and Gage, P.W., *Dengue virus M protein C-terminal peptide (DVM-C) forms ion channels.* The Journal of Membrane Biology, 2005. **204**(1): p. 33-8.
544. Wong, S.S., et al., *Dengue virus PrM/M proteins fail to show pH-dependent ion channel activity in Xenopus oocytes.* Virology, 2011. **412**(1): p. 83-90.

545. Shoshan-Barmatz, V., et al., *VDAC, a multi-functional mitochondrial protein regulating cell life and death.* Molecular Aspects of Medicine, 2010. **31**(3): p. 227-85.
546. Tangsongcharoen, C., Roytrakul, S. and Smith, D.R., *Analysis of cellular proteome changes in response to ZIKV NS2B-NS3 protease expression.* Biochimica et Biophysica Acta (BBA) - Proteins and Proteomics, 2019. **1867**(2): p. 89-97.
547. Rinkenberger, N. and Schoggins, J.W., *Mucolipin-2 cation channel increases trafficking efficiency of endocytosed viruses.* mBio, 2018. **9**(1): p. e02314-17.
548. Doñate-Macián, P., et al., *The TRPV4 channel links calcium influx to DDX3X activity and viral infectivity.* Nature Communications, 2018. **9**(1): p. 2307.
549. Norez, C., et al., *Rescue of functional delF508-CFTR channels in cystic fibrosis epithelial cells by the α-glucosidase inhibitor miglustat.* FEBS Letters, 2006. **580**(8): p. 2081-6.
550. Norez, C., et al., *A cystic fibrosis respiratory epithelial cell chronically treated by miglustat acquires a non–cystic fibrosis–like phenotype.* American Journal of Respiratory Cell and Molecular Biology, 2009. **41**(2): p. 217-25.
551. Angiari, S., et al., *TIM-1 glycoprotein binds the adhesion receptor P-selectin and mediates T cell trafficking during inflammation and autoimmunity.* Immunity, 2014. **40**(4): p. 542-53.
552. Quicke, K.M., et al., *Zika virus infects human placental macrophages.* Cell Host & Microbe, 2016. **20**(1): p. 83-90.
553. Lang, J., et al., *An hPSC-derived tissue-resident macrophage model reveals differential responses of macrophages to ZIKV and DENV infection.* Stem Cell Reports, 2018. **11**(2): p. 348-62.
554. Cox, T.M., et al., *The role of the iminosugar N-butyldeoxynojirimycin (miglustat) in the management of type I (non-neuronopathic) Gaucher disease: a position statement.* Journal of Inherited Metabolic Disease, 2003. **26**(6): p. 513-26.
555. Bertolotti-Ciarlet, A., et al., *Cellular localization and antigenic characterization of Crimean-Congo hemorrhagic fever virus glycoproteins.* Journal of Virology, 2005. **79**(10): p. 6152-61.
556. Steentoft, C., et al., *Precision mapping of the human O-GalNAc glycoproteome through SimpleCell technology.* The EMBO Journal, 2013. **32**(10): p. 1478-88.
557. Roversi, P., et al., *Interdomain conformational flexibility underpins the activity of UGGT, the eukaryotic glycoprotein secretion checkpoint.* Proceedings of the National Academy of Sciences, 2017. **114**(32): p. 8544-9.
558. Inada, H., et al., *Keratin attenuates tumor necrosis factor–induced cytotoxicity through association with TRADD.* The Journal of Cell Biology, 2001. **155**(3): p. 415-26.
559. Takahashi, K., et al., *Production and secretion of two vasoactive peptides, adrenomedullin and endothelin-1, by cultured human adrenocortical carcinoma cells.* Peptides, 2000. **21**(2): p. 251-56.
560. Zhang, L., et al., *Versatile reporter systems show that transactivation by human T-cell leukemia virus type 1 Tax occurs independently of chromatin remodeling factor BRG1.* Journal of Virology, 2006. **80**(15): p. 7459-68.
561. Vershinina, M., et al., *Regulation of cytokine mRNAs by interferon and interferon inducers [abstract only].* Russian Journal of Immunology, 2002. **7**(2): p. 161-6.
562. Narovlianskiĭ, A., et al., *[Effect of interferon inductors on infection induced by hepatitis C virus and activity of mRNA cytokines in cell cultures SW-13 and MT-4][Article in Russian][Abstract only].* Voprosy Virusologii, 2002. **47**(6): p. 17-21.
563. Messina, J.P., et al., *The global distribution of Crimean-Congo hemorrhagic fever.* Transactions of The Royal Society of Tropical Medicine and Hygiene, 2015. **109**(8): p. 503-13.

564. Watts, D.M., et al., *Inhibition of Crimean-Congo hemorrhagic fever viral infectivity yields in vitro by ribavirin.* American Journal of Tropical Medicine and Hygiene, 1989. **41**(5): p. 581-5.
565. Paragas, J., et al., *A simple assay for determining antiviral activity against Crimean-Congo hemorrhagic fever virus.* Antiviral Research, 2004. **62**(1): p. 21-5.
566. Tignor, G.H. and Hanham, C.A., *Ribavirin efficacy in an in vivo model of Crimean-Congo hemorrhagic fever virus (CCHF) infection.* Antiviral Research, 1993. **22**(4): p. 309-25.
567. Bente, D.A., et al., *Pathogenesis and immune response of Crimean-Congo hemorrhagic fever virus in a STAT-1 knockout mouse model.* Journal of Virology, 2010. **84**(21): p. 11089-100.
568. Oestereich, L., et al., *Evaluation of antiviral efficacy of ribavirin, arbidol, and T-705 (favipiravir) in a mouse model for Crimean-Congo hemorrhagic fever.* PLoS Neglected Tropical Diseases, 2014. **8**(5): p. e2804.
569. Hawman, D.W., et al., *Favipiravir (T-705) but not ribavirin is effective against two distinct strains of Crimean-Congo hemorrhagic fever virus in mice.* Antiviral Research, 2018. **157**: p. 18-26.
570. Hurtley, S.M., et al., *Interactions of misfolded influenza virus hemagglutinin with binding protein (BiP).* Journal of Cell Biology, 1989. **108**(6): p. 2117-26.
571. Zivcec, M., et al., *Molecular insights into Crimean-Congo hemorrhagic fever virus.* Viruses, 2016. **8**(4): p. 106.
572. Bereczky, S., et al., *Crimean–Congo hemorrhagic fever virus infection is lethal for adult type I interferon receptor-knockout mice.* Journal of General Virology, 2010. **91**(6): p. 1473-7.
573. Zivcec, M., et al., *Lethal Crimean-Congo hemorrhagic fever virus infection in interferon α/β receptor knockout mice is associated with high viral loads, pro-inflammatory responses and coagulopathy.* Journal of Infectious Diseases, 2013. **207**(12): p. 1909-21.
574. Royall, J.A., et al., *Tumor necrosis factor and interleukin 1 alpha increase vascular endothelial permeability.* Am J Physiol, 1989. **257**(6 Pt 1): p. 399-410.
575. Hoang, L.T., et al., *The early whole-blood transcriptional signature of dengue virus and features associated with progression to dengue shock syndrome in Vietnamese children and young adults.* Journal of Virology, 2010. **84**(24): p. 12982-94.
576. Chen, Y.C. and S.Y. Wang, *Activation of terminally differentiated human monocytes/macrophages by dengue virus: productive infection, hierarchical production of innate cytokines and chemokines, and the synergistic effect of lipopolysaccharide.* Journal of Virology, 2002. **76**(19): p. 9877-87.
577. Czura, C.J., *Merinoff symposium 2010: sepsis - speaking with one voice.* Molecular Medicine (Cambridge, Mass.), 2011. **17**(1-2): p. 2-3.
578. Hotchkiss, R.S. and Karl, I.E., *The pathophysiology and treatment of sepsis.* New England Journal of Medicine, 2003. **348**(2): p. 138-50.
579. Hotchkiss, R.S., Monneret, G., and Payen, D., *Sepsis-induced immunosuppression: from cellular dysfunctions to immunotherapy.* Nature Reviews Immunology, 2013. **13**: p. 862-74.
580. Otto, G.P., et al., *The late phase of sepsis is characterized by an increased microbiological burden and death rate.* Critical Care, 2011. **15**(4): p. R183.
581. Lv, S., et al., *Anti-TNF-α therapy for patients with sepsis: a systematic meta-analysis.* International Journal of Clinical Practice, 2014. **68**(4): p. 520-8.
582. Pennica, D., et al., *Cloning and expression in Escherichia coli of the cDNA for murine tumor necrosis factor.* Proceedings of the National Academy of Sciences of the United States of America, 1985. **82**(18): p. 6060-4.

583. Zoon, K.C., et al., *Purification and characterization of multiple components of human lymphoblastoid interferon-alpha.* Journal of Biological Chemistry, 1992. **267**(21): p. 15210-6.
584. Capobianchi, M.R., et al., *Acid lability is not an intrinsic property of interferon-alpha induced by HIV-infected cells.* Journal of Interferon Research, 1992. **12**(6): p. 431-8.
585. Nyman, T.A., et al., *Identification of nine interferon-alpha subtypes produced by Sendai virus-induced human peripheral blood leucocytes.* Biochemical Journal, 1998. **329**(Pt 2): p. 295-302.
586. Karpusas, M., et al., *The crystal structure of human interferon β at 2.2-Å resolution.* Proceedings of the National Academy of Sciences of the United States of America, 1997. **94**(22): p. 11813-8.
587. Benarroch, D., et al., *A structural basis for the inhibition of the NS5 dengue virus mRNA 2'-O-methyltransferase domain by ribavirin 5'-triphosphate.* Journal of Biological Chemistry, 2004. **279**(34): p. 35638-43.
588. Graci, J.D. and Cameron, C.E., *Mechanisms of action of ribavirin against distinct viruses.* Reviews in Medical Virology, 2005. **16**(1): p. 37-48.
589. Tam, R.C., et al., *Ribavirin polarizes human T cell responses towards a Type 1 cytokine profile.* Journal of Hepatology, 1999. **30**(3): p. 376-82.
590. Conte, E., et al., *Ribavirin up-regulates IL-12 p40 gene expression and restores IL-12 levels in Leishmania-treated PBMCs.* Parasite Immunology, 2005. **27**(12): p. 447-51.
591. Ning, Q., et al., *Ribavirin inhibits viral-induced macrophage production of TNF, IL-1, the procoagulant fgl2 prothrombinase and preserves Th1 cytokine production but inhibits Th2 cytokine response.* The Journal of Immunology, 1998. **160**(7): p. 3487-93.
592. Malinoski, F.J., et al., *Prophylactic ribavirin treatment of dengue type 1 infection in rhesus monkeys.* Antiviral Research, 1990. **13**(3): p. 139-49.
593. Chan, K.W.K., et al., *Animal models for studying dengue pathogenesis and therapy.* Antiviral Research, 2015. **123**: p. 5-14.
594. Gray, S.B., et al., *Single-nucleotide polymorphisms in the TNF gene are associated with obesity-related phenotypes in vervet monkeys.* Obesity, 2012. **19**(7): p. 1427-32.
595. Souza-Neto, J.A., Sim, S. and Dimopoulos, G., *An evolutionary conserved function of the JAK-STAT pathway in anti-dengue defense.* Proceedings of the National Academy of Sciences, 2009. **106**(42): p. 17841-6.
596. Xi, Z., Ramirez, J.L., and Dimopoulos, G., *The Aedes aegypti Toll pathway controls dengue virus infection.* PLoS Pathogens, 2008. **4**(7): p. e1000098.
597. Scott, J.C., et al., *Comparison of dengue virus type 2-specific small RNAs from RNA interference-competent and –incompetent mosquito cells.* PLoS Neglected Tropical Diseases, 2010. **4**(10): p. e848.
598. Kanthong, N., Laosutthipong, C., and Flegel, T.W., *Response to Dengue virus infections altered by cytokine-like substances from mosquito cell cultures.* BMC Microbiology, 2010. **10**(1): p. 290.
599. Seeds, R.E., et al., *The role of myeloid receptors on murine plasmacytoid dendritic cells in induction of type I interferon.* International Immunopharmacology, 2011. **11**(7): p. 794-801.
600. Uchida, L., et al., *The dengue virus conceals double-stranded RNA in the intracellular membrane to escape from an interferon response.* Scientific Reports, 2014. **4**: p. 7395.
601. Scaffidi, P., Misteli, T., and Bianchi, M.E., *Release of chromatin protein HMGB1 by necrotic cells triggers inflammation.* Nature, 2002. **418**: p. 191-5.
602. Wang, H., et al., *HMG-1 as a late mediator of endotoxin lethality in mice.* Science, 1999. **285**(5425): p. 248-51.

603. Gardella, S., et al., *The nuclear protein HMGB1 is secreted by monocytes via a non-classical, vesicle-mediated secretory pathway.* EMBO Reports, 2002. **3**(10): p. 995-1001.
604. Bonaldi, T., et al., *Monocytic cells hyperacetylate chromatin protein HMGB1 to redirect it towards secretion.* The EMBO Journal, 2003. **22**(20): p. 5551-60.
605. Youn, J.H. and J.S. Shin, *Nucleocytoplasmic shuttling of HMGB1 is regulated by phosphorylation that redirects it toward secretion.* The Journal of Immunology, 2006. **177**(11): p. 7889-97.
606. Andersson, U., et al., *High mobility group 1 protein (Hmg-1) stimulates proinflammatory cytokine synthesis in human monocytes.* The Journal of Experimental Medicine, 2000. **192**(4): p. 565-70.
607. Dumitriu, I.E., et al., *Release of high mobility group box 1 by dendritic cells controls T cell activation via the receptor for advanced glycation end products.* The Journal of Immunology, 2005. **174**(12): p. 7506-15.
608. Park, J.S., et al., *Involvement of Toll-like receptors 2 and 4 in cellular activation by high mobility group box 1 protein.* Journal of Biological Chemistry, 2004. **279**(9): p. 7370-7.
609. Ong, S.P., et al., *Dengue virus infection mediates HMGB1 release from monocytes involving PCAF acetylase complex and induces vascular leakage in endothelial cells.* PLoS ONE, 2012. **7**(7): p. e41932.
610. Kamau, E., et al., *Dengue virus infection promotes translocation of high mobility group box 1 protein from the nucleus to the cytosol in dendritic cells, upregulates cytokine production and modulates virus replication.* Journal of General Virology, 2009. **90**(8): p. 1827-35.
611. Chen, L.C., et al., *Dengue virus infection induces passive release of high mobility group box 1 protein by epithelial cells.* Journal of Infection, 2008. **56**(2): p. 143-50.
612. Allonso, D., et al., *Elevated serum levels of high mobility group box 1 (HMGB1) protein in dengue-infected patients are associated with disease symptoms and secondary infection.* Journal of Clinical Virology, 2012. **55**(3): p. 214-9.
613. Yi, G., et al., *Hepatitis C virus NS4B can suppress STING accumulation to evade innate immune responses.* Journal of Virology, 2016. **90**(1): p. 254-65.
614. Sauder, D.N., *Immunomodulatory and pharmacologic properties of imiquimod.* Journal of the American Academy of Dermatology, 2000. **43**(1, Part 2): p. S6-S11.
615. Yamamoto, M., et al., *Role of adaptor TRIF in the MyD88-independent Toll-like receptor signaling pathway.* Science, 2003. **301**(5633): p. 640-3.
616. Kawai, T., et al., *Unresponsiveness of MyD88-deficient mice to endotoxin.* Immunity, 1999. **11**(1): p. 115-22.
617. Kaisho, T., et al., *Endotoxin-induced maturation of MyD88-deficient dendritic cells.* The Journal of Immunology, 2001. **166**(9): p. 5688-94.
618. Shen, H., et al., *Dual signaling of MyD88 and TRIF is critical for maximal TLR4-induced dendritic cell maturation.* Journal of Immunology, 2008. **181**(3): p. 1849-58.
619. Muzio, M., et al., *Differential expression and regulation of Toll-like receptors (TLR) in human leukocytes: selective expression of TLR3 in dendritic cells.* The Journal of Immunology, 2000. **164**(11): p. 5998-6004.
620. Visintin, A., et al., *Regulation of Toll-like receptors in human monocytes and dendritic cells.* The Journal of Immunology, 2001. **166**(1): p. 249-55.
621. Zarember, K.A. and Godowski, P.J., *Tissue expression of human Toll-like receptors and differential regulation of Toll-like receptor mRNAs in leukocytes in response to microbes, their products, and cytokines.* The Journal of Immunology, 2002. **168**(2): p. 554-61.
622. Miettinen, M., et al., *IFNs activate toll-like receptor gene expression in viral infections.* Genes And Immunity, 2001. **2**: p. 349-55.

623. Heinz, S., et al., *Species-specific regulation of Toll-like receptor 3 genes in men and mice.* Journal of Biological Chemistry, 2003. **278**(24): p. 21502-9.
624. Pålsson-McDermott, E.M. and O'Neill, L.A.J., *Signal transduction by the lipopolysaccharide receptor, Toll-like receptor-4.* Immunology, 2004. **113**(2): p. 153-62.
625. Rinderknecht, E., O'Connor, B.H. and Rodriguez, H., *Natural human interferon-gamma. Complete amino acid sequence and determination of sites of glycosylation.* Journal of Biological Chemistry, 1984. **259**(11): p. 6790-7.
626. Sareneva, T., et al., *Role of N-glycosylation in the synthesis, dimerization and secretion of human interferon-gamma.* Biochemical Journal, 1994. **303**(3): p. 831-40.
627. Rubartelli, A., et al., *A novel secretory pathway for interleukin-1 beta, a protein lacking a signal sequence.* The EMBO Journal, 1990. **9**(5): p. 1503-10.
628. Mortier, A., et al., *Effect of posttranslational processing on the in vitro and in vivo activity of chemokines.* Experimental Cell Research, 2011. **317**(5): p. 642-54.
629. Botos, I., Segal, D.M. and Davies, D.R., *The structural biology of Toll-like receptors.* Structure, 2011. **19**(4): p. 447-59.
630. Leifer, C.A. and Medvedev, A.E., *Molecular mechanisms of regulation of Toll-like receptor signaling.* Journal of Leukocyte Biology, 2016. **100**(5): p. 927-41.
631. da Silva Correia, J. and Ulevitch, R.J., *MD-2 and TLR4 N-linked glycosylations are important for a functional lipopolysaccharide receptor.* Journal of Biological Chemistry, 2002. **277**(3): p. 1845-54.
632. Ohnishi, T., Muroi, M. and Tanamoto, K.I., *N-linked glycosylations at Asn26 and Asn114 of human MD-2 are required for Toll-like receptor 4-mediated activation of NF-κB by lipopolysaccharide.* The Journal of Immunology, 2001. **167**(6): p. 3354-9.
633. Amith, S.R., et al., *Neu1 desialylation of sialyl α-2,3-linked β-galactosyl residues of TOLL-like receptor 4 is essential for receptor activation and cellular signaling.* Cellular Signalling, 2010. **22**(2): p. 314-24.
634. Feng, C., et al., *Sialyl residues modulate LPS-mediated signaling through the Toll-like receptor 4 complex.* PLoS ONE, 2012. **7**(4): p. e32359.
635. Iijima, J., et al., *Core fucose is critical for CD14-dependent Toll-like receptor 4 signaling.* Glycobiology, 2017. **27**(11): p. 1006-15.
636. Nakayama, K., et al., *Core fucose is essential glycosylation for CD14-dependent Toll-like receptor 4 and Toll-like receptor 2 signaling in macrophages.* The Journal of Biochemistry, 2018: p. mvy098.
637. Kataoka, H., et al., *Roles of N-linked glycans in the recognition of microbial lipopeptides and lipoproteins by TLR2.* Cellular Microbiology, 2006. **8**(7): p. 1199-1209.
638. Sun, J., et al., *Structural and functional analyses of the human Toll-like receptor 3: role of glycosylation.* Journal of Biological Chemistry, 2006. **281**(16): p. 11144-51.
639. Sato, R., et al., *Requirement of glycosylation machinery in TLR responses revealed by CRISPR/Cas9 screening.* International Immunology, 2017. **29**(8): p. 347-55.
640. Zhu, J., et al., *Characterization of bovine Toll-like receptor 8: Ligand specificity, signaling essential sites and dimerization.* Molecular Immunology, 2009. **46**(5): p. 978-90.
641. Kato, Y., Adachi, Y. and Ohno, N., *Contribution of N-linked oligosaccharides to the expression and functions of beta-glucan receptor, Dectin-1.* Biological and Pharmaceutical Bulletin, 2006. **29**(8): p. 1580-6.
642. Ron, D. and Walter, P., *Signal integration in the endoplasmic reticulum unfolded protein response.* Nature Reviews Molecular Cell Biology, 2007. **8**: p. 519-29.
643. Liu, Y.P., et al., *Endoplasmic reticulum stress regulates the innate immunity critical transcription factor IRF3.* The Journal of Immunology, 2012. **189**(9): p. 4630-9.
644. Martinon, F., et al., *TLR activation of the transcription factor XBP1 regulates innate immune responses in macrophages.* Nature Immunology, 2010. **11**: p. 411-8.

645. Zeng, L., et al., *XBP-1 couples endoplasmic reticulum stress to augmented IFN-β induction via a cis-acting enhancer in macrophages.* The Journal of Immunology, 2010. **185**(4): p. 2324-30.
646. Goodall, J.C., et al., *Endoplasmic reticulum stress-induced transcription factor, CHOP, is crucial for dendritic cell IL-23 expression.* Proceedings of the National Academy of Sciences, 2010. **107**(41): p. 17698-703.
647. Iwasaki, Y., et al., *Activating transcription factor 4 links metabolic stress to interleukin-6 expression in macrophages.* Diabetes, 2014. **63**(1): p. 152-61.
648. Leonard, A., et al., *Preconditioning with endoplasmic reticulum stress ameliorates endothelial cell inflammation.* PLoS ONE, 2014. **9**(10): p. e110949.
649. Komura, T., et al., *ER stress induced impaired TLR signaling and macrophage differentiation of human monocytes.* Cellular Immunology, 2013. **282**(1): p. 44-52.
650. Kim, S.Y., J.S. Hwang, and I.O. Han, *Tunicamycin inhibits Toll-like receptor-activated inflammation in RAW264.7 cells by suppression of NF-κB and c-Jun activity via a mechanism that is independent of ER-stress and N-glycosylation.* European Journal of Pharmacology, 2013. **721**(1): p. 294-300.
651. Nishiyama, K., et al., *Fatty acid transport protein 1 enhances the macrophage inflammatory response by coupling with ceramide and c-Jun N-terminal kinase signaling.* International Immunopharmacology, 2018. **55**: p. 205-15.
652. Allen, M.J., et al., *Pro-inflammatory cytokines and the pathogenesis of Gaucher's disease: increased release of interleukin-6 and interleukin-10.* QJM: An International Journal of Medicine, 1997. **90**(1): p. 19-25.
653. Köberlin, M.S., et al., *A conserved circular network of coregulated lipids modulates innate immune responses.* Cell, 2015. **162**(1): p. 170-83.
654. MacKichan, M.L. and DeFranco, A.L., *Role of ceramide in lipopolysaccharide (LPS)-induced signaling: LPS increases ceramide rather than acting as a structural homolog.* Journal of Biological Chemistry, 1999. **274**(3): p. 1767-75.
655. Józefowski, S., et al., *Ceramide and ceramide 1-phosphate are negative regulators of TNF-α production induced by lipopolysaccharide.* The Journal of Immunology, 2010. **185**(11): p. 6960-73.
656. Borkowski, A.W., et al., *Activation of TLR3 in keratinocytes increases expression of genes involved in formation of the epidermis, lipid accumulation, and epidermal organelles.* Journal of Investigative Dermatology, 2013. **133**(8): p. 2031-40.
657. Warke, R.V., et al., *Dengue virus induces novel changes in gene expression of human umbilical vein endothelial cells.* Journal of Virology, 2003. **77**(21): p. 11822-32.
658. Black, R.A., et al., *A metalloproteinase disintegrin that releases tumour-necrosis factor-α from cells.* Nature, 1997. **385**: p. 729-33.
659. Moss, M.L., et al., *Cloning of a disintegrin metalloproteinase that processes precursor tumour-necrosis factor-α.* Nature, 1997. **385**: p. 733-6.
660. Horiuchi, K., et al., *Cutting edge: TNF-α-converting enzyme (TACE/ADAM17) inactivation in mouse myeloid cells prevents lethality from endotoxin shock.* The Journal of Immunology, 2007. **179**(5): p. 2686-9.
661. Armstrong, L., et al., *Contribution of TNF-α converting enzyme and proteinase-3 to TNF-α processing in human alveolar macrophages.* American Journal of Respiratory Cell and Molecular Biology, 2006. **34**(2): p. 219-25.
662. Robache-Gallea, S., et al., *In vitro processing of human tumor necrosis factor-α.* Journal of Biological Chemistry, 1995. **270**(40): p. 23688-92.
663. Vandenbroucke, R.E., et al., *Matrix metalloproteinase 13 modulates intestinal epithelial barrier integrity in inflammatory diseases by activating TNF.* EMBO Molecular Medicine, 2013. **5**(7): p. 1000-16.

664. Blaydon, D.C., et al., *Inflammatory skin and bowel disease linked to ADAM17 deletion.* New England Journal of Medicine, 2011. **365**(16): p. 1502-8.
665. Dreymueller, D., et al., *Lung endothelial ADAM17 regulates the acute inflammatory response to lipopolysaccharide.* EMBO Molecular Medicine, 2012. **4**(5): p. 412-23.
666. Chavaroche, A., et al., *Glycosylation of a disintegrin and metalloprotease 17 affects its activity and inhibition.* Analytical Biochemistry, 2014. **449**: p. 68-75.
667. Yan, J.P., et al., *3'-azidothymidine (zidovudine) inhibits glycosylation and dramatically alters glycosphingolipid synthesis in whole cells at clinically relevant concentrations.* Journal of Biological Chemistry, 1995. **270**(39): p. 22836-41.
668. Chen, S., et al., *Zidovudine-based treatments inhibit the glycosylation of ADAM17 and reduce CD163 shedding from monocytes.* Journal of Acquired Immune Deficiency Syndromes, 2018. **79**(1): p. 126-34.
669. Chang, T.H., Liao, C.L. and Lin, Y.L., *Flavivirus induces interferon-beta gene expression through a pathway involving RIG-I-dependent IRF-3 and PI3K-dependent NF-κB activation.* Microbes and Infection, 2006. **8**(1): p. 157-71.
670. Rolph, M.S., et al., *Downregulation of interferon-β in antibody-dependent enhancement of dengue viral infections of human macrophages is dependent on interleukin-6.* The Journal of Infectious Diseases, 2011. **204**(3): p. 489-91.
671. Brown, M.G., et al., *RNA sensors enable human mast cell anti-viral chemokine production and IFN-mediated protection in response to antibody-enhanced dengue virus infection.* PLoS ONE, 2012. **7**(3): p. e34055.
672. Savan, R., *Post-transcriptional regulation of interferons and their signaling pathways.* Journal of Interferon & Cytokine Research, 2014. **34**(5): p. 318-29.
673. Bogdan, C. and Schleicher, U., *Production of interferon-γ by myeloid cells – fact or fancy?* Trends in Immunology, 2006. **27**(6): p. 282-90.
674. Nedwin, G.E., et al., *Effect of interleukin 2, interferon-gamma, and mitogens on the production of tumor necrosis factors alpha and beta.* The Journal of Immunology, 1985. **135**(4): p. 2492-7.
675. Collart, M.A., et al., *Gamma interferon enhances macrophage transcription of the tumor necrosis factor/cachectin, interleukin 1, and urokinase genes, which are controlled by short-lived repressors.* The Journal of Experimental Medicine, 1986. **164**(6): p. 2113.
676. Matic, M. and Simon, S.R., *Effects of gamma interferon on release of tumor necrosis factor alpha from lipopolysaccharide-tolerant human monocyte-derived macrophages.* Infection and Immunity, 1992. **60**(9): p. 3756.
677. Kitchens, R.L., Wang, P.Y., and Munford, R.S., *Bacterial lipopolysaccharide can enter monocytes via two CD14-dependent pathways.* The Journal of Immunology, 1998. **161**(10): p. 5534-45.
678. Husebye, H., et al., *Endocytic pathways regulate Toll-like receptor 4 signaling and link innate and adaptive immunity.* The EMBO Journal, 2006. **25**(4): p. 683-92.
679. Chuang, T.H. and Ulevitch, R.J., *Triad3A, an E3 ubiquitin-protein ligase regulating Toll-like receptors.* Nature Immunology, 2004. **5**: p. 495-502.
680. Ling, L.E., et al., *Human type I interferon receptor, IFNAR, is a heavily glycosylated 120-130 kD membrane protein.* Journal of Interferon & Cytokine Research, 1995. **15**(1): p. 55-61.
681. Pennica, D., et al., *Biochemical characterization of the extracellular domain of the 75-kilodalton tumor necrosis factor receptor.* Biochemistry, 1993. **32**(12): p. 3131-8.
682. Ruiz Silva, M., et al., *Suppression of chikungunya virus replication and differential innate responses of human peripheral blood mononuclear cells during co-infection with dengue virus.* PLoS Neglected Tropical Diseases, 2017. **11**(6): p. e0005712.

683. Rückert, C., et al., *Impact of simultaneous exposure to arboviruses on infection and transmission by Aedes aegypti mosquitoes.* Nature Communications, 2017. **8**: p. 15412.
684. Chaves, B.A., et al., *Coinfection with Zika virus (ZIKV) and dengue virus results in preferential ZIKV transmission by vector bite to vertebrate host.* The Journal of Infectious Diseases, 2018. **218**(4): p. 563-71.
685. Mourya, D., et al., *Experimental Zika virus infection in Aedes aegypti: susceptibility, transmission & co-infection with dengue & chikungunya viruses.* Indian Journal of Medical Research, 2018. **147**(1): p. 88-96.
686. Myrielle, D.R., et al., *Co-infection with Zika and dengue viruses in 2 patients, New Caledonia, 2014.* Emerging Infectious Disease Journal, 2015. **21**(2): p. 381-2.
687. Pessôa, R., et al., *Investigation into an outbreak of dengue-like Illness in Pernambuco, Brazil, revealed a cocirculation of Zika, chikungunya, and dengue virus type 1.* Medicine, 2016. **95**(12): p. e3201.
688. Chia, P.Y., et al., *Clinical features of patients with Zika and dengue virus co-infection in Singapore.* Journal of Infection, 2017. **74**(6): p. 611-5.
689. Iovine, N.M., et al., *Coinfection with Zika and dengue-2 viruses in a traveler returning from Haiti, 2016: clinical presentation and genetic analysis.* Clinical Infectious Diseases, 2017. **64**(1): p. 72-5.
690. Badolato-Corrêa, J., et al., *Human T cell responses to Dengue and Zika virus infection compared to Dengue/Zika coinfection.* Immunity, Inflammation and Disease, 2018. **6**(2): p. 194-206.
691. Estofolete, C.F., et al., *Co-infection between Zika and different dengue serotypes during DENV outbreak in Brazil.* Journal of Infection and Public Health, 2019. **12**(2): p. 178-81.
692. Villamil-Gómez, W.E., et al., *Dengue, chikungunya and Zika co-infection in a patient from Colombia.* Journal of Infection and Public Health, 2016. **9**(5): p. 684-6.
693. Villamil-Gómez, W.E., et al., *Zika, dengue, and chikungunya co-infection in a pregnant woman from Colombia.* International Journal of Infectious Diseases, 2016. **51**: p. 135-8.
694. Carrillo-Hernández, M.Y., et al., *Co-circulation and simultaneous co-infection of dengue, chikungunya, and zika viruses in patients with febrile syndrome at the Colombian-Venezuelan border.* BMC Infectious Diseases, 2018. **18**(1): p. 61.
695. Waggoner, J.J., et al., *Viremia and clinical presentation in Nicaraguan patients infected with Zika virus, chikungunya virus, and dengue virus.* Clinical Infectious Diseases, 2016. **63**(12): p. 1584-90.
696. Smee, D.F., Bray, M., and Huggins, J.W., *Antiviral activity and mode of action studies of ribavirin and mycophenolic acid against orthopoxviruses in vitro.* Antiviral Chemistry and Chemotherapy, 2001. **12**(6): p. 327-35.
697. Day, C.W., et al., *Error-prone replication of West Nile virus caused by ribavirin.* Antiviral Research, 2005. **67**(1): p. 38-45.